



Sylen OWF

Sediment Dispersal modelling

Svea Vind Offshore

Date: 21 December 2023



Prepared by Verified by Description Rev.no. **Date** Approved by 01 20231124 Version 1 AIRN/TEB GVIG TEB 02 20231221 Version 2 TEB GVIG TEB



Contents

1.	Introduction	6
2.	Scope of Work	6
3.	Abbreviation	6
4.	Summary	7
4.1.	Baseline and representative year	7
4.2.	Sediment dispersal	7
5.	Methodology	8
5.1.1.		
5.1.2.	Sediment model	9
6.	Background data	10
6.1.	Layout, Project description	
6.1.1.	Wind farm Layout	10
6.1.2.	Sediment sources - Construction Phase	10
6.1.3.	Dimensions and gross sediment spill	11
6.2.	Bathymetry data	12
6.3.	Observations	12
6.3.1.	Water levels	13
6.3.2.	Currents	14
6.3.3.	Salinity	16
6.3.4.	Vertical Profiles (CTD) Measurements of Salinity	17
6.3.5.	Water temperature	18
6.3.6.	Vertical Profiles (CTD) Measurements of Temperature	19
6.4.	Hydrodynamic data from models	20
6.4.1.	Water levels	20
6.4.2.	Currents	20
6.4.3.	Salinity and Temperature	20
6.5.	Wind, Air Pressure, Air Temperature, Net long and short-wave radiations	20
6.6.	Sea ice	20
6.7.	Run-off	22
6.8.	Surficial sediments, seabed geology	25



6.9.	Baseline description	26
7 . I	Hydrodynamic 3D model (Regional & Local)	28
7.1.	Bathymetry and mesh	28
7.1.1.	Regional model	28
7.1.2.	Local sediment model	28
7.2.	Boundary data	29
7.3.	Model setup and calibration	30
7.4.	Identification of a representative period	30
7.5.	Verification	31
7.5.1.	Water levels	31
7.5.2.	Salinity	33
7.5.3.	Salinity Profiles	34
7.5.4.	Water temperature	35
7.5.5.	Temperature Profiles	36
8.	Sediment dispersal model	40
8.1.	Sediment sources and spill program	40
8.2.	Sediment type	41
8.3.	Estimated spill	42
8.4.	Estimated sediment concentrations and associated durations	43
8.4.1.	Surface	44
8.4.2.	Distribution over the water column	45
8.4.3.	At the bottom	46
8.1.	Estimated sedimentation	50
9. I	References	53

Appendix

Appendix 1: Grain sieve analyses

Appendix 2 Current field (SMHI)

Appendix 3: Sylen OWF, Temperature profiles (SMHI, modelled 4x4km)

Appendix 4 Sylen OWF, Temperature profiles (SMHI, modelled 2x2km)

Appendix 5 Sylen OWF, Salinity profiles (SMHI, modelled 4x4km)

Appendix 6 Sylen OWF, Salinity profiles (SMHI, modelled 2x2km)

Appendix 7 Sylen OWF, Current roses (SMHI, modelled 4x4km)

Appendix 8 Sylen OWF, Current roses (SMHI, modelled 2x2km)

Appendix 9 Sylen OWF, Simplified Particle Tracks

Appendix 10 Observations: Water levels

Appendix 11 Observations: CTD-Measuring sites

Appendix 12 Observations: Surface temperature

Appendix 13 Model verification: Water levels



Appendix 14 Model verification: Salinity profiles

Appendix 15 Model verification: Timeseries of surface temperature

Appendix 16 Model verification: Temperature profiles

Appendix 17 Sediment dispersal: Concentration – Season 1

Appendix 18 Sediment dispersal: Concentration – Season 2

Appendix 19 Sediment dispersal: Sedimentation – season 1

Appendix 20 Sediment dispersal: Sedimentation – season 2



1. Introduction

Sylen OWF has appointed NIRAS to quantify the impact on the dispersal of sediment in the construction phase.

During the construction of the wind farm, installation activities such as seabed preparations and cable burial may involves dredging at the foundation location and jetting of the cables to bury them safe for fishing activities, anchors, etc. This will potentially release sediments to the water resulting in excess sediment concentrations and when the sediments settle excess sedimentations rates.

The effects on the physical environment are analysed using numerical models.

2. Scope of Work

The purpose of the sediment dispersion study is to present the potential impact of sediment dispersal due to dredging, jetting etc. during the construction of the wind farm.

3. Abbreviation

Current direction Going towards

GBS Gravity Based Structure

IAC Inter array cable

MP Monopile

OSS Offshore substation
OWF Offshore Wind Farm

TP Transition piece, substructure

Wave direction Coming from Wind direction Coming from

WTG Wind turbine generator



4. Summary

The main objective of this study is to investigate sediment dispersion during the construction phase. For this purpose, two types of numerical models were used:

- 1) A 3D hydrodynamic model to simulate water level, currents, salinity, and temperature.
- 2) A sediment model to simulate the spreading and deposition of sediments stirred up during the construction.

Prior to assessing the sediment dispersal, the hydrodynamic model was calibrated using publicly available water level, salinity, and temperature data from Sweden and Finland.

While the final wind farm layout is still open, the impact is investigated based on a case with 347 20 MW turbines and 8 offshore substations all on gravity-based substructures expected to be constructed over a period of 2 years each with 2 phases.

4.1. Baseline and representative year

The Sylen OWF is located in the south-western part of the Bothnian Sea, approximately 120 kilometres north of the narrowest zone of the Åland Sea.

The hydrographic conditions for Sylen OWF and the southern part of the Bothnia Bay (based on SMHI's 3D model, (Copernicus, Baltic Sea Physics Analysis and Forecast, 2x2km, 2022) (Copernicus, Baltic Sea Physics Reanalysis 4x4km, 2022)) are characterised by a relatively low salinity (4.5-6.5 PSU). The interannual variability is so pronounced that no clear seasonal pattern is discernible.

Sea surface temperature varies from 0-2°C during the winter to over >20°C in July and August. Temperature is strongly stratified during the summer with a thermocline (zone of maximum temperature gradient) at around 10-30m depth. Between September and October, the water may warm up to 12-15° over the entire depth. The water depths at Style OWF is between 40 to 60 m.

Ice cover spreads from north to south starting in December and reaches a maximum extent in March, with the entire length of the west coast of Finland covered with ice. From June, the entire Gulf of Bothnia is ice-free again.

Due to the absence of tides, water level variations are mostly driven by variations at the Åland boundary, wind and pressure differences and account for ± 100 cm around their average during the year.

Currents are generally weak (around 0.1 m/s), and mostly driven by wind as well as temperature and salinity differences. The strongest currents occur in the summer months. The average circulation in the Bothnian Sea is counter clockwise, which generally leads to a southward current along the Swedish coast. However, this large-scale pattern is interrupted by local eddies.

Based on data from SMHI's 3D model of the Baltic Sea the year-to-year variations were investigated and the year 2022 was found to be close to an average year and thus to be used as a baseline for description of the potential impact. In general, the year-to-year variation is small and unlikely to impact the conclusion.

4.2. Sediment dispersal

For the purpose of investigating the sediment spreading the following four types of sources were considered:



- 1) Dredging of the gravity-based substructures and offshore substations with a dredge capacity of 1000m³/hour with 5% spill dispersed just above the seabed (released 2 meters over the seabed). The coarse sediment fraction settles next to the GBS (Gravity Base Structure, or the WTG and the OSS), and the finer ones are available for transport in the surrounding waters.
- 2) 10% of the total dredged sediments are assumed to overflow from the barge and are released at the surface and available for transport in the surrounding waters.
- 3) Burial of the inter array cable via jetting of a 1.5 x 2 m trench whereof 100% the sediments are assumed to be brought into suspension and released 2 m over the seabed.
- 4) Burial of the export cable via jetting of a 1.5 x 2 m trench whereof 100% the sediments are assumed to be brought into suspension and released 2 m over the seabed.

It is assumed that the construction will be conducted during two seasons with two phases per season each. In total, 2 419 914 m³ sediment (including coarse material) are released (15% close to the surface and 85% at the bottom). Due to the composition of the soil, the amount of fine sediment (finer than sand) accounts to 46% in season 1 and to 40% in season 2.

Sediment concentrations: As a result of the significantly larger volumes released near the seabed,

- the greatest concentrations occur near the seabed (e.g. 1000 mg/l is reached or exceed during 6 hours over an area of 195 ha in season 1, and on 4 ha in season 2),
- the sediment reaches the greatest extent close to the seabed (e.g. 10mg/l is reached or exceeded during season 1 on an area of > 43,000 ha),
- and the duration in which a certain concentration is reached or exceeded is the longest close to the seabed (the concentration of 10 mg/l is reached or exceeded for a maximum 15 days, season 1).

Due to the larger proportion of fine sediment released in the first season, the concentrations, the affected area and duration tend to be greater in season 1.

Sedimentation: The sedimented sediments originate from the dredging of the gravity-based substructures and the offshore substations and the burying of the inter-array and export cables using jetting. The resulting sediment heights are most pronounced along the inter-array and export cables (maximum 30 mm, density 1,650 kg/m³), where the largest amount of sediment is released. Sedimentation of at least 1 mm can be expected over an area of 19,365 ha (season 1), respectively 18,139 ha (season 2). Sedimentation > 0.01 mm extends approximately 38 kilometres to the south and 24 kilometres to the south-west (season 1).

5. Methodology

To estimate the dispersal of sediment two types of numerical models are used:

- 1) A 3D hydrodynamic model to simulate water levels, currents, salinity and temperature.
- 2) A sediment model to simulate the dispersal and deposit of the sediments dispersed due to the installation.

Before any evaluation of potential impacts the base model is calibrated toward the and publicly available water level, salinity and temperature data from Sweden and Finland.

Project ID: 10418781



Based on 10 years of data the Baseline is described and a representative period is identified and used for the simulation of the constriction and operation phase.

Bathymetric data for the model domain are extracted from the Baltic Sea Bathymetry Database (BSBD, last updated on 16/10/2017 (HELCOM, 2017)) which is based on modelled data from the countries around the Baltic Sea and is delivered as a grid with 500 meter resolution. Freely available boundary data of water level conditions will be applied at the boundary towards the Baltic Sea (Copernicus, Baltic Sea Physics Analysis and Forecast, 2x2km, 2022) combined with wind fields and air pressure at the surface of the model domain. Wind data is obtained from ECMWF, ERA5 (ECMWF, 2022).

Two models will be set up:

- 1) A general model of the Gulf of Bothnia (regional model) and
- 2) A detailed model covering the same extent as the regional model, but with a better spatial (vertical and horizontal) resolution in the vicinity of the project area.

5.1.1. Hydrodynamic model

MIKE 3 HD FM (Hydrodynamics) is a hydrodynamic model with a flexible mesh. Based on tidal, current, salinity and temperature inputs along the open boundaries together with the meteorological conditions at the sea surface, the model simulates tide, current speed and direction, temperature, and salinity throughout the model domain across the water column. The benefit of a flexible mesh is the possibility of using varying sizes of the mesh across the domain. Therefore, the focus area can have a high resolution, and areas further away can have a coarser resolution. This makes the model run faster, with a minor impact on the simulation results.

5.1.2. Sediment model

MIKE 21/3 PT (Particle Tracking) is a so-called Lagrangian model which over time considers both the position and properties of the particles e.g., keeping track of the particle position in both x, y- and z-direction according to the local current field. This is the opposite of a Eulerian model which does this cell-wise where e.g. the concentration will be an average of the volume over each cell. This type of model is extremely sensitive to the model resolution both horizontally and vertically, whereas the Lagrangian approach is independent of cell sizes.

The selection of MIKE 21/3 PT for modelling the sediment dispersal is due to the nature of the plumes created by dredging, drilling, ploughing, and jetting. The plumes are initially narrow and occur in various water column depths. This is difficult to describe in a traditional model e.g., MIKE 21 MT (Mud Transport) mesh while maintaining a reasonable calculation time.

To assess the quantity and duration of spillage, it is important to understand the construction activities. Will they be carried out simultaneously or will they be carried out independently at short intervals from each other? This will have an impact on the modelling study as in the former scenario, a higher quantity of sediments will be spilled in a shorter duration and in the latter scenario, spillage will occur in smaller quantities but repeatedly at certain intervals.



6. Background data

This chapter presents the background data used in the numerical modelling and the description of the seabed geology, oceanographic and hydraulic conditions for the wind farm. This includes project specifications, metocean data, soil data and bathymetric data.

6.1. Layout, Project description

6.1.1. Wind farm Layout

The layout of Sylen Offshore Wind Farm is illustrated in Figure 6.1. The footprint covers an area of 524 km², the total number of turbines for the 20 MW case is 347, there are 8 offshore substation, 465 km infield cables and 163 km export cable in the economical zone.

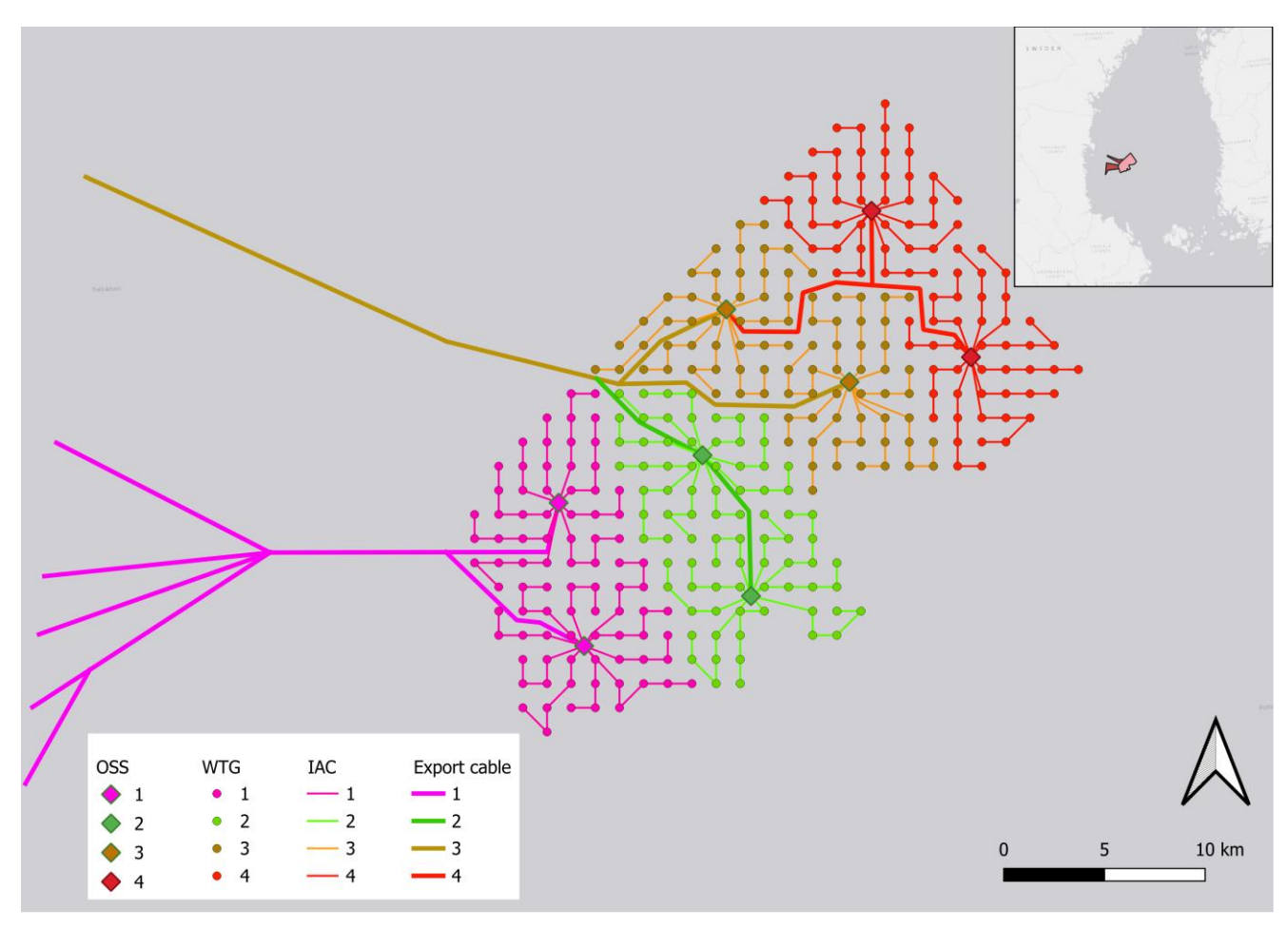


Figure 6.1: Sylen, wind farm layout coloured according to the phase.

6.1.2. Sediment sources - Construction Phase

The considered cases are as listed Table 6-1 based on the use of GBS that requires levelling/excavation of the seabed prior to installation. Afterwards are the cables between foundations first surfaced laid on the seabed and then jetted down to 2 metres. Similar with the export cables.

The sediment spills from these activities are assumed to be:



- Levelling/ excavation 5% of the fines released 2 m above the seabed.
- Overrun from the barge discharging another 10% of the fines at the surface.
- Jetting of the export and inter-array cables where all the sediment in the trench is brought into suspension releasing some of the fine sediments 2 m above the seabed i.e. 100%.

Where the fines are defined as the sediment with a grain size smaller than 0.25 mm i.e. fine sand, silt and clay. Coarser sediment is for the jetting assumed to settle in the trench and for the dredging not to released. It is assumed that the construction will be conducted in two simultaneous phases during two different seasons (phases 1 and 2 will be constructed during season 1, phases 3 and 4 during season 2).

6.1.3. Dimensions and gross sediment spill

In Table 6-1 the dimensions of the supporting substructures to be used for the modelling are listed per phase and installation season.



Table 6-1: Substructure dimensions inclusive spill percentage and gross spill.

Case	-	25MW GBS Season 1, Phase 1	25MW GBS Season 1, Phase 2	25MW GBS Season 2, Phase 3	25MW GBS Season 2, Phase 4	Total
Capacity	MW/Unit	25	25	25	25	
Substructure	-	GBS	GBS	GBS	GBS	
Capacity, total	MW	2,150	2,050	2,225	2,250	8,675
Nos	#	86	82	89	90	347
Bottom diameter, base	m	45	45	45	45	
Top diameter, base	m	8	8	8	8	
Drilling/dredging depth	m	5	5	5	5	
Spill percentage, dredging	%	5%	5%	5%	5%	
Spill percentage, overrun	%	10%	10%	10%	10%	
Vol. to be removed	m³/pos.	9,817	9,817	9,817	9,817	
Total drilled/dredged vol.	m ³	844,303	805,033	873,755	883,573	3,406,665
Spill, gross foundation	m ³	126,645	120,755	131,063	132,536	511,000
Length infield cable	m	112,947	111,036	121,311	120,113	465,407
Trench 1.5x2m, Dispersed	m ³	338,841	333,108	363,933	360,339	1,396,221
Spill percentage	%	100%	100%	100%	100%	
Spill gross	m ³	338,841	333,108	363,933	360,339	1,396,221
Spill, gross infield cable	m ³	338,841	333,108	363,933	360,339	1,396,221
Length export cable	m	80,768	14,406	47,205	20,674	163,053
Trench 1.5x2m, Dispersed	m ³	242,304	43,218	141,615	62,022	
Spill percentage	%	100%	100%	100%	100%	
Spill gross	m ³	242,304	43,218	141,615	62,022	489,159
Spill, gross export cable	m ³	242,304	43,218	141,615	62,022	489,159
No. OSS	#	2	2	2	2	8
Bottom diameter, base	m	55	55	55	55	
Dredging depth	m	5	5	5	5	
Spill percentage, dredging	%	5%	5%	5%	5%	
Spill percentage, overrun	%	10%	10%	10%	10%	
Vol. to be removed	m³/pos.	11,879	11,879	11,879	11,879	47,517
Spill, gross OSS	m ³	3,564	3,564	3,564	3,564	14,255
Spill, gross	m ³	711,354	500,645	640,175	558,461	2,410,635
Spill, net	m ³	489,412	344,444	440,440	384,221	1,658,517

6.2. Bathymetry data

The water depths in the model are based on the Baltic Sea Bathymetry Database (BSBD, last updated on 16/10/2017 (HELCOM, 2017) presented in Figure 7.1 (together with the mesh).

6.3. Observations

Observational data are used for model calibration. Figure 6.2 provides an overview of the locations of the measuring points for the individual parameters.



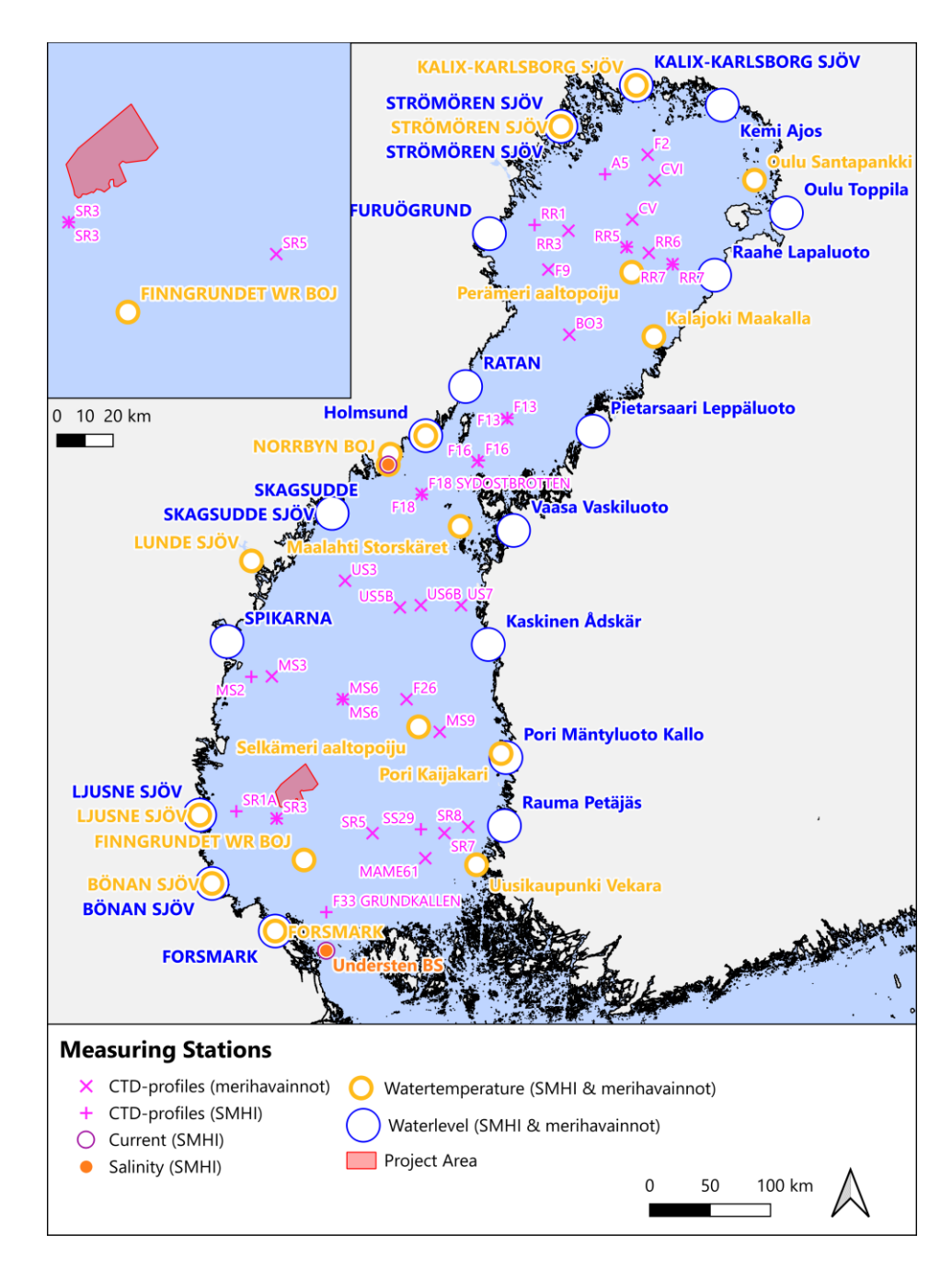


Figure 6.2: Location of water level, current, water temperature, and salinity monitoring stations used for calibration and validation of the hydrodynamic model.

6.3.1. Water levels

Water levels with an hourly resolution have been obtained from the SMHI (Swedish) and the FMI (Finish) stations (see table in Appendix 10), extracted for the period available. The locations of the water level stations are displayed in Figure 6.2. Due to the large number of available stations, the water level variations are discussed using two stations located in the immediate vicinity of the project (Figure 6.2). Water levels for these stations are displayed in Figure 6.3 to Figure 6.4, showing a maximum variation of \pm 1.00 m around a mean of approximately 0 m. No dominant tidal pattern is evident.



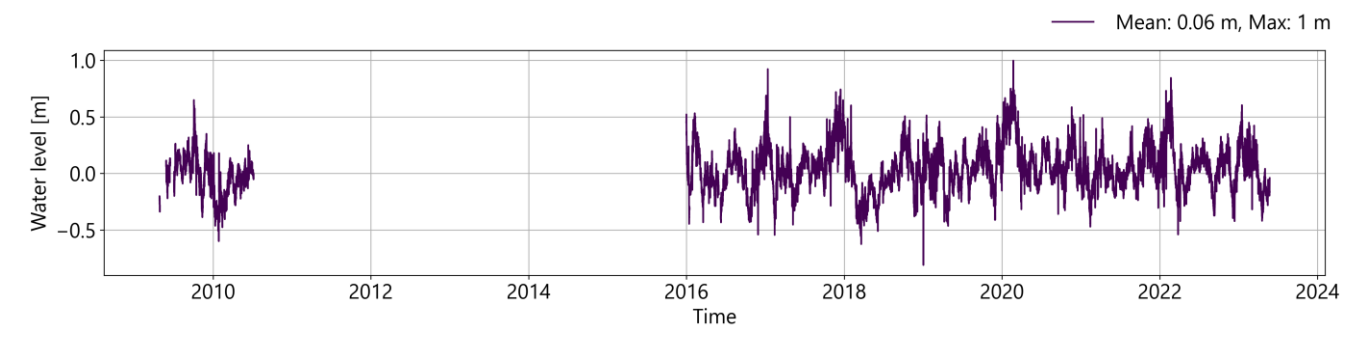


Figure 6.3: Measured water level at LJUSNE SJÖV (SMHI-Station).

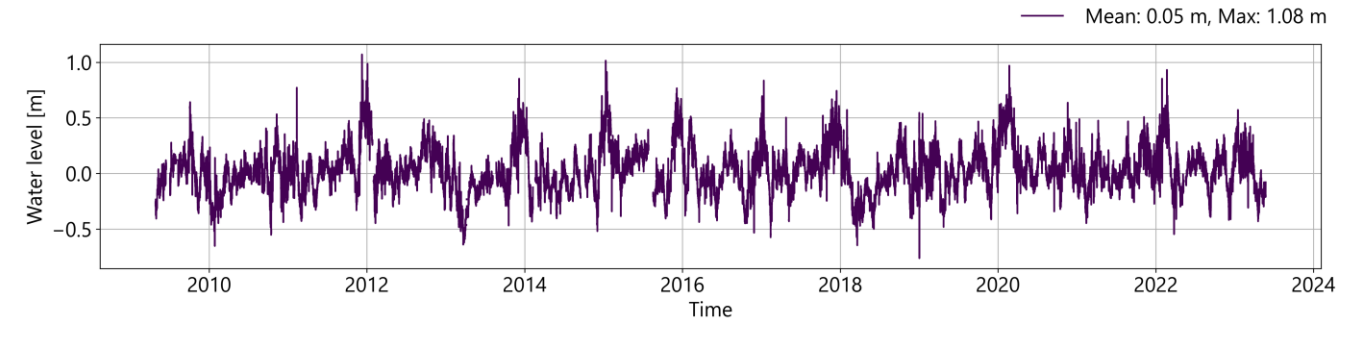


Figure 6.4: Measured water level at BÖNAN SJÖV (SMHI-Station).

6.3.2. Currents

Current speeds and directions with an hourly resolution have been obtained from the following SMHI stations (Table 6-2)

- NORRBYN BOJ between 1 and 41 m depths for the period 2016-2021 (Figure 6.5 and Figure 6.6) and
- Understen BS at 217-219 m depth for the year 2021 (Figure 6.7 and Figure 6.8).

Table 6-2: Current measuring stations used in the present study.

Name	ID	Lat	Long	Source
NORRBYN BOJ	33021	63.4990	19.8044	SMHI
Understen BS	33038	60.2715	19.9302	SMHI

Speed: The speeds recorded at the measurement station Understen BS, Figure 6.7 & Figure 6.8, with a mean of approx. 20 cm/s are significantly higher than at NORRBYN, Figure 6.5 & Figure 6.6, with means < 10 cm/s. This is due to the location of the measuring stations. While Understen BS is located in the narrows of the Åland Sea at least 13 km from the coast, NORRBYN BOJ is located further north, in a wider section approximately 3 kilometres from the coast.

Direction: A dominant current in the north, north-east direction can be identified at the measuring station Understen BS. In contrast, the flow direction at NORRBYN BOJ is evenly distributed, with a slight trend towards the east, increasing with depth.



Both measuring station are not suited for the model calibration due to their location (immediate proximity to the open model boundary (Understen BS) or to the coast (NORRBYN BOY)).



Figure 6.5: Measured current speed at NORRBYN at 5 m, 15 m, and 25 m depth (from top to bottom).

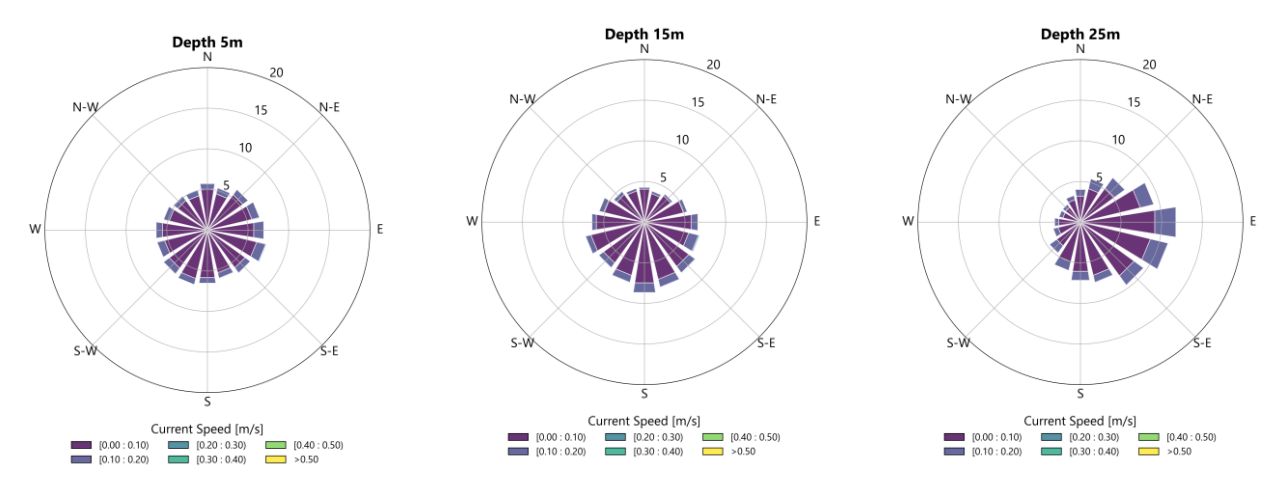


Figure 6.6: Measured current direction at NORRBYN at 5 m, 15 m, and 25 m depth (from left to right).



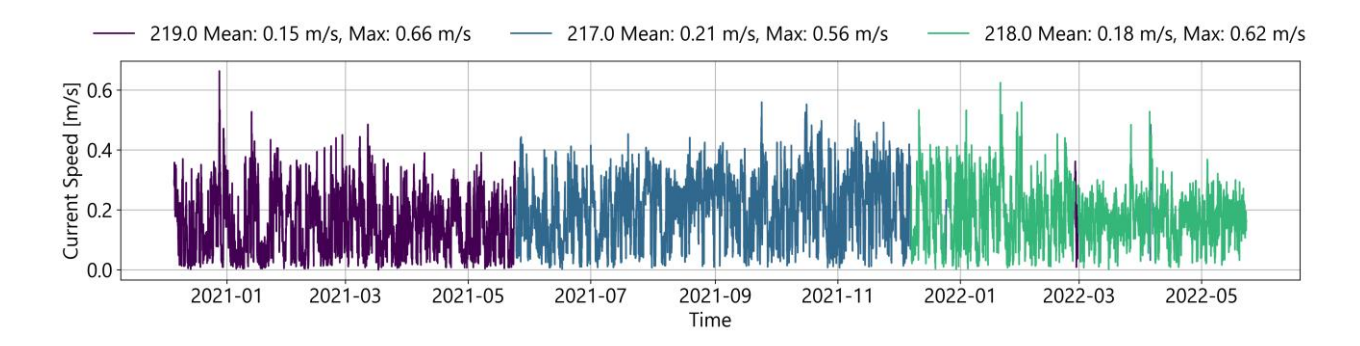


Figure 6.7: Measured current speed at Understen BS between 217 and 219 m.

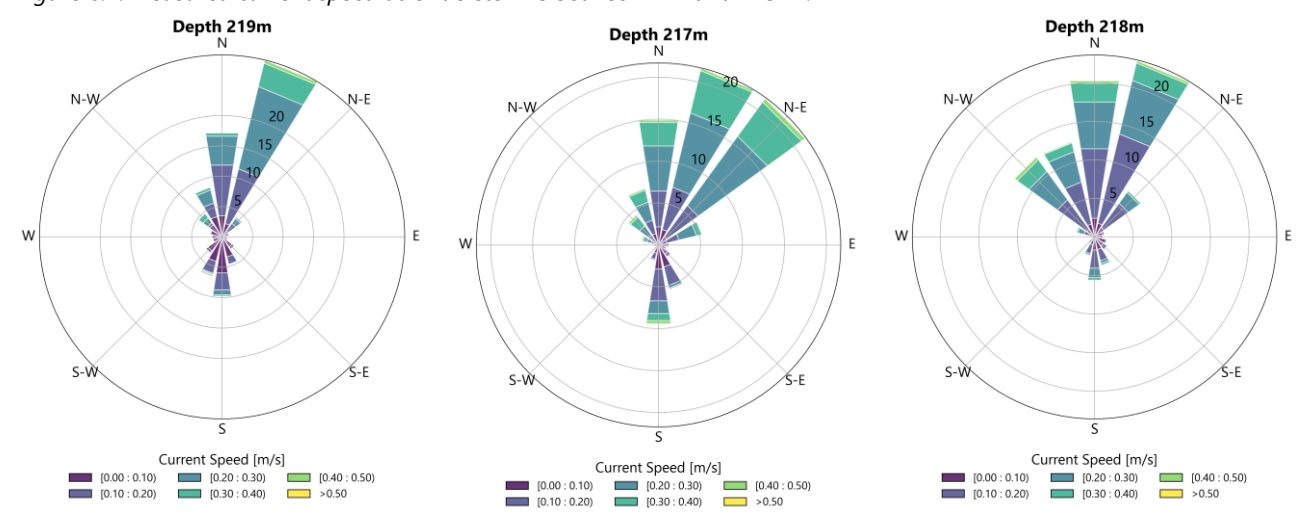


Figure 6.8: Measured current direction at Understen BS between 217 m and 219 m (the corresponding time period of the measurment is depicted in Figure 6.7).

6.3.3. Salinity

Salinity data with an hourly resolution have been obtained from the SMHI stations NORRBYN BOJ (lat: 63.499, long: 19.8044, depth: 7 m) for the period 2016-2021 (Figure 6.9) and Understen BS (lat: 60.2715, long: 18.9302 depth: 220 m) for the year 2021 (Figure 6.10). Despite the large data gaps, the following two patterns are recognisable:

- Spatial pattern tending towards lower salinity in the northern area (as there are no strong vertical variations, see chapter 6.3.4).
- Annual pattern with tendency towards lower salinity between February and April.



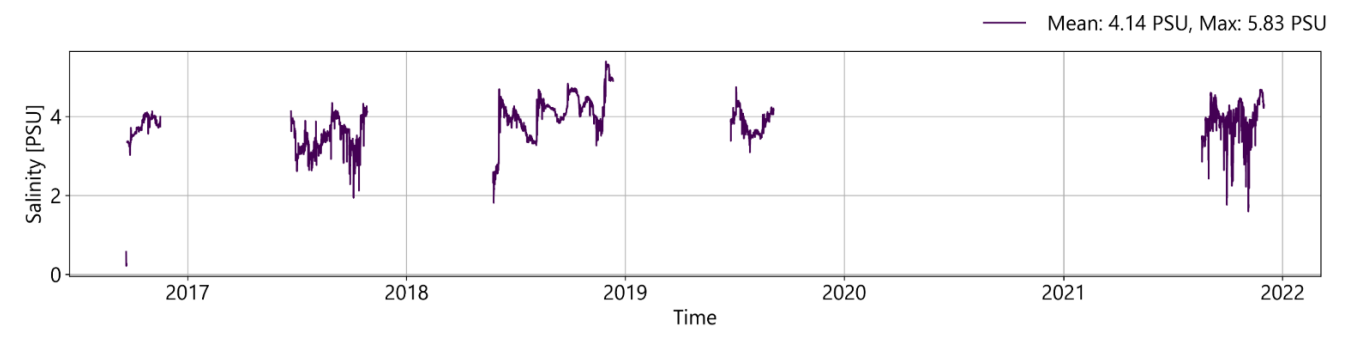


Figure 6.9: Measured salinity at NORRBYN BOJ at 7 m (SMHI-Station).

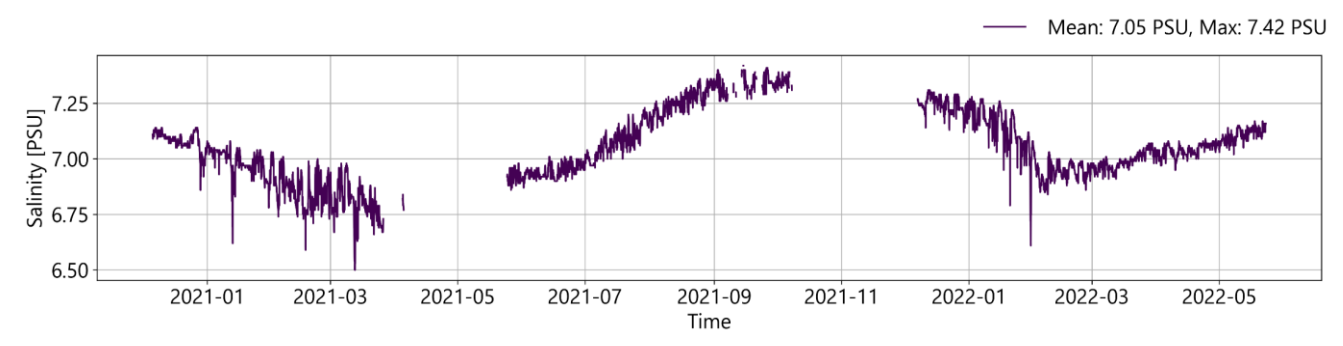


Figure 6.10: Measured surface salinity at Understen BS at 220 m (SMHI-Station).

6.3.4. Vertical Profiles (CTD) Measurements of Salinity

Publicly available vertical salinity profiles have been downloaded from SMHI (Swedish) and Merihavainnot.fi (an open-access marine data service maintained by the Finnish Environment Institute (SYKE)). Out of the approximately 230 available monitoring stations, 14 Swedish and 25 Finish (partly overlapping) stations were considered in more detail and used for model verification (see table in Appendix 11).

Due to the large number of available stations, salinity profiles and their temporal evolution are discussed based on the example of two stations only; F2 (Figure 6.11) and SR5 (Figure 6.12) in the northern (Bothnian Bay) and southern (Bothnian Sea) parts, respectively (see Figure 6.2). While the temporal and vertical variations are small regardless of location, there is a significant difference in salinity between the two stations. Similar to the surface salinity, lower salinity concentrations are measured at the station further north (F2, Figure 6.11), where almost no halocline is evident. In contrast, there is a clear halocline between 50 m and 80 m at SR5.

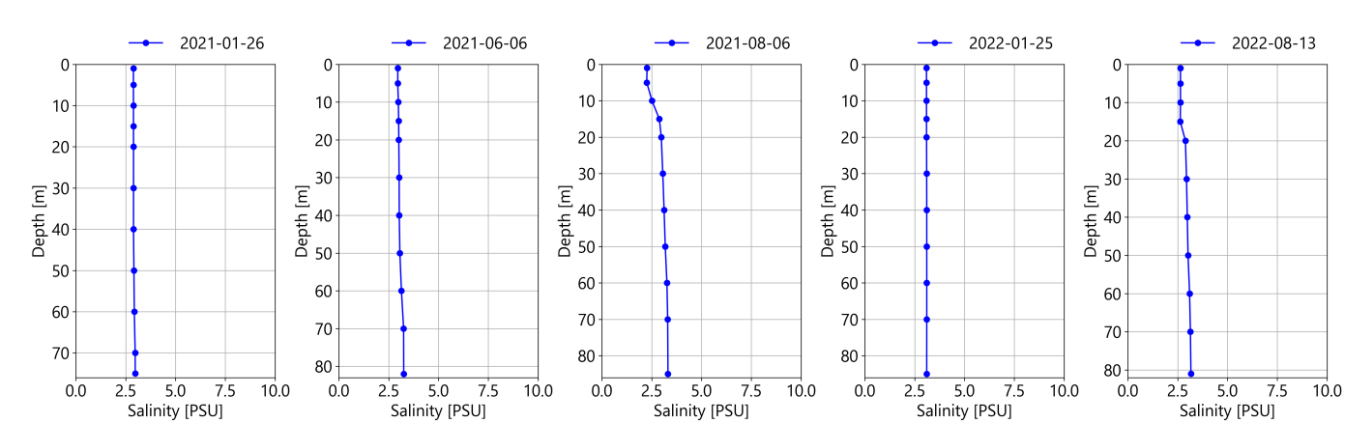


Figure 6.11: Measured Salinity profile at station F2 (source: merihavainnot.fi, location see Figure 6.2).



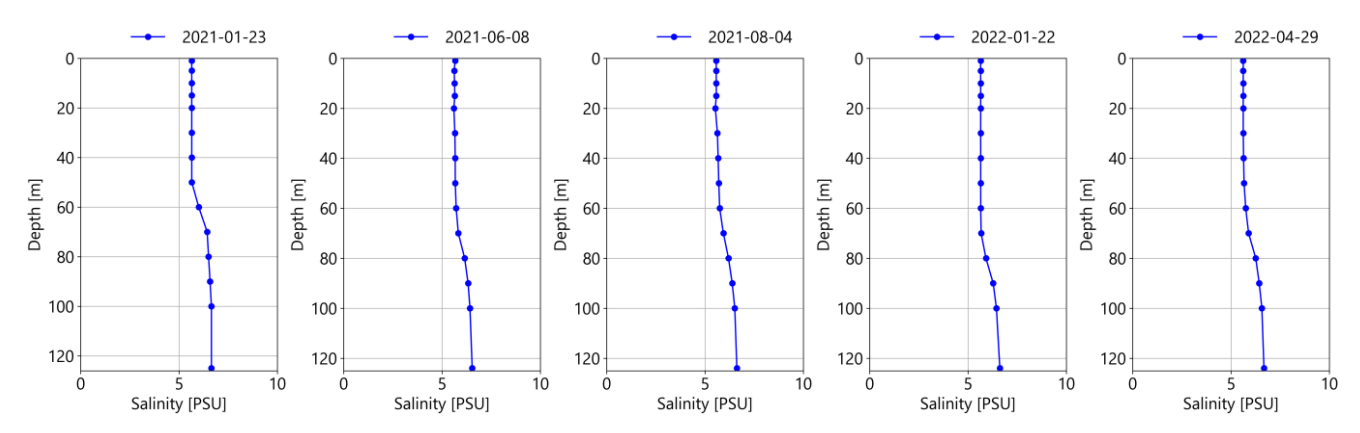


Figure 6.12: Measured Salinity profile at station SR5 (source: merihavainnot.fi, location see Figure 6.2).

6.3.5. Water temperature

Surface temperature with an hourly resolution have been obtained from 9 SMHI (Swedish) and 7 FMI (Finish) stations (see table in Appendix 12). The locations of the surface temperature stations are displayed in Figure 6.2. Due to the large number of available stations, the temporal surface temperature variations are discussed based on two locations, located either in the northern part (STRÖMÖREN SJÖV Figure 6.13) or in the southern part (LJUSNE SJÖV, Figure 6.14).

Significant annual fluctuations can be observed at both stations. While the measured minimum and maximum temperatures are at both stations varying between 0° and approx. 25°, the northern station (KALIX-KARLSBORG SJÖV Figure 6.13) shows a clearly longer period (approx. November to May) during which the surface temperatures stands at around 0°. At the southern station (LJUSNE SJÖV, Figure 6.14), the surface temperature is only around 0° for about 3 months (January-March) explaining the 1.5° higher annual mean value.

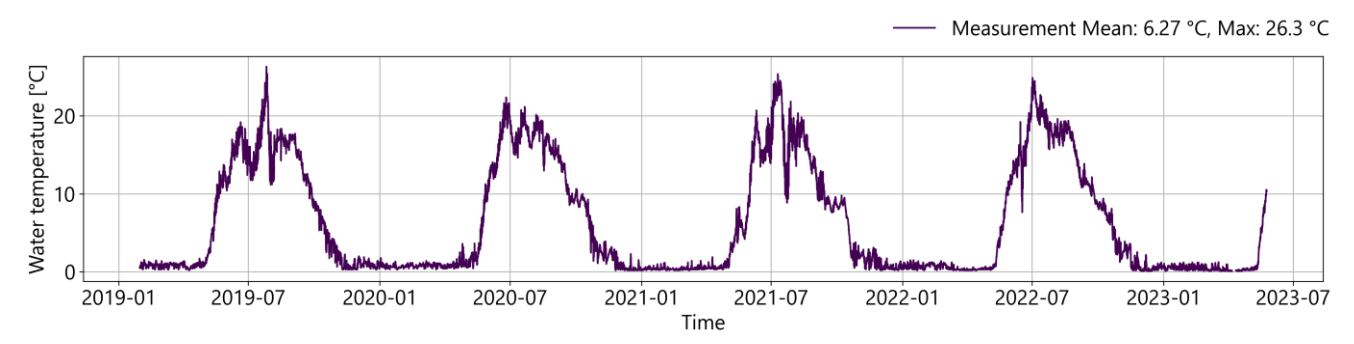


Figure 6.13: Measured surface water temperature at STRÖMÖREN SJÖV (SMHI-Station).

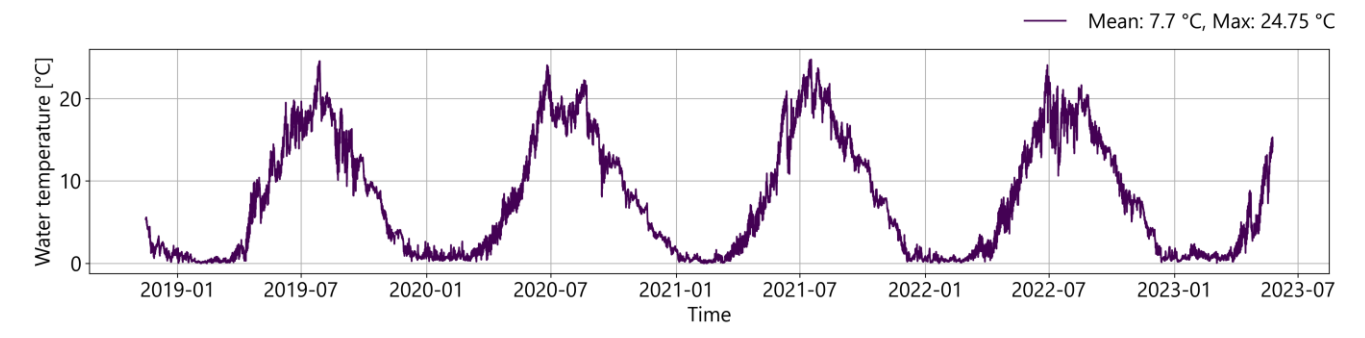


Figure 6.14: Measured surface water temperature at LJUSNE SJÖV (SMHI-Station).



6.3.6. Vertical Profiles (CTD) Measurements of Temperature

Temperature profiles are available at the same locations as salinity (see table in Appendix 11 and Figure 6.2). As with the salinity, due to the large number of available stations, the temperature profiles and their temporal evolution are discussed for two stations only, namely F2 and SR5 (in the northern and southern part respectively, see Figure 6.2).

The measurements of the temperature profiles (in contrast to the vertical profiles of salinity) show seasonal and vertical fluctuations in temperature at both stations. While the vertical variations in temperature are relatively small in January, there is a thermocline visible between 10-30 m in August. Comparing the two stations, it can be seen that the water at station SR5 (in the southern part) tends to be warmer, while the surface temperature at F2 fluctuates more.

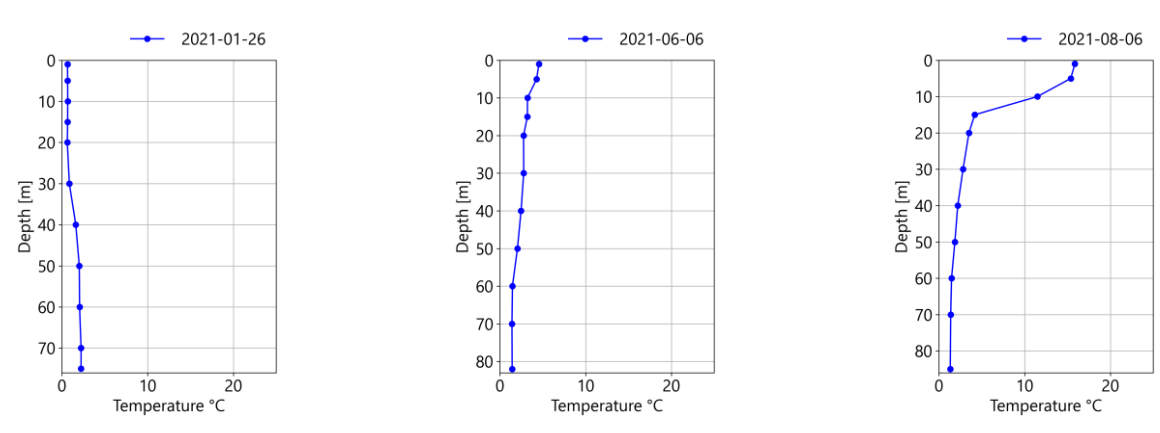


Figure 6.15: Measured temperature profile at station F2 (source: merihavainnot.fi, location see Figure 6.2).

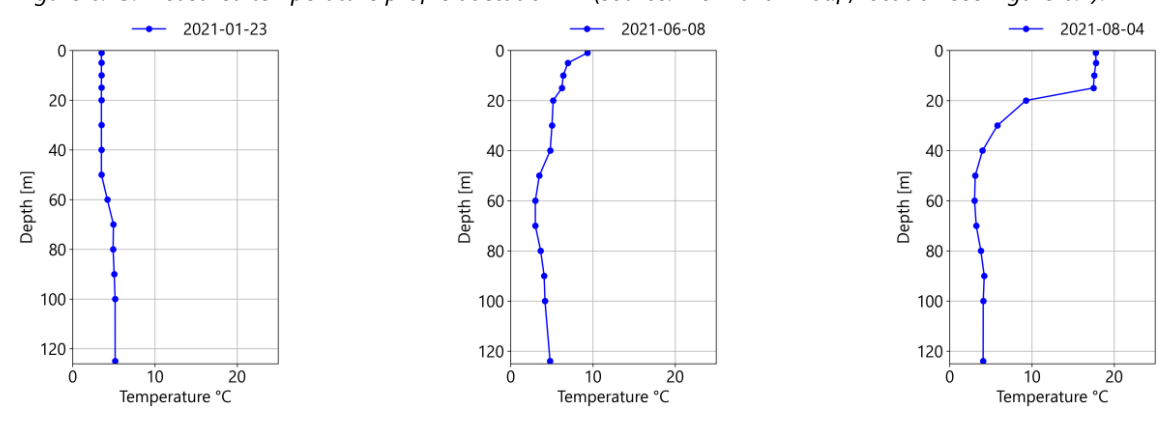


Figure 6.16: Measured temperature profile at station SR5 (source: merihavainnot.fi, location see Figure 6.2).



6.4. Hydrodynamic data from models

6.4.1. Water levels

Data from the 2km by 2km SMHI 3D Baltic Sea model are used at the Åland Sea boundary conditions to feed the MIKE model (Copernicus, Baltic Sea Physics Analysis and Forecast, 2x2km, 2022) and (Copernicus, Baltic Sea Physics Reanalysis 4x4km, 2022).

6.4.2. Currents

To identify a representative year for simulating impacts on hydrodynamics and sediment dispersal, SMHI 3D Baltic Sea model results at Sylen OWF (Copernicus, Baltic Sea Physics Analysis and Forecast, 2x2km, 2022) and (Copernicus, Baltic Sea Physics Reanalysis 4x4km, 2022) are presented in Appendix 2, Appendix 7 and Appendix 8.

6.4.3. Salinity and Temperature

For initialisation and to feed the model at the boundary, data from SMHI's numerical model of the Baltic Sea are used, (Copernicus, Baltic Sea Physics Analysis and Forecast, 2x2km, 2022) and (Copernicus, Baltic Sea Physics Reanalysis 4x4km, 2022).

Data from selected years are presented in Appendix 3 to Appendix 6.

6.5. Wind, Air Pressure, Air Temperature, Net long and short-wave radiations

Atmospheric data in the form of instantaneous wind speed at 10 mMSL in x and y-directions, air pressure at the surface, air temperature at 2 m above the surface, relative air humidity, and net long and short-wave radiation at the surface have been extracted from ECMWF (ECMWF, 2022). The data have a horizontal resolution of 0.25 degrees and a temporal resolution of 1 hour.

6.6. Sea ice

The presence of sea ice is based on data produced by SMHI, (Copernicus, Baltic Sea Physics Analysis and Forecast, 2x2km, 2022) and (Copernicus, Baltic Sea Physics Reanalysis 4x4km, 2022) as ice thickness and concentration (Figure 6.17 and Figure 6.18). As the figures illustrate, the ice cover spreads from north to south starting in December and reaches a maximum extent in March, with the entire length of the west coast of Finland covered with ice. From June, the entire Gulf of Bothnia is ice-free again. The project area is not affected by long-lasting ice cover (at least in 2021).



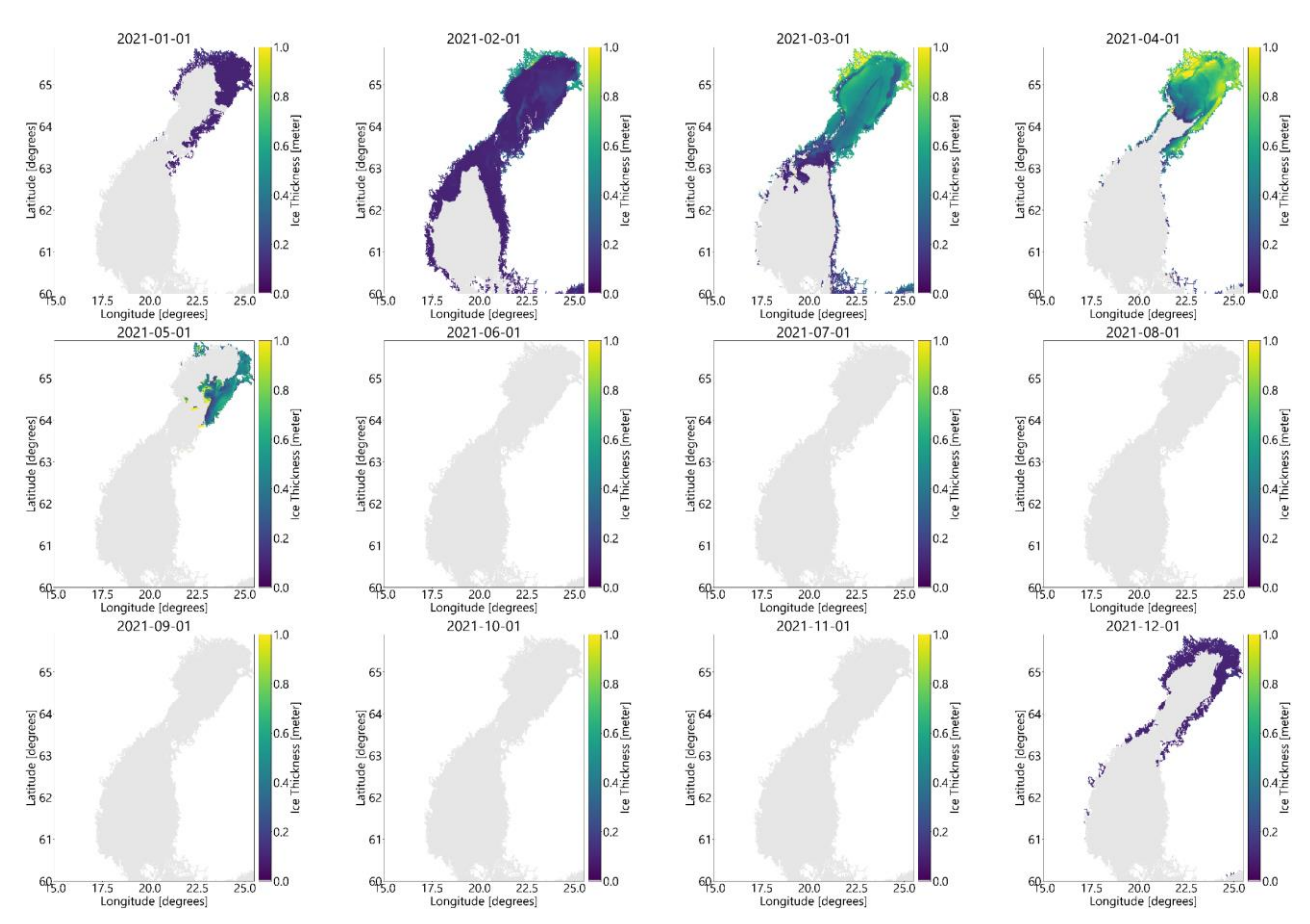


Figure 6.17: Temporal evolution of the ice thickness in during the year of 2021.



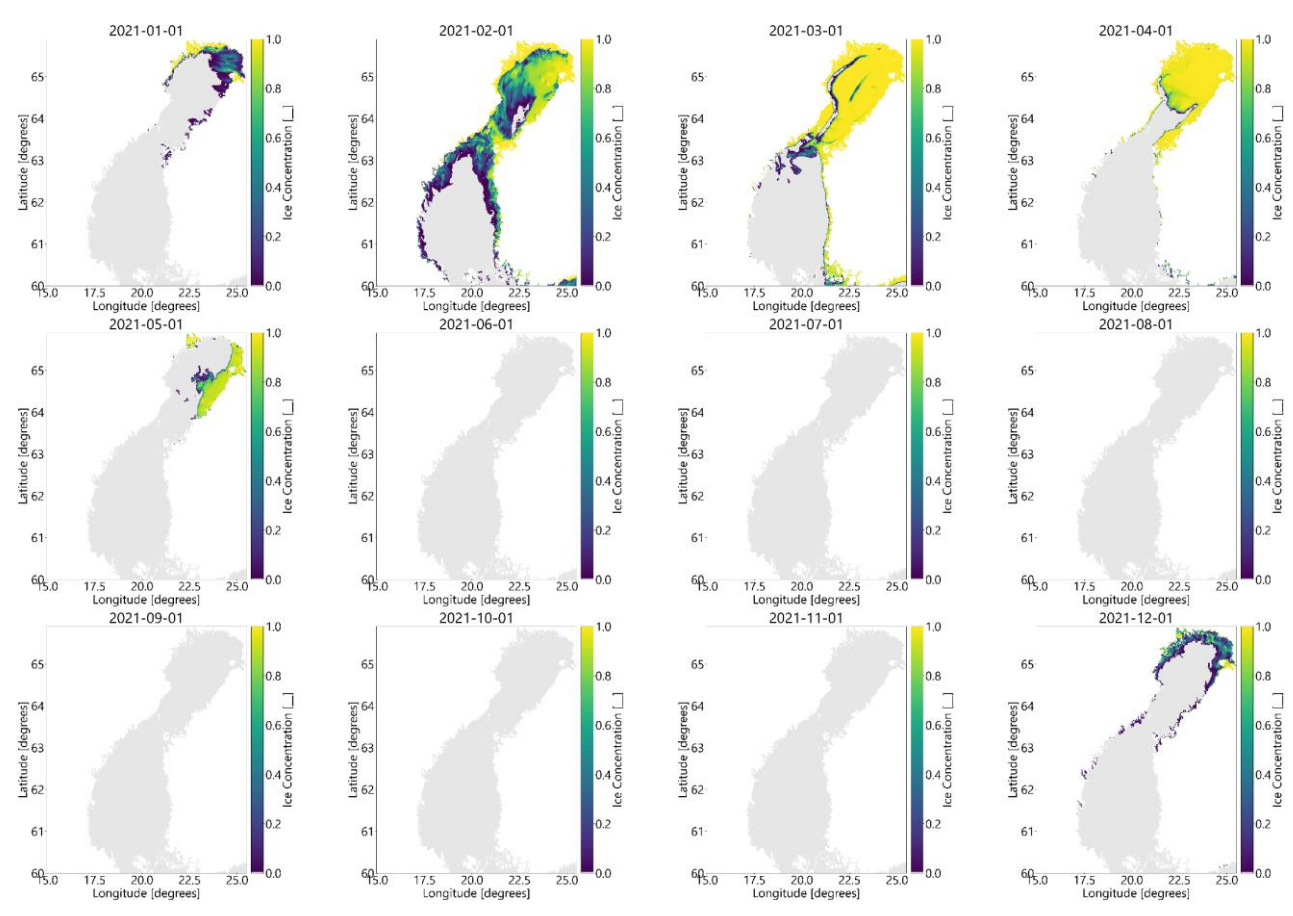


Figure 6.18: Temporal evolution of the ice concentration during the year of 2021.

6.7. Run-off

The following major freshwater discharges (average discharge greater than 100m³/s) to the Gulf of Bothnia are used as input to the model:

- Kokemäenjoki (Harjavalta station, lat: 61.34, long: 22.11; Finland)
- Oulujoki (Merikoski station, lat: 65.023, long: 25.47; Finland)
- lijoki (Raasakka station, lat: 65.33, long: 25.41; Finland)
- Kemijoki (Taivalkoski station, lat: 65.93, long: 24.71; Finland)
- Tornionjoki (Karunki station, lat: 66.03, long: 24.02; Finland)
- Kalixälven (lat: 65.8, long: 23.25; Sweden)
- Luleälven (lat: 65.56, long: 22.05; Sweden)
- Piteälven (lat:65.30, long: 21.44; Sweden)
- Skellefteälven (lat: 64.71, long: 21.18; Sweden)
- Umeälven (lat: 63.74, long: 20.36; Sweden)
- Ångerman (lat: 63.03, long: 17.78; Sweden)
- Indalsälven (lat: 62.5, long: 17.5; Sweden)
- Ljungan (lat: 62.28, long: 17.4; Sweden)
- Ljusnan (lat: 61.2, long: 17.13; Sweden)
- Dalälven (lat: 60.62, long: 17.49; Sweden)



For the Swedish rivers, modelled and station-corrected daily discharges and temperatures have been obtained from the SMHI VattenWebb platform for the years 2020-2023. For the Finnish rivers, observed daily discharges have been obtained from the Finnish environmental institute Ymparisto, and water temperatures have been assumed similar to those of the Swedish river at the closest latitude. The discharges and temperatures of the main rivers are shown in Figure 6.20 and Figure 6.22, respectively, the total river discharge in Figure 6.21 and their location in Figure 6.19.

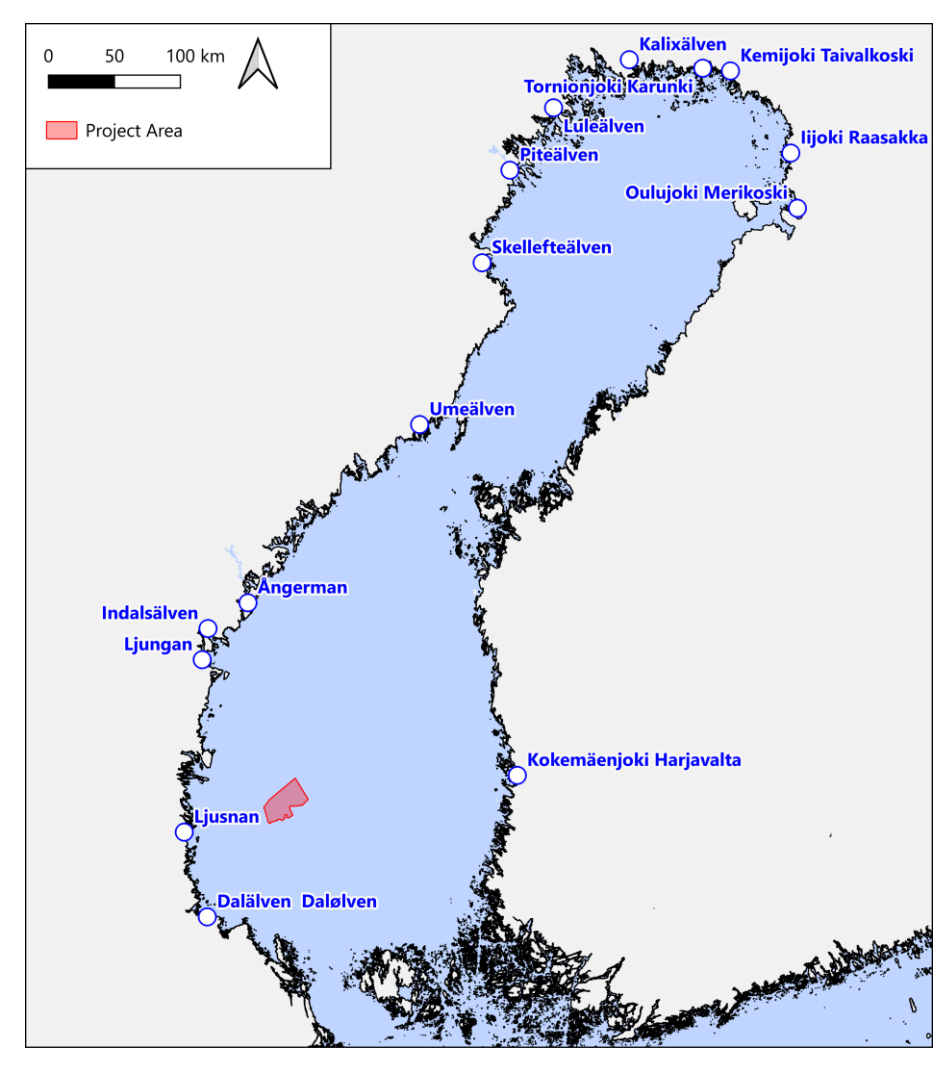


Figure 6.19: Location of the main rivers included in the model.



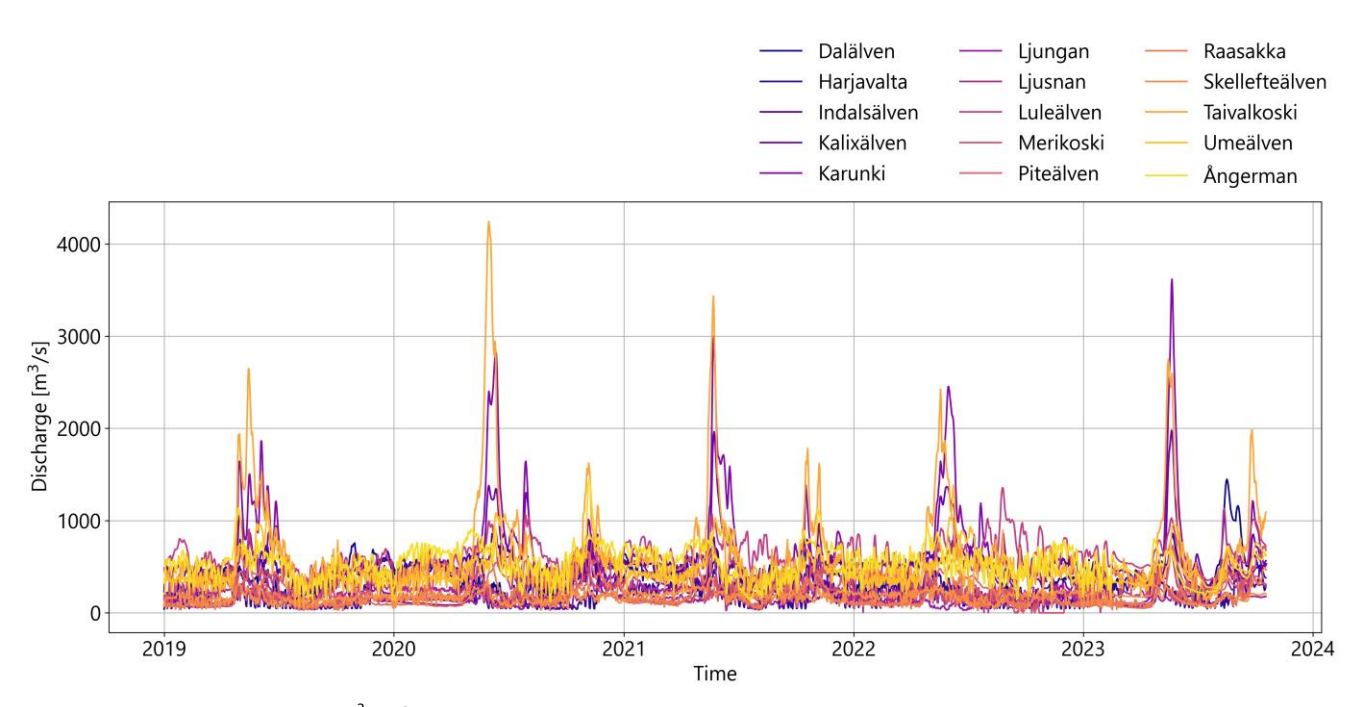


Figure 6.20: Daily discharges $[m^3/s]$ for the main rivers considered in the model.

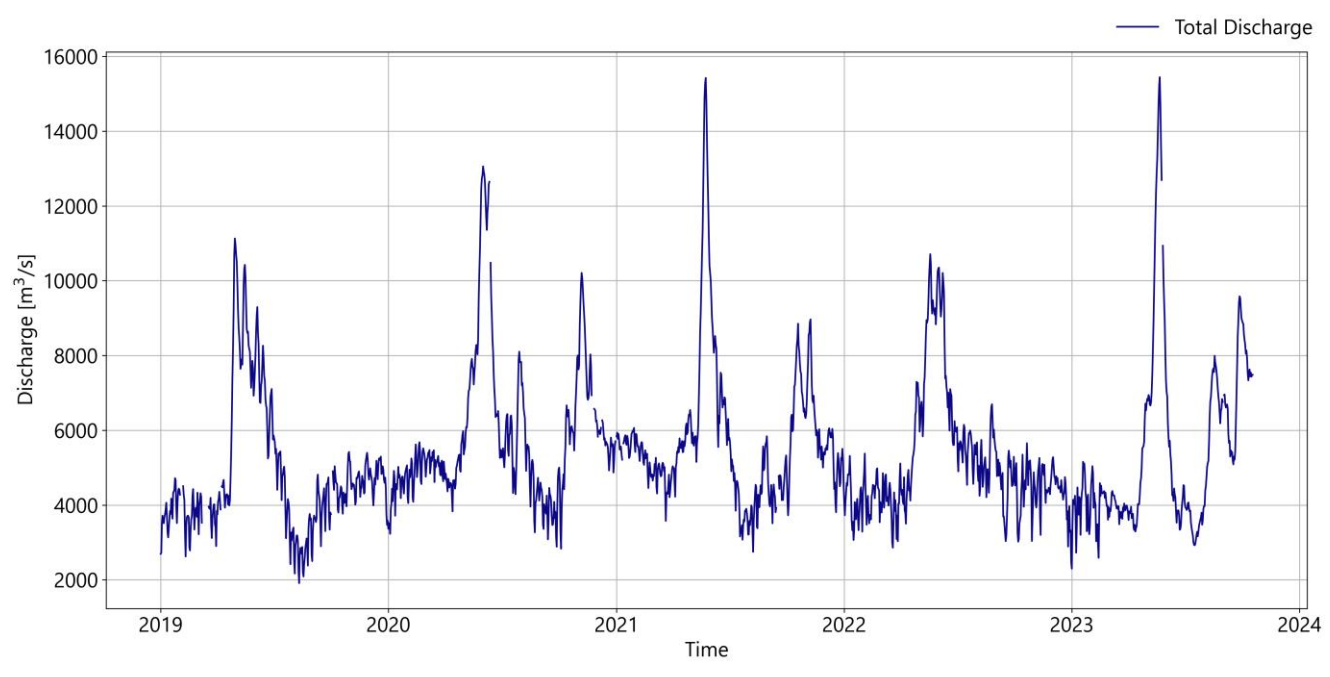


Figure 6.21: Total river discharge [m³/s] into the model.



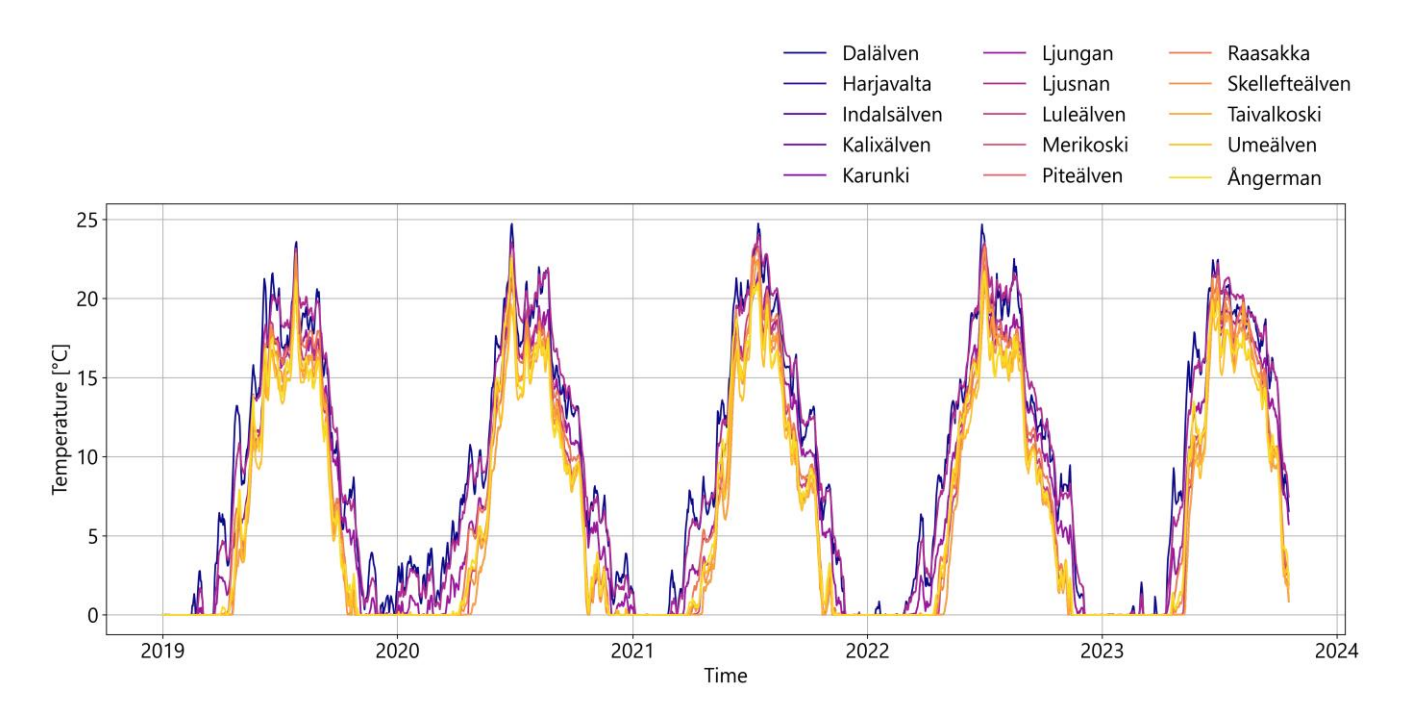


Figure 6.22: Daily water temperatures [°C] for the main rivers considered in the model.

6.8. Surficial sediments, seabed geology

The general image of the surficial sediments present in the wind farm and the surrounding area is based on data provided by the client as grains sieves analyses, Appendix 1, and backscatter data, Figure 6.23.

The seabed within the wind farm and along the export cable is classified into 2 categories. For each of the categories, the grain size distribution for the spill sources located in that category is represented by an average value based on the grain sieve data from the Sylen OWF representing the same category.



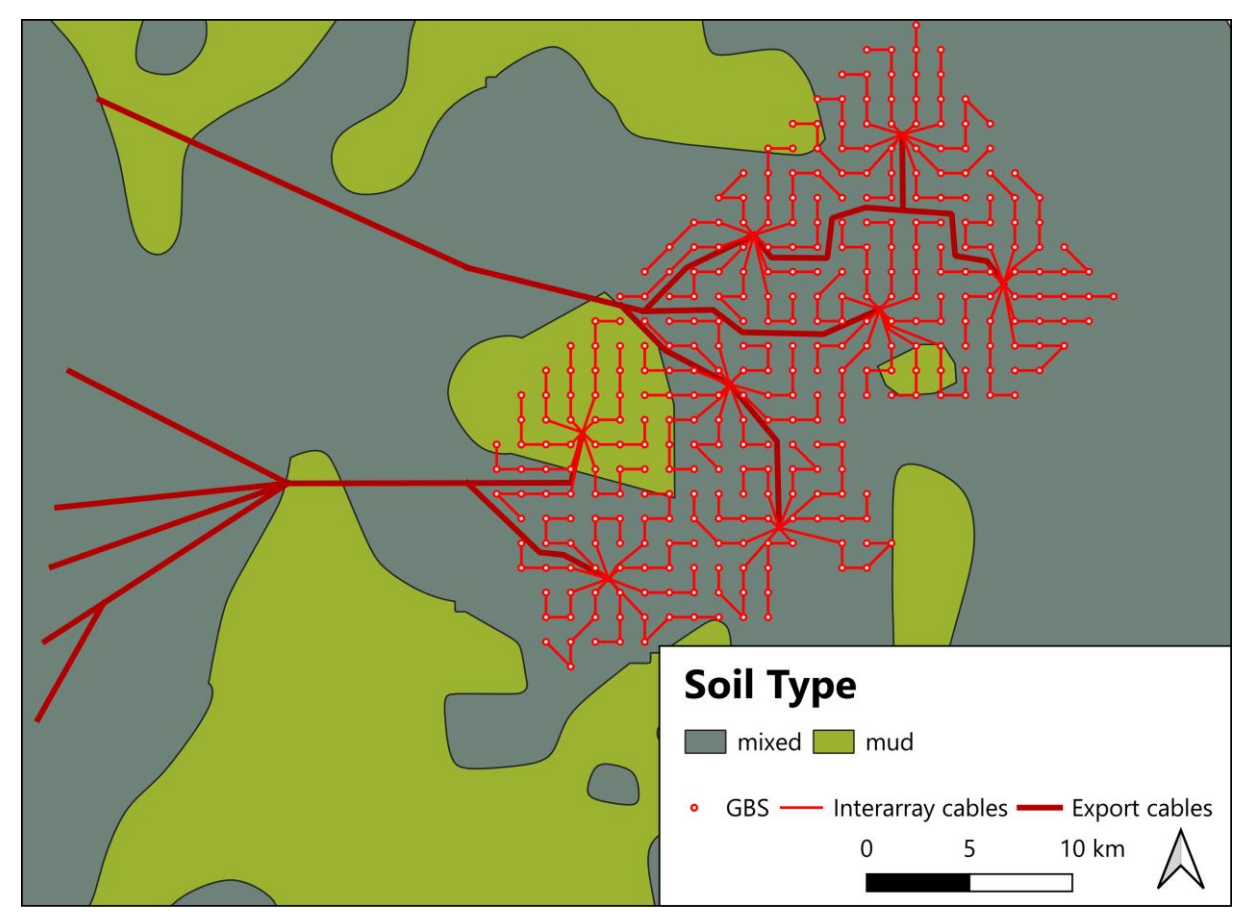


Figure 6.23: Interpretation of surficial sediments from backscatter data.

6.9. Baseline description

The Sylen OWF is located in the south-western part of the Bothnian sea, approximately 120 kilometres north of the narrowest zone of the Åland Sea.

Hydrographic conditions at the Sylen OWF southern part of the Bothnia Bay are characterised by a relatively low salinity (4.5-6.5 PSU). Salinity varies within and also between years (Appendix 5 and Appendix 6), with the generally higher values presented in Appendix 6 probably due to the different resolution. The interannual variability is so pronounced that no clear seasonal pattern is discernible.

Water temperature varies from 0°C during the winter to up to >22°C occurring in July and August. According to the SMHI model results (Appendix 3 and Appendix 4) the water temperature dropped below 0° for a maximum of two months (February and Mach) in 2010, 2011, 2013 and 2018, with the cooling extending a maximum depth of 25 m (2010). Since 2019, no temperatures below 0° have been documented. Temperature is strongly stratified during the summer with a thermocline (zone of maximum temperature gradient) around 10-30 m depth. Between September and October, the water may warm up to 12-15° over the entire depth.

Due to the absence of tides, water level variations are mostly driven by variations at the Åland boundary, wind and pressure differences and amount to ± 100 cm around their average during the year. Currents are generally weak, around 0.15m/s at the surface (maximum of 0.5m/s) and less than 0.07m/s below 30m, and mostly driven by wind as well as temperature and salinity differences. The strongest currents occur in the summer months



(May to August, especially July see Appendix 2). The average circulation in the Bothnian Sea is counter clockwise, which generally leads to a southward flow along the Swedish coast. This large-scale pattern is interrupted by local eddies, which is why no dominant flow direction is recognisable in the flow roses (Appendix 7 and Appendix 8).



7. Hydrodynamic 3D model (Regional & Local)

7.1. Bathymetry and mesh

7.1.1. Regional model

To account for regional circulation patterns, the regional 3D hydrodynamic model encompasses the whole Gulf of Bothnia (see Figure 7.1, Bothnian Sea and Bothnian Bay). The boundary with the Baltic Proper is located at the narrowest zone of the Åland Sea. The regional model is used for calibration and validation of the hydrodynamic processes, and to force the local pressure model (see below). To maintain reasonable simulation times, the model has a relatively coarse horizontal resolution (16 km²). The mesh constitutes of 12,934 elements and 7,486 nodes. To capture temperature and salinity stratification, which are more pronounced in the surface layer, the water column is divided into 15 vertical elements for depths up to 30 meters (hybrid sigma layers), giving a minimum vertical resolution of 3 meters. The part of the water column deeper than 30 meters is described using constant depth layers of 12 meters. The bathymetry in the Gulf of Bothnia varies between 0 meter at the coast to 250 meters for the north-western Bothnian Sea.

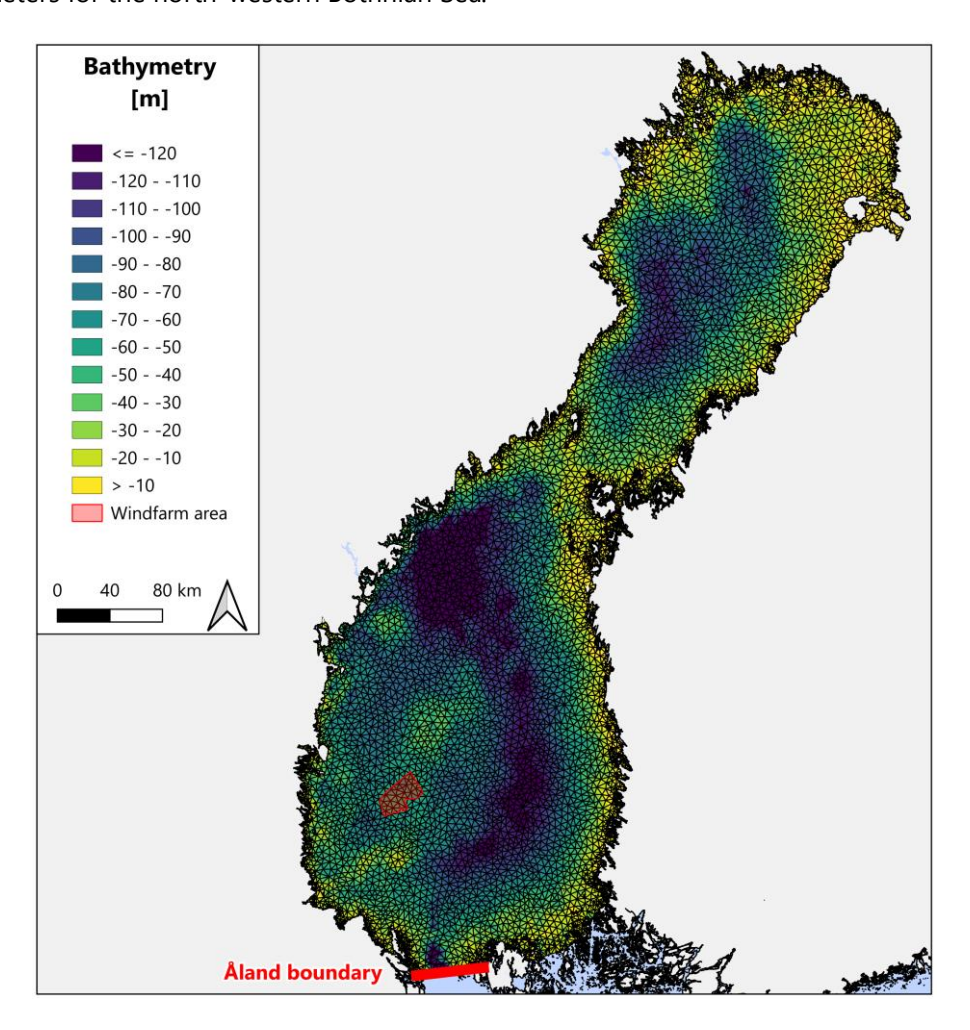


Figure 7.1: Mesh and associated bathymetry (MSL) of the regional model

7.1.2. Local sediment model

To model sediment dispersal (Figure 7.2), the local sediment model represents the same area as the regional model with the difference that the vertical resolution instead of a combination of sigma and z-layer only consist



of sigma-layers to avoid artificial sediment traps due to the z-layers. The model consists of 50,539 elements and 26,318 nodes, and its vertical resolution is 21 sigma layers spanning over a depth of -73.5 m.

The local model has a varying horizontal resolution, continuously increasing towards the windfarm area and the export cables (from 16 km² to 4 km² given a distance of more than 50 km, 15 km respectively). In the area within a distance of 15 km the resolution is increased to 0.5km^2 . Along the export cables and within the windfarm area, where the impacts of sediment dispersal are expected to be the strongest, the maximum cell size is set to 0.09km^2 . The sediment model is forced by the same boundary data as the regional model.

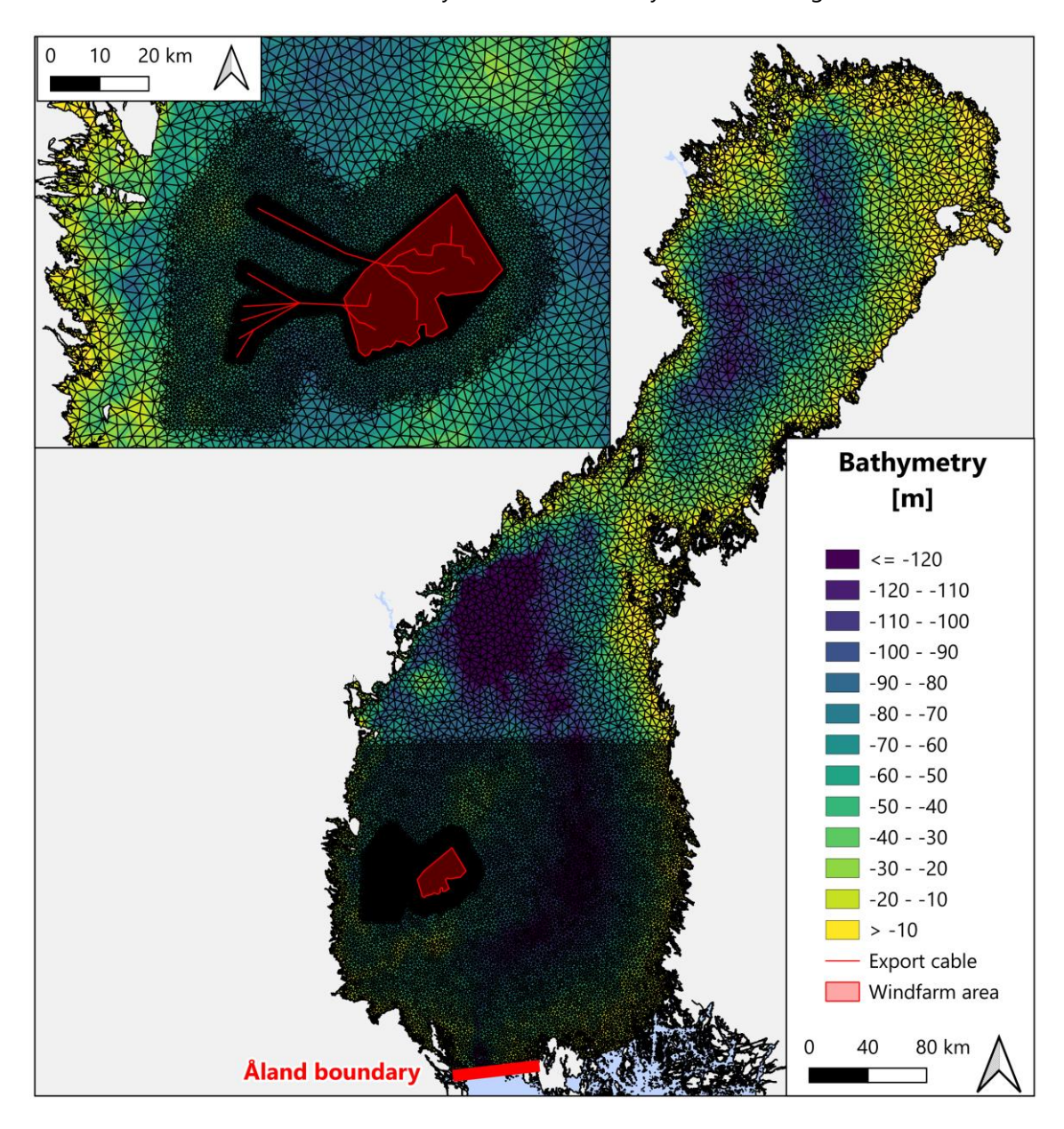


Figure 7.2: Zoom of the mesh and associated bathymetry of the local sediment model for analysis of sediment dispersal.

7.2. Boundary data

The regional model at the open boundary towards the Baltic Sea is forced with modelled SMHI data regarding salinity, temperature, and water level. At the surface, ECMWF's ERA5 wind data in the form of wind fields, air pressure, precipitation and evaporation, and sea ice concentration and thickness from the Baltic SMHI model

Prepared by: AIRN Verified by: GVIG Approved by: TEB Document ID: 4S6X2MX43VNH-1644138503-81



are considered. Heat exchange with the atmosphere has been taken into account via data from ECMWF's ERA5 of net short and longwave radiation, air temperature and humidity at the sea surface. Forcings from the catchment are also considered through the freshwater discharges temperatures from the major rivers listed in chapter 6.7.

To minimize the spin-up period the model is for the first time-step initialized with salinity, temperature and surface elevation from the Baltic Sea SMHI model.

7.3. Model setup and calibration

The regional model is forced at the southern boundary using specified water levels, and salinity and temperature profiles from the Baltic SMHI model. Water levels have been calibrated by adjusting the wind friction coefficients to get a reasonable agreement with observation data.

To account for salinity and temperature stratification, the vertical eddy viscosity is resolved using the k-ε turbulence model. Salinity and temperature profiles have been calibrated against available measurements within the project area by adjusting the vertical and horizontal dispersion coefficients, and surface temperatures have been calibrated through the light extinction coefficient determining the depth of the light penetration in the water column.

7.4. Identification of a representative period

Based on modelled temperature, salinity and currents at Sylen OWF from SMHI Baltic Sea model, presented in Appendix 2, Appendix 3 to Appendix 8, and a simplified particle tracking analyses based on the horizontal currents of the SMHI Baltic Sea model (Copernicus, Baltic Sea Physics Analysis and Forecast, 2x2km, 2022), shown in Appendix 9, an average year is identified by comparing yearly conditions.

Interannual variations are generally small for temperature, but significant for salinity and current. There is a general counter-clockwise circulation pattern in the Bothnian Sea, but this is disturbed by local eddies. There is a clear seasonal pattern in the modelled particle trajectories (Appendix 9), with stronger transport in the winter months and less dispersion in the summer months (May - August).

The year 2022 has been chosen as a representative year as it follows the general increase in salinity end of spring and the lower surface salinity end of summer as well as the seasonal pattern in modelled particle trajectories, Appendix 9. Temperature is highest in late summer with a thermocline going down to 15 meters. Thermocline depth in this area varies between 10-30 m, so that 15m is on the lower side and indicates slightly reduced vertical mixing.

Comparison between modelled currents by the 2km by 2km and 4km by 4km SMHI models indicate increased current speeds and more evenly spread direction components in the finer version. The average magnitude of the current is in general around than 0.1 m/s with an anti-clockwise circulation (Appendix 2). Within the project area, currents flow in general southwards.

The year 2022 experiences anti-clockwise currents circulation aligned with the general variations in the current pattern. On that background the year 2022 was chosen to investigate the effects of the wind farm on hydrodynamics and of its construction on sediment spreading.



7.5. Verification

The verification of the regional model is based on the comparison of the simulated and measured, publicly available data from 2021. The following parameters are taken into account:

- Observed water levels.
- Observed timeseries of surface temperature and salinity.
- Observed CTD measurements.

Due to the inappropriate location of the current measuring stations (distance to the project area, close vicinity to the shore or the boundary), a comparison of the measured and simulated currents is not carried out.

7.5.1. Water levels

The visual comparison of the calculated water levels with the observed water levels in 2021 (Figure 7.3 to Figure 7.5, as well as entire overview of all stations in Appendix 13 demonstrates good agreement for all stations in the period mid-May and mid-November with correlation coefficients varying between 0.89 - 0.95 (July in Appendix 13) and between 0.92-0.97 (September in Appendix 13).

While the agreement between calculated and measured water levels at the southwestern stations (FORSMARK, BÖNAN SJÖV(Figure 7.3), LJUSNE SJÖV, SPIKARNA, SKAGSUDDE SJÖV (see Appendix 13) is comparably good over the entire year with correlation coefficients between 0.93 -0.95 (Table 7-1), lower correlation coefficients are observed at the remaining stations.

The visual comparison (Appendix 13) reveals an underestimation of the water levels by the model between December and May. The further north or east the station lies, the more pronounced the difference is. For example, the calculated water levels at the RATAN station in March show a mean error of -0.39 m (Figure 7.4), while those at the STRÖMÖREN SJÖV (Figure 7.5) station show a mean error of -0.76 m (see Appendix 13). As shown by the comparison of the location of stations with ice cover (Figure 6.17 and Figure 6.18), there is a correlation between ice cover and low water levels in the model compared to the measurements (as the difference occurs mainly at stations and in the period when ice cover is documented). The underestimation can be explained by the fact that ice thickness is not included in water levels in MIKE.

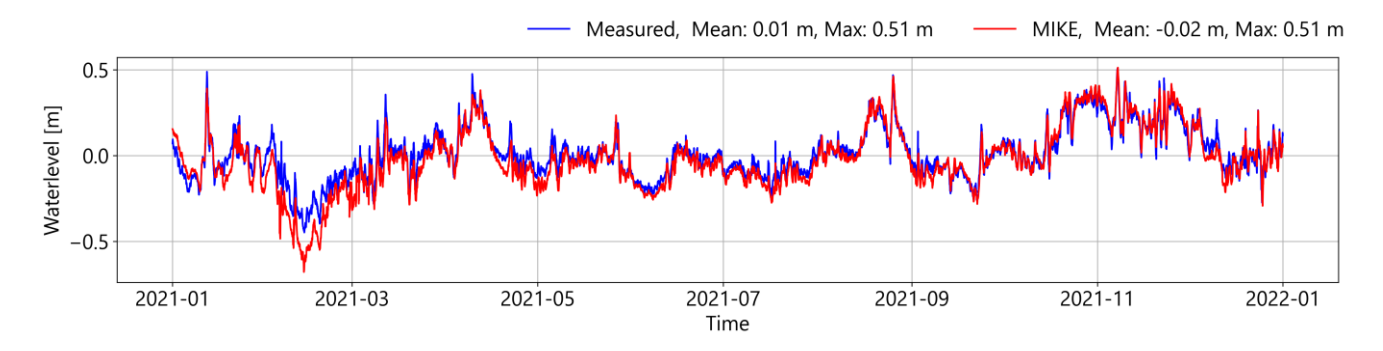


Figure 7.3: Comparison between observed water level in mMSL (blue line) and modelled water level (red line) for BÖNAN SJÖV (SMHI-Station).



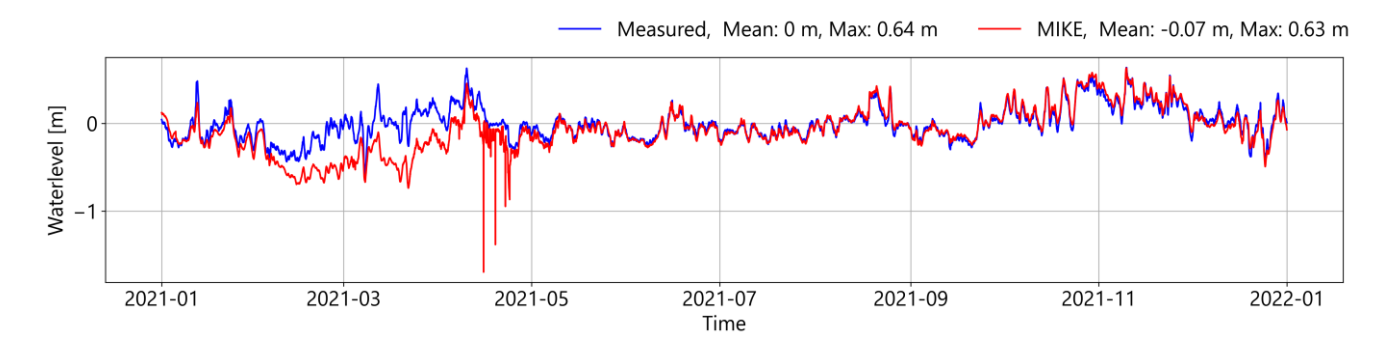


Figure 7.4: Comparison between observed water level in mMSL (blue line) and modelled water level (red line) for RATAN (SMHI-Station).

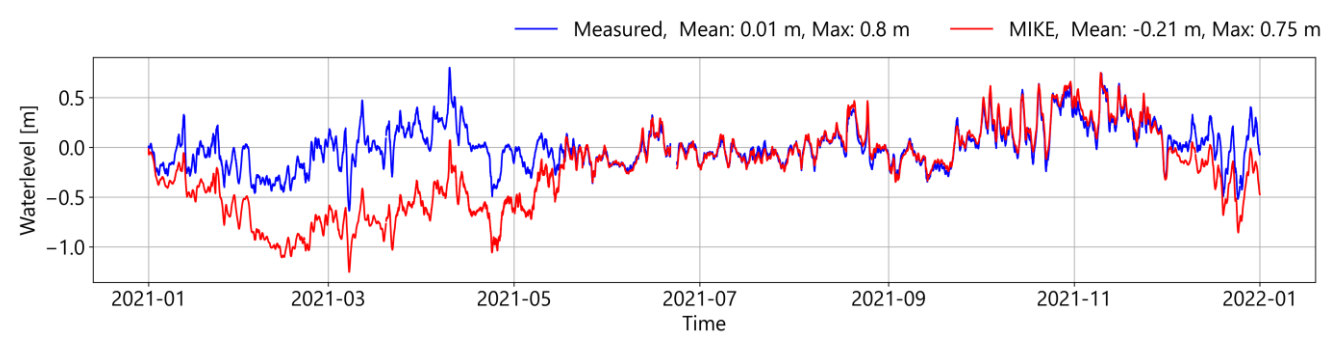


Figure 7.5: Comparison between observed water level in mMSL (blue line) and modelled water level (red line) for STRÖMÖREN SJÖV (SMHI-Station).

Table 7-1: Performance Metrics of the HD-Model in respect to the Water levels (over 2021).

Name	ME [m]	MAE [m]	RMSE [m]	Std. of Residuals [m]	Correlation Coefficients [-]
FORSMARK	-0.01	0.04	0.06	0.06	0.95
BÖNAN SJÖV	-0.03	0.05	0.06	0.06	0.95
LJUSNE SJÖV	-0.04	0.06	0.07	0.06	0.94
SPIKARNA	-0.04	0.05	0.07	0.06	0.96
SKAGSUDDE SJÖV	-0.05	0.06	0.09	0.08	0.93
Holmsund	-0.10	0.11	0.18	0.16	0.81
RATAN	-0.07	0.10	0.17	0.15	0.80
FURUÖGRUND	-0.18	0.20	0.33	0.27	0.66
STRÖMÖREN SJÖV	-0.22	0.25	0.37	0.30	0.65
KALIX-KARLSBORG SJÖV	-0.17	0.21	0.33	0.29	0.67
Kemi Ajos	-0.11	0.18	0.28	0.25	0.69
Oulu Toppila	-0.13	0.20	0.29	0.26	0.69
Raahe Lapaluoto	-0.11	0.17	0.28	0.26	0.65
Pietarsaari Leppäluoto	-0.09	0.13	0.21	0.19	0.76



7.5.2. Salinity

The model performance with respect to the temporal evolution of the salinity is presented on the basis of the available measurement data at the surface from the stations NORRBYN BOJ and Understen BS (see locations in Figure 6.2). While the salinity at the southern station (Understen BS, Figure 7.6) tends to be underestimated by the model (mean error of -0.61 PSU, see Table 7-2), the model overestimates the salinity at the northern station NORRBYN BOJ (Figure 7.7 and Table 7-2, mean error of +0.79 PSU). Due to the temporally incomplete measurement data and the sparse spatial distribution of the measurement sites, the significance of the comparison is limited and in view of the large number of CTD measurements, a detailed analysis of the temporal evolution of the salinity at these two stations is dispensed with.

Table 7-2: Performance Metrics of the HD-Model in respect to the salinity (over 2021, given the measurement periods available).

Name	ME [PSU]	MAE [PSU]	RMSE [PSU]	Std. of Residuals [PSU]	Correlation Coefficients [-]
NORRBYN BOJ	0.79	0.79	0.89	0.41	0.44
Understen BS	-0.61	0.61	0.63	0.17	0.63

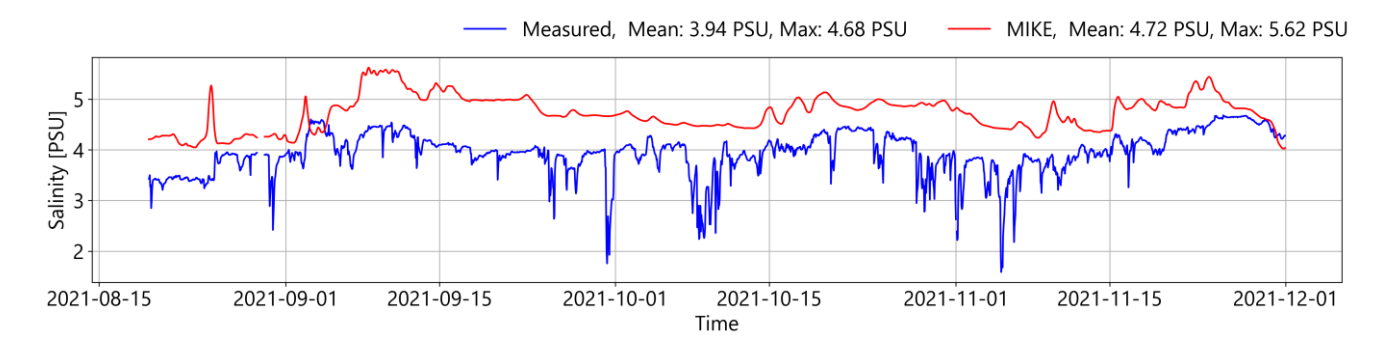


Figure 7.6: Comparison between observed salinity (blue line) and modelled salinity (red line) for NORRBYN BOJ (SMHI-Station).

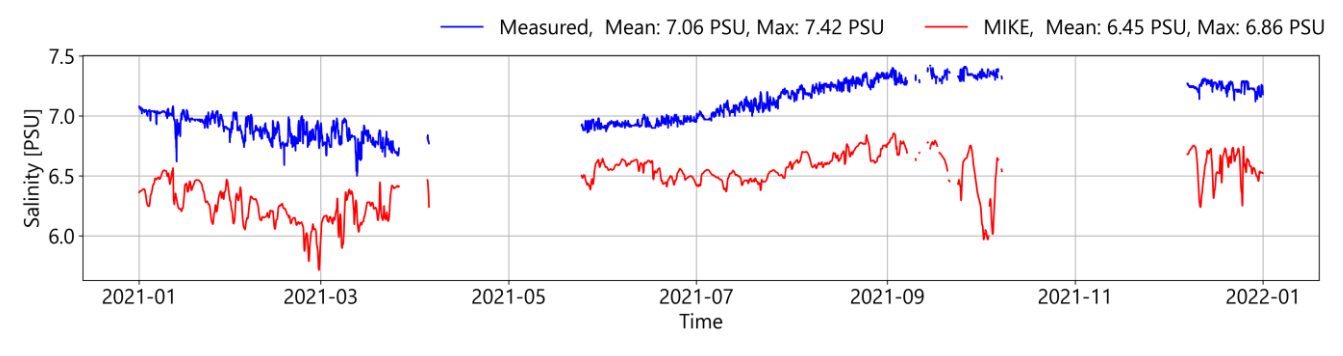


Figure 7.7: Comparison between observed salinity (blue line) and modelled salinity (red line) for Understen BS (SMHI-Station).



7.5.3. Salinity Profiles

The comparison of the calculated and measured vertical salinity profiles (Figure 7.8 and Figure 7.9, as well as figures in Appendix 14) indicates good agreement for the majority of the profiles. The slight stratification occurring towards summer can be reproduced with the model. However, the MIKE model tends to overestimate the salinity at the measuring points to the north (as already observed in chapter 7.5.2) (e.g. compare Figure 7.8 (located in the south) vs. Figure 7.9 (located in the north).

Observed discrepancies in water depth can be explained by the grid resolution. The regional model is based on a coarse mesh (to shorten the computation time), which leads to an averaging out of local lows.

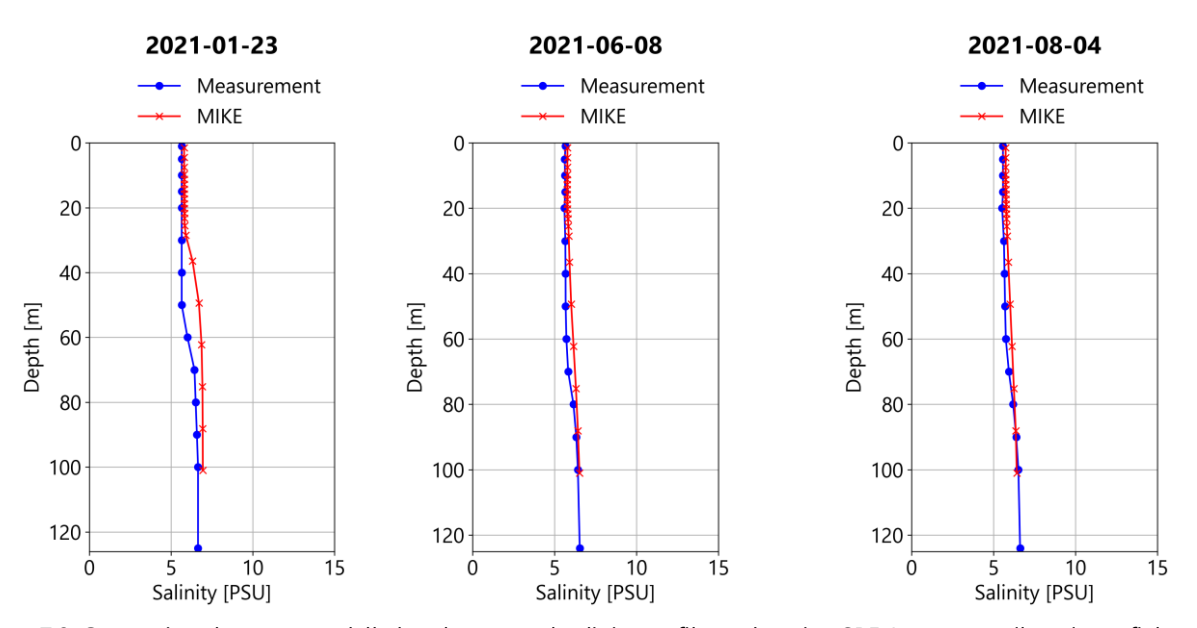


Figure 7.8: Comparison between modelled and measured salinity profiles at location SR5 (source: merihavainnot.fi, location see Figure 6.2).

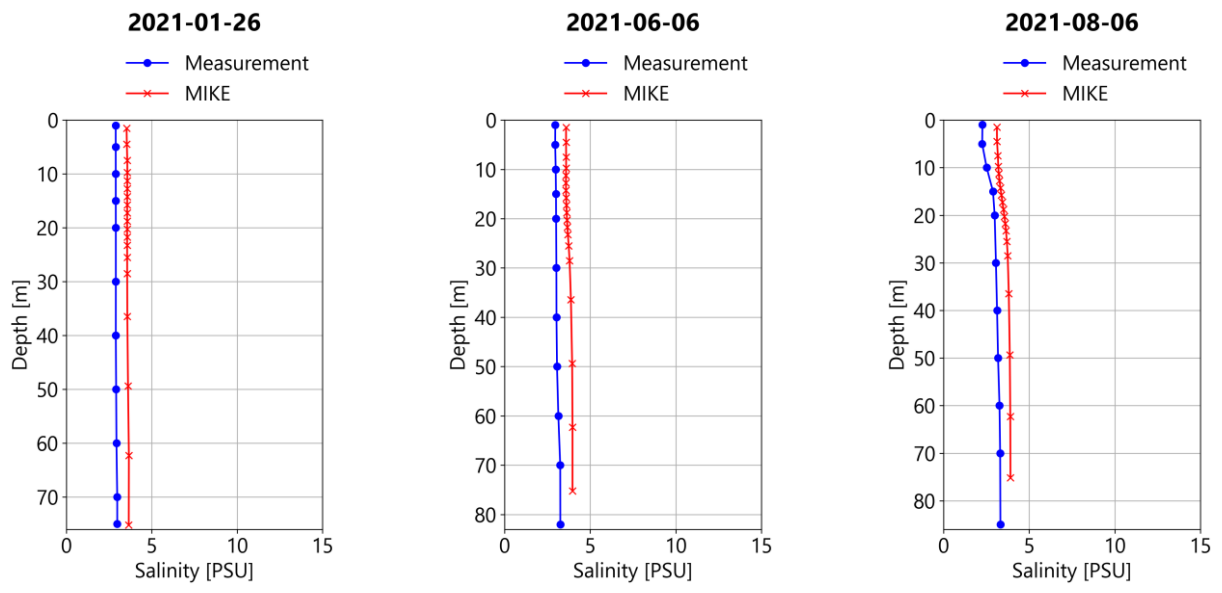


Figure 7.9: Comparison between modelled and measured salinity profiles at location F2 (source: merihavainnot.fi, location see Figure 6.2).



Station SR3 lies only about 10 kilometres south of the planned wind farm (see Figure 6.2). Measurements at this location are therefore well suited to assess the model quality in the project area. The comparison (Figure 7.10) reveals a general good agreement of the salinity by the model, regardless of depth.

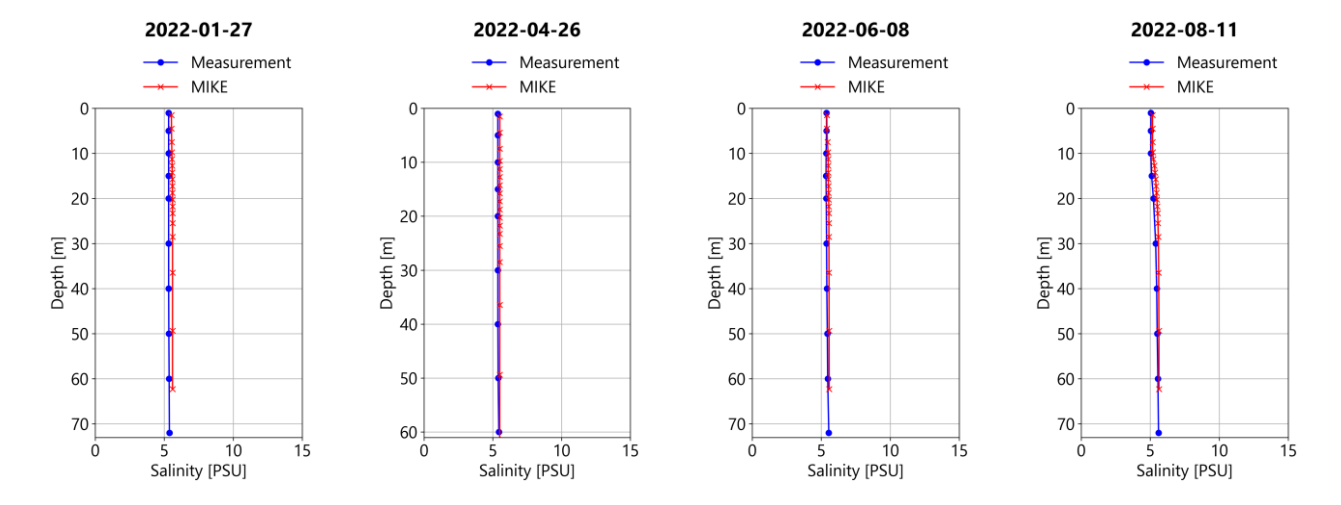


Figure 7.10: Comparison between modelled and measured salinity profiles at location F2 (source: merihavainnot.fi, location see Figure 6.2).

7.5.4. Water temperature

For the evaluation of the MIKE model with regard to the surface temperature, 17 measuring stations are available (Figure 7.11 and Figure 7.12 and Appendix 15). The surface temperatures calculated with the model, with correlation coefficients between 0.90-0.99 and a mean error -2.5 to +1.0° (Table 7-3, Figure 7.11 and Figure 7.12), agree well with the (partly incomplete) measured values, regardless of spatial location and season.

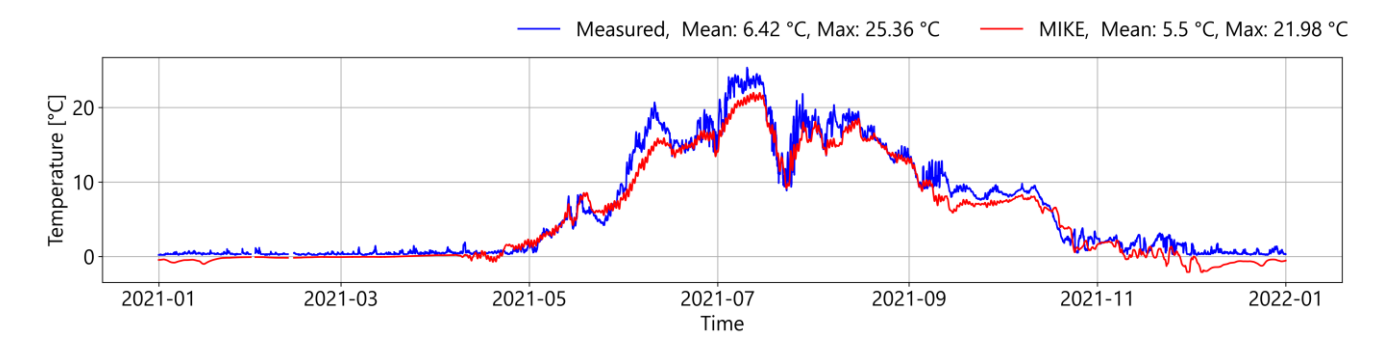


Figure 7.11: Comparison observed surface water temperature (blue line) and modelled surface water temperature (red line) for KALIX-KARLSBORG SJÖV (SMHI-Station).



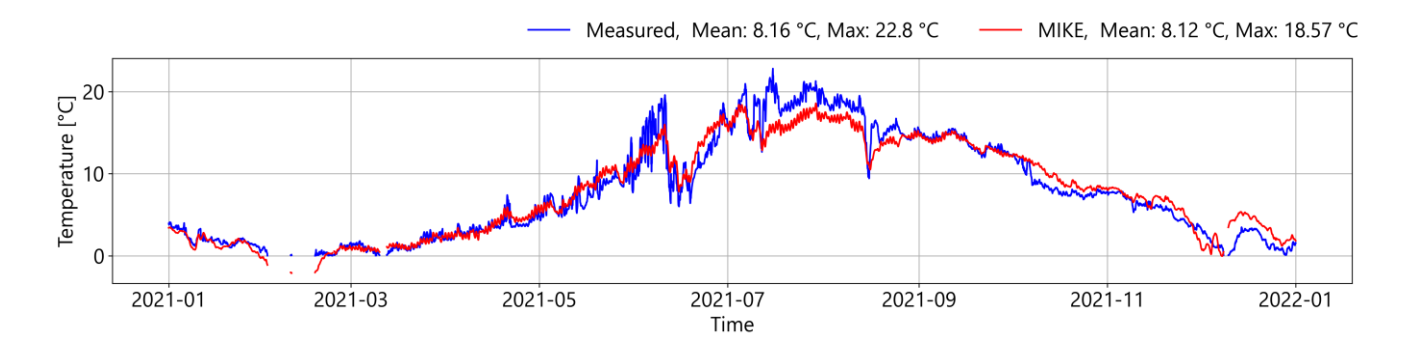


Figure 7.12: Comparison between observed surface water temperature (blue line) and modelled surface water temperature (red line) for BÖNAN SJÖV (SMHI-Station).

Table 7-3: Performance Metrics of the HD-Model in respect to the surface temperature (over 2021).

Name	ME [°C]	MAE [°C]	RMSE [°C]	Std. of Residu- als [°C]	Correlation Coefficients [°C]
FORSMARK	-0.74	0.99	1.29	1.05	0.99
BÖNAN SJÖV	-0.05	1.08	1.48	1.47	0.97
FINNGRUNDET WR BOJ	0.34	0.81	1.12	1.07	0.98
LJUSNE SJÖV	-0.29	1.02	1.55	1.53	0.98
NORRBYN SST	-0.13	0.99	1.43	1.43	0.97
NORRBYN BOJ	0.96	1.17	1.40	1.02	0.95
Holmsund	-2.48	2.50	2.74	1.15	0.99
STRÖMÖREN SJÖV	-0.60	1.58	1.79	1.69	0.98
KALIX-KARLSBORG SJÖV	-0.92	1.15	1.51	1.20	0.99
Oulu Santapankki	-0.12	0.68	0.98	0.97	0.98
Perämeri aaltopoiju	0.50	1.12	1.46	1.38	0.96
Kalajoki Maakalla	0.70	1.57	2.06	1.94	0.92
Maalahti Storskäret	0.15	1.04	1.36	1.35	0.96
Selkämeri aaltopoiju	0.19	0.83	1.21	1.20	0.98
Pori Kaijakari	-0.24	1.59	2.14	2.13	0.90
Uusikaupunki Vekara	-0.32	1.13	1.60	1.57	0.94

7.5.5. Temperature Profiles

Not only does the comparison of the over 60 modelled and measured vertical temperature profiles (in Appendix 16) demonstrate the model's capability to reproduce the temporal evolution of the water temperature in the Gulf of Bothnia, but it also reveals an overall satisfactory reproduction of the vertical profiles. Despite the general good agreement between modelled and measured profiles, the following limitations of the model can be observed:



- overestimation of stratification (i.e. overestimation of the warming of the upper water layers, underestimation of the mixture respectively) in June (e.g. F26, MS3, F18, BO3, RR3, CV, CVI, F2 (e.g. Figure 7.13))
- underestimation of the water depth, which is warmed in August (affecting mainly southern sites, e.g. F26 (Figure 7.14))
- overestimation of the water depth, which is warmed in August (affecting mainly northern sites, e.g. US7, CV (Figure 7.15) and RR7).

Observed discrepancies in water depth can be explained by the grid resolution. The regional model is based on a coarse mesh (to shorten the computation time), which leads to an averaging out of local lows.

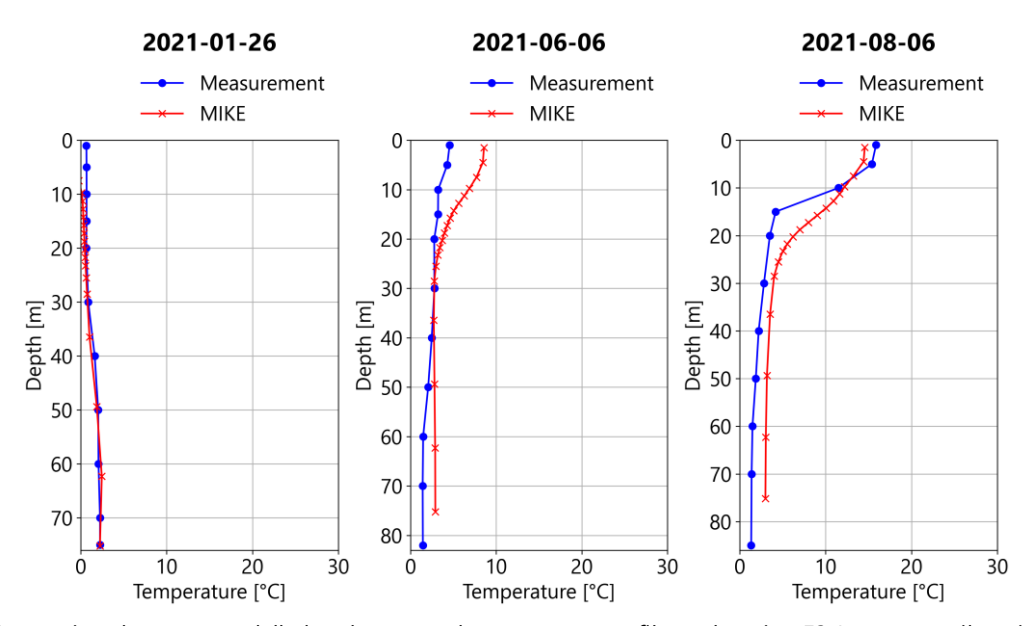


Figure 7.13: Comparison between modelled and measured temperature profiles at location F2 (source: merihavainnot.fi, location see Figure 6.2).



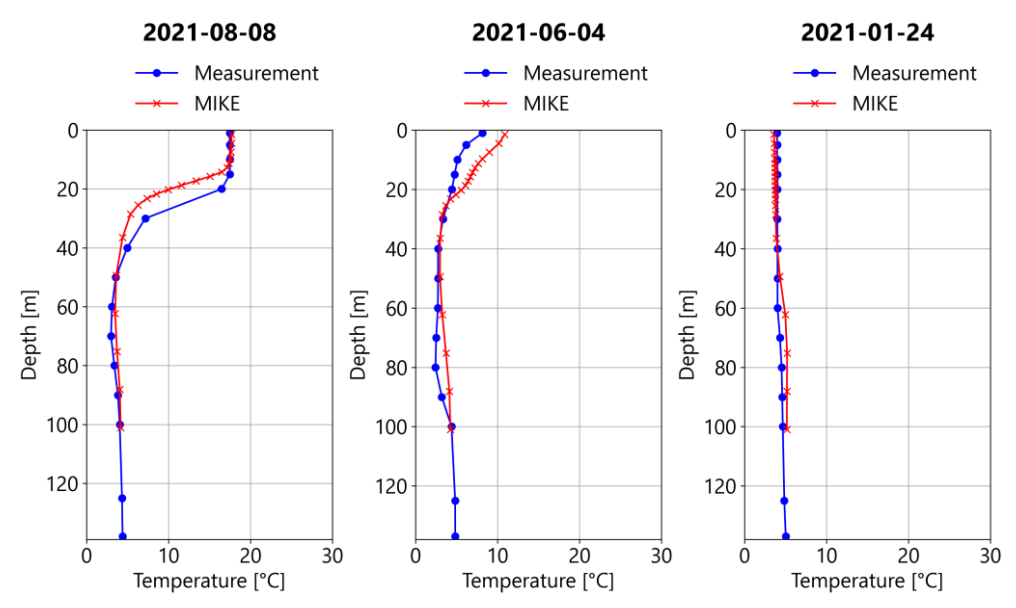


Figure 7.14: Comparison between modelled and measured temperature profiles at location F26 (source: merihavainnot.fi, location see Figure 6.2).

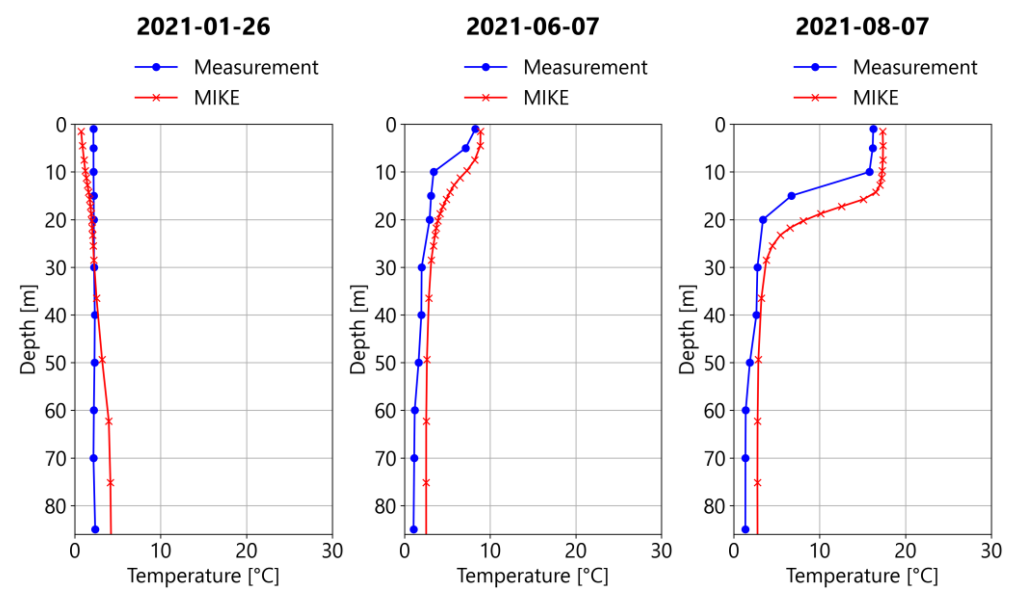


Figure 7.15: Comparison between modelled and measured temperature profiles at location CV (source: merihavainnot.fi, location see Figure 6.2).

Aligned with the salinity, the model quality in the project area is assessed by comparing the measured and calculated temperature profiles at station SR3 (Figure 7.16). The seasonal variation in 2022 can be represented with the model.



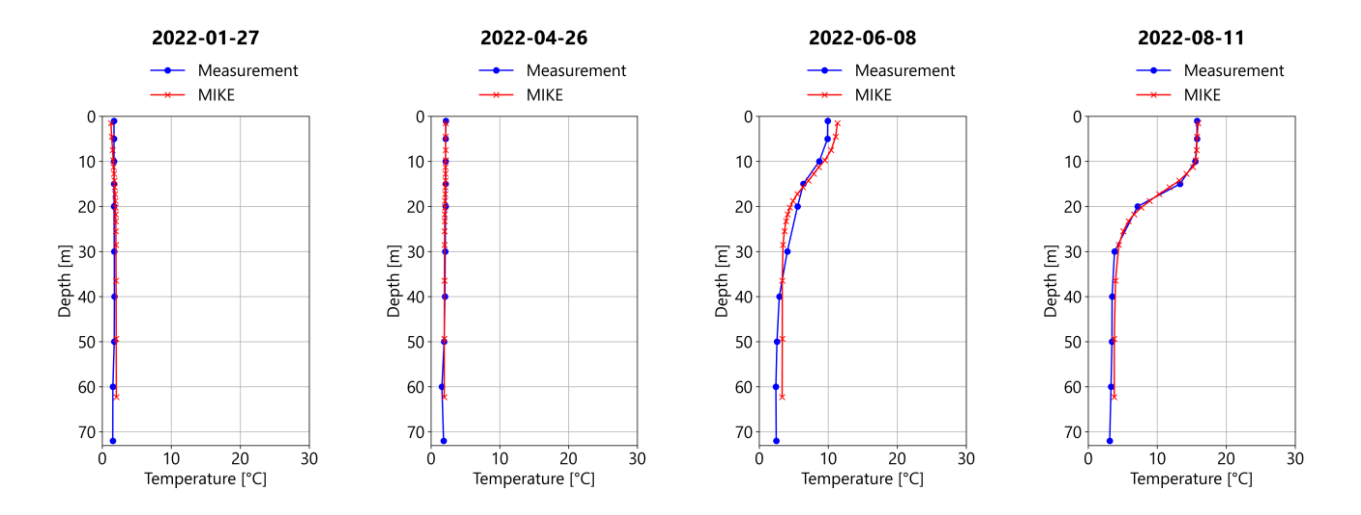


Figure 7.16: Comparison between modelled and measured temperature profiles at location SR3 (source: merihavainnot.fi, location see Figure 6.2).



8. Sediment dispersal model

The input to the sediment model is described in the first three sections of this chapter and the outcome of the model in the last two sections.

8.1. Sediment sources and spill program

One case (25MW) with four types of sources is considered:

- 1) Dredging of the gravity-based substructures and offshore substations with a dredge capacity of 1000m³/hour with 5% spill dispersed just above the seabed (released 2 meters over the seabed). The coarse sediment fraction settles next to the GBS (Gravity Base Structure, or the WTG and the OSS), and the finer ones are available for transport in the surrounding waters.
- 2) 10% of the total dredged sediments are assumed to overflow from the barge and are released at the surface and available for transport in the surrounding waters.
- 3) Burial of the inter array cable via jetting of a 1.5 x 2 m trench whereof 100% the sediments are assumed to be brought into suspension and released 2 m over the seabed.
- 4) Burial of the inter array cable via jetting of a 1.5 x 2 m trench whereof 100% the sediments are assumed to be brought into suspension and released 2 m over the seabed.

Each of the 347 WTGs can generate 25MW and the GBS has a base slab with a diameter of 45m, yielding an excavation of 9,817 m³ for each GBS. The installation program is described Table 8-1, starting with the dredging of the GBS and offshore substations, and parallel installation of the foundations and laying of the inter array cables (IAC) and redundancy cables. It is assumed that the construction will be conducted in two simultaneous phases during two seasons or years (four phases in total).

Table 8-1: Installation program for the 25MW case, starting April 1st and ending around 23 weeks later, September 6th (per season or year).

season or year).							
25MW GBS Season 1, Phase 1							
Activity	Amount	Unit	Capacity	Unit	Days	Start	End
1 OSS, installation	2	#	7.00	days/(FOU+topside)	14	2030-04-01	2030-04-15
1 OSS, dredging	23,758	m3	500	m3/hour+0.5 day/OSS	3	2030-04-01	2030-04-03
1 GBS installation	86	#	1.00	days/FOU + 0.5 day/FOU	129	2030-04-28	2030-09-04
1 GBS seabed preparation	844,303	m3	500	m3/hour + 1 day/FOU	156	2030-04-01	2030-09-04
1 Infield cable, laying + pull in	112,947	m	300	m/hour + 6 hours/pull in	37	2030-07-29	2030-09-04
1 Infield cable, burial	112,947	m	150	m/hour + 6 hours/WTG	53	2030-07-15	2030-09-06
Export cable, laying	80,768	m	300	m/hour	11	2030-04-15	2030-04-26
Export cable, burial	80,768	m	150	m/hour	22	2030-04-20	2030-05-12
25MW GBS Season 1, Phase 2							
Activity	Amount	Unit	Capacity	Unit	Days	Start	End
1 OSS, installation	2	#	7.00	days/(FOU+topside)	14	2030-04-01	2030-04-15
1 OSS, dredging	23,758	m3	500	m3/hour+0.5 day/OSS	3	2030-04-01	2030-04-03
1 GBS installation	82	#	1.00	days/FOU + 0.5 day/FOU	123	2030-04-27	2030-08-28
1 GBS seabed preparation	805,033	m3	500	m3/hour + 1 day/FOU	149	2030-04-01	2030-08-28
1 Infield cable, laying + pull in	111,036	m	300	m/hour + 6 hours/pull in	36	2030-07-23	2030-08-28
1 Infield cable, burial	111,036	m	150	m/hour + 6 hours/WTG	51	2030-07-09	2030-08-30
Export cable	14,406	m	300	m/hour	2	2030-04-15	2030-04-17
Export cable, burial	14,406	m	150	m/hour	4	2030-04-20	2030-04-24



25MW GBS Season 2, Phase 3							
Activity	Amount	Unit	Capacity	Unit	Days	Start	End
1 OSS, installation	2	#	7.00	days/(FOU+topside)	14	2030-04-01	2030-04-15
1 OSS, dredging	23,758	m3	500	m3/hour+0.5 day/OSS	3	2030-04-01	2030-04-03
1 GBS installation	89	#	1.00	days/FOU + 0.5 day/FOU	134	2030-04-29	2030-09-09
1 GBS seabed preparation	873,755	m3	500	m3/hour + 1 day/FOU	162	2030-04-01	2030-09-09
1 Infield cable, laying + pull in	121,311	m	300	m/hour + 6 hours/pull in	39	2030-08-01	2030-09-09
1 Infield cable, burial	121,311	m	150	m/hour + 6 hours/WTG	56	2030-07-17	2030-09-11
Export cable, laying	47,205	m	300	m/hour	7	2030-04-15	2030-04-21
Export cable, burial	47,205	m	150	m/hour	13	2030-04-20	2030-05-03
25MW GBS Season 2, Phase 4							
Activity	Amount	Unit	Capacity	Unit	Days	Start	End
1 OSS, installation	2	#	7.00	days/(FOU+topside)	14	2030-04-01	2030-04-15
1 OSS, dredging	23,758	m3	500	m3/hour+0.5 day/OSS	3	2030-04-01	2030-04-03
1 GBS installation	90	#	1.00	days/FOU + 0.5 day/FOU	135	2030-04-29	2030-09-11
1 GBS seabed preparation	883,573	m3	500	m3/hour + 1 day/FOU	164	2030-04-01	2030-09-11
1 Infield cable, laying + pull in	120,113	m	300	m/hour + 6 hours/pull in	39	2030-08-03	2030-09-11
1 Infield cable, burial	120,113	m	150	m/hour + 6 hours/WTG	56	2030-07-19	2030-09-13
Export cable	20,674	m	300	m/hour	3	2030-04-15	2030-04-17

8.2. Sediment type

The expected types of sediments are defined along the cables per 200 m section and at the substructures according to the sediment classification based on the backscatter data in combination with sediment samples for Sylen OWF (see Figure 8.1 and Appendix 1). Each sediment type is spatially associated with the sediment samples and an average grain size distribution per sediment type is calculated as described in chapter 6.8.

The sediment model is an add-on to the hydrodynamic thus current data and water level data are transferred by time step for advective transport of the sediment and deposition/resuspension of near-bottom sediments.

The sediment model itself contains information as follow:

- 1) The sediment types are split into 6 categories based on grain sizes and settling velocities, Table 8.2.
- 2) Coarse sediment is not modelled as this settles close to the source.
- 3) For erosion a critical shear stress e.g., 0.3 N/m² (DHI/IOW Consortium, 2013).
- 4) Dispersion both horizontal and vertical.
- 5) A description of the sediment source in time and space.

Table 8.2: Sediment categories and settling velocities (DHI/IOW Consortium, 2013) used for the modelling of the sediment dispersal.

Туре	coarse	fine sand	coarse silt	medium silt	fine silt	Clay
Settling velocity	-	15.0 mm/s	2.90 mm/s	0.560 mm/s	0.070 mm/s	0.030 mm/s
d, mean	-	0.130 mm	0.040 mm	0.0130 mm	0.0040 mm	0.0010 mm
d, minimum	-	0.060 mm	0.020 mm	0.0060 mm	0.0020 mm	0.0000 mm
d, maximum	-	0.200 mm	0.060 mm	0.020 mm	0.0060 mm	0.0020 mm
mud	1.7%	14.3%	11.3%	3.7%	16.3%	52.7%
mixed	39.4%	23.2%	10.6%	4.6%	6.7%	15.5%



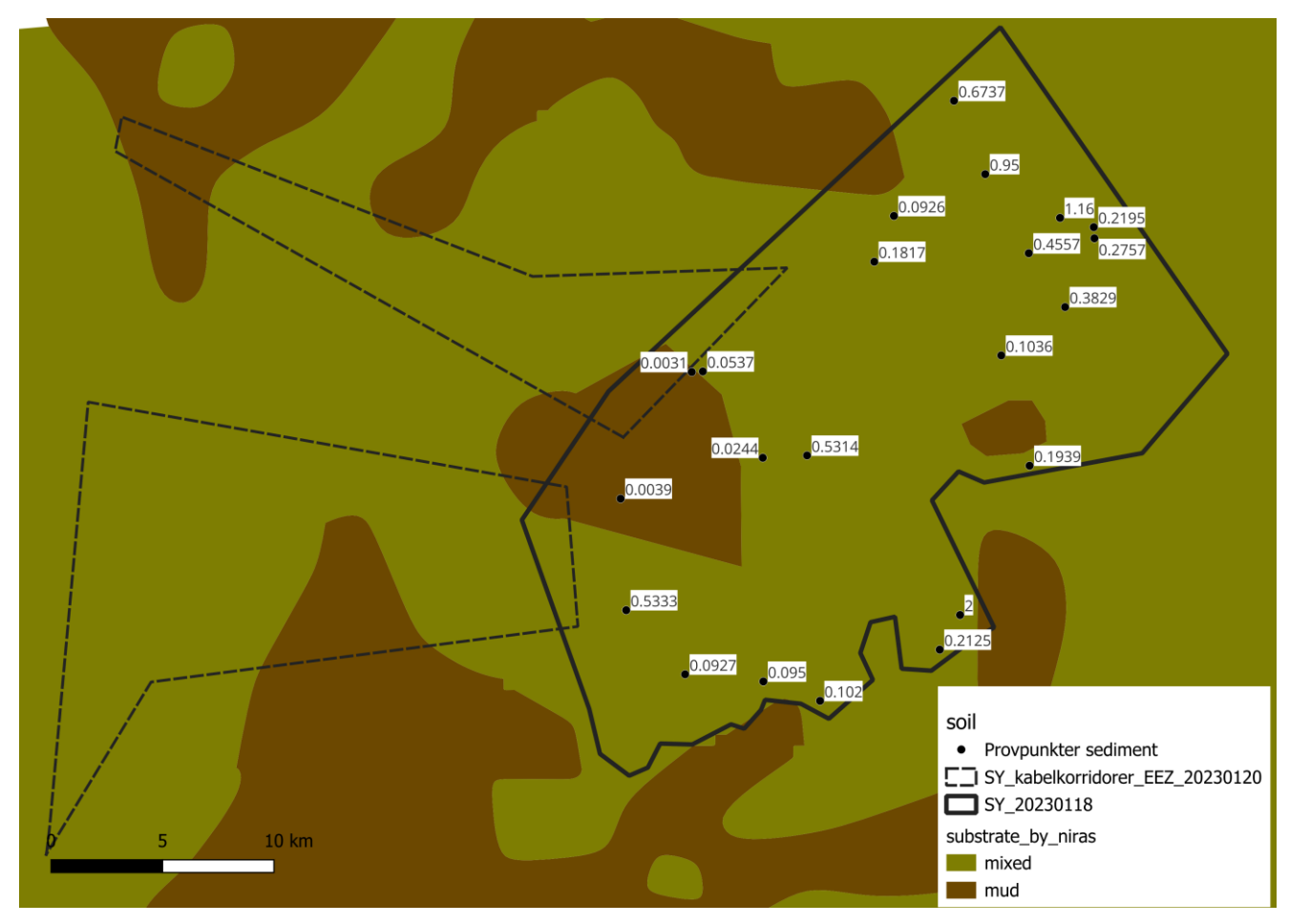


Figure 8.1: Sylen OWF and cable corridors together with the identified soil types and measured mean grain diameter in mm.

8.3. Estimated spill

In total is the spill estimated to 2,420,00 m³ (1,570,770 m³ exclusive the coarse sediments), Table 8-3. Furthermore, it should be highlighted, that significantly more sediment is released near the bottom (85% compared to the surface with 15%).



Sediment →	coarse	fine sand	coarse silt	medium silt	fine silt	Clay	Sum
Activity ↓	m³	m ³	m ³	m ³	m³	m³	m³
OSS-25MW-bottom_1	246	225	131	49	138	408	1,196
OSS-25MW-bottom_2	472	278	127	55	81	185	1,196
OSS-25MW-surface_1	492	449	262	99	276	815	2,392
OSS-25MW-surface_2	943	555	253	110	161	370	2,392
WTG-25MW-bottom_1	10,802	8,475	4,623	1,805	4,388	12,479	42,571
WTG-25MW-bottom_2	14,693	9,114	4,320	1,827	3,067	7,570	40,591
WTG-25MW-surface_1	21,603	16,950	9,246	3,610	8,776	24,958	85,142
WTG-25MW-surface_2	29,386	18,228	8,641	3,654	6,134	15,139	81,182
IAC-25MW_1	88,161	68,100	36,860	14,452	34,528	97,681	339,783
IAC-25MW_2	124,630	75,877	35,481	15,126	24,300	58,647	334,061
Export-C-25MW_1	90,498	55,120	25,782	10,989	17,672	42,673	242,735
Export-C-25MW_2	15,284	9,640	4,624	1,942	3,382	8,496	43,368
Sum - Season 1	397,209	263,009	130,351	53,717	102,904	269,421	1,216,611
Proportion	33%	22%	11%	4%	8%	22%	
OSS-25MW-bottom_3	472	278	127	55	81	185	1,196
OSS-25MW-bottom_4	472	278	127	55	81	185	1,196
OSS-25MW-surface_3	943	555	253	110	161	370	2,392
OSS-25MW-surface_4	943	555	253	110	161	370	2,392
WTG-25MW-bottom_3	16,246	9,962	4,683	1,990	3,253	7,922	44,056
WTG-25MW-bottom_4	17,189	10,253	4,721	2,031	3,096	7,262	44,551
WTG-25MW-surface_3	32,492	19,924	9,366	3,980	6,506	15,844	88,112
WTG-25MW-surface_4	34,378	20,505	9,441	4,062	6,193	14,524	89,103
IAC-25MW_3	135,236	82,676	38,779	16,502	26,778	64,968	364,938
IAC-25MW_4	139,941	83,283	38,278	16,486	24,982	58,389	361,359
Export-C-25MW_3	49,116	31,322	15,140	6,330	11,282	28,642	141,833
Export-C-25MW_4	24,509	14,431	6,577	2,847	4,188	9,620	62,173
Sum - Season 2	451,936	274,022	127,745	54,557	86,763	208,281	1,203,303
Proportion	38%	23%	11%	5%	7%	17%	
Sum - Total	849,145	537,031	258,096	108,274	189,667	477,702	2,419,914

Table 8-3: Total spill per source and sediment category.

8.4. Estimated sediment concentrations and associated durations

The sediment concentrations expected according to the simulation and the associated total time periods during which they will be reached or exceeded (not necessarily consecutive) are discussed hereafter. The results are shown separately for the different water depths, whereas within the wind farm area, the depth varies between 30 and 60 metres. Greater depths (locally up to max. 80 m) can also be observed along the export cables (Figure 8.2).

Results relevant to the sediment distribution assessment are presented in **Error! Reference source not found.** to Figure 8.5, Table 8-4 to Table 8-5, and Appendix 17 to Appendix 18.



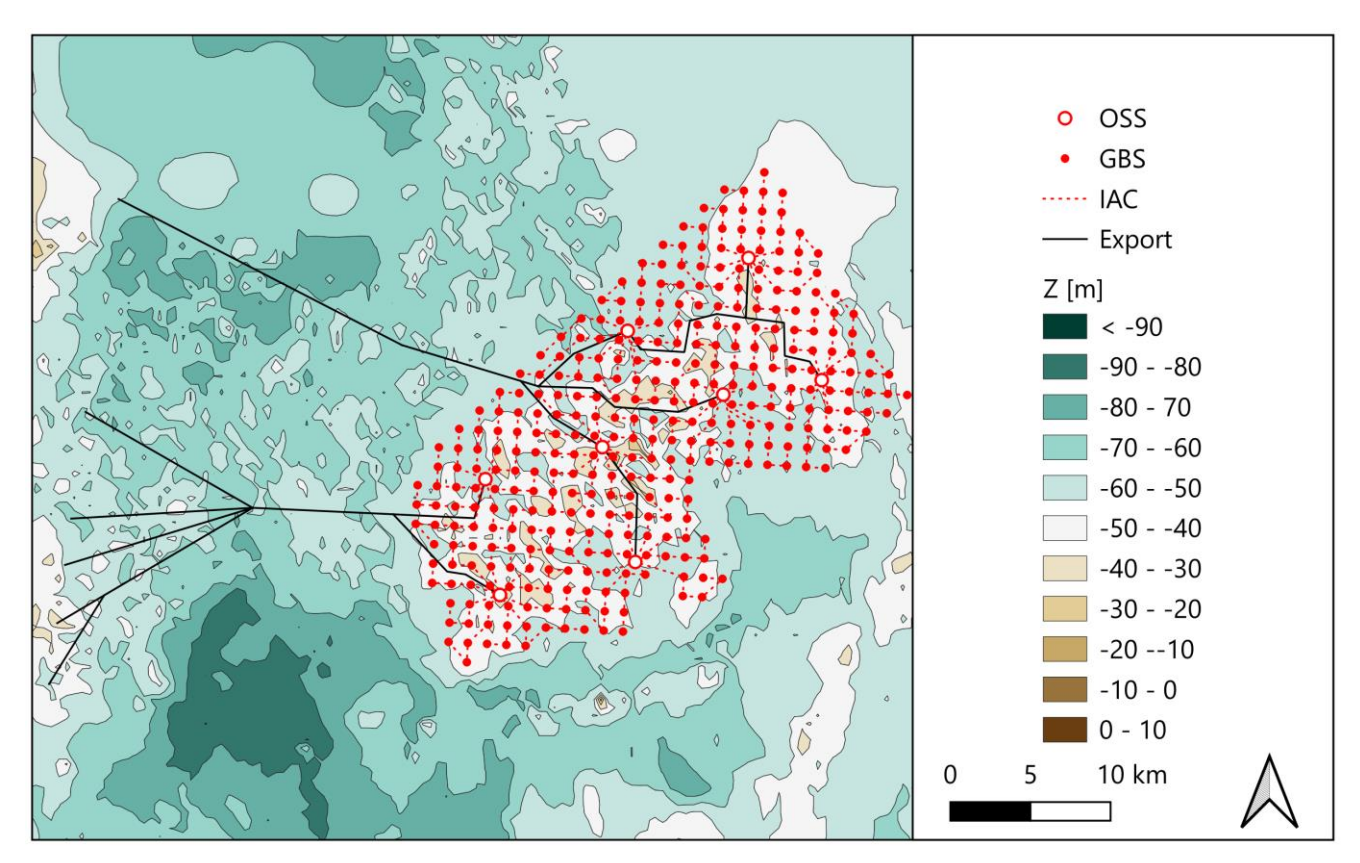


Figure 8.2: Bathymetry within the project area (source : Database (BSBD, last updated on 16/10/2017 (HELCOM, 2023)).

8.4.1. **Surface**

The total duration of the construction period during which the sediment concentrations in the surface layer reach or exceed 10 mg/l is presented in **Error! Reference source not found.**.

The shown sediment originates from the overflow from the barge (within the wind farm site) during the dredging of the gravity-based substructures and offshore substations. The released sediments are transported and dispersed with surface currents while sinking through the water column. The fact that the individual sources (locations of gravity-based substructures and offshore substations) cannot be identified in **Error! Reference source not found.**, indicates pronounced transport and dispersion.

In addition, the results (Error! Reference source not found., Table 8-4 and Table 8-5) show, that

- The observed concentrations and their exceedance durations tend to be higher in season 1, due to the larger proportion of fine material released (see Table 8-3).
- After a maximum of 2 days, the concentration falls below 10 mg/l in the top 10 meters.
- Regardless of the season under consideration, a concentration of 500 mg/l in the top 10 metres is neither reached nor exceeded.



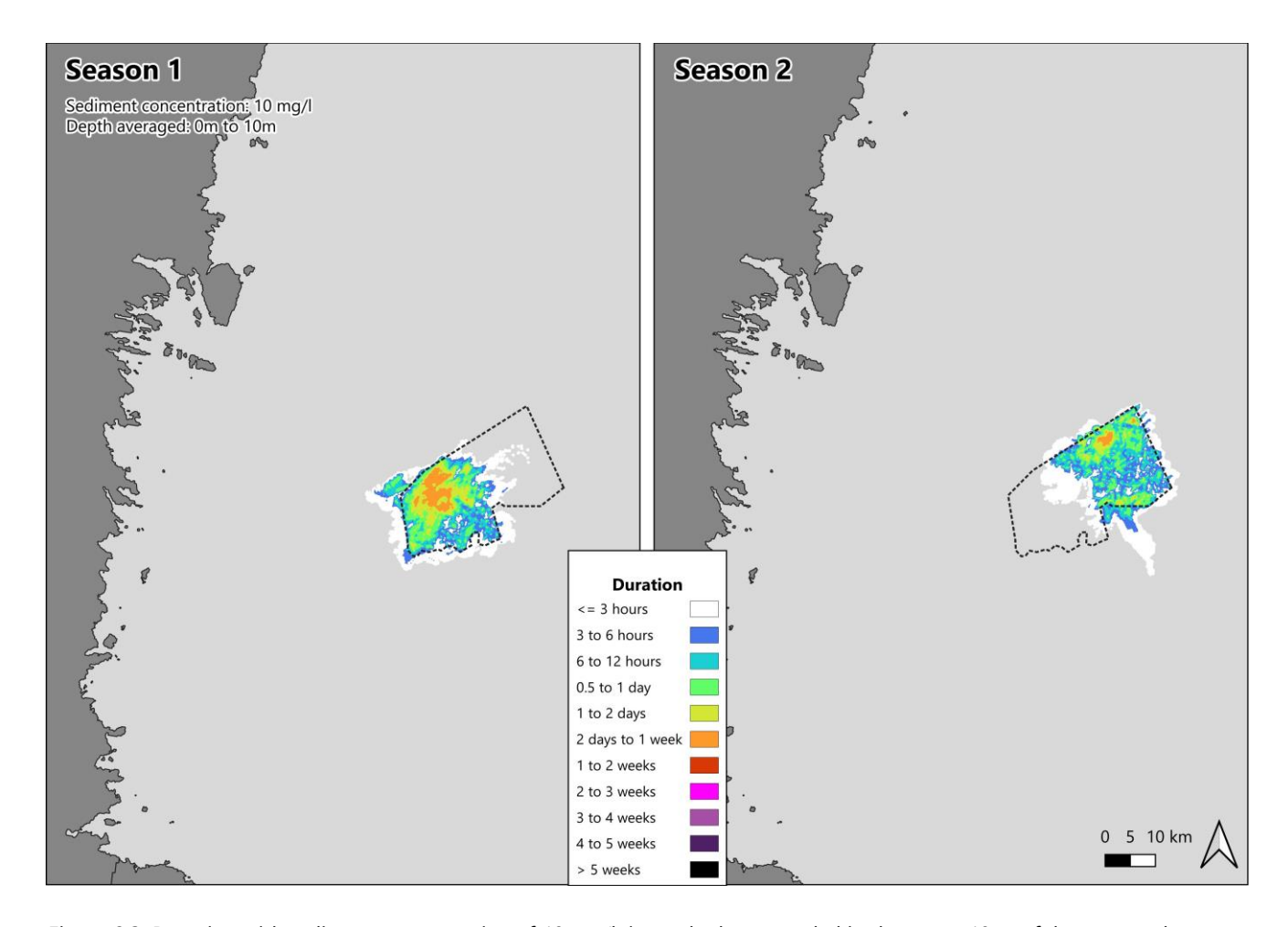


Figure 8.3: Duration with sediment concentration of 10 mg/l is reached or exceeded in the upper 10 m of the water column during season 1 (left) and season 2 (right). The seabed is shown in light gray, indicating the areas where no spilled sediments are observed).

8.4.2. Distribution over the water column

The released sediments sink through the water column, while being transported and dispersed with surface currents. Therefore, the sediment concentration decreases up to a depth of approximately 30 m (see e.g. **Error! Reference source not found.**, Table 8-4 and Table 8-5, and Appendix 17 to Appendix 18). The concentration increases again at greater depths as the bottom is reached. The material documented in these layers no longer originates solely from the settling of the material released by the overflow of the barge but is released by the activities near the bottom.



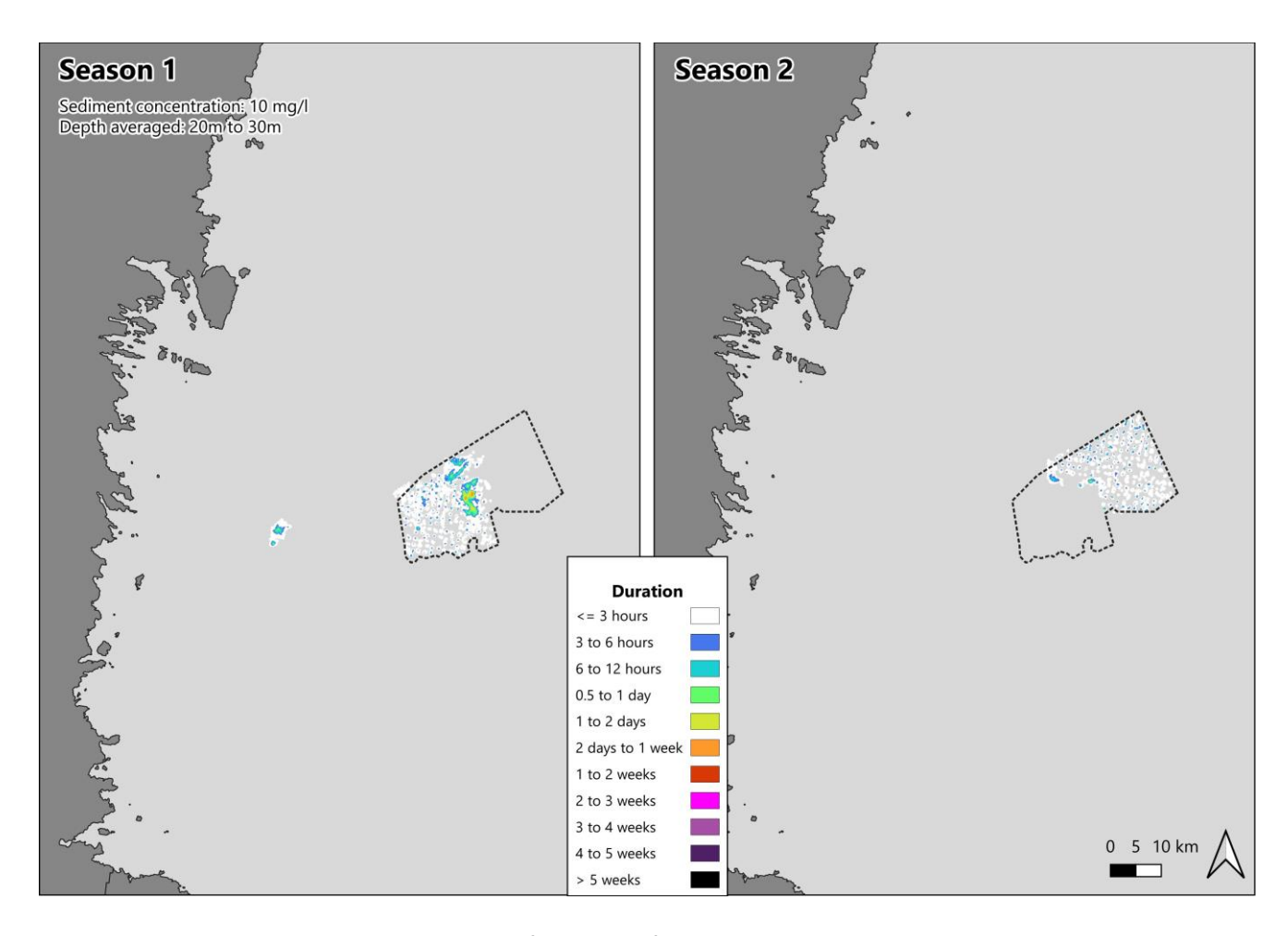


Figure 8.4: Duration with sediment concentration of 10 mg/l (Left: Season 1, right: Season 2) is reached or exceeded in at a depth of 20-30 m of the water column during season 1 (left) and season 2 (right). The seabed is shown in light gray, indicating the areas where no spilled sediments are observed).

8.4.3. At the bottom

Sediment is released near the bottom by dredging of the gravity-based substructures and the offshore substations, and by burying the inter-array and export cables using jets. Compared to the surface, significantly more sediment is released near the bottom (Table 8-3). However, in addition, sediments that are released at the surface arrive at the bottom through sedimentation processes before settling.

The results shown in Figure 8.5, Table 8-4, and Table 8-5, and Appendix 17 to Appendix 18 depict the following points:

- Aligned with the observations of sediment distribution at the surface, greater concentrations are observed in season 1 over a larger area and for a longer duration. This is due to the larger proportion of fines (see Table 8-3).
- The relatively large sediment volumes released directly near the seabed explain why:
 - the highest concentrations occur near the seabed (e.g. 1000 mg/l is reached or exceed during 6 hours on an area of 195 ha in season 1, and on 4 ha in season 2)



- Sediment spreading reaches the maximum extent near the seabed (e.g. 10mg/l is reached or exceeded during season 1 on an area of > 43,000 ha, Table 8-4).
- The concentration of 10 mg/l is reached or exceeded during a maximum period duration of 15 days (Figure 8.5, season 1).
- Due to transport and dispersion with bottom currents, the concentration decreases with increasing distance from the source, this is clearly visible when comparing the areas on which 10 mg/l or 100 mg/l are reached or exceeded (see Figure 8.5, Table 8-4 and Table 8-5). Regardless of the season, the area where 100 mg/l is reached or exceeded for 6 hours is 3.5 times smaller than the area with a minimum concentration of 10 mg/l.



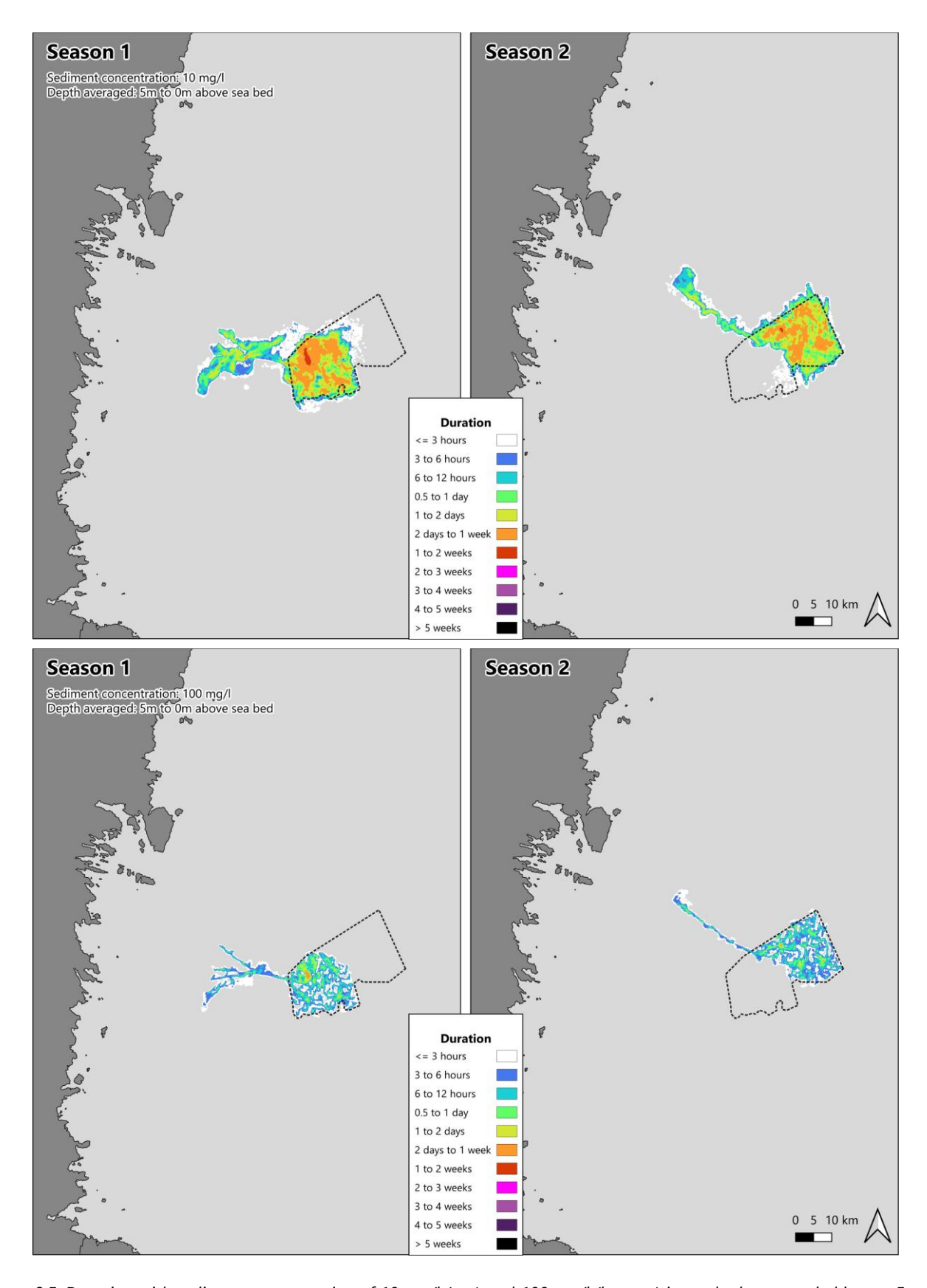


Figure 8.5: Duration with sediment concentration of 10 mg/l (top) and 100 mg/l (bottom) is reached or exceeded lowest 5 m of the water column, 5 m above the sea bed, during season 1 (left) and season 2 (right). The seabed is shown in light gray, indicating the areas where no spilled sediments are observed).



			Duration 6 h 12 h 24 h 2 d 1 week 2 weeks 3 weeks 4 weeks 5 w 23,010 15,652 8,834 3,243 -														
	Concentration	6 h	12 h	24 h	2 d	1 week	2 weeks	3 weeks	4 weeks	5 weeks							
	10 mg/l	23,010	15,652	8,834	3,243	-	-	-	-	-							
٤	20 mg/l	9,835	6,243	2,828	318	-	-	-		-							
10	100 mg/l	379	85	5	-	-	-	-	-	-							
- 0	500 mg/l	-	-	-	-	-	-	-	-	-							
	1000 mg /l	-	-	-	-	-	-	-	-	-							
	10 mg/l	6,354	3,643	1,309	23	-	-	-		-							
- 20 m	20 mg/l	592	179	11	-	-	•	-	-	-							
- 50	100 mg/l	-	-	-	-	-	•	-	-	-							
10	500 mg/l	-	-	-	-	-	ı	-	-	-							
	1000 mg /l	-	-	-	ī	-	ı	-	-	-							
	10 mg/l	2,206	914	345	69	-	-	-	-	-							
E	20 mg/l	461	175	46	0	-	-	-	-	-							
- 30 m	100 mg/l	24	4	-	-	-	-	-	-	-							
20	500 mg/l	-	-	-	-	-	-	-	-	-							
	1000 mg /l	-	-	-	-	-	-	-	-	-							
_	10 mg/l	15,141	11,725	6,943	2,871	-	-	-	-	-							
E	20 mg/l	8,276	5,468	2,291	291	-	-	-	-	-							
- 40 m	100 mg/l	1,127	270	5	-	-	-	-	-	-							
30	500 mg/l	3	-	-	-	-	-	-	-	-							
	1000 mg /l	-	-	-	-	-	-	-	-	-							
_	10 mg/l	29,963	24,595	17,937	8,975	502	-	-	-	-							
E	20 mg/l	22,341	16,923	9,095	2,833	74	-	-	-	-							
- 50	100 mg/l	6,080	1,853	366	3	-	-	-	-	-							
40	500 mg/l	129	12	-	-	-	-	-	-	-							
	1000 mg /l	1	-	-	-	-	-	-	-	-							
_	10 mg/l	22,629	15,652	8,608	3,002	342	22	-	-	-							
E	20 mg/l	15,515	9,248	3,947	1,020	125	-	-	-	-							
- 60	100 mg/l	3,993	1,458	483	165	-	-	-	-	-							
20	500 mg/l	428	176	27	-	-	-	-	-	-							
	1000 mg /l	135	11	-	-	-	-	-	-	-							
a	10 mg/l	43,073	35,267	24,964	12,156	544	16	-	-	-							
o pa	20 mg/l	34,391	25,857	13,917	4,138	161	-	-	-	-							
m above seabed	100 mg/l	12,893	4,524	903	191	-	-	-	-	-							
5 m S	500 mg/l	791	210	33	-	-	-	-	-	-							
	1000 mg /l	195	30	-	-	-	-	-	-	-							

Table 8-4: Area (ha) experiencing sediment concentration equal or greater than 10, 20, 100, 500, and 1000 mg/l for during varying durations and at different depths during season 1. For Info: $100 \text{ ha} = 1 \text{km}^2$.



		20,405 10,480 2,952 539 - - - - 6,077 2,364 628 12 - - - - 114 11 - - - - - - - - - - - - - - - - - - - - - - 2,280 786 95 0 - - - -														
	Concentration	6 h	12 h	24 h	2 d	1 week	2 weeks	3 weeks	4 weeks	5 weeks						
	10 mg/l	20,405	10,480	2,952	539	1	-	-	-	-						
Ε	20 mg/l	6,077	2,364	628	12	-	-	-	-	-						
- 10 m	100 mg/l	114	11	-	-	-	-	-	-	-						
- 0	500 mg/l	-	-	-	-	-	-	-	-							
	1000 mg /l	-	-	-	-	-	-	-	-	-						
	10 mg/l	2,280	786	95	0	-	-	-	-	-						
- 20 m	20 mg/l	46	3	-	-	1	-	-	-	-						
- 50	100 mg/l	-	-	-	ı	ı	1	-	-	-						
10	500 mg/l	-	-	-	ı	ı	-	-	-	-						
	1000 mg /l	1	-	-	ı	ı	-	-	-	-						
	10 mg/l	441	69	1	-	1	-	-	-	-						
- 30 m	20 mg/l	5	-	-	ı	ı	-	-	-	-						
- 3	100 mg/l	-	-	-	ı	ı	-	-	-	-						
70	500 mg/l	-	-	-	-	ı	-	-	-	-						
	1000 mg /l	1	-	-	ı	ı	-	-	-	1						
	10 mg/l	8,044	5,255	2,371	445	ı	-	-	-	-						
40 m	20 mg/l	4,114	2,316	596	29	ı	-	-	-	-						
- 4	100 mg/l	317	29	-	ı	ı	-	-	-	-						
30	500 mg/l	-	-	-	ı	ı	-	-	-	-						
	1000 mg /l	-	-	-	-	-	-	-	-	-						
_	10 mg/l	26,982	22,433	15,518	6,830	8	-	-	-	-						
- 50 m	20 mg/l	20,394	14,898	7,514	1,222	-	-	-	-	-						
- 56	100 mg/l	4,778	1,191	91	16	ı	-	-	-	-						
40	500 mg/l	64	1	-	-	-	-	-	-	-						
	1000 mg /l	-	-	-	-	-	-	-		-						
_	10 mg/l	20,143	14,202	7,806	2,305	75	-	-	-	-						
_ E	20 mg/l	13,328	8,619	3,650	703	12	-	-	-	-						
- 60 ш	100 mg/l	4,081	1,282	173	23	-	-	-	-	-						
20	500 mg/l	156	15	-	-	-	-	-	-	-						
	1000 mg /l	7	-	-	-	-	-	-	-	-						
o.	10 mg/l	39,091	32,666	22,746	9,588	92	-	-	-	-						
m above seabed	20 mg/l	31,188	23,761	12,515	2,328	12	-	-	-	-						
m abov seabed	100 mg/l	11,420	3,468	336	37	-	-	-	-	-						
Se Se	500 mg/l	254	14	-	-	-	-	-	-	-						
۳,	1000 mg /l	4	-	-	-	-	-	-	-	-						

Table 8-5: Area (ha) experiencing sediment concentration equal or greater than 10, 20, 100, 500, and 1000 mg/l for during varying durations and at different depths during season 2 For Info: $100 \text{ ha} = 1 \text{km}^2$.

8.1. Estimated sedimentation

The sedimented sediments originate from the dredging of the gravity-based substructures and the offshore substations and the burying of the inter-array and export cables using jetting.

Results of the sedimentation case are presented in Figure 8.6, Table 8-6 and Table 8-7, Appendix 19 and Appendix 20. The results can be summarised as follows:

- There is no outstanding difference in respect to the maximum sedimentation height between the seasons considered.
- The strongest sedimentation is observed along the inter-array and export cables, where the largest amount of sediment is released.
- Sedimentation of at least 1 mm must be expected over an area of 19,365 ha (season 1), respectively 18,139 ha (season 2).



- As a result of the construction phase a maximum sedimentation height of 30 mm (1,650 kg/m³, over an area of 3 ha (season 1), 6 h respectively (season 2)) is reached.
- The greatest distance for a sedimentation of less than 1 mm between the source and sedimentation accounts to approximately 38 kilometres to the south and 24 kilometres to the south-west (season 1). Larger sedimentation occur in a short distance to the source, approximately +/-500m.

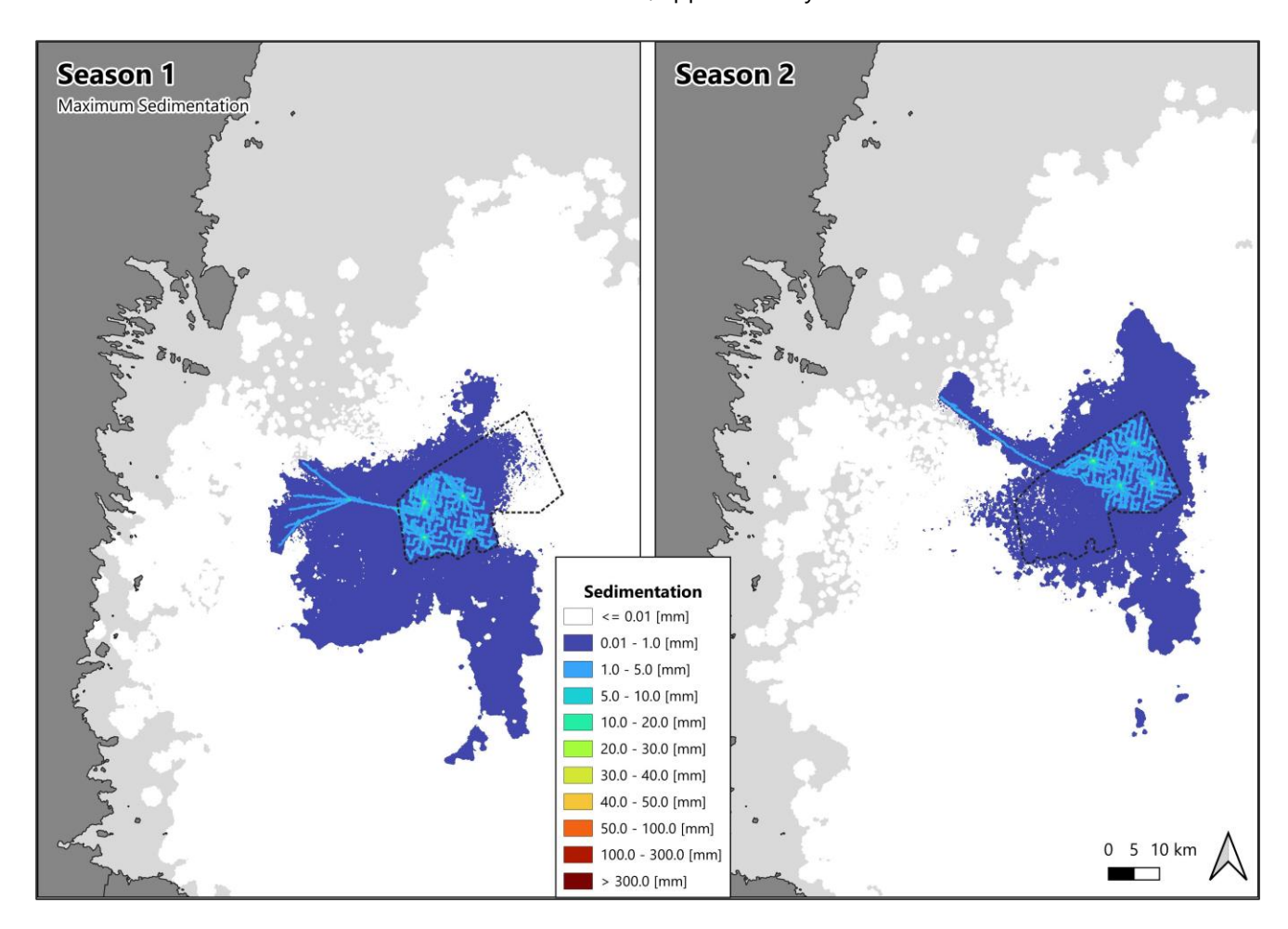


Figure 8.6: Maximum recorded sedimentation (10 minutes value, 1,650 kg/ m^3) resulting from season 1 (top) and season 2 (bottom).

Table 8-6: Area (ha) experiencing sedimentation due to the sediment disposal during season 1 case. For info: $100 \text{ ha} = 1 \text{ km}^2$.

				Sedin	nentation	[mm]			
	1	1 5 19,365 3,680		10 20		40	50	100	300
Maximum	19,365	3,680	465	47	3	-	-	-	-
End	19,365	3,680	465	465 47		-	-	-	-



Table 8-7: Area (ha) experiencing sedimentation due to the sediment disposal during season 1 case. For info: $100 \text{ ha} = 1 \text{ km}^2$.

				Sedin	nentation	[mm]			
	1	5	10 20		30	40	50	100	300
Maximum	18,139	3,374	323	35	6	-	-	-	-
End	18,139	3,374	323	35	6	-	-	-	-



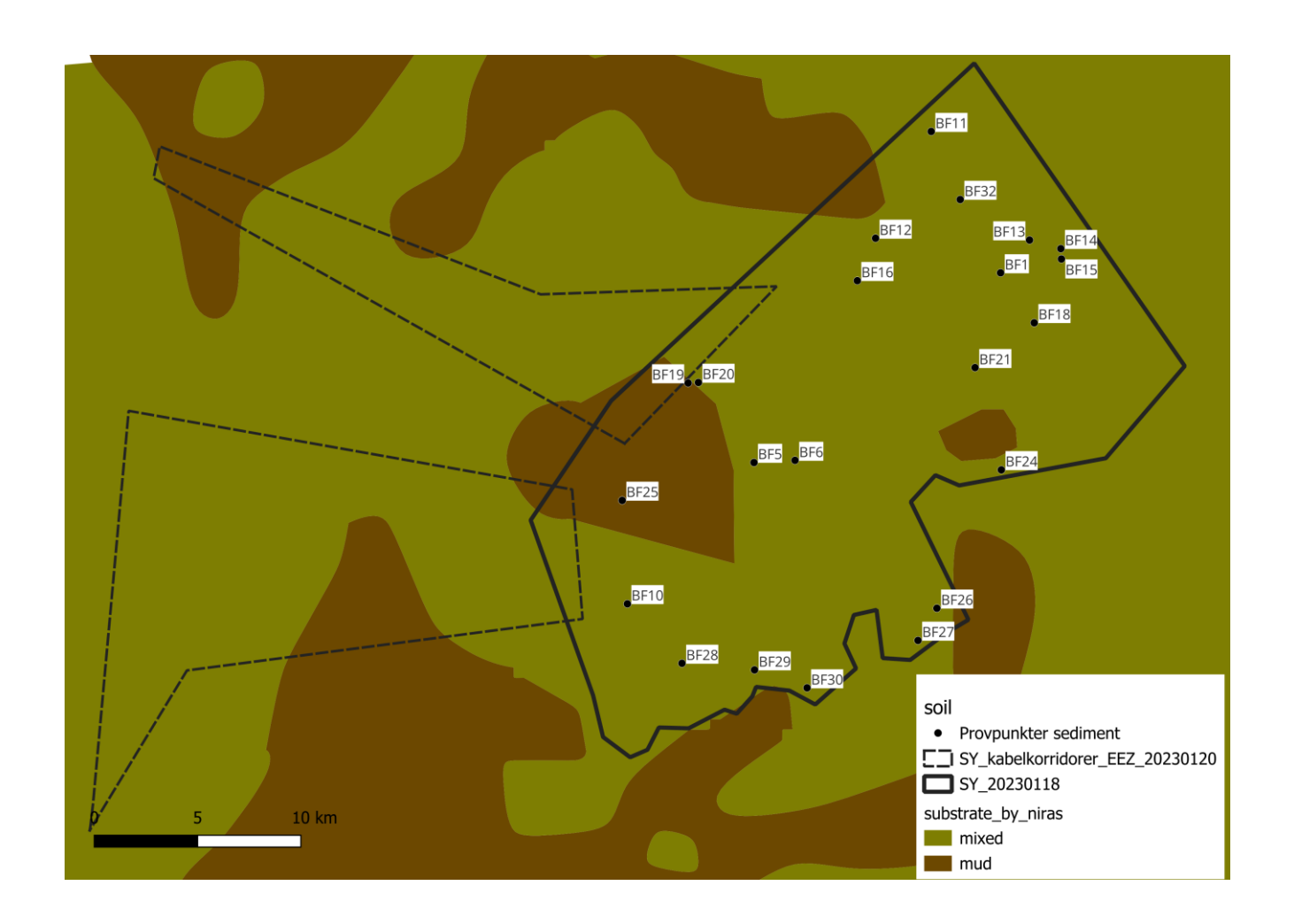
9. References

- Copernicus. (2022, 10). *Baltic Sea Physics Analysis and Forecast, 2x2km*. Retrieved from https://resources.marine.copernicus.eu/product
 - detail/BALTICSEA_ANALYSISFORECAST_PHY_003_006/INFORMATION
- Copernicus. (2022, 10). Baltic Sea Physics Reanalysis 4x4km. Retrieved from Copernicus:
 - https://resources.marine.copernicus.eu/product-
 - detail/BALTICSEA_REANALYSIS_PHY_003_011/INFORMATION
- DHI/IOW Consortium. (2013). Fehmarnbelt Fixed Link EIA. Marine Soil Impact Assessment. Sediment Spill during Construction of the Fehmarnbelt Fixed Link. Report No. E1TR0059 Voume II. https://vvmdocumentation.femern.com/8.%20E1TR0059%20Vol%20II6fdc.pdf?filename=files/BR/8.%20 E1TR0059%20Vol%20II.pdf.
- ECMWF, C. C. (2022, 12 01). *Climate Data Store*. (ECMWF) Retrieved from https://cds.climate.copernicus.eu/cdsapp#!/dataset/reanalysis-era5-single-levels?tab=form
- EMODnet. (2022). *EMODnet geology*. Retrieved from https://www.emodnet-geology.eu/map-viewer/?p=sea_floor_geology
- EMODnet. (2023, 03 15). *Bathymetry 2022*. Retrieved from portal.emodnet-bathymetry.eu/#: portal.emodnet-bathymetry.eu/#
- HELCOM. (2017). *Baltic Sea Bathymetry Database*. Retrieved from https://metadata.helcom.fi/geonetwork/srv/eng/catalog.search#/metadata/8b46e4c7-f911-44ab-89e6-2c8b8d9fa2c0
- HELCOM. (2023). *Baltic Sea Bathymetry Database*. Retrieved from https://metadata.helcom.fi/geonetwork/srv/eng/catalog.search#/metadata/8b46e4c7-f911-44ab-89e6-2c8b8d9fa2c0
- Jensen, N.O. (1983). A note on wind generator interaction. DTU.
- SGU. (2020). https://resource.sgu.se/service/wms/130/maringeologi-100-tusen. Retrieved from Maringeologi 1:100 000: https://resource.sgu.se/service/wms/130/maringeologi-100-tusen



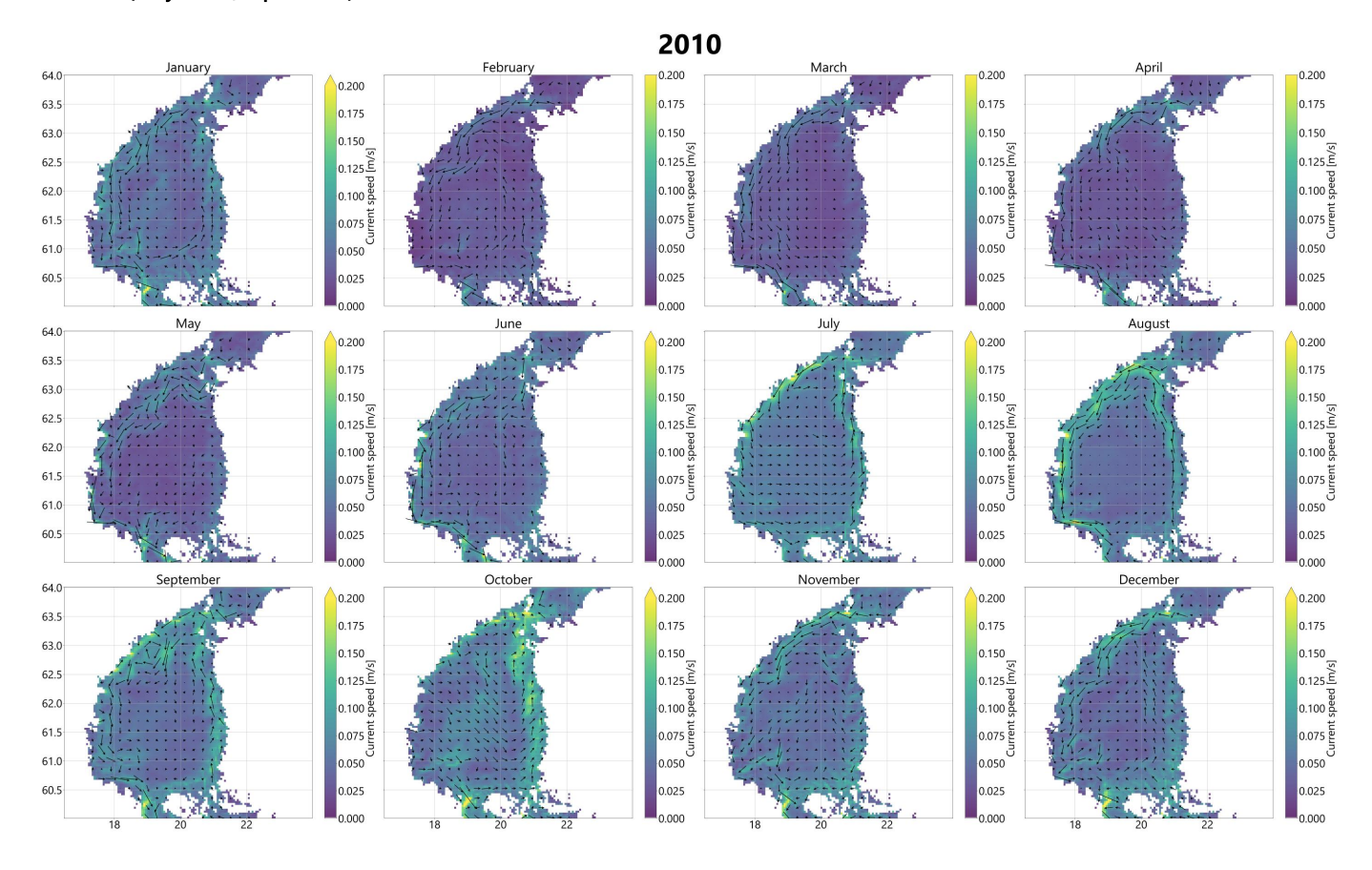
Appendix 1: Grain sieve analyses

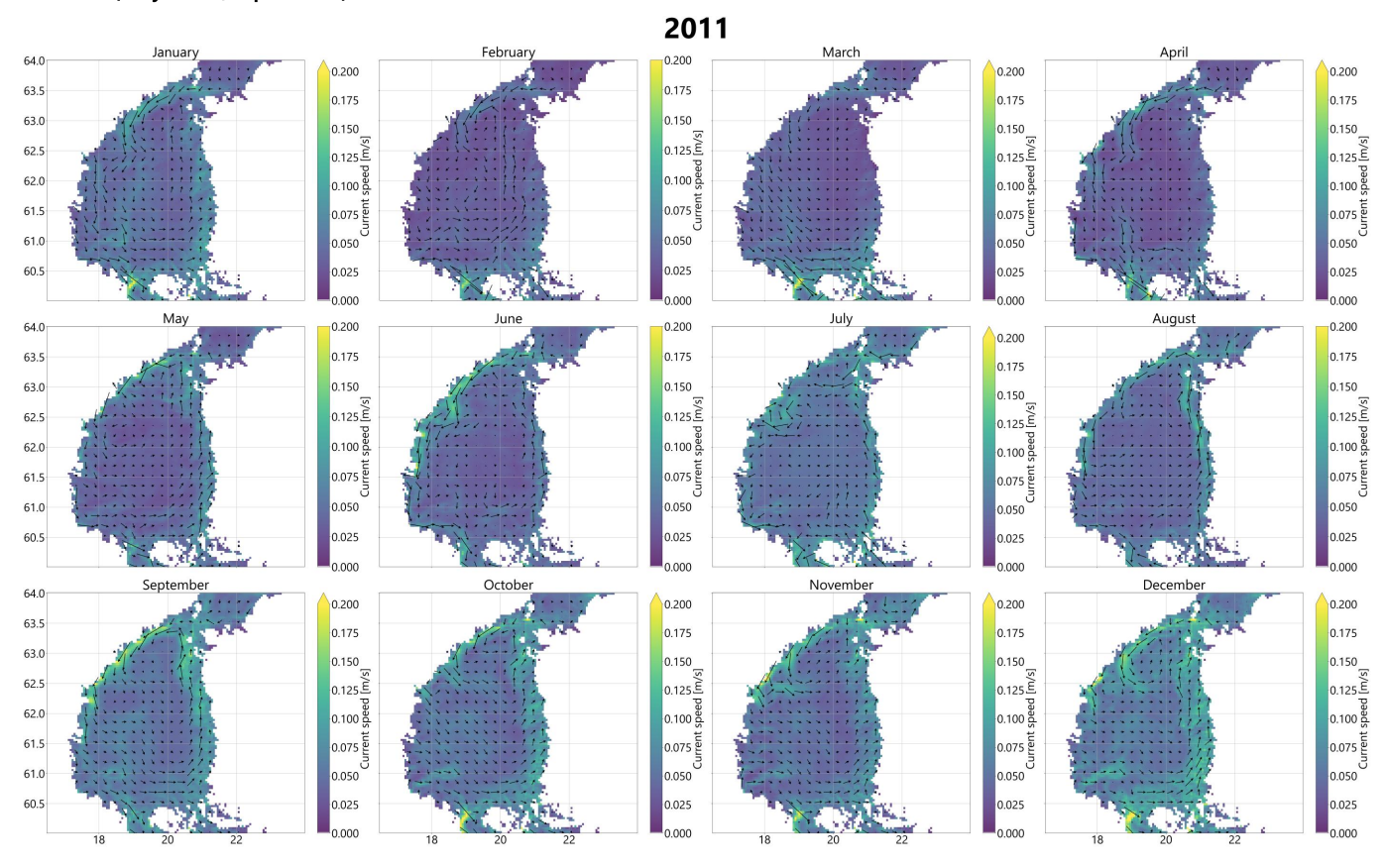
Туре	ID:	BF1	BF5	BF6	BF10	BF11	BF12	BF13	BF14	BF15	BF16	BF18	BF19	BF20	BF21	BF23	BF24	BF25	BF26	BF27	BF28	BF29	BF30	BF32
Ler	<0,002 mm	1	25	2	5	7	15	3	10	9	8	5	46	20	4	70	7	42	7	9	6	4	16	8
Finsilt	0,002-0,006 mm	1	16	2	5	2	8	2	6	6	4	3	15	9	3	17	5	17	3	3	4	3	8	4
Mellansilt	0,006-0,02 mm	1	8	2	8	2	5	3	6	6	6	3	1	5	3	2	3	8	4	2	4	4	9	5
Grovsilt	0,02-0,06 mm	4	9	4	9	3	12	5	11	10	12	6	17	19	21	2	13	15	4	8	22	24	11	0
Finsand	0,06-0,2 mm	4	21	11	3	12	43	8	15	12	23	17	19	23	61	7	23	17	7	27	60	60	20	5
Mellansand	0,2-0,6 mm	61	16	35	24	23	1	19	41	37	23	35	2	18	8	0	15	1	15	32	4	3	16	25
Grovsand	0,6-2 mm	12	3	35	46	19	6	25	7	9	16	11	0	3	0	0	16	0	10	11	1	0	11	12
Fingrus	2-6 mm	4	1	7	1	18	11	19	3	4	6	12	0	1	0	1	8	0	15	6	0	0	6	18
Mellangrus	6-20 mm	12	1	3	0	15	0	18	1	7	1	9	0	1	0	0	10	0	36	1	0	0	4	23

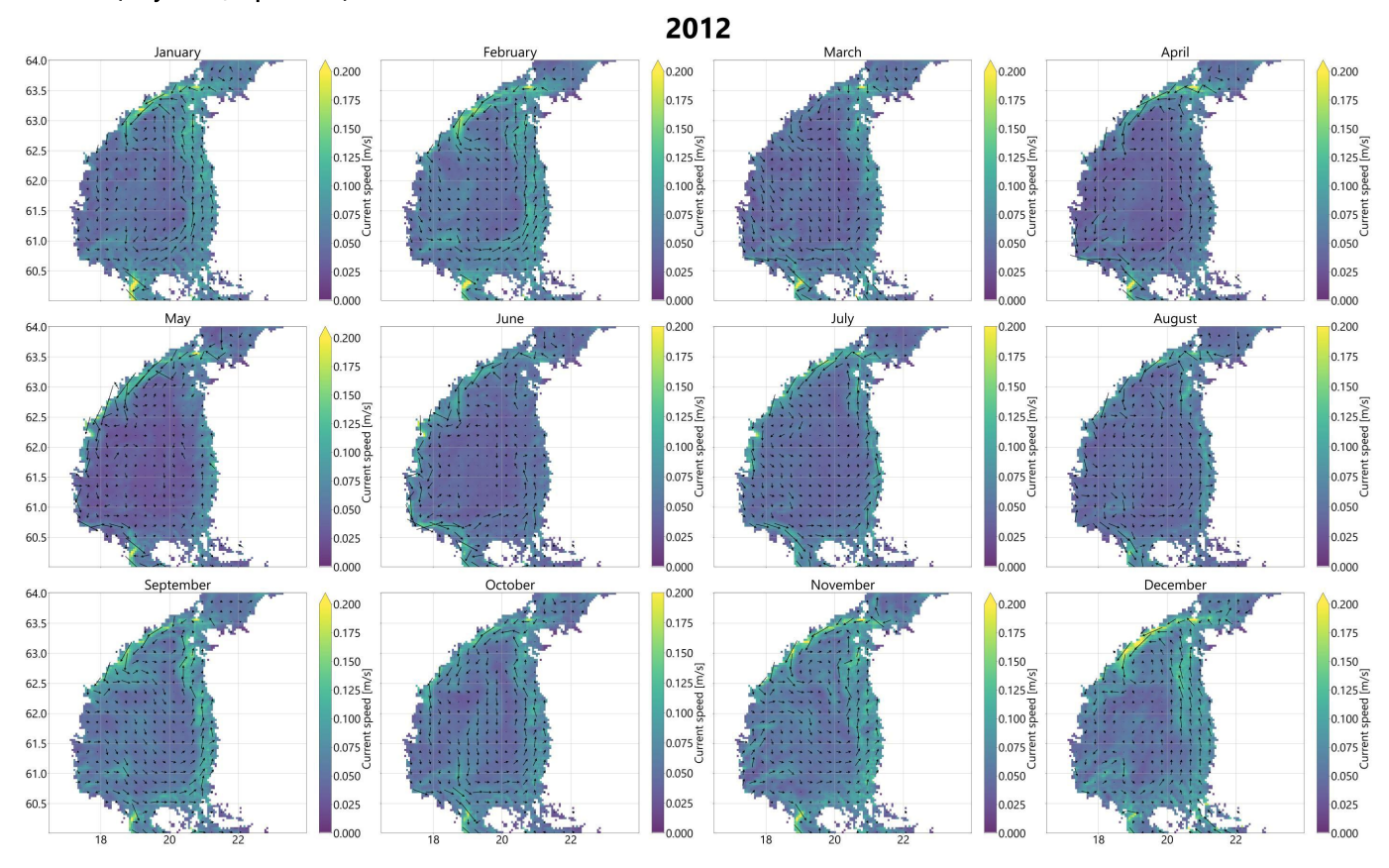


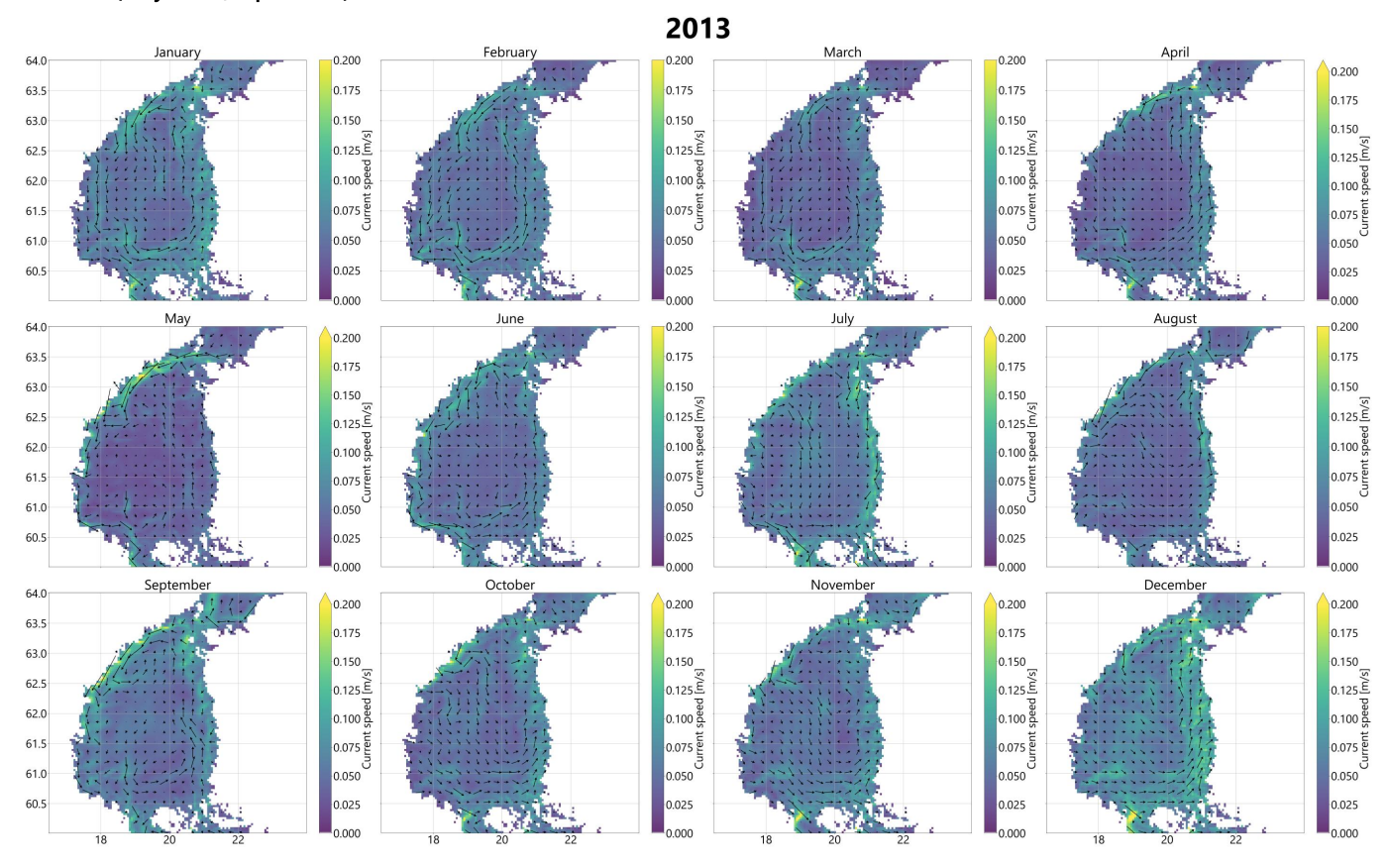


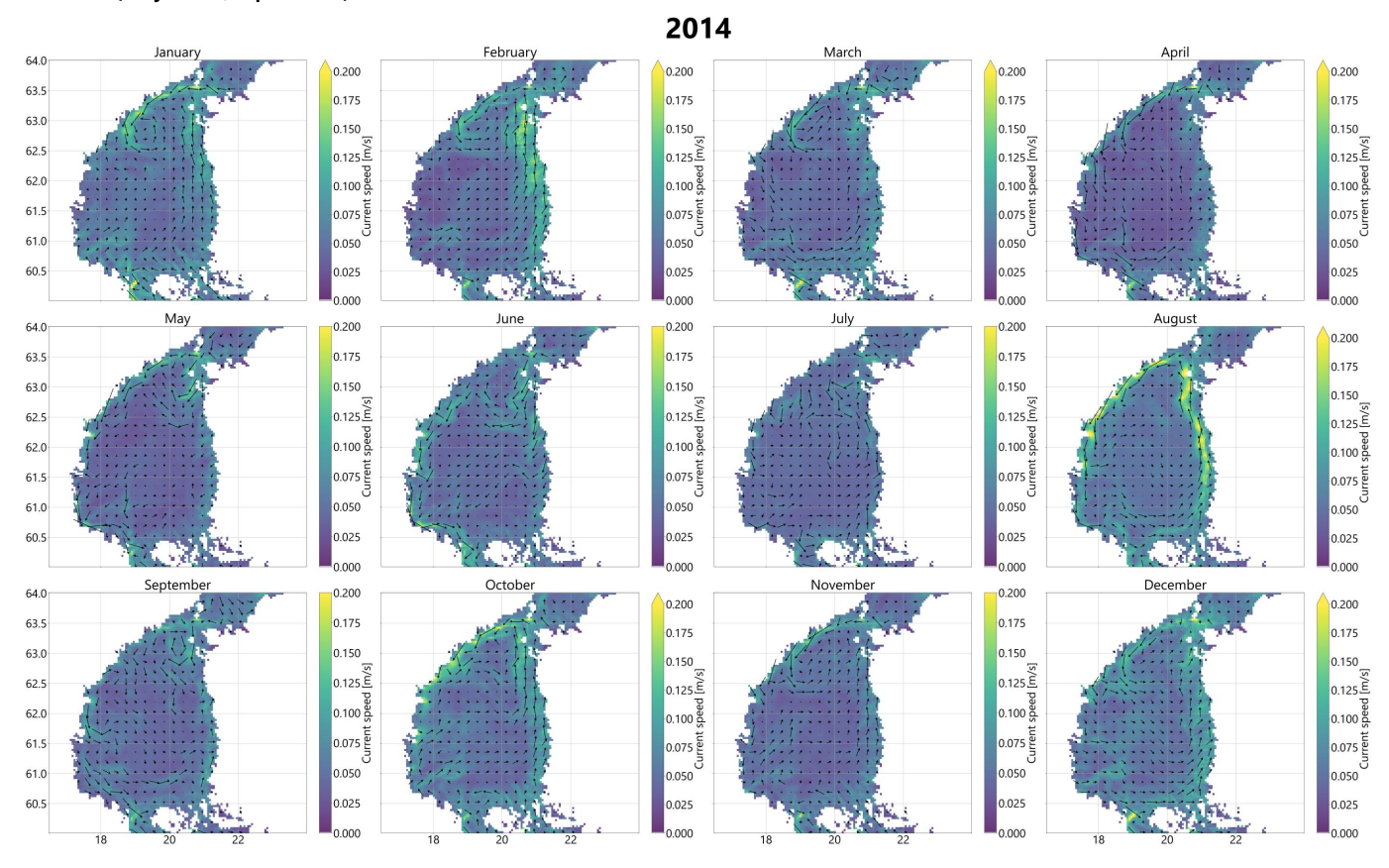
Appendix 2 Current field (SMHI)

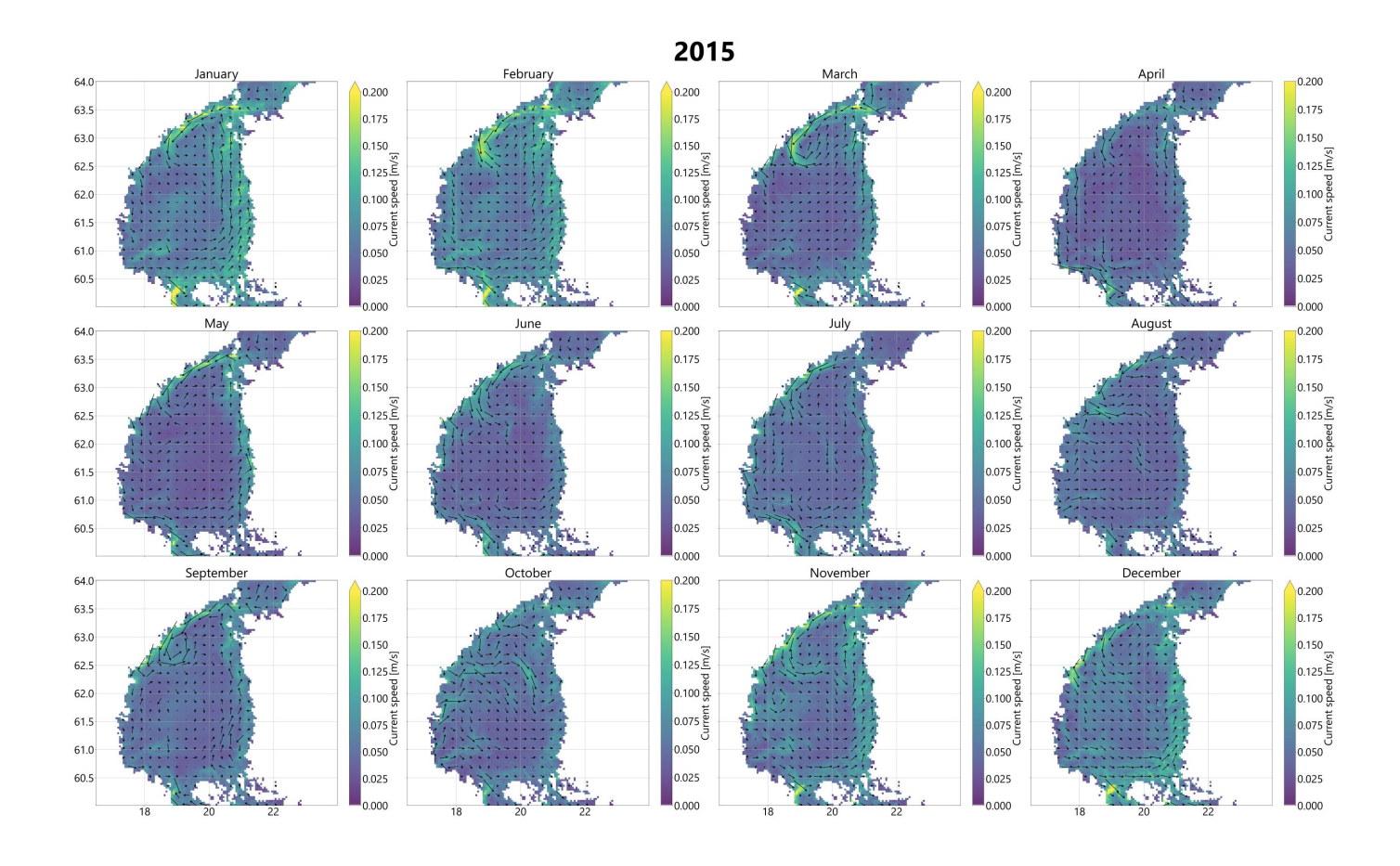


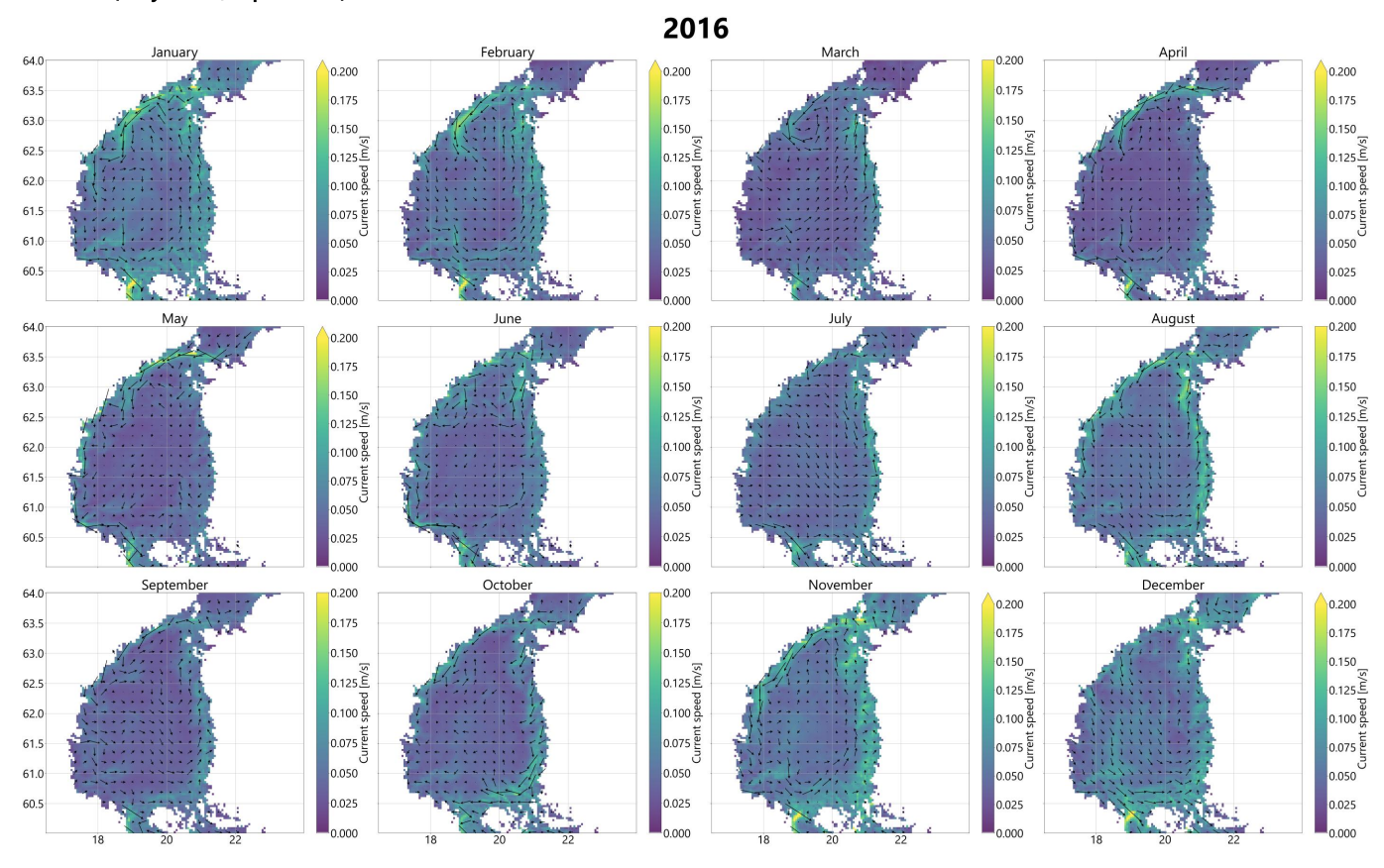


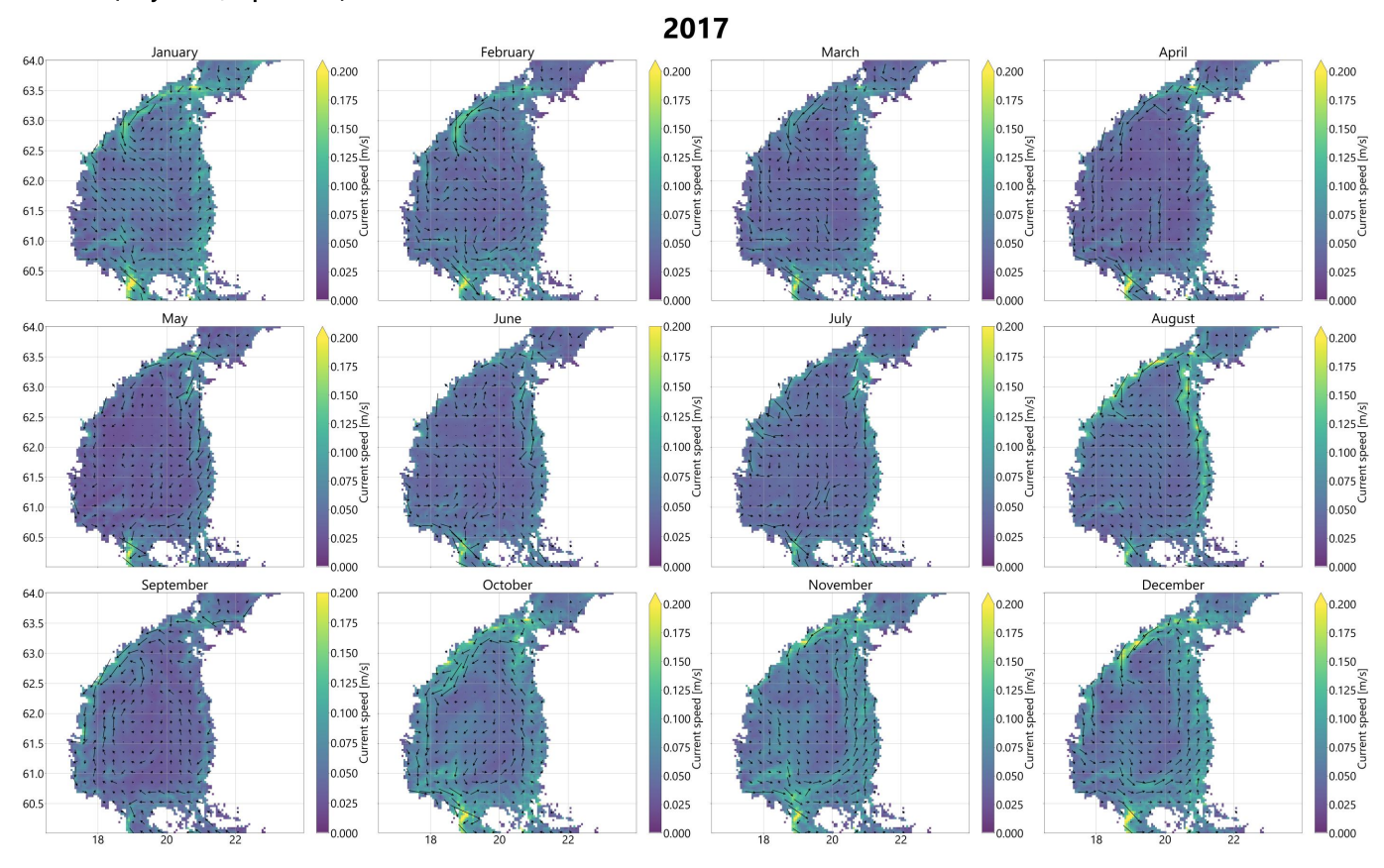


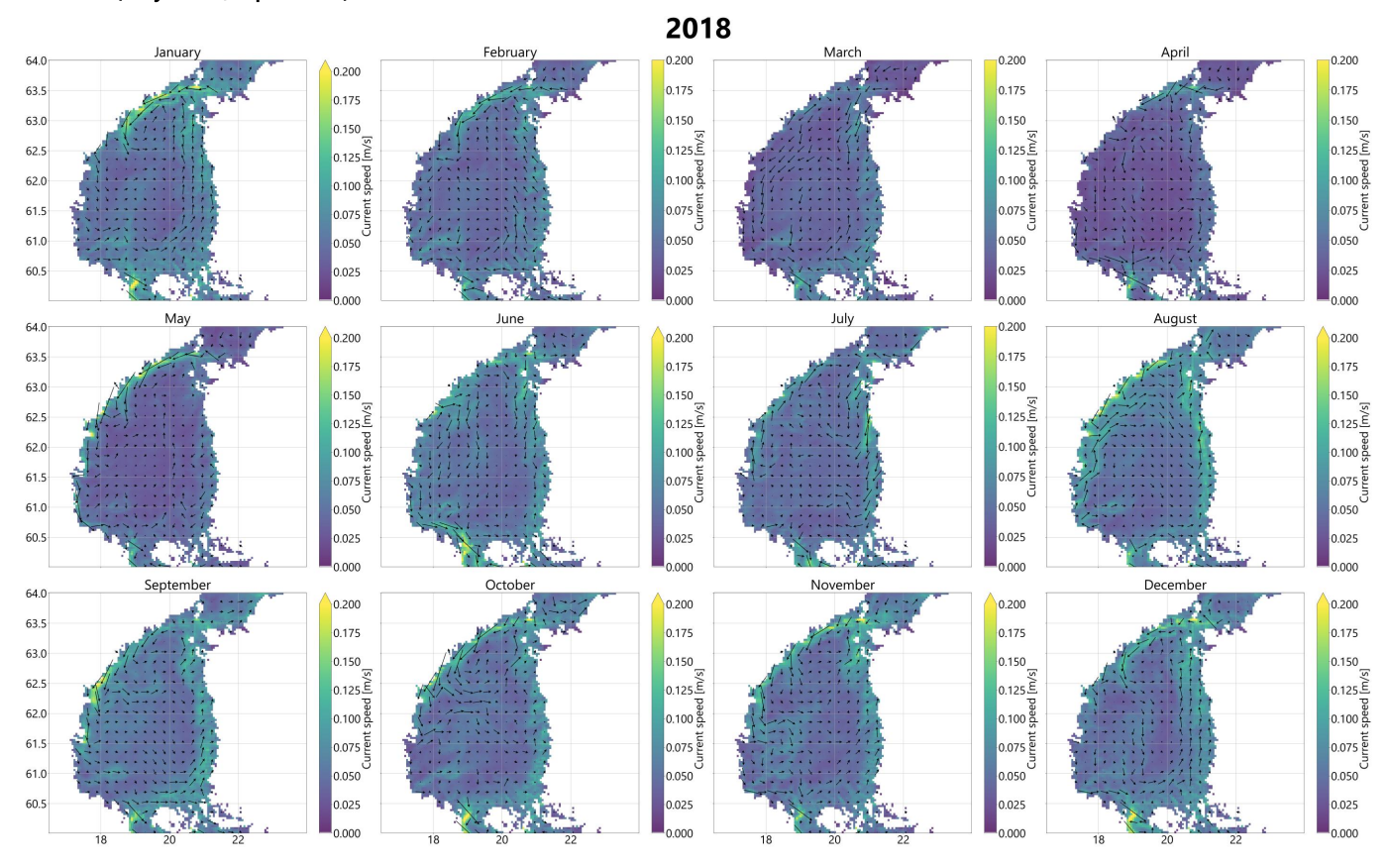


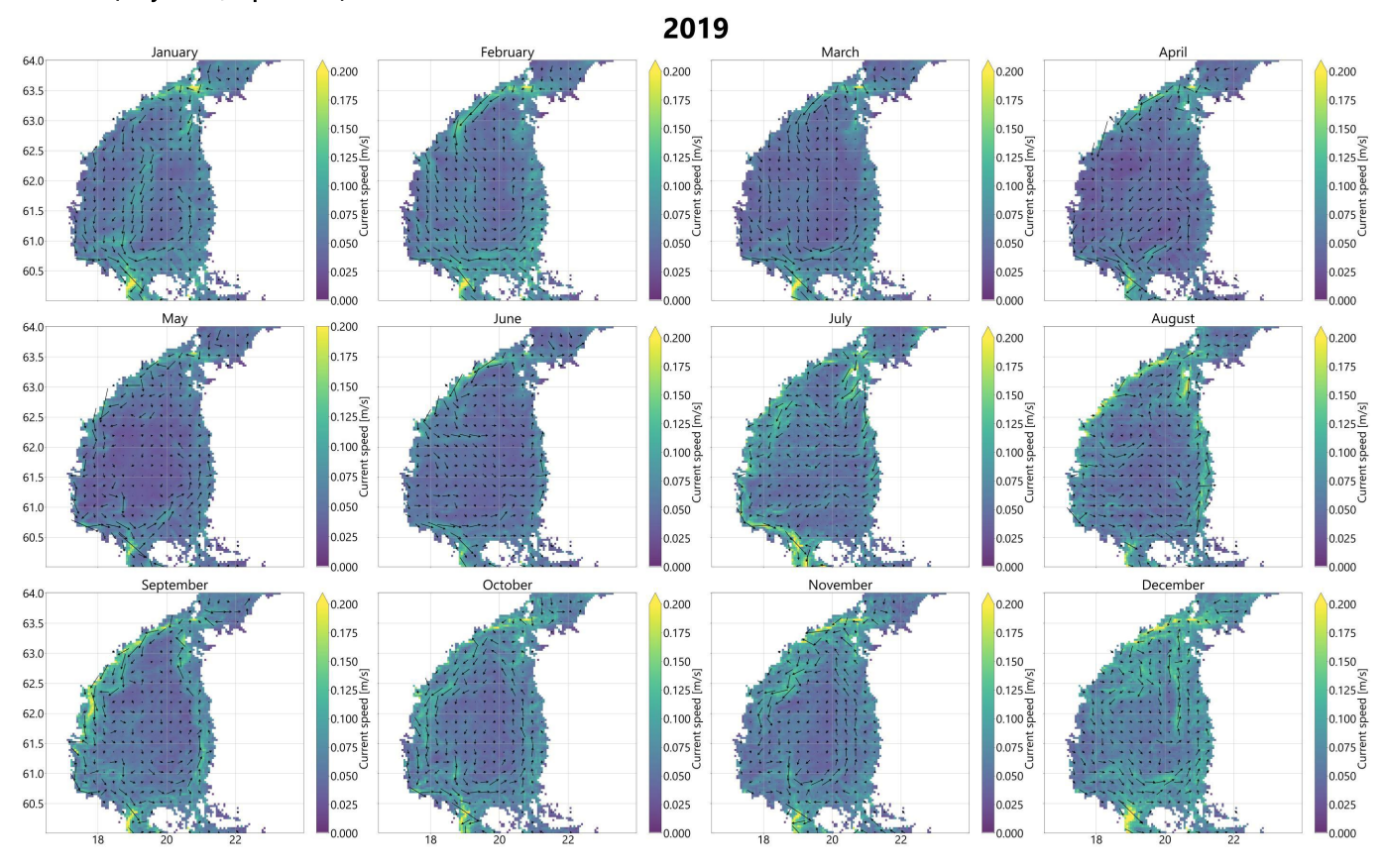


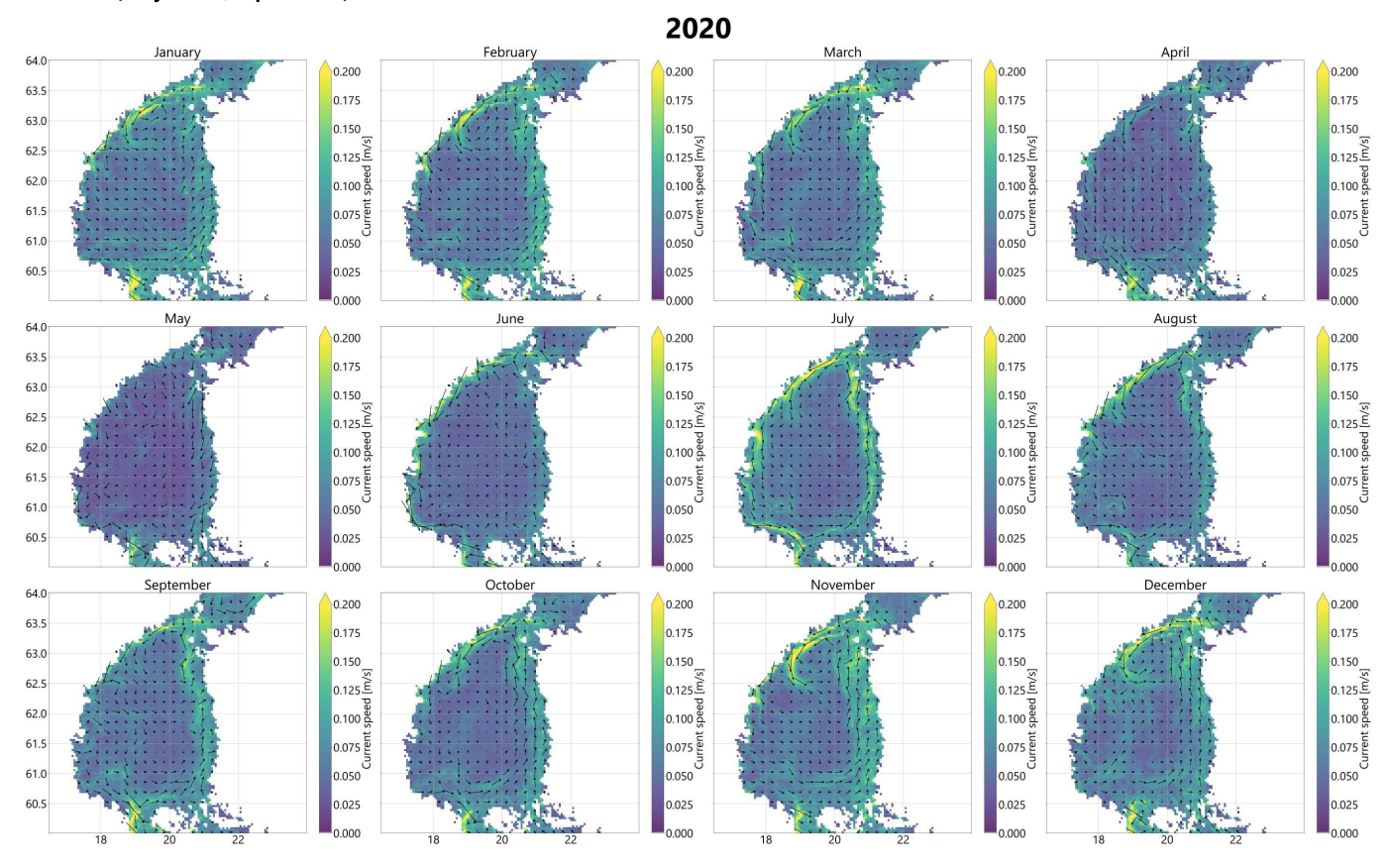




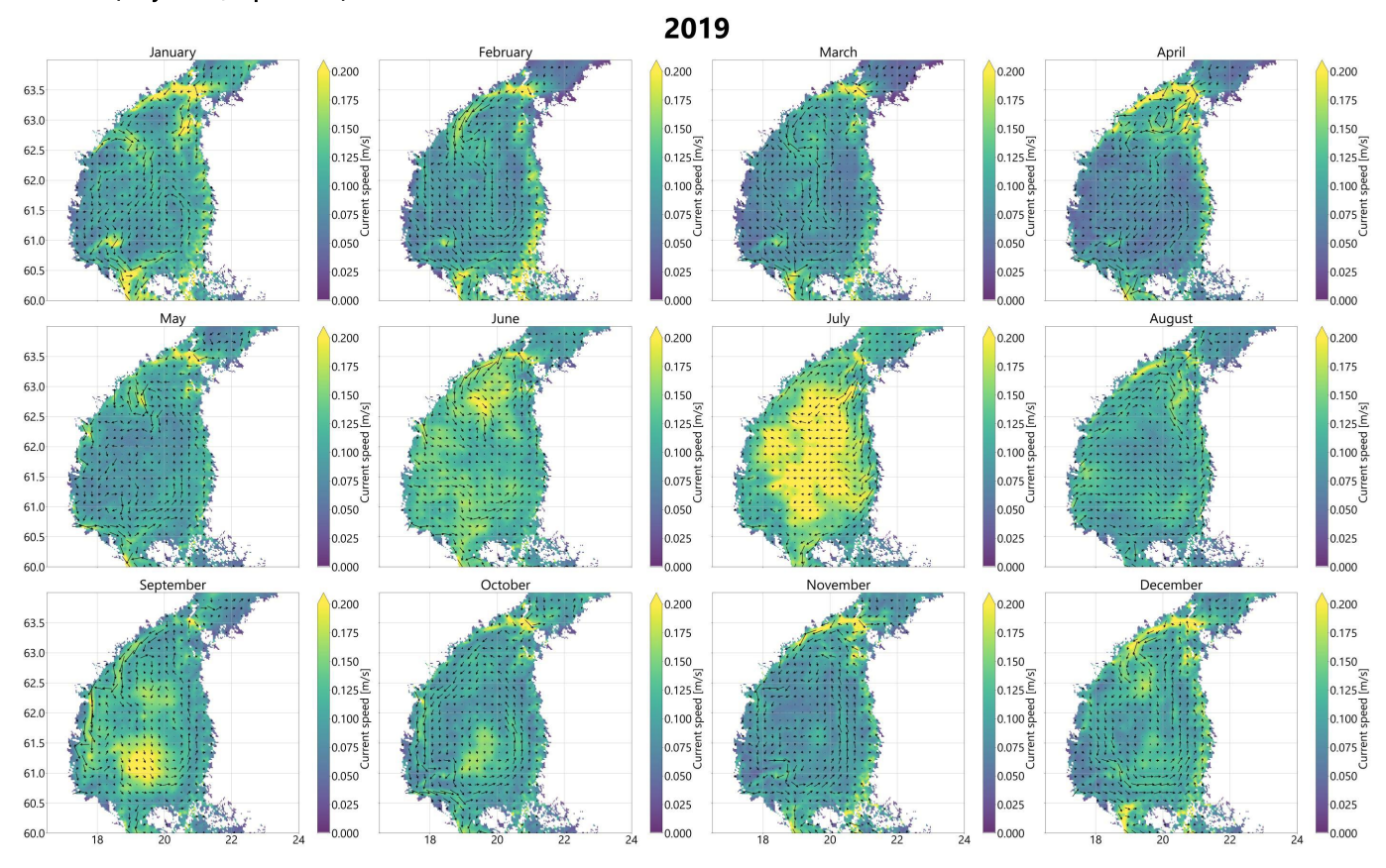




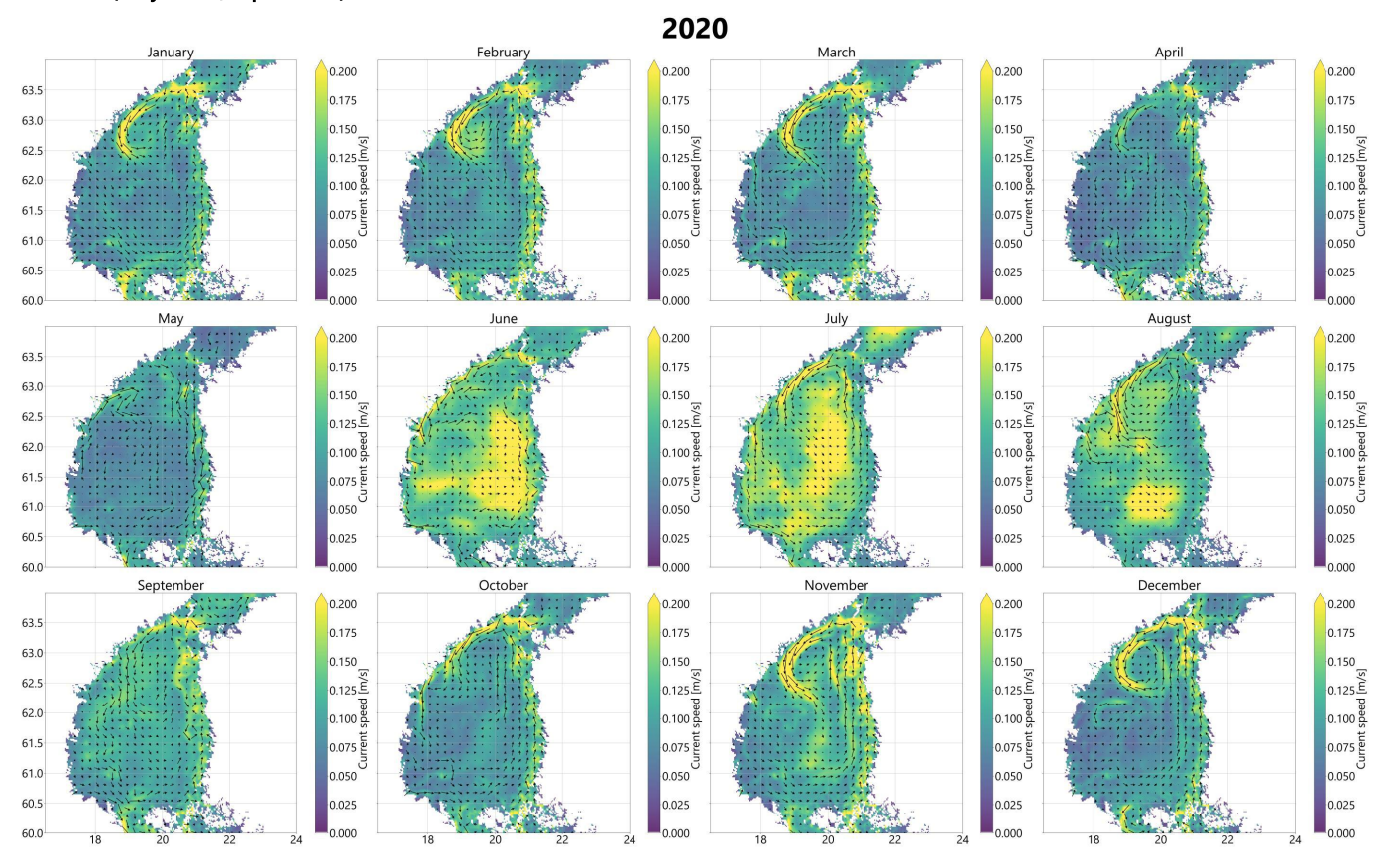




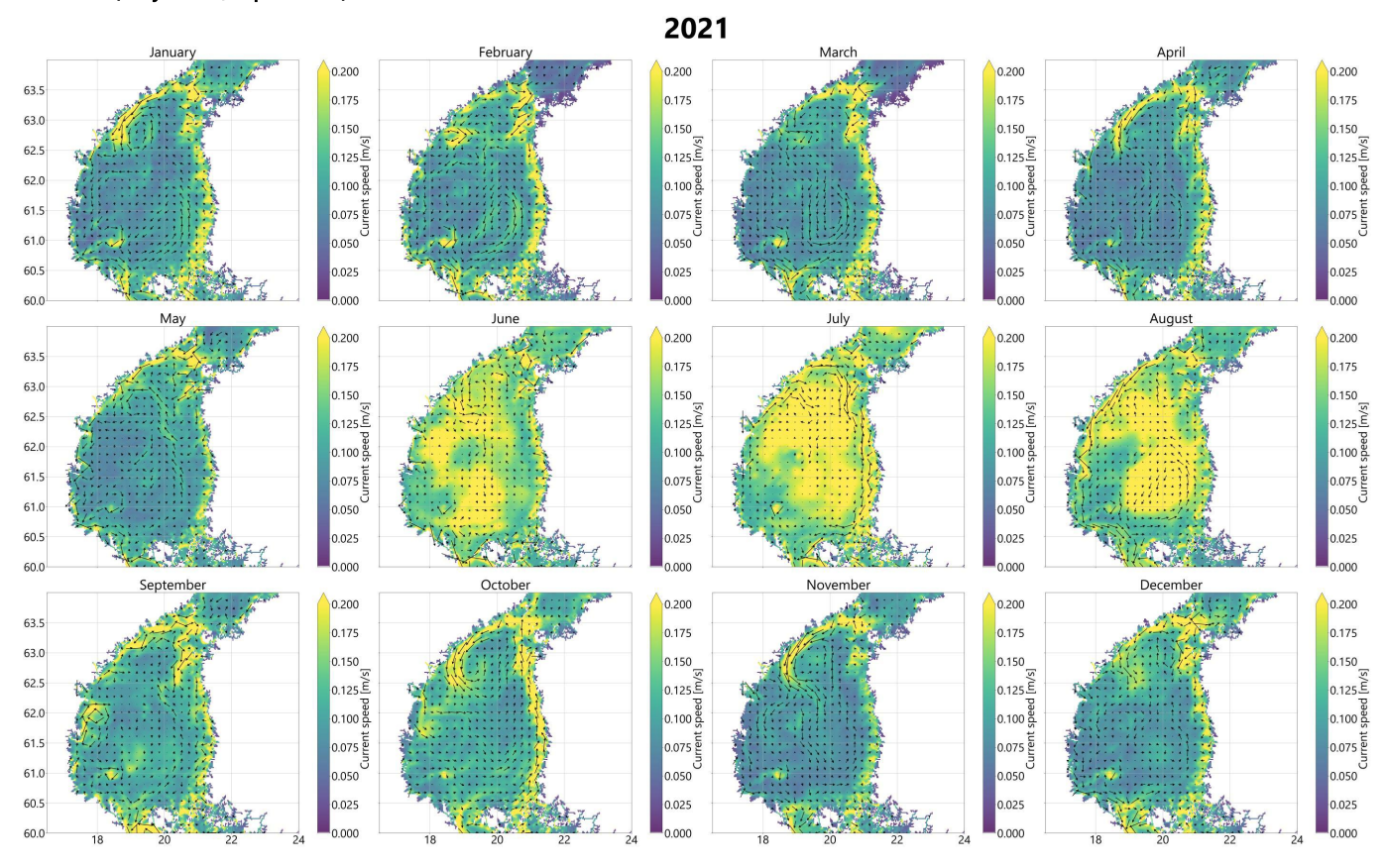
SMHI 2x2 (daily values, depth: 1.5 m)



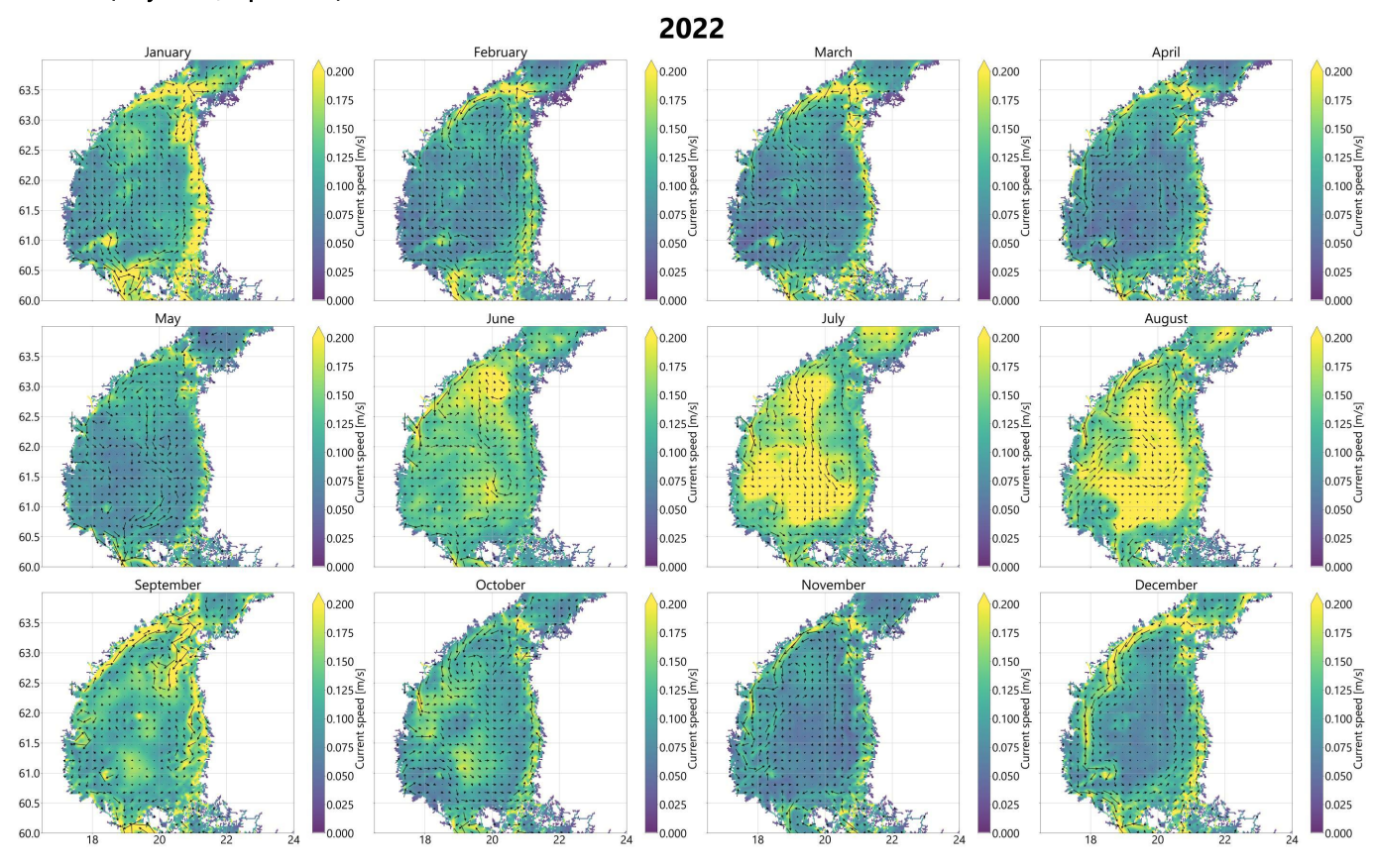
SMHI 2x2 (daily values, depth: 1.5 m)

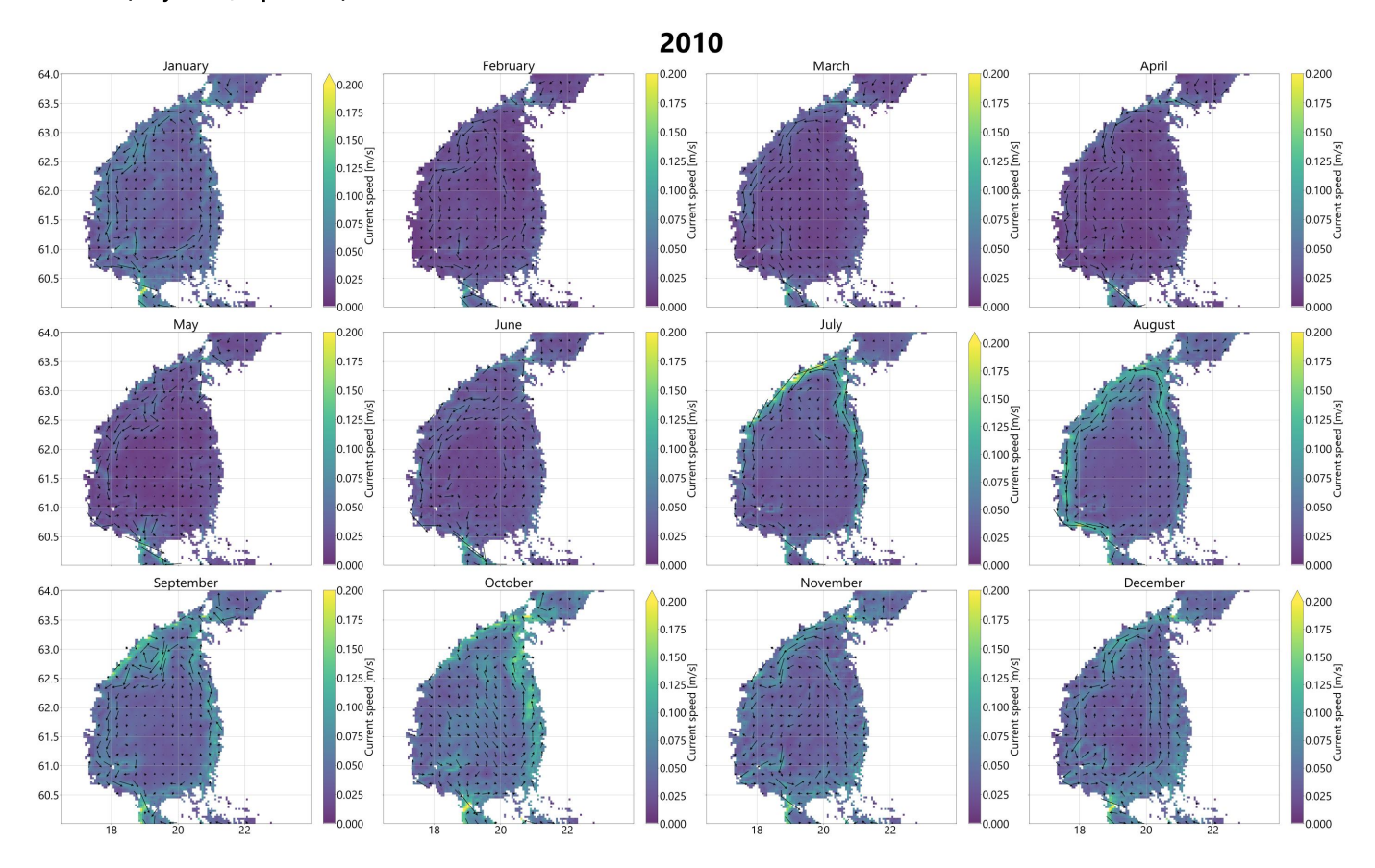


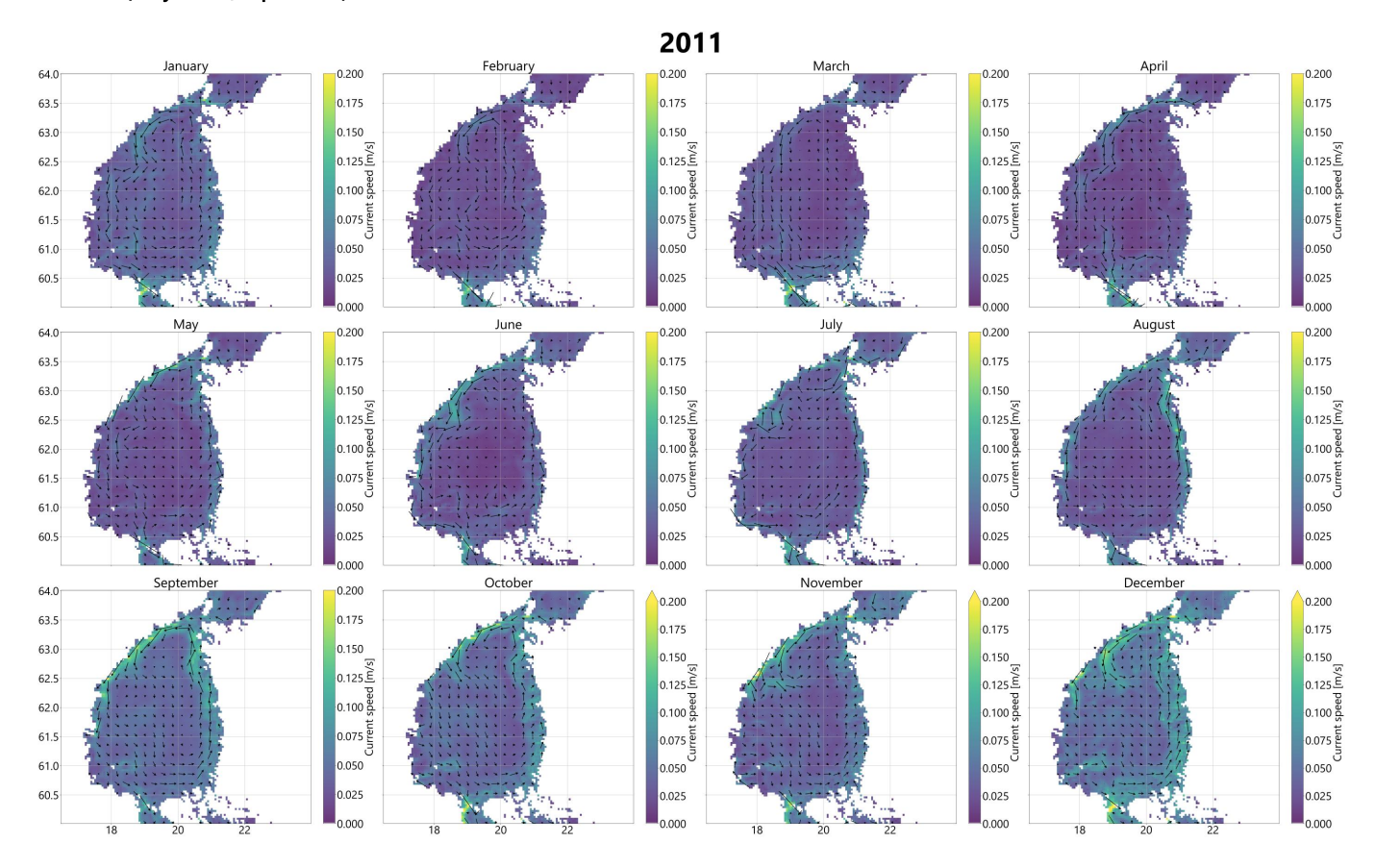
SMHI 2x2 (daily values, depth: 1.5 m)

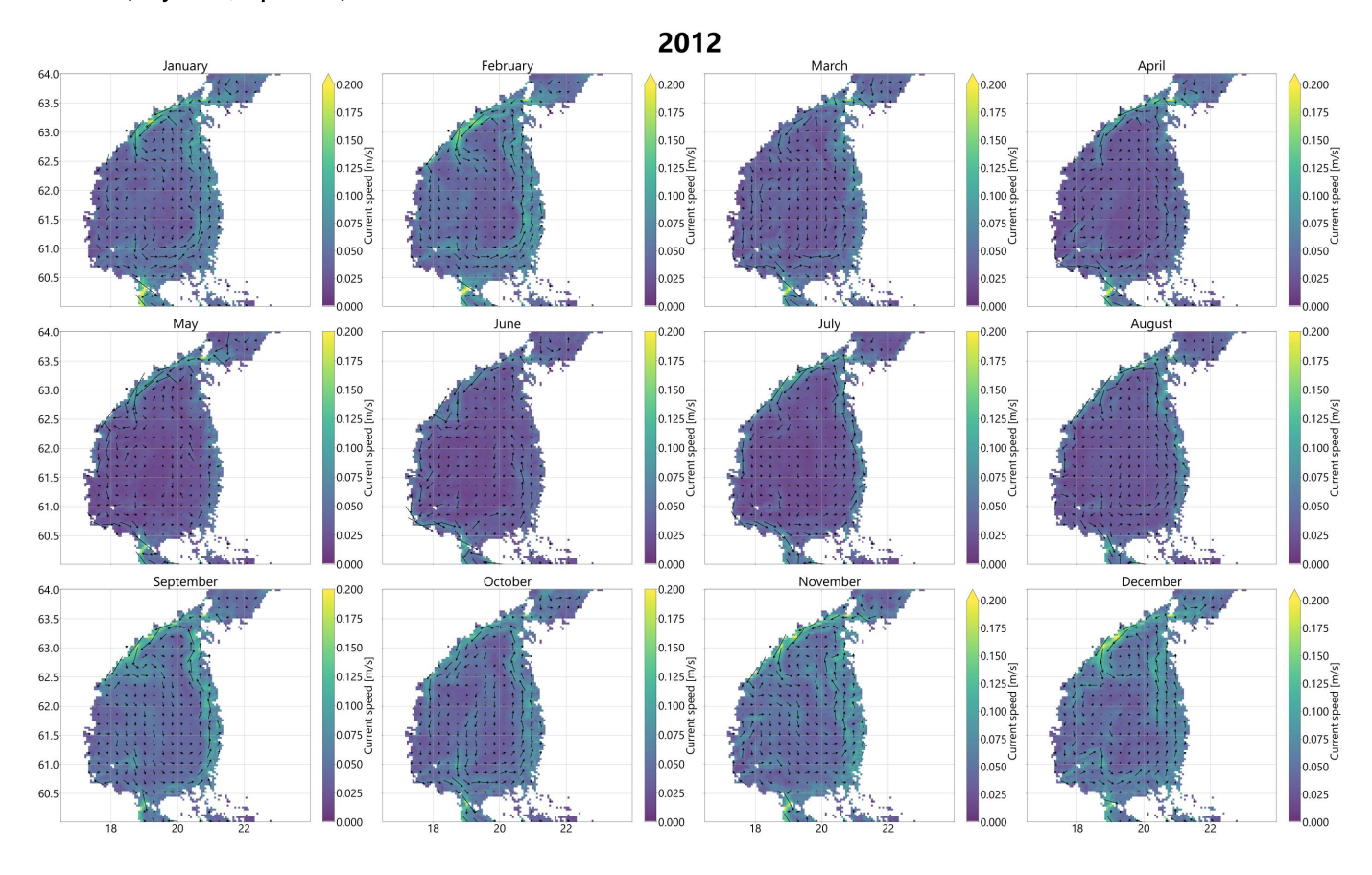


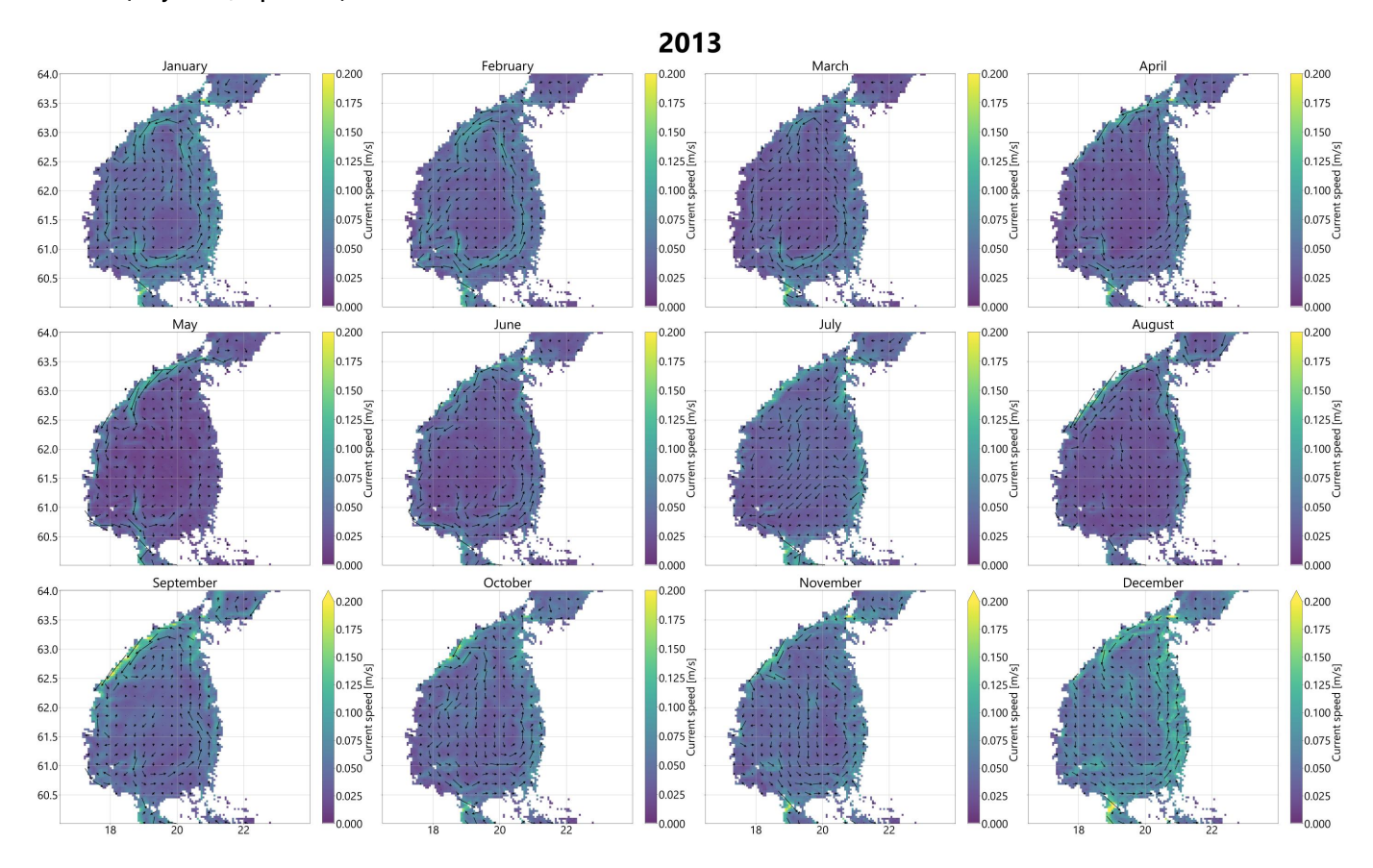
SMHI 2x2 (daily values, depth: 1.5 m)

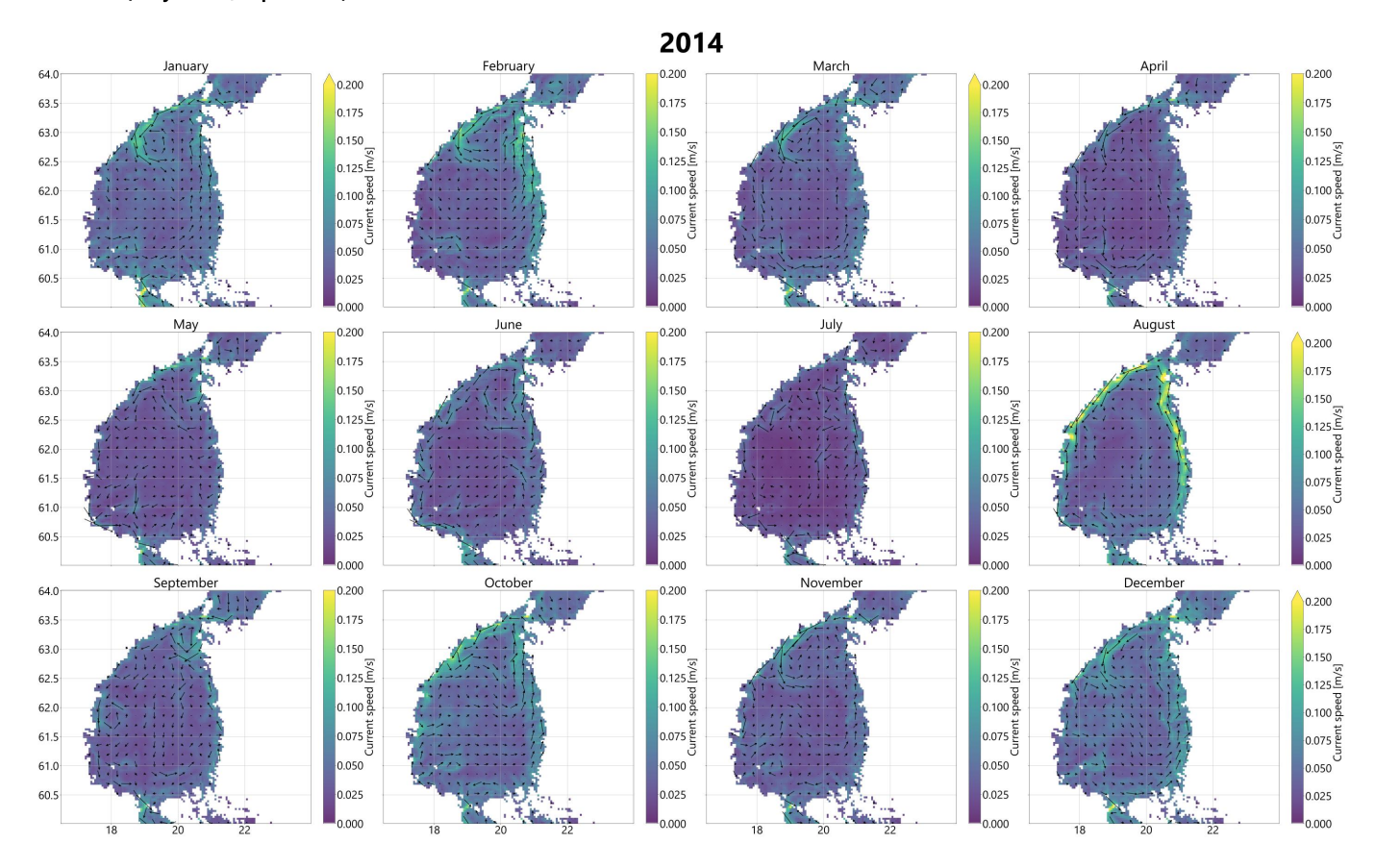


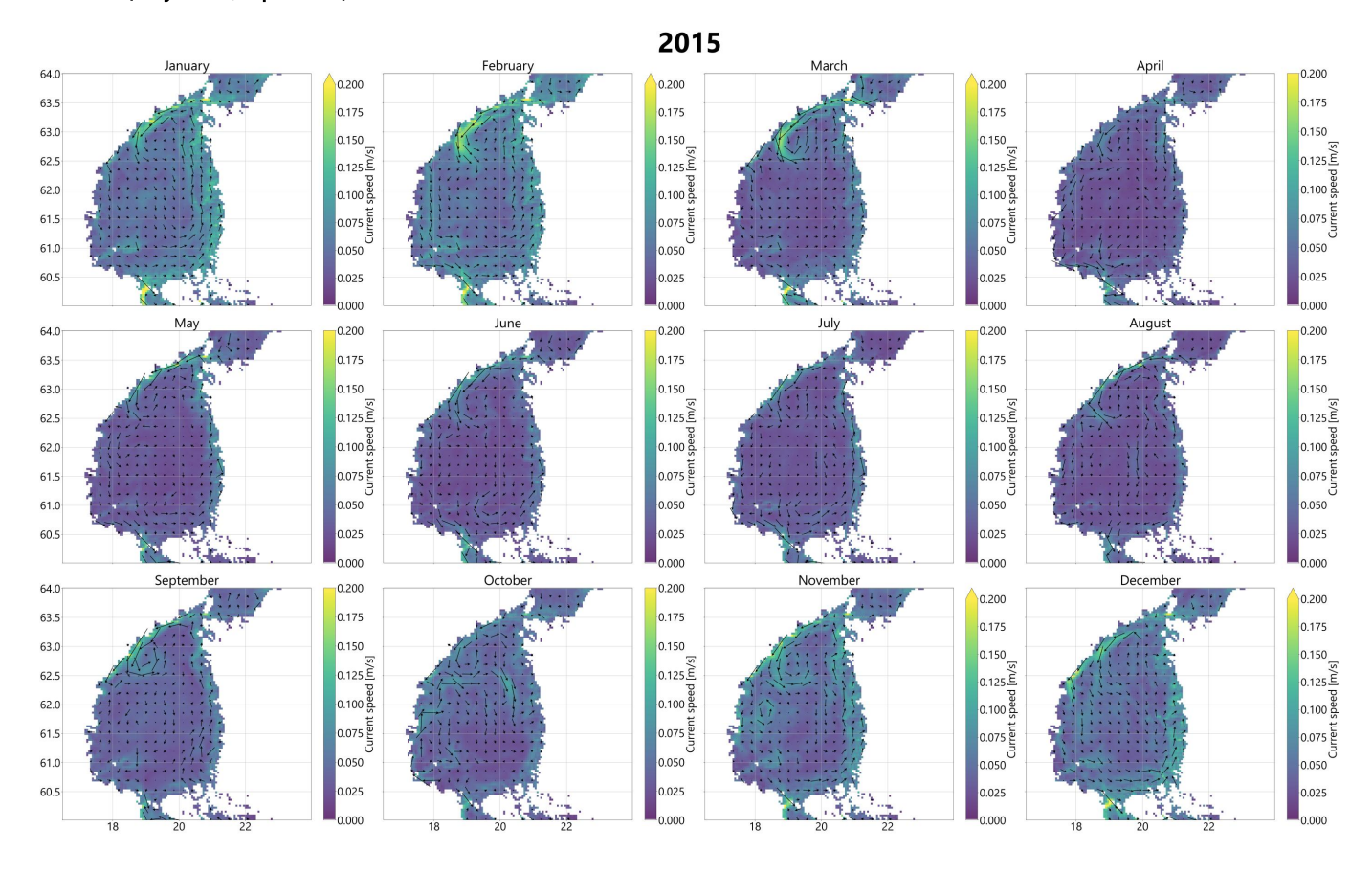


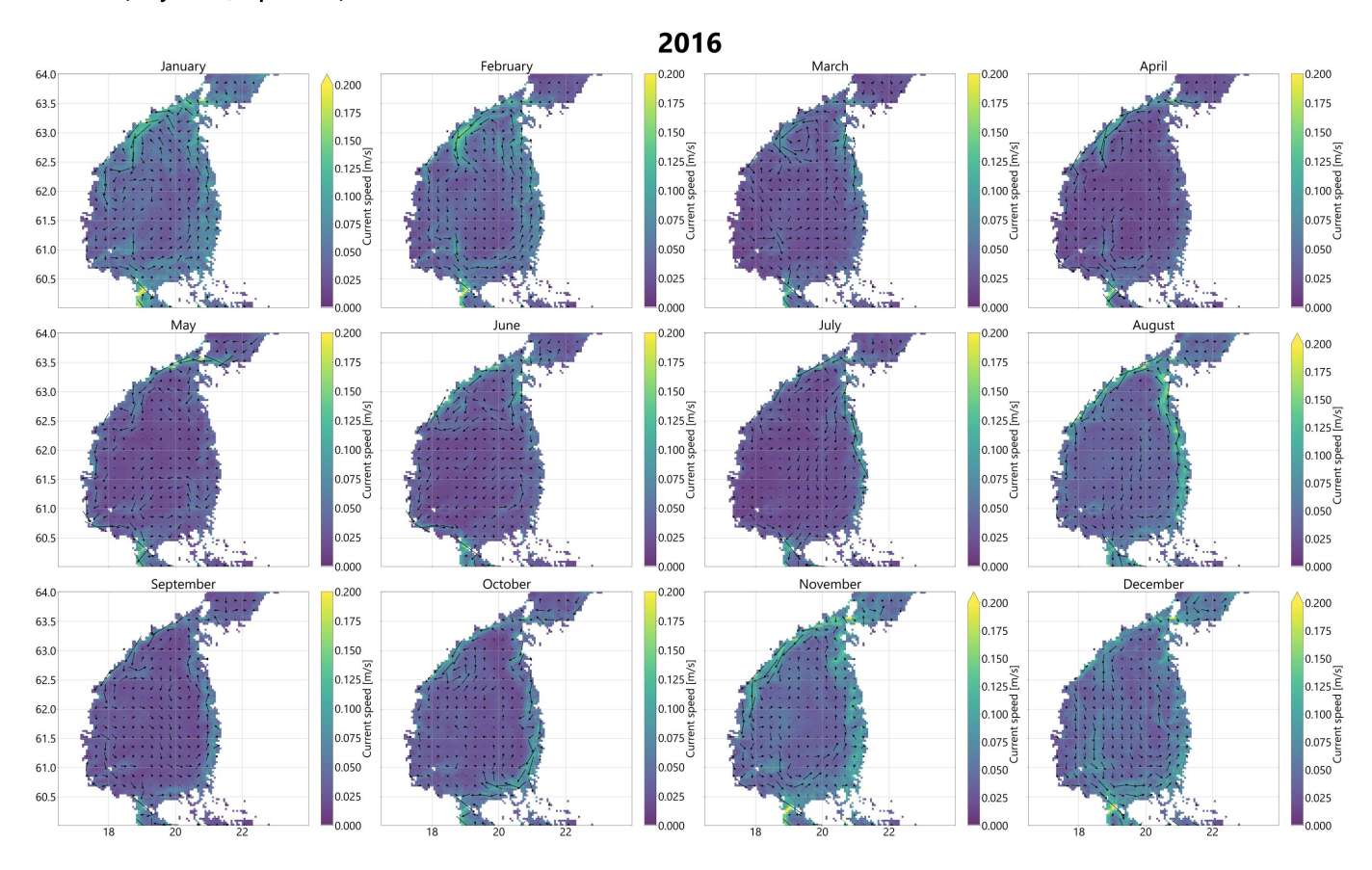


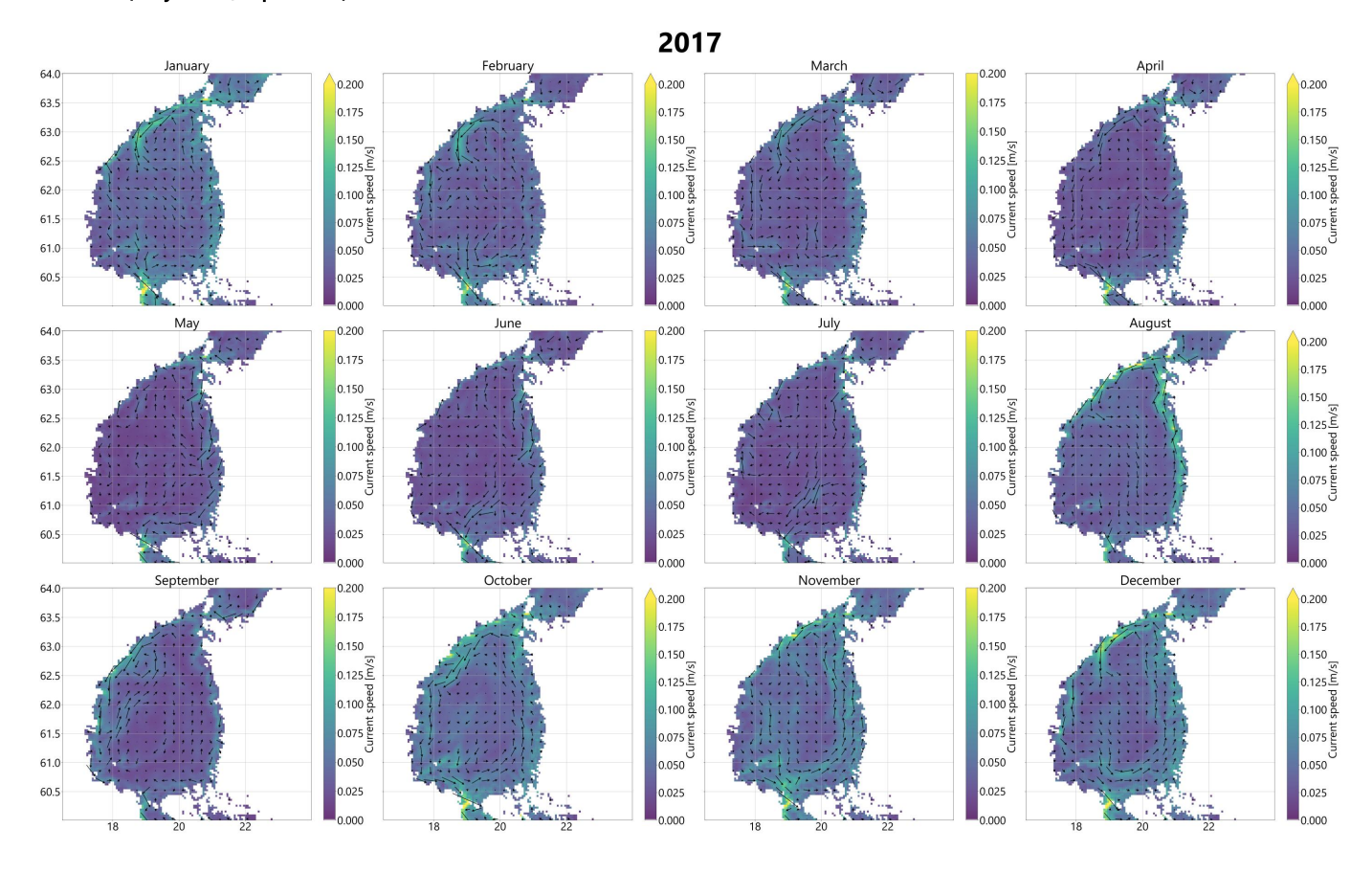


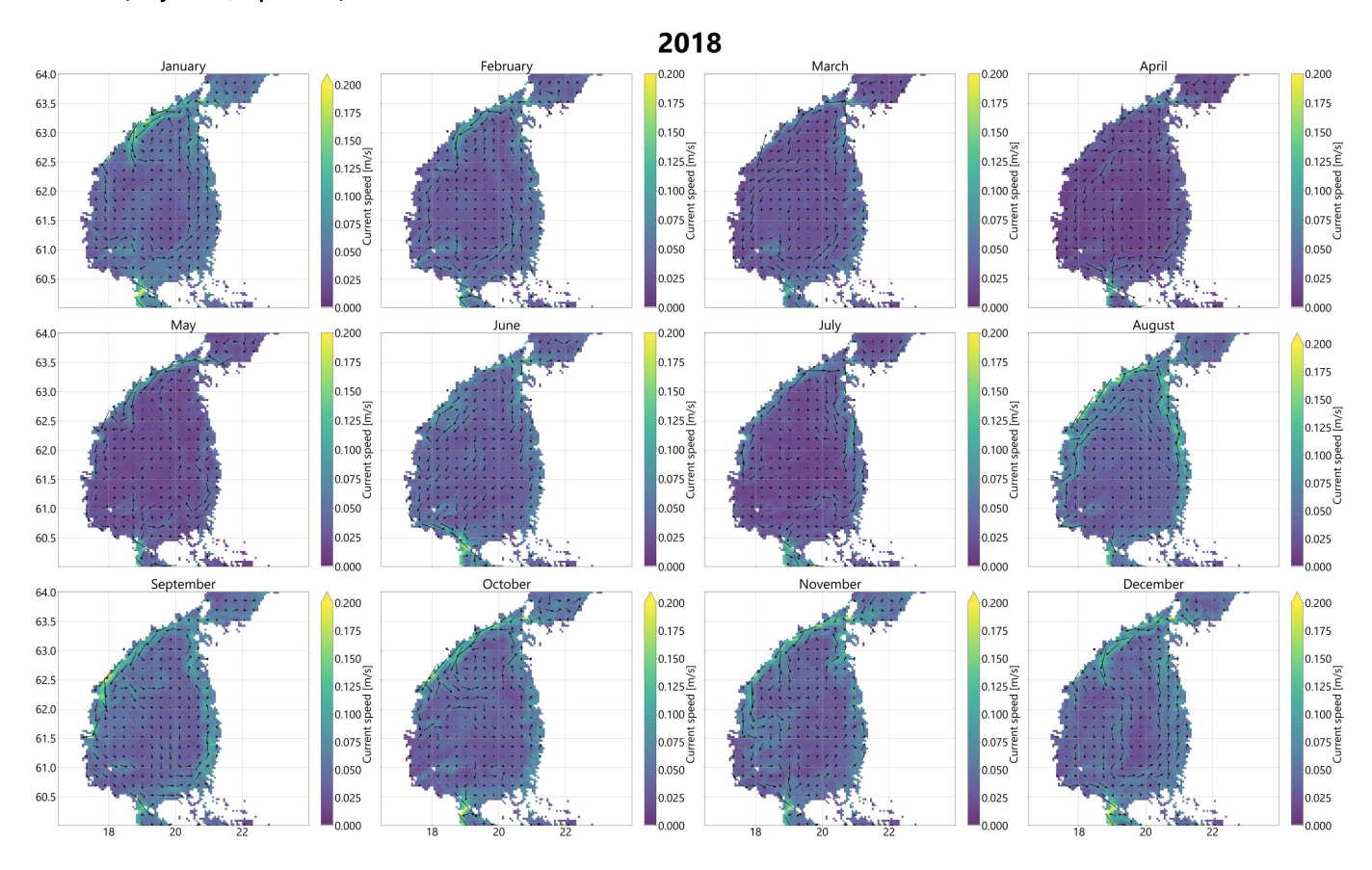


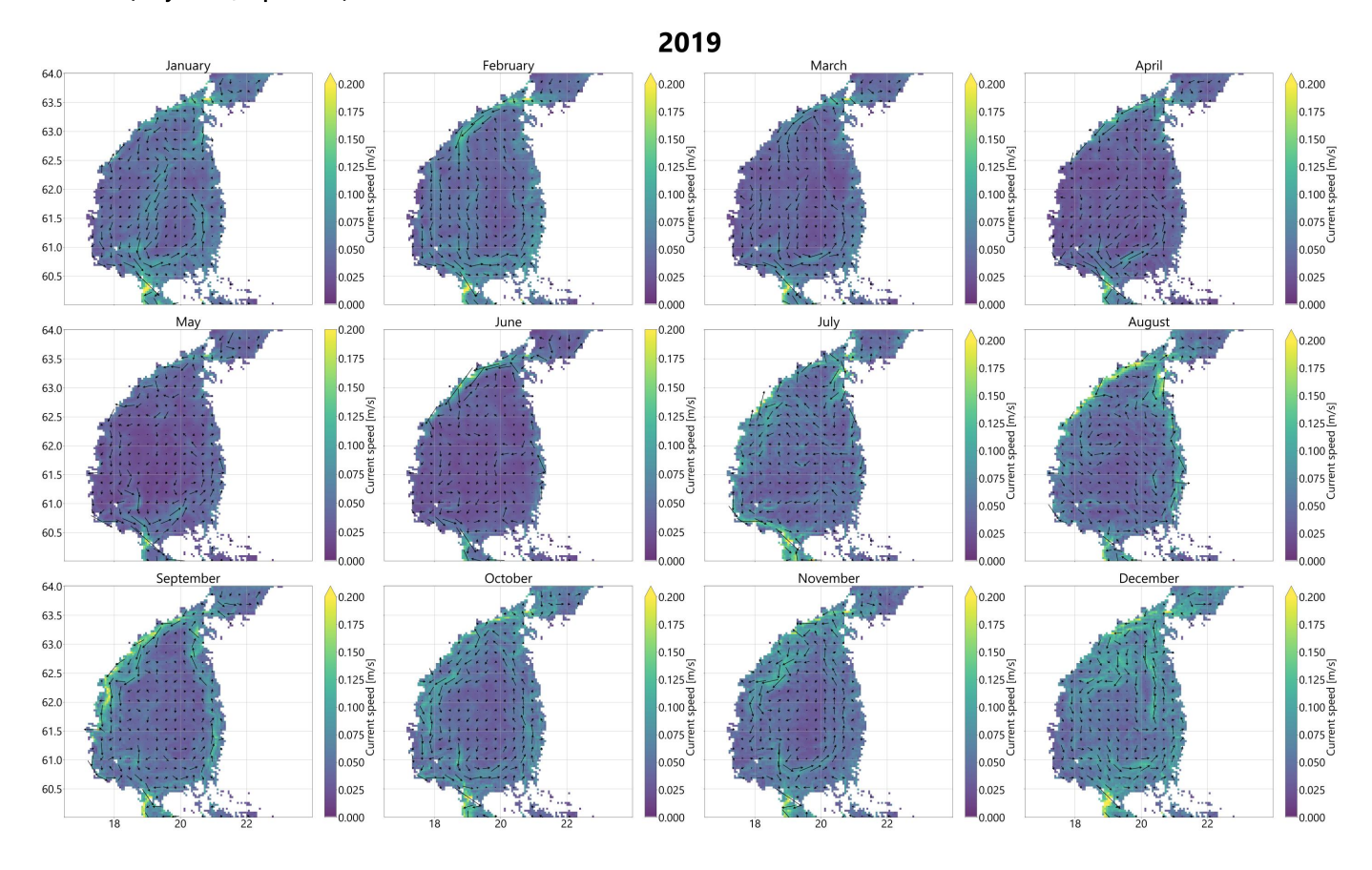


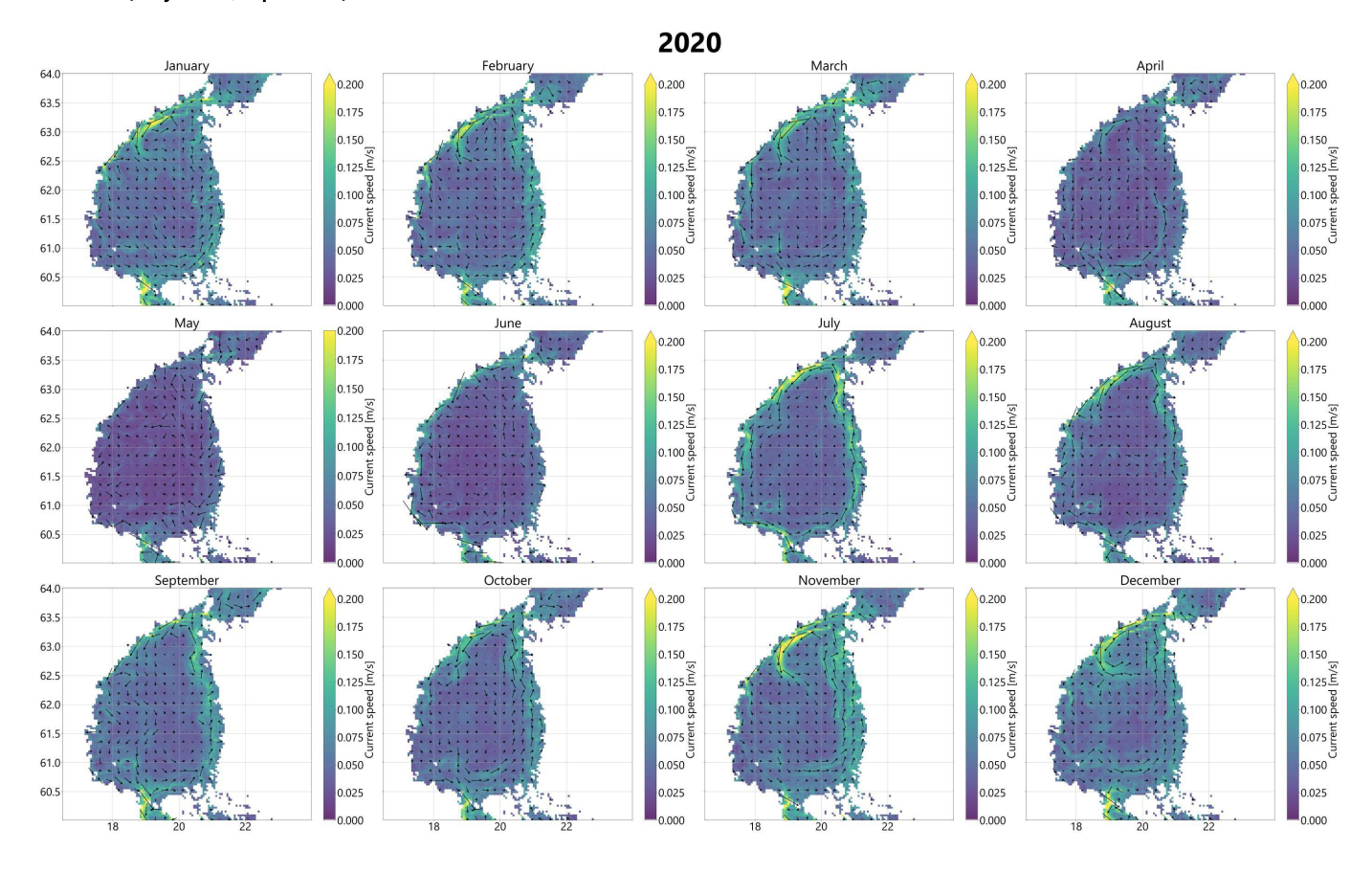


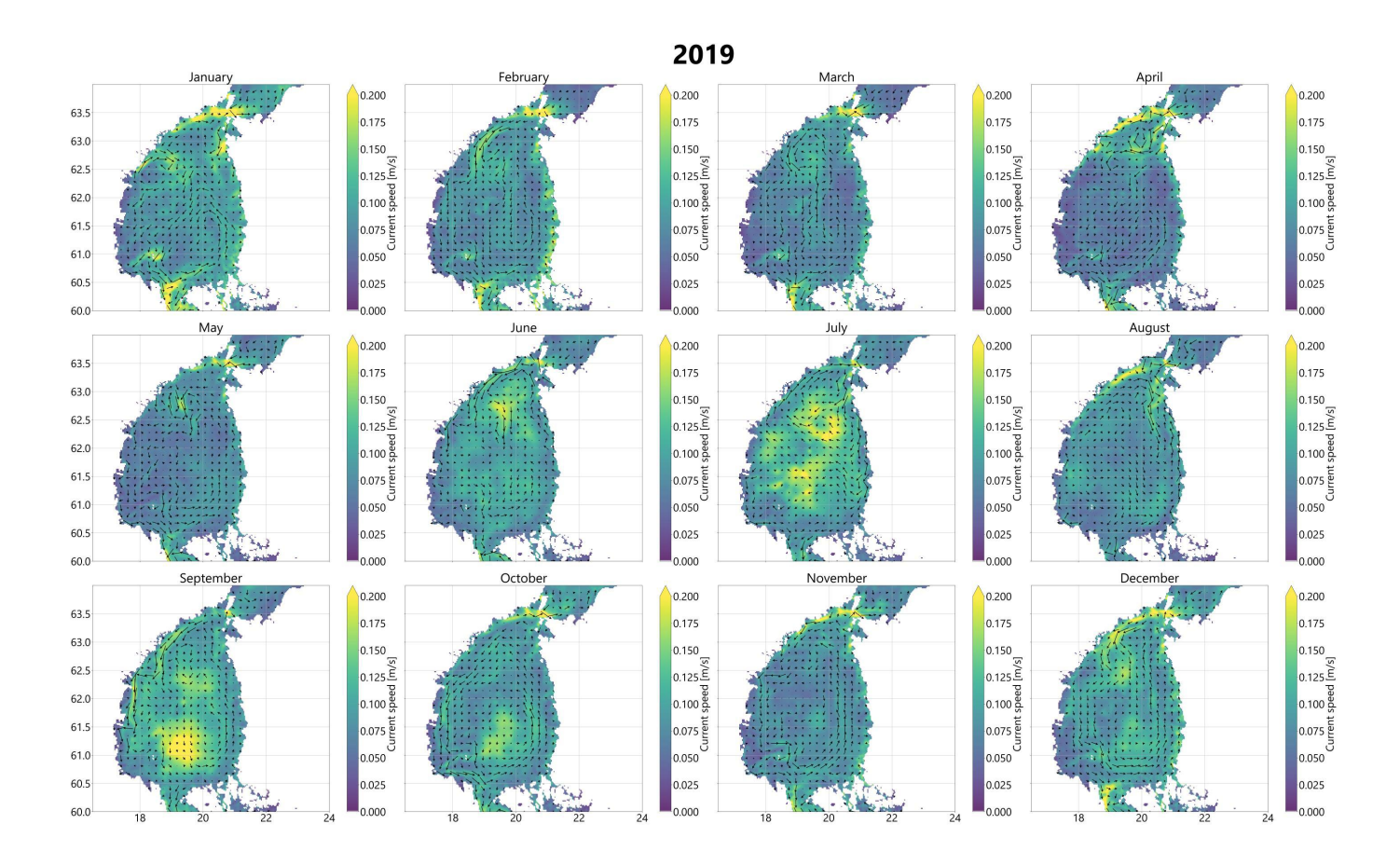


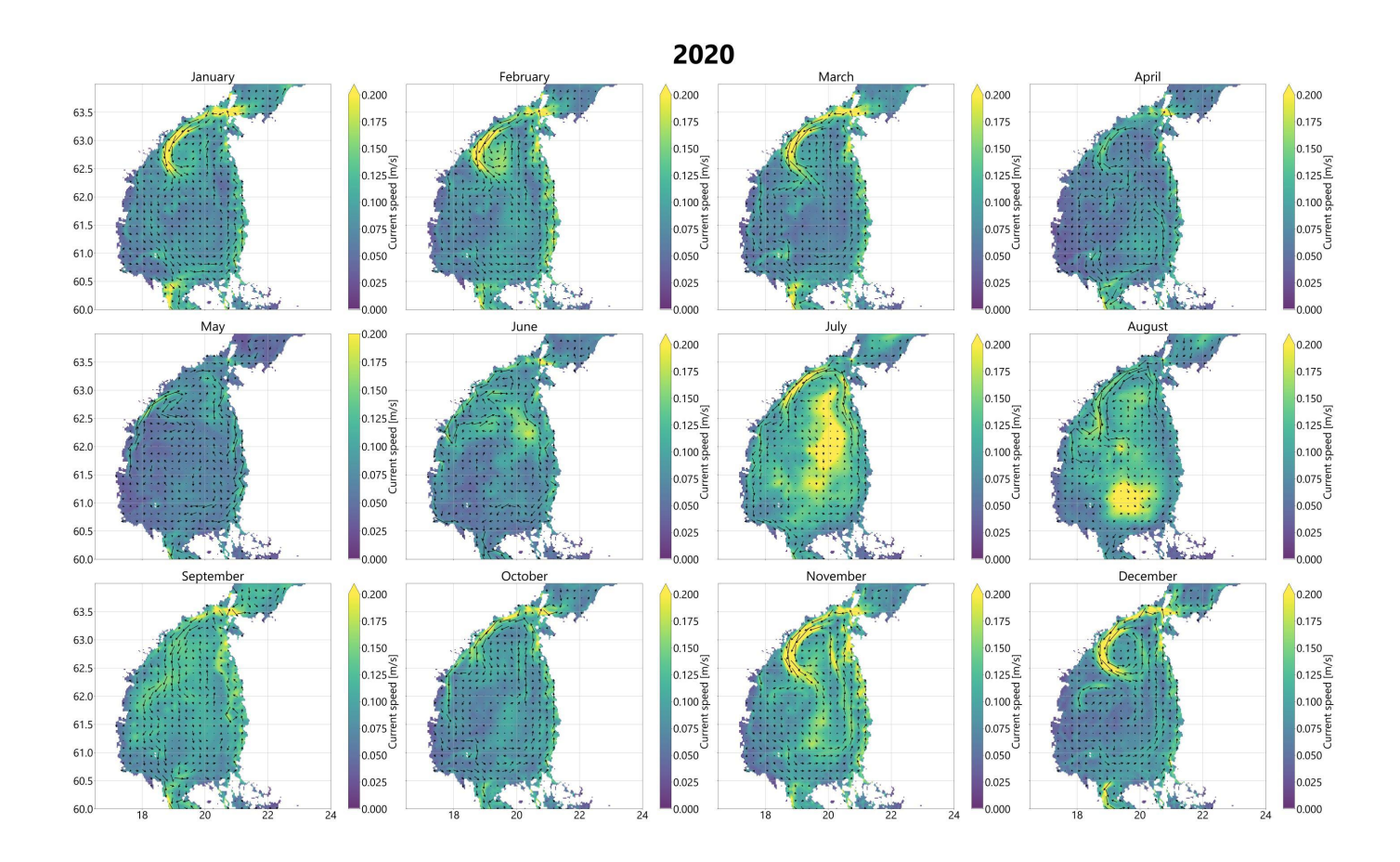




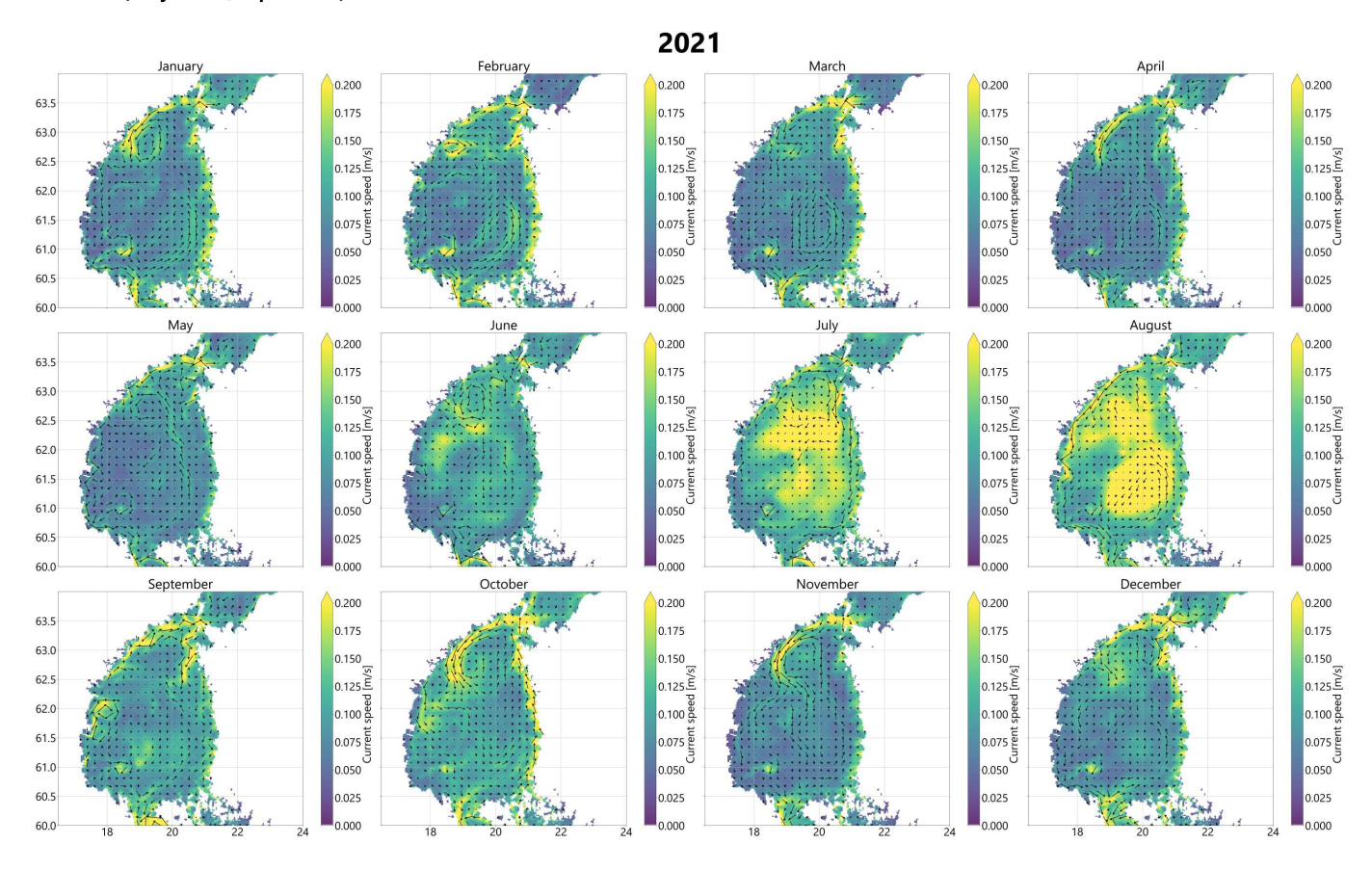




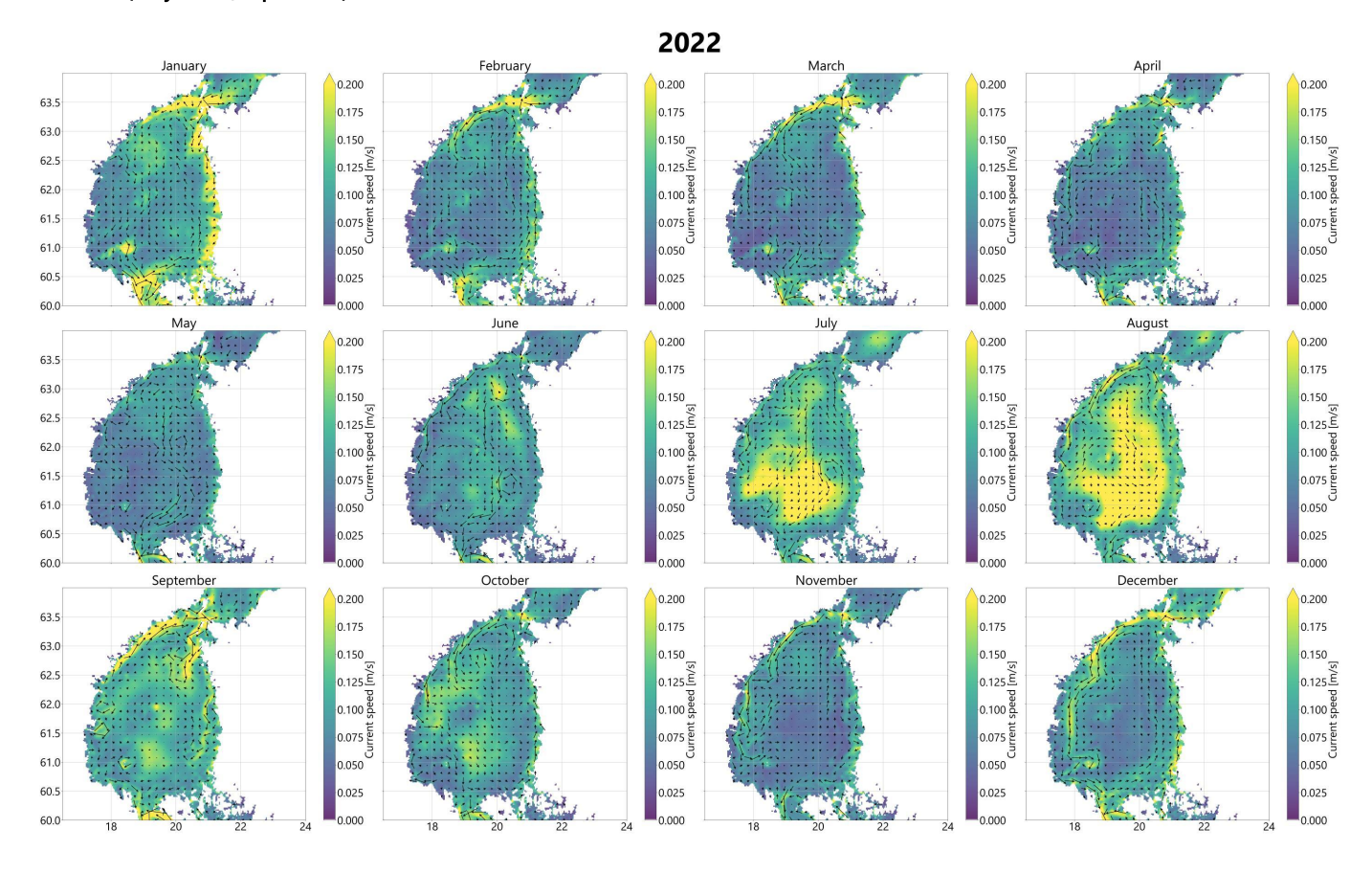


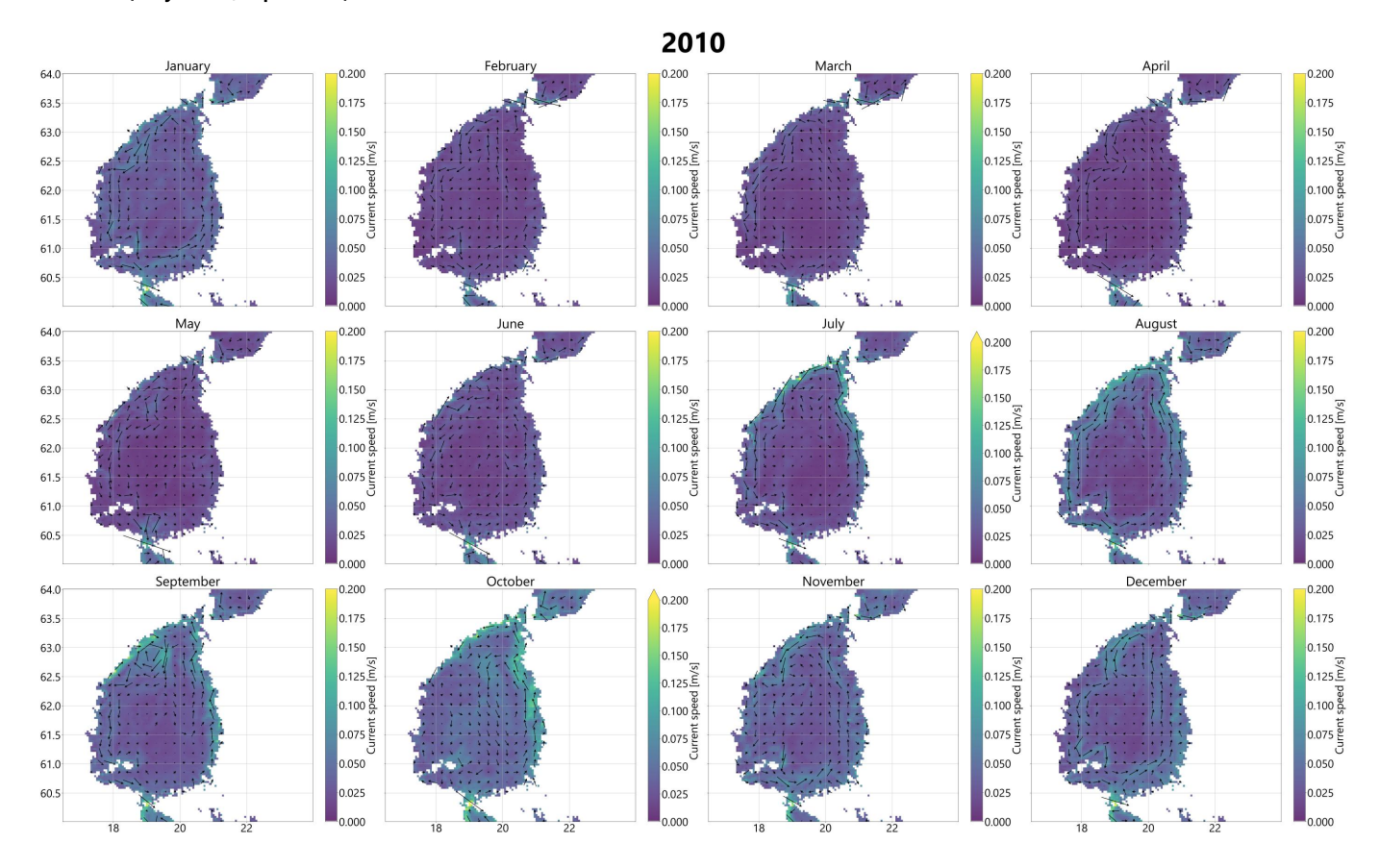


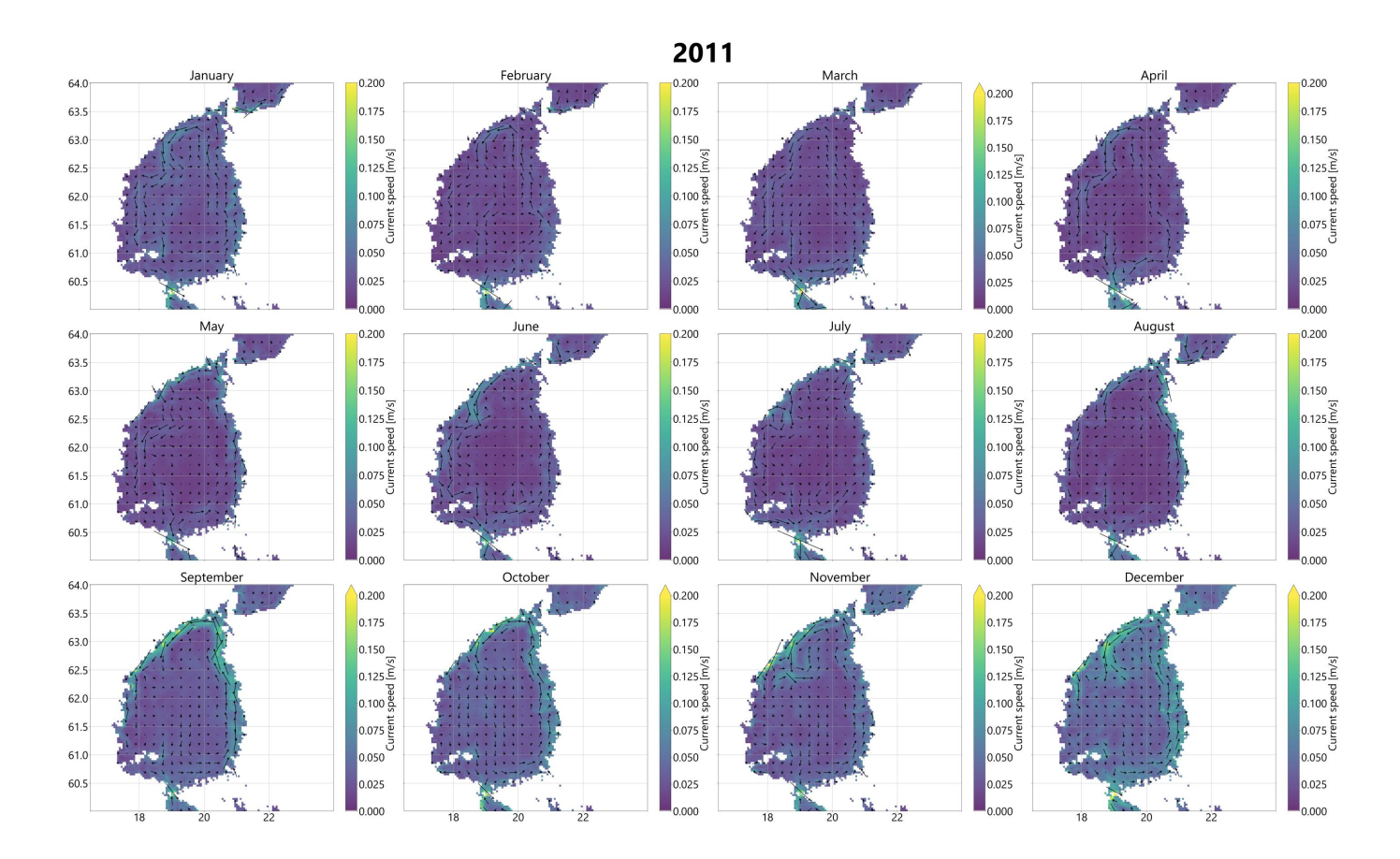
SMHI 2x2 (daily values, depth: 10 m)

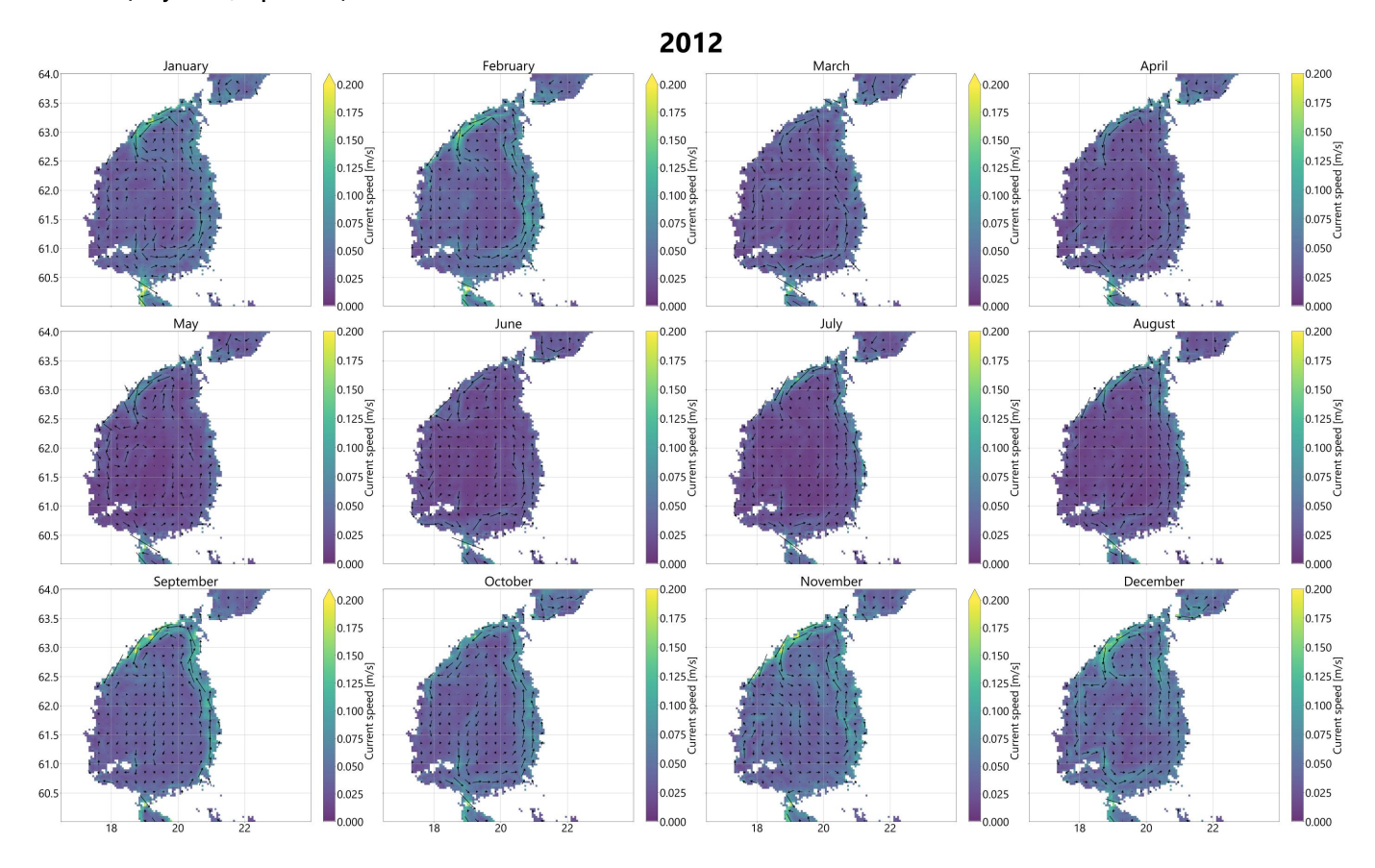


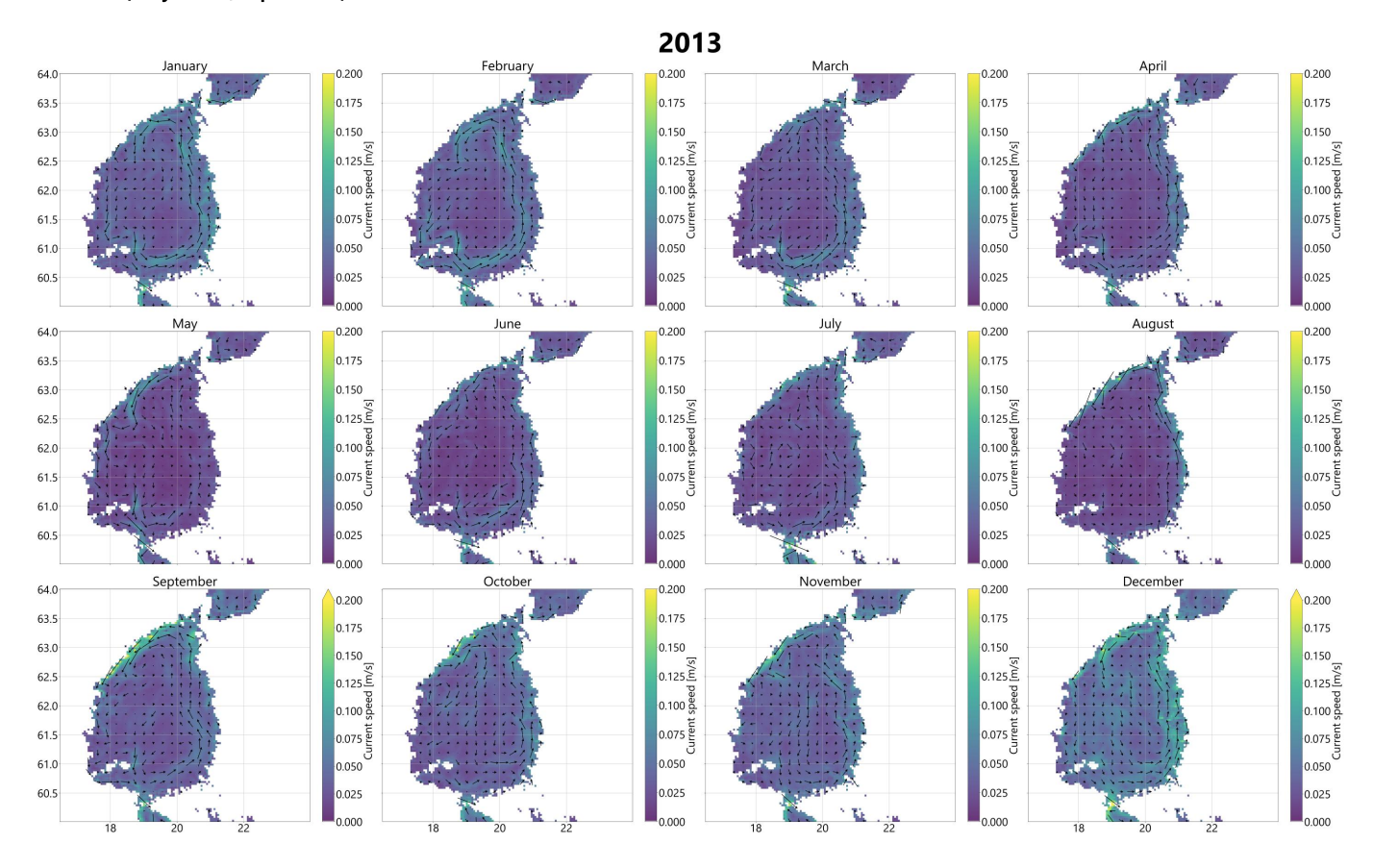
SMHI 2x2 (daily values, depth: 10 m)

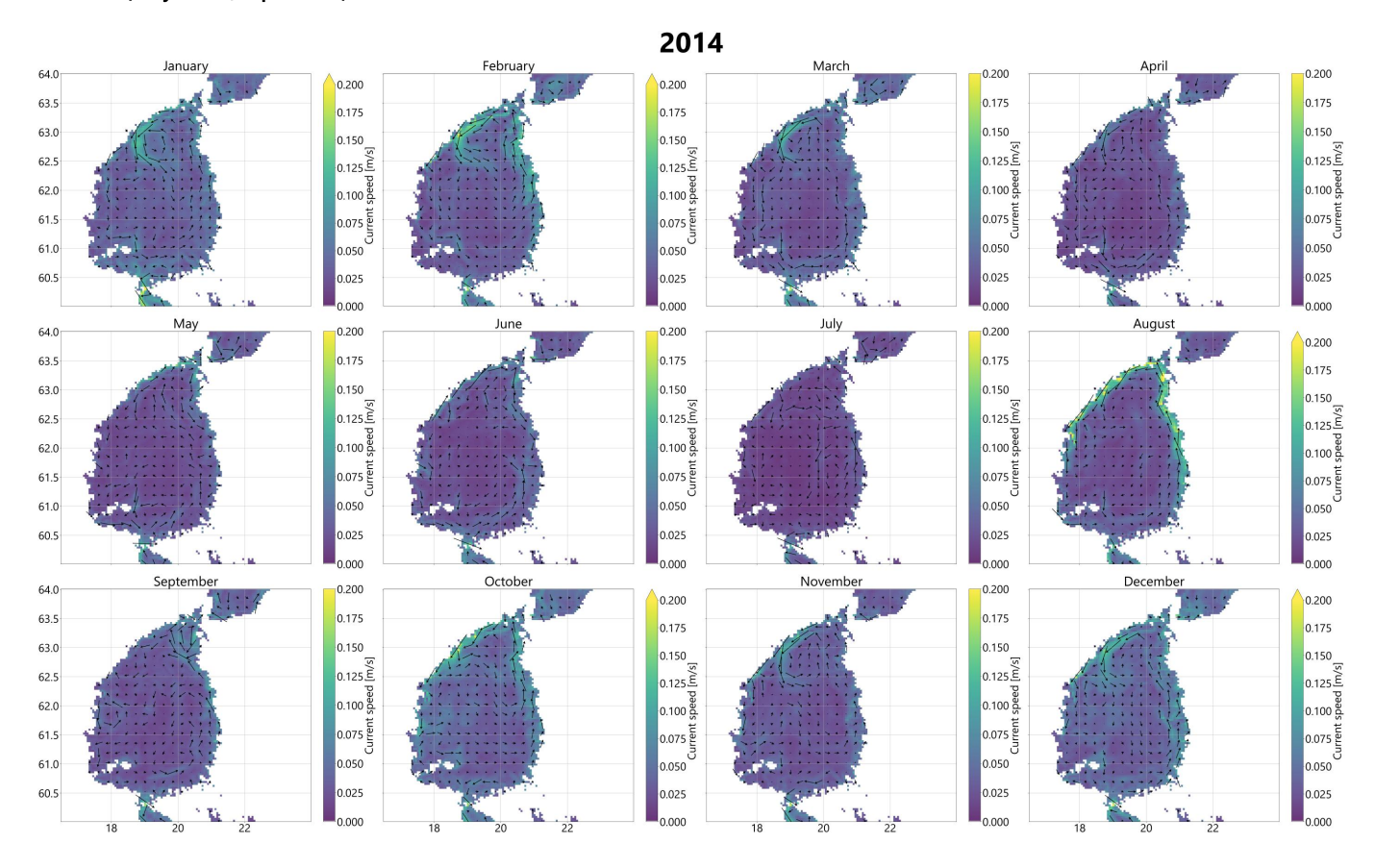


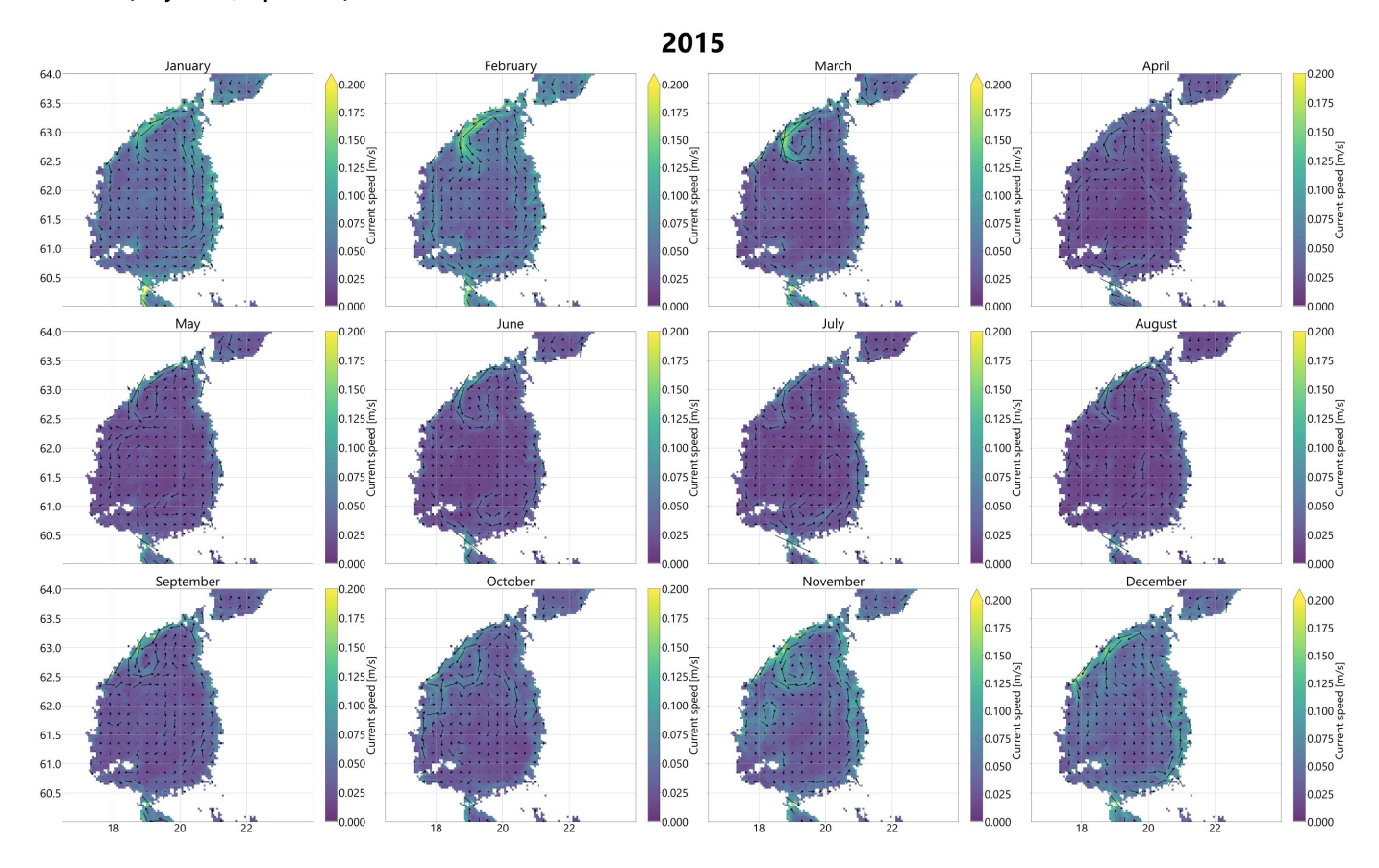


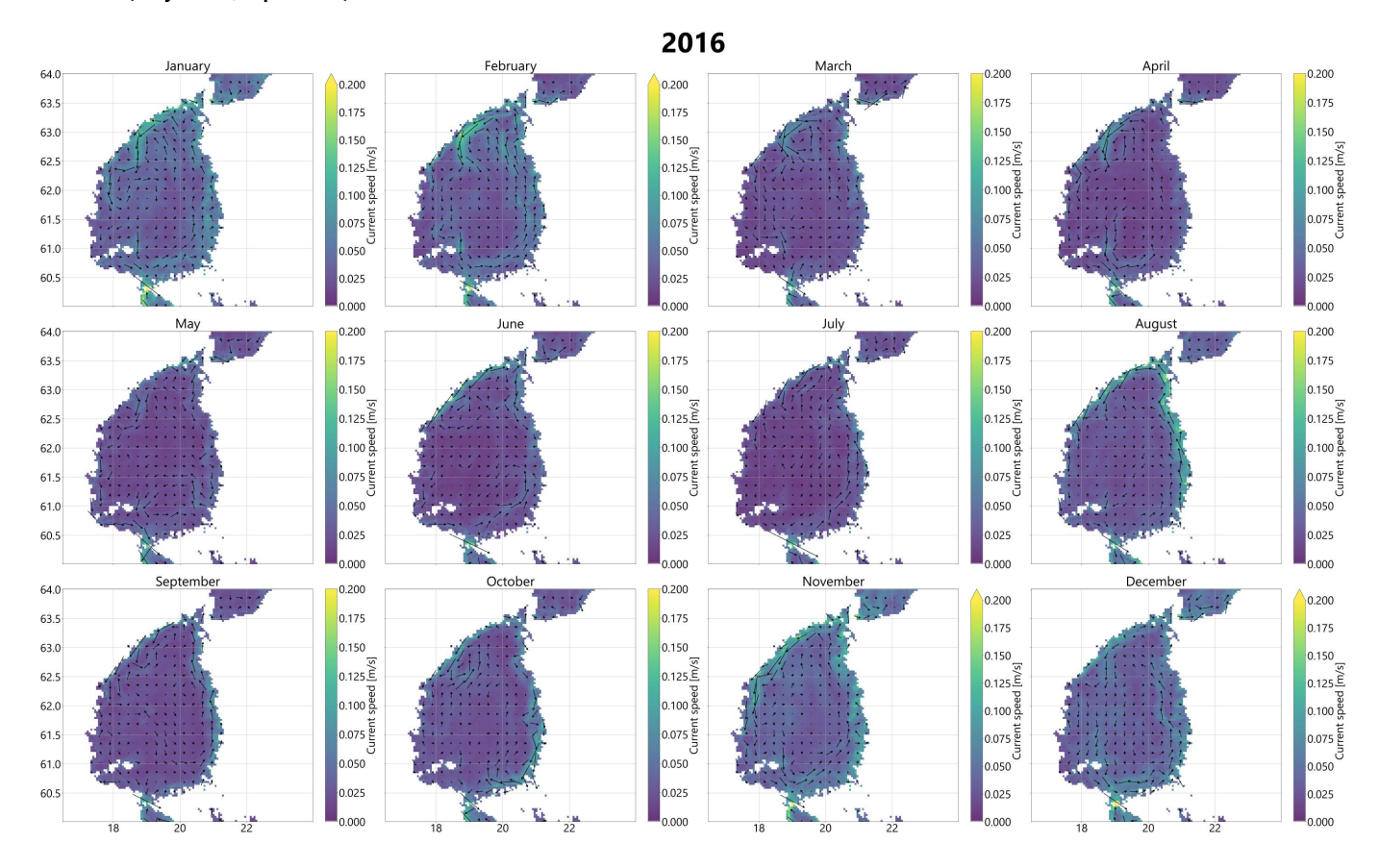


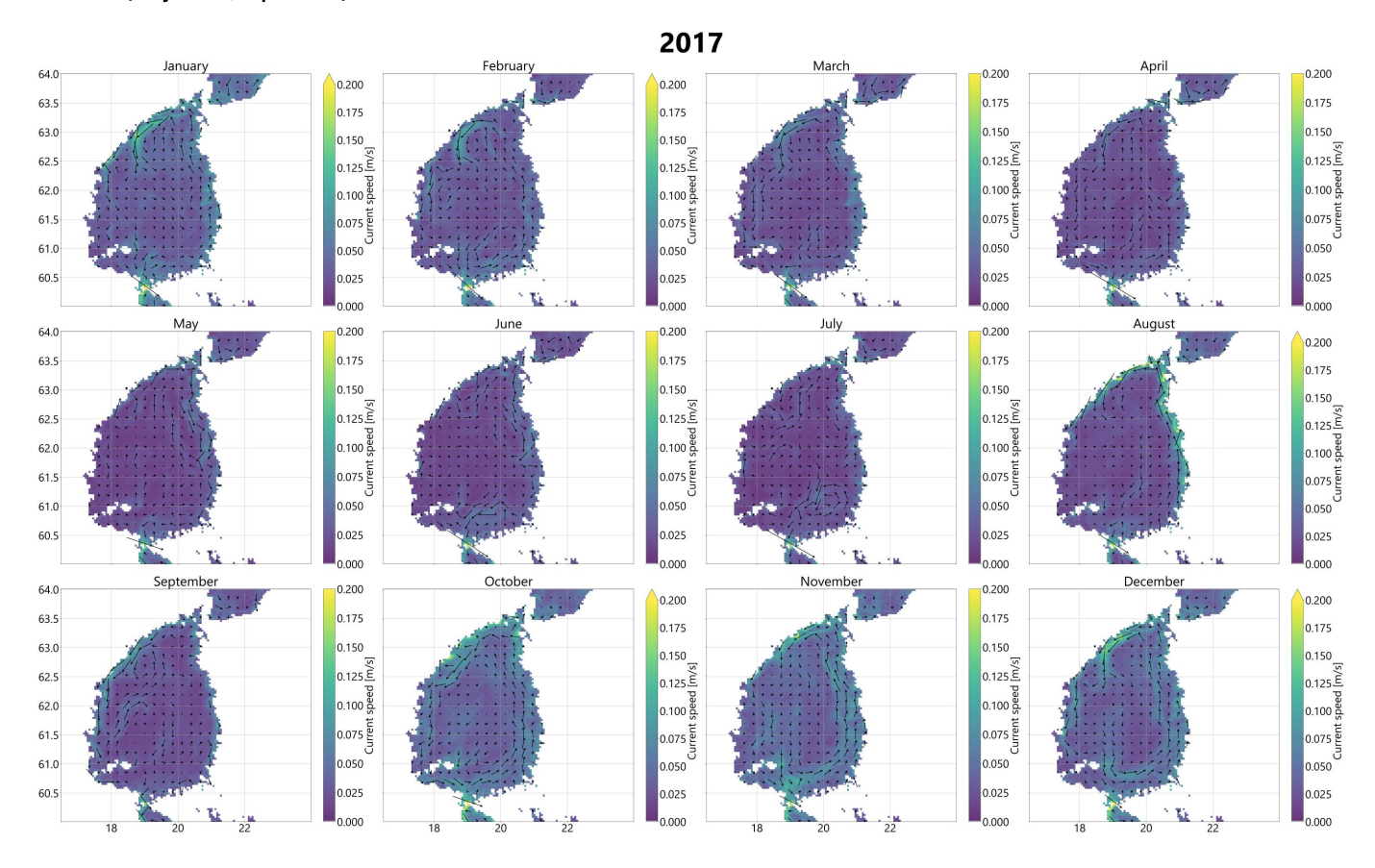


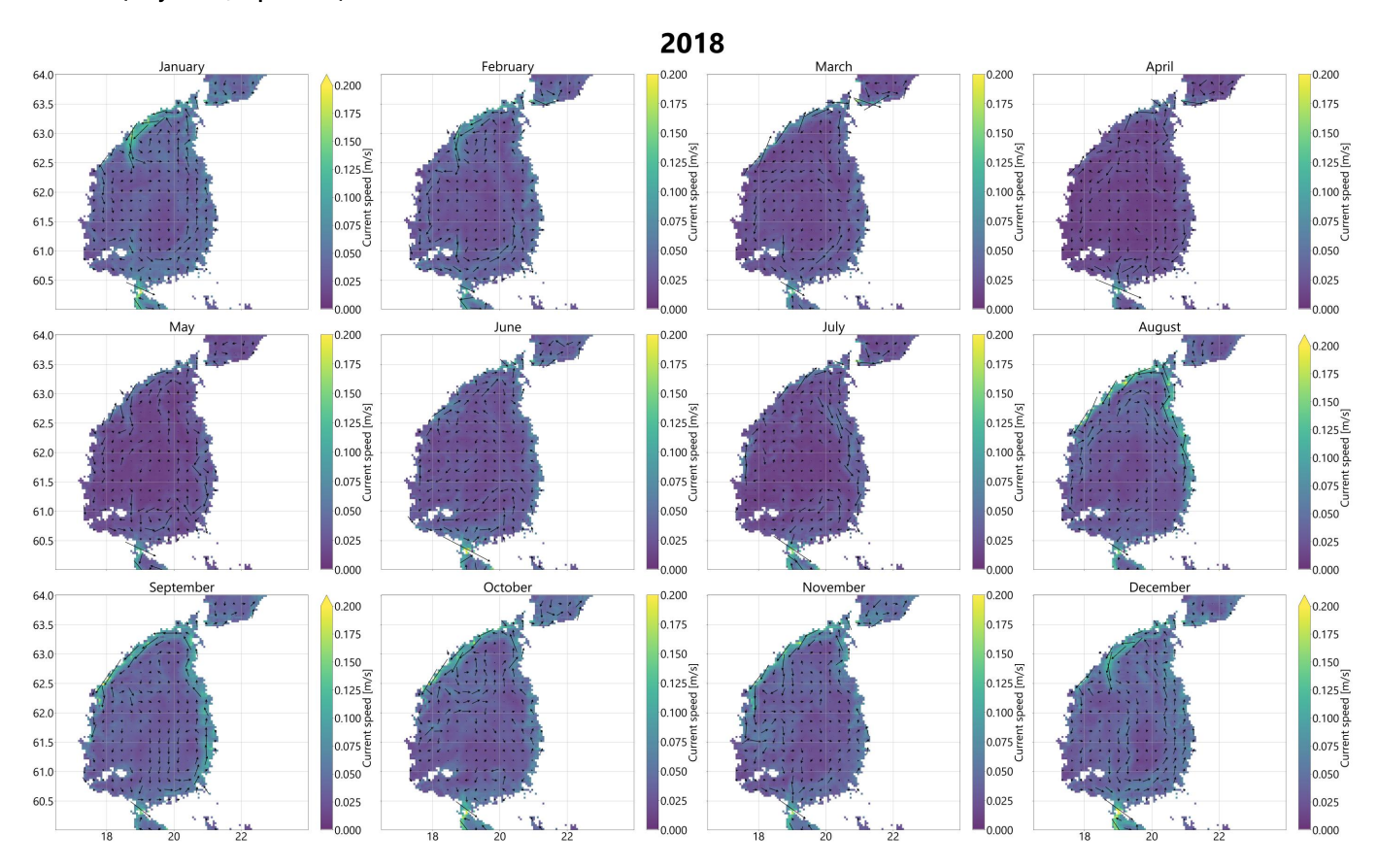


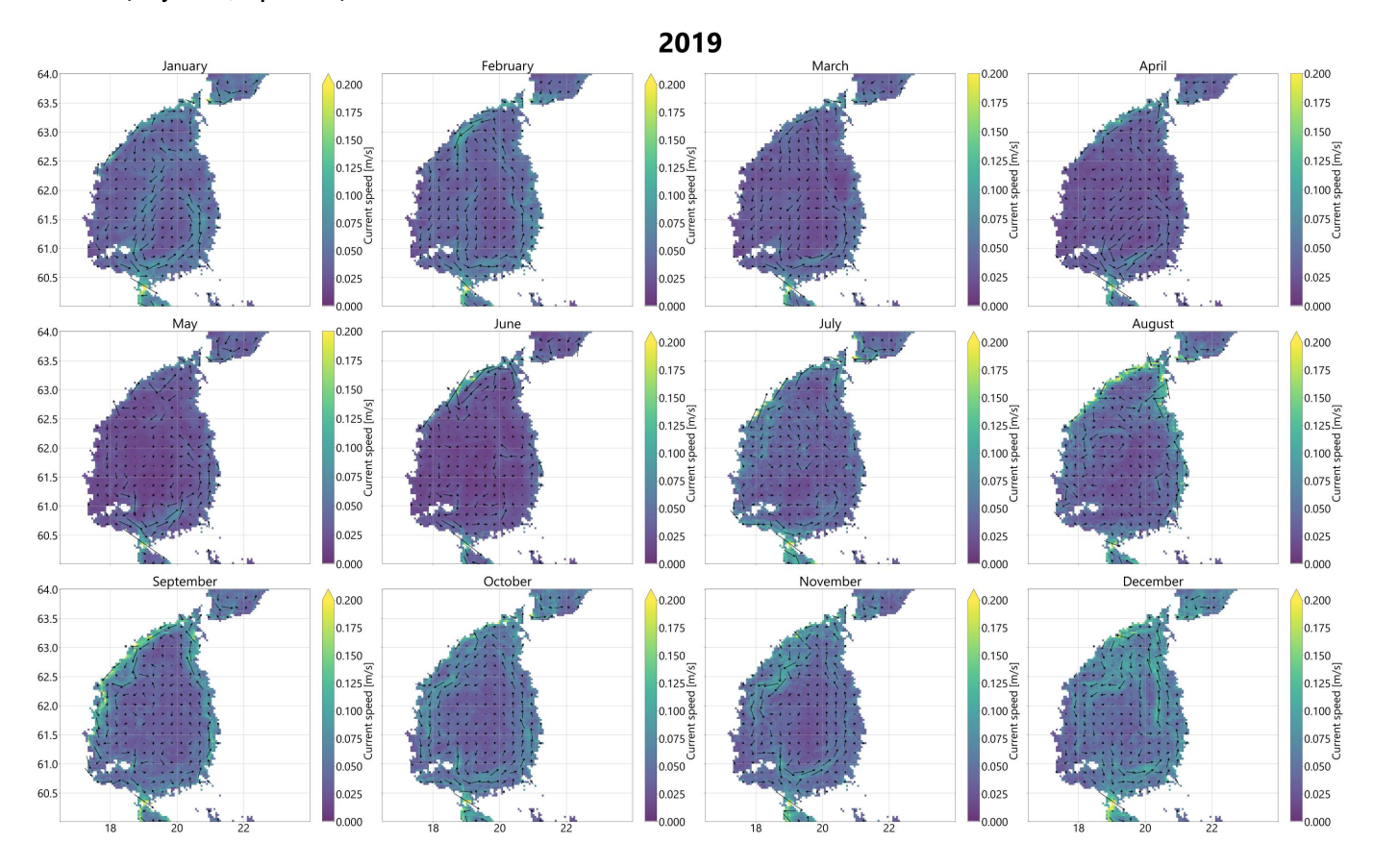


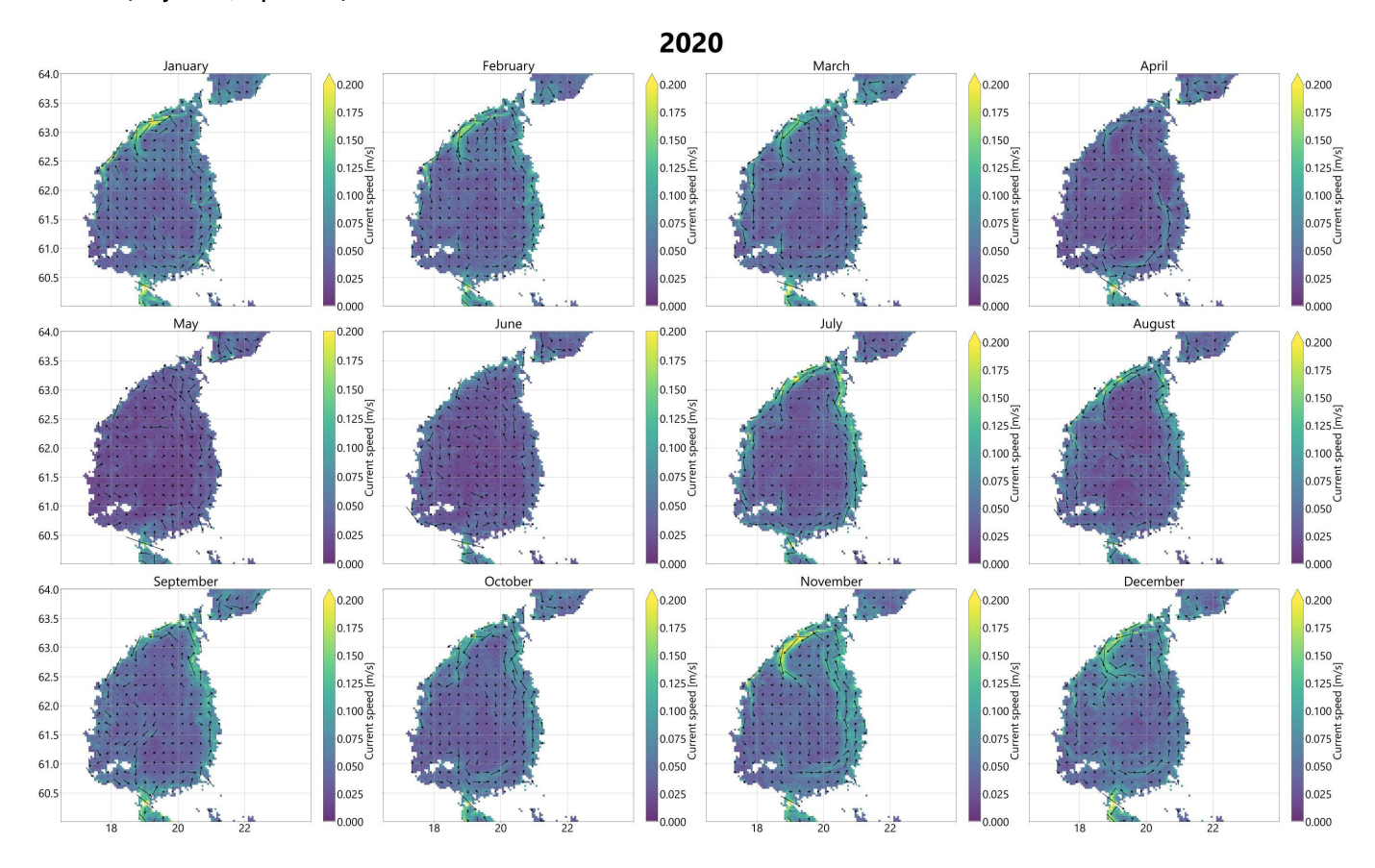




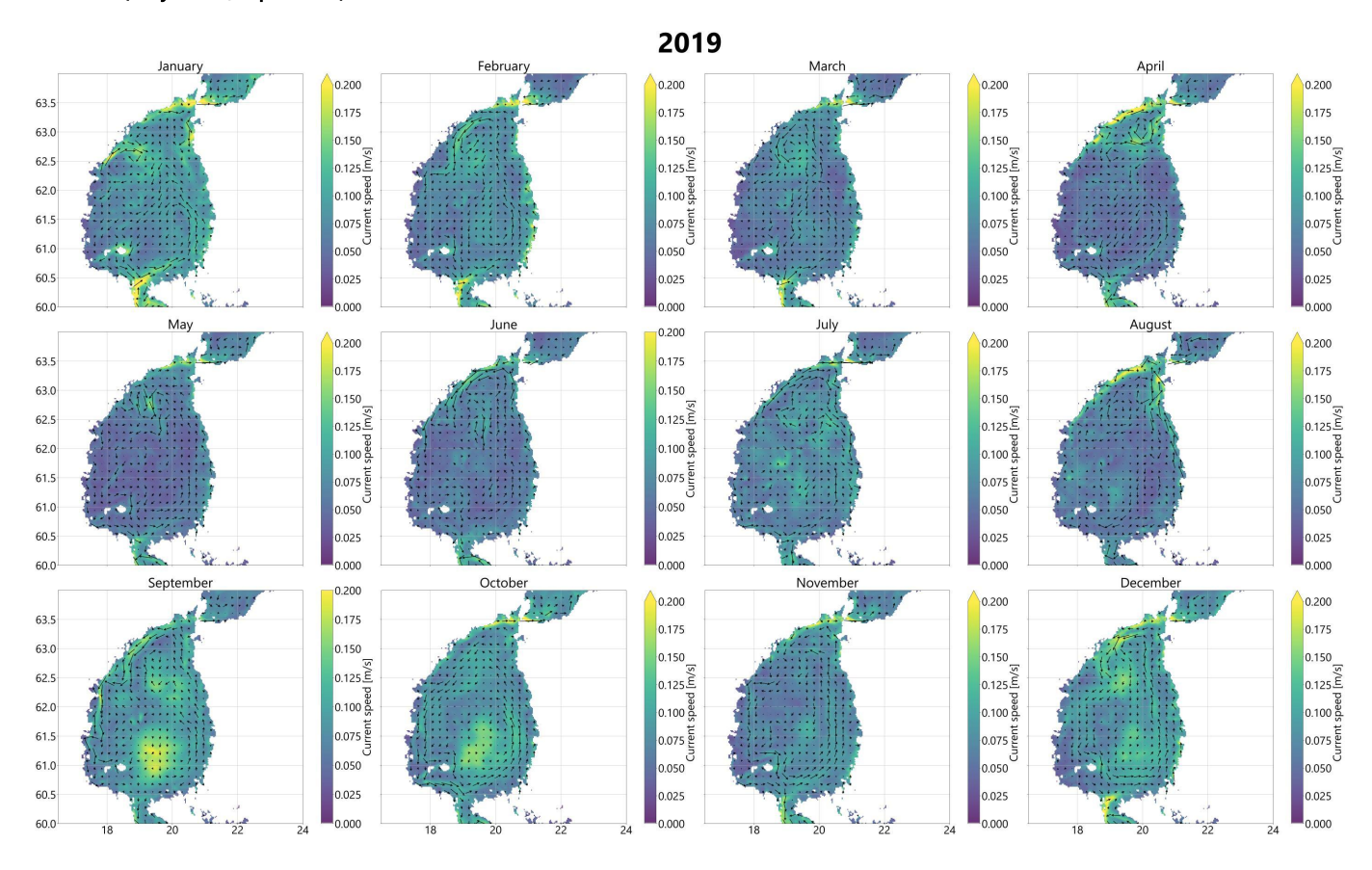


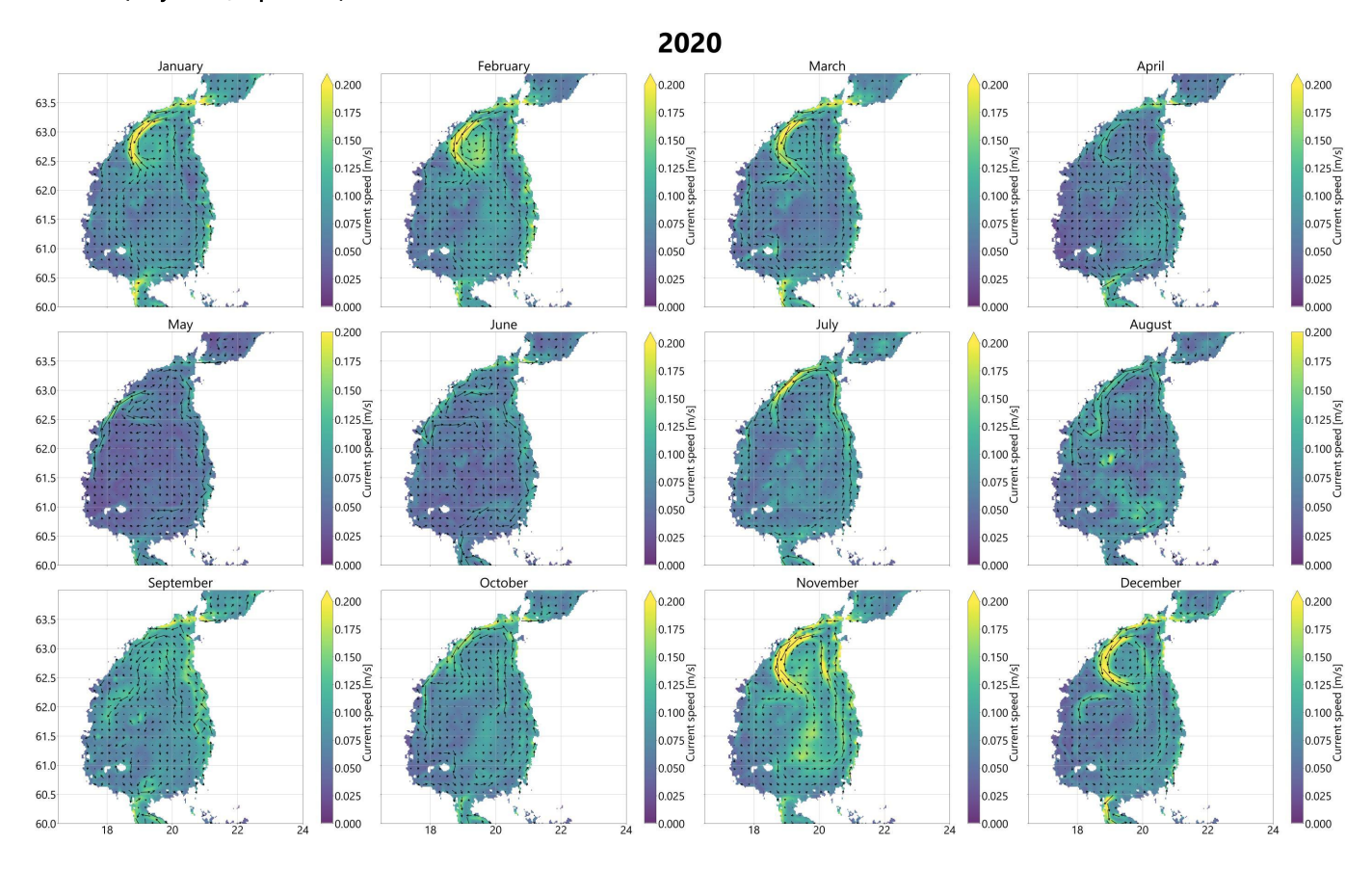




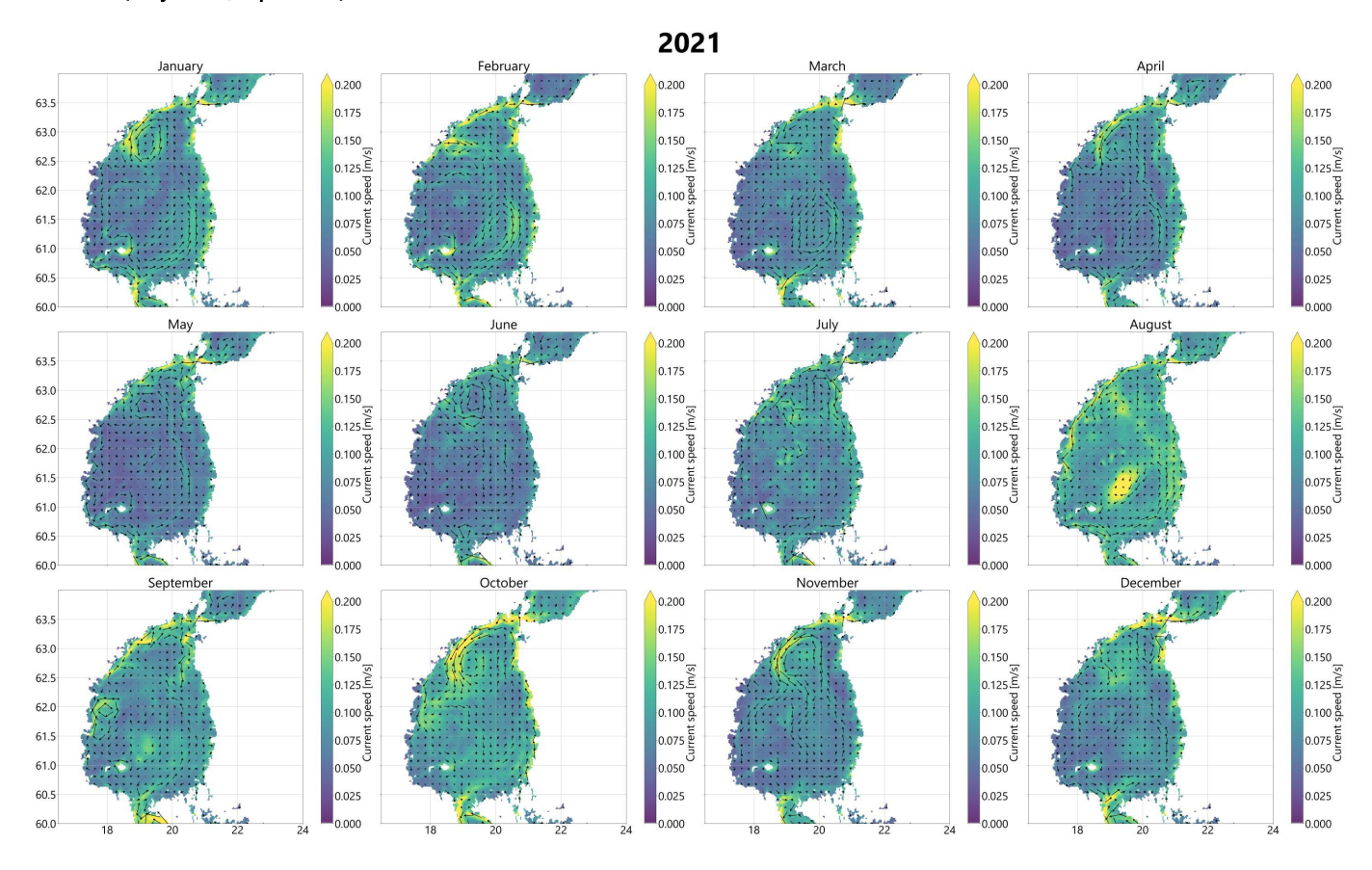


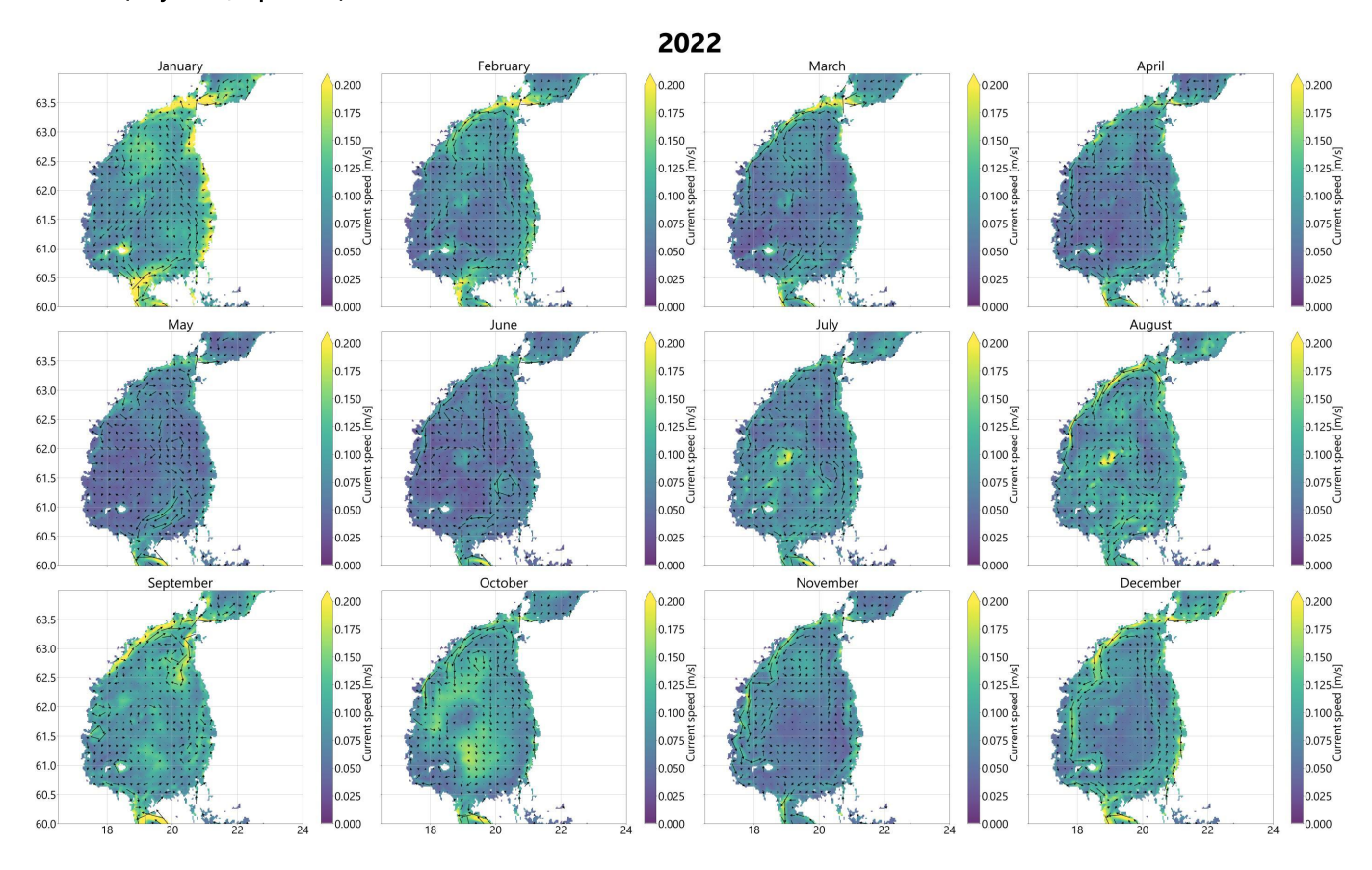
SMHI 2x2 (daily values, depth: 20 m)





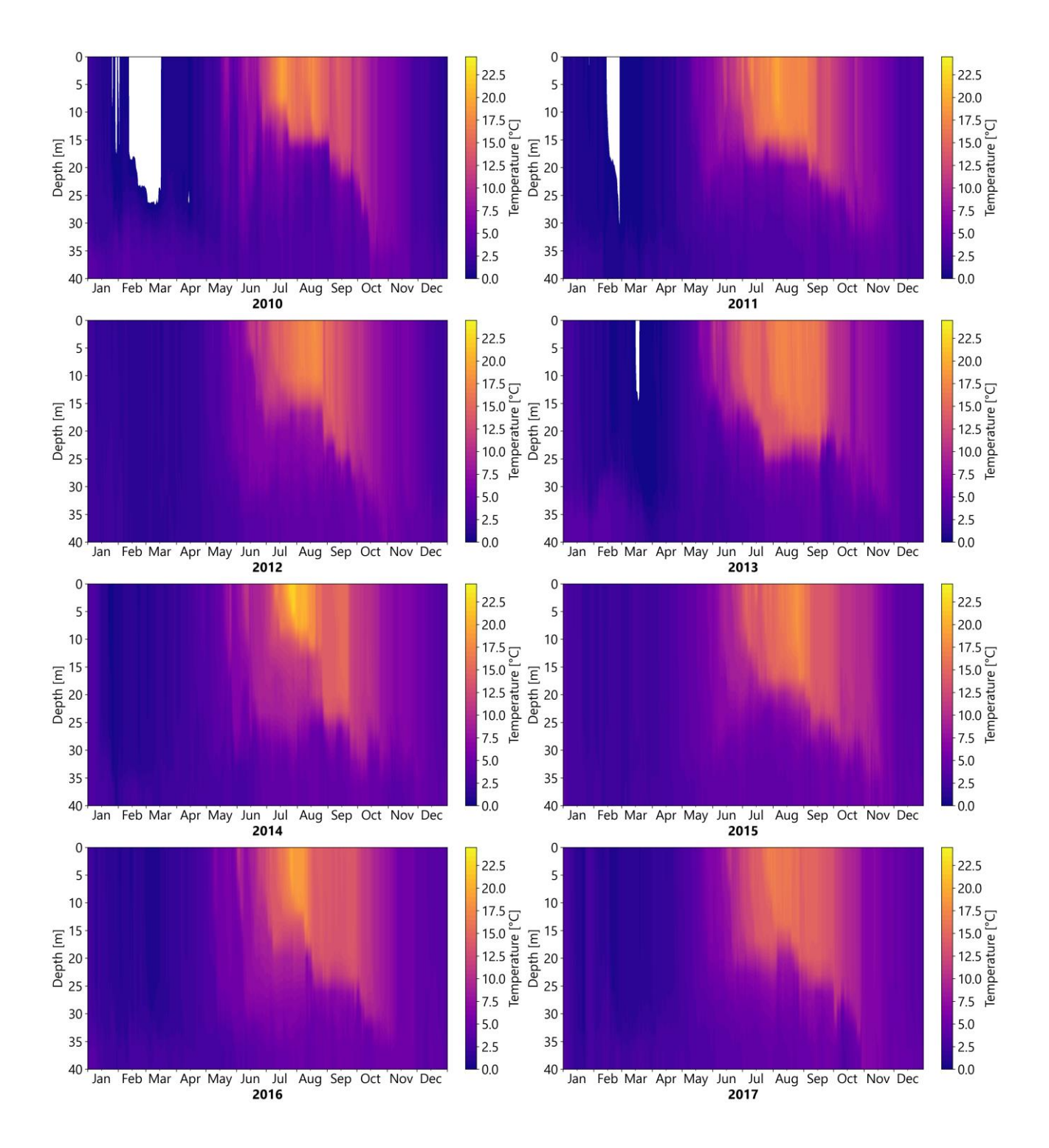
SMHI 2x2 (daily values, depth: 20 m)

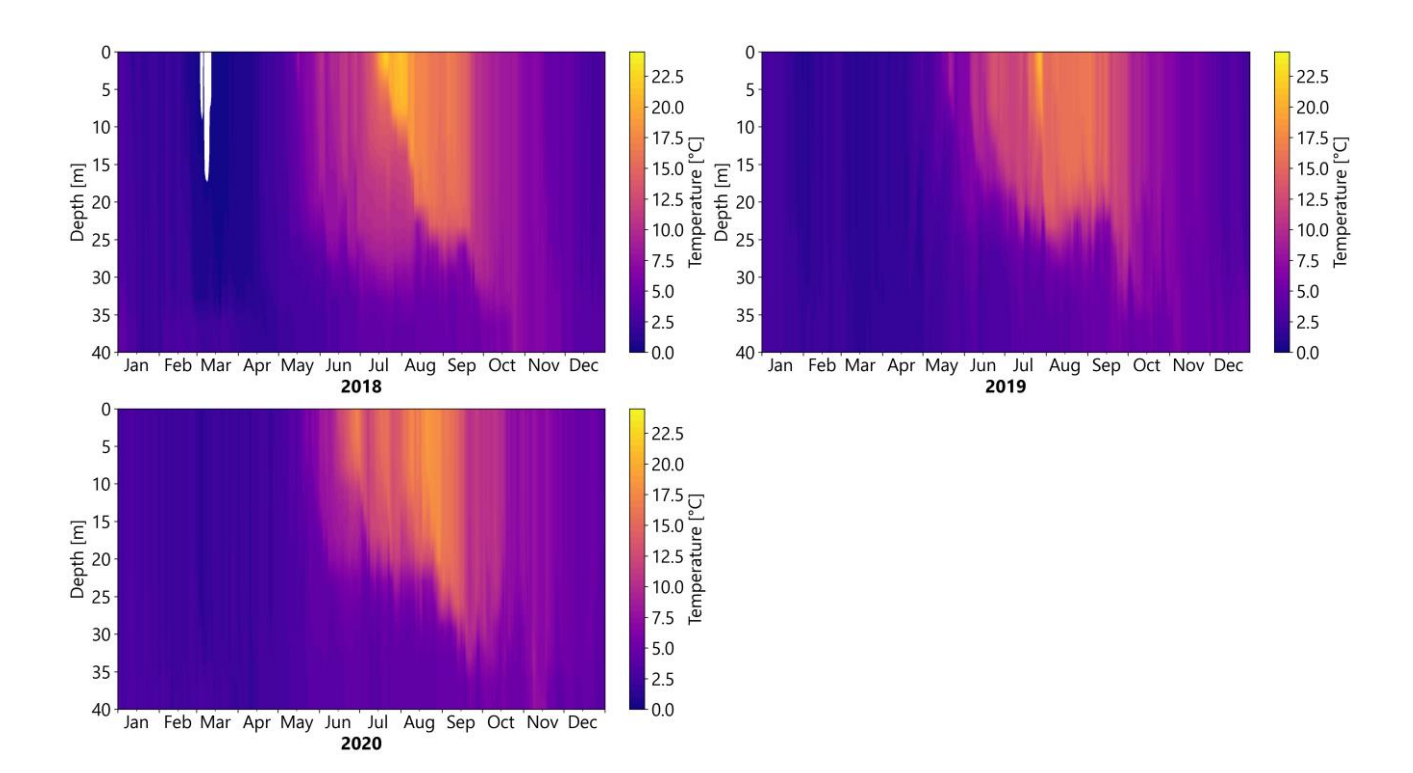






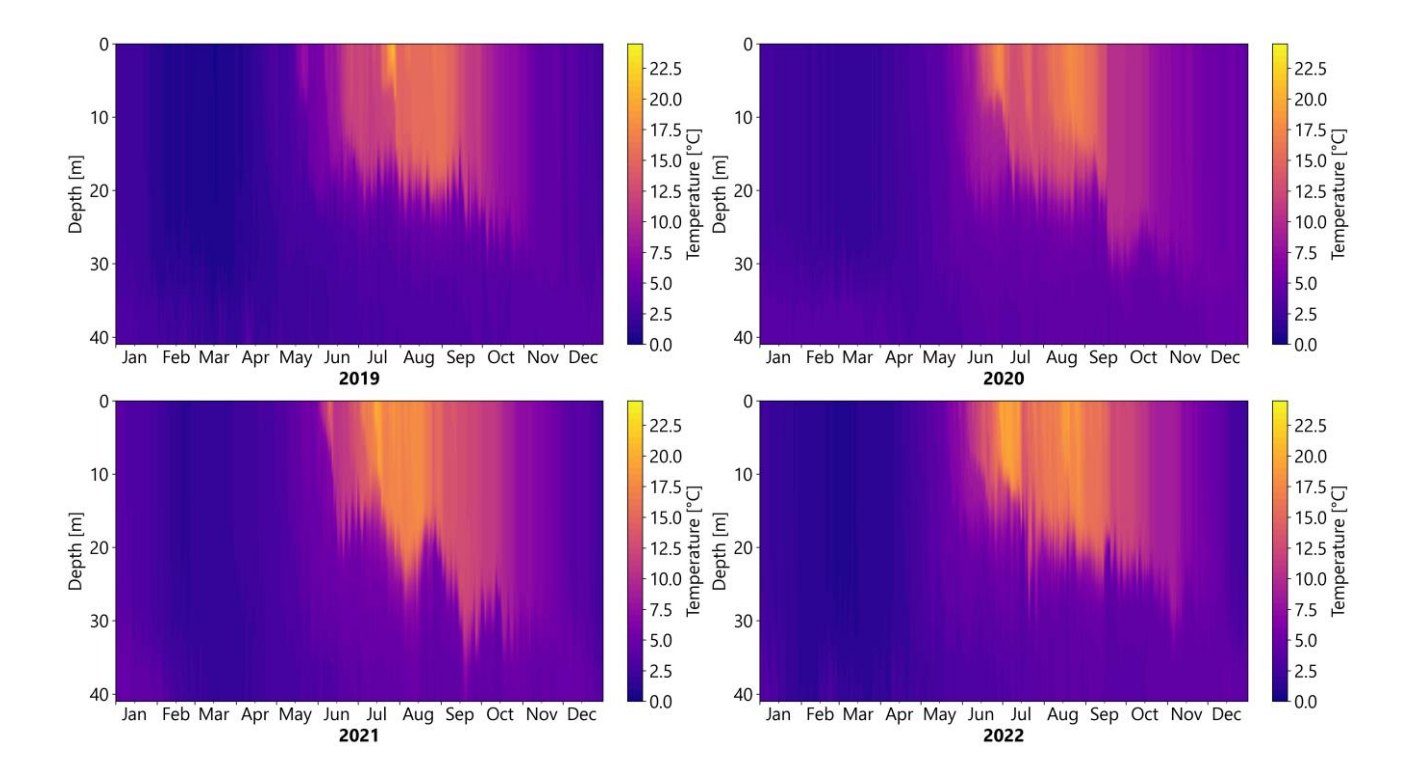
Appendix 3: Sylen OWF,	Tomporature profiles	(CN/ILI)	modelled (v/km)
Appendix 5. Sylen Owr,	remperature profiles	(SIVIHI)	, modelied 4x4km)





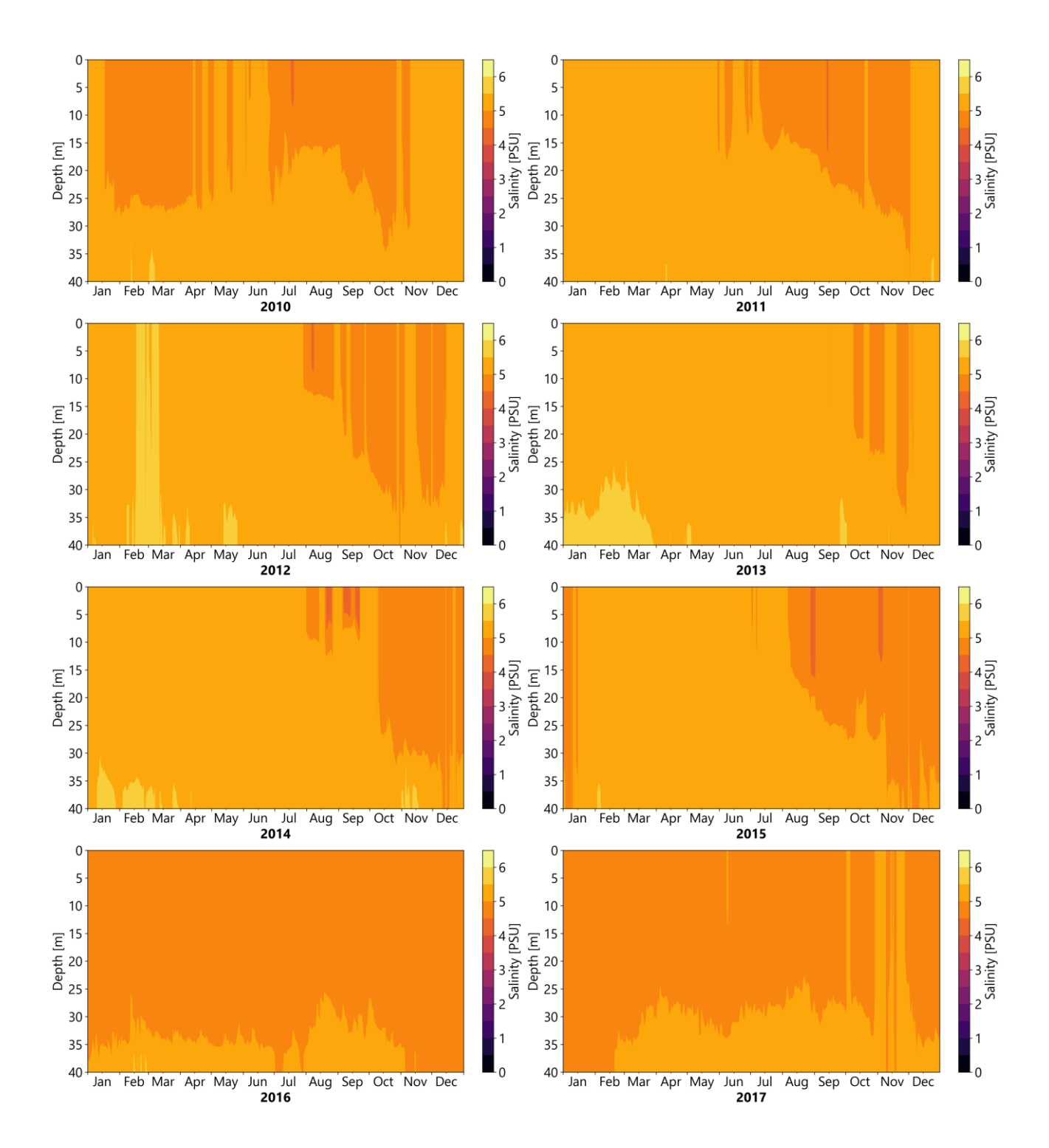


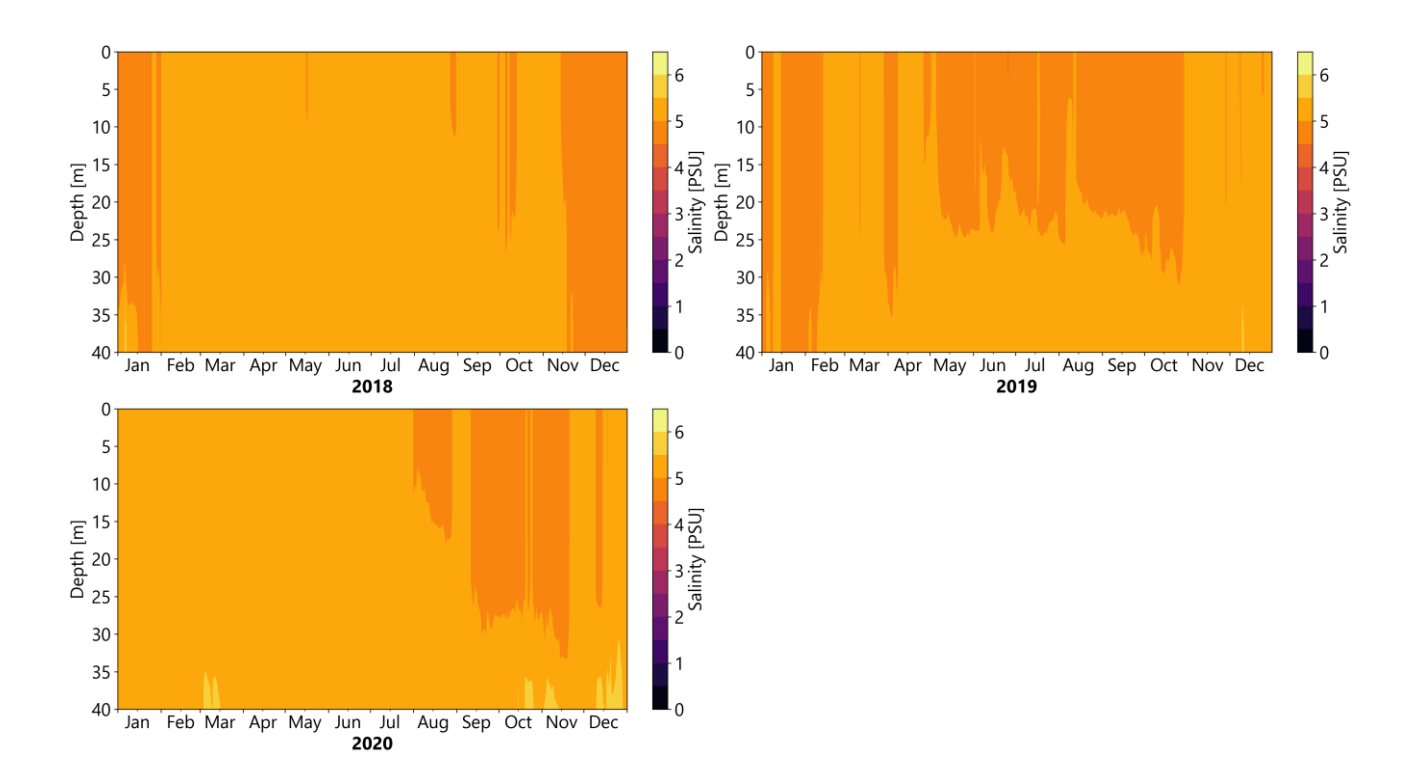
Apr	oendix 4	4 Sylen	OWF,	Temper	ature pr	rofiles ((SMHI,	modelled	2x2km)
רן דן:		,	,		J. J. J. J. J.	,	(





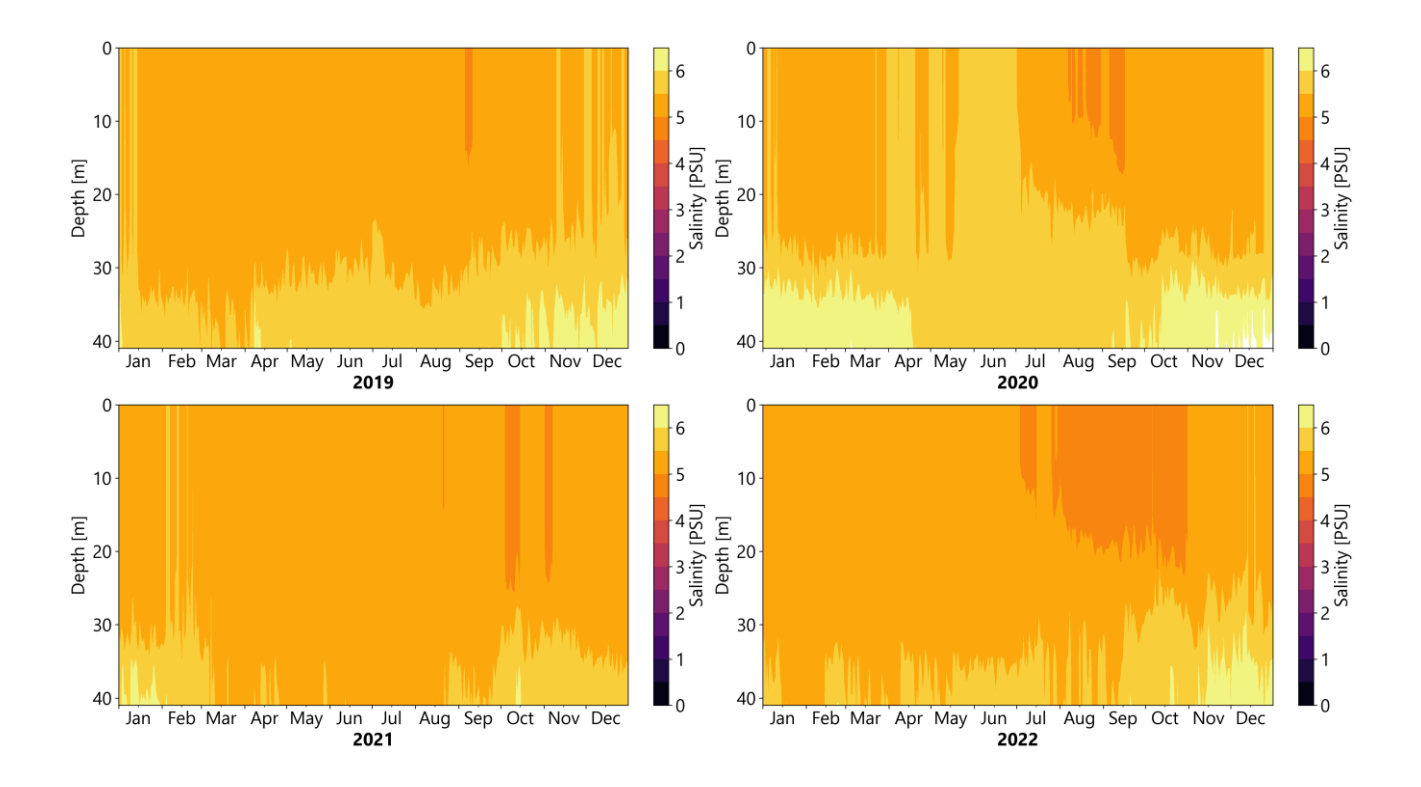
Appendix 5 Sylen OWF, Salinity profiles (SMHI, modelled 4x4km	Appen-	dix 5	Sylen	OWF,	Salinity	profiles	(SMHI,	modelled 4x4kn	n)
---	--------	-------	-------	------	----------	----------	--------	----------------	----





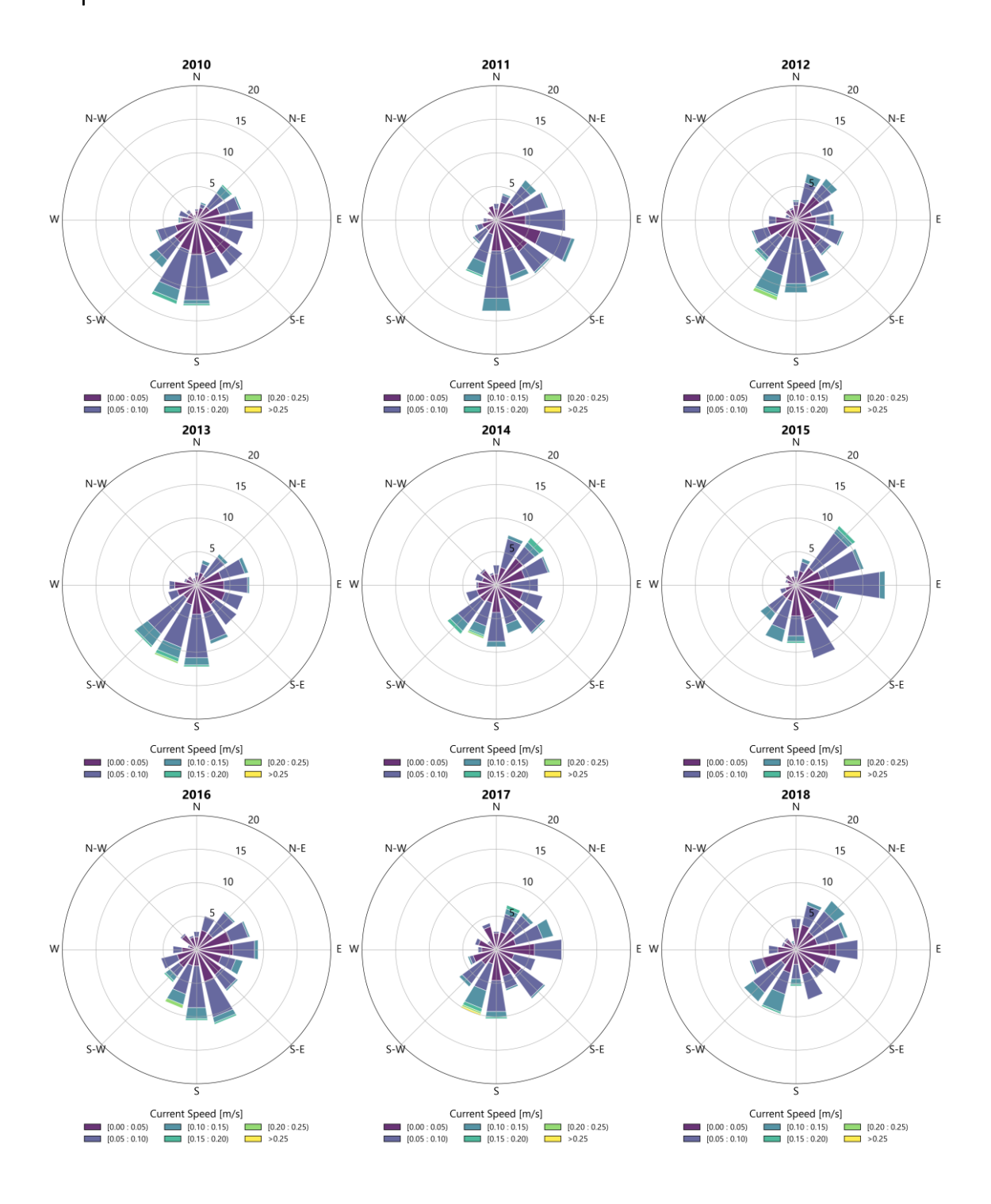


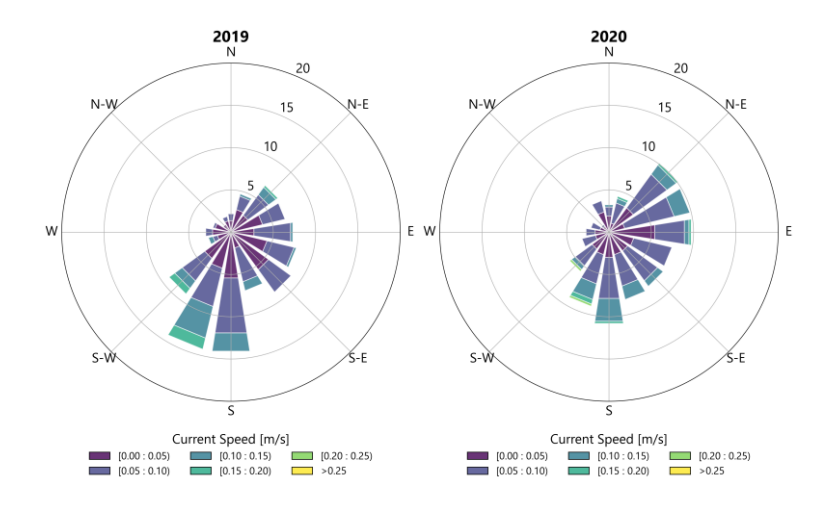
Appendix 6 Sylen OWF, Salinity profiles (SMHI, modelled 2x2km	Аp	pendix	6 9	Sylen	OWF,	Salinity	y profiles	(SMHI,	modelled	2x2km
---	----	--------	-----	-------	------	----------	------------	--------	----------	-------



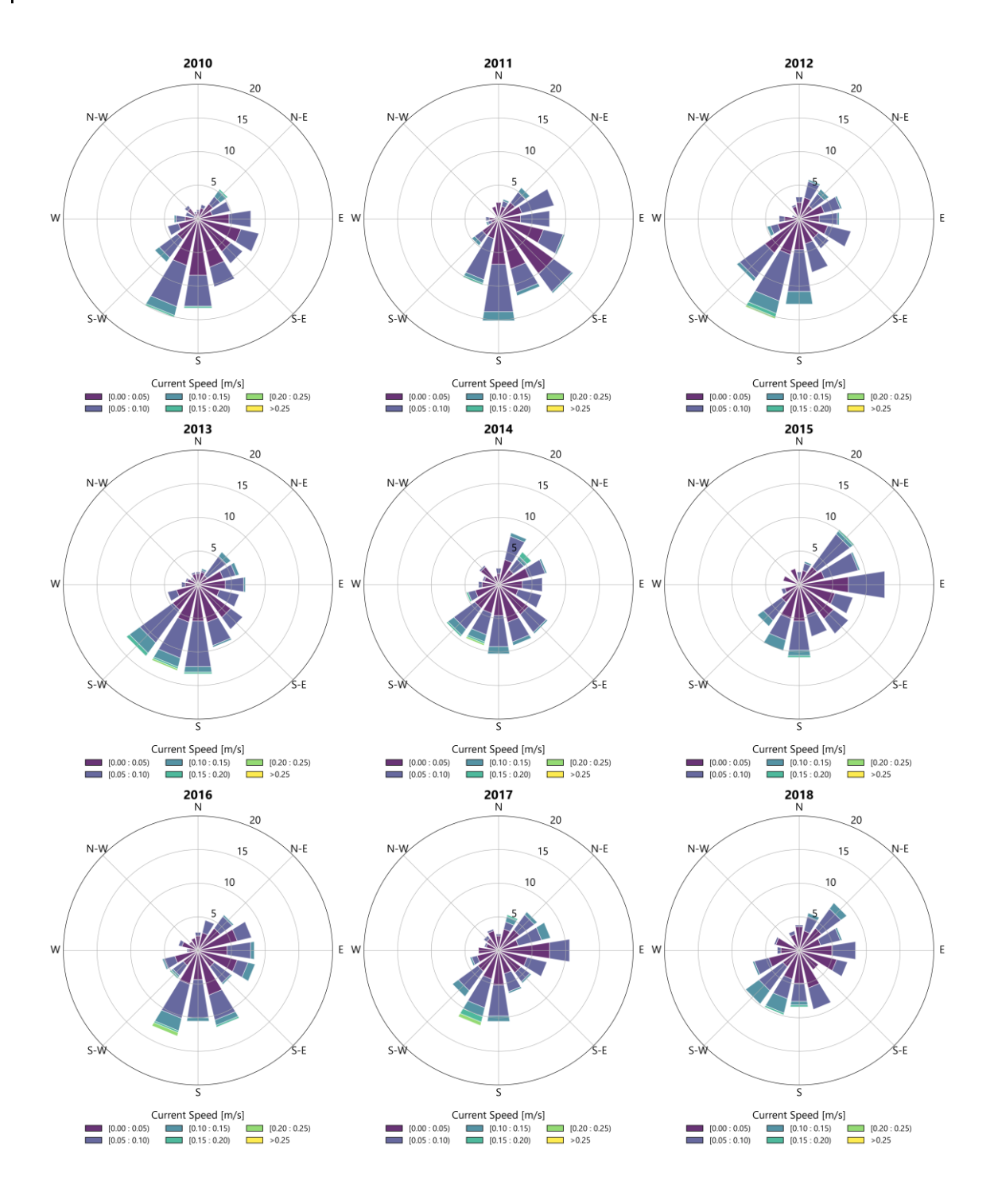


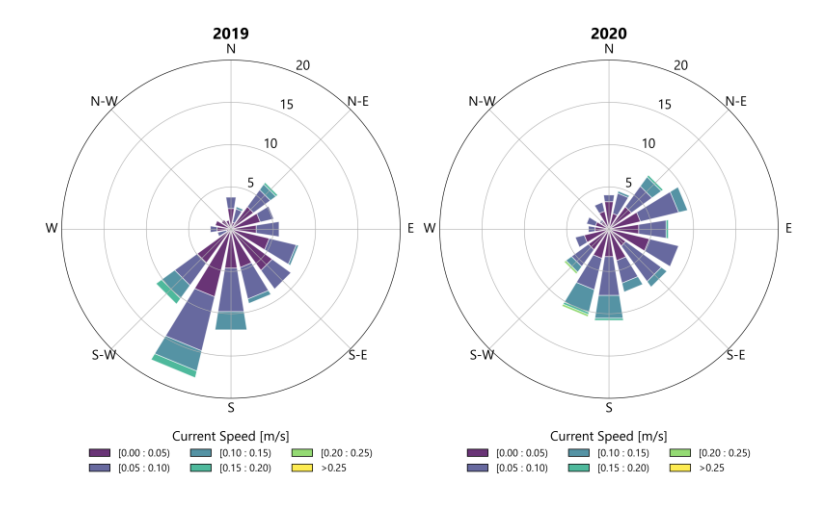
Depth 1 m



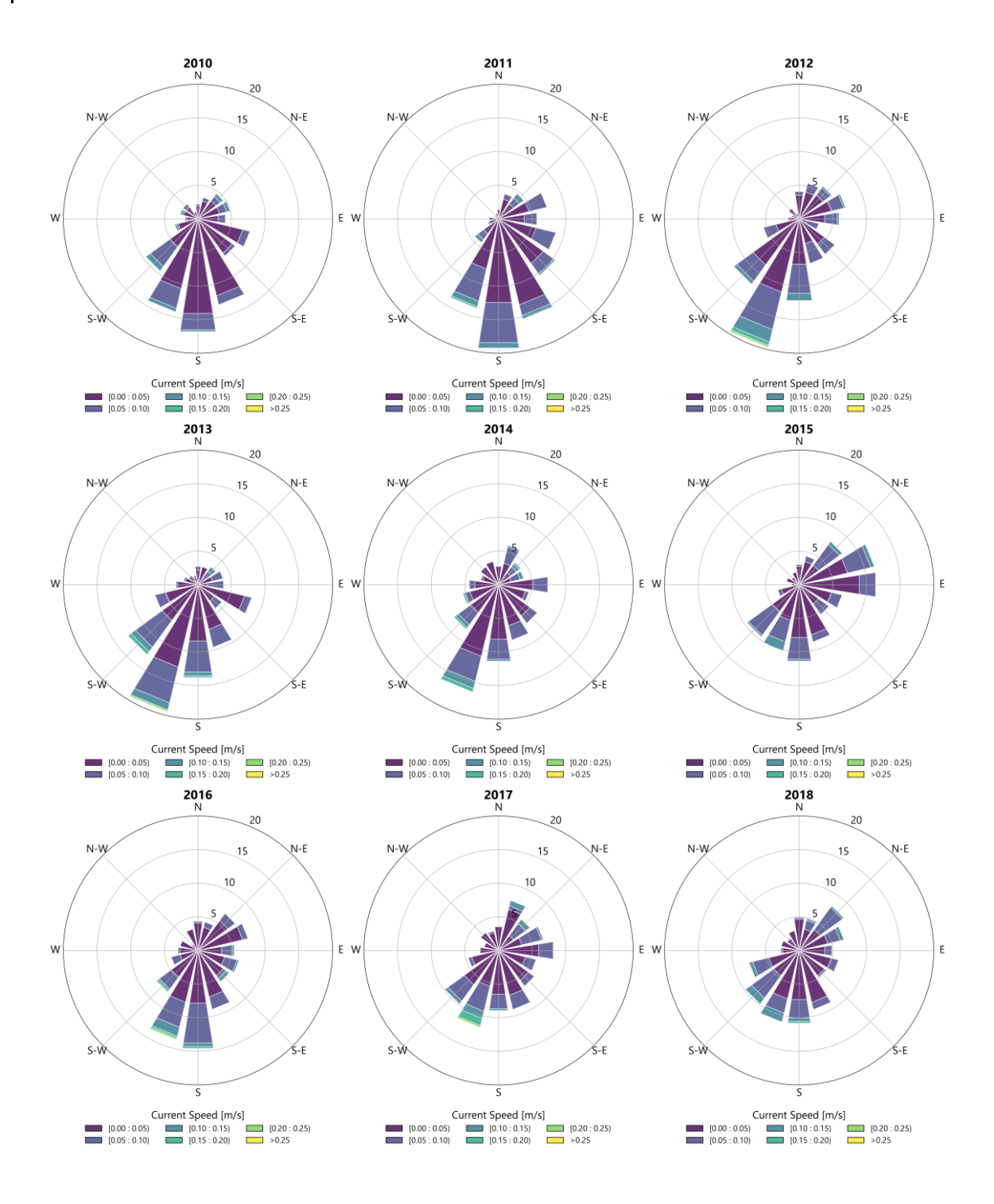


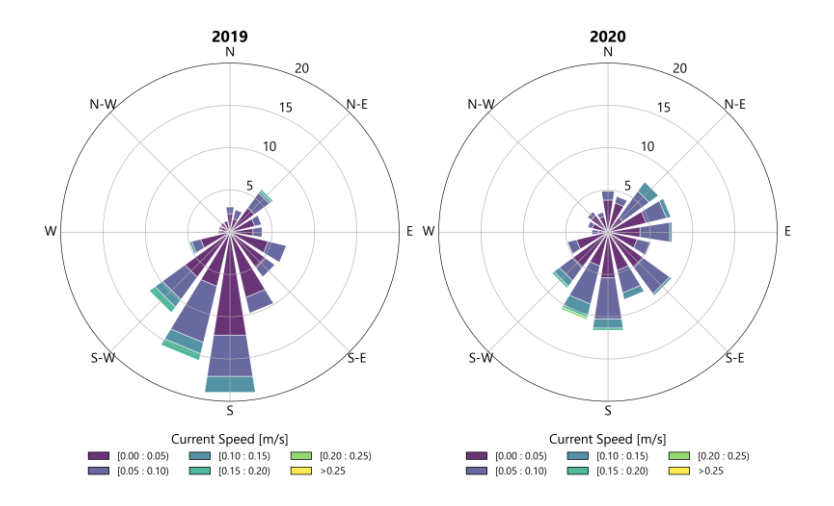
Depth 4 m





Depth 10 m

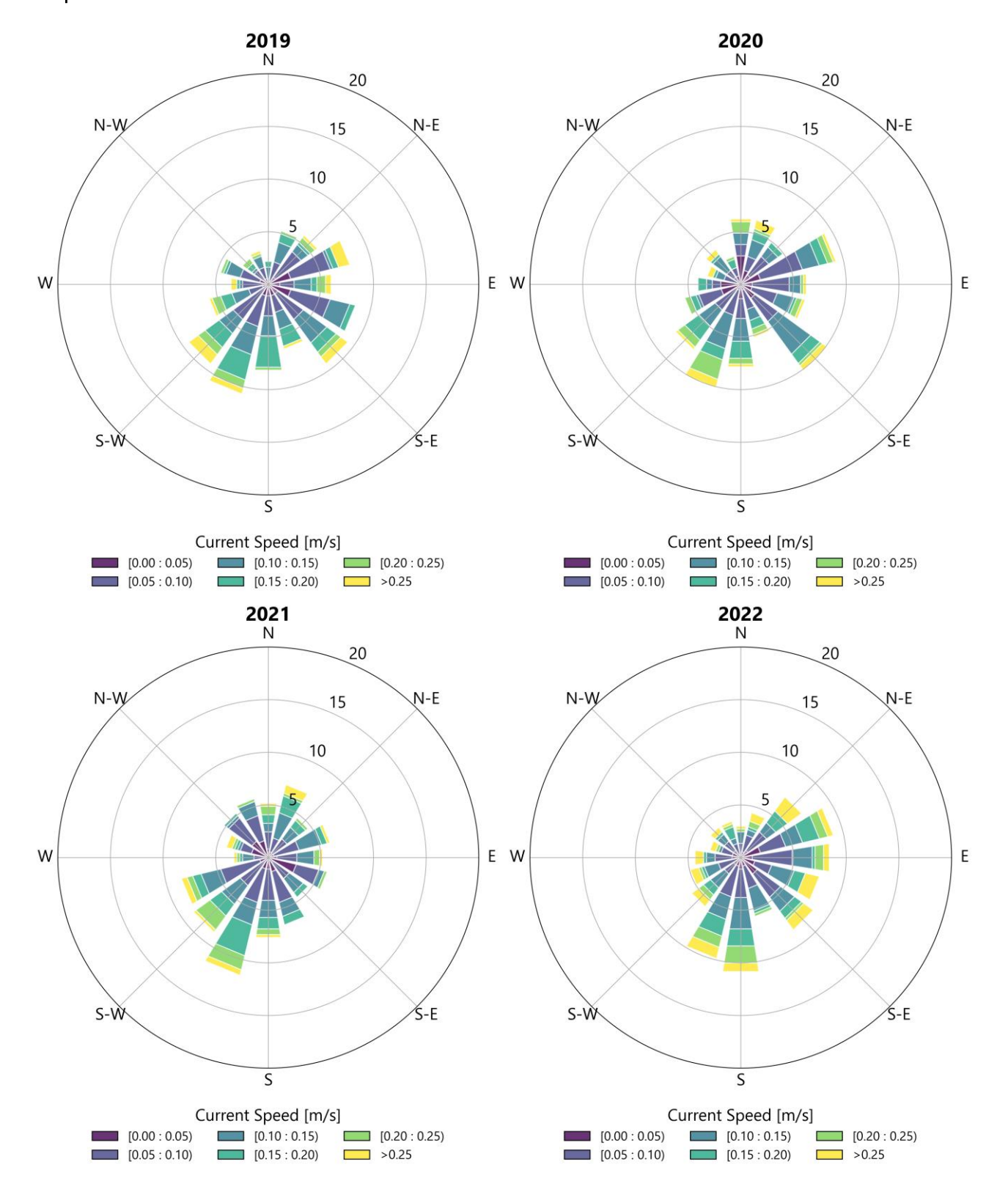




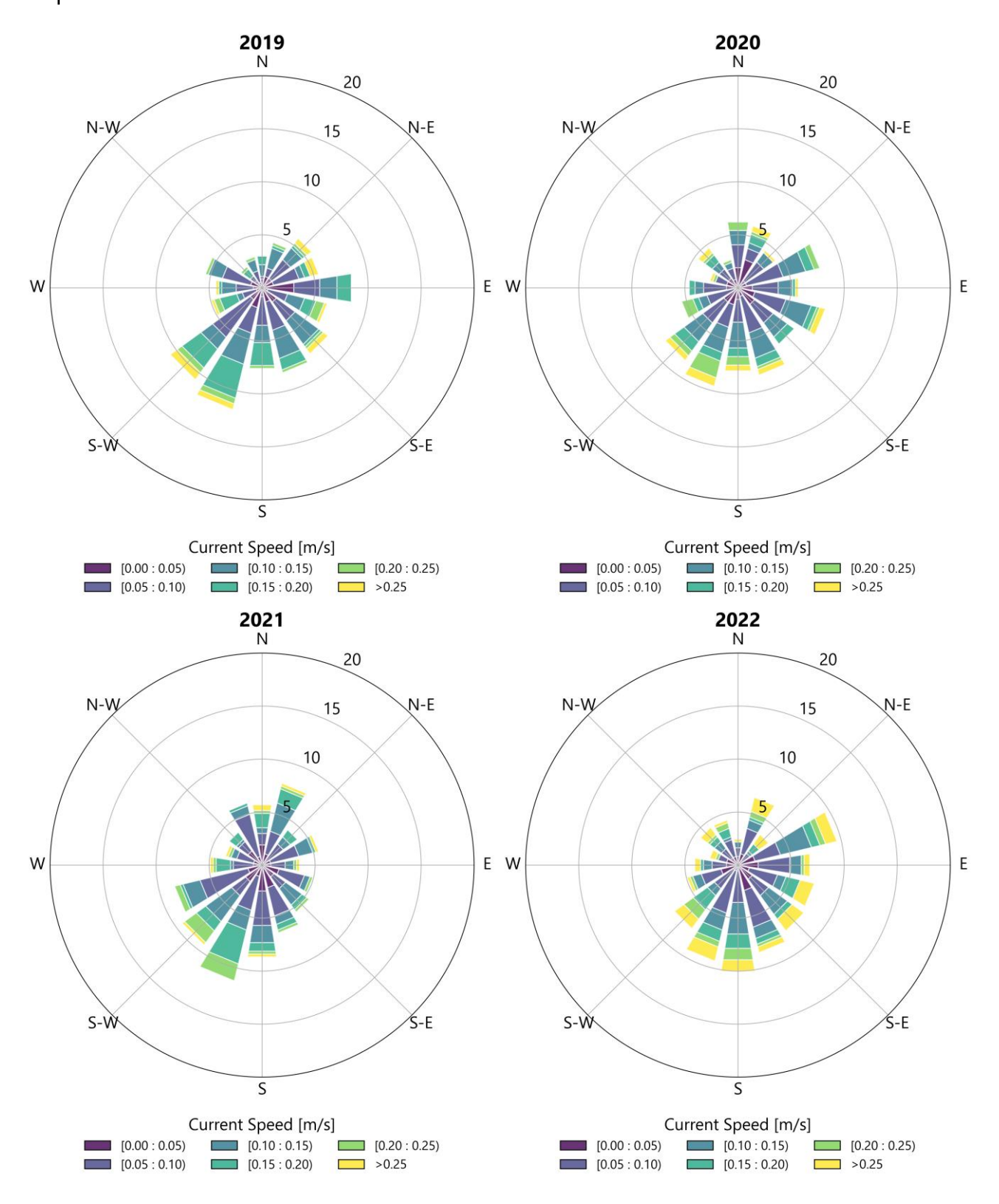


App	pendix	8 S [,]	ylen OW	, Current	roses	(SMHI,	modelled 2x	(2km)
-----	--------	------------------	---------	-----------	-------	--------	-------------	-------

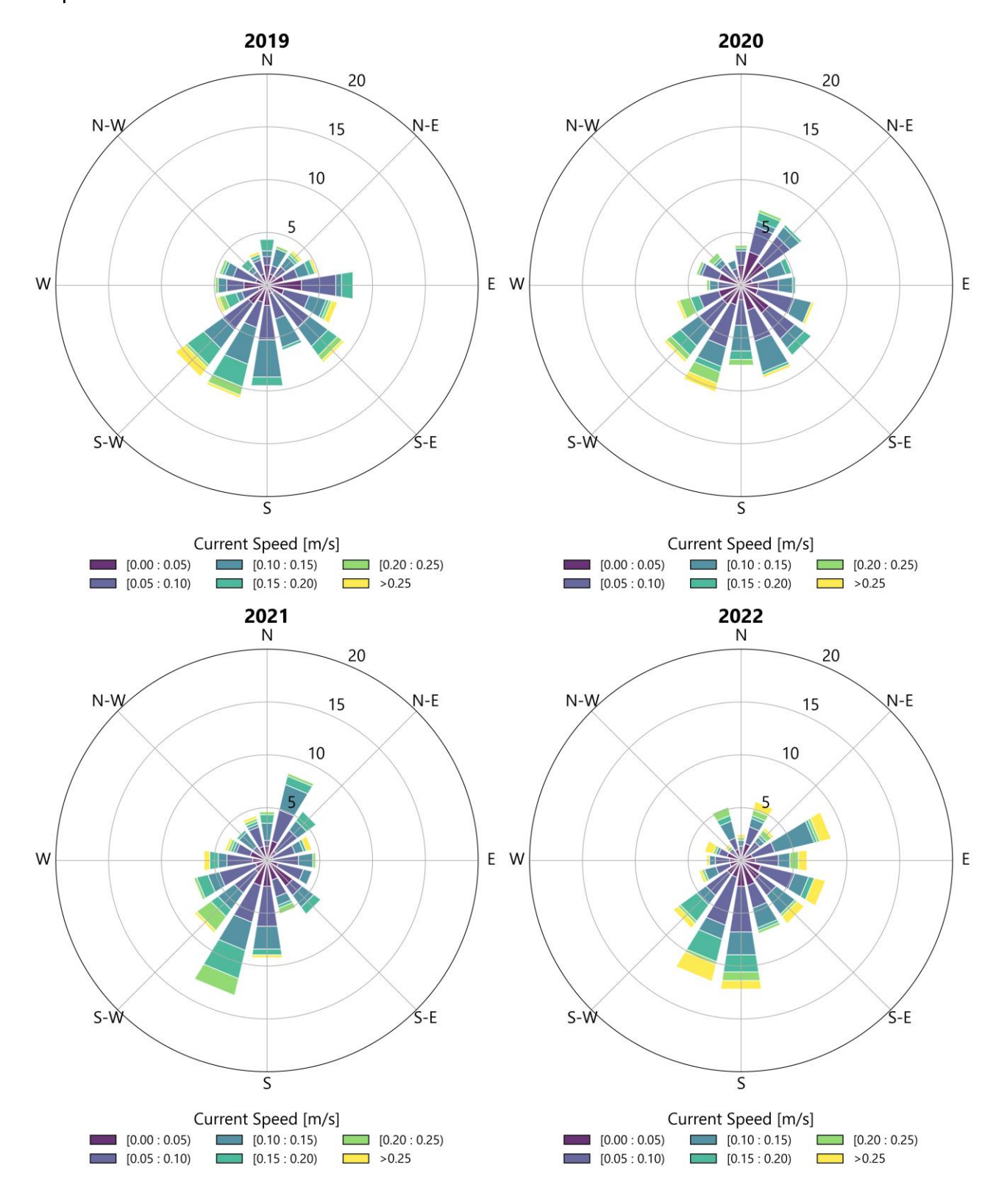
Depth 1 m



Depth 5 m



Depth 10 m

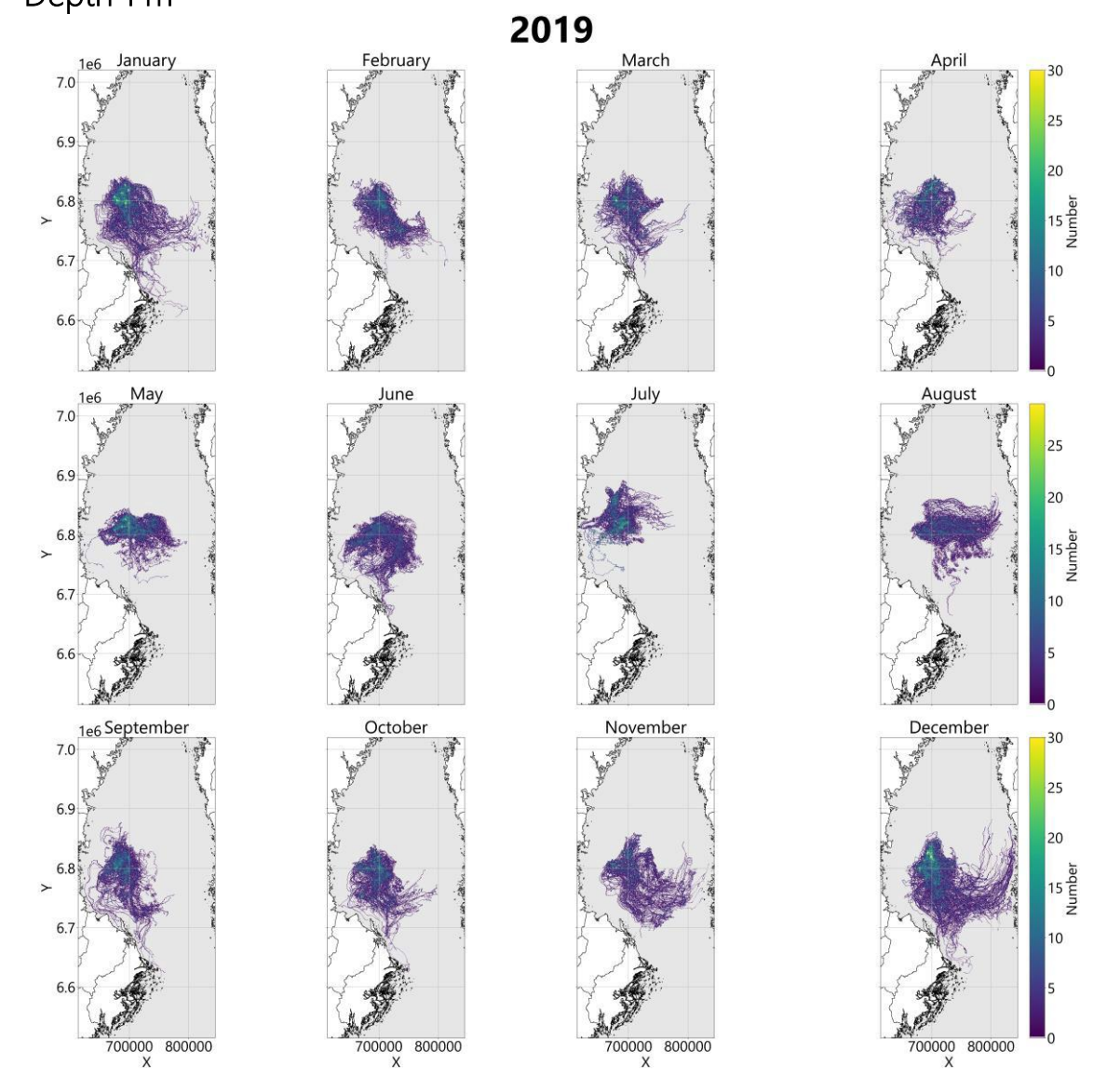


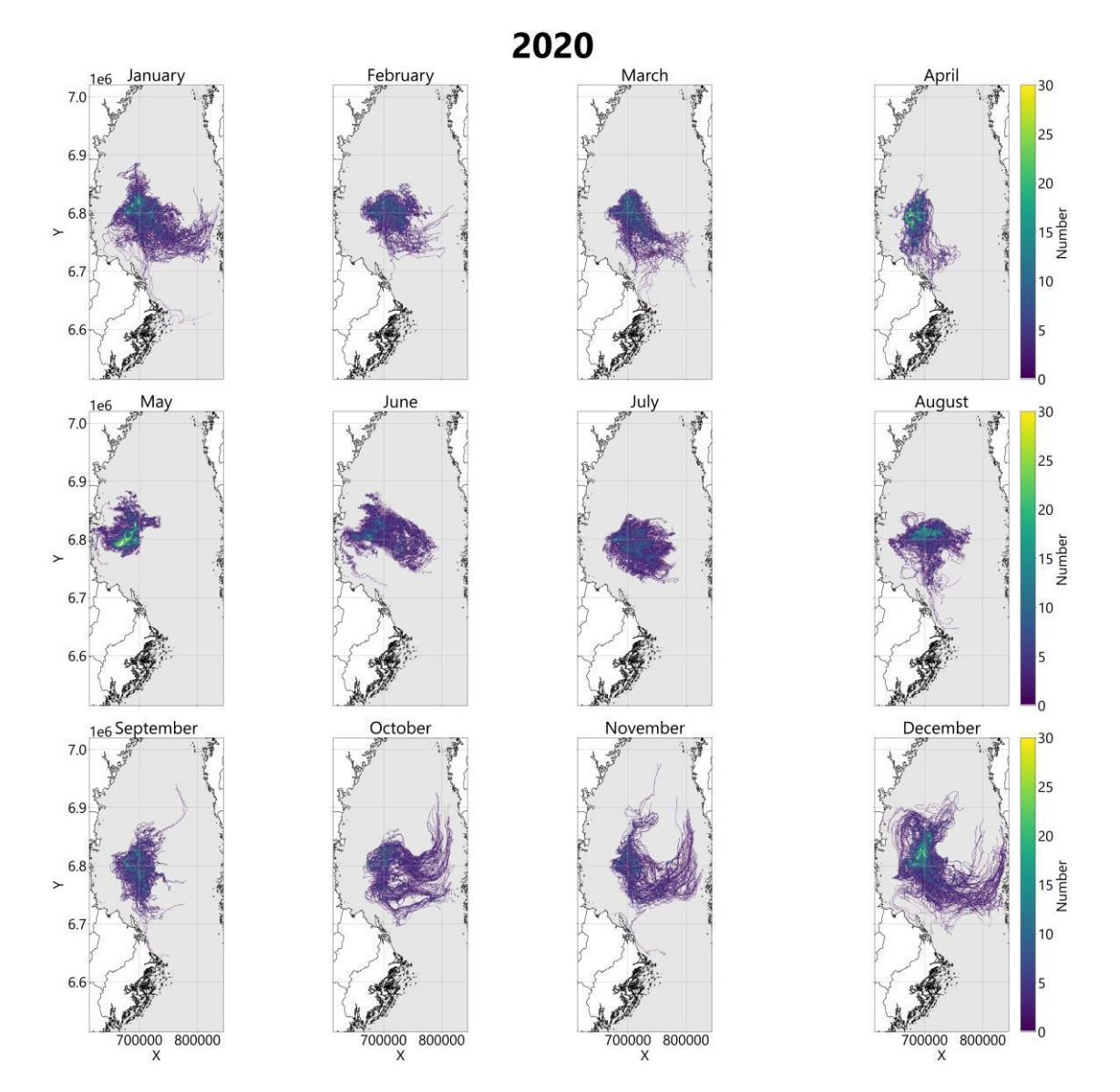


Appendix 9 Sylen OWF, Simplified Particle Tracks

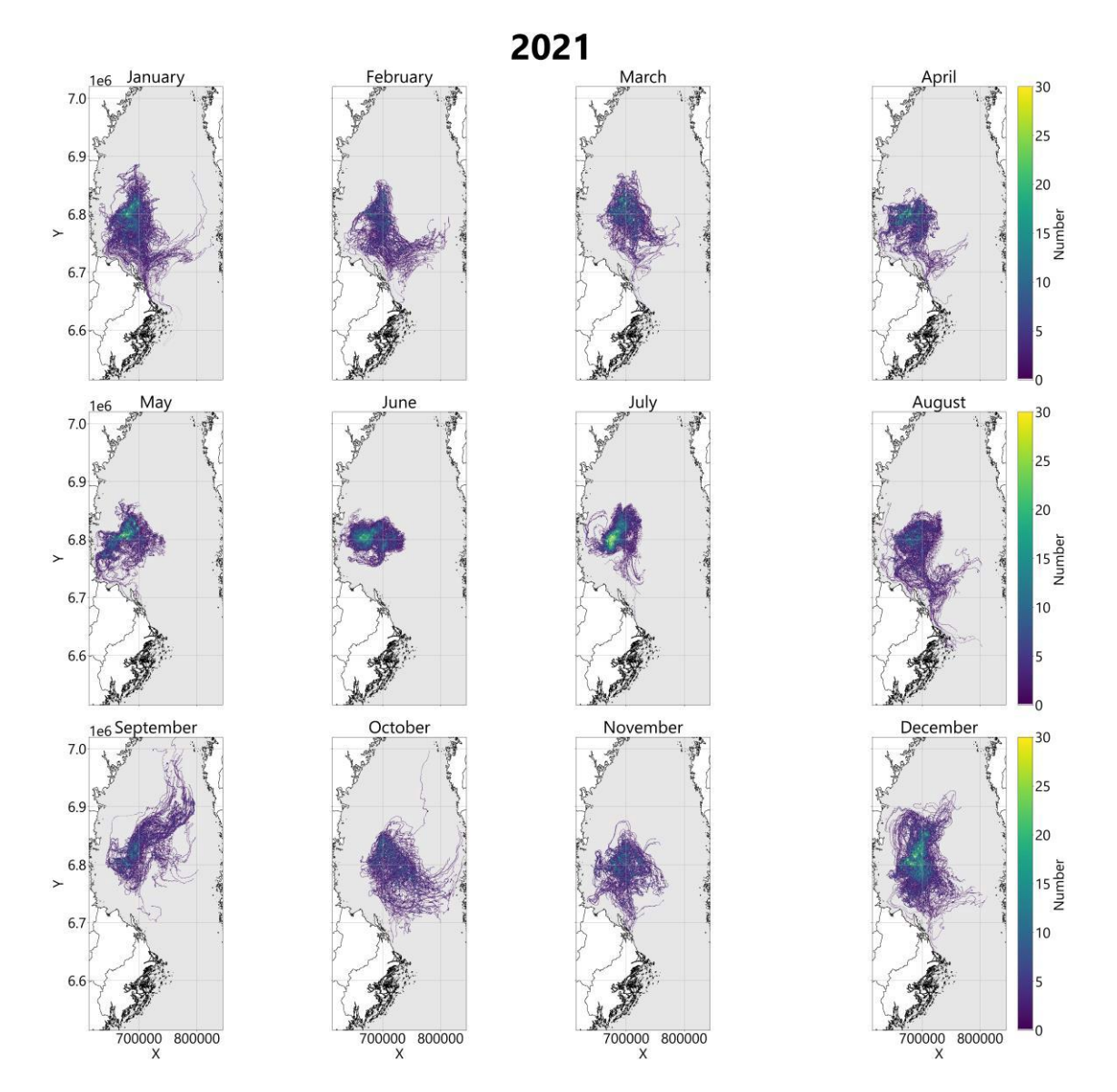
The following maps show the resulting tracks of a simplified particle tracking model based on the horizontal currents of the SMHI Baltic Sea model (Copernicus, Baltic Sea Physics Analysis and Forecast, 2x2km, 2022). Every day, one particle is released at each of five locations in the wind farm area, and its horizontal path is tracked for 30 days before the particle disappears again. The maps show all paths of the particles released in the respective month.

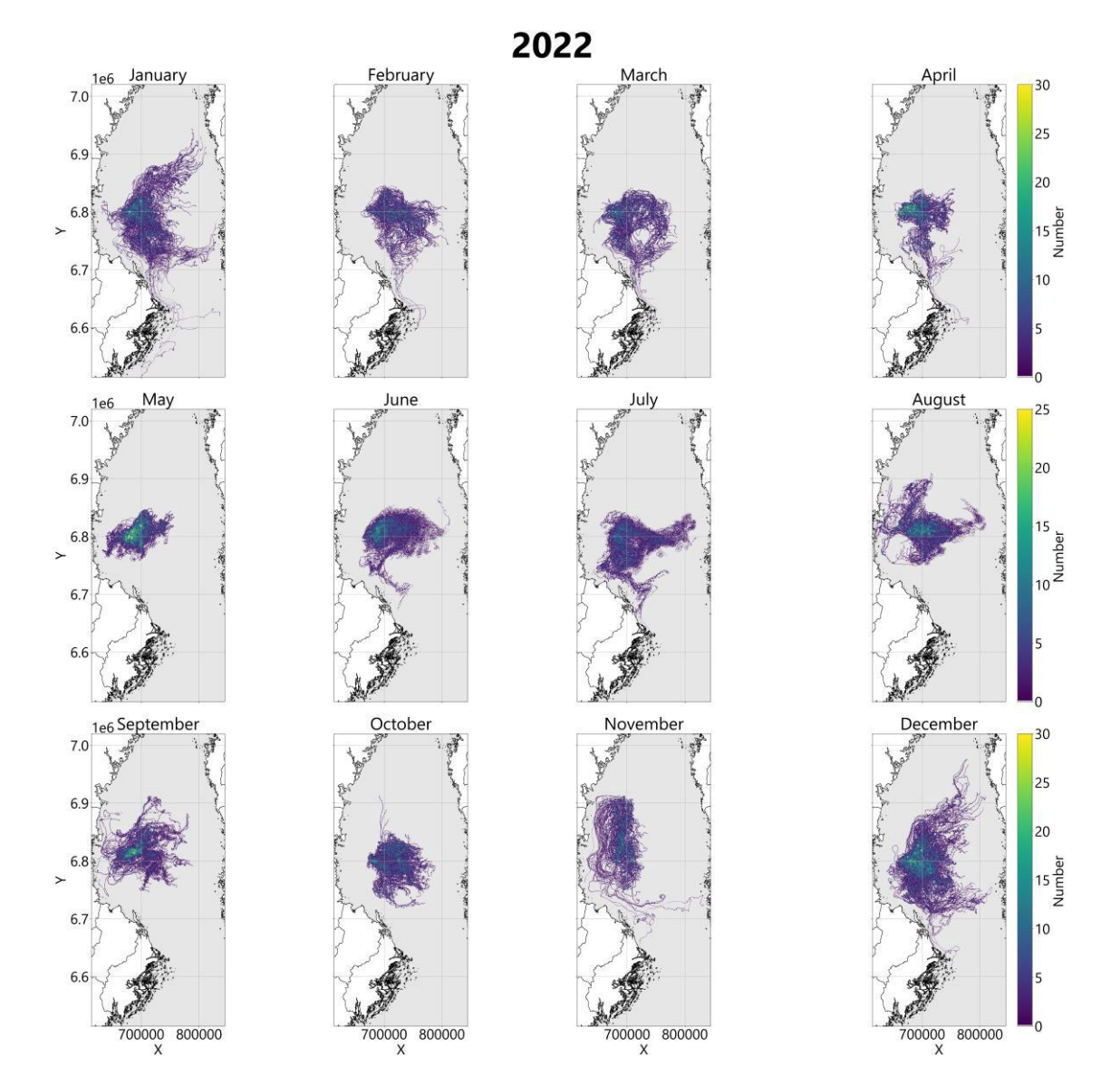
Depth 1 m





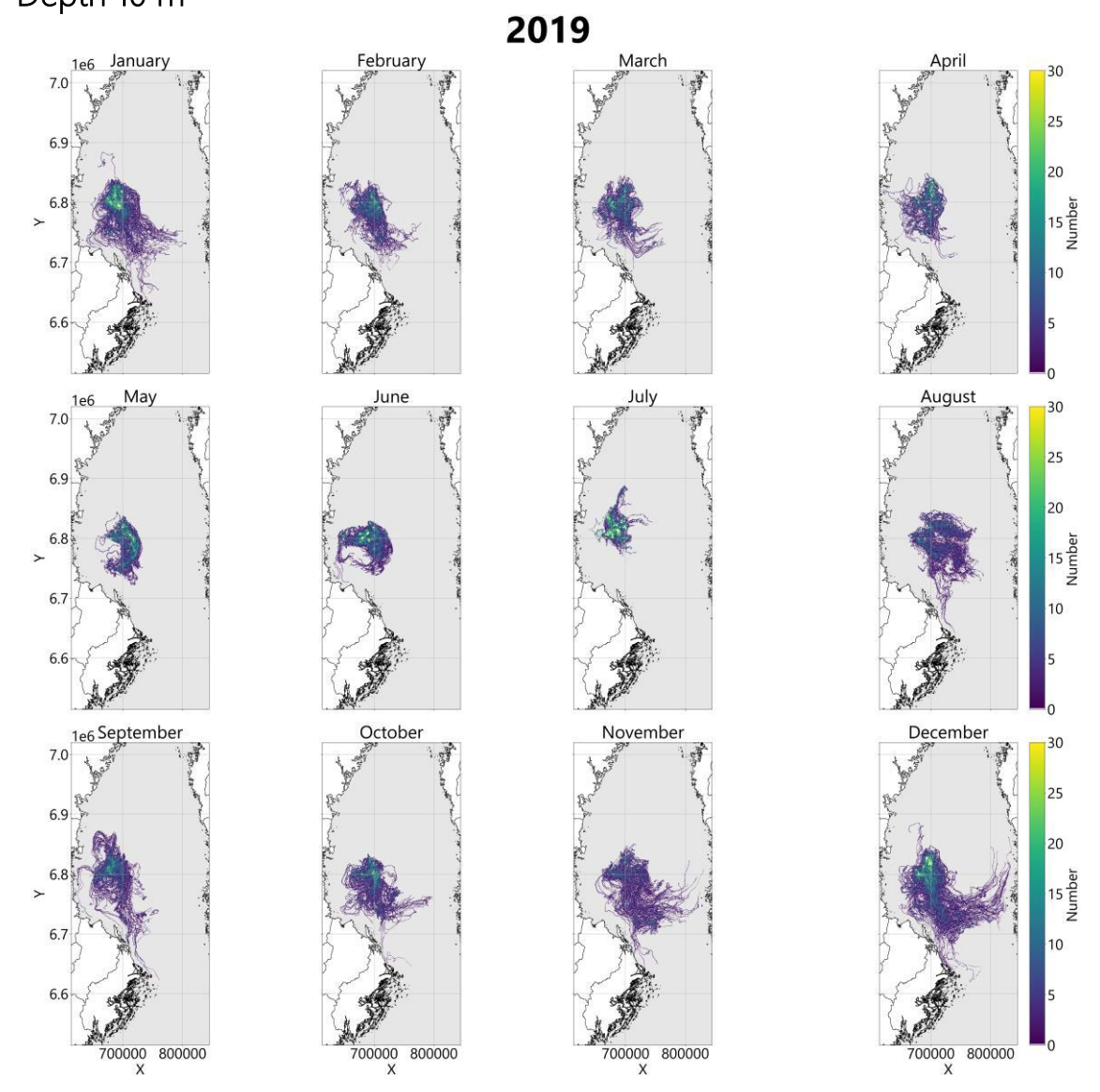
Document ID: 4S6X2MX43VNH-1644138503-43



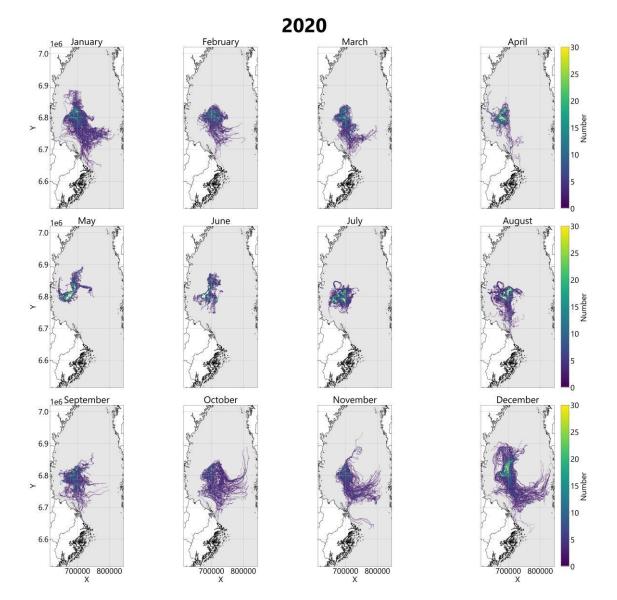


Document ID: 4S6X2MX43VNH-1644138503-43

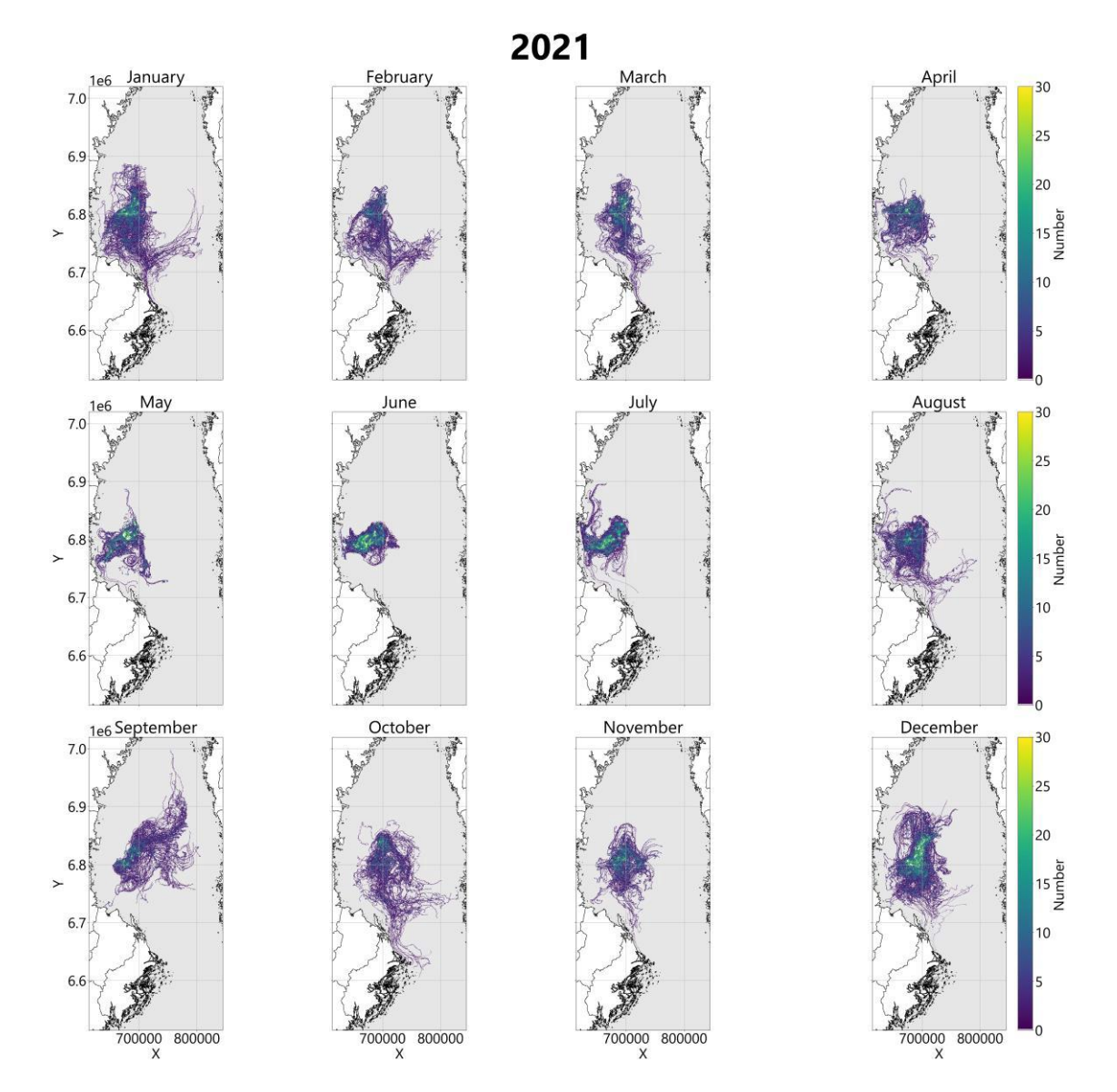


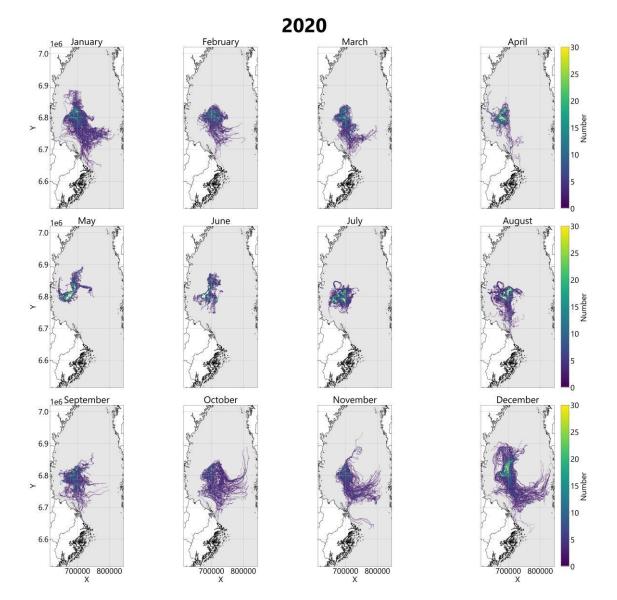


Document ID: 4S6X2MX43VNH-1644138503-44



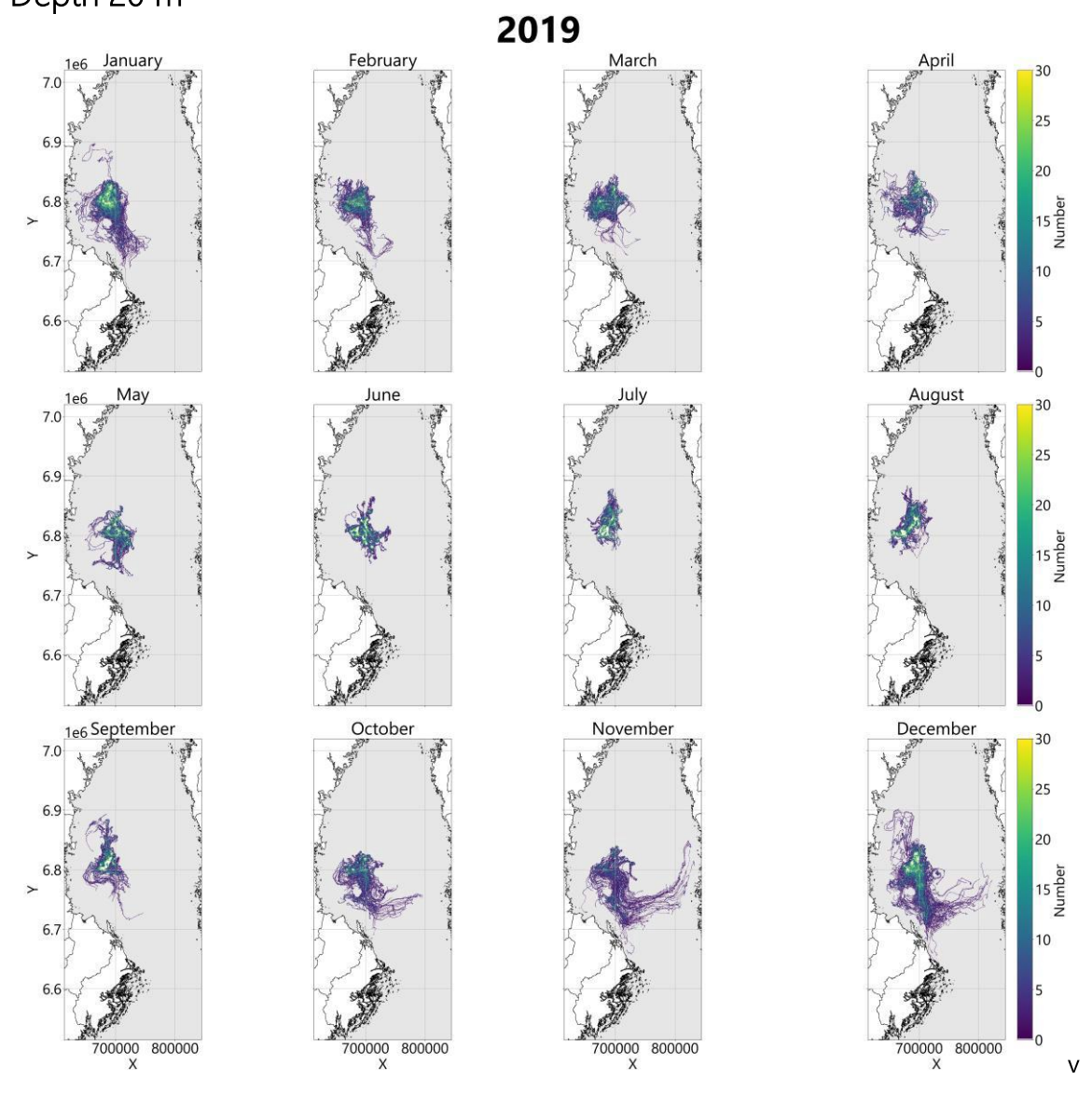
Document ID: 4S6X2MX43VNH-1644138503-44

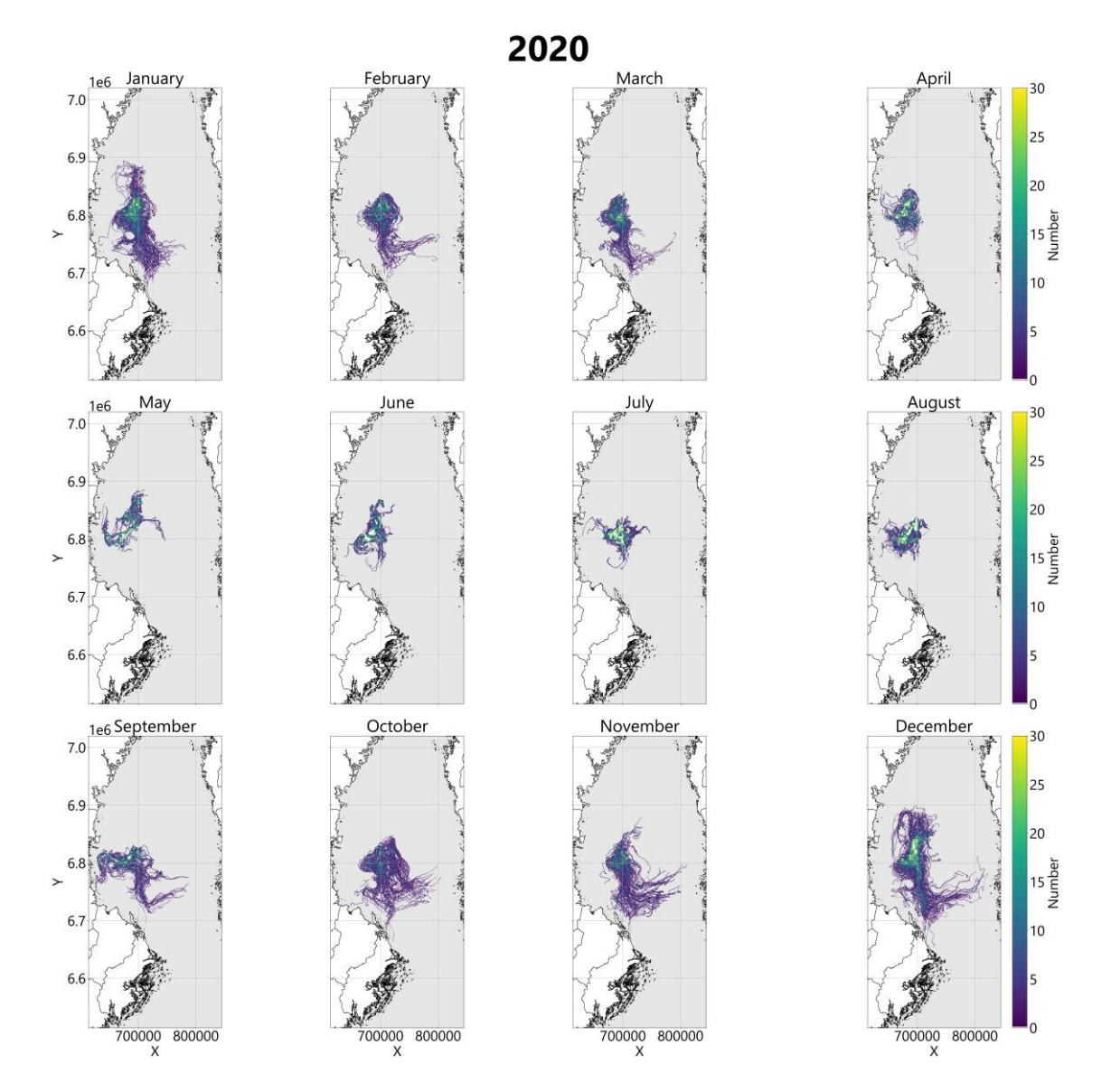




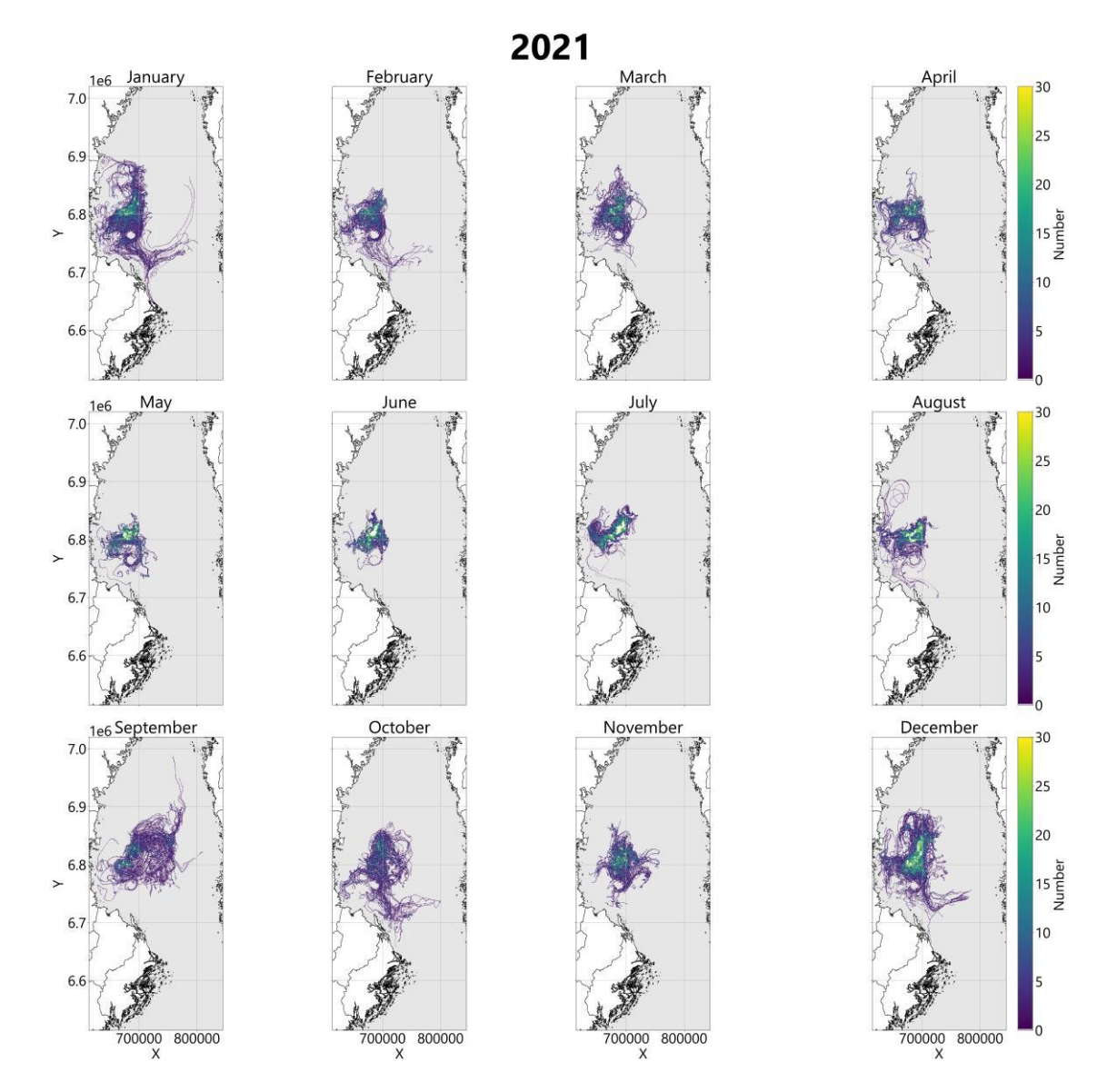
Document ID: 4S6X2MX43VNH-1644138503-44

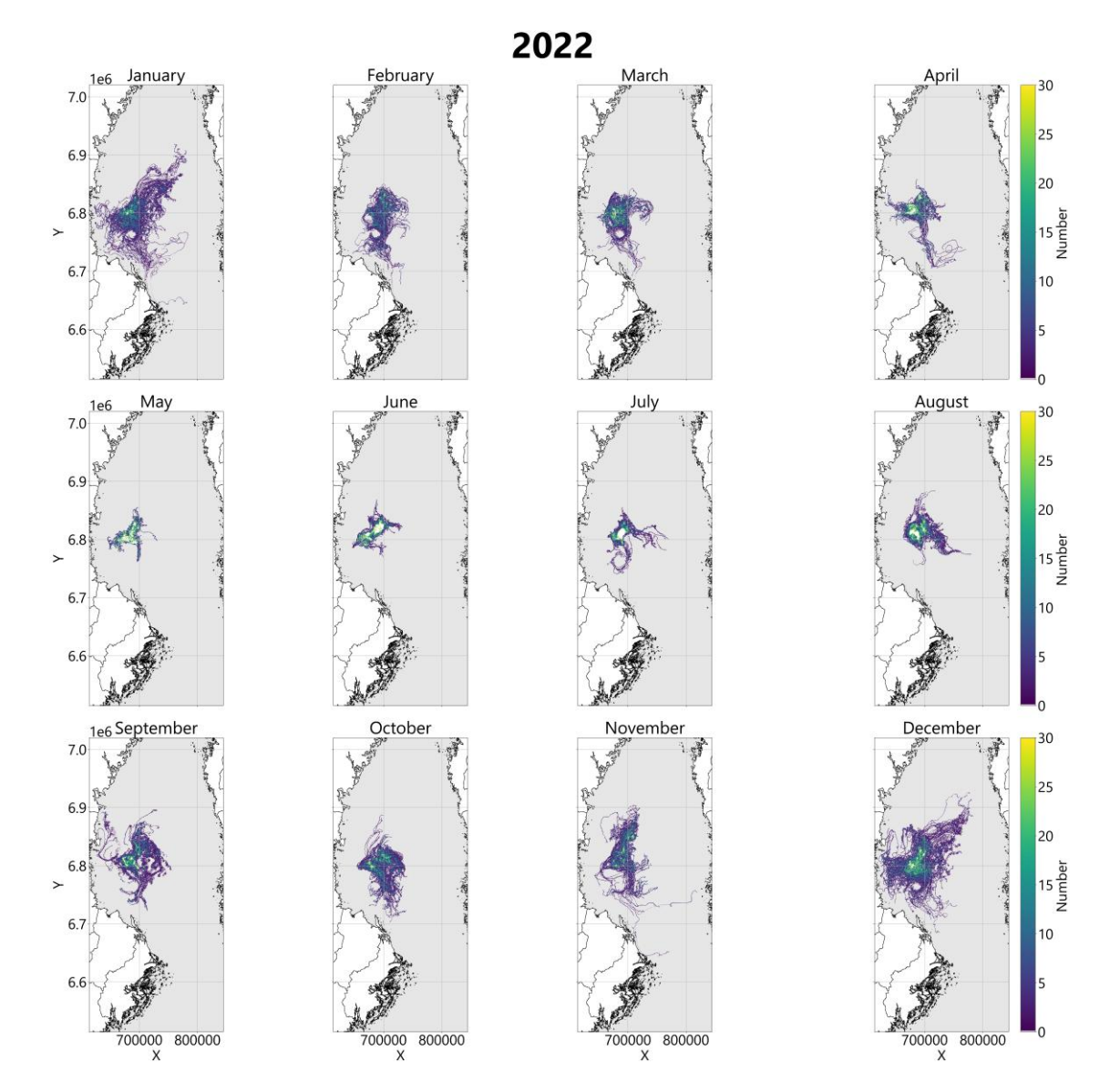






Document ID: 4S6X2MX43VNH-1644138503-46





Document ID: 4S6X2MX43VNH-1644138503-46



Appendix 10 Observations: Water level

Water level measuring stations used in the present study

Name	ID	Lat	Long	Source
FURUÍGRUND	2055	64.9158	21.2306	SMHI
RATAN	2056	63.9861	20.8950	SMHI
SPIKARNA	2061	62.3633	17.5311	SMHI
FORSMARK	2179	60.4086	18.2108	SMHI
FORSMARK	2179	60.4086	18.2108	SMHI
SKAGSUDDE	2321	63.1906	19.0125	SMHI
KALIX-KARLSBORG SJÍV	35103	65.7887	23.3027	SMHI
BÍNAN SJÍV	35119	60.7384	17.3186	SMHI
Holmsund	35124	63.6803	20.3331	SMHI
LJUSNE SJÍV	35127	61.2067	17.1452	SMHI
SKAGSUDDE SJÍV	35138	63.1906	19.0119	SMHI
STRÍMÍREN SJÍV	35183	65.5497	22.2383	SMHI
Kemi Ajos	100539	65.6734	24.5153	FMI
Raahe Lapaluoto	100540	64.6663	24.4071	FMI
Vaasa Vaskiluoto	134223	63.0815	21.5712	FMI
Rauma Petäjäs	134224	61.1339	21.4426	FMI
Oulu Toppila	134248	65.0403	25.4182	FMI
Pietarsaari Leppäluoto	134250	63.7086	22.6896	FMI
Kaskinen Ådskär	134251	62.3440	21.2148	FMI
Pori Mäntyluoto Kallo	134266	61.5944	21.4634	FMI



۸r	ϽI	pendix	11	Observations:	CTD-I	Measuring	sites

Location of CTD-Measurements used in the present study

Name	ID	Lat	Long	Source
MAME61	91607	60.9119	20.3272	Merihavainnot.fi
SR5	70676	61.0833	19.5833	Merihavainnot.fi
SR7	70677	61.0835	20.5965	Merihavainnot.fi
SR8	78292	61.1265	20.9300	Merihavainnot.fi
SR3	71073	61.1833	18.2300	Merihavainnot.fi
MS9	77892	61.7668	20.5305	Merihavainnot.fi
F26	77178	61.9835	20.0630	Merihavainnot.fi
MS6	70670	61.9837	19.1635	Merihavainnot.fi
MS3	77880	62.1345	18.1630	Merihavainnot.fi
US5B	70683	62.5862	19.9688	Merihavainnot.fi
US6B	70684	62.6002	20.2630	Merihavainnot.fi
US7	70685	62.6002	20.8297	Merihavainnot.fi
US3	70681	62.7588	19.1957	Merihavainnot.fi
F18	70656	63.3143	20.2727	Merihavainnot.fi
F18	70656	63.3143	20.2727	Merihavainnot.fi
F16	70679	63.5168	21.0628	Merihavainnot.fi
F13	77162	63.7835	21.4795	Merihavainnot.fi
воз	70647	64.3050	22.3583	Merihavainnot.fi
F9	77223	64.7003	22.0628	Merihavainnot.fi
RR7	78138	64.7337	23.8128	Merihavainnot.fi
RR6	70674	64.8003	23.4795	Merihavainnot.fi
RR5	70673	64.8337	23.1628	Merihavainnot.fi
RR3	70644	64.9337	22.3460	Merihavainnot.fi
CV	77045	65.0003	23.2462	Merihavainnot.fi
CVI	70650	65.2337	23.5620	Merihavainnot.fi
F2	70658	65.3837	23.4627	Merihavainnot.fi
A5		65.2690	22.8618	SMHI
F13		63.7912	21.4836	SMHI
F16		63.5257	21.0817	SMHI
F18 SYDOSTBROTTEN		63.3092	20.2803	SMHI
F33 GRUNDKALLEN		60.5402	18.9309	SMHI
MS2		62.1320	17.8736	SMHI
MS6		61.9835	19.1646	SMHI
RR1		64.9680	21.8680	SMHI
RR5		64.8376	23.1696	SMHI

Name	. ID	Lat	Long	Source
RR7		64.7320	23.8167	SMHI
SR1A		61.2321	17.6620	SMHI
SR3		61.1838	18.2323	SMHI
SS29		61.1096	20.2654	SMHI



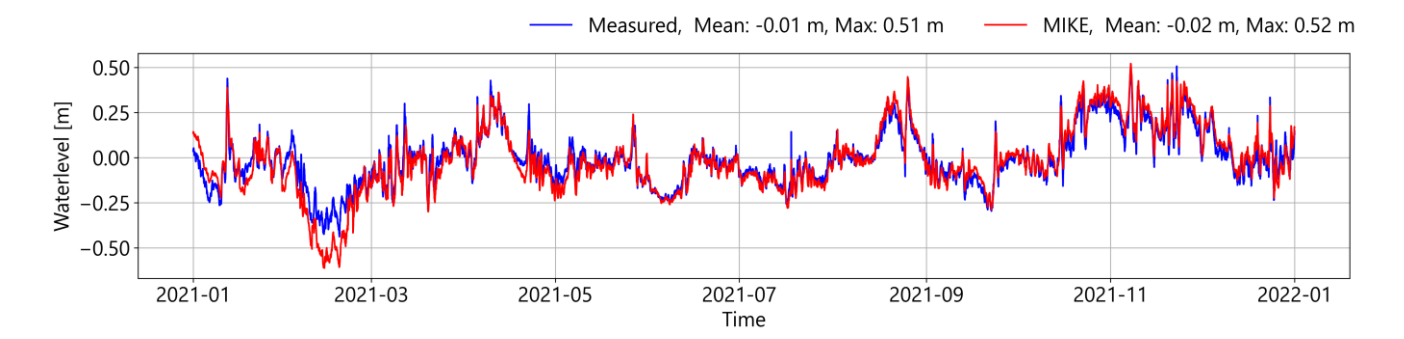
Append	dix 12	Observations:	Surface	temperature
--------	--------	---------------	---------	-------------

Surface temperature measuring stations used in the present study

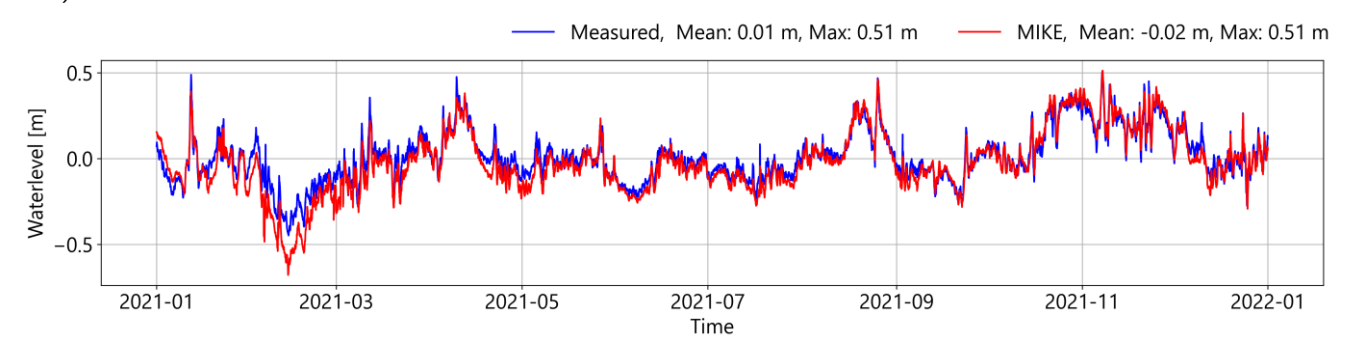
Name	ID	Lat	Long	Source
FORSMARK	2179	60.4086	18.2108	SMHI
FINNGRUNDET WR BOJ	33003	60.9000	18.6167	SMHI
NORRBYN BOJ	33021	63.4990	19.8044	SMHI
KALIX-KARLSBORG SJÖV	35103	65.7887	23.3027	SMHI
BÍNAN SJÍV	35119	60.7384	17.3186	SMHI
Holmsund	35124	63.6803	20.3331	SMHI
LJUSNE SJÍV	35127	61.2067	17.1452	SMHI
STRÍMÍREN SJÍV	35183	65.5497	22.2383	SMHI
NORRBYN SST	37110	63.5642	19.8331	SMHI
Oulu Santapankki	103807	65.2340	24.9692	FMI
Kalajoki Maakalla	103808	64.2938	23.5506	FMI
Pori Kaijakari	104600	61.6218	21.3956	FMI
Uusikaupunki Vekara	106631	60.8670	21.0494	FMI
Maalahti Storskõret	107033	63.1076	20.8185	FMI
Selkõmeri aaltopoiju	134246	61.8001	20.2327	FMI
Perõmeri aaltopoiju	137228	64.6841	23.2380	FMI



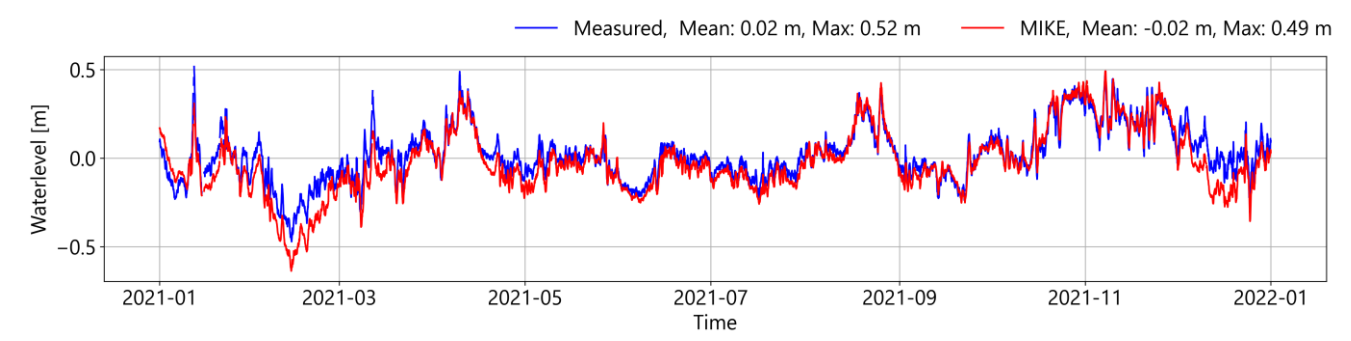
Appendix 13 Model verification: Water leve
--



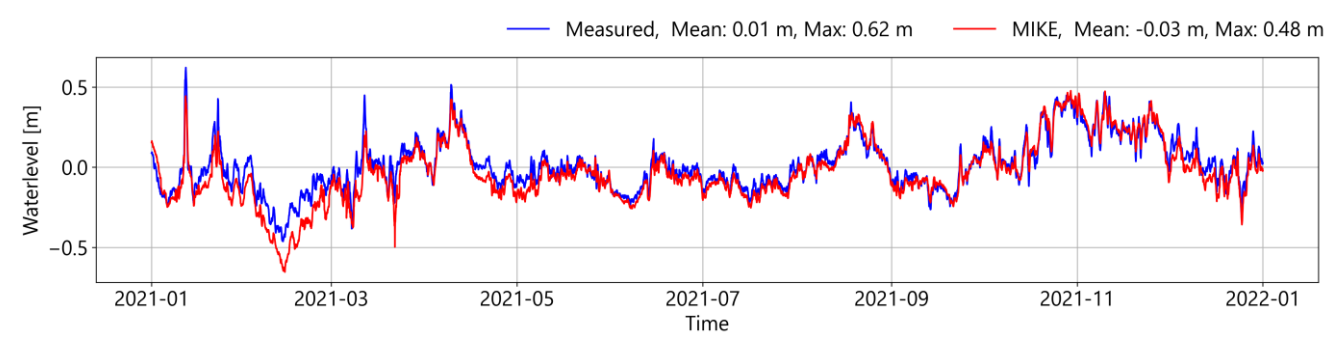
Comparison between observed water level in mMSL (blue line) and modelled water level (red line) for FORSMARK (SMHI-Station).



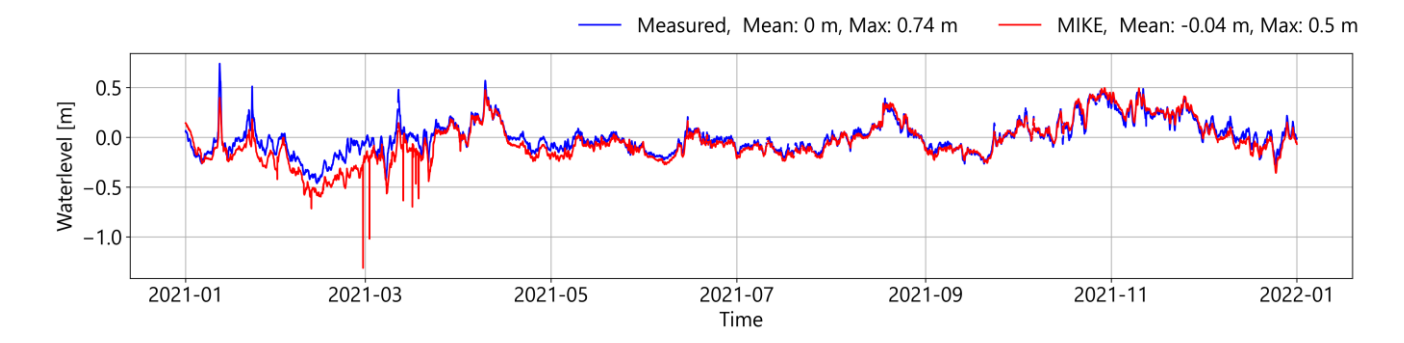
Comparison between observed water level in mMSL (blue line) and modelled water level (red line) for BÖNAN SJÖV. (SMHI-Station).



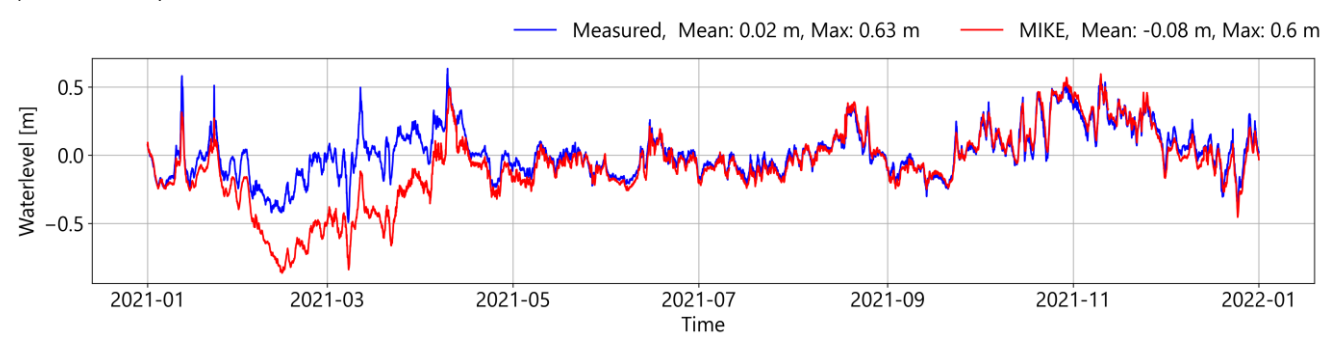
Comparison between observed water level in mMSL (blue line) and modelled water level (red line) for LJUSNE SJÖV (SMHI-Station).



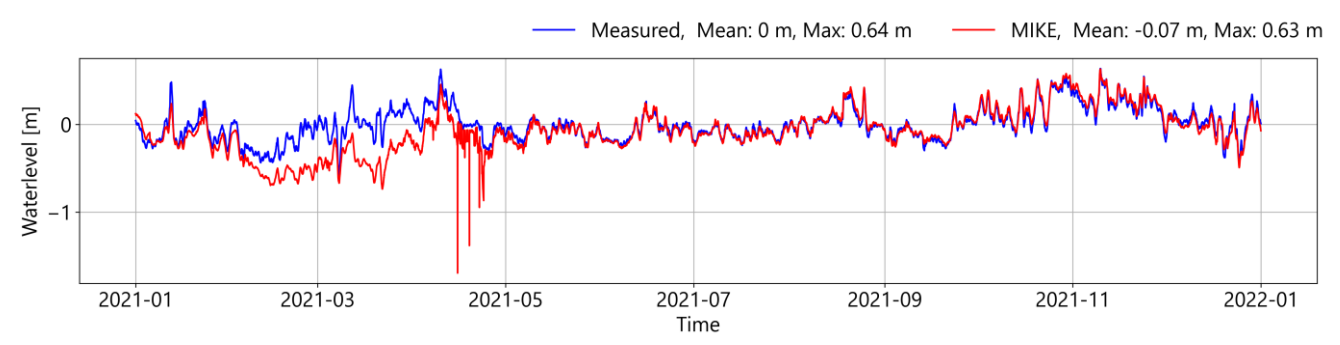
Comparison between observed water level in mMSL (blue line) and modelled water level (red line) for SPIKARNA (SMHI-Station).



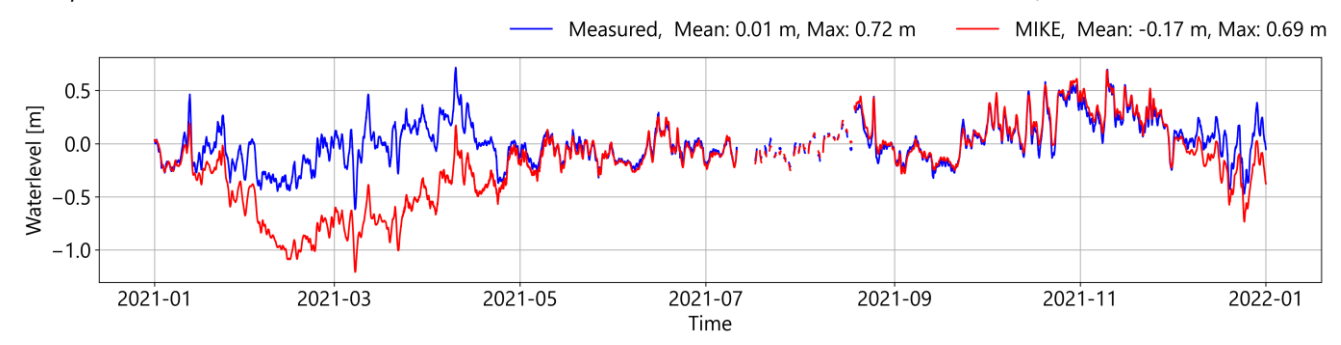
Comparison between observed water level in mMSL (blue line) and modelled water level (red line) for SKAGSUDDE SJÖV (SMHI-Station).



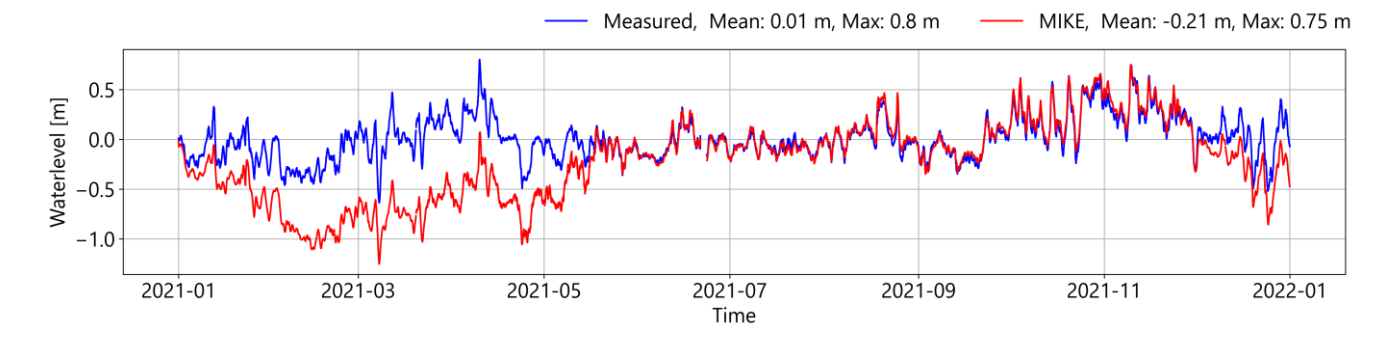
Comparison between observed water level in mMSL (blue line) and modelled water level (red line) for Holmsund (SMHI-Station).



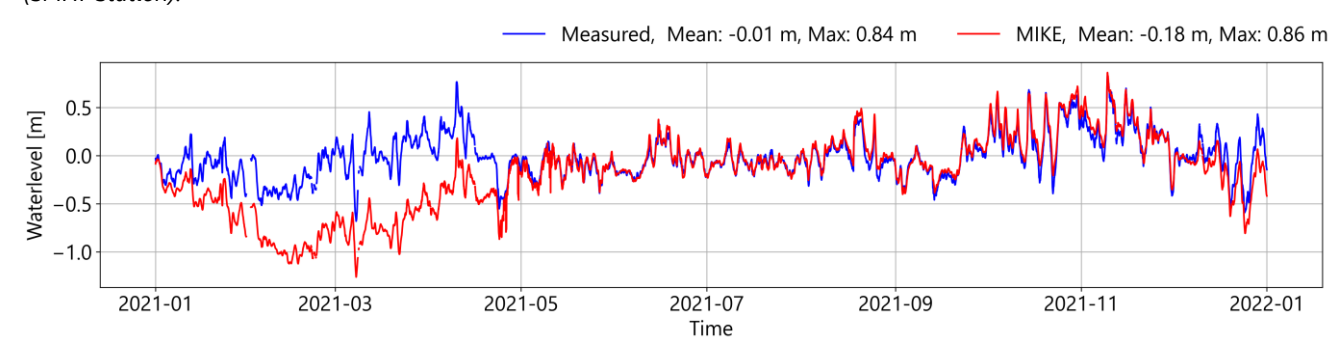
Comparison between observed water level in mMSL (blue line) and modelled water level (red line) for RATAN (SMHI-Station).



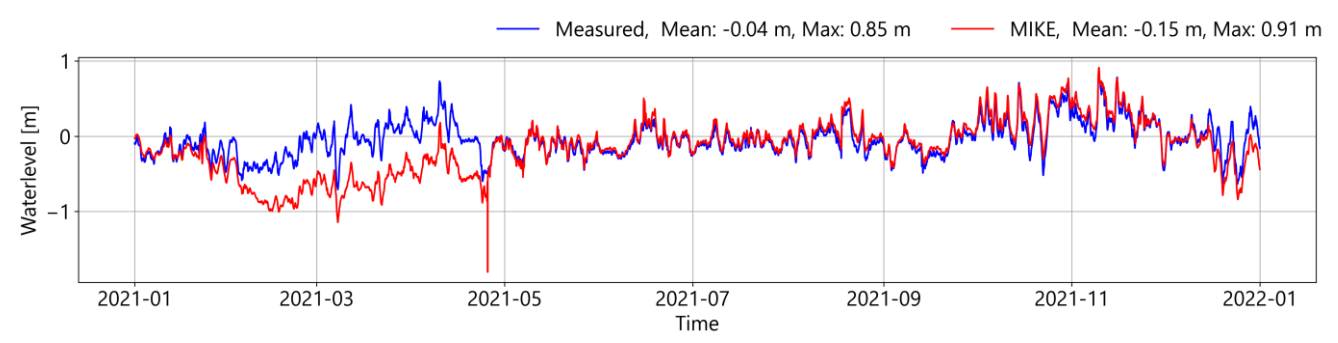
Comparison between observed water level in mMSL (blue line) and modelled water level (red line) for FURUGÖRUND (SMHI-Station).



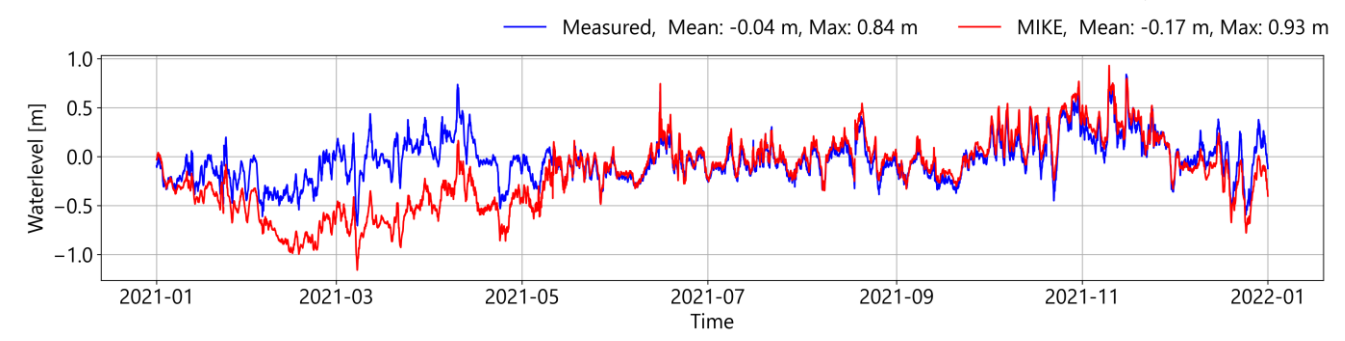
Comparison between observed water level in mMSL (blue line) and modelled water level (red line) for STRÖMÖREN SJÖV (SMHI-Station).



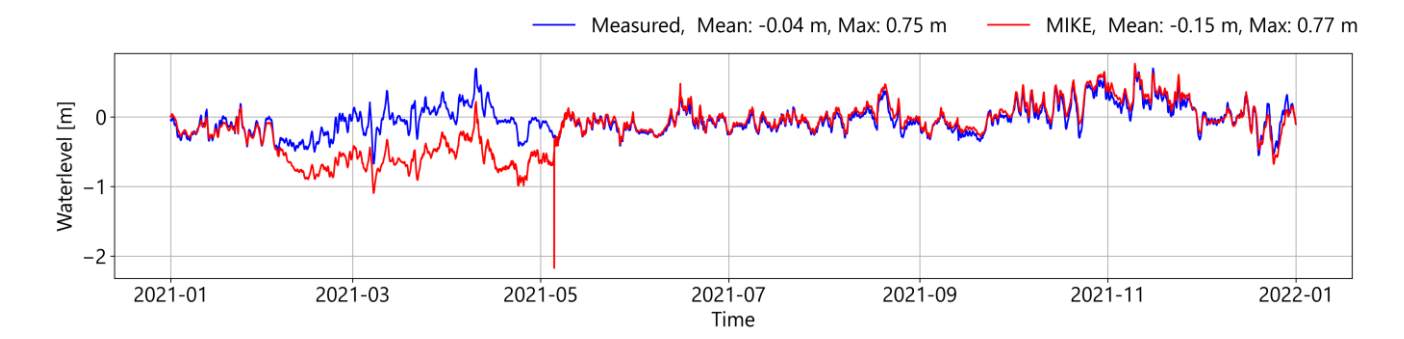
Comparison between observed water level in mMSL (blue line) and modelled water level (red line) for KALIX-KARLSBORG SJÖV (SMHI-Station).



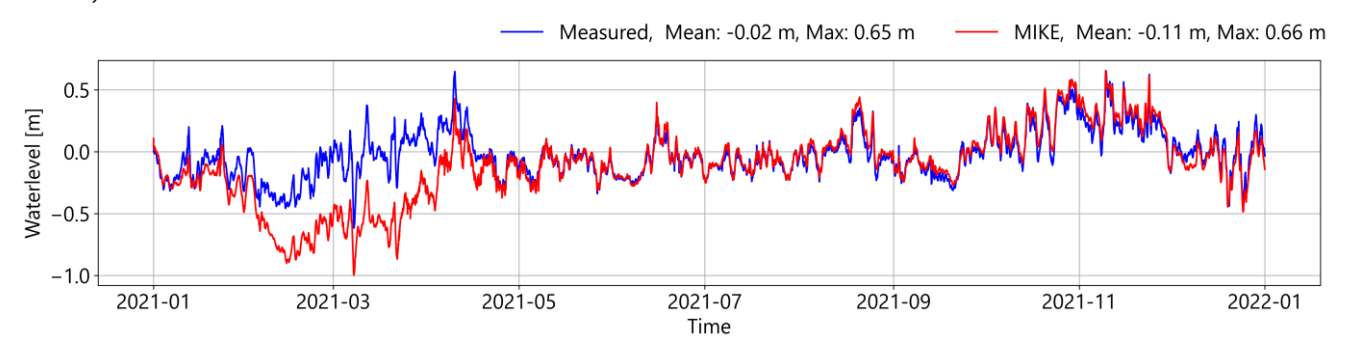
Comparison between observed water level in mMSL (blue line) and modelled water level (red line) for Kemi Ajos (FMI-Station).



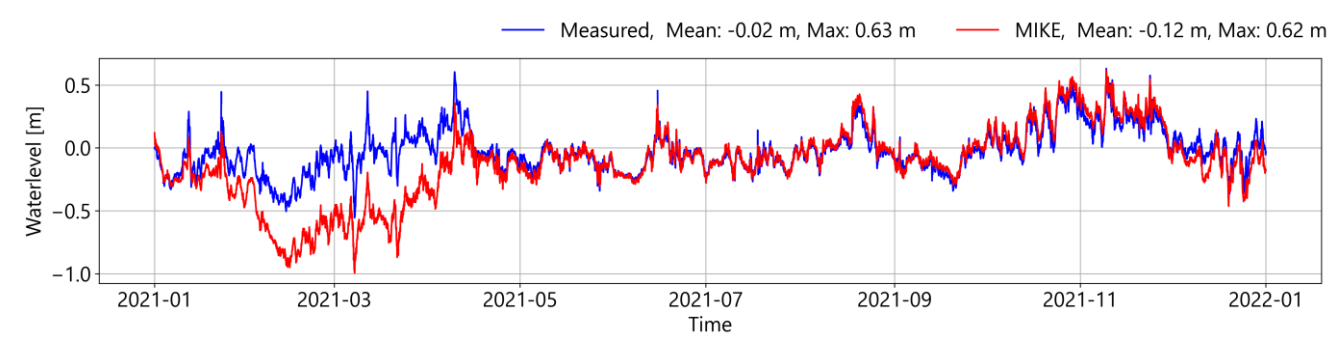
Comparison between observed water level in mMSL (blue line) and modelled water level (red line) for Oulu Toppila (FMI-Station).



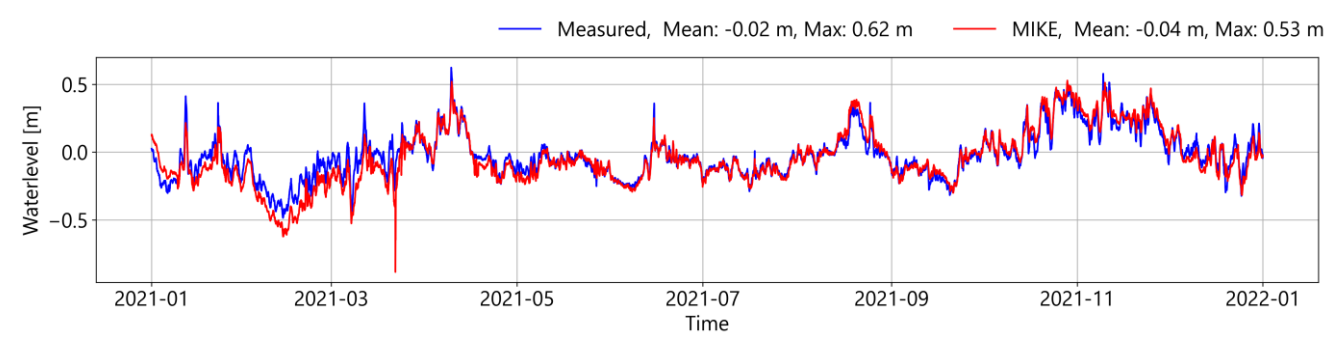
Comparison between observed water level in mMSL (blue line) and modelled water level (red line) for Raahe Lapaluoto (FMI-Station).



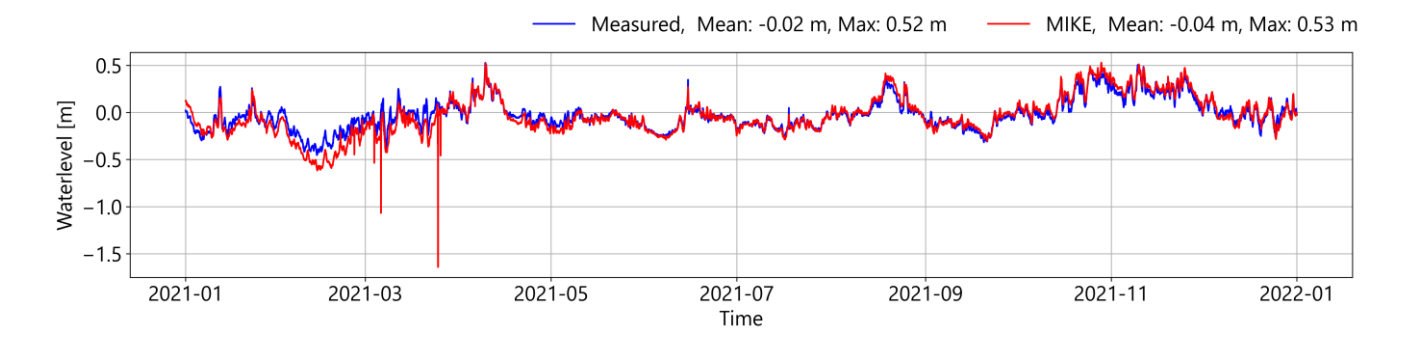
Comparison between observed water level in mMSL (blue line) and modelled water level (red line) for Pietarsaari Leppäluoto (FMI-Station).



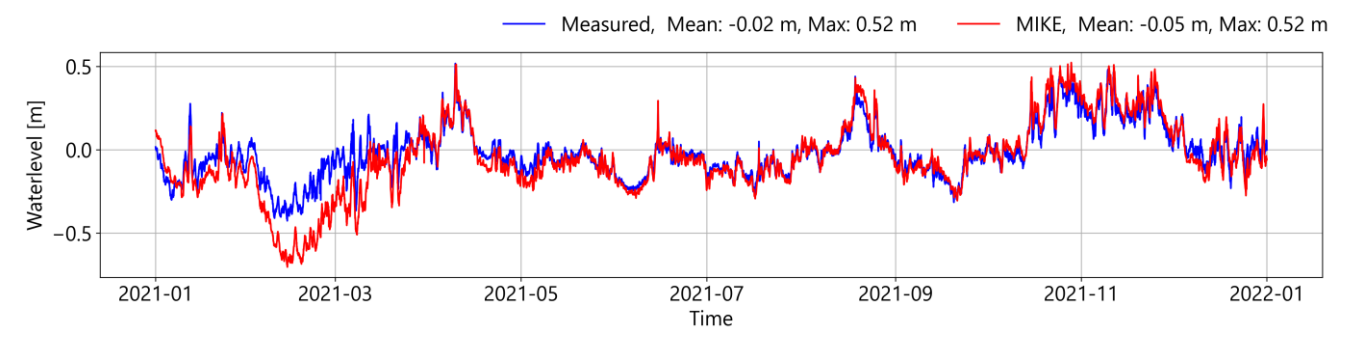
Comparison between observed water level in mMSL (blue line) and modelled water level (red line) for Vaasa Vaskiluoto (FMI-Station).



Comparison between observed water level in mMSL (blue line) and modelled water level (red line) for Kaskinen Ådskär (FMI-Station).



Comparison between observed water level in mMSL (blue line) and modelled water level (red line) for Pori Mäntyluoto Kallo (FMI-Station).



Comparison between observed water level in mMSL (blue line) and modelled water level (red line) for Rauma Petäjäs (FMI-Station).

Performance Metrics of the HD-Model in respect to the Waterlevels (March 2021)

Name	ME	MAE	RMSE	Correlation Coefficients	
	[m]	[m]	[m]	[m]	[-]
FORSMARK	-0.03	0.04	0.05	0.04	0.90
BÖNAN SJÖV	-0.06	0.06	0.08	0.05	0.88
LJUSNE SJÖV	-0.07	0.07	0.09	0.06	0.87
SPIKARNA	-0.07	0.07	0.10	0.07	0.87
SKAGSUDDE SJÖV	-0.11	0.11	0.15	0.10	0.79
Holmsund	-0.43	0.43	0.44	0.06	0.92
RATAN	-0.39	0.39	0.41	0.11	0.75
FURUÖGRUND	-0.73	0.73	0.73	0.06	0.94
STRÖMÖREN SJÖV	-0.76	0.76	0.77	0.07	0.95
KALIX-KARLSBORG SJÖV	-0.75	0.75	0.75	0.07	0.93
Kemi Ajos	-0.62	0.62	0.62	0.08	0.93
Oulu Toppila	-0.63	0.63	0.64	0.08	0.91
Raahe Lapaluoto	-0.59	0.59	0.60	0.07	0.93
Pietarsaari Leppäluoto	-0.52	0.52	0.53	0.06	0.92

Performance Metrics of the HD-Model in respect to the Waterlevels (July 2021)

Name	ME	MAE	RMSE	Std. of Residuals	Correlation Coefficients
	[m]	[m]	[m]	[m]	[-]
FORSMARK	-0.02	0.03	0.03	0.02	0.91
BÖNAN SJÖV	-0.04	0.04	0.05	0.02	0.89
LJUSNE SJÖV	-0.05	0.05	0.05	0.02	0.89
SPIKARNA	-0.04	0.04	0.04	0.02	0.93
SKAGSUDDE SJÖV	-0.03	0.03	0.04	0.02	0.93
Holmsund	-0.03	0.03	0.04	0.02	0.93
RATAN	-0.02	0.02	0.03	0.02	0.94
FURUÖGRUND	-0.02	0.02	0.03	0.02	0.95
STRÖMÖREN SJÖV	-0.01	0.03	0.03	0.03	0.92
KALIX-KARLSBORG SJÖV	0.00	0.02	0.03	0.03	0.94
Kemi Ajos	0.04	0.04	0.05	0.03	0.95
Oulu Toppila	0.04	0.04	0.05	0.04	0.94
Raahe Lapaluoto	0.03	0.03	0.04	0.03	0.95
Pietarsaari Leppäluoto	0.01	0.02	0.03	0.02	0.95

Performance Metrics of the HD-Model in respect to the Waterlevels (September 2021)

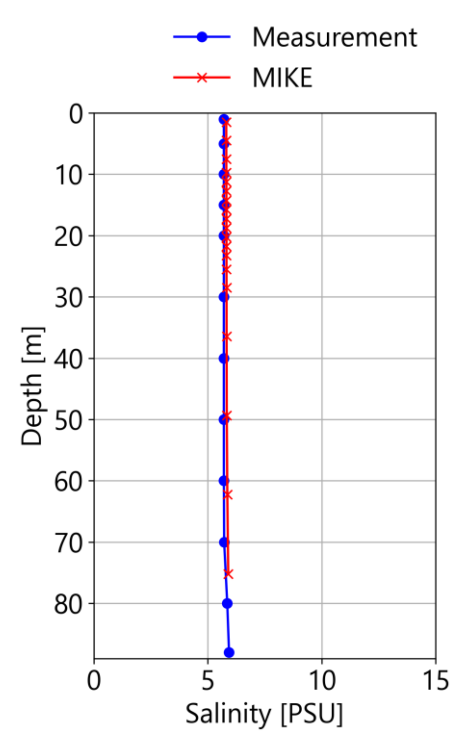
Name	ME	MAE	RMSE	Std. of Residuals	Correlation Coefficients
	[m]	[m]	[m]	[m]	[-]
FORSMARK	0.01	0.03	0.03	0.03	0.92
BÖNAN SJÖV	-0.01	0.03	0.03	0.03	0.92
LJUSNE SJÖV	-0.02	0.03	0.04	0.03	0.92
SPIKARNA	-0.01	0.02	0.03	0.03	0.94
SKAGSUDDE SJÖV	-0.01	0.02	0.03	0.03	0.95
Holmsund	-0.01	0.03	0.03	0.03	0.95
RATAN	0.01	0.03	0.03	0.03	0.95
FURUÖGRUND	0.00	0.03	0.03	0.03	0.96
STRÖMÖREN SJÖV	0.01	0.03	0.04	0.04	0.96
KALIX-KARLSBORG SJÖV	0.02	0.03	0.04	0.04	0.97
Kemi Ajos	0.05	0.05	0.06	0.04	0.97
Oulu Toppila	0.04	0.05	0.06	0.04	0.95
Raahe Lapaluoto	0.04	0.05	0.06	0.03	0.96
Pietarsaari Leppäluoto	0.02	0.03	0.04	0.03	0.95



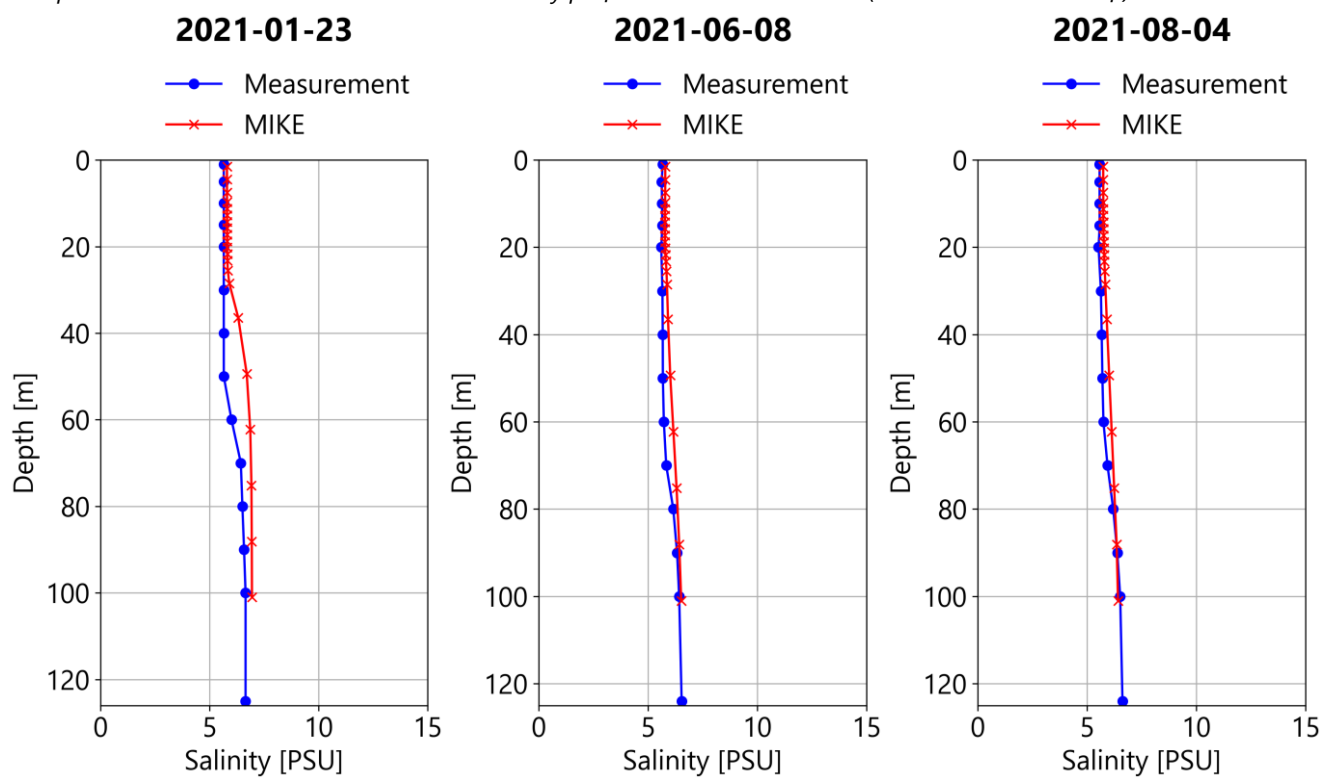
Appendix 14 Model verification: Salinity p	profiles
--	----------

Profiles from merihavainnot.fi

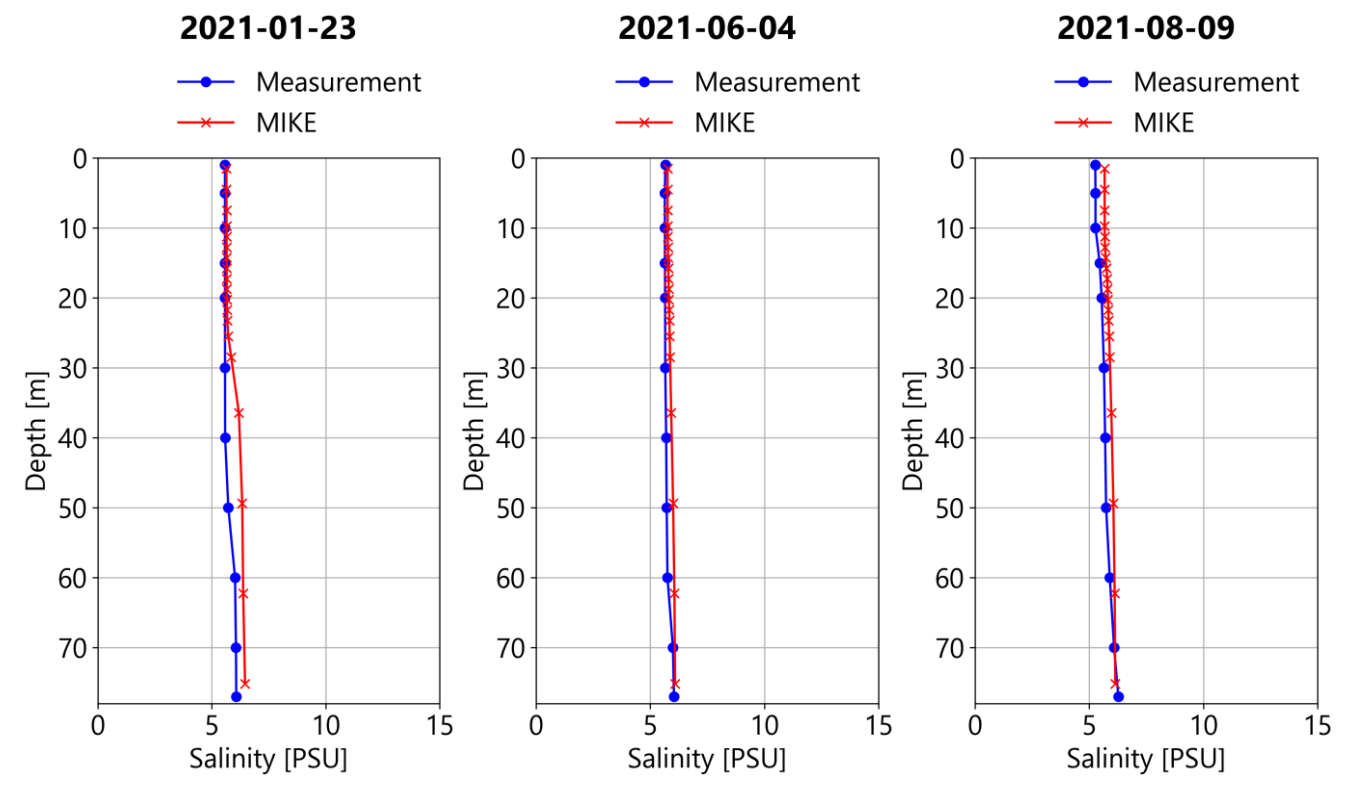




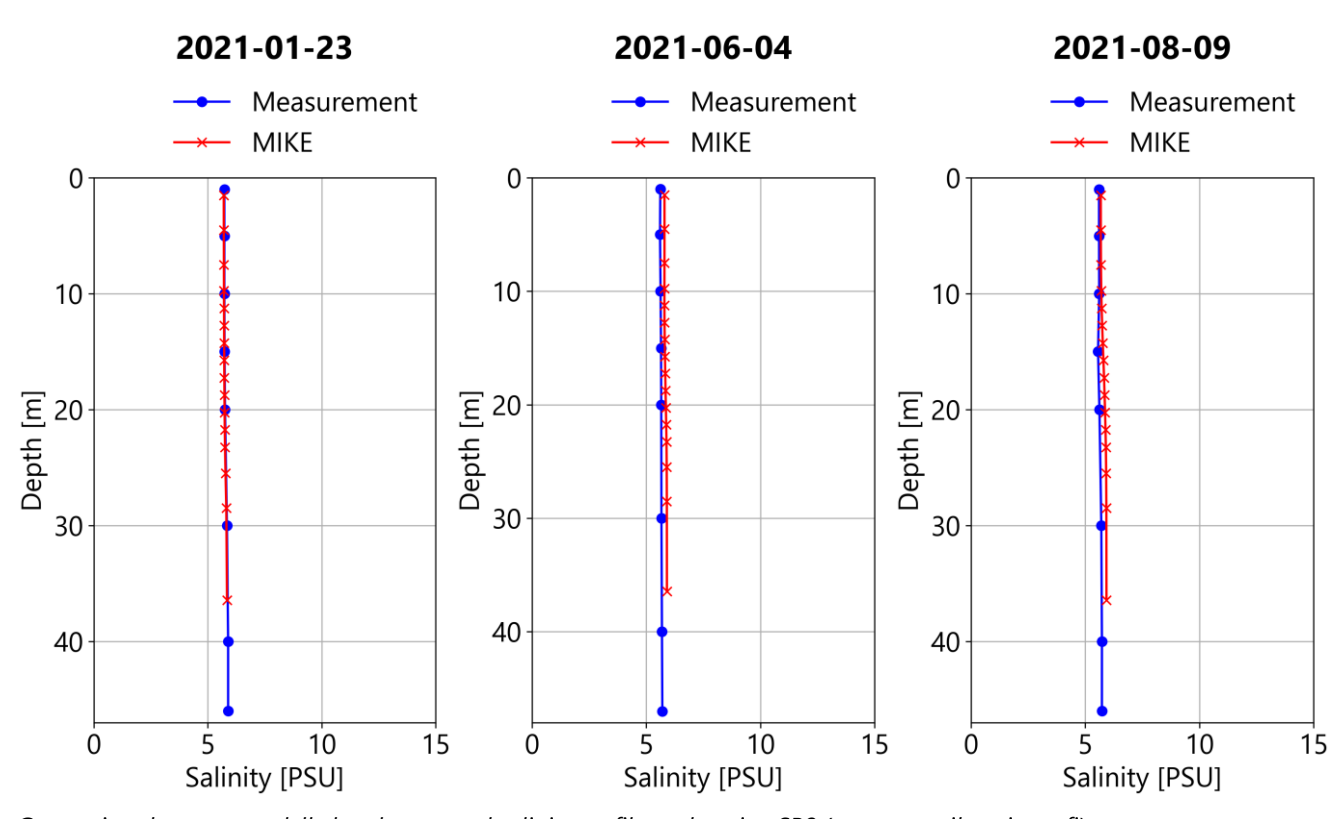
Comparison between modelled and measured salinity profiles at location MAME61 (source: merihavainnot.fi)



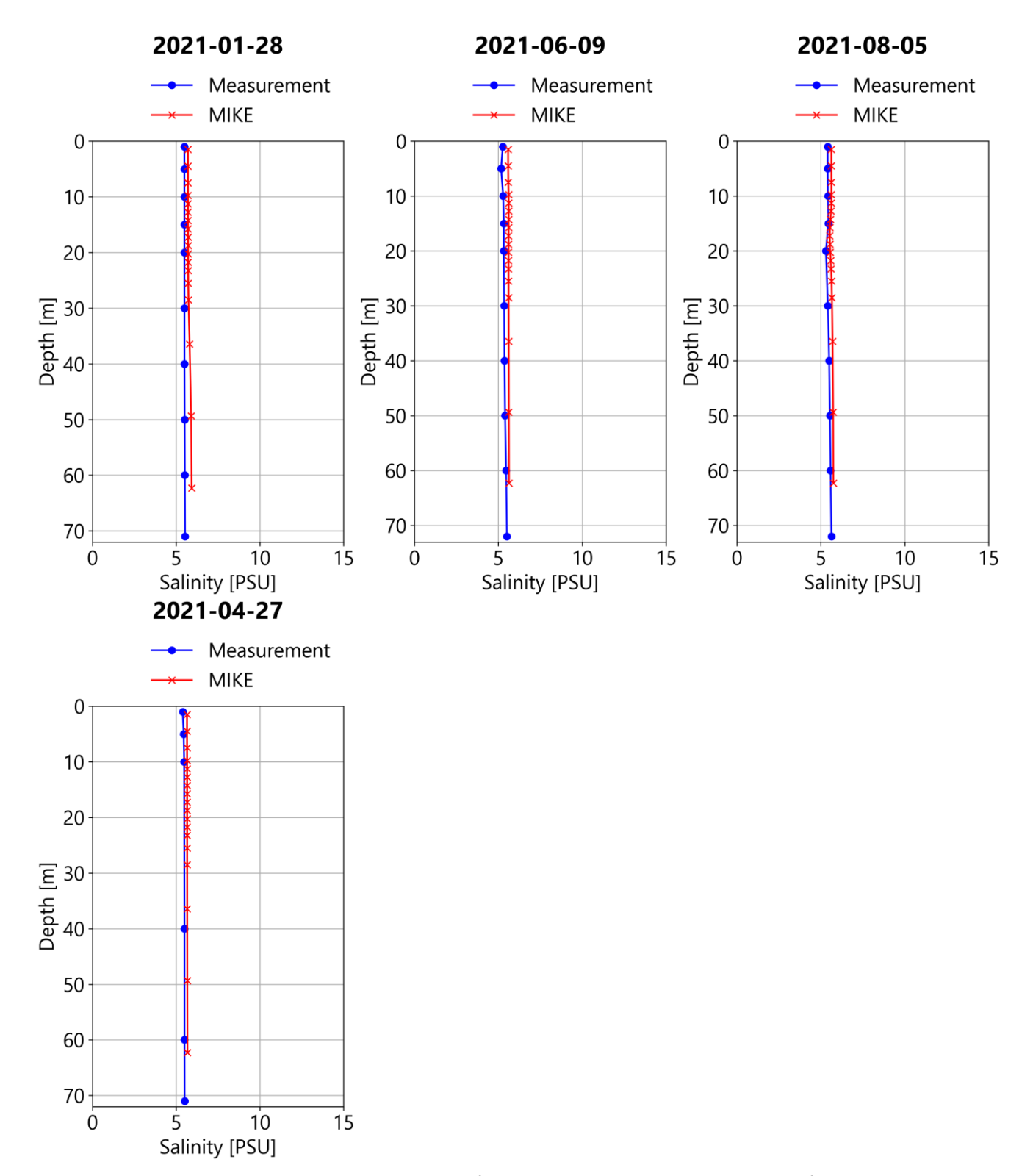
Comparison between modelled and measured salinity profiles at location SR5 (source: merihavainnot.fi)



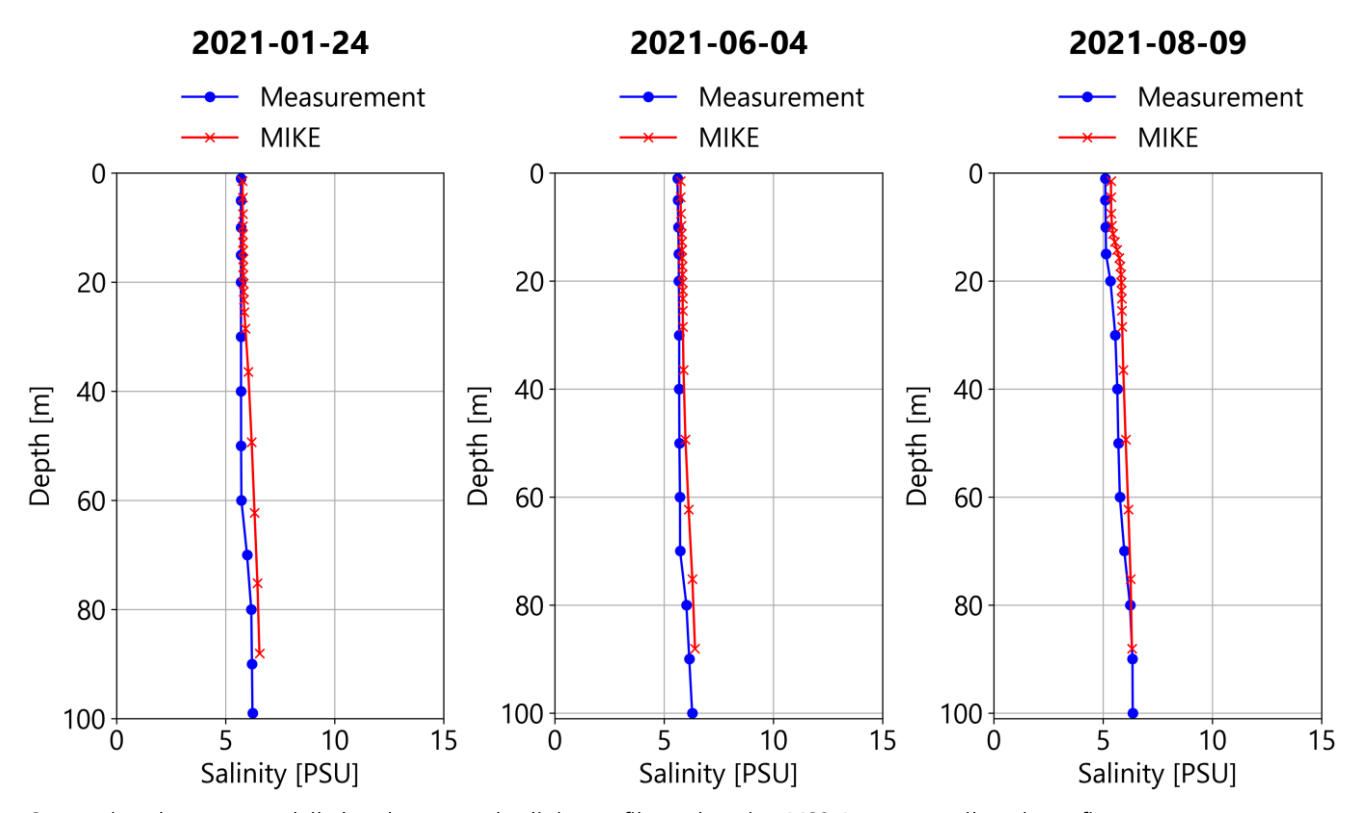
Comparison between modelled and measured salinity profiles at location SR7 (source: merihavainnot.fi)



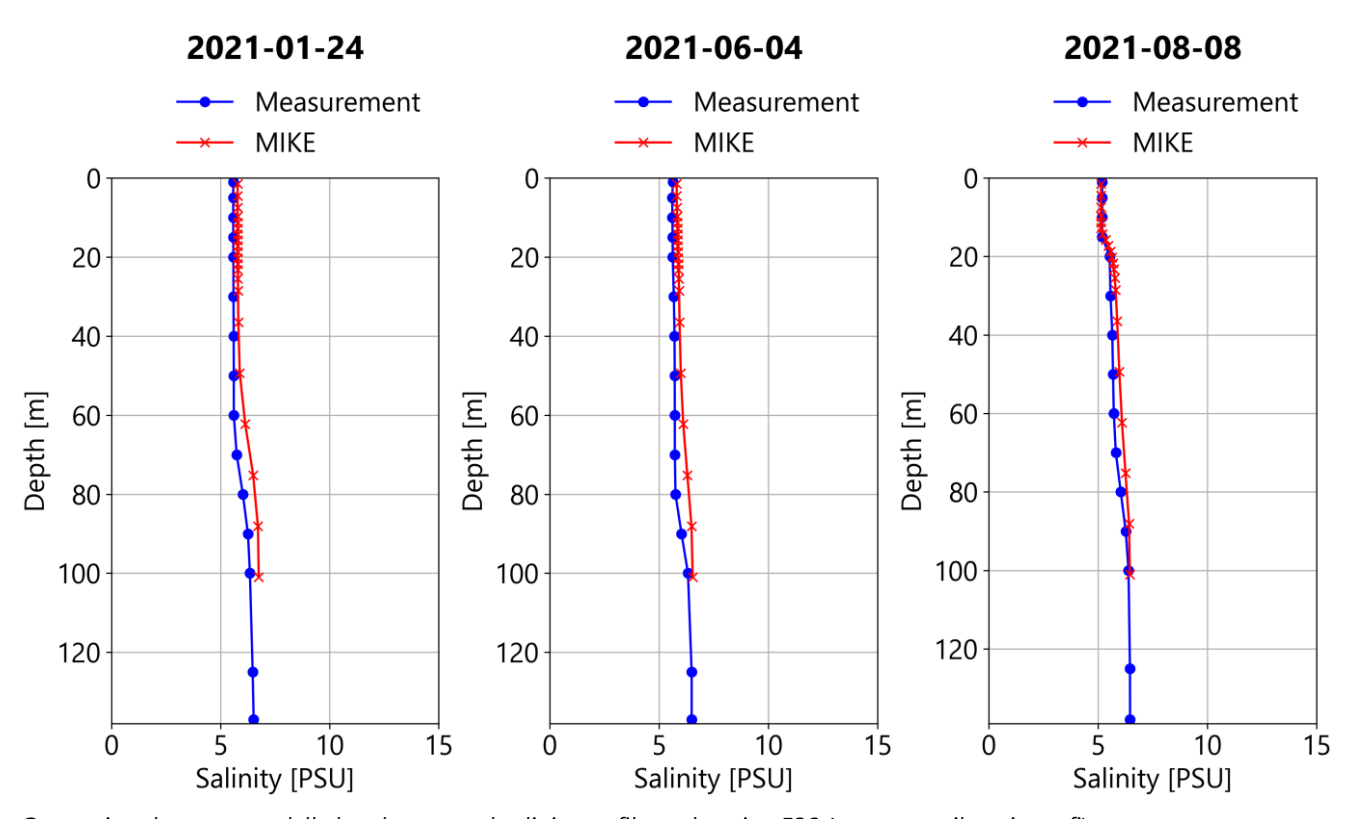
Comparison between modelled and measured salinity profiles at location SR8 (source: merihavainnot.fi)



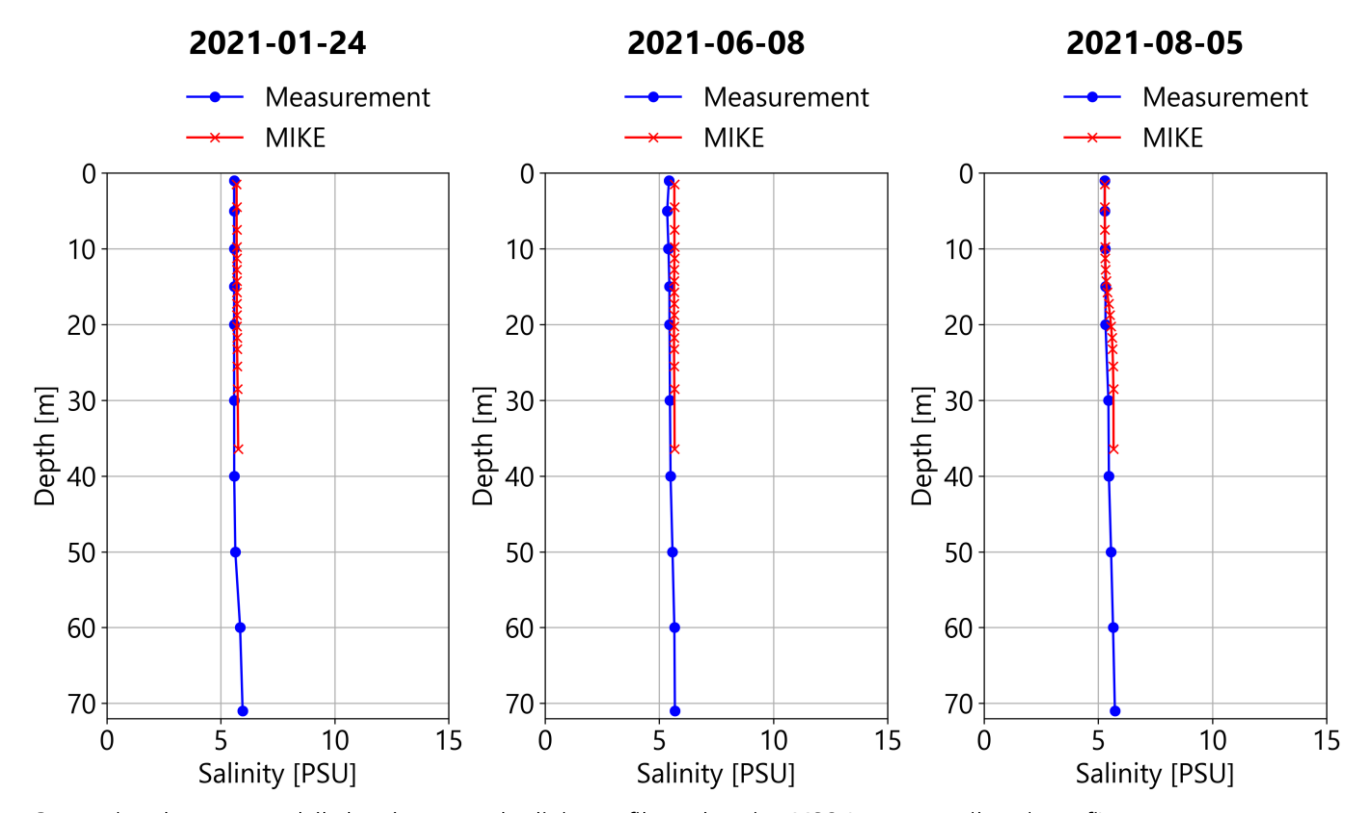
Comparison between modelled and measured salinity profiles at location SR3 (source: merihavainnot.fi)



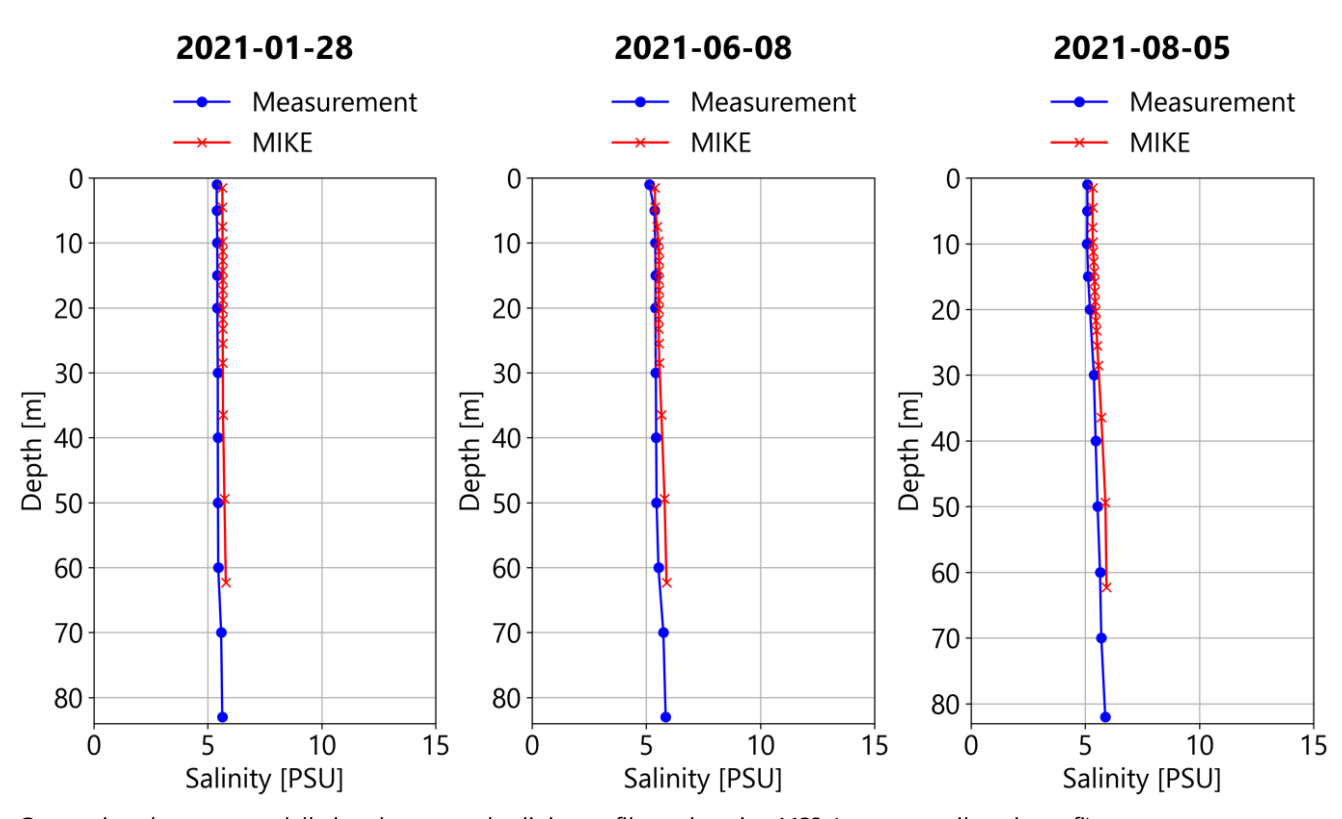
Comparison between modelled and measured salinity profiles at location MS9 (source: merihavainnot.fi)



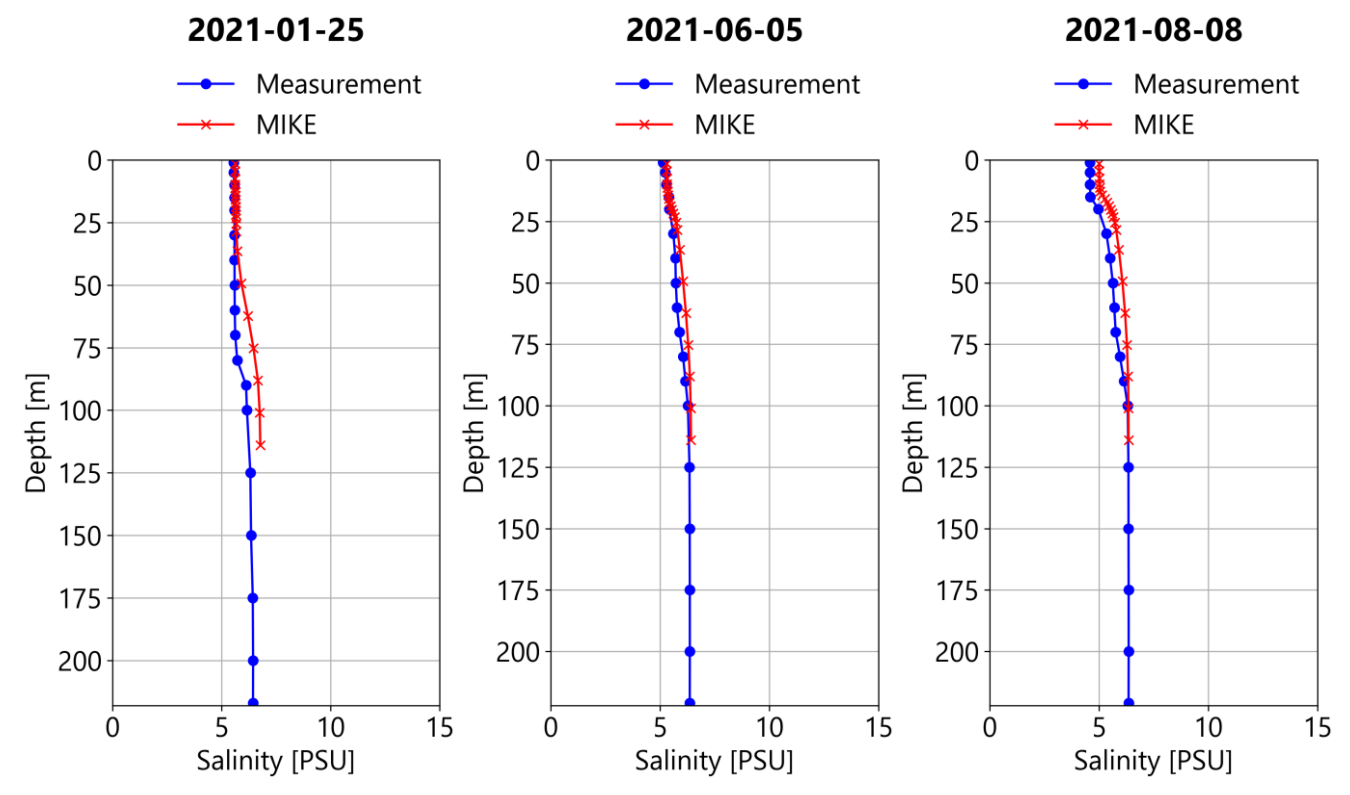
Comparison between modelled and measured salinity profiles at location F26 (source: merihavainnot.fi)



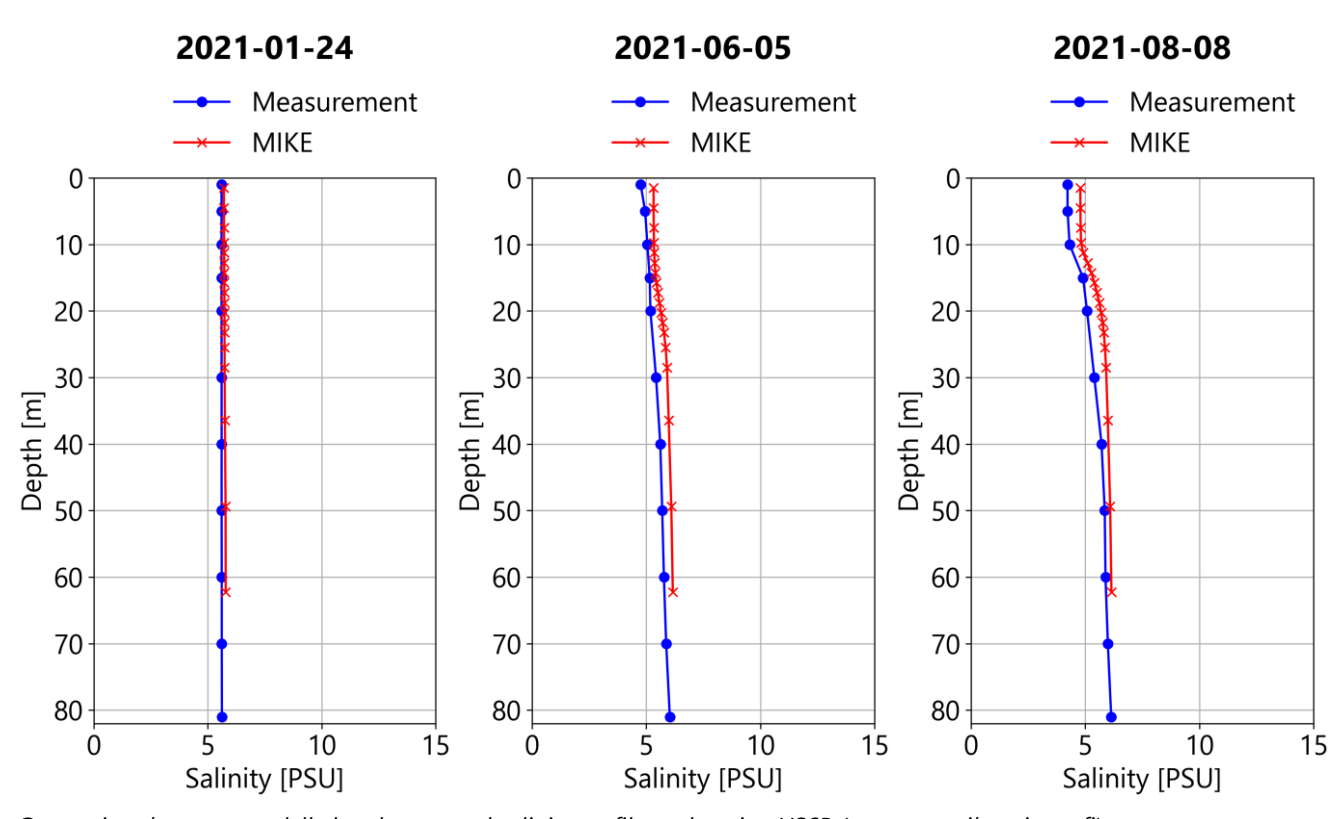
Comparison between modelled and measured salinity profiles at location MS6 (source: merihavainnot.fi)



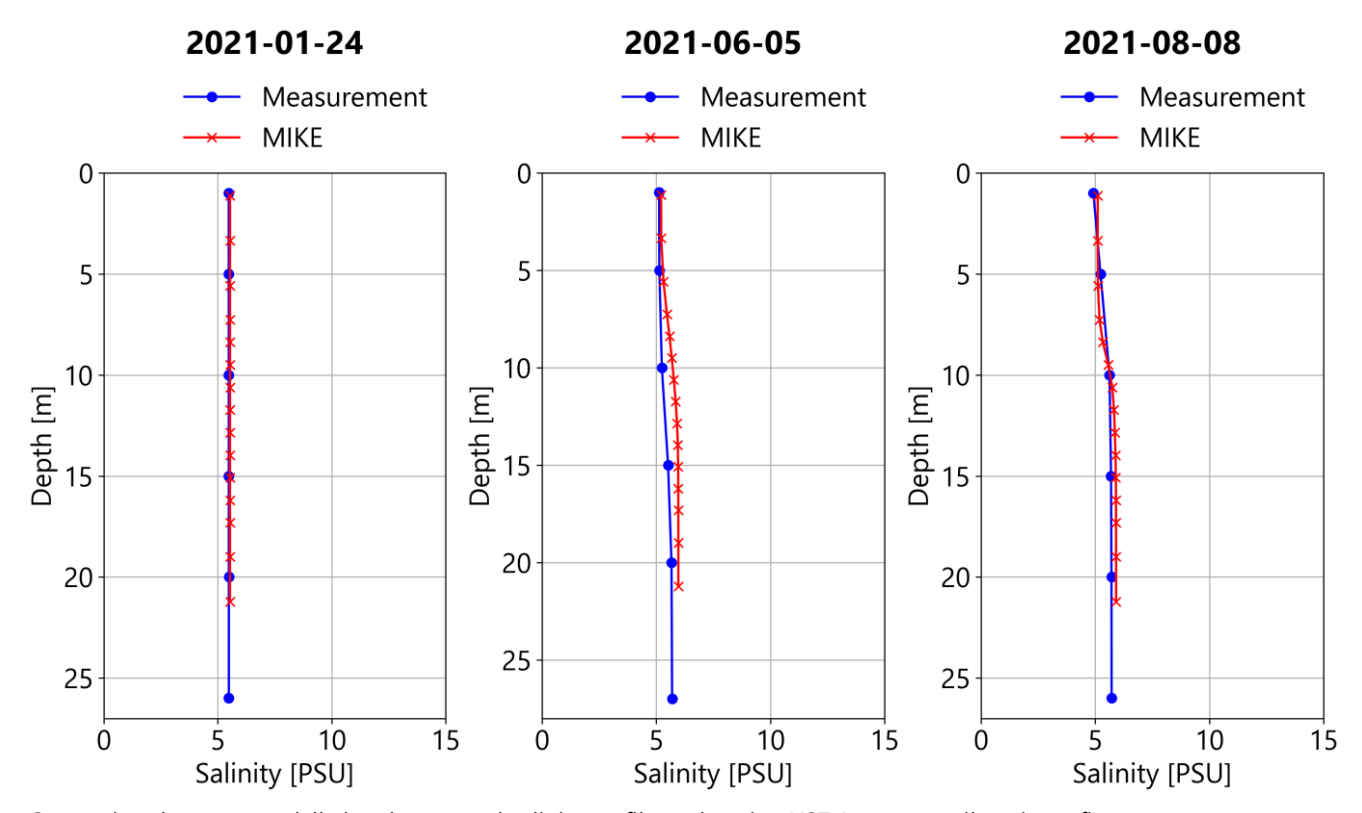
Comparison between modelled and measured salinity profiles at location MS3 (source: merihavainnot.fi)



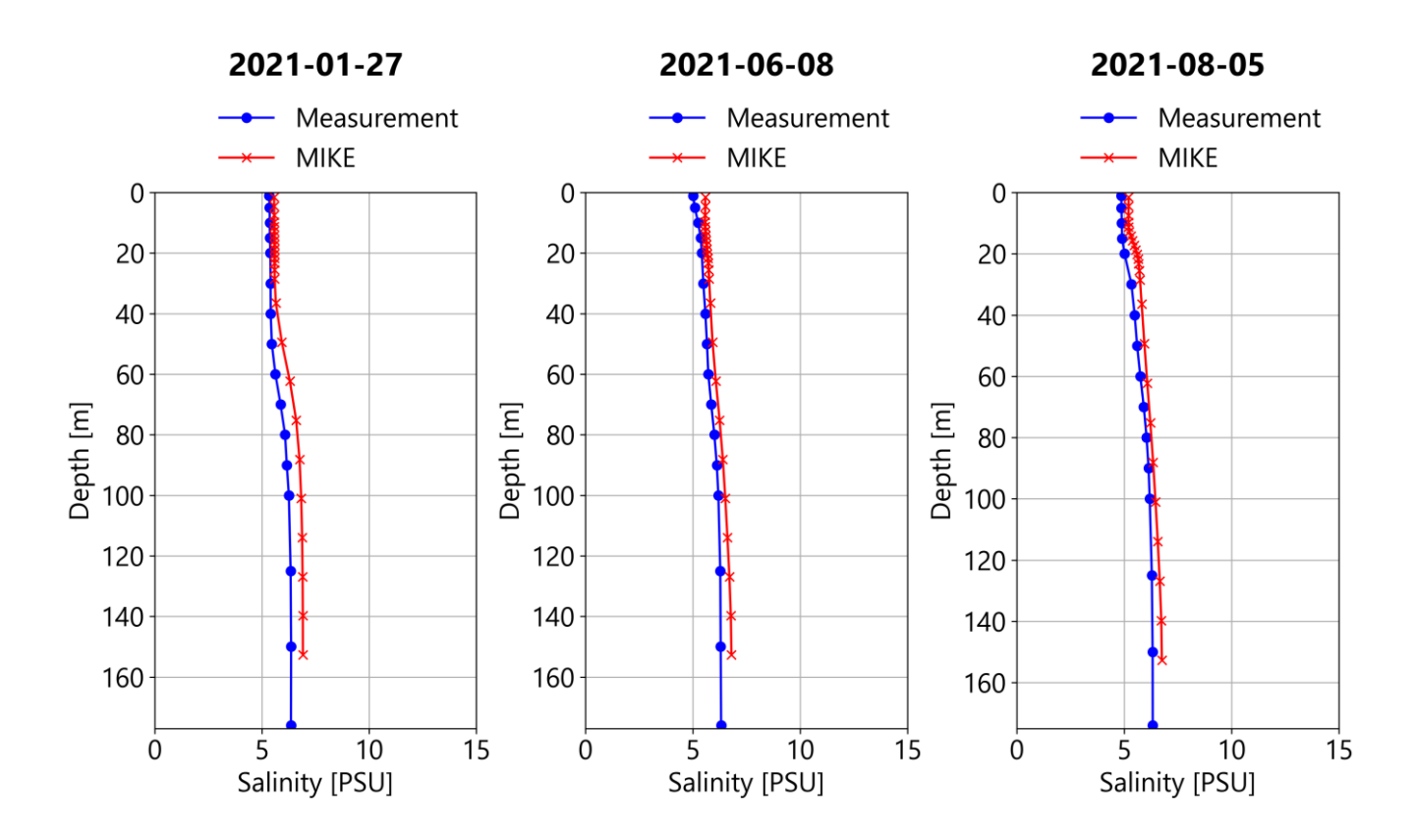
Comparison between modelled and measured salinity profiles at location US5B (source: merihavainnot.fi)



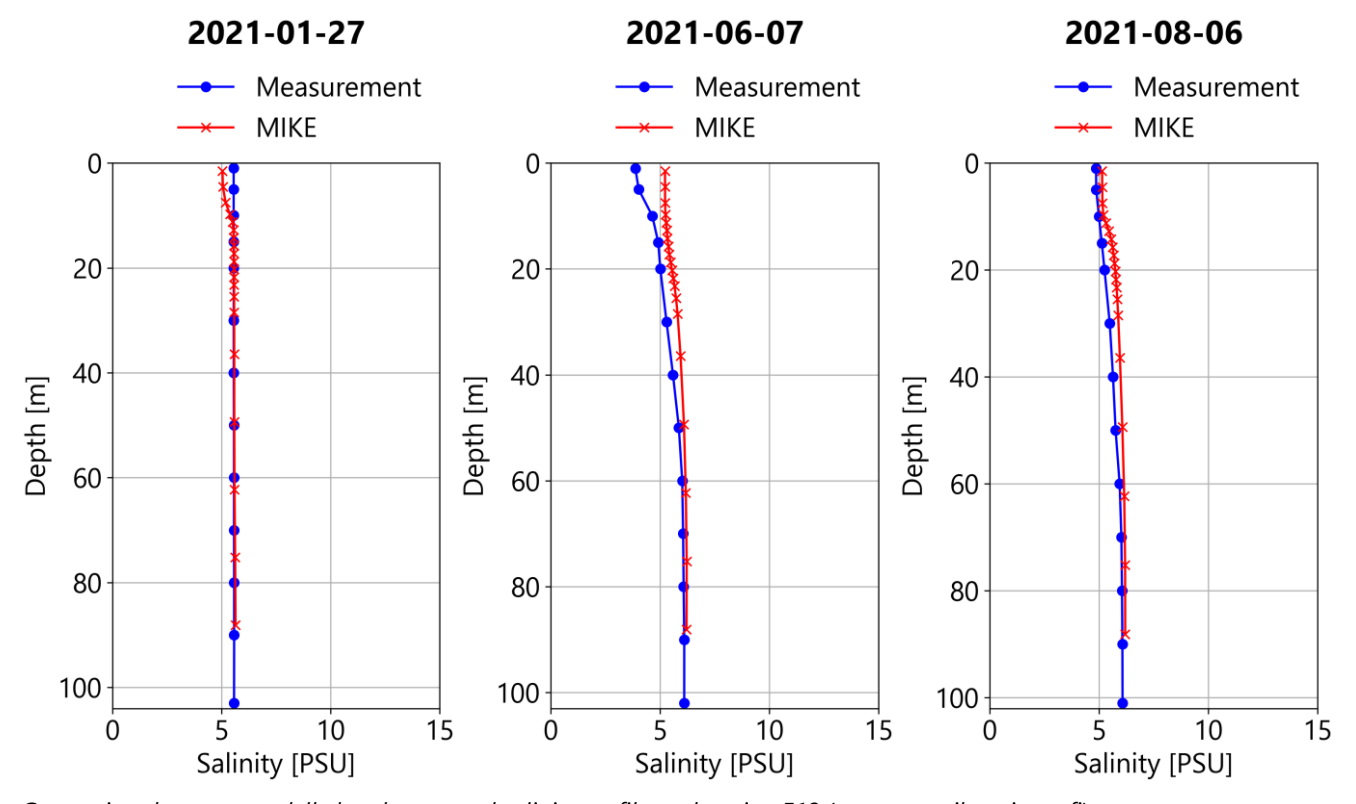
Comparison between modelled and measured salinity profiles at location US6B (source: merihavainnot.fi)



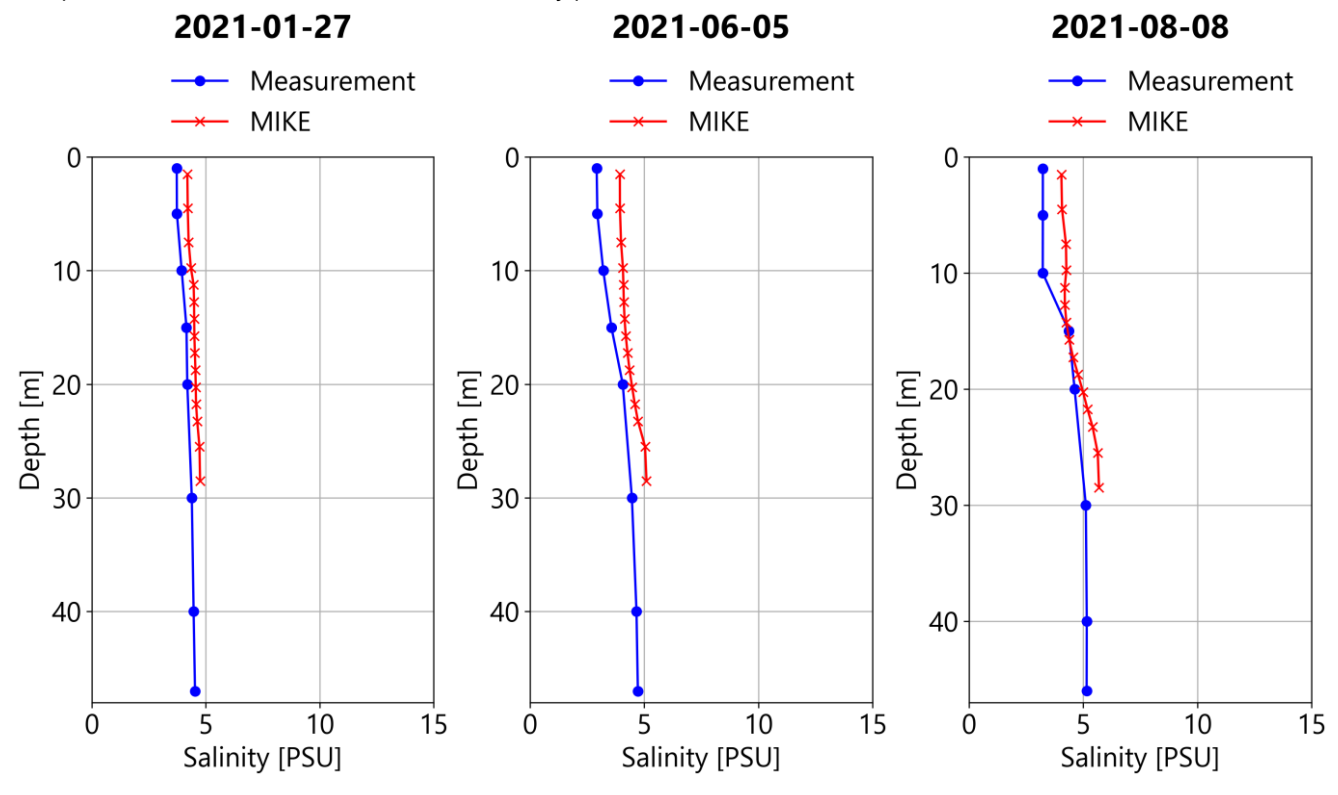
Comparison between modelled and measured salinity profiles at location US7 (source: merihavainnot.fi)



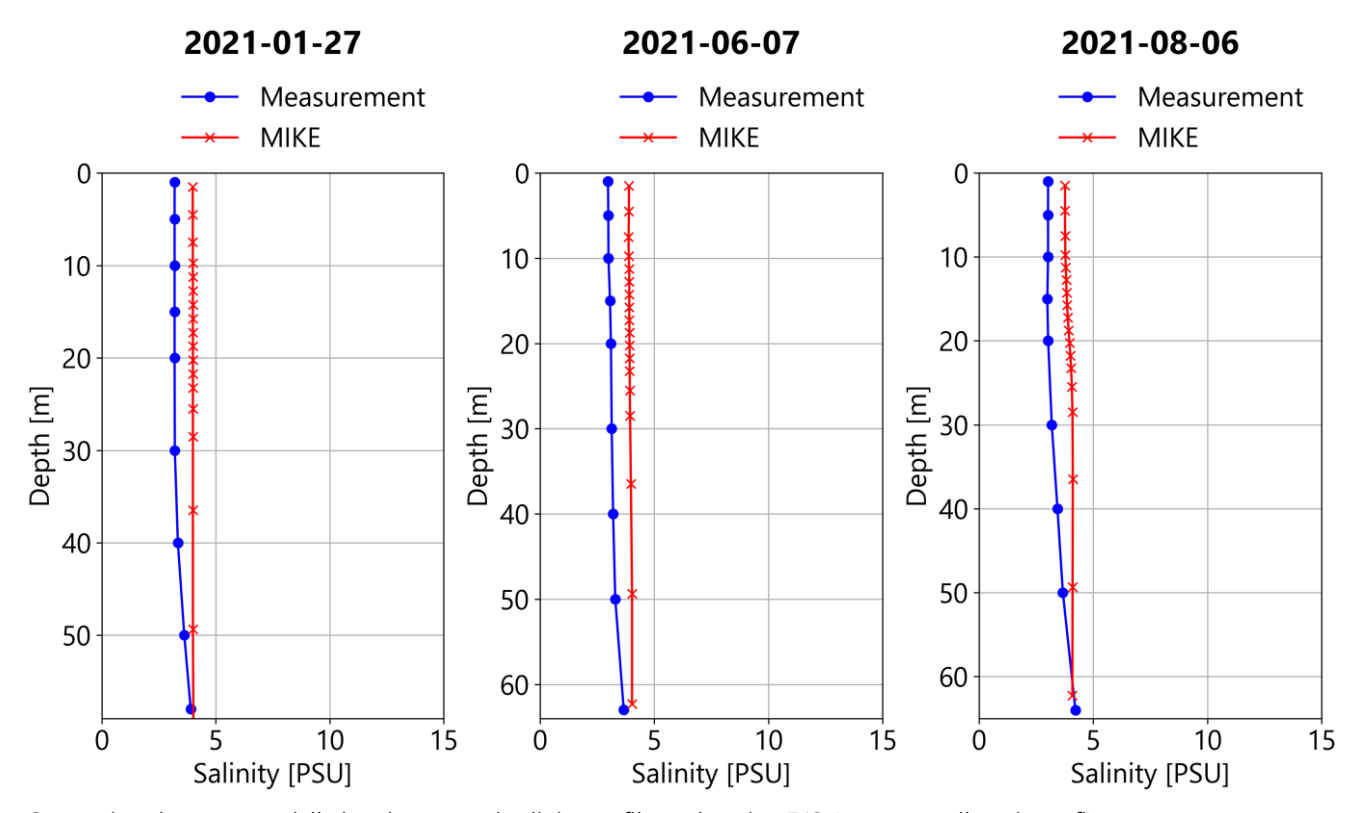
Comparison between modelled and measured salinity profiles at location US3 (source: merihavainnot.fi)



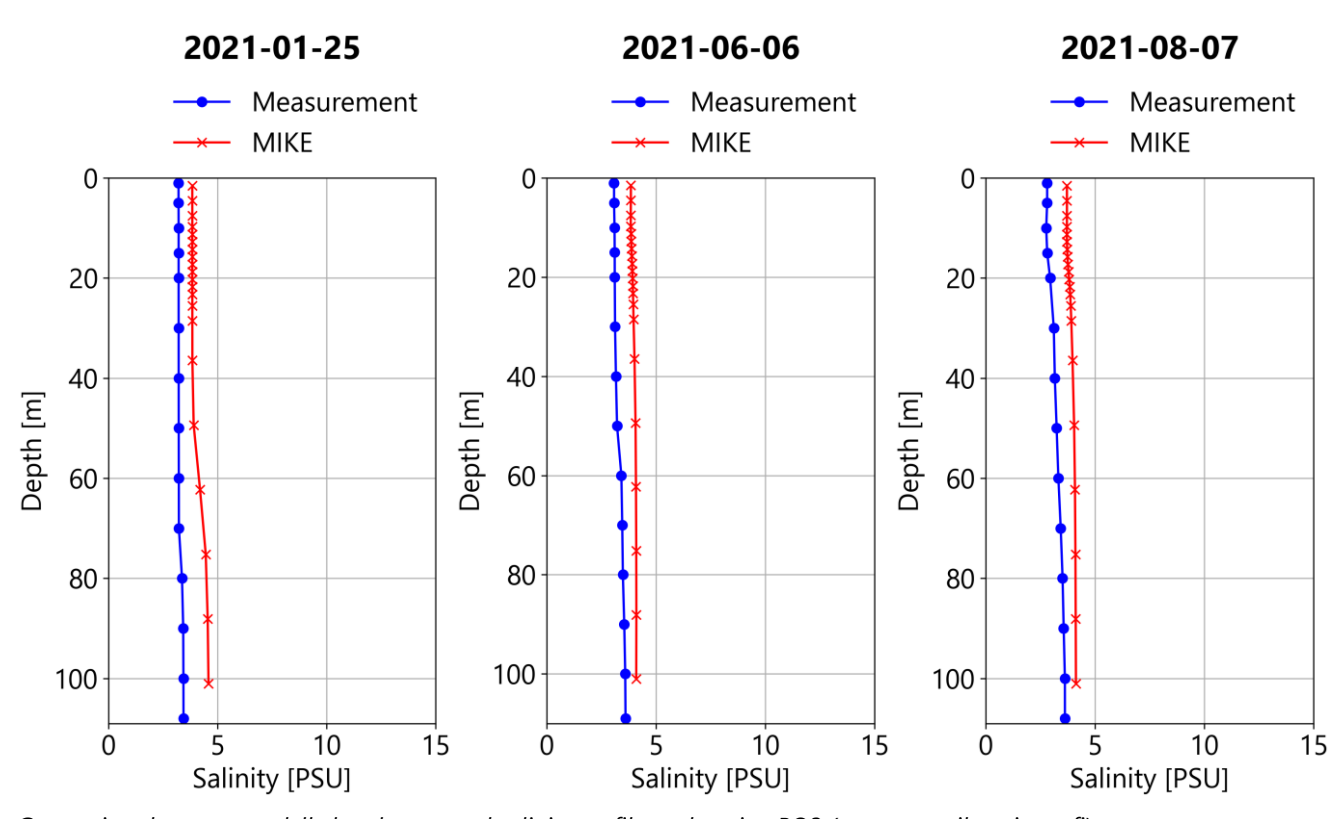
Comparison between modelled and measured salinity profiles at location F18 (source: merihavainnot.fi)



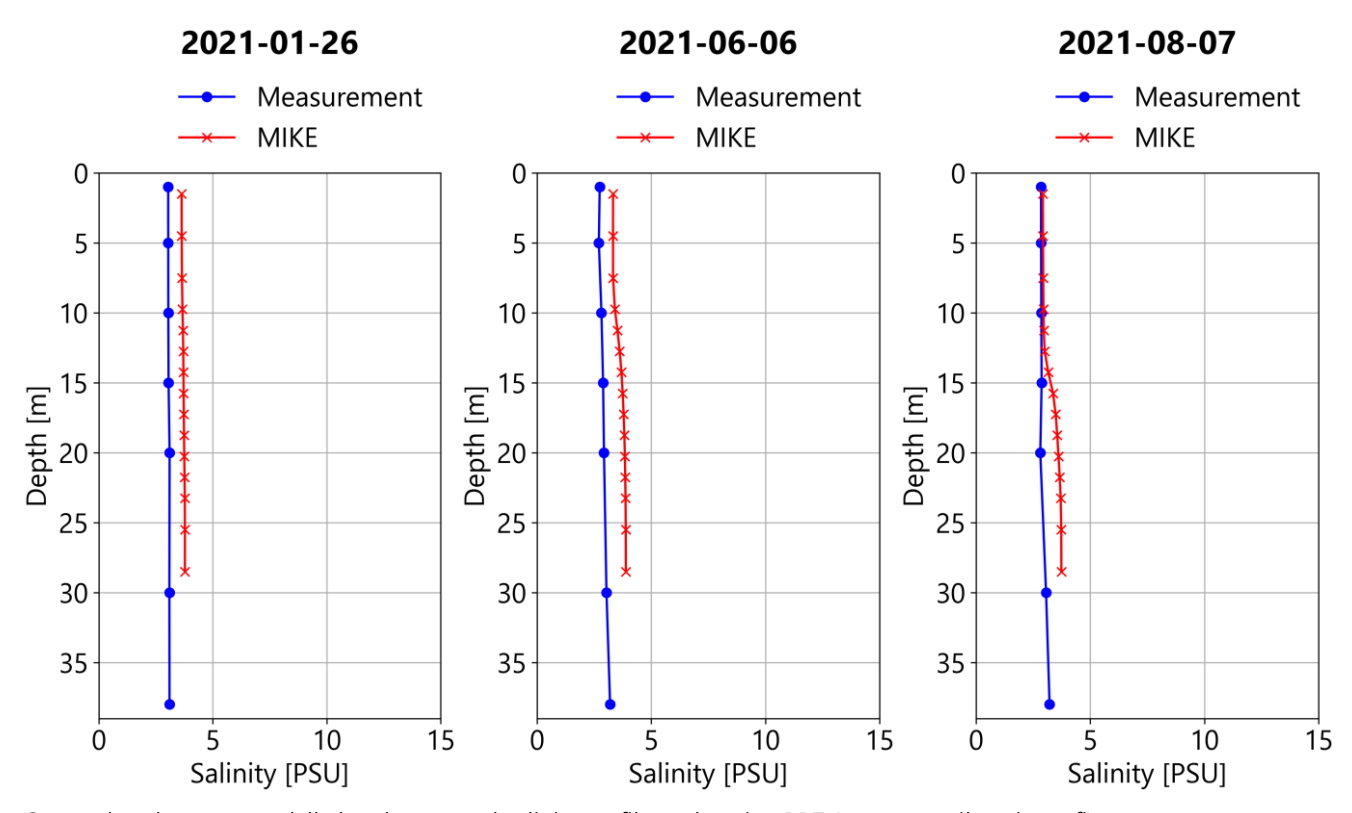
Comparison between modelled and measured salinity profiles at location F16 (source: merihavainnot.fi)



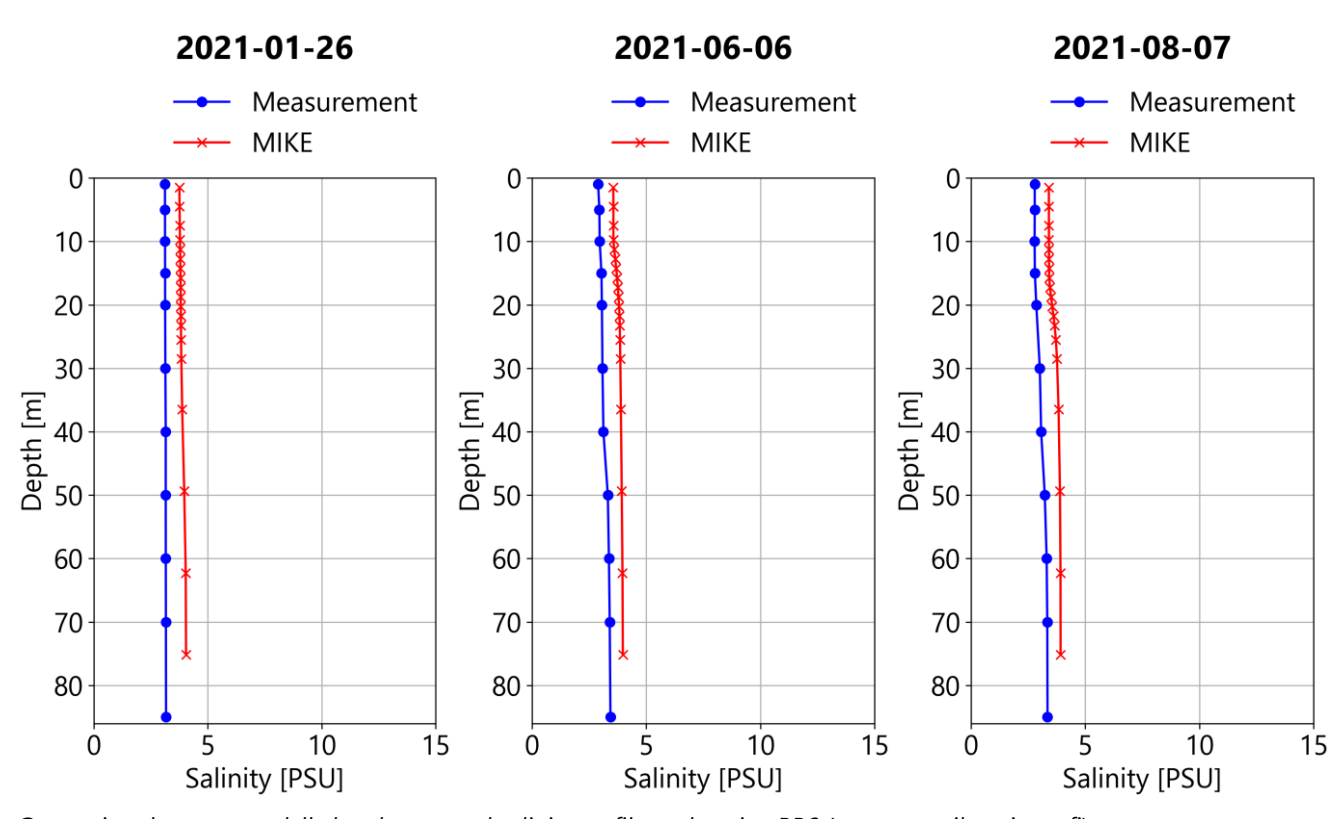
Comparison between modelled and measured salinity profiles at location F13 (source: merihavainnot.fi)



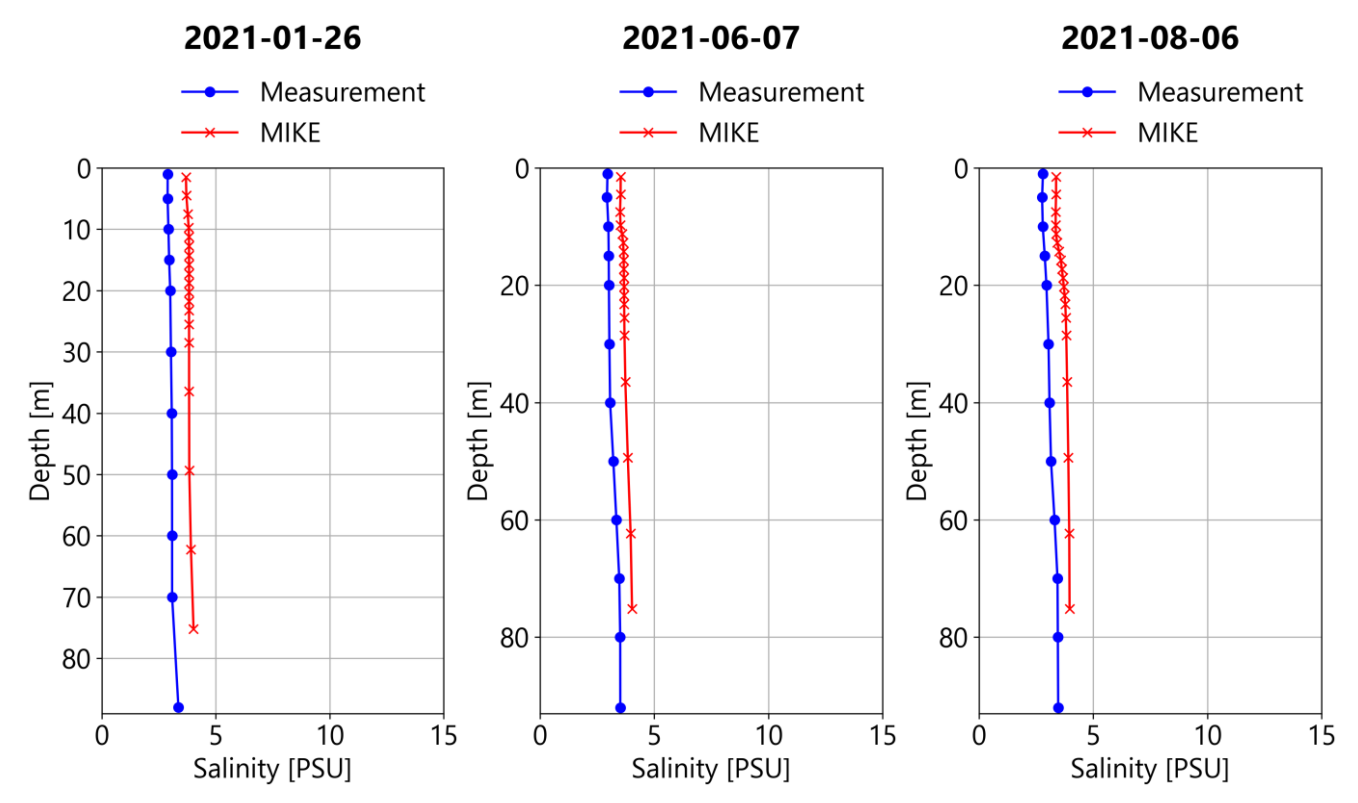
Comparison between modelled and measured salinity profiles at location BO3 (source: merihavainnot.fi)



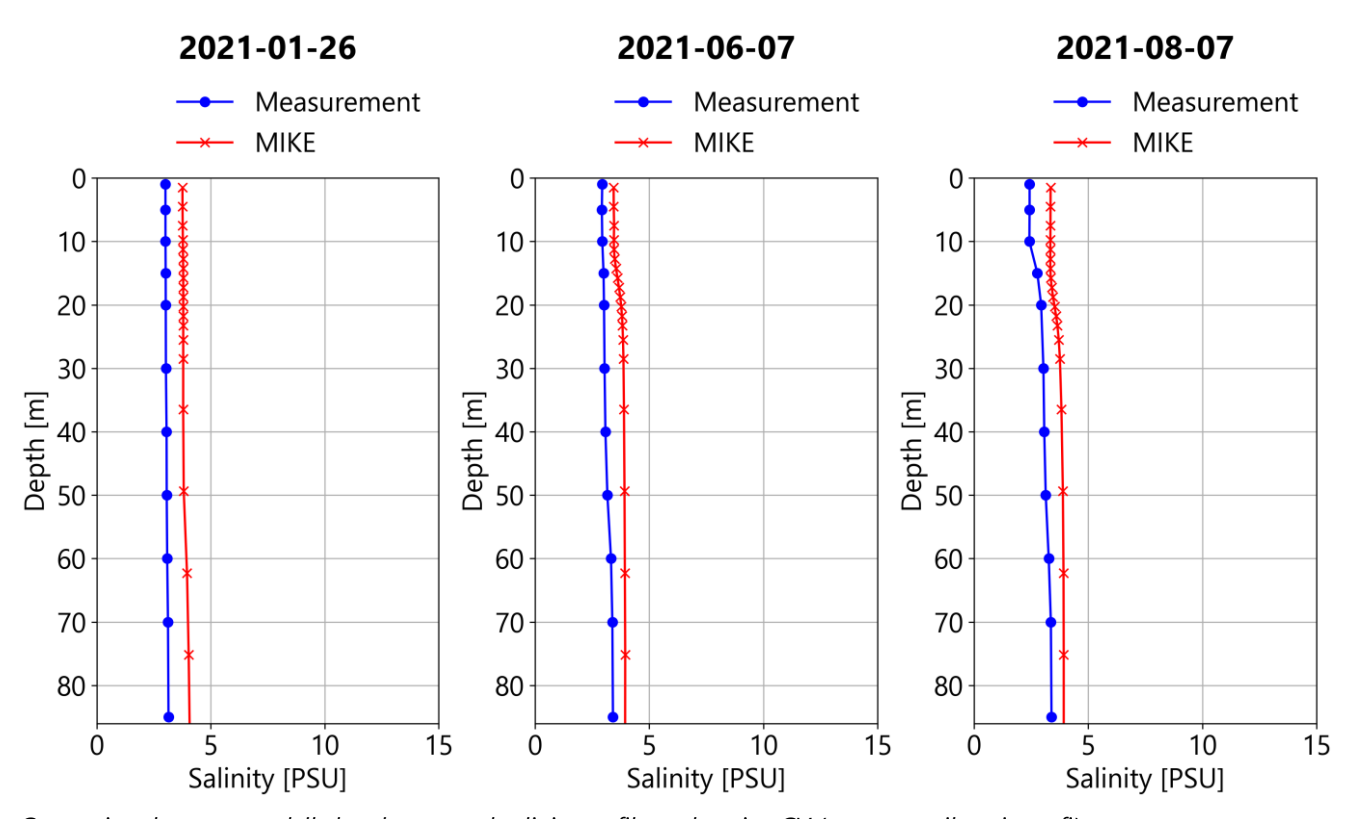
Comparison between modelled and measured salinity profiles at location RR7 (source: merihavainnot.fi)



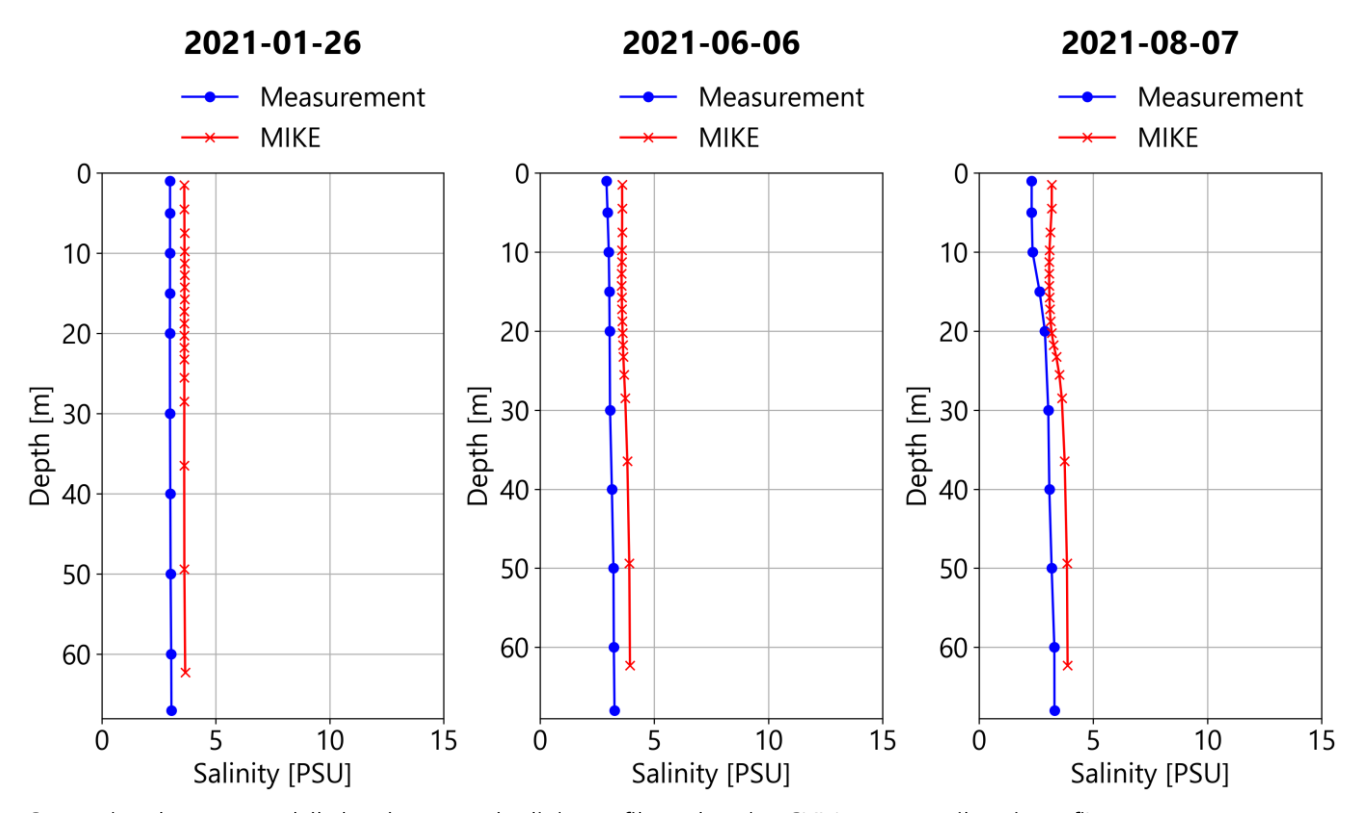
Comparison between modelled and measured salinity profiles at location RR6 (source: merihavainnot.fi)



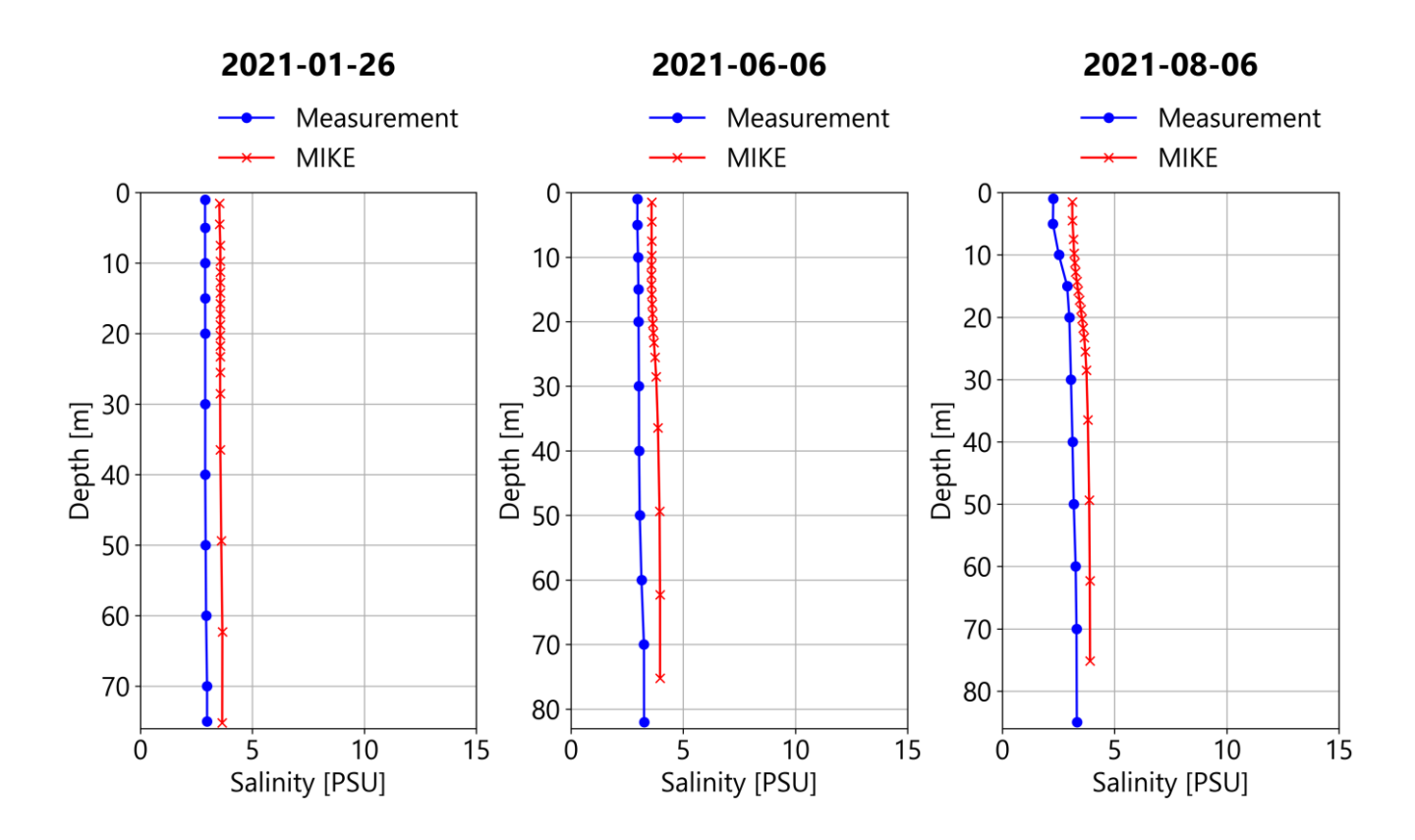
Comparison between modelled and measured salinity profiles at location RR3 (source: merihavainnot.fi)



Comparison between modelled and measured salinity profiles at location CV (source: merihavainnot.fi)

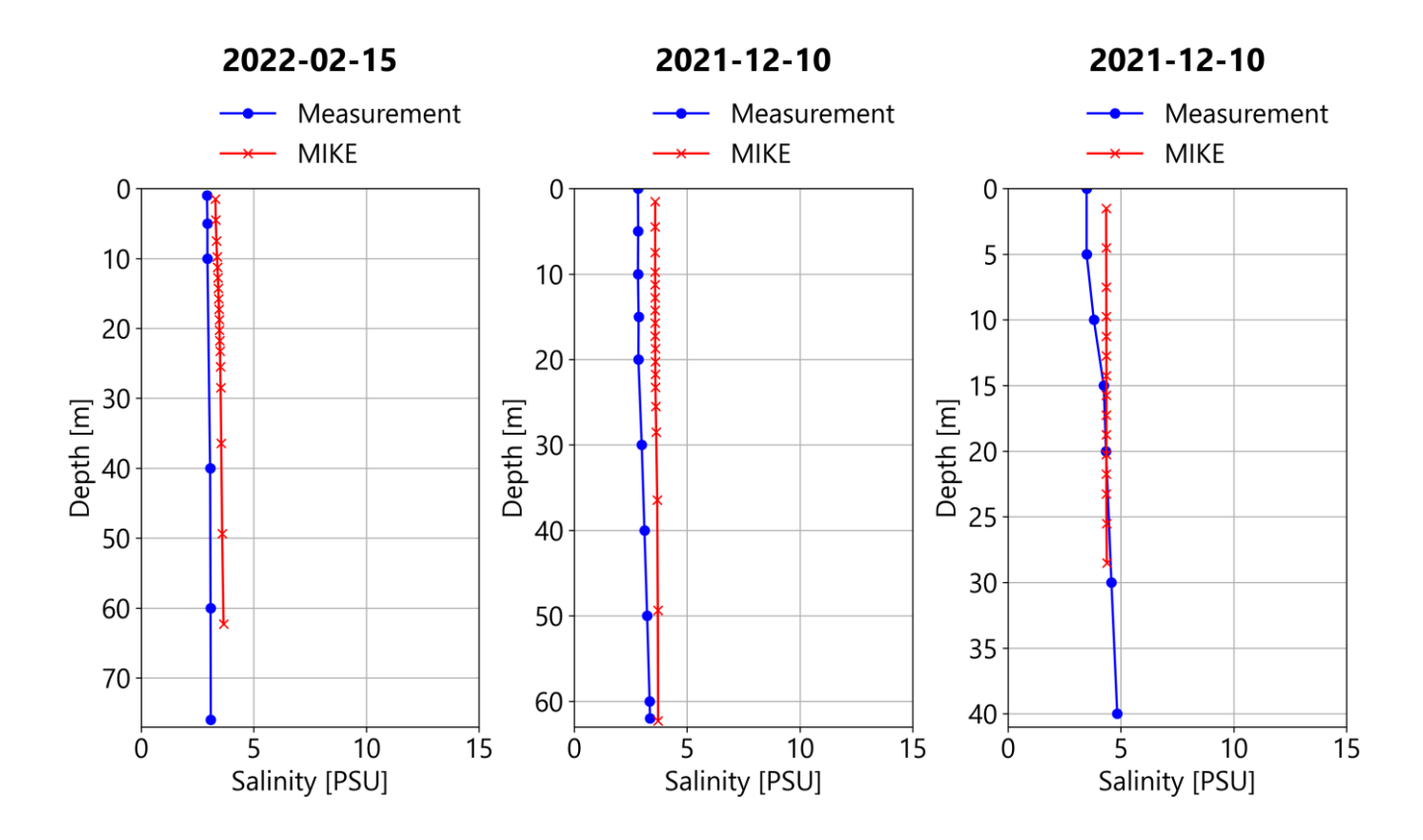


Comparison between modelled and measured salinity profiles at location CVI (source: merihavainnot.fi)

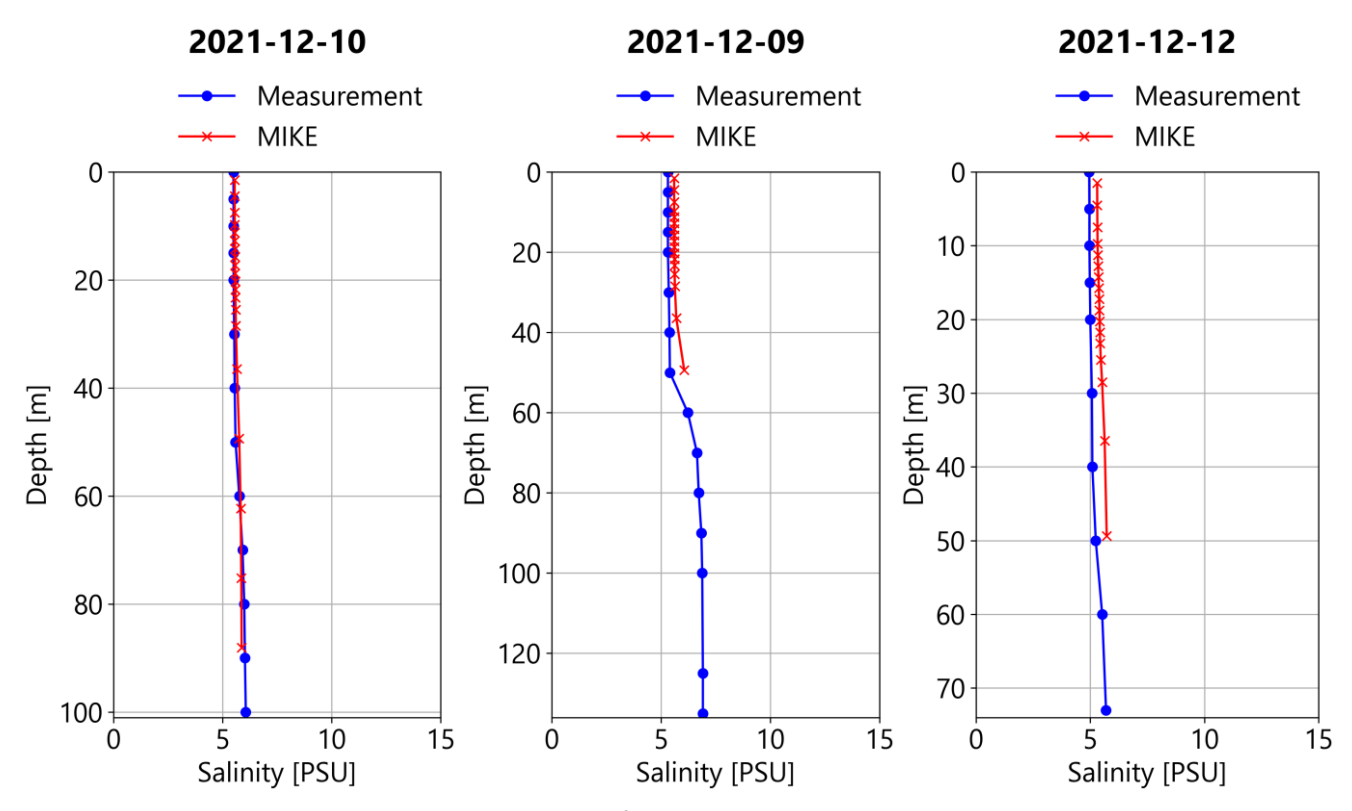


Comparison between modelled and measured salinity profiles at location F2 (source: merihavainnot.fi)

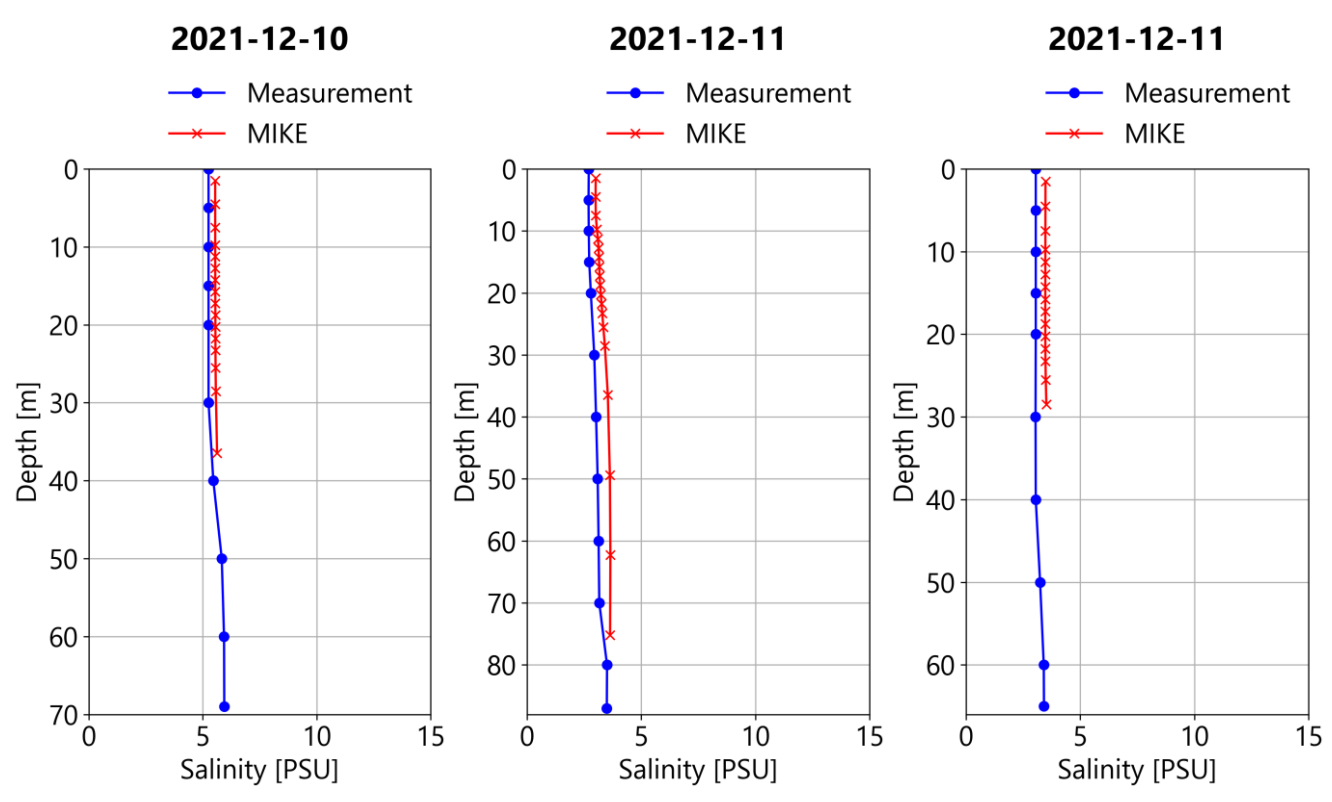
Profiles from SMHI



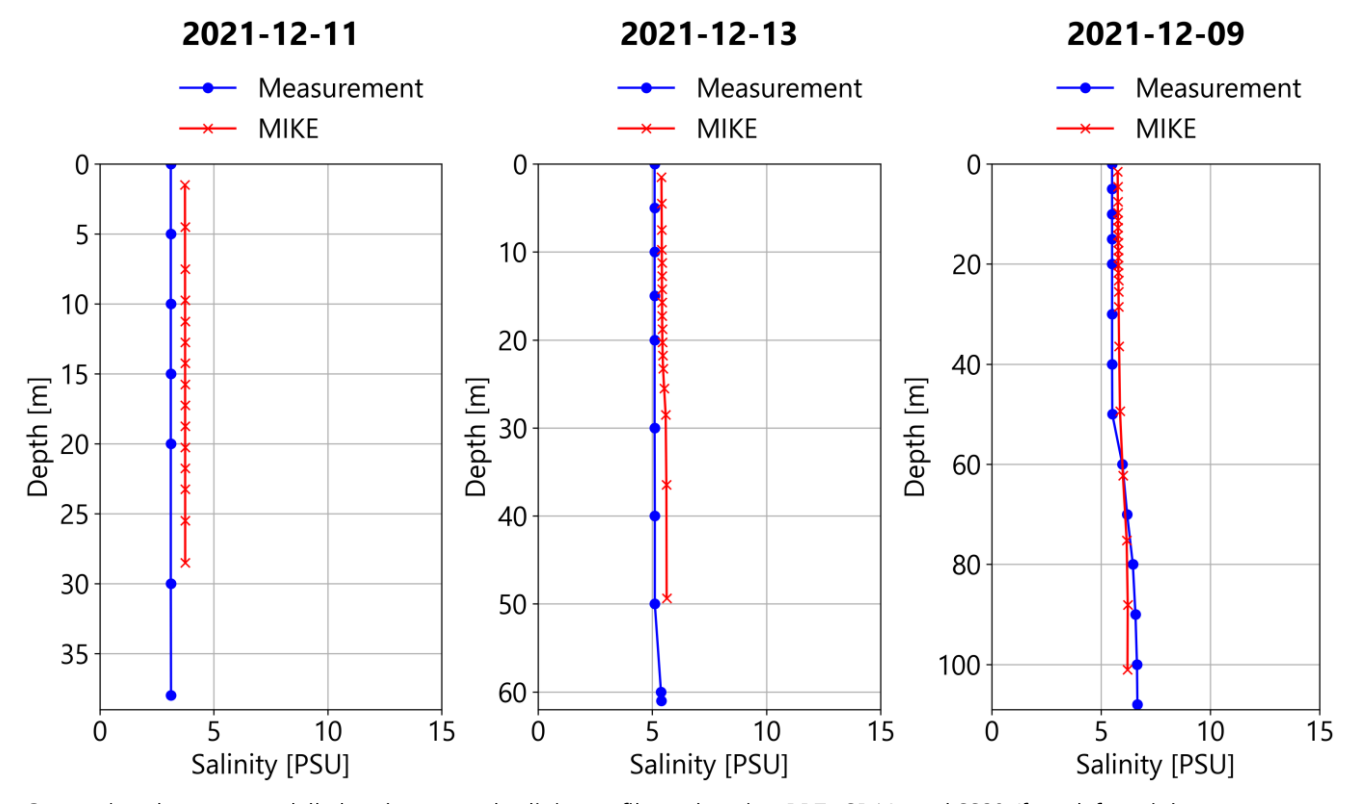
Comparison between modelled and measured salinity profiles at location A5, F13, and F16 (from left to right, source: SMHI)



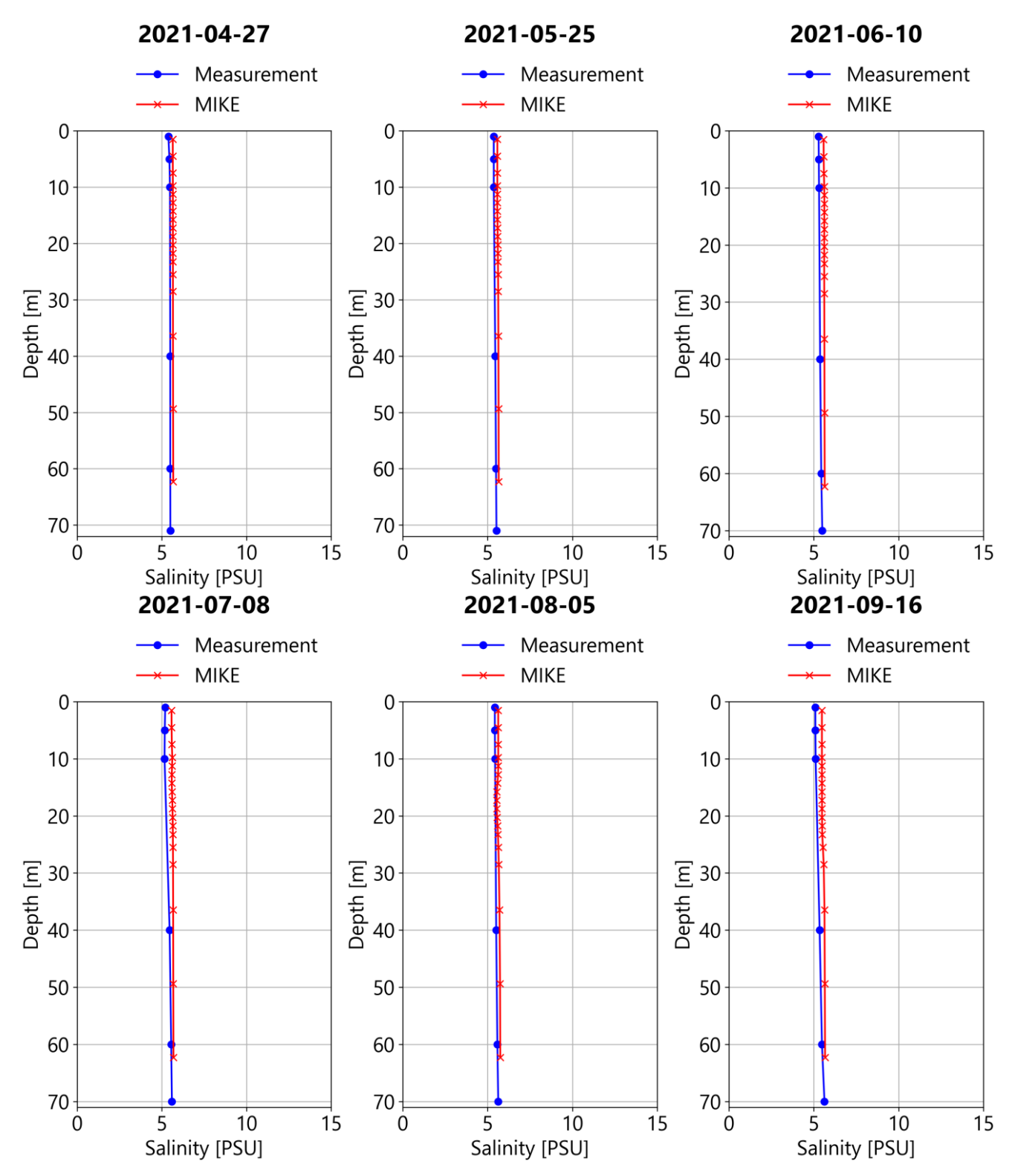
Comparison between modelled and measured salinity profiles at location F18 SYDOSTBROTTEN, F33 GRUNDKALLEN, and MS2 (from left to right, source: SMHI)



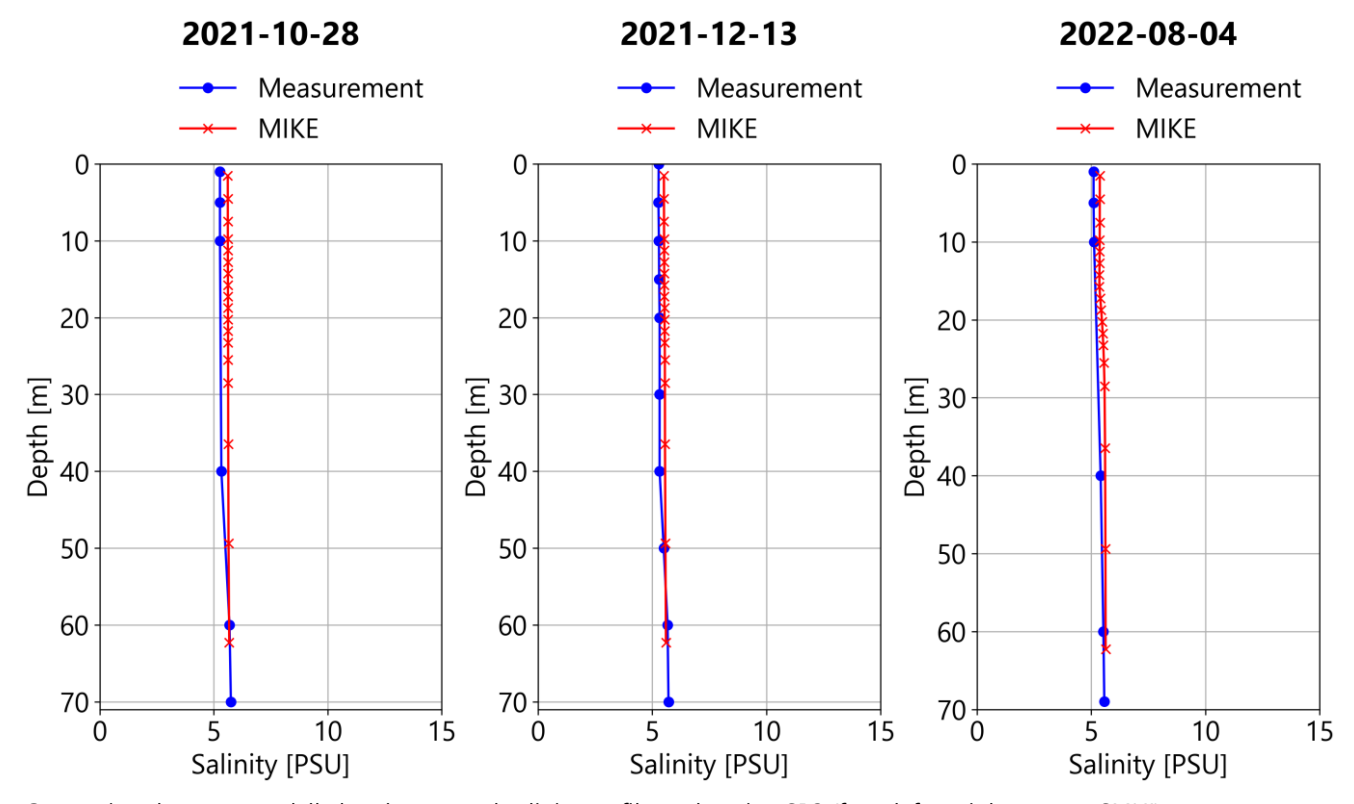
Comparison between modelled and measured salinity profiles at location MS6, RR1, and RR5 (from left to right, source: SMHI)



Comparison between modelled and measured salinity profiles at location RR7, SR1A, and SS29 (from left to right, source: SMHI)



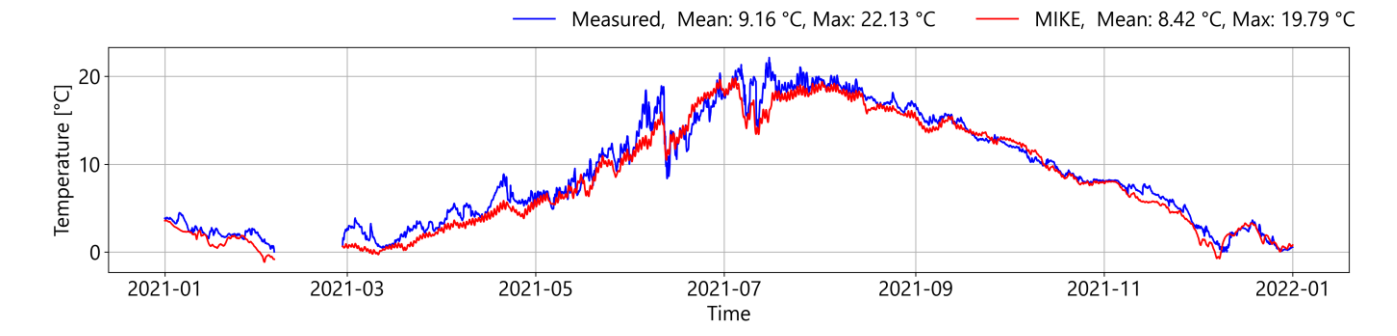
Comparison between modelled and measured salinity profiles at location SR3 (from left to right, source: SMHI)



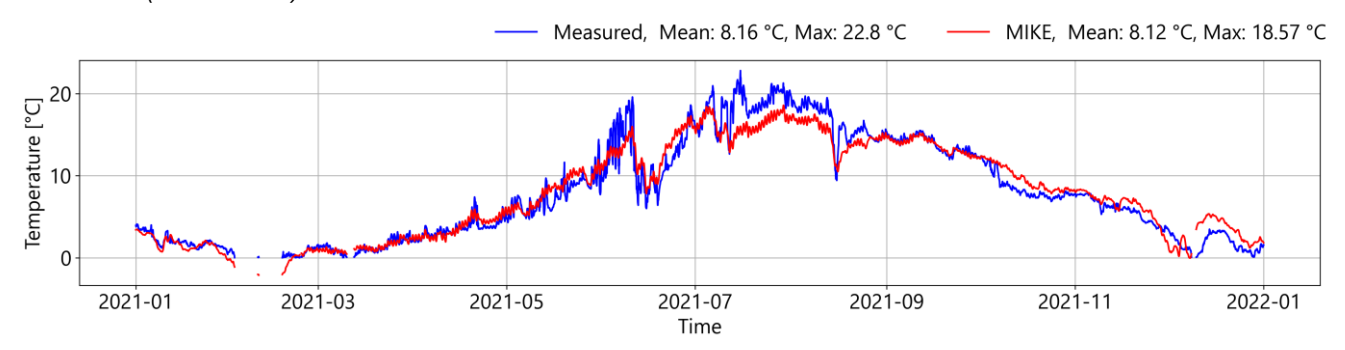
Comparison between modelled and measured salinity profiles at location SR3 (from left to right, source: SMHI)



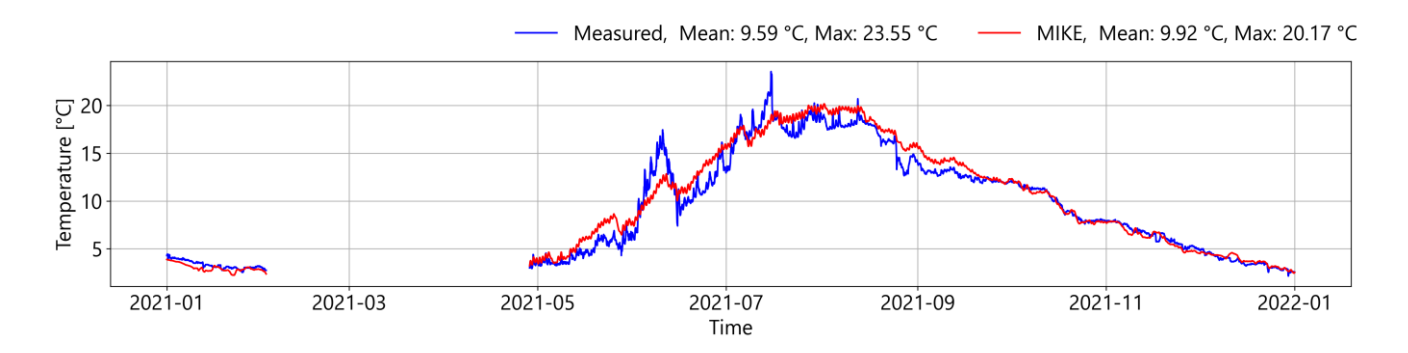
_		_		_	_	
1	110000	varification	Timesassias	~£ ~.	f-	temperature
ADDEDOIX IS	MODEL	verilication:	Timesenes	O(S)	mace	iemberallire.
APPCHAIN IS	IVICACI	VCI IIICAGOII.	111110301103	01 00	ai iacc	componatare



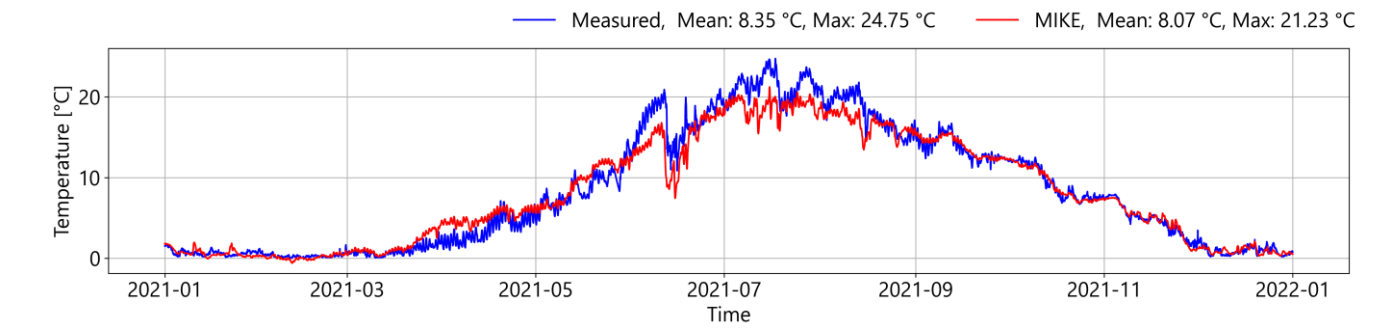
Comparison between observed surface water temperature (blue line) and modelled surface water temperature (red line) for FORSMARK (SMHI-Station).



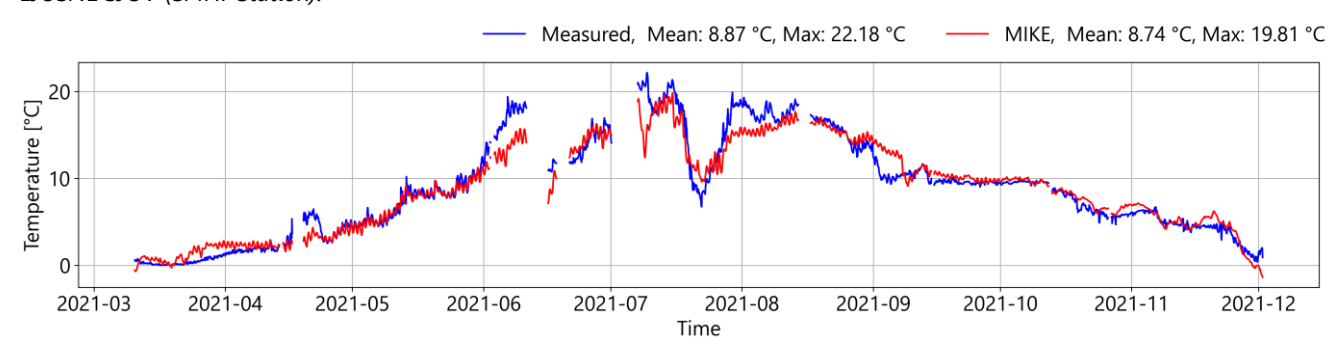
Comparison between observed surface water temperature (blue line) and modelled surface water temperature (red line) for BÖNAN SJÖV (SMHI-Station).



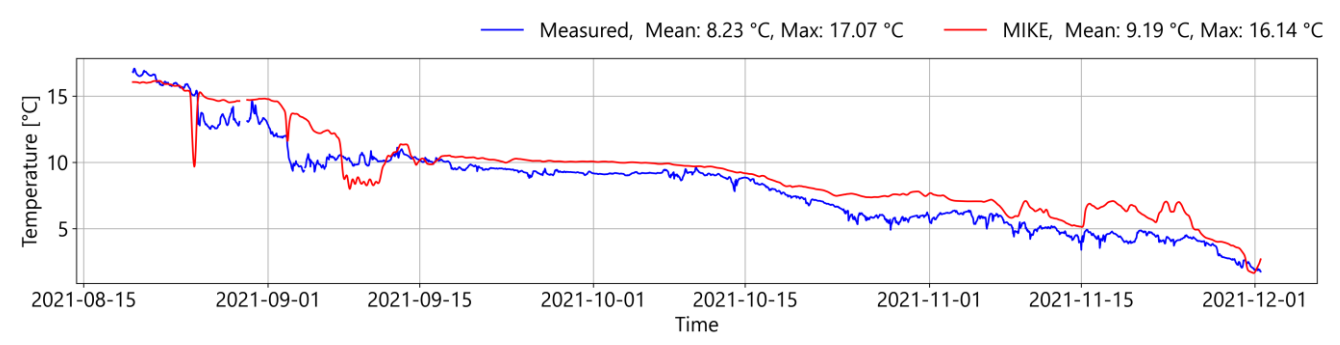
Comparison between observed surface water temperature (blue line) and modelled surface water temperature (red line) for FINNGRUNDET WR BOJ (SMHI-Station).



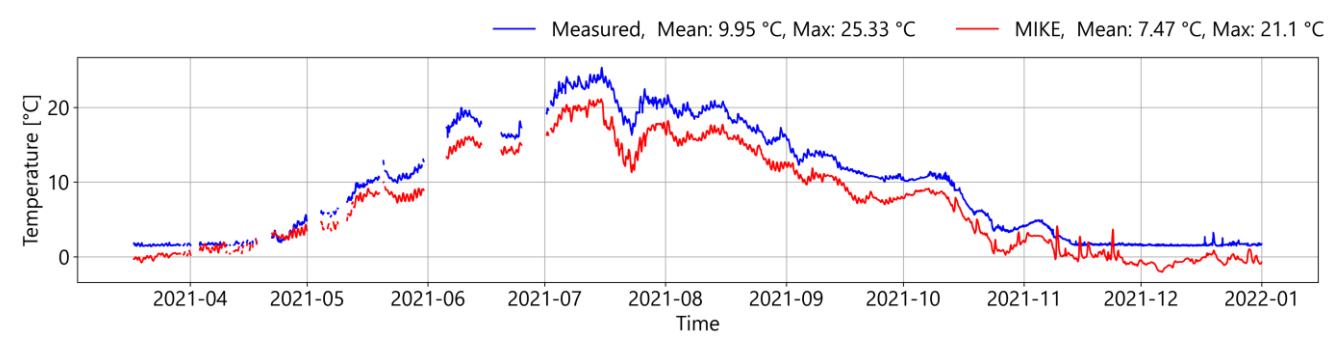
Comparison between observed surface water temperature (blue line) and modelled surface water temperature (red line) for LJUSNE SJÖV (SMHI-Station).



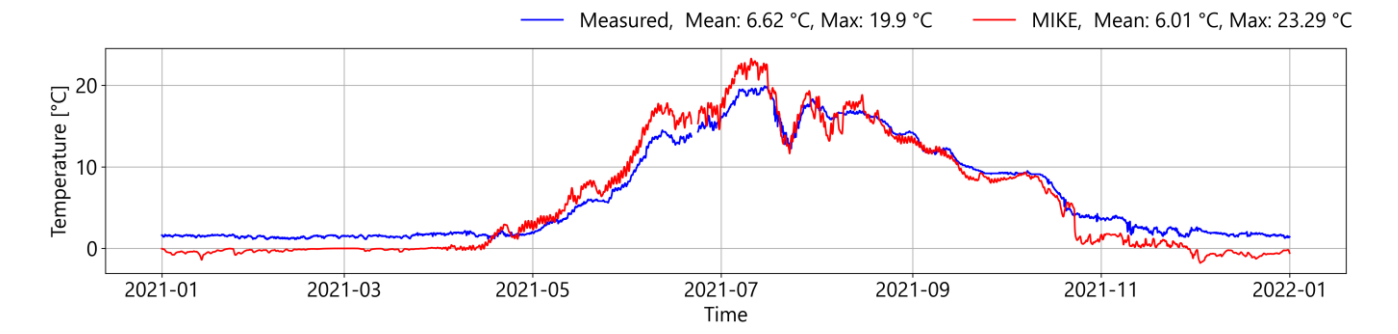
Comparison between observed surface water temperature (blue line) and modelled surface water temperature (red line) for NORRBYN SST (SMHI-Station).



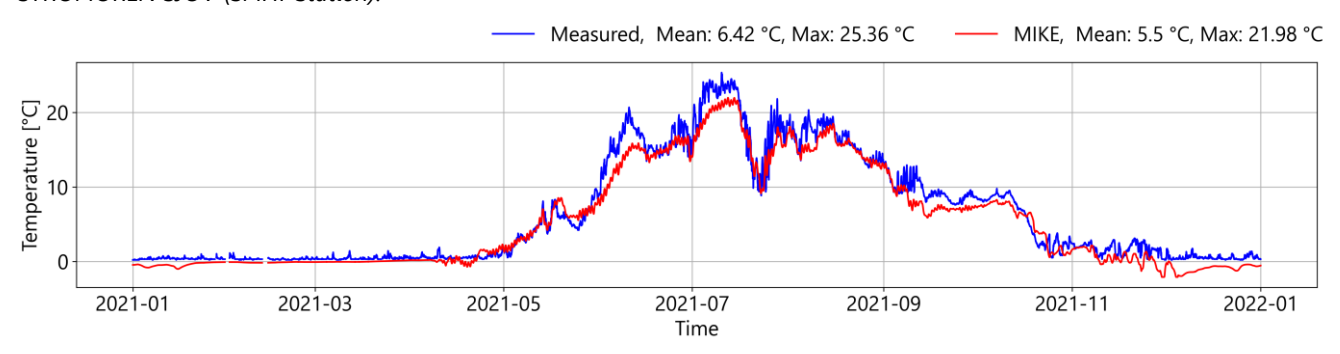
Comparison between observed surface water temperature (blue line) and modelled surface water temperature (red line) for NORRBYN BOJ (SMHI-Station).



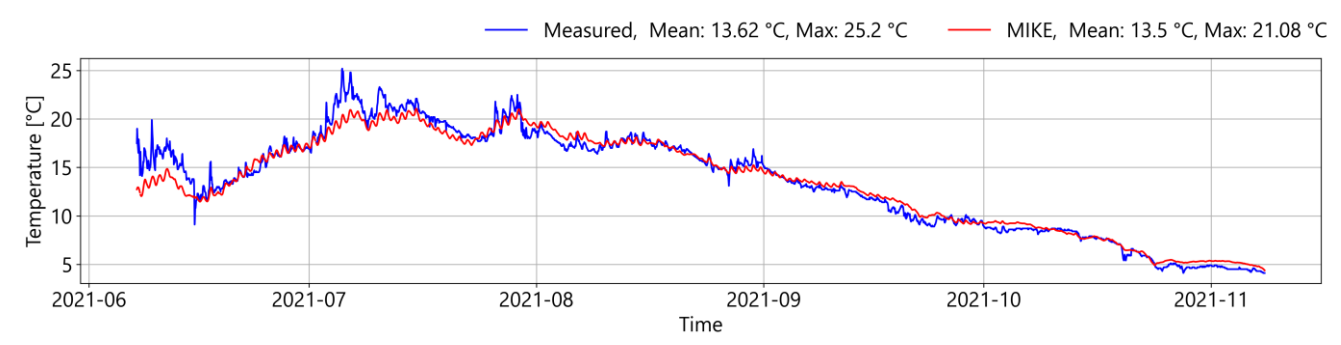
Comparison between observed surface water temperature (blue line) and modelled surface water temperature (red line) for Holmsund (SMHI-Station).



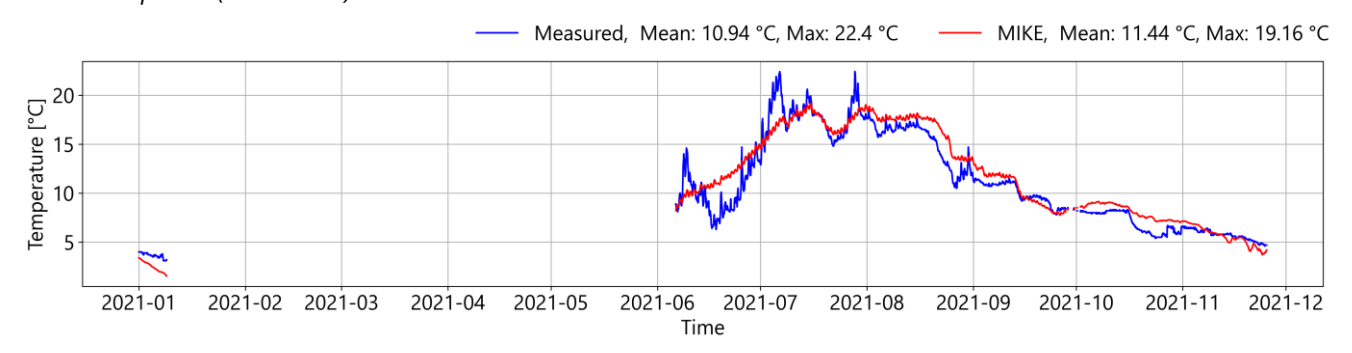
Comparison between observed surface water temperature (blue line) and modelled surface water temperature (red line) for STRÖMÖREN SJÖV (SMHI-Station).



Comparison between observed surface water temperature (blue line) and modelled surface water temperature (red line) for KALIX-KARLSBORG SJÖV (SMHI-Station).



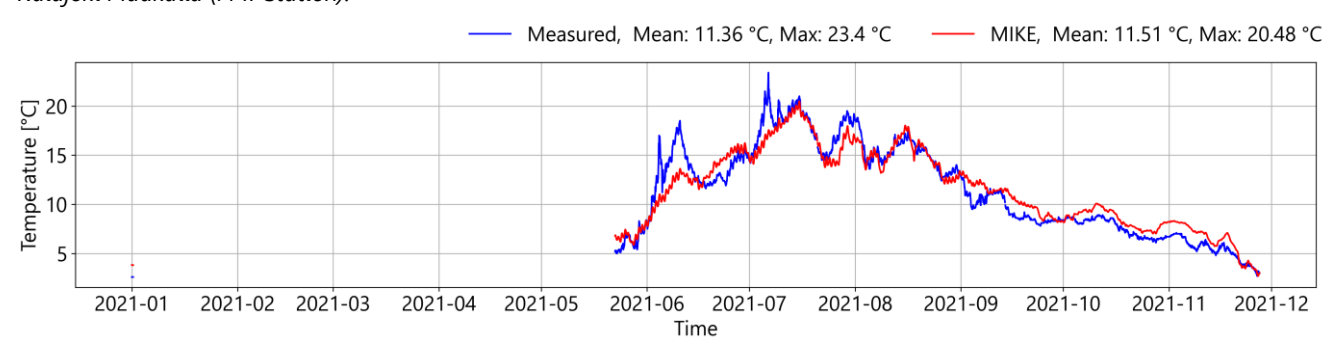
Comparison between observed surface water temperature (blue line) and modelled surface water temperature (red line) for Oulu Santapankki (FMI-Station).



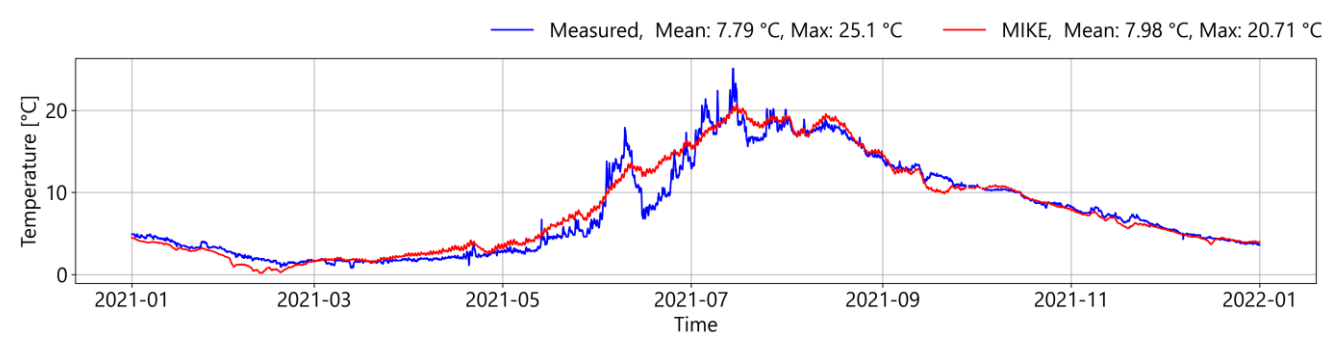
Comparison between observed surface water temperature (blue line) and modelled surface water temperature (red line) for Perämeri aaltopoiju (FMI-Station).



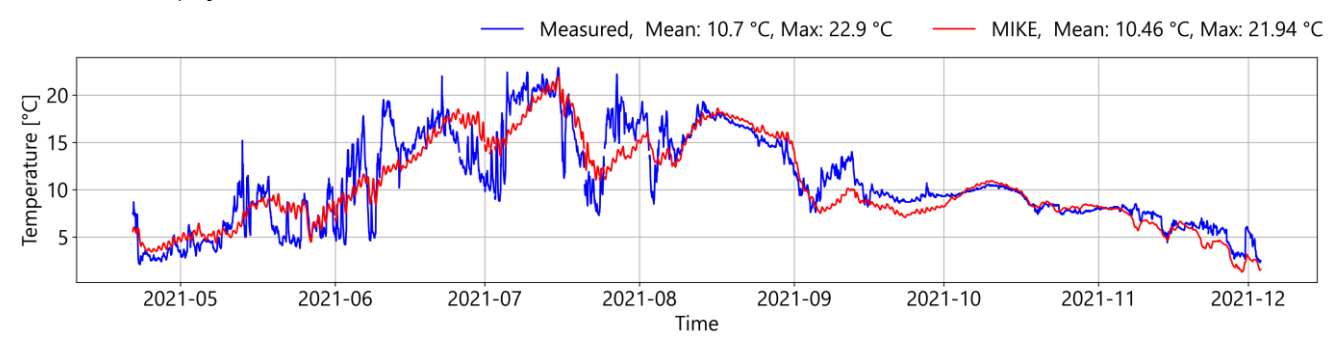
Comparison between observed surface water temperature (blue line) and modelled surface water temperature (red line) for Kalajoki Maakalla (FMI-Station).



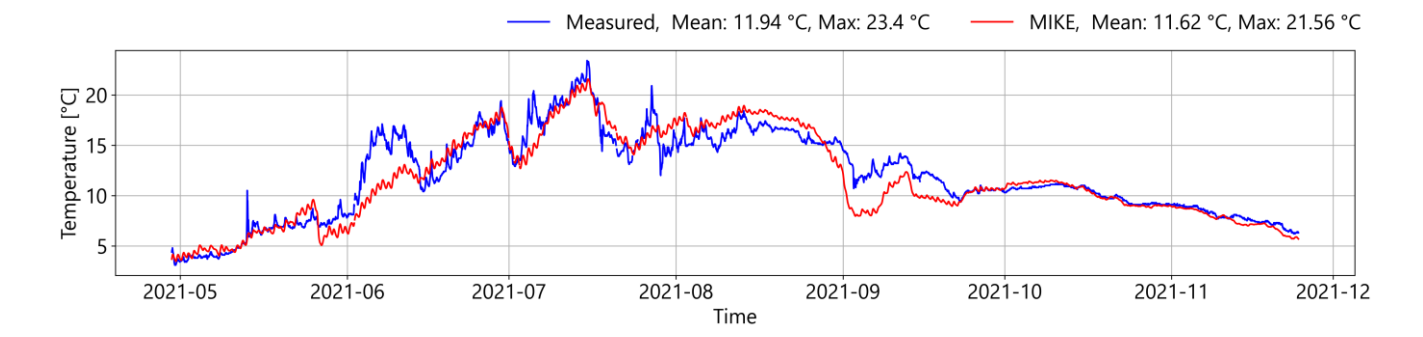
Comparison between observed surface water temperature (blue line) and modelled surface water temperature (red line) for Maalahti Storskäret (FMI-Station).



Comparison between observed surface water temperature (blue line) and modelled surface water temperature (red line) for Selkämeri aaltopoiju (FMI-Station).



Comparison between observed surface water temperature (blue line) and modelled surface water temperature (red line) for Pori Kaijakari (FMI-Station).



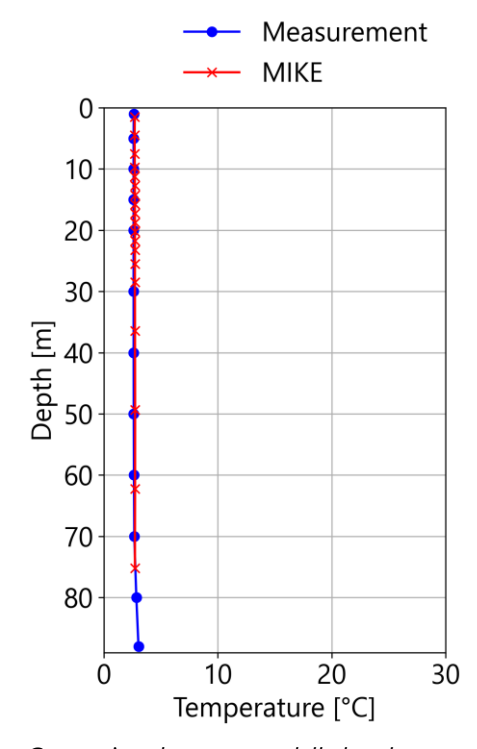
Comparison between observed surface water temperature (blue line) and modelled surface water temperature (red line) for Uusikaupunki Vekara (FMI-Station).



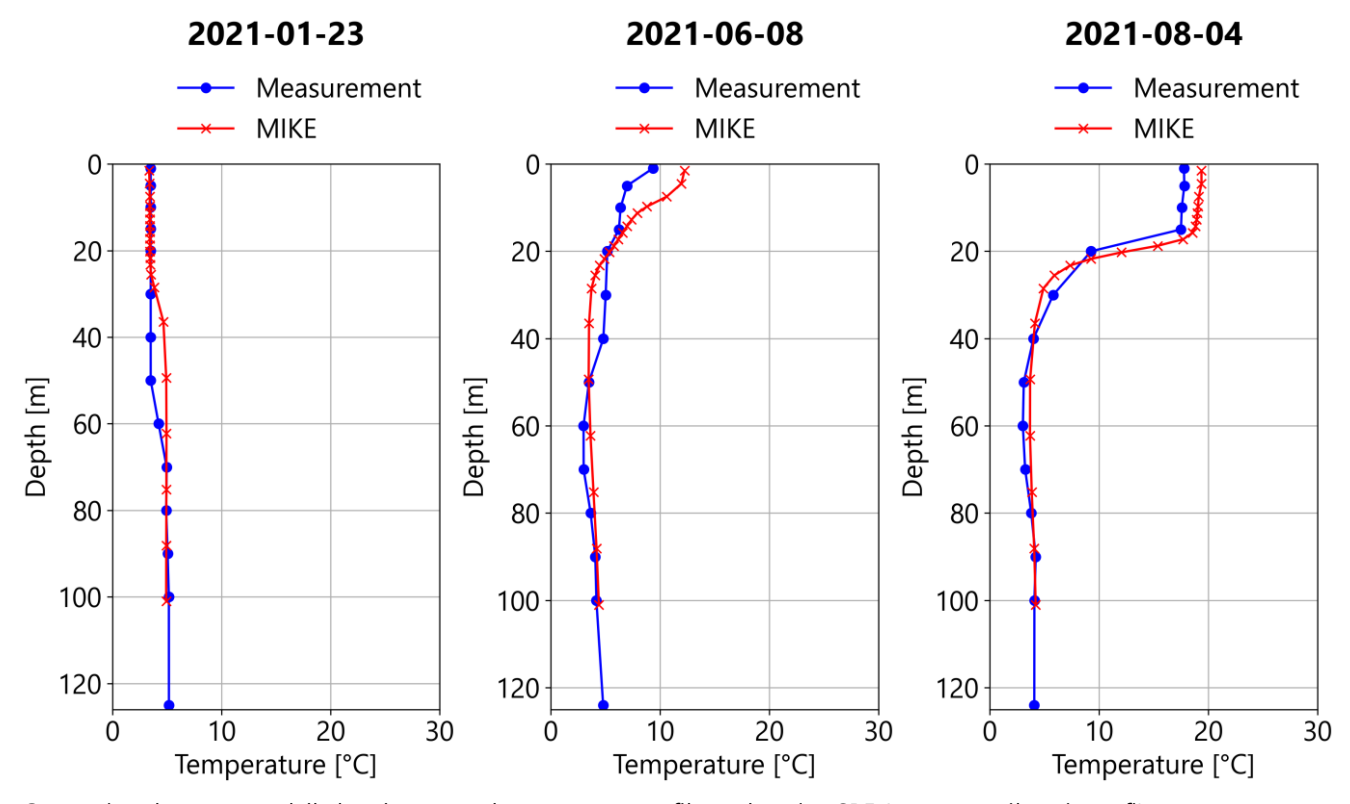
Appendix 16 Model verification:	Temperature	profiles
---------------------------------	-------------	----------

Profiles from merihavainnot.fi

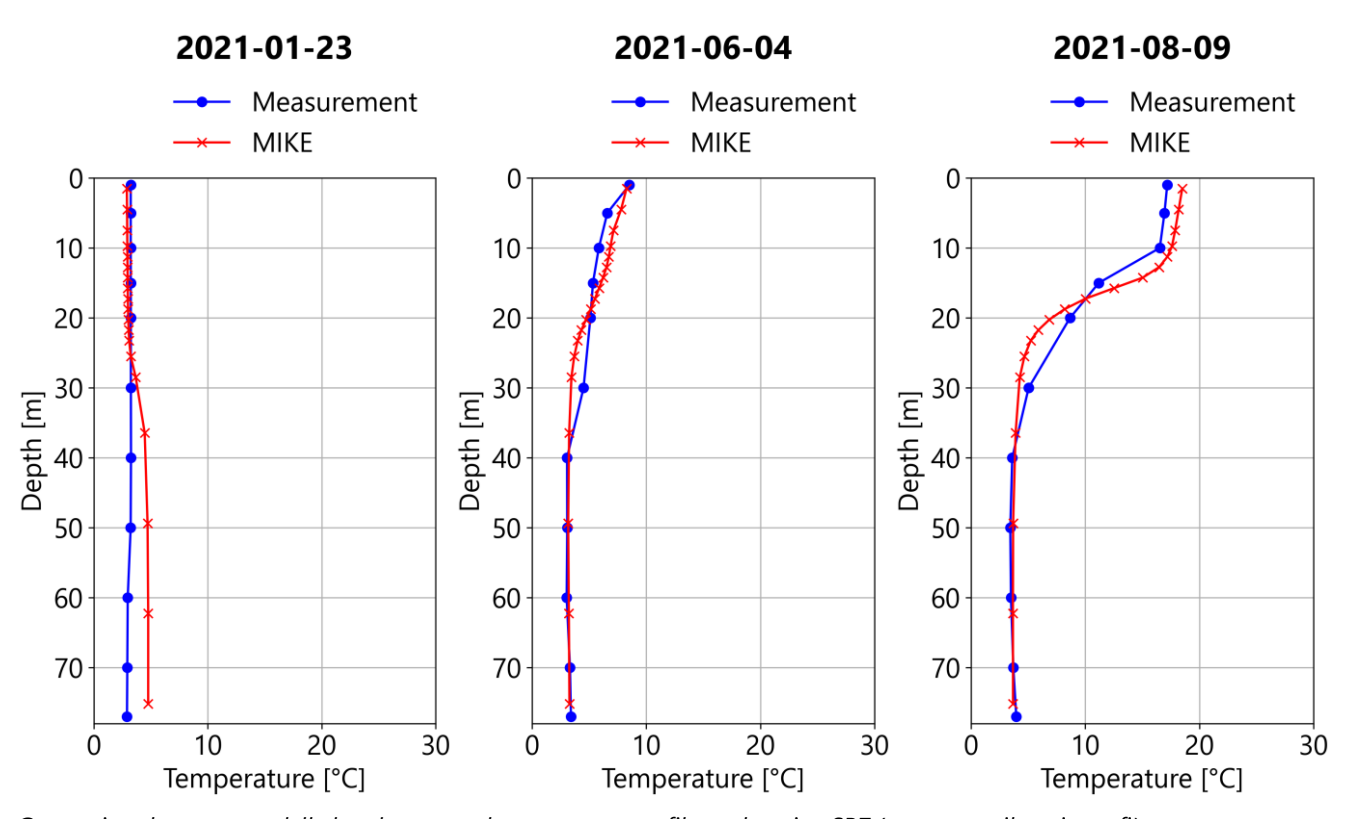




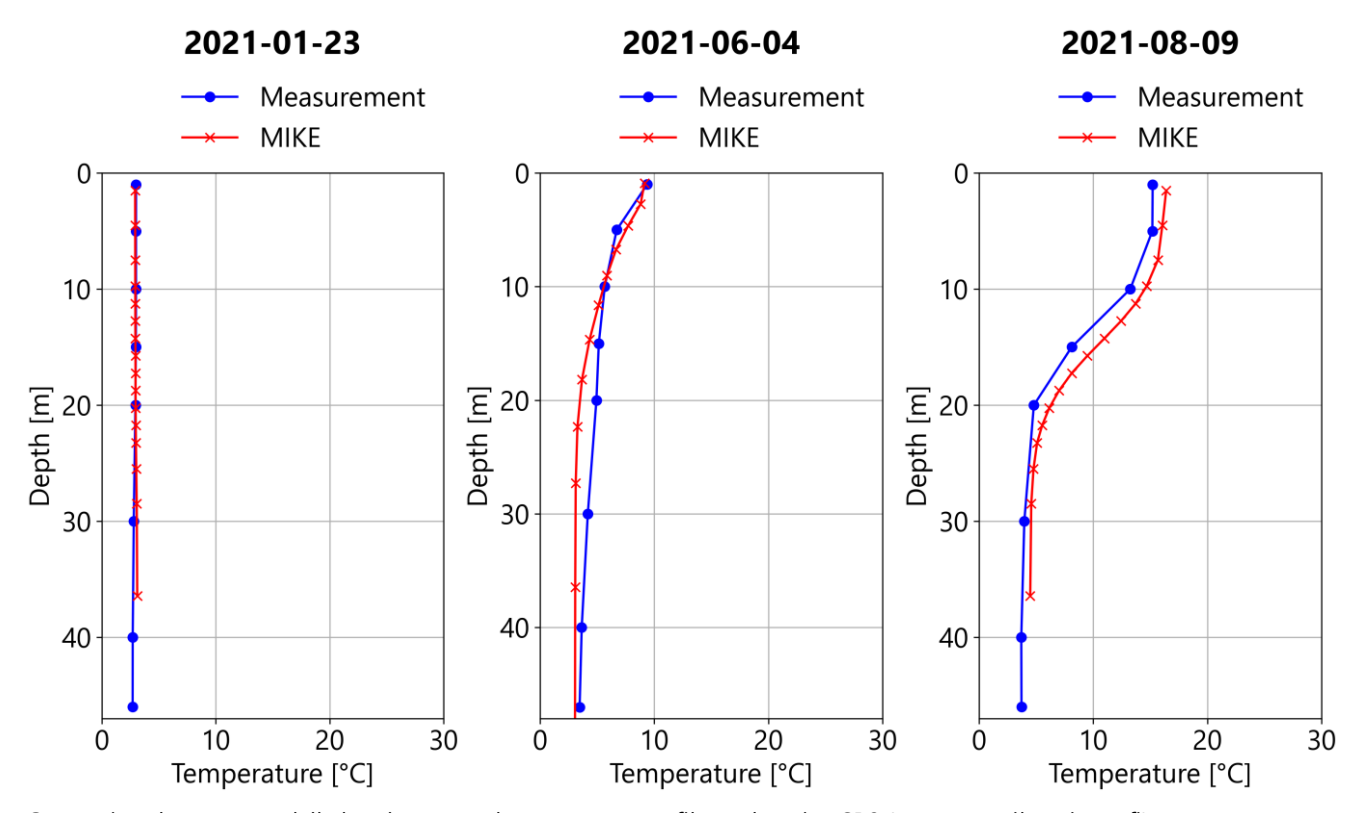
Comparison between modelled and measured temperature profiles at location MAME61 (source: merihavainnot.fi)



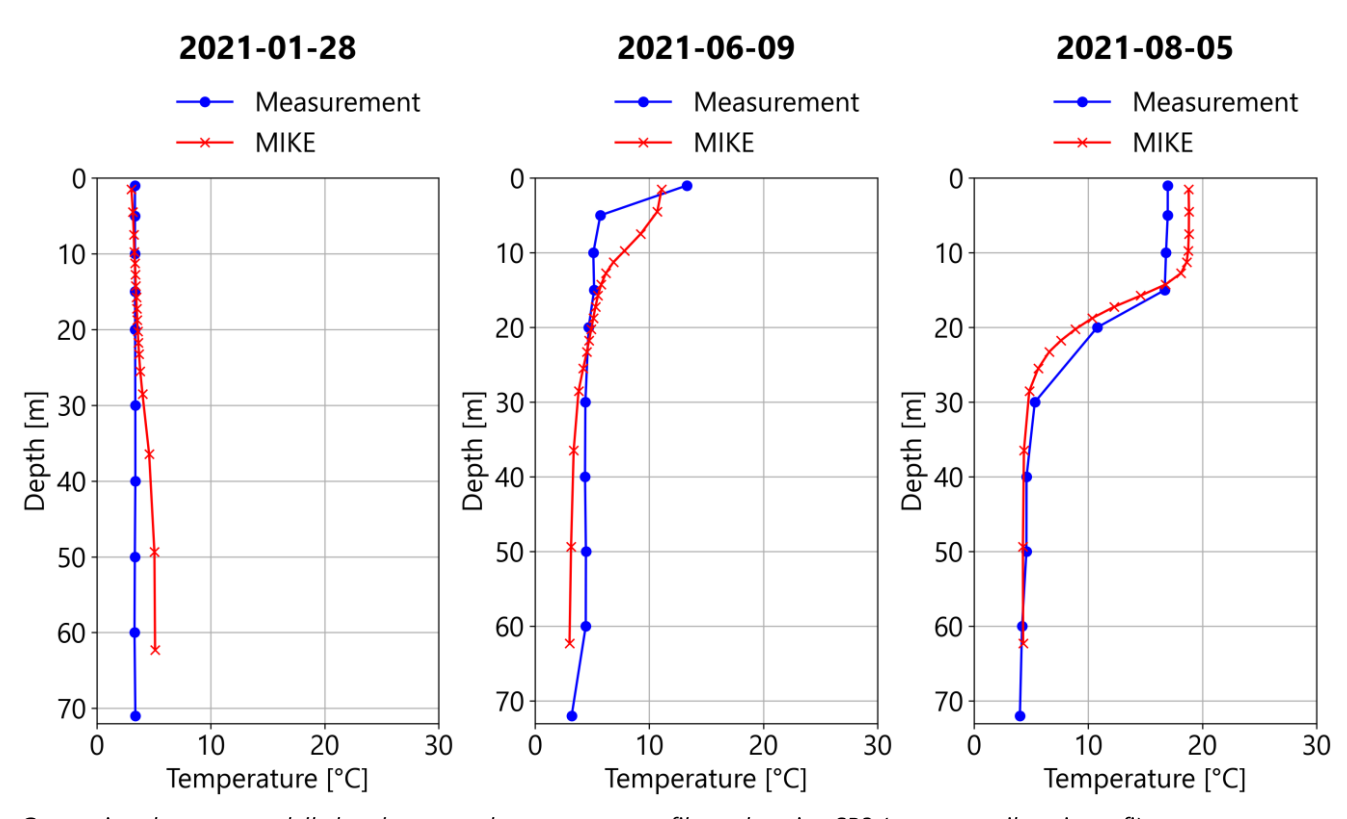
Comparison between modelled and measured temperature profiles at location SR5 (source: merihavainnot.fi)



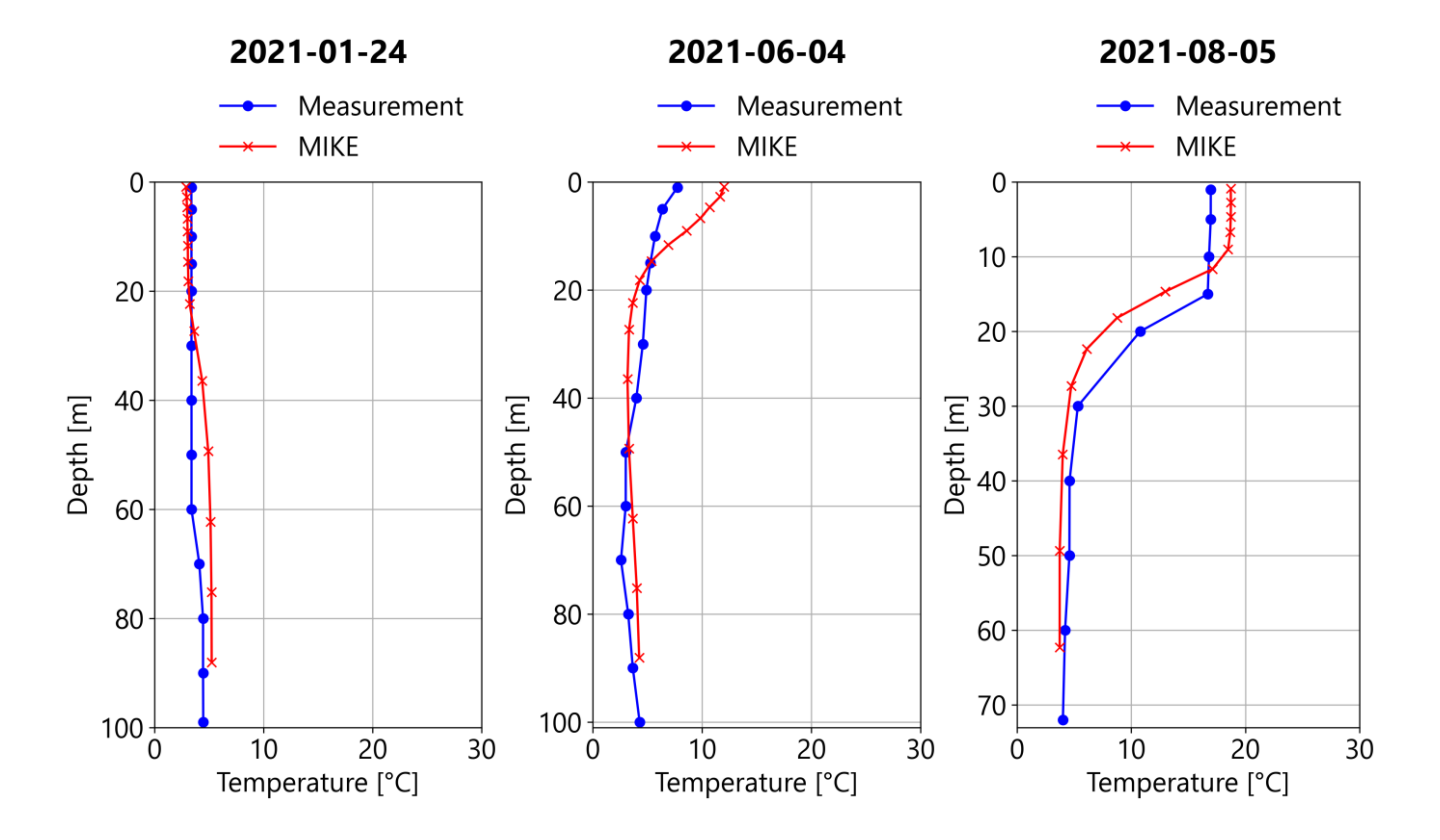
Comparison between modelled and measured temperature profiles at location SR7 (source: merihavainnot.fi)



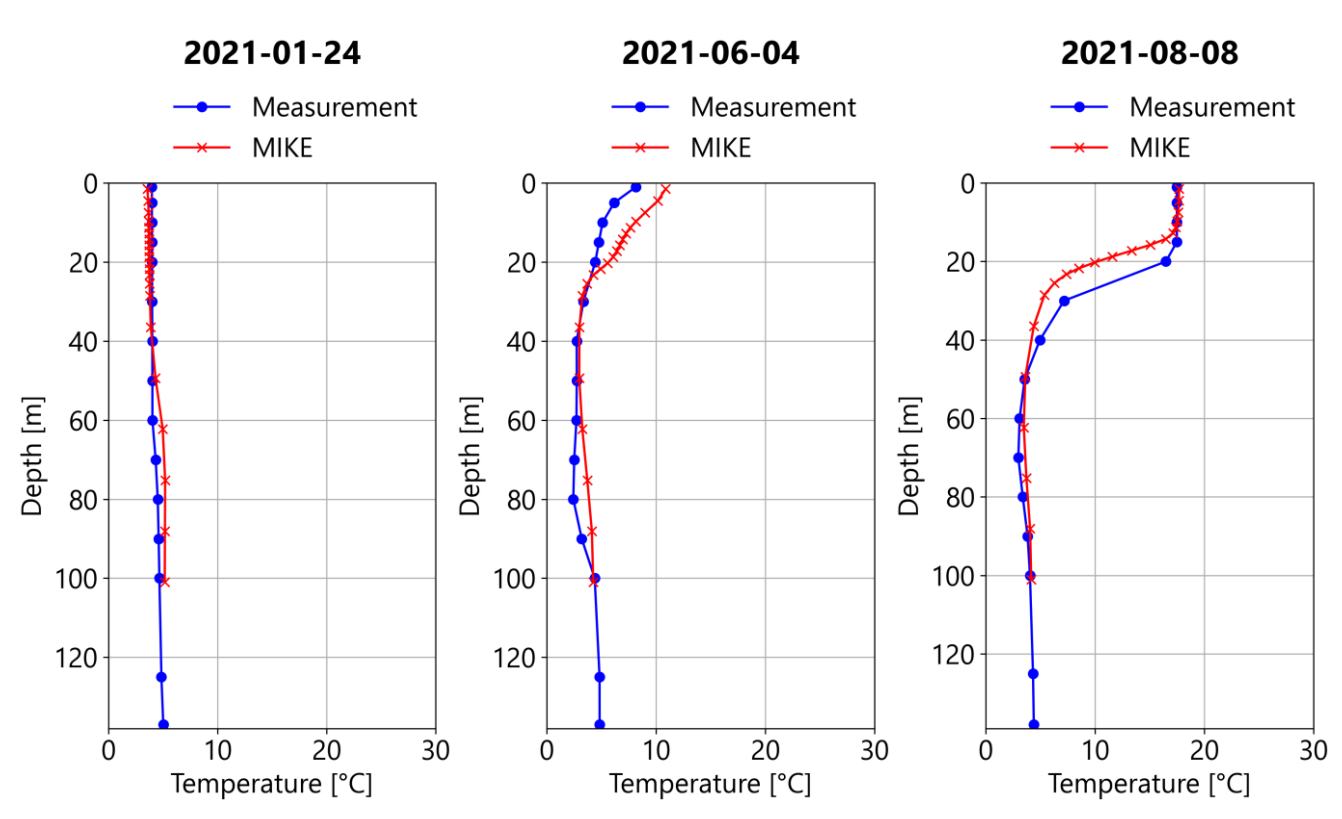
Comparison between modelled and measured temperature profiles at location SR8 (source: merihavainnot.fi)



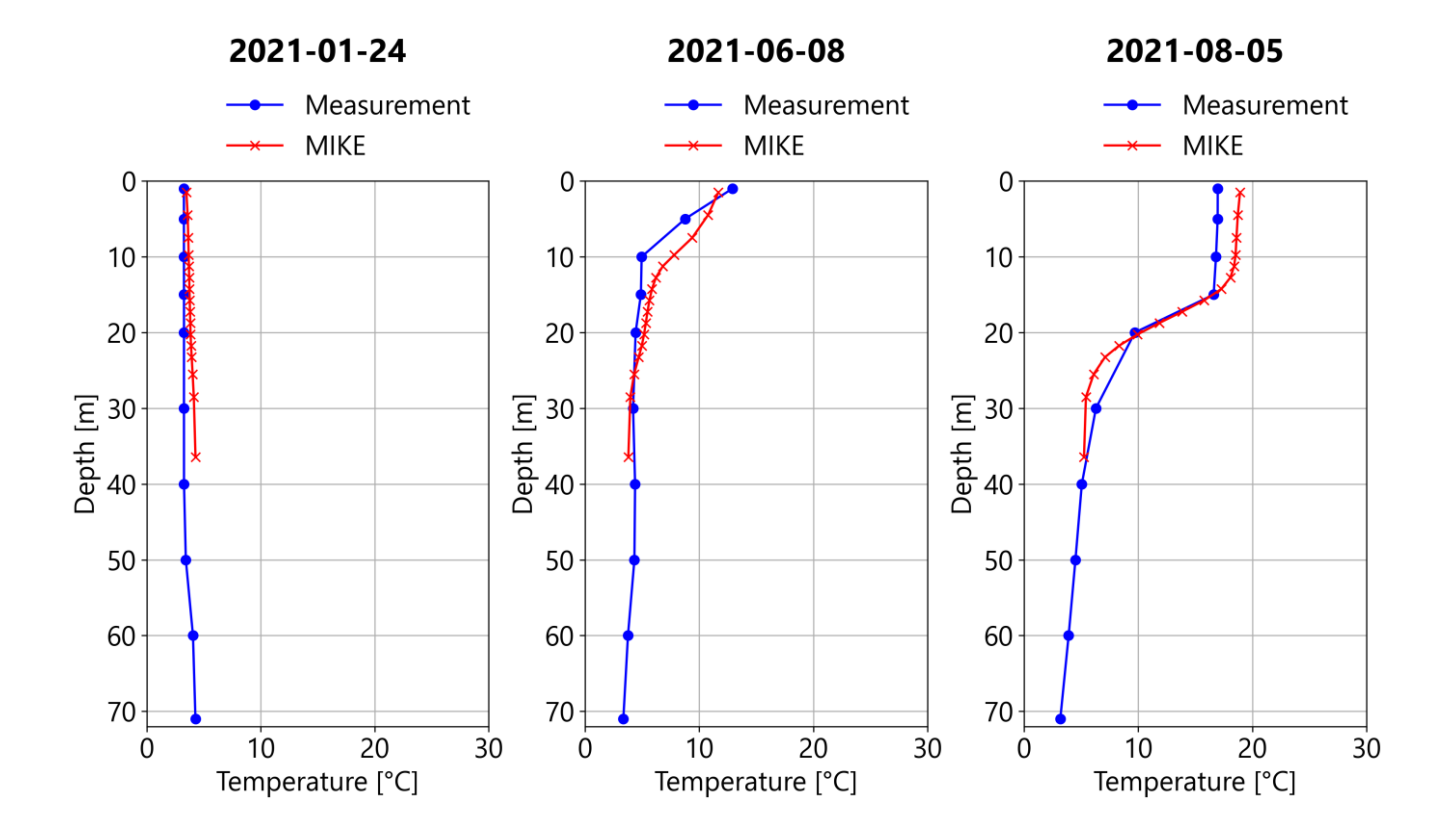
Comparison between modelled and measured temperature profiles at location SR3 (source: merihavainnot.fi)



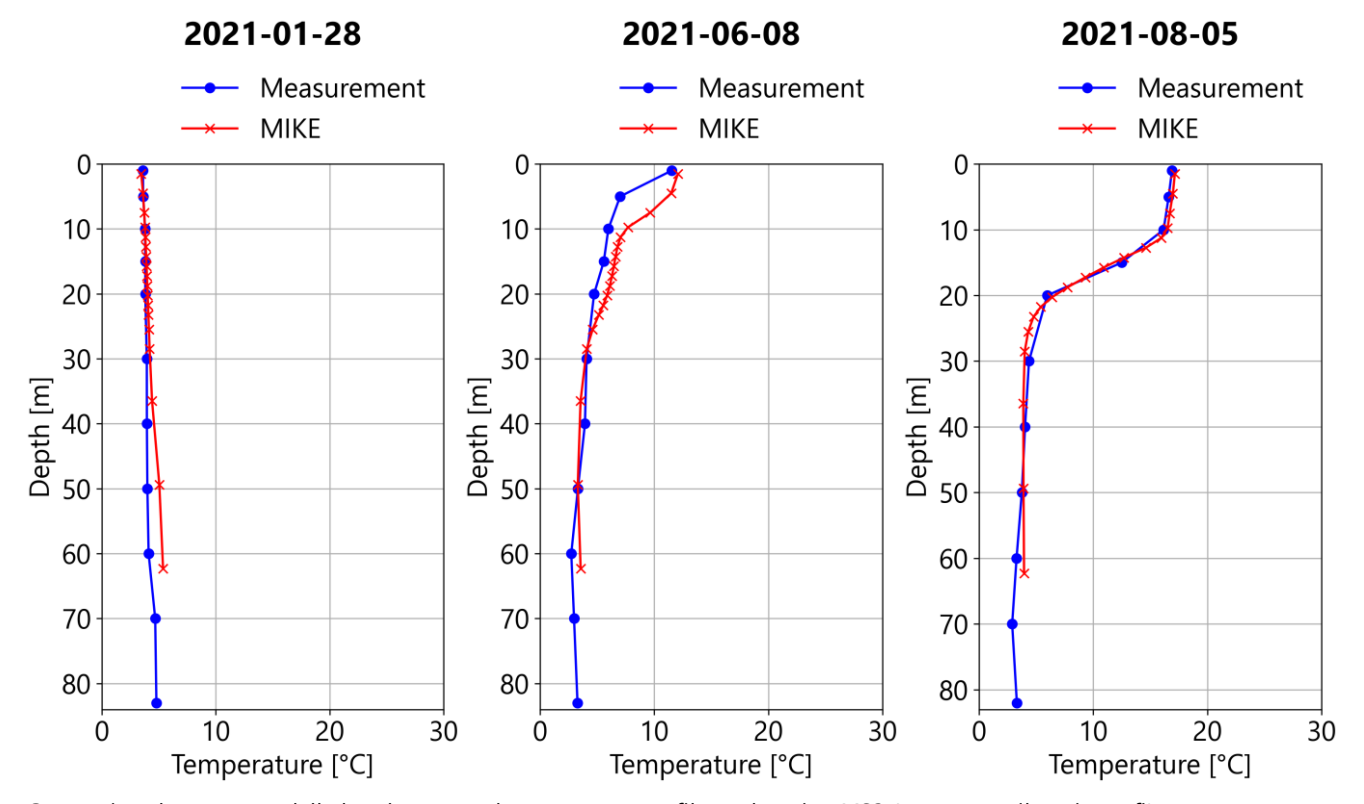
Comparison between modelled and measured temperature profiles at location MS9 (source: merihavainnot.fi)



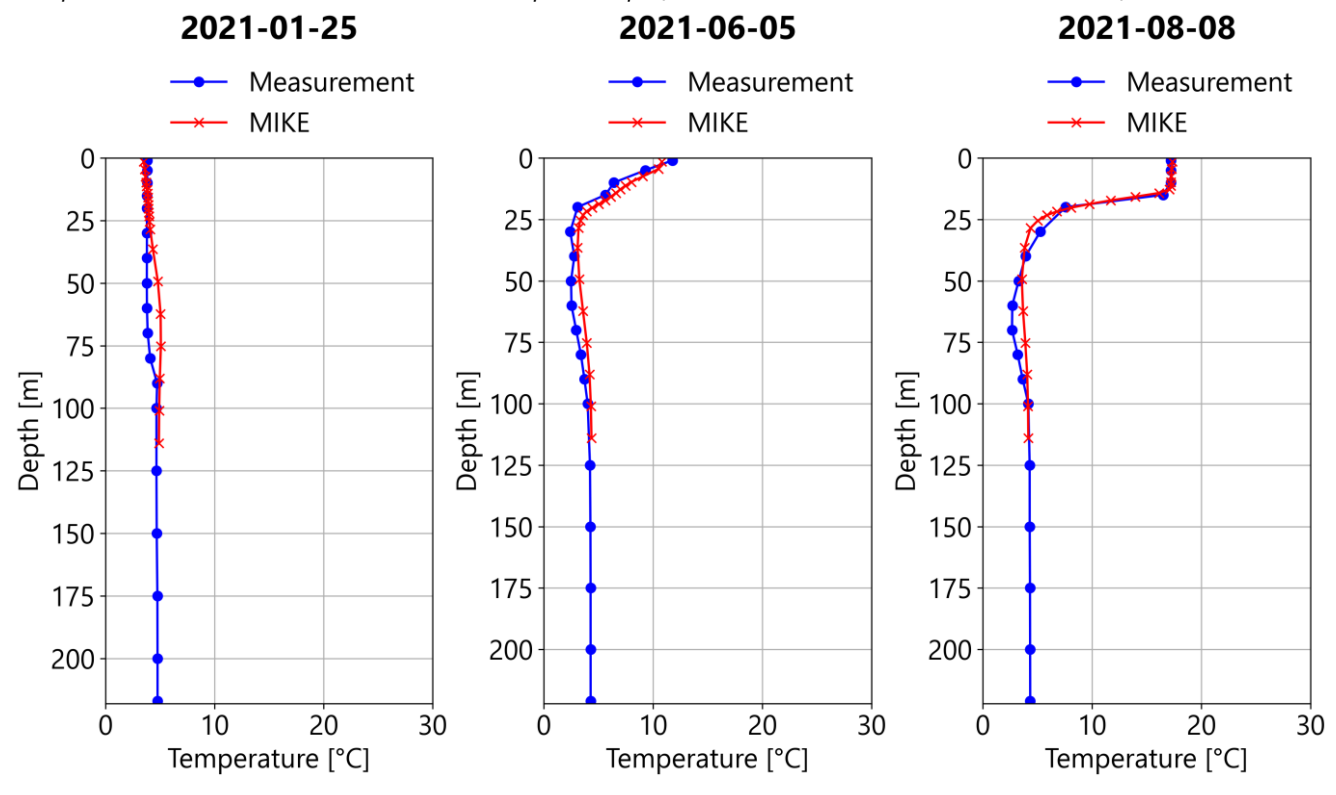
Comparison between modelled and measured temperature profiles at location F26 (source: merihavainnot.fi, location)



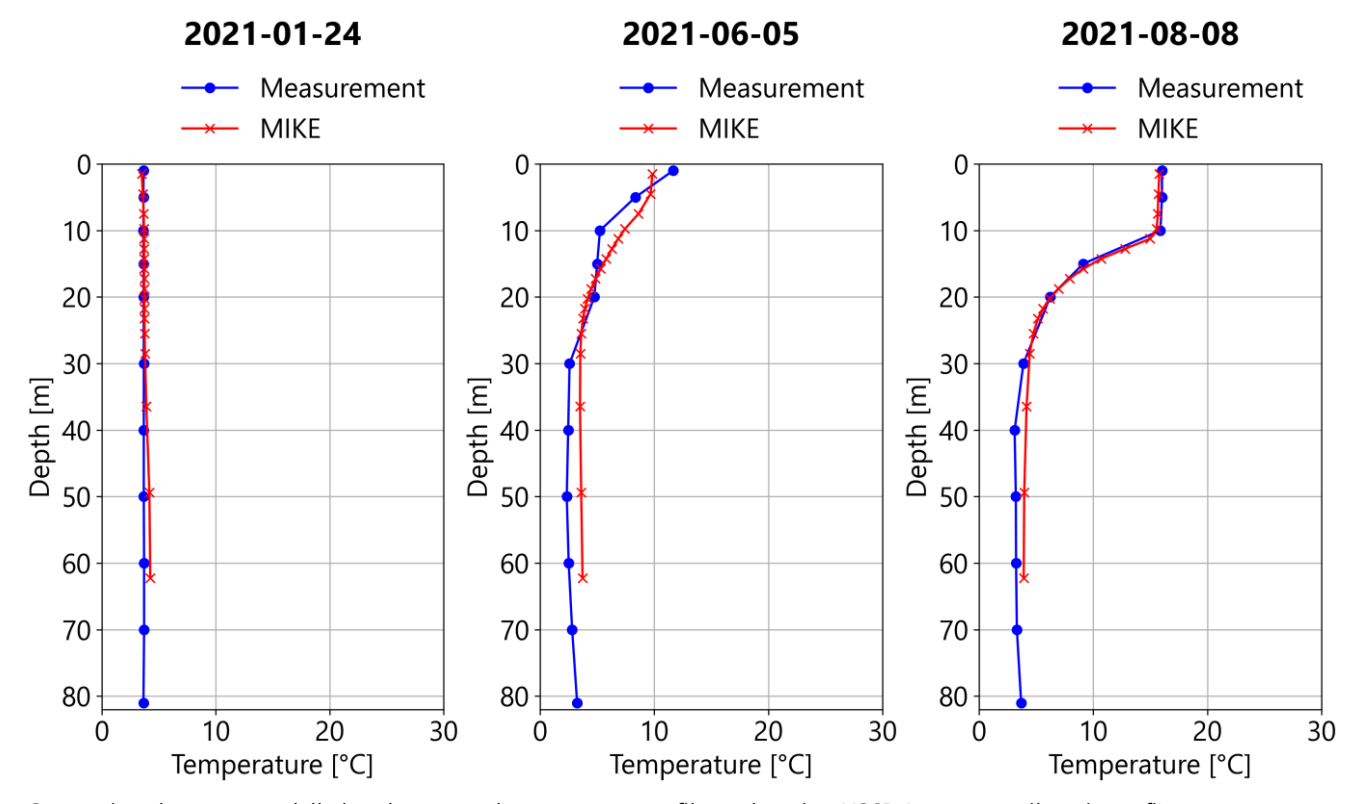
Comparison between modelled and measured temperature profiles at location MS6 (source: merihavainnot.fi)



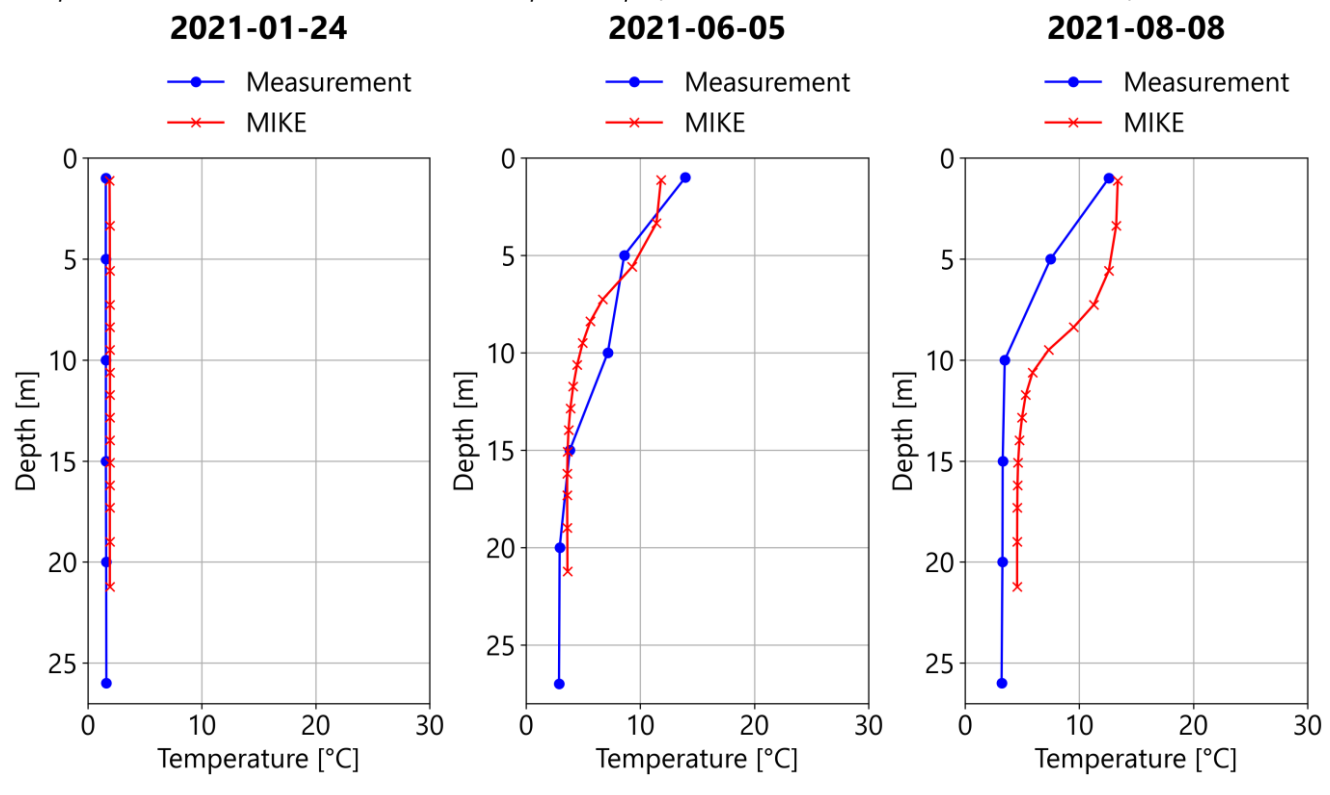
Comparison between modelled and measured temperature profiles at location MS3 (source: merihavainnot.fi)



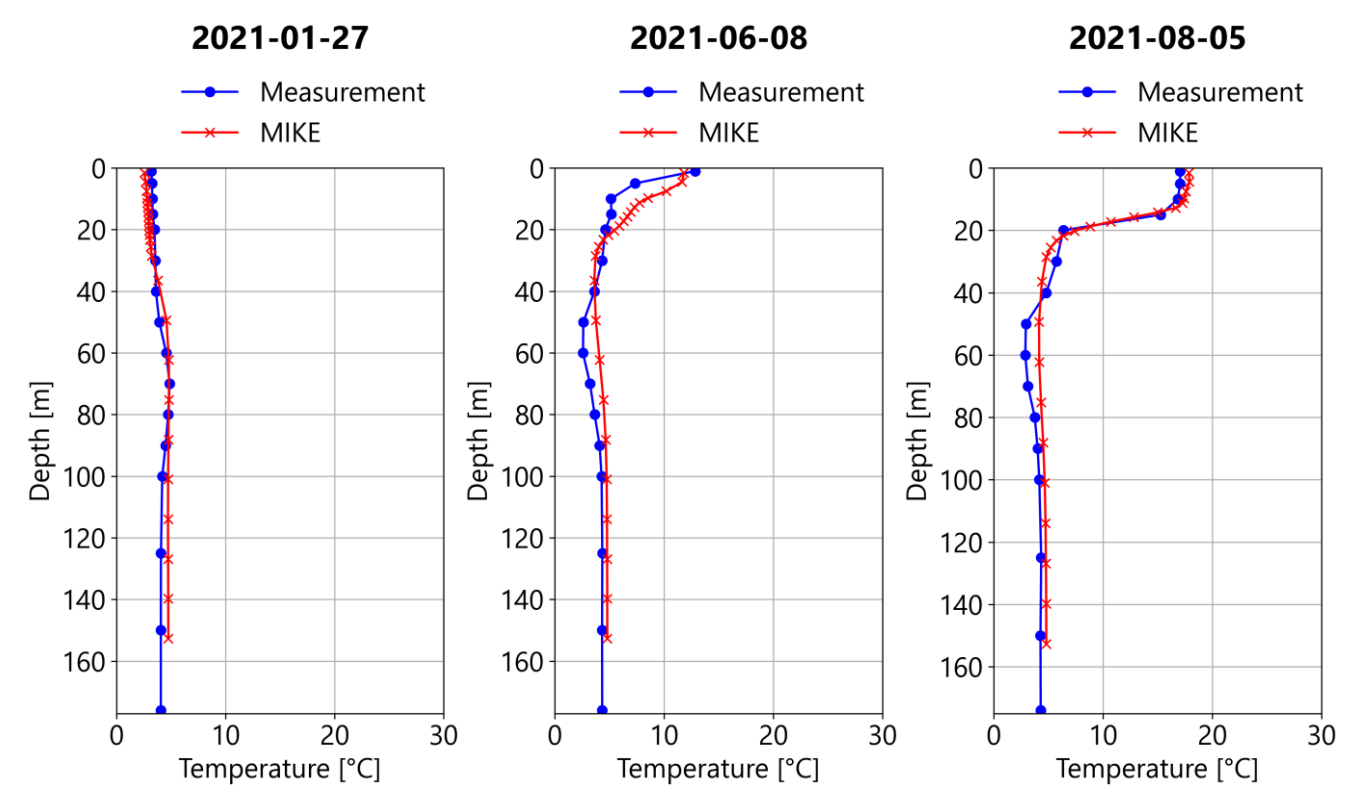
Comparison between modelled and measured temperature profiles at location US5B (source: merihavainnot.fi)



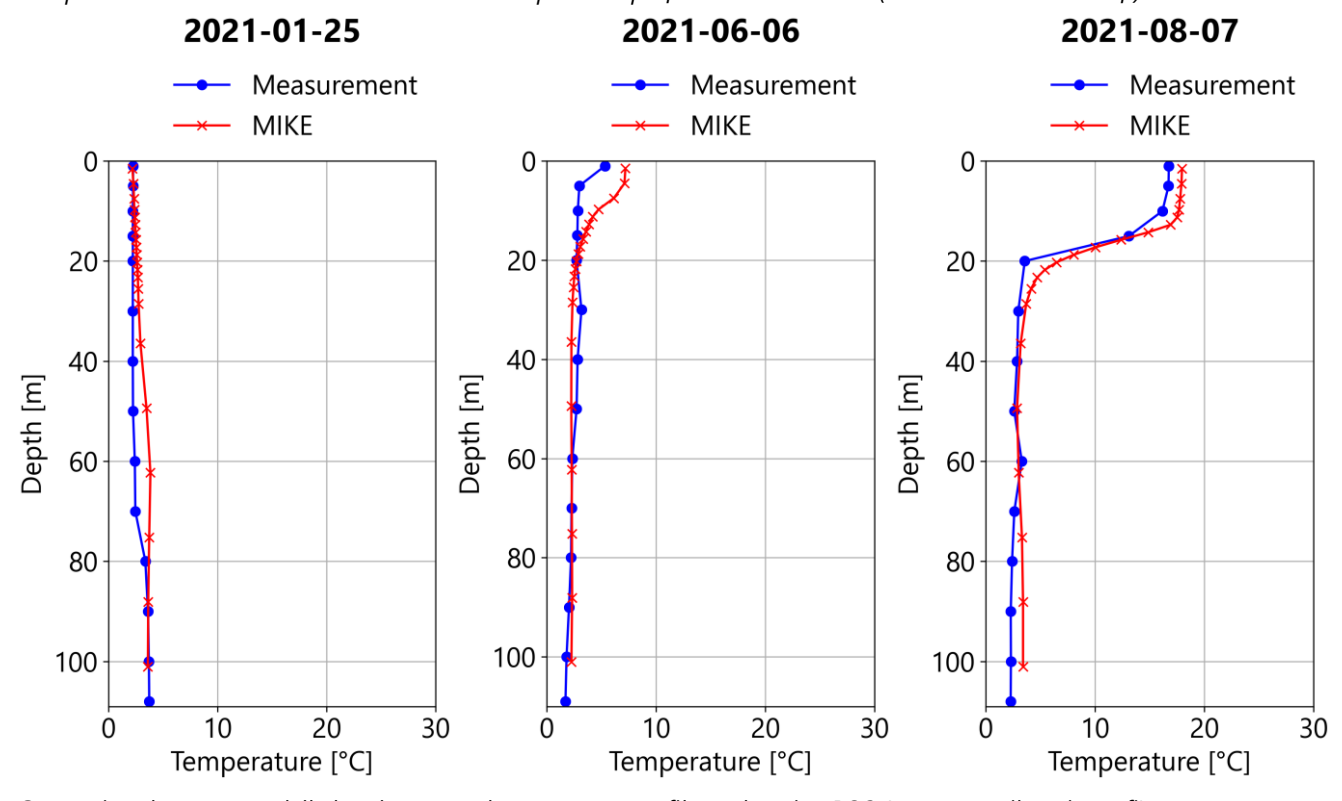
Comparison between modelled and measured temperature profiles at location US6B (source: merihavainnot.fi)



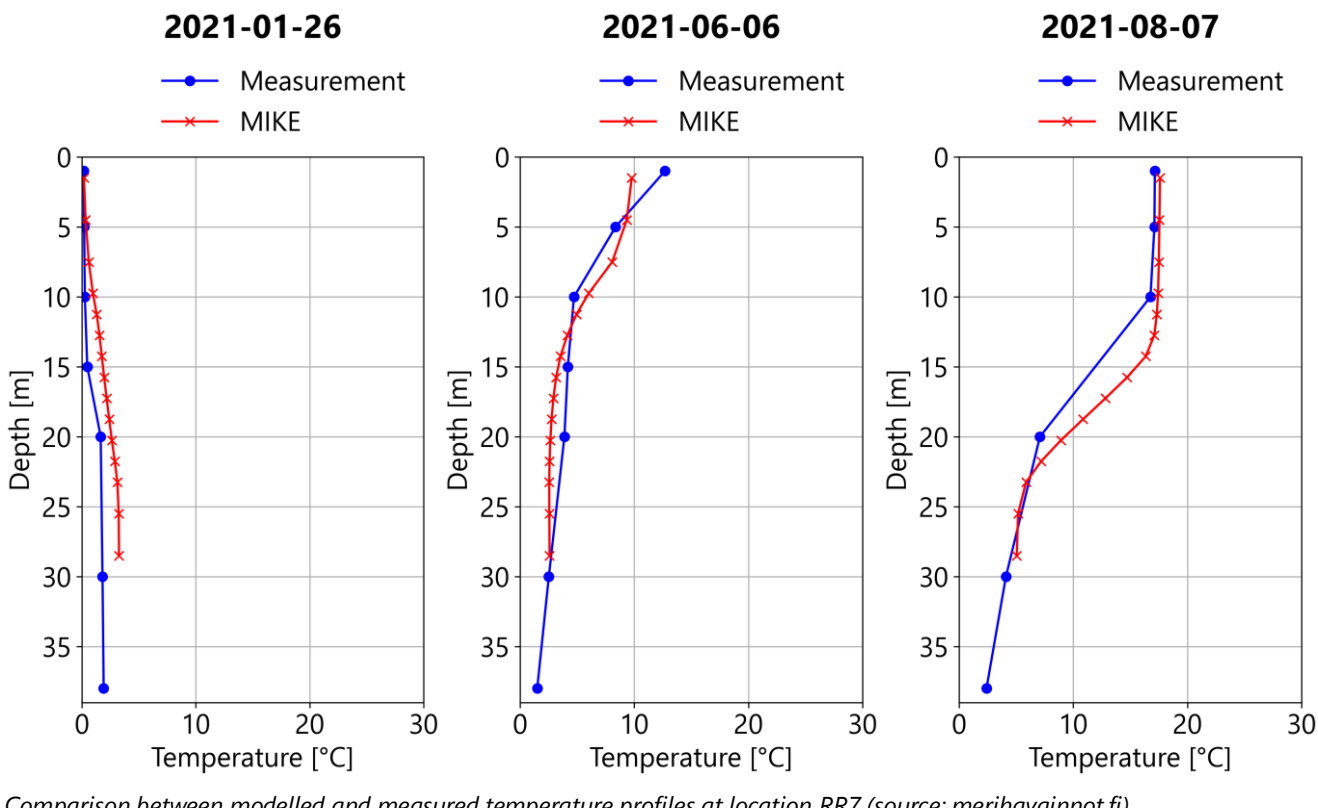
Comparison between modelled and measured temperature profiles at location US7 (source: merihavainnot.fi)



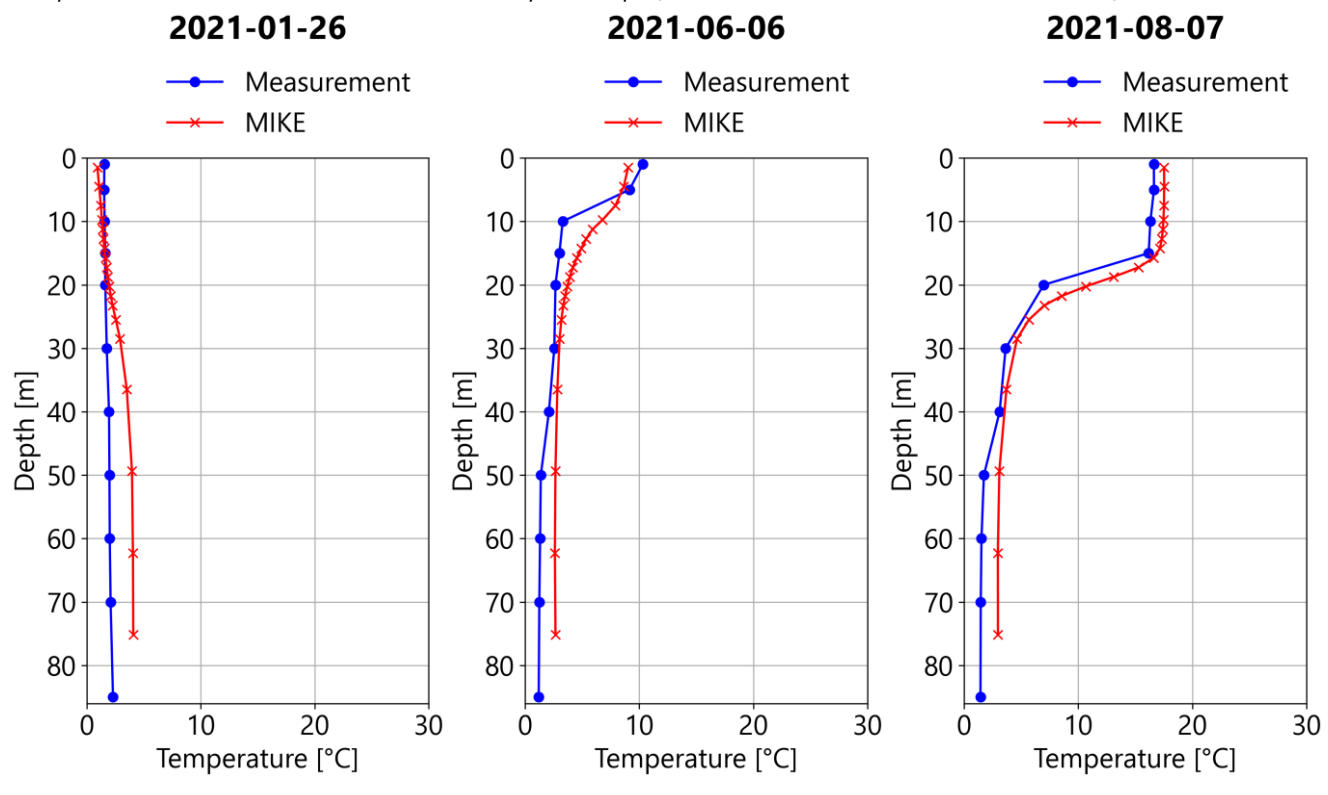
Comparison between modelled and measured temperature profiles at location US3 (source: merihavainnot.fi)



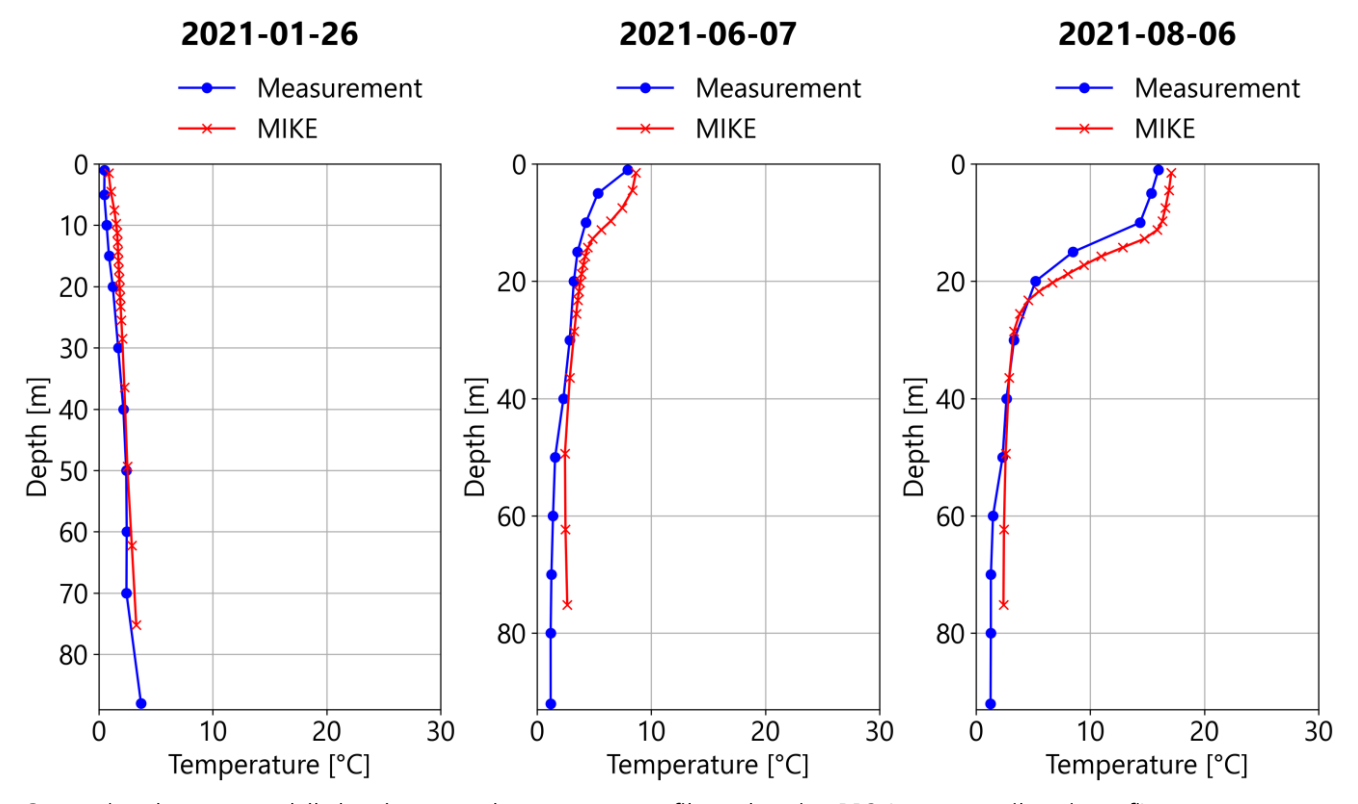
Comparison between modelled and measured temperature profiles at location BO3 (source: merihavainnot.fi)



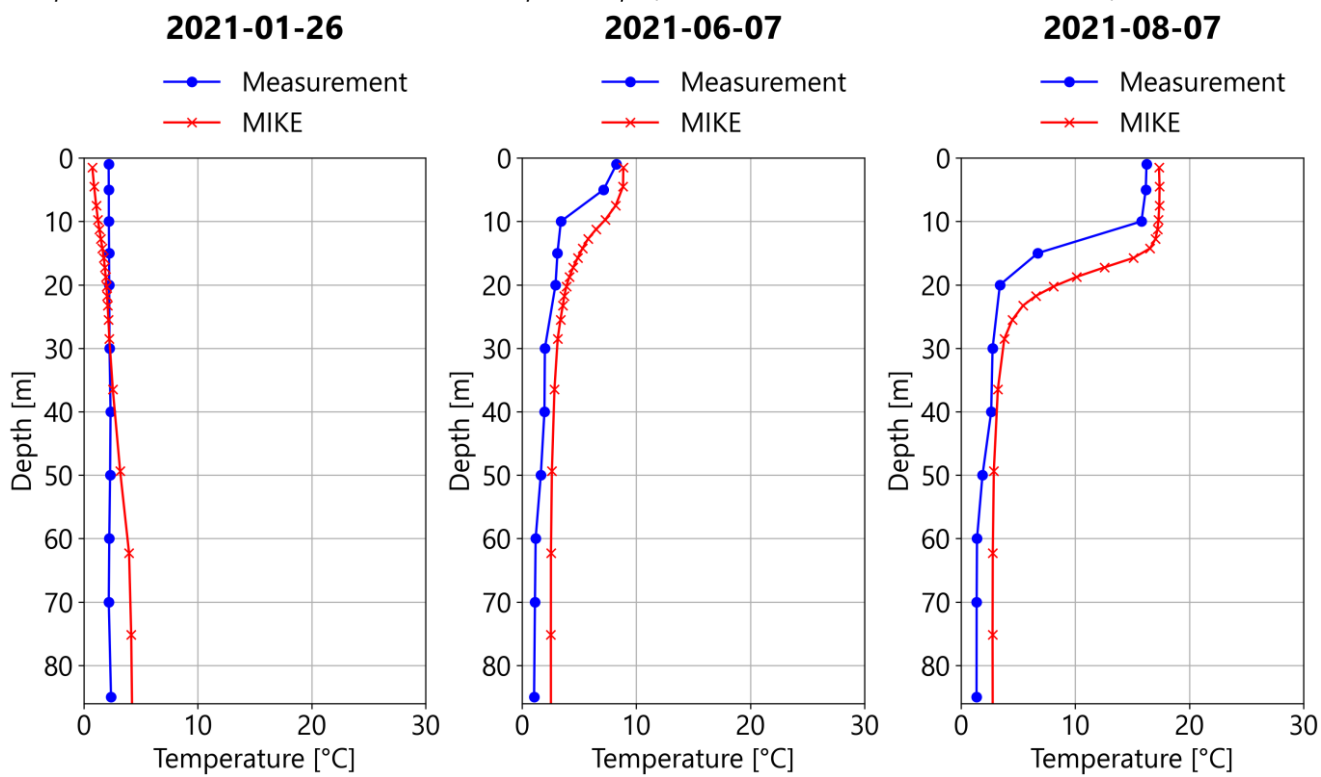
Comparison between modelled and measured temperature profiles at location RR7 (source: merihavainnot.fi)



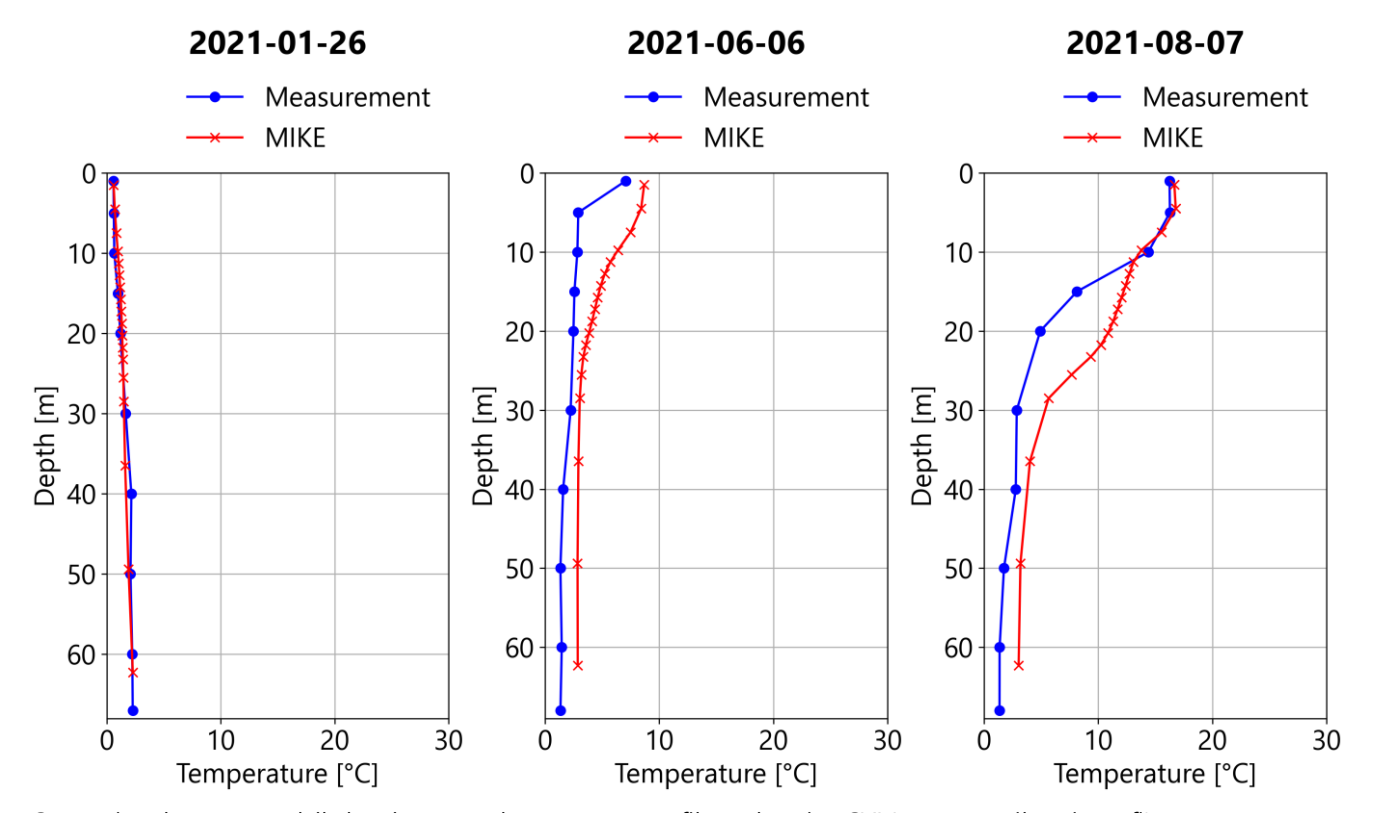
Comparison between modelled and measured temperature profiles at location RR6 (source: merihavainnot.fi)



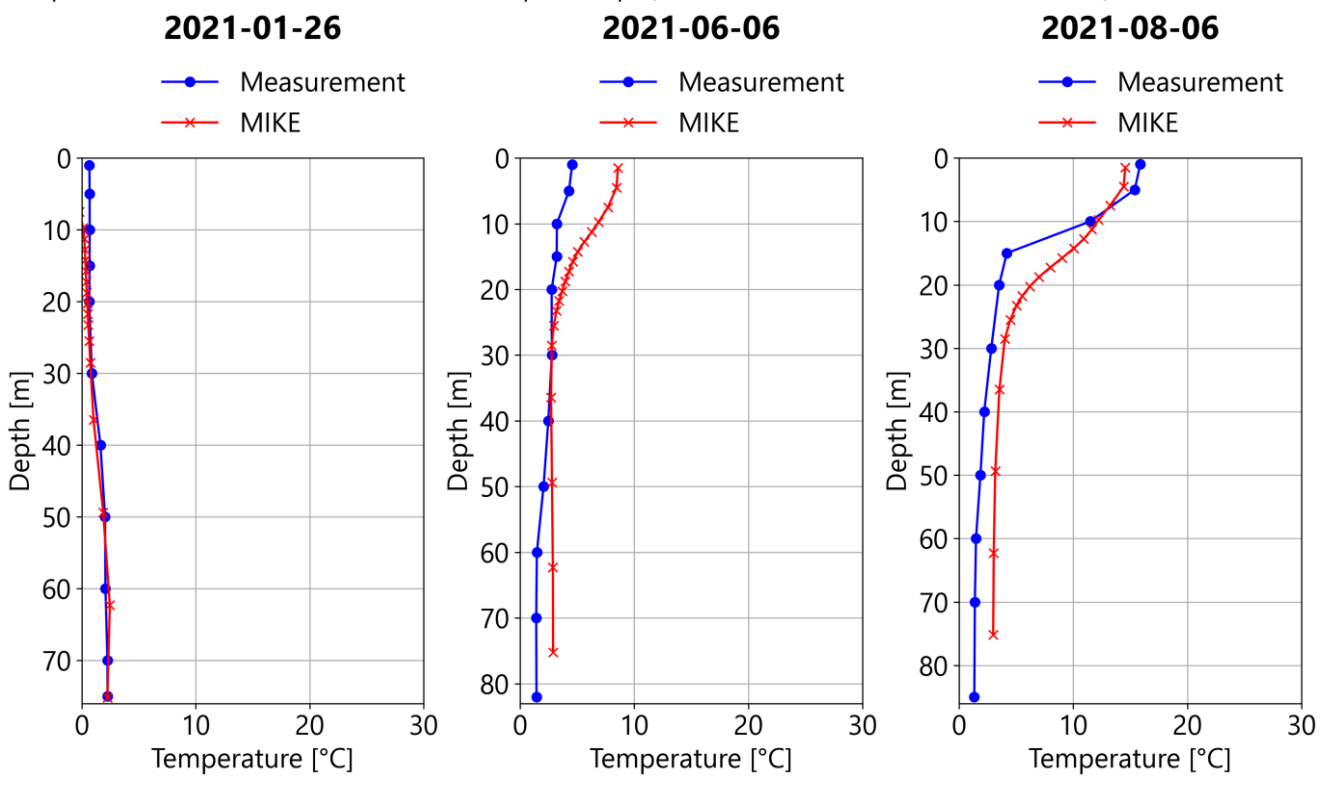
Comparison between modelled and measured temperature profiles at location RR3 (source: merihavainnot.fi)



Comparison between modelled and measured temperature profiles at location CV (source: merihavainnot.fi)

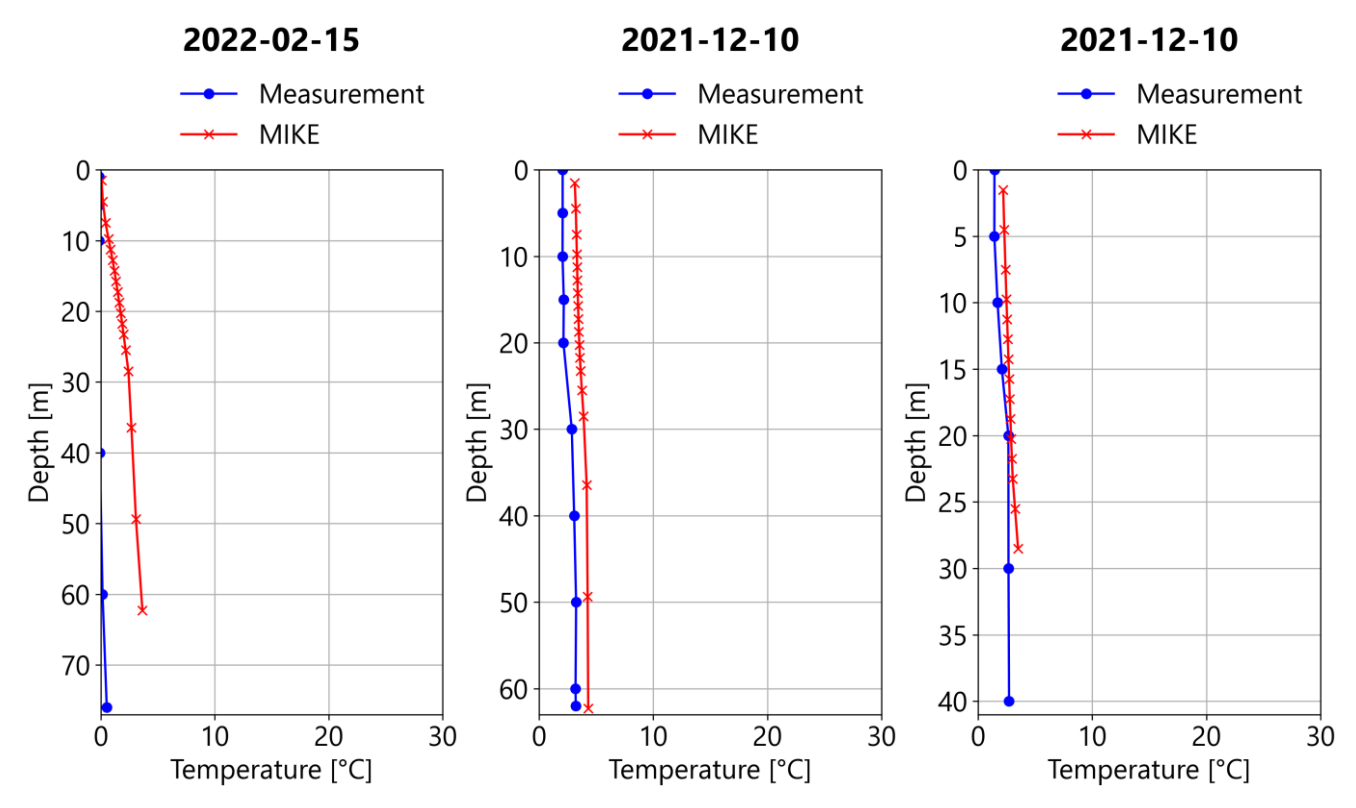


Comparison between modelled and measured temperature profiles at location CVI (source: merihavainnot.fi)

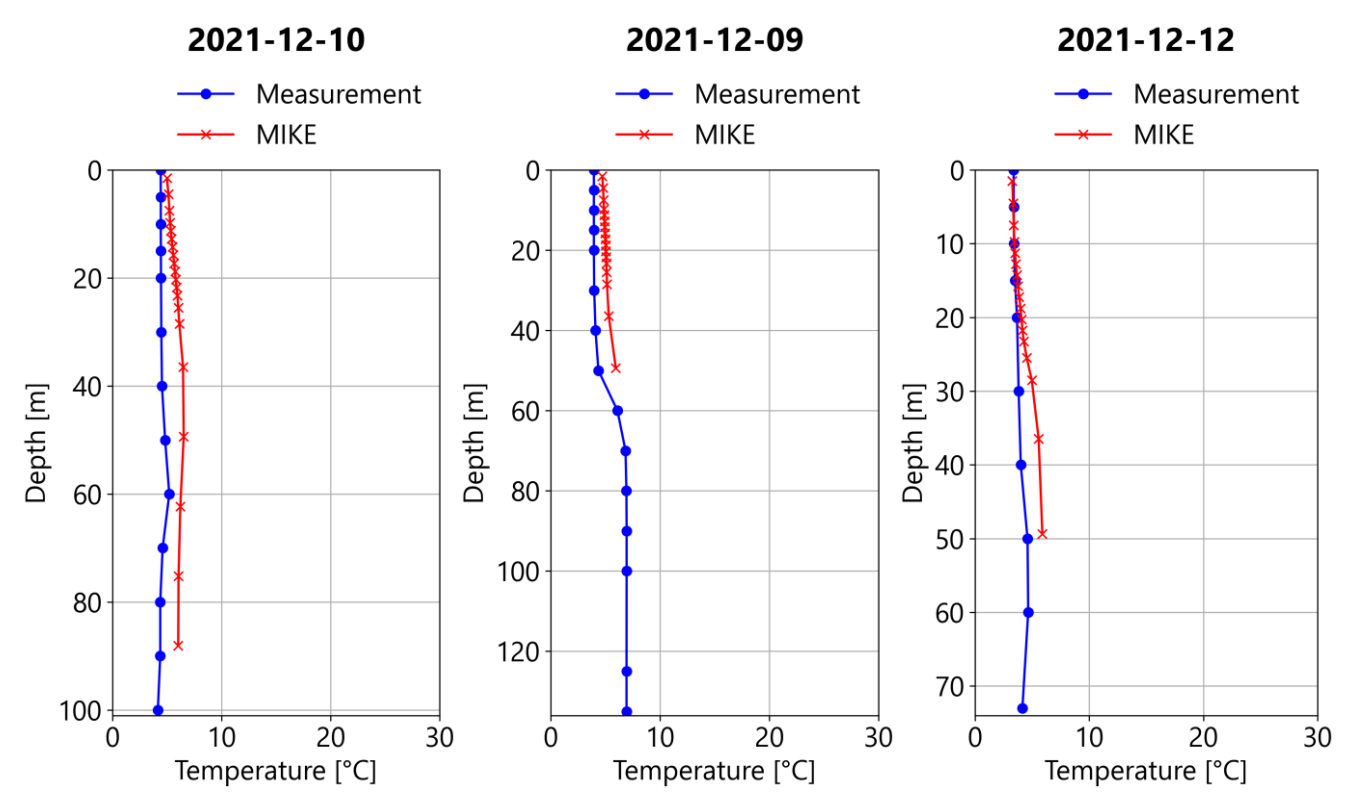


Comparison between modelled and measured temperature profiles at location F2 (source: merihavainnot.fi)

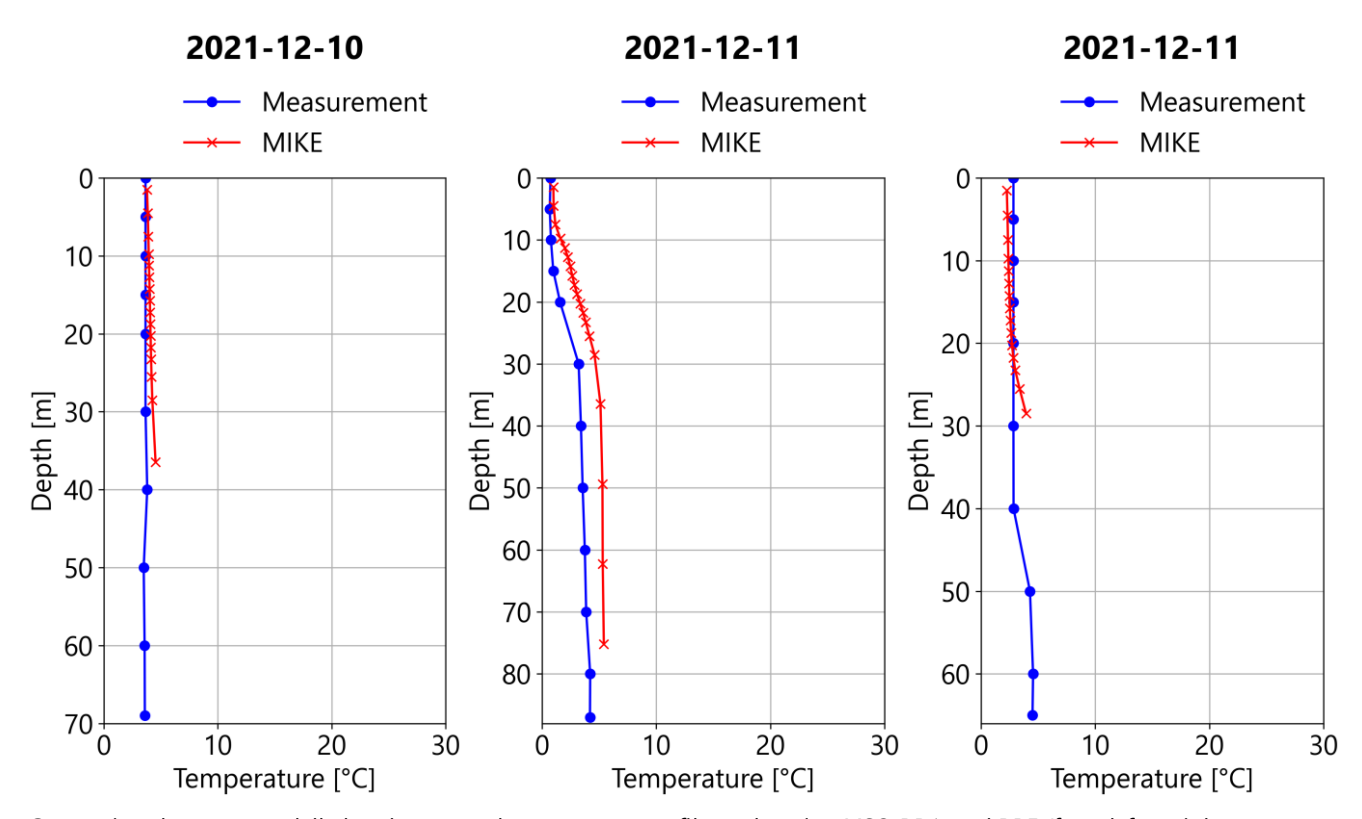
Profiles from SMHI



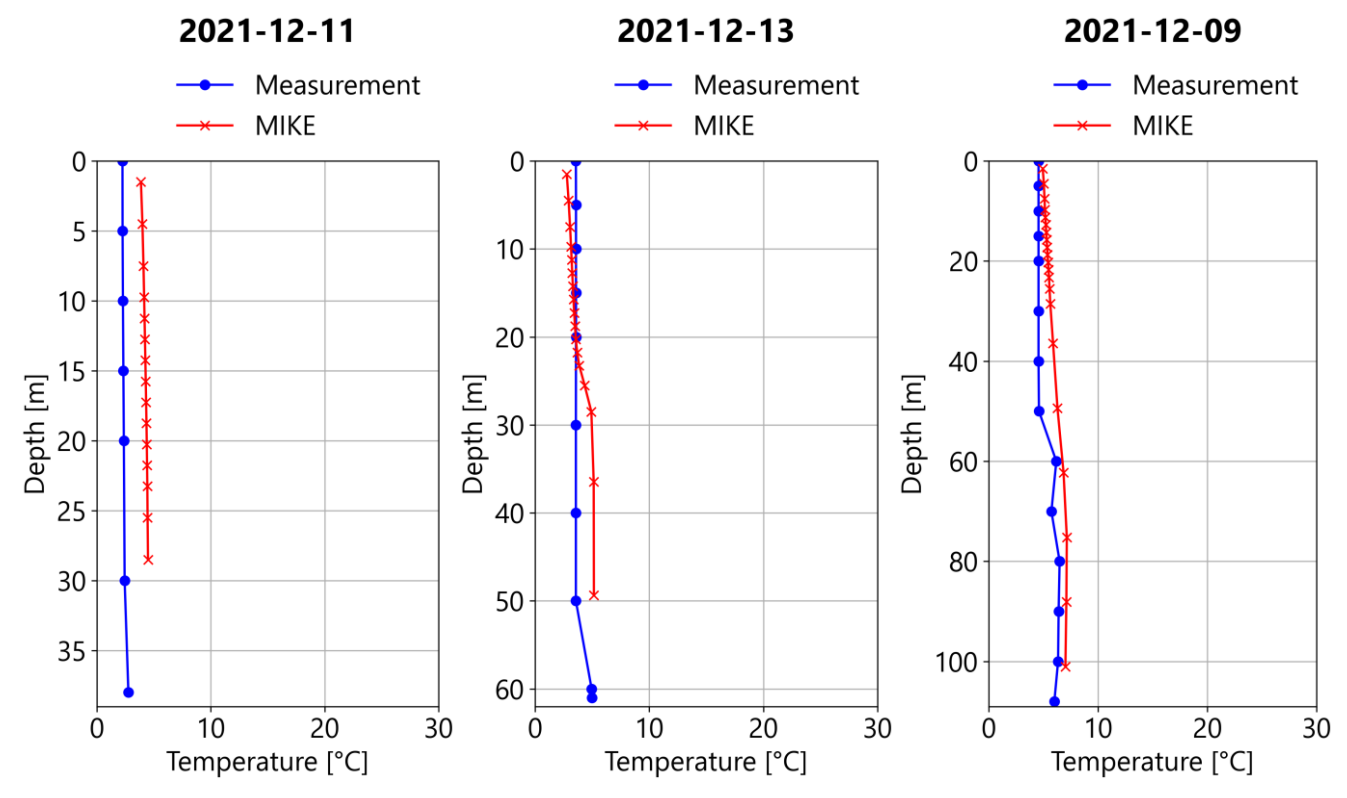
Comparison between modelled and measured temperature profiles at location A5, F13, and F16 (from left to right, source: SMHI)



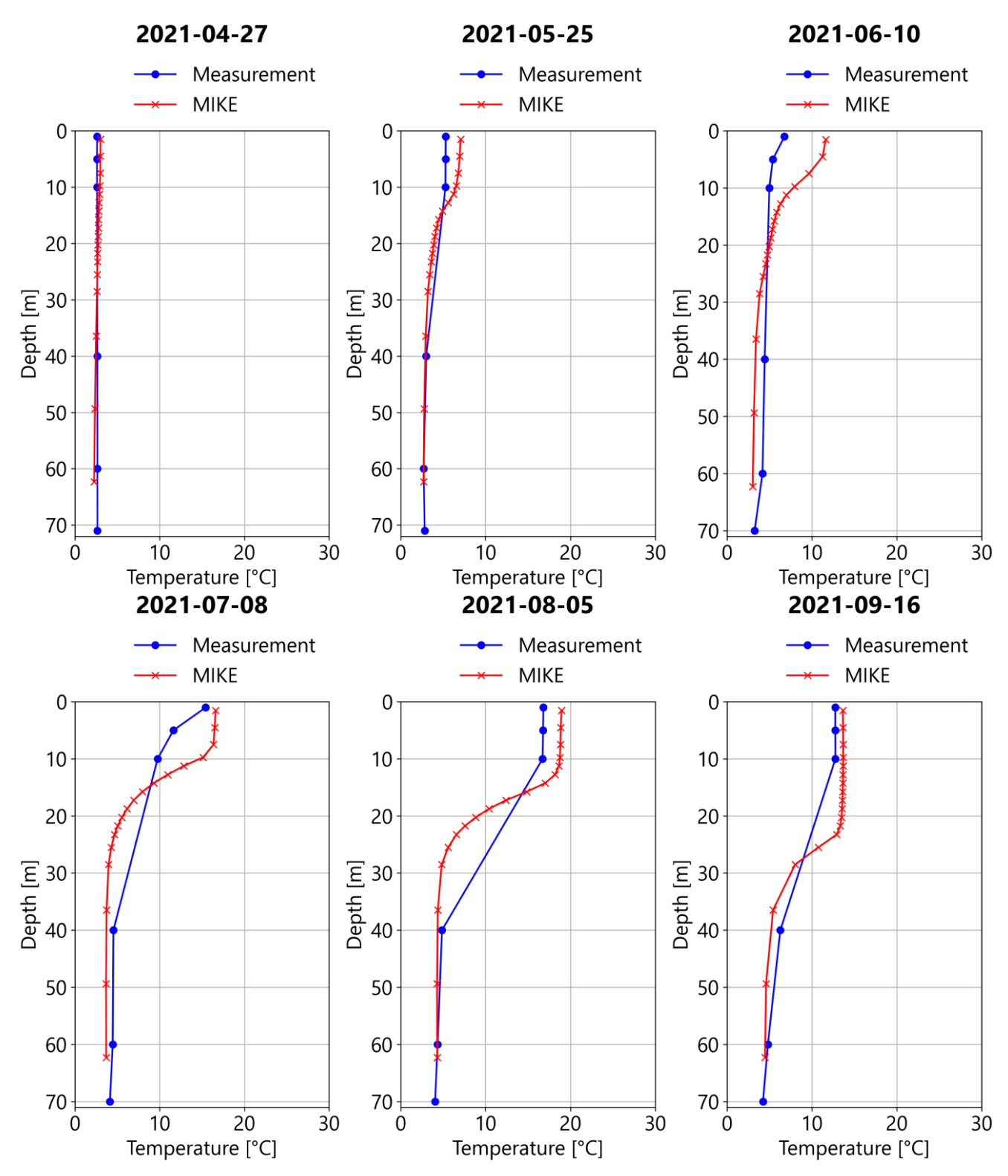
Comparison between modelled and measured temperature profiles at location F18 SYDOSTBROTTEN, F33 GRUNDKALLEN, and MS2 (from left to right, source: SMHI)



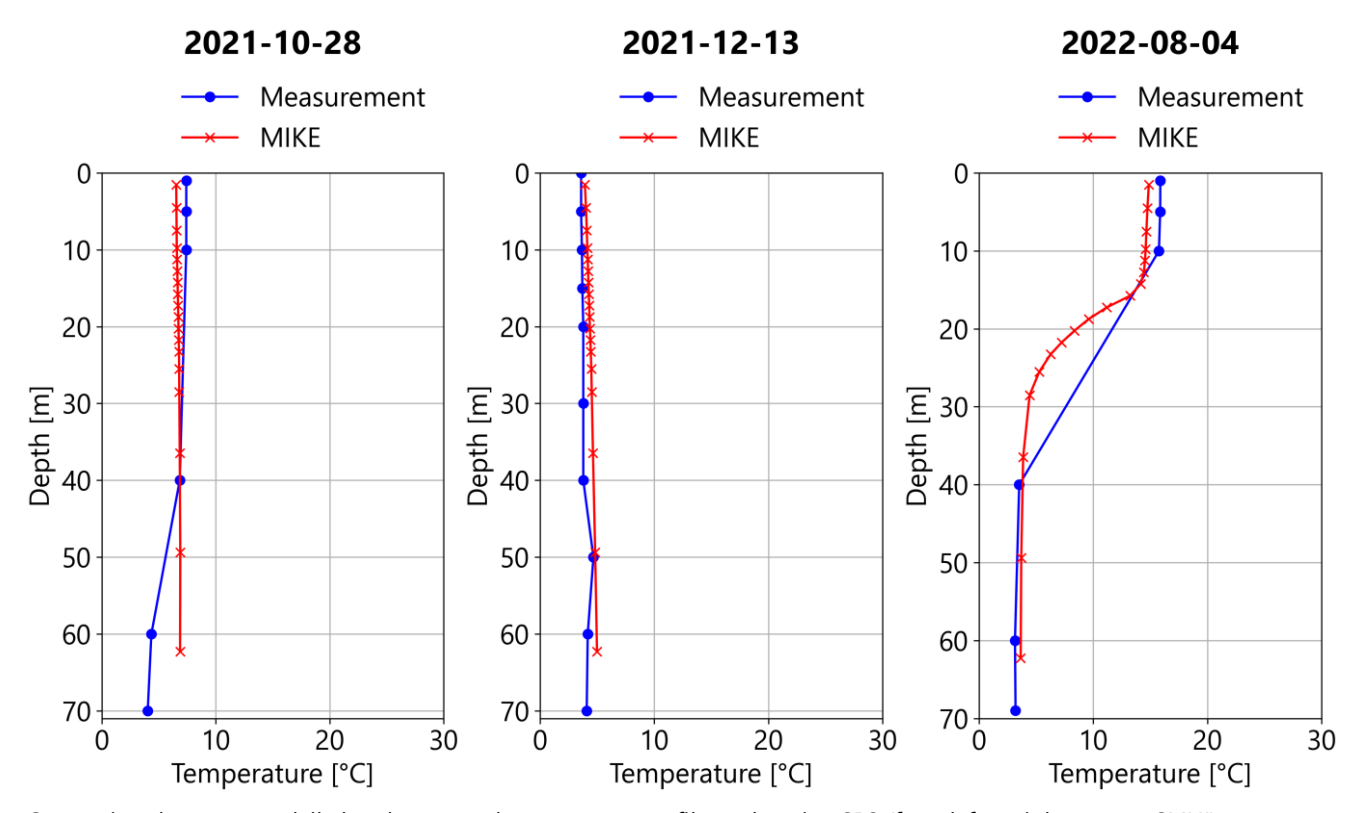
Comparison between modelled and measured temperature profiles at location MS6, RR1, and RR5 (from left to right, source: SMHI)



Comparison between modelled and measured temperature profiles at location SR1A, and SS29 (from left to right, source: SMHI)

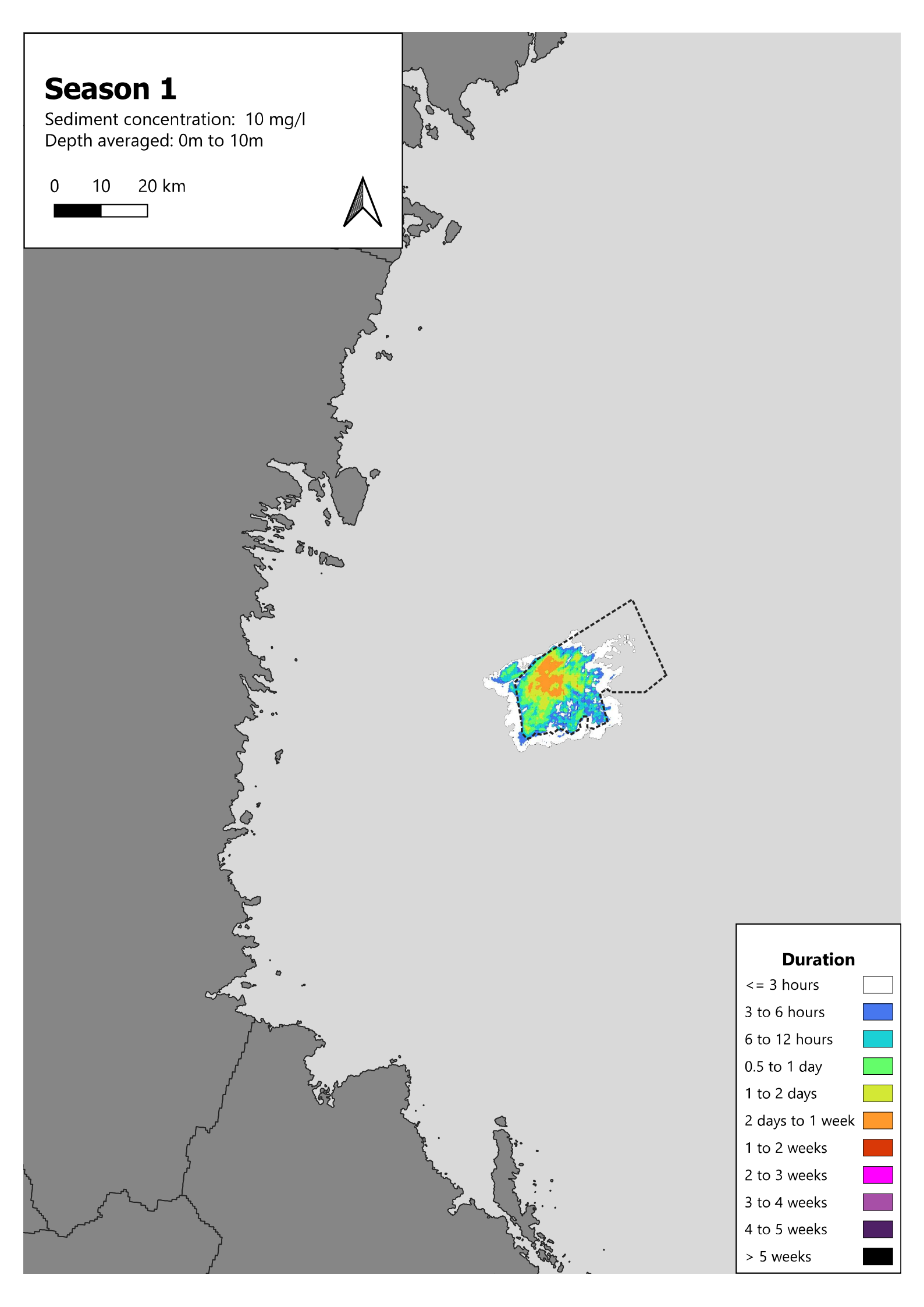


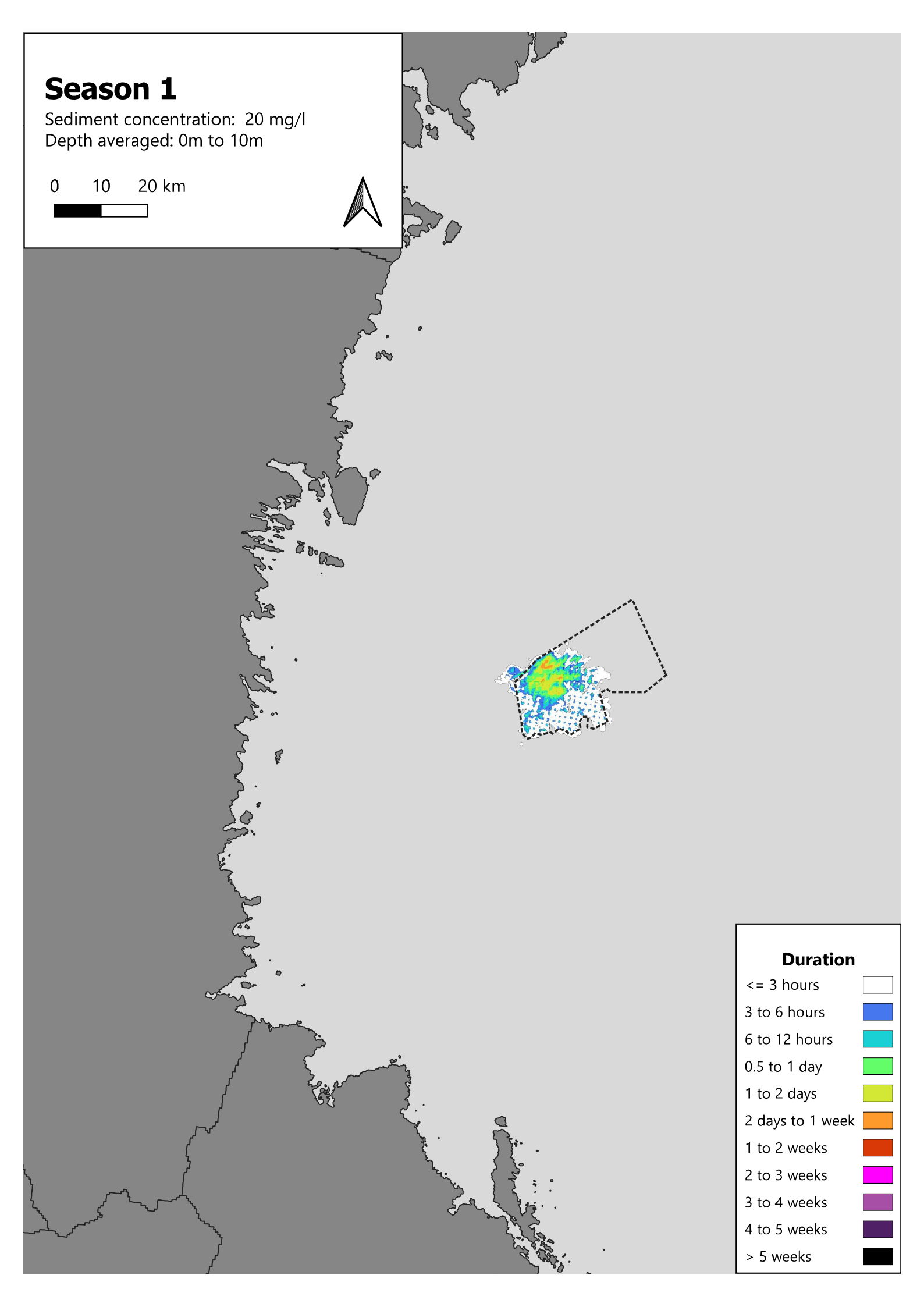
Comparison between modelled and measured temperature profiles at location SR3 (from left to right, source: SMHI)

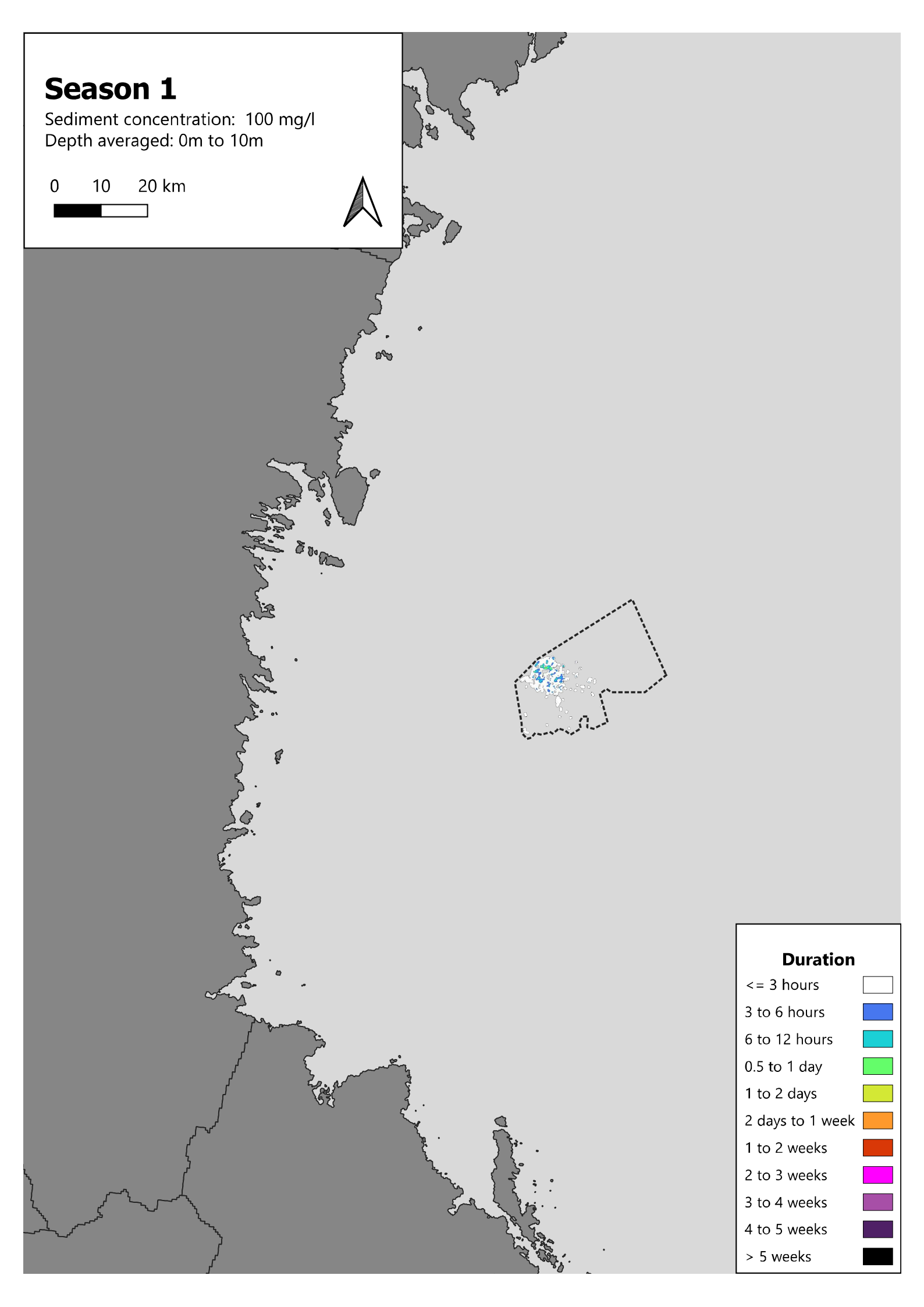


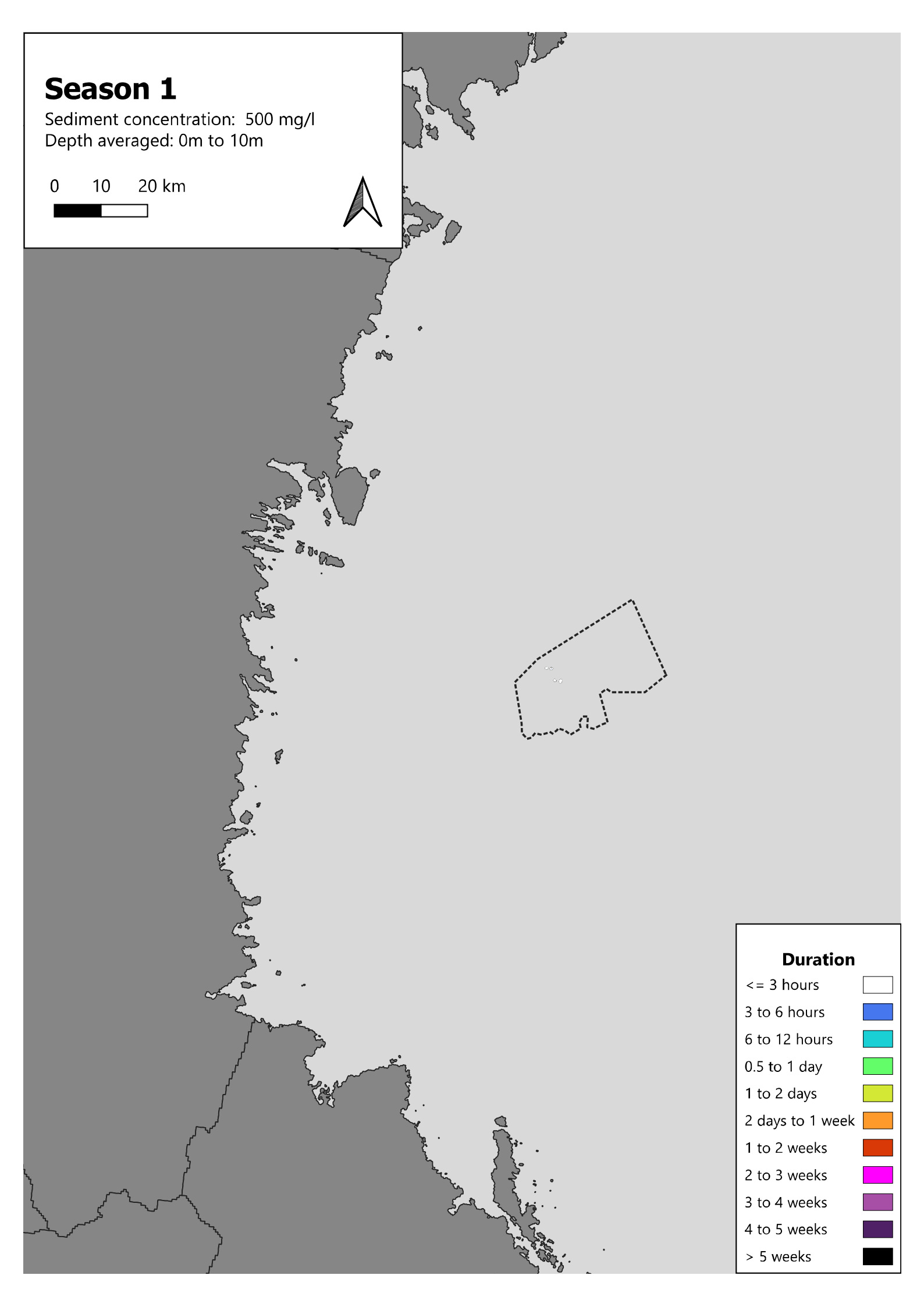
Comparison between modelled and measured temperature profiles at location SR3 (from left to right, source: SMHI)

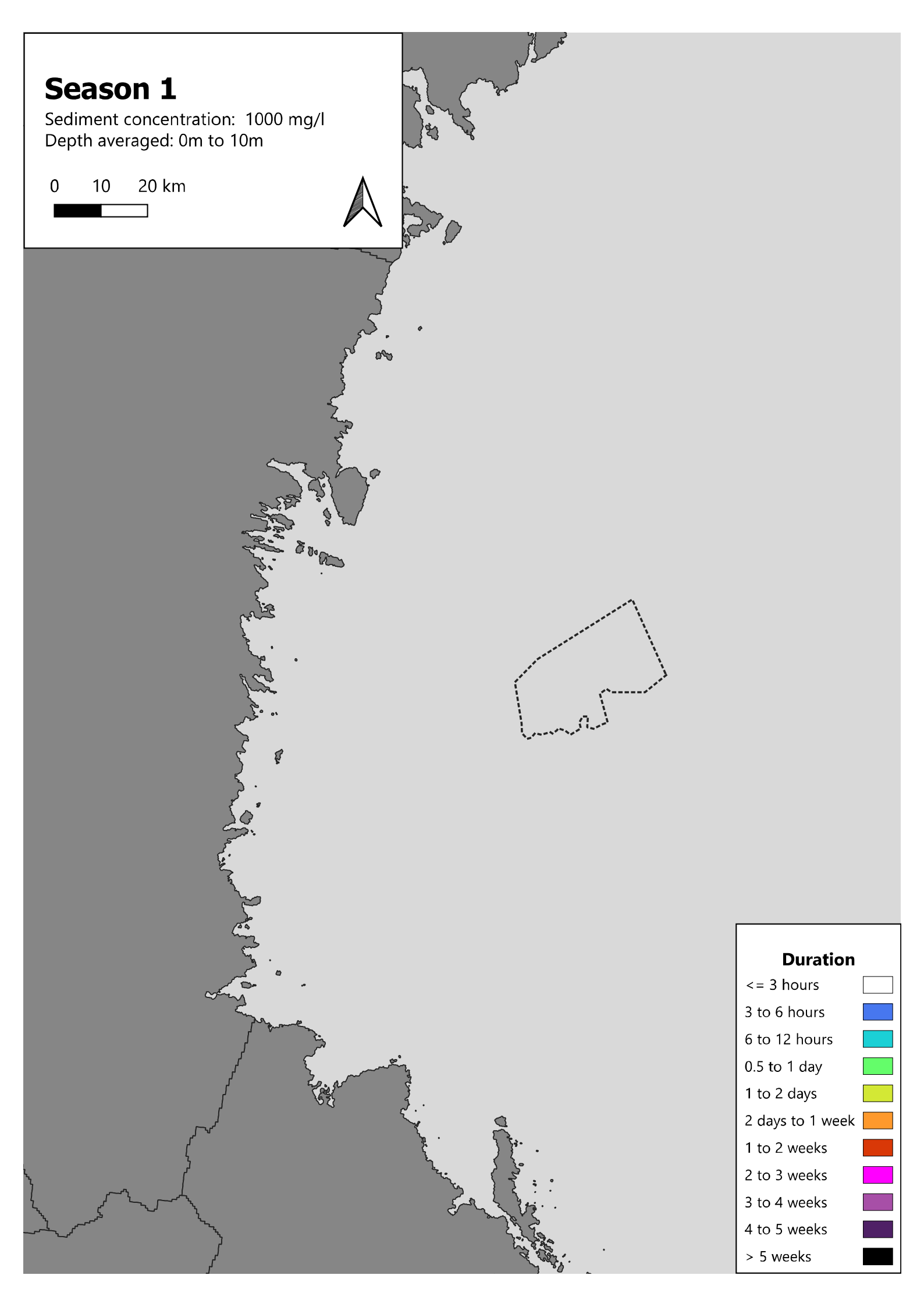


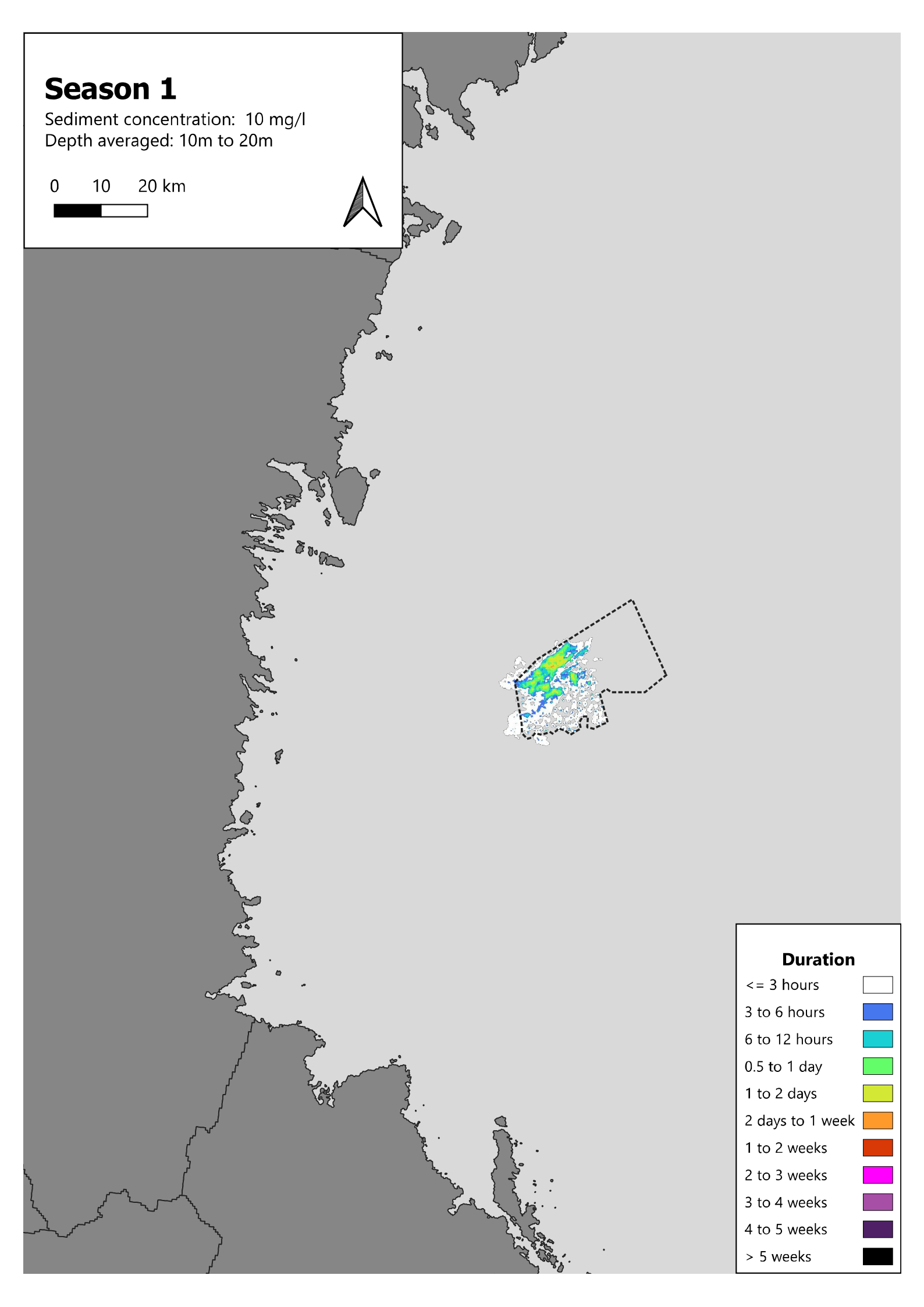


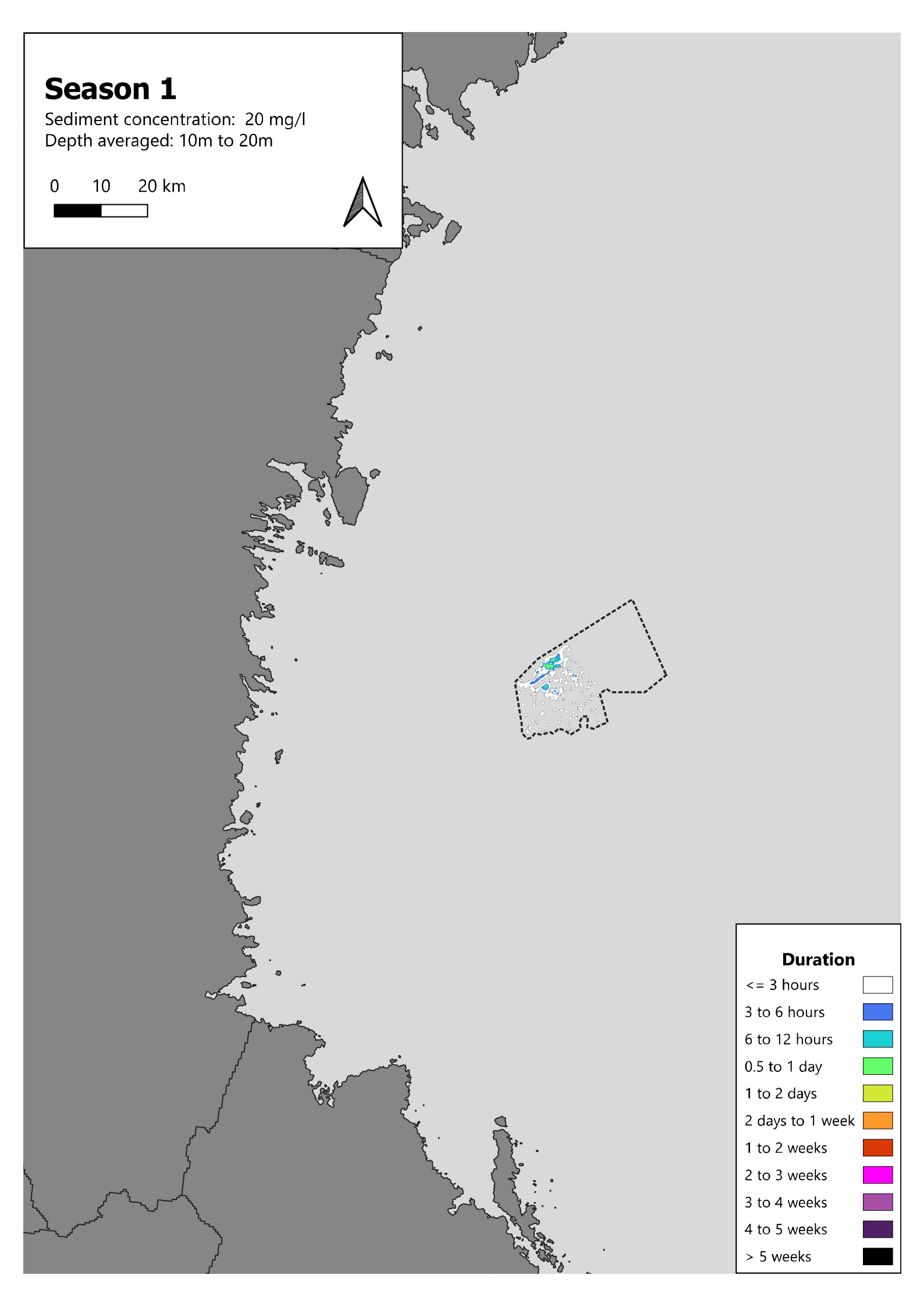


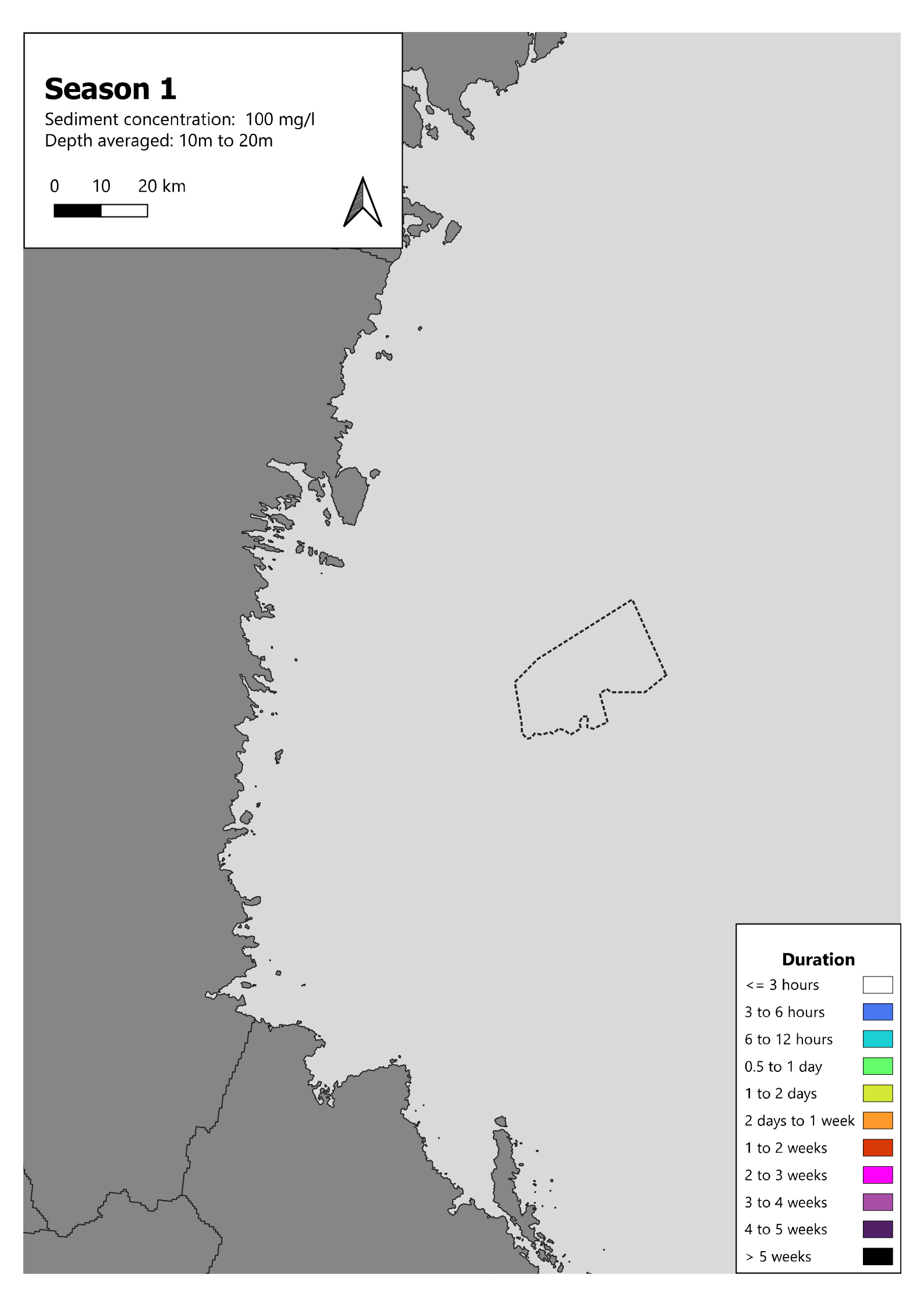


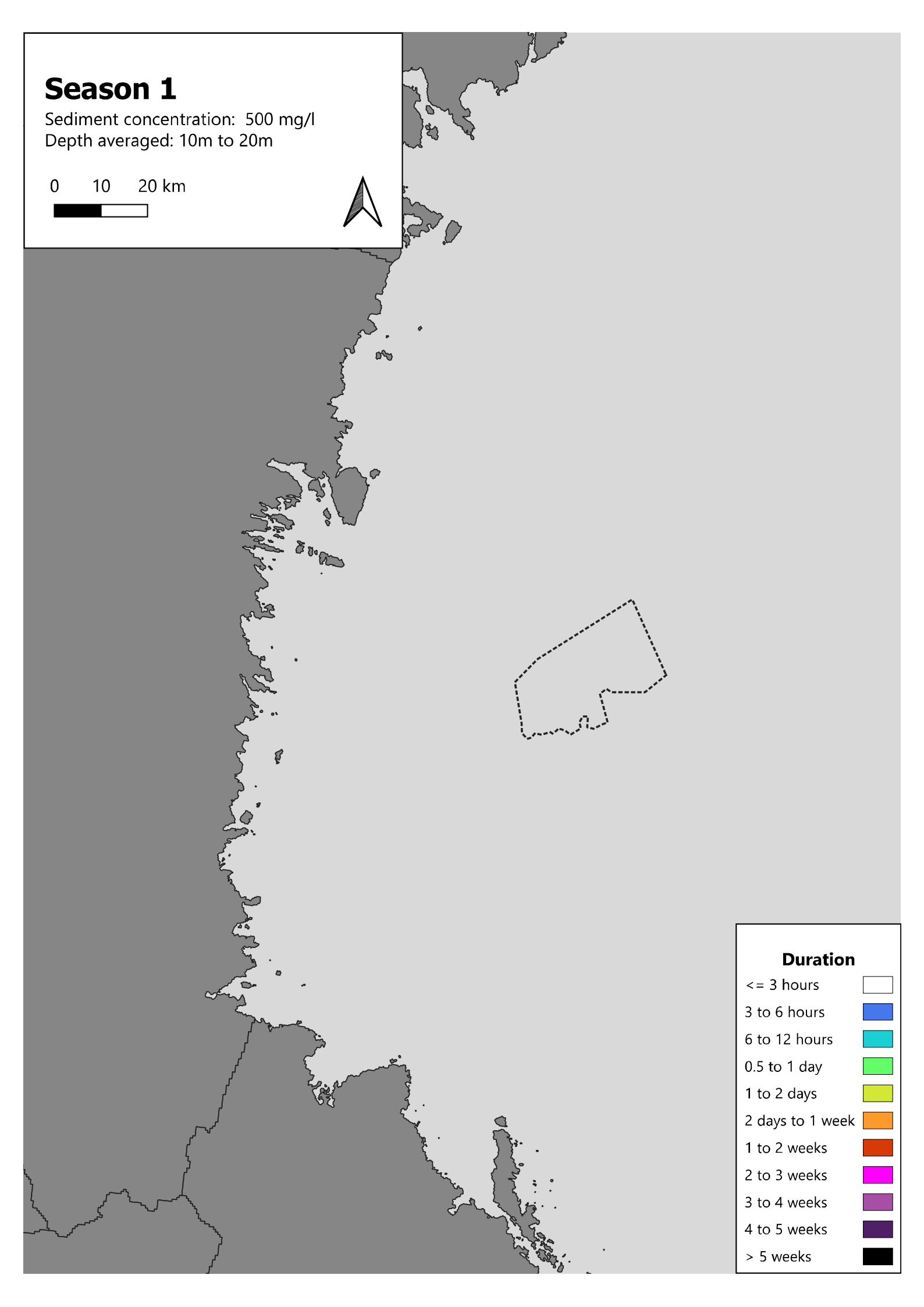


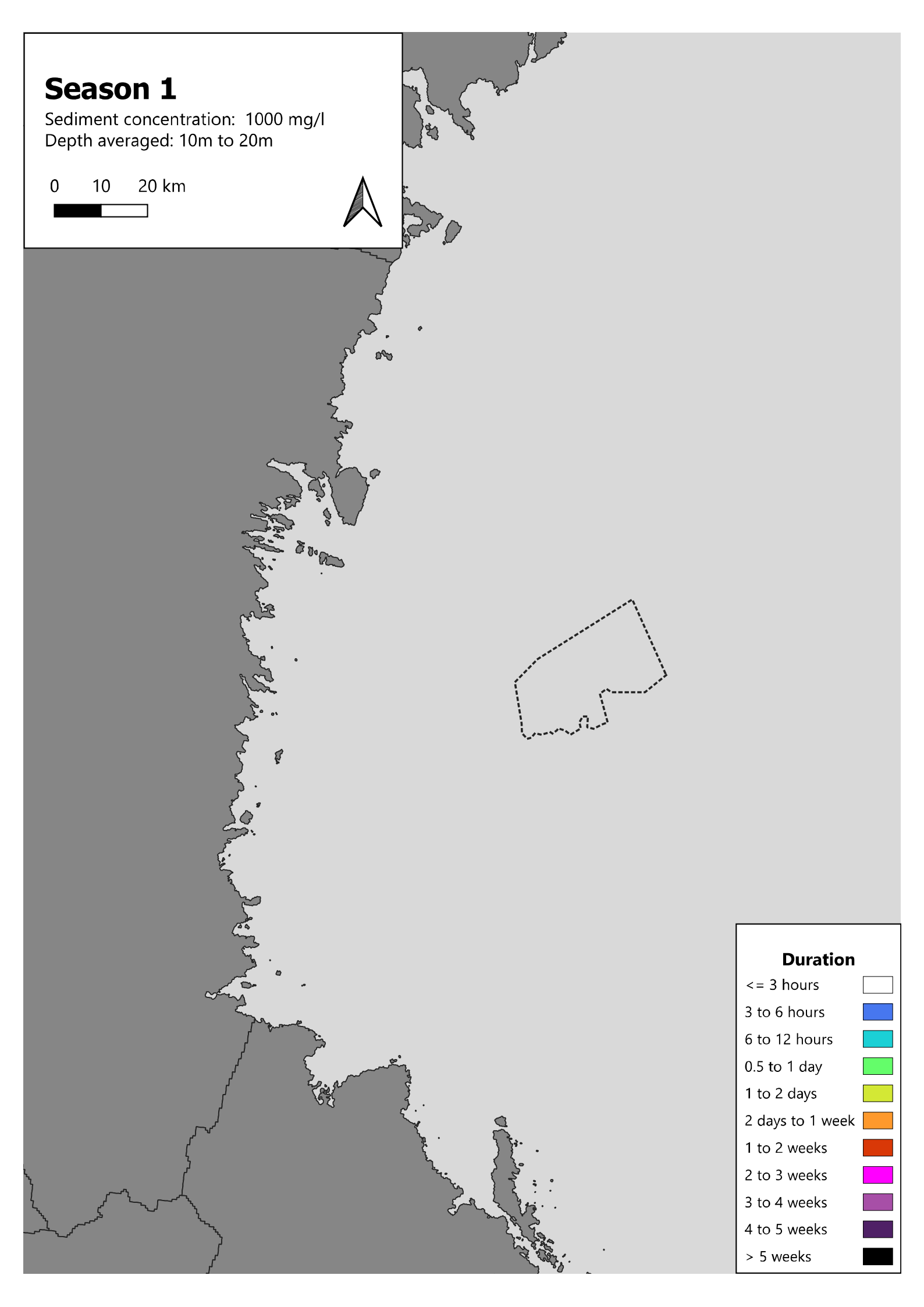


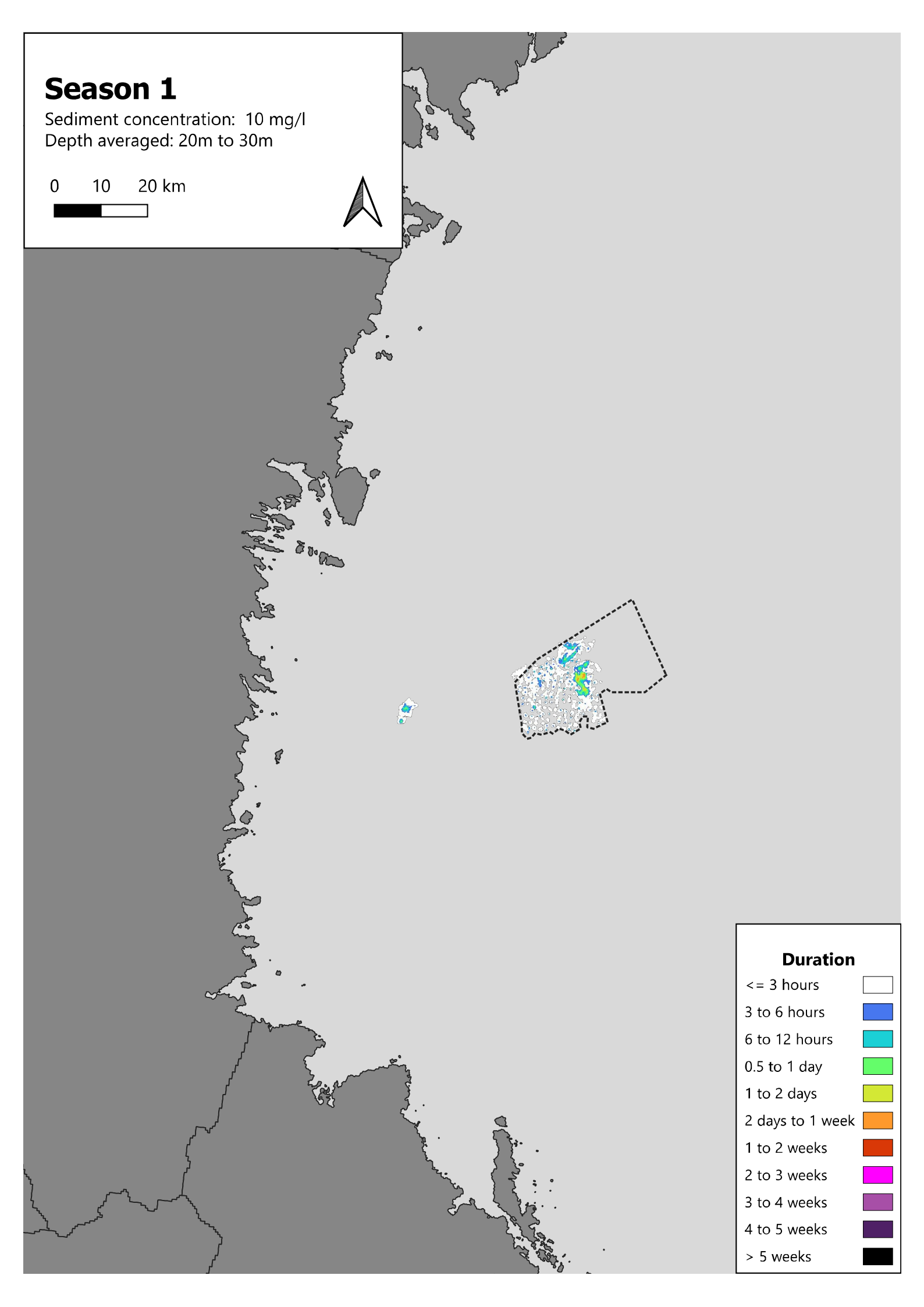


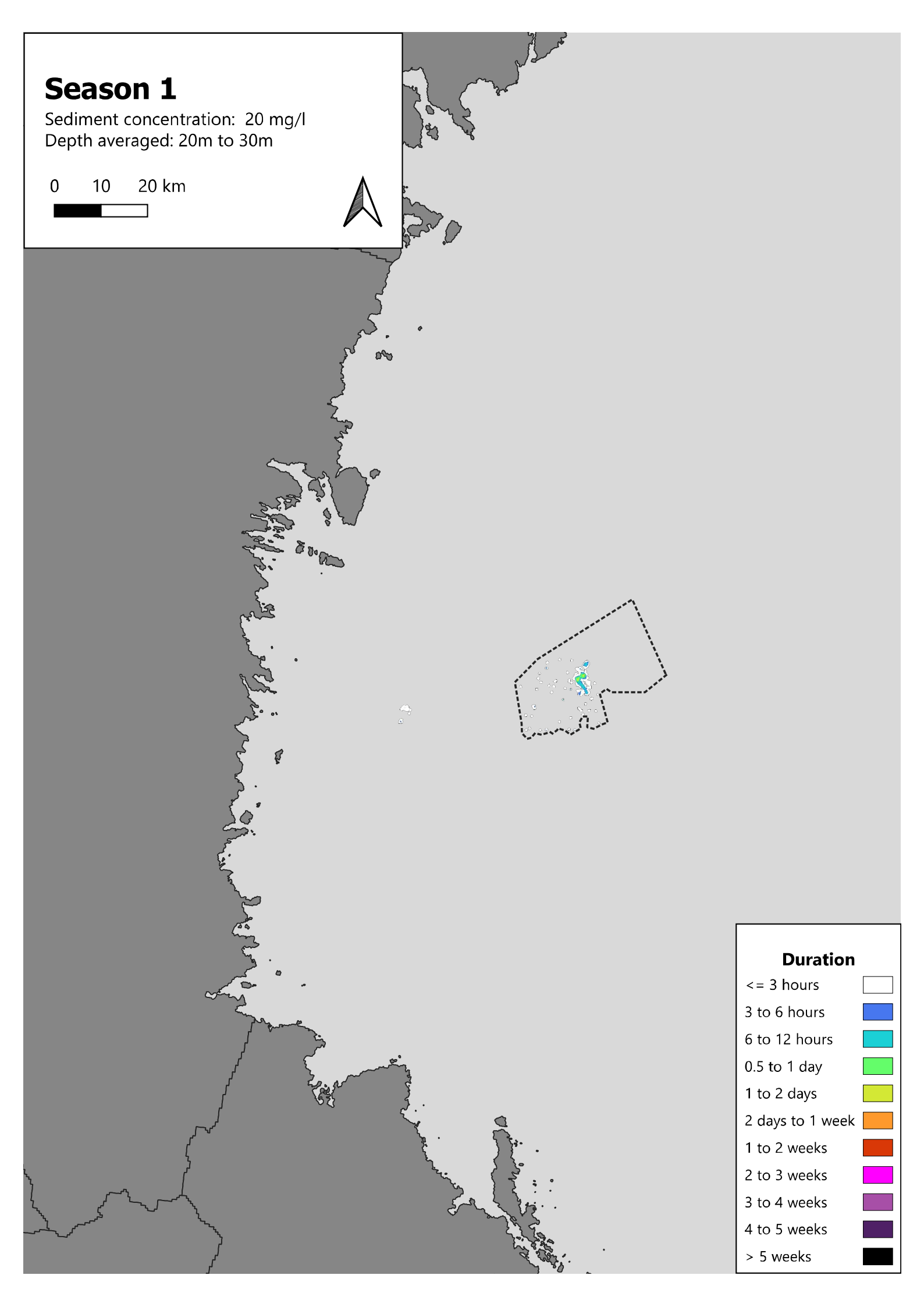


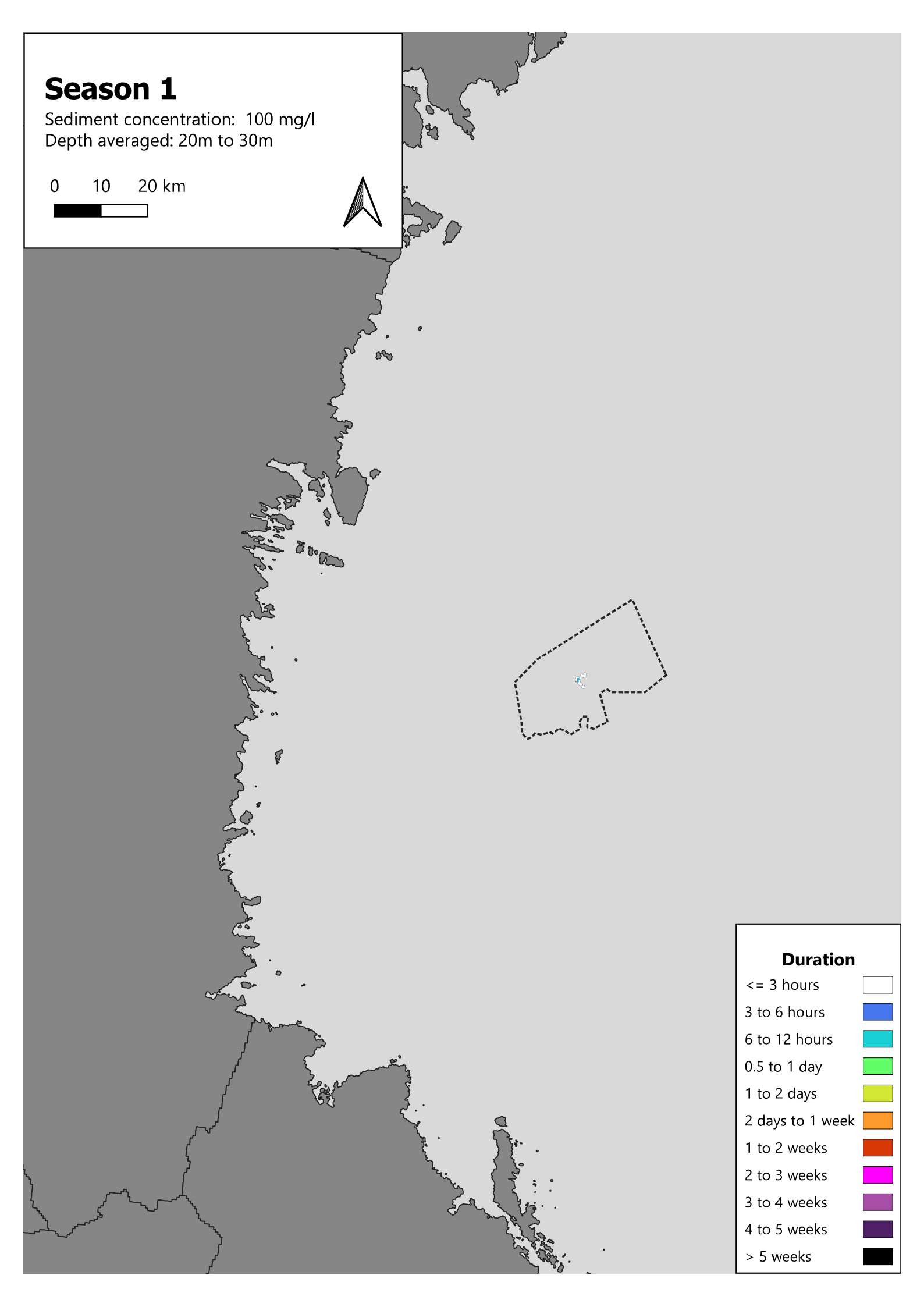


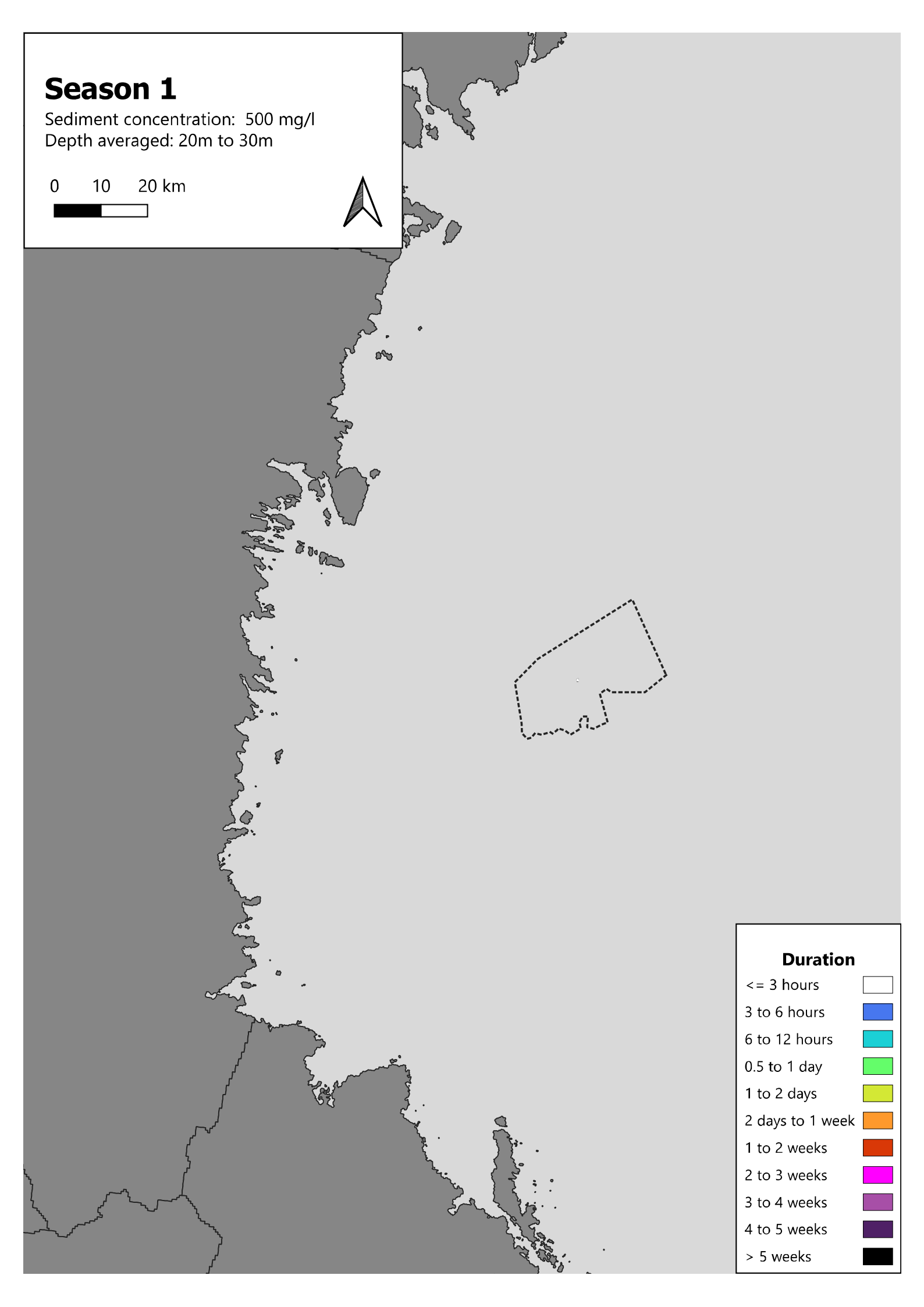


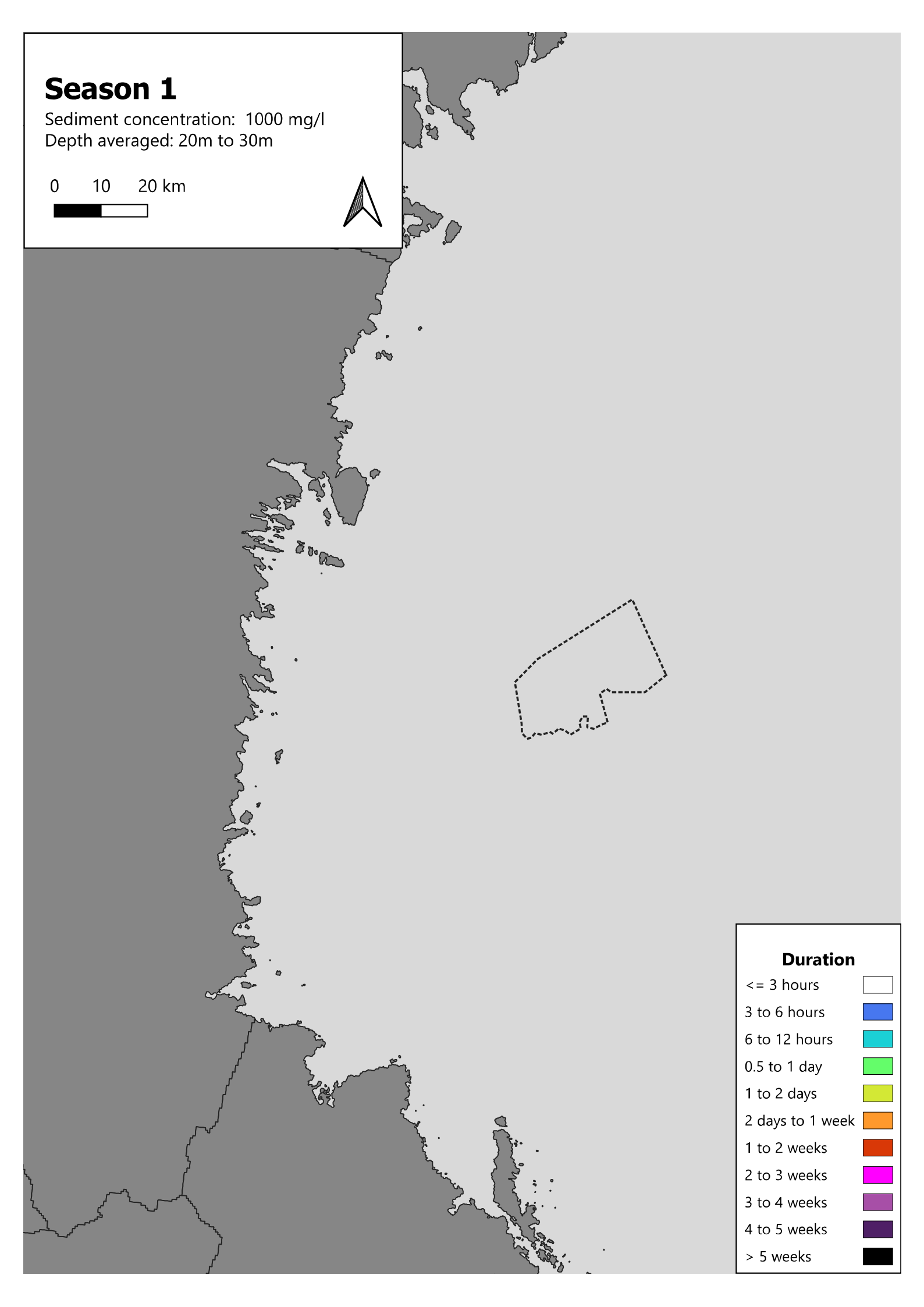


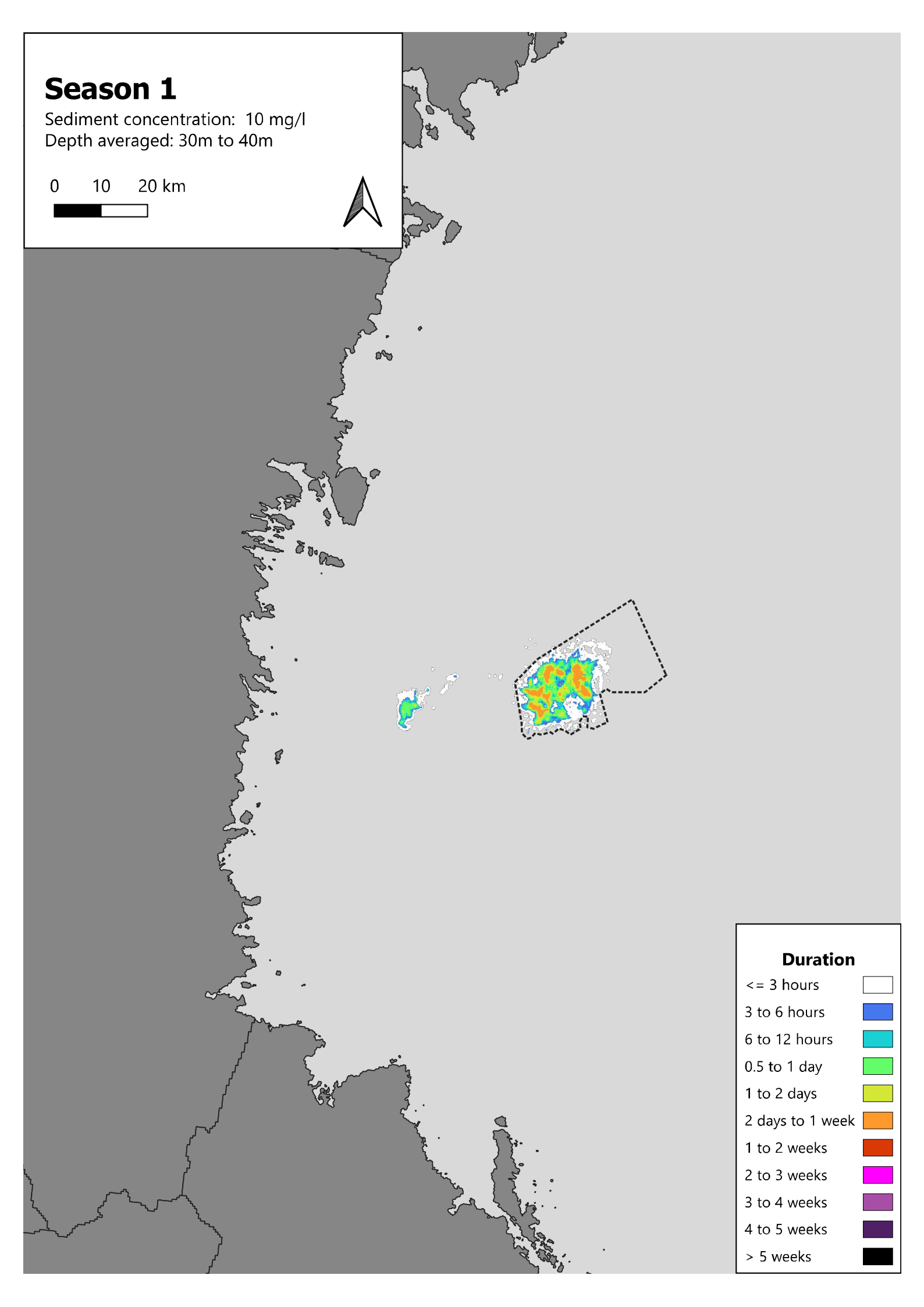


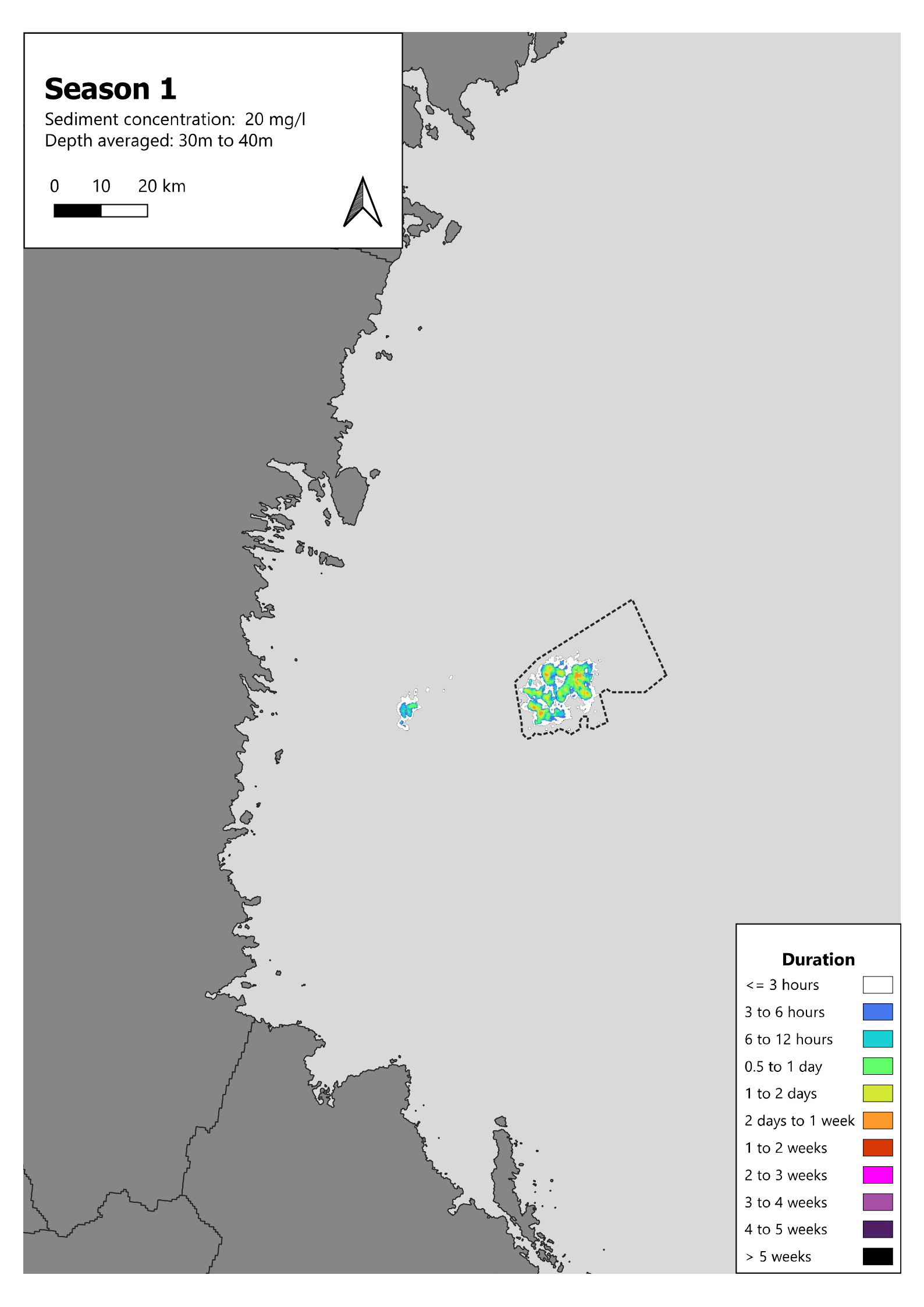


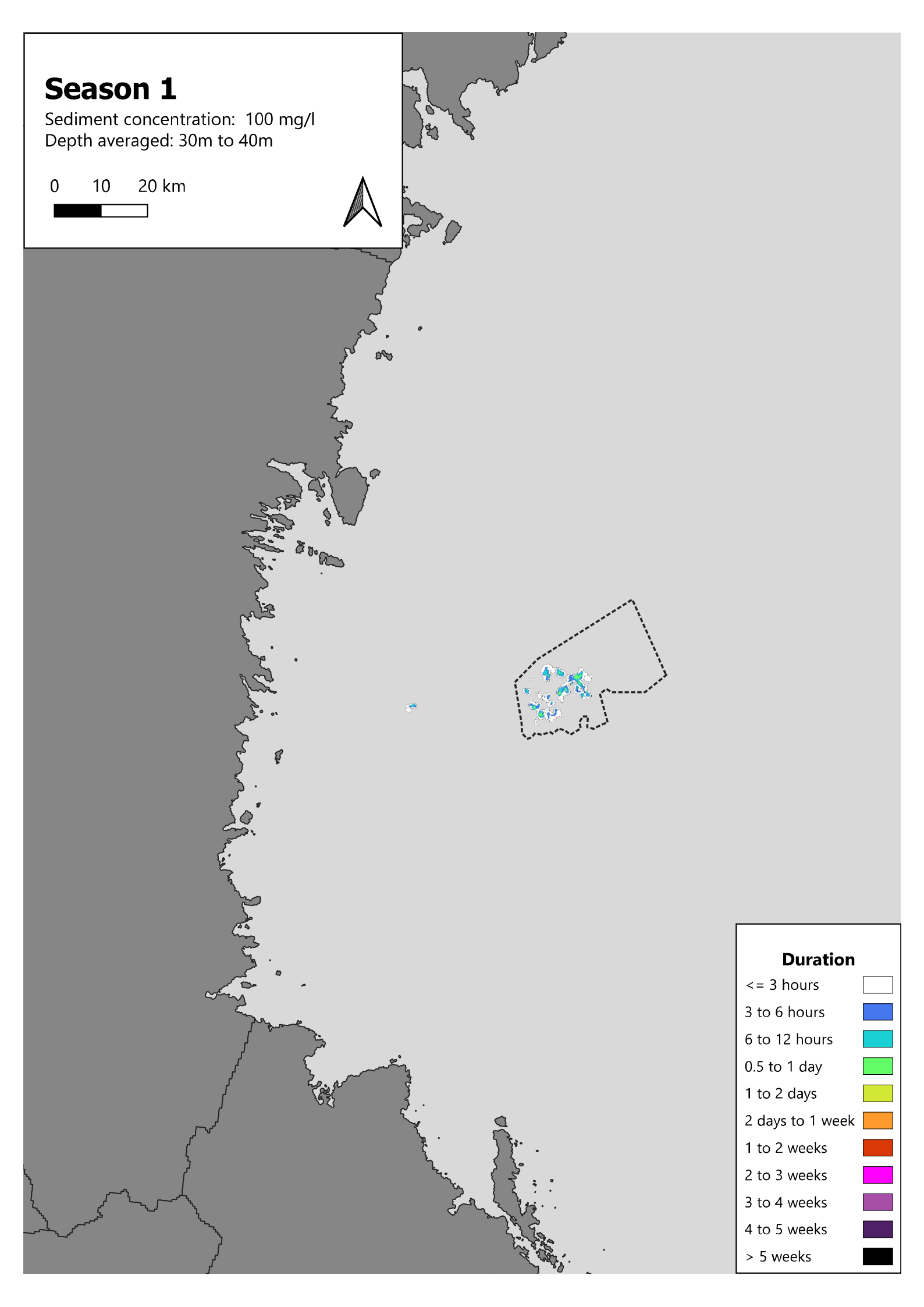


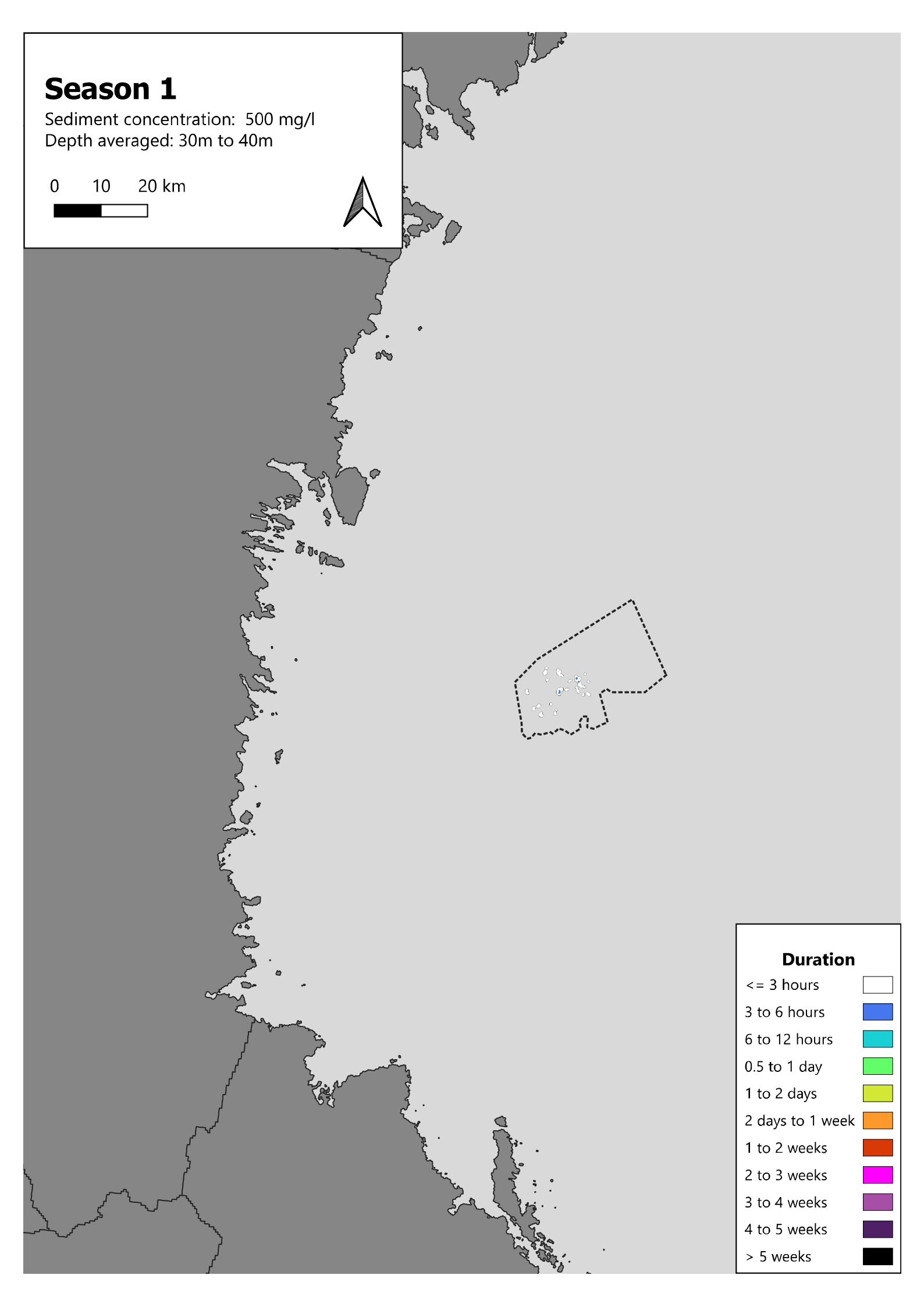


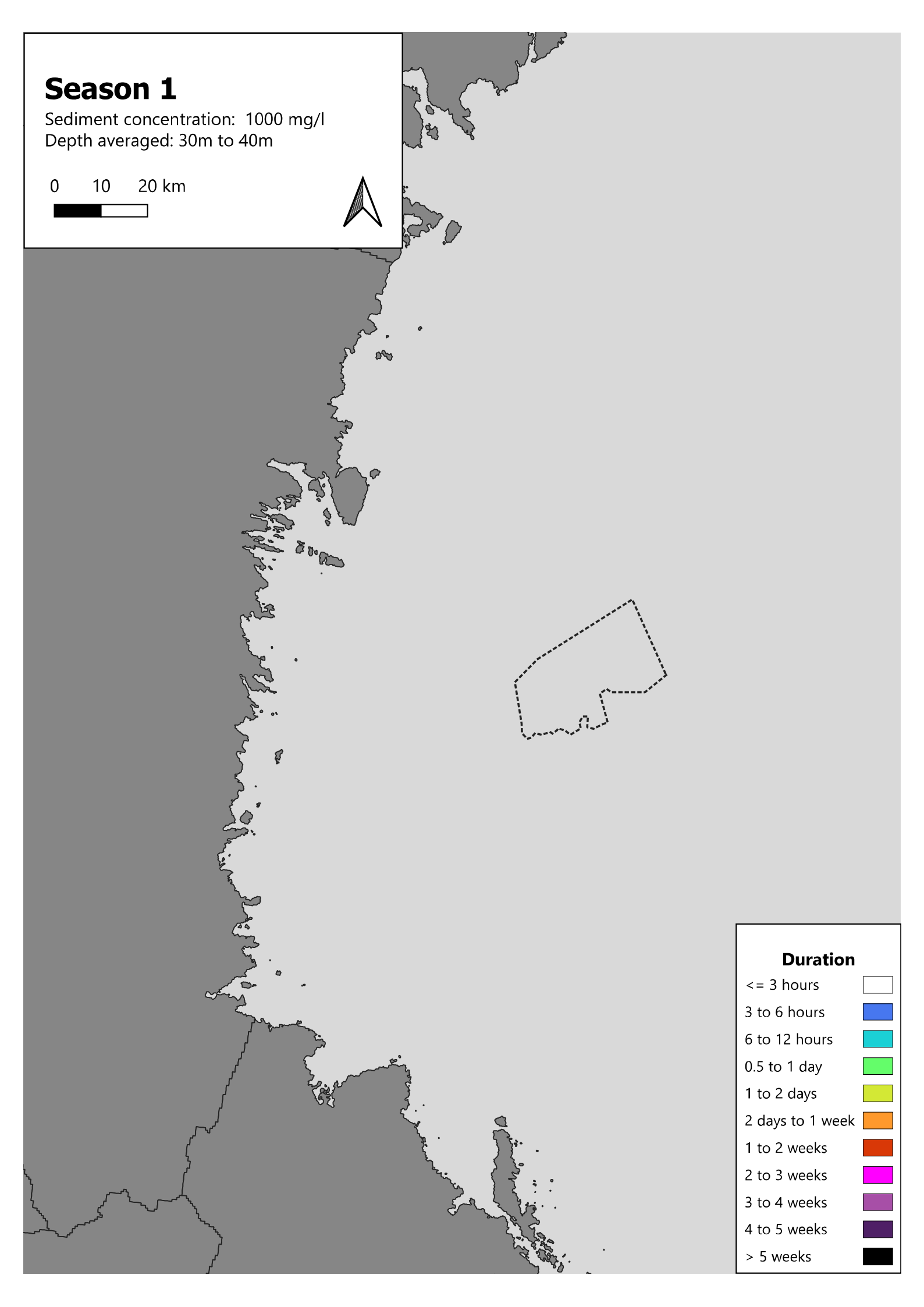


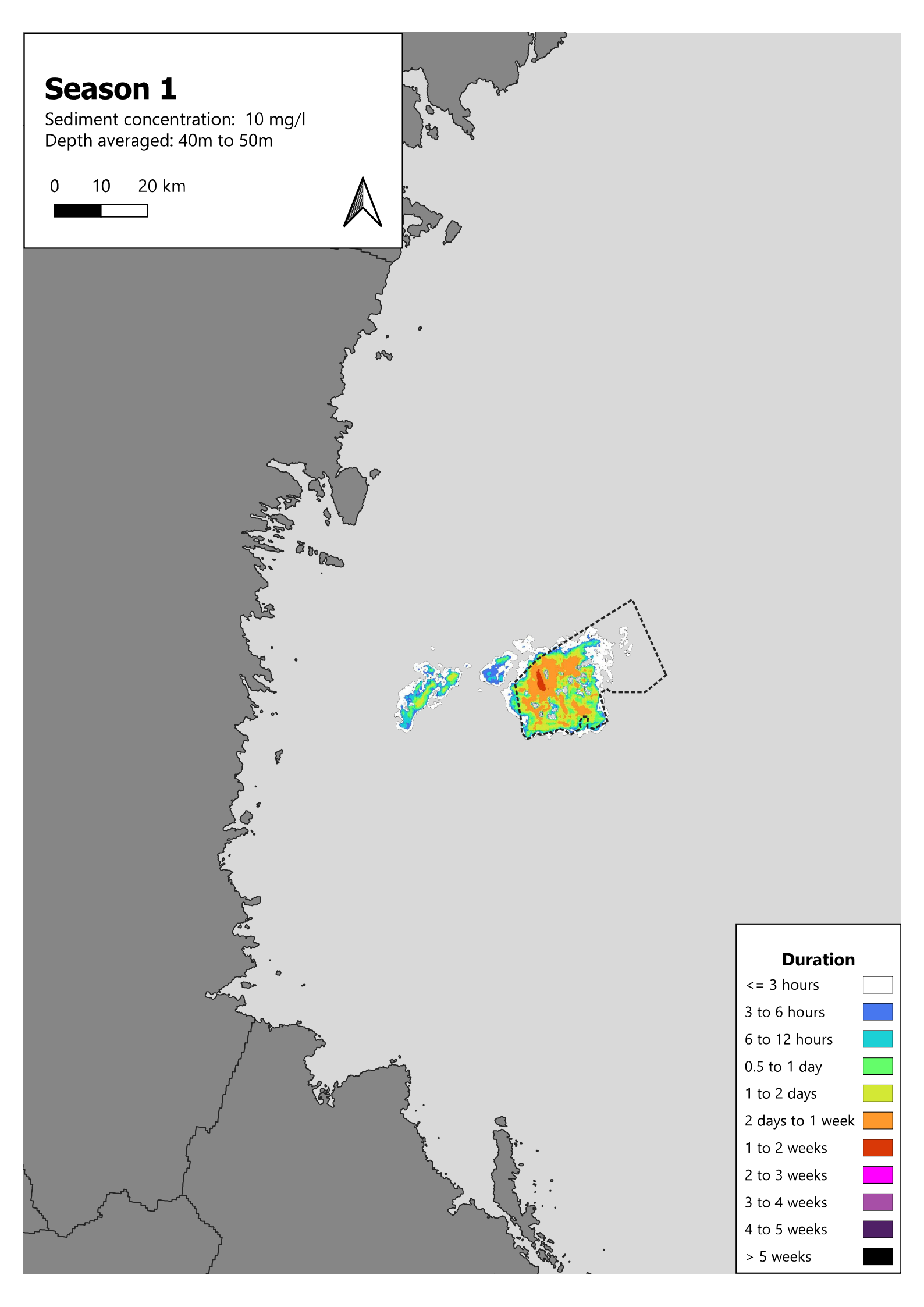


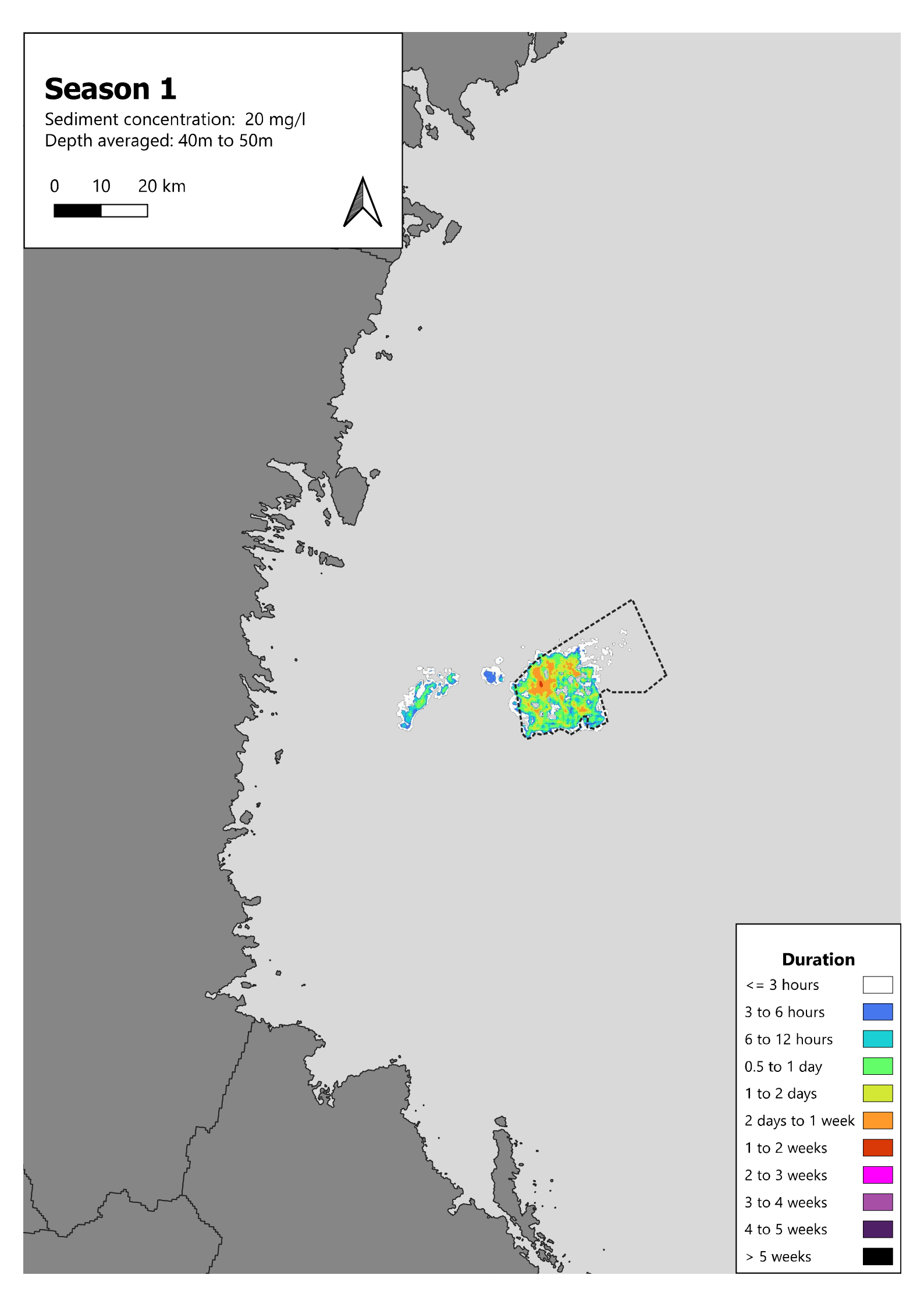


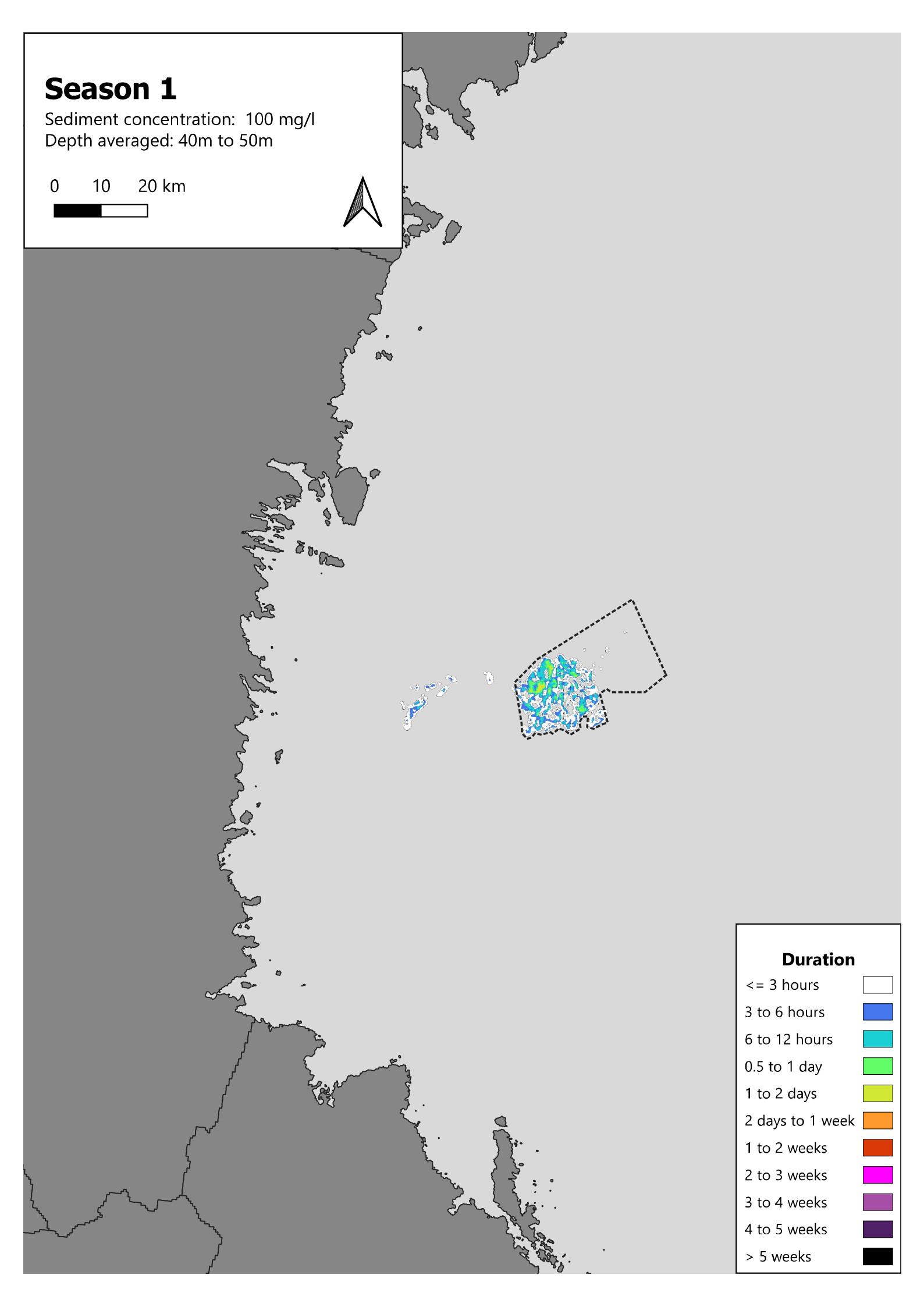


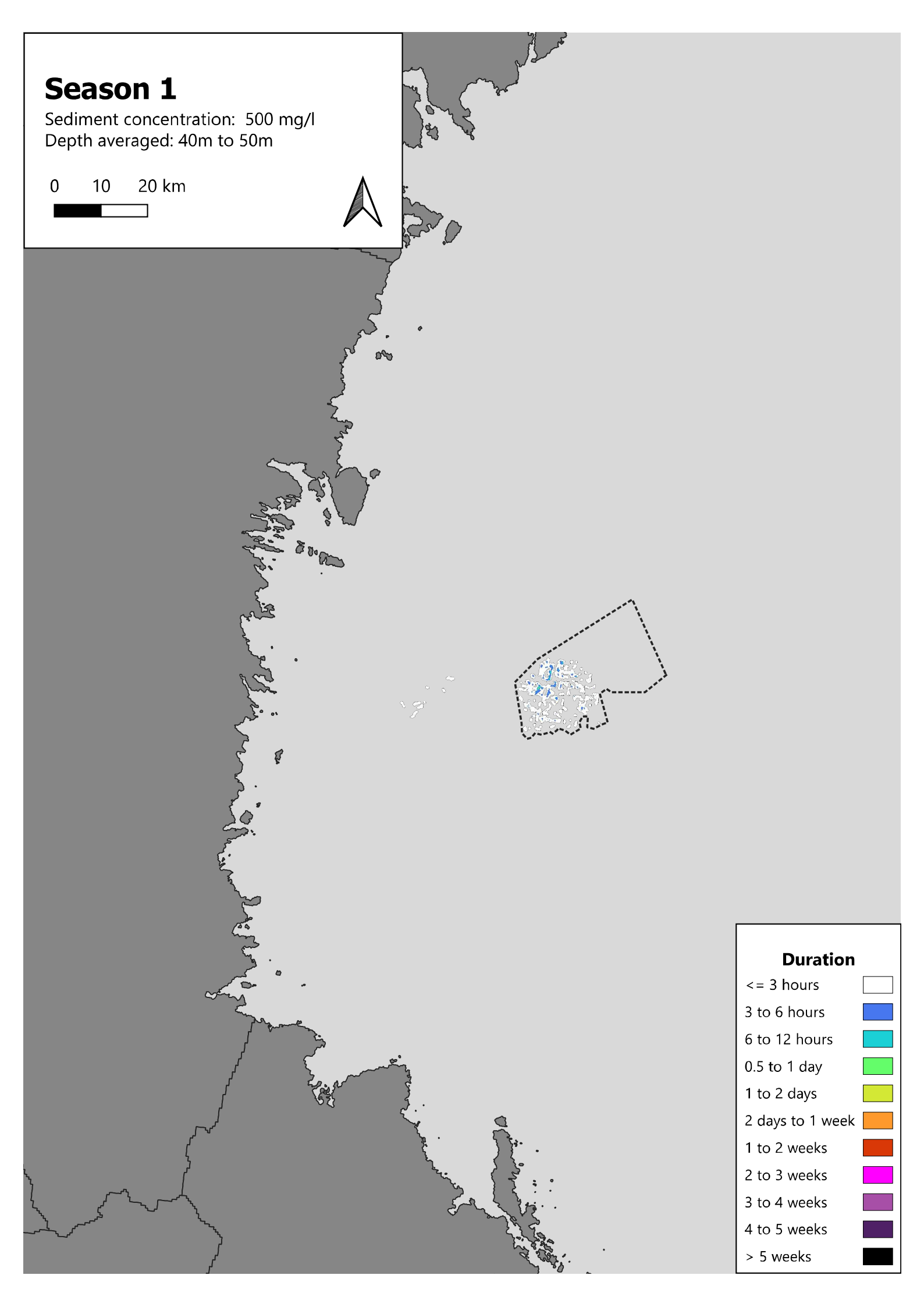


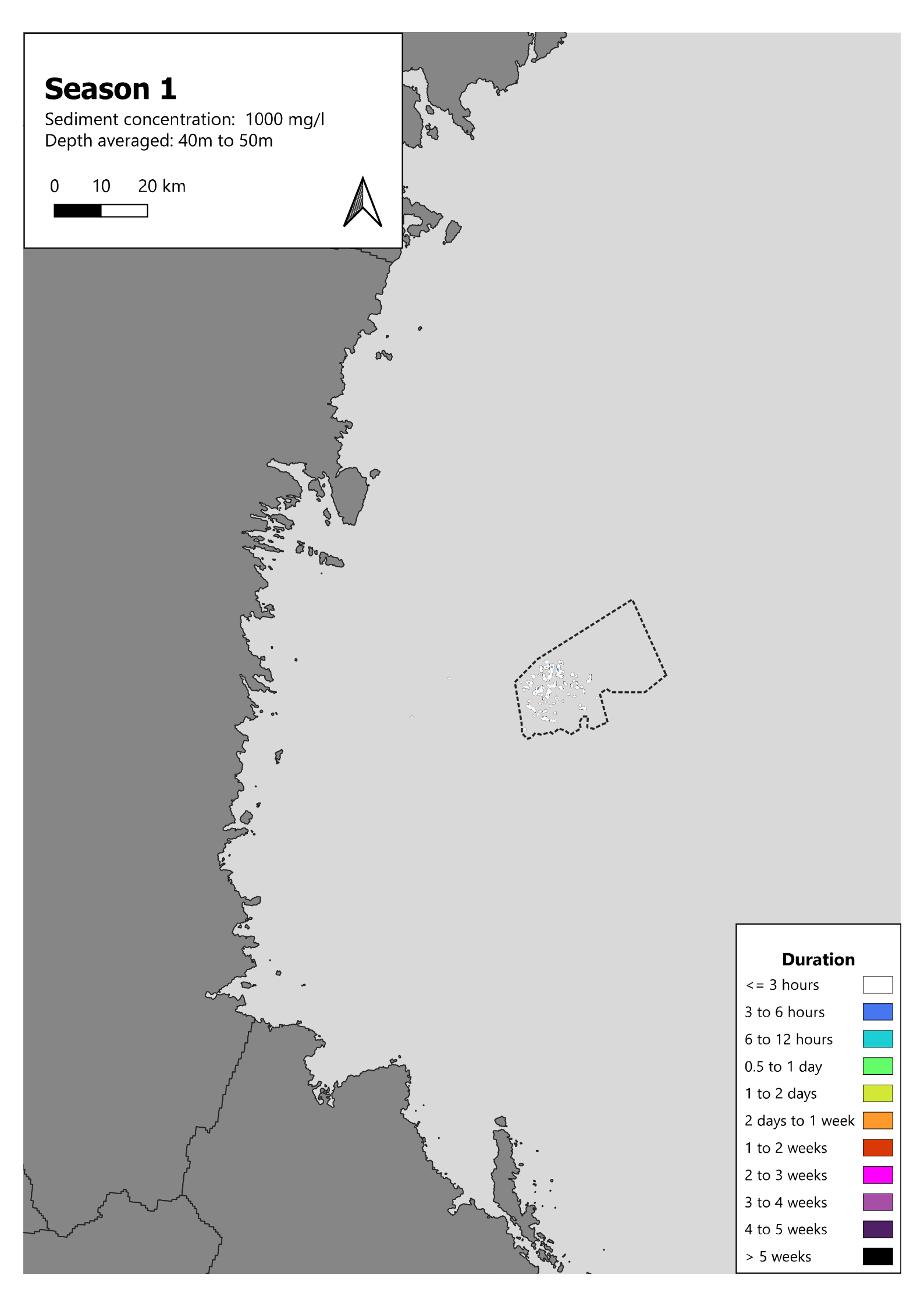


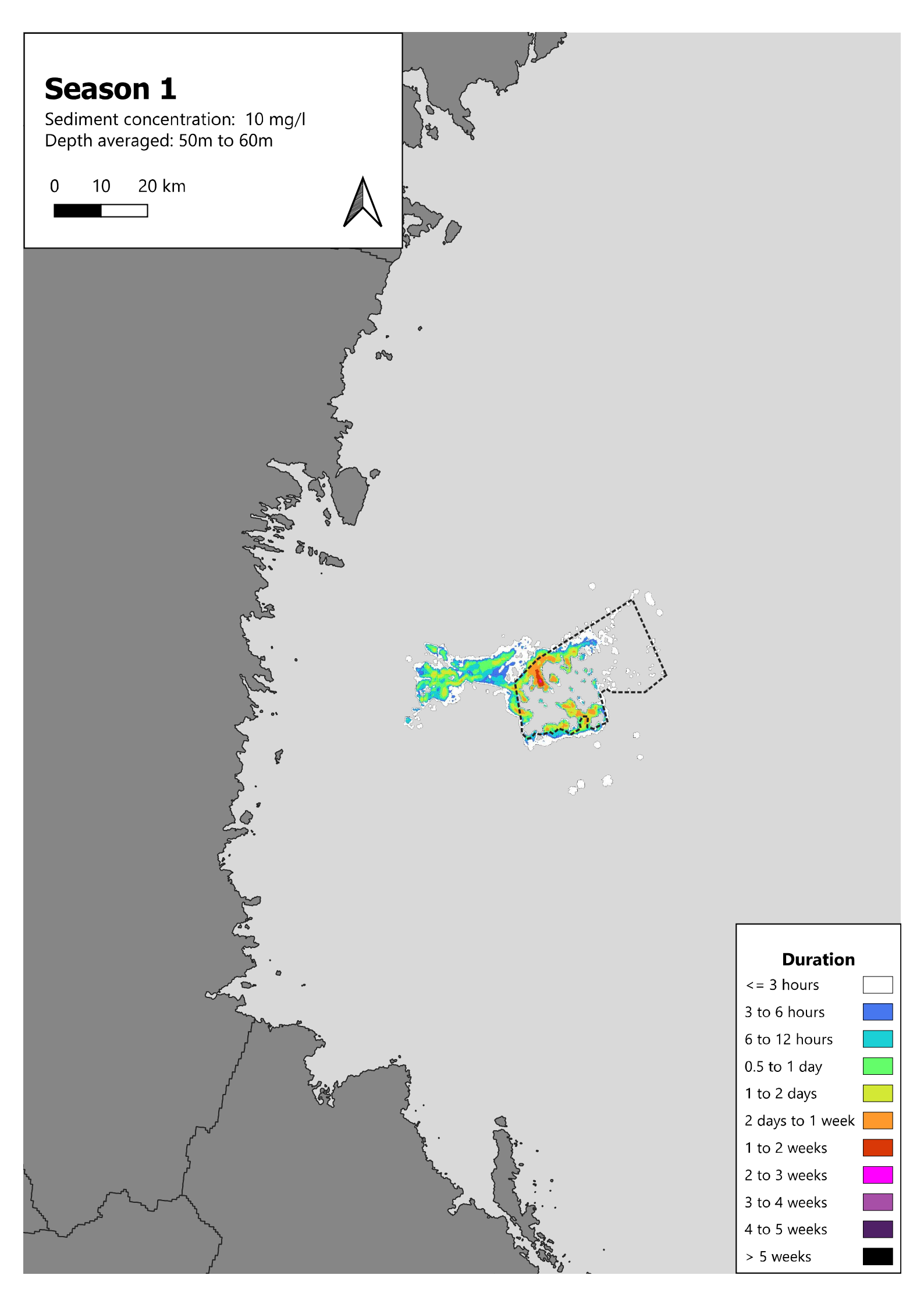


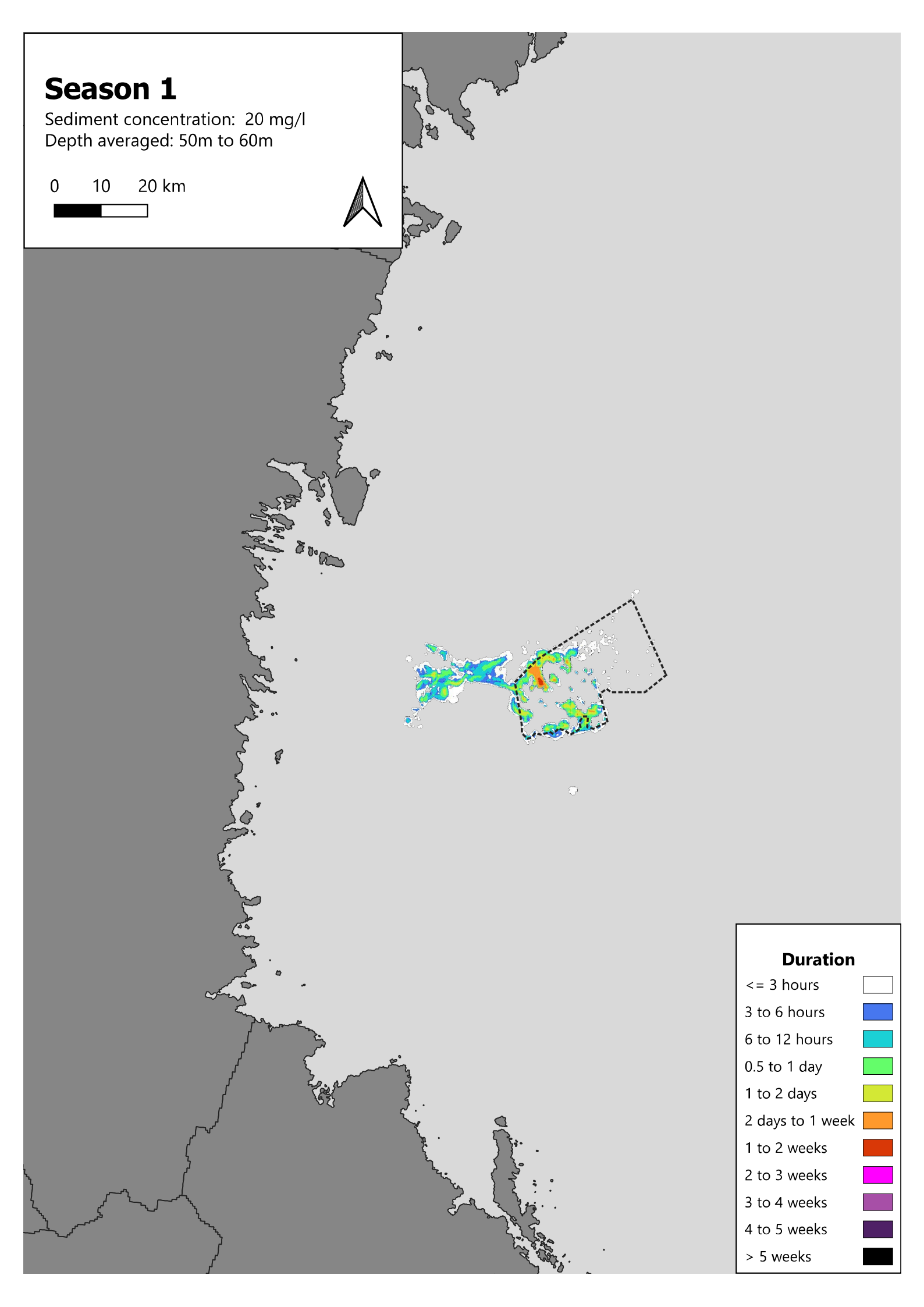


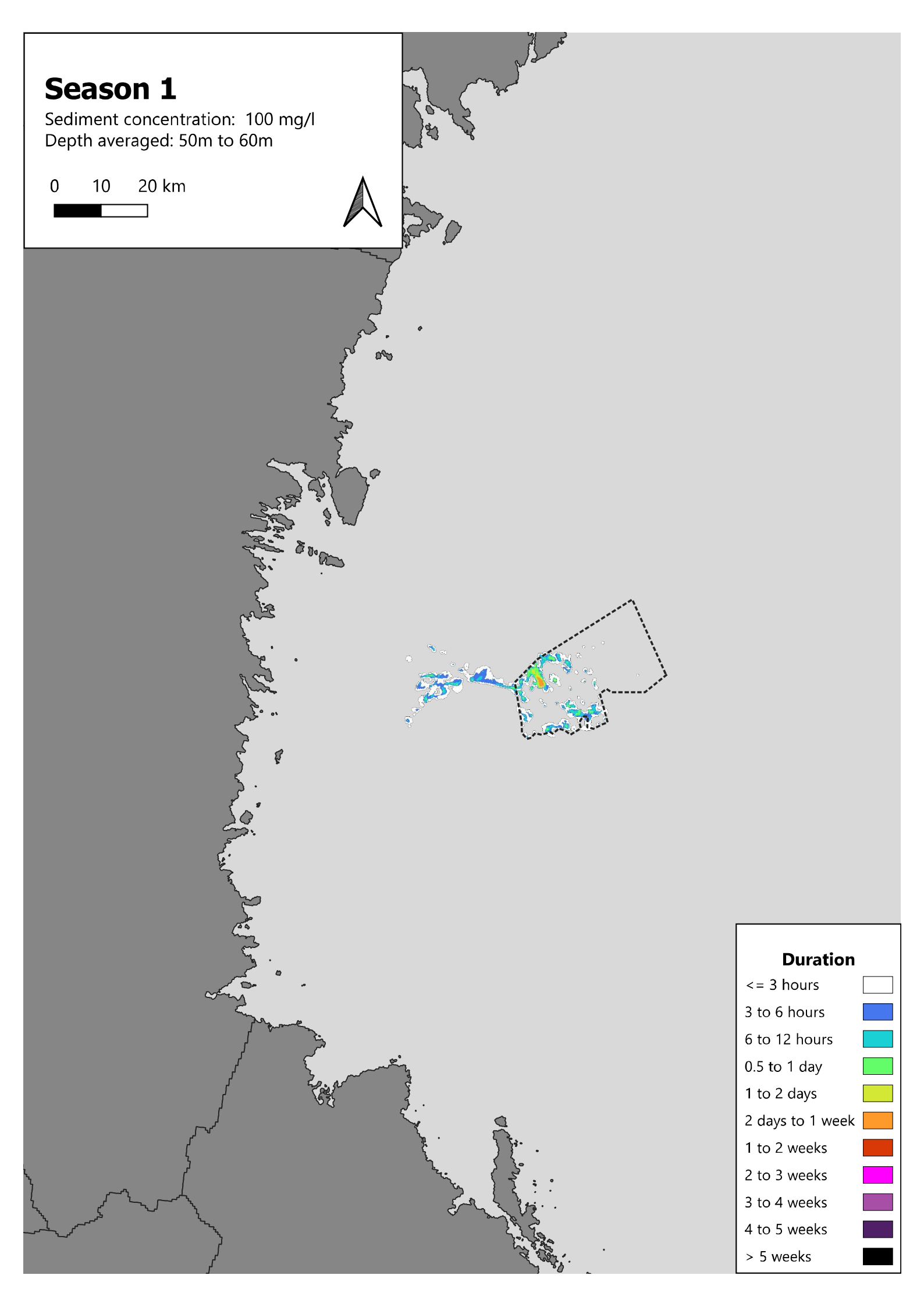


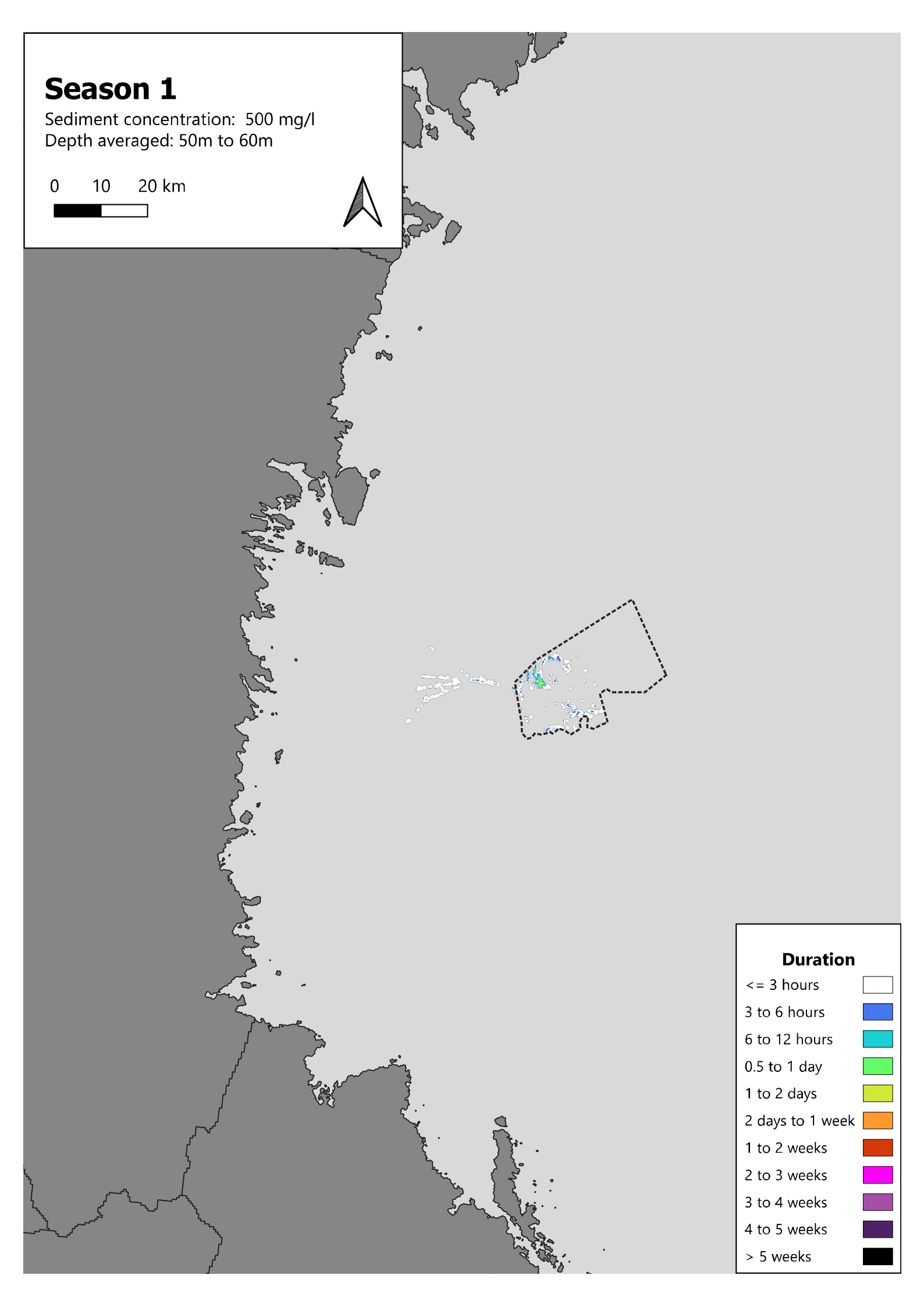


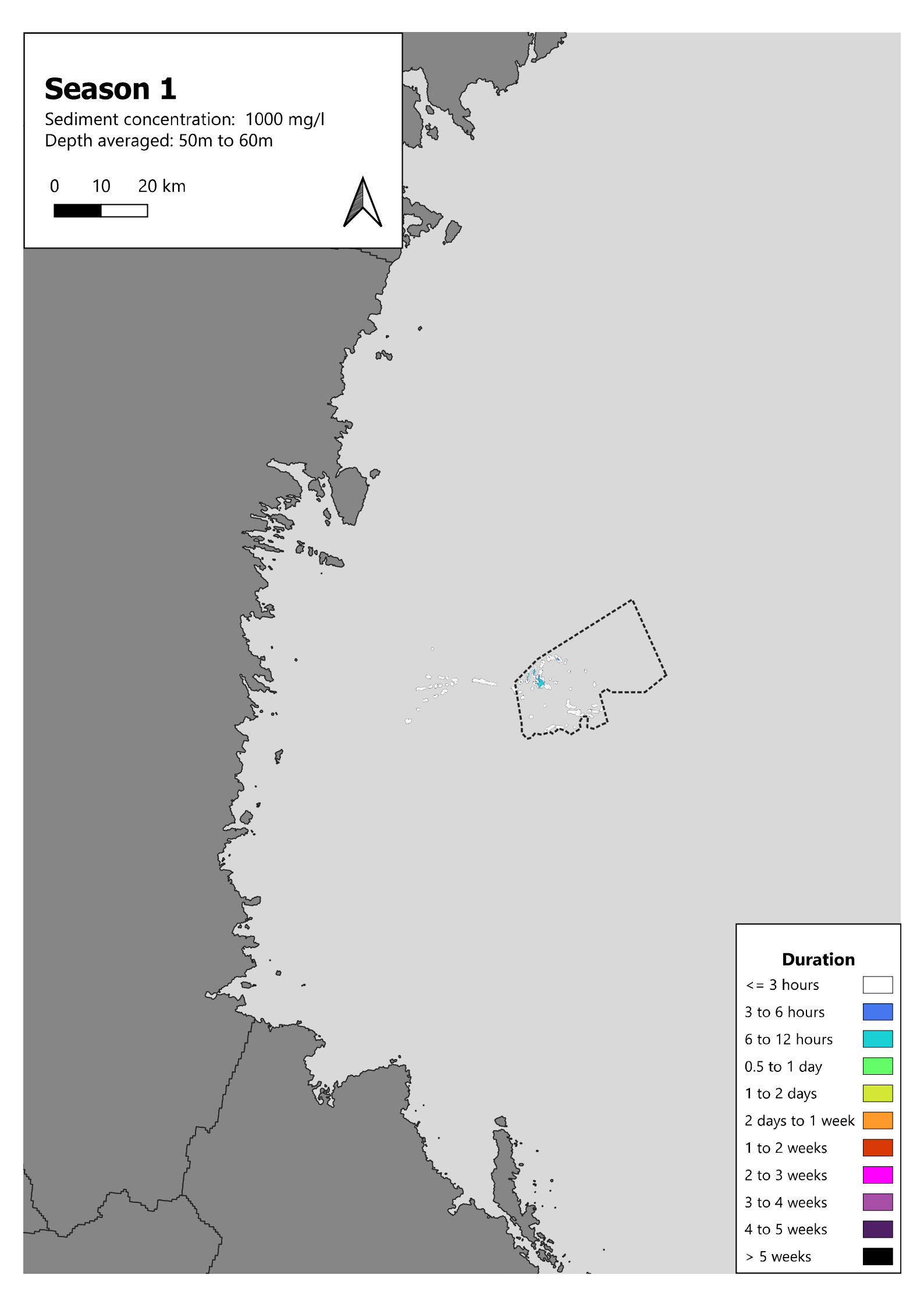


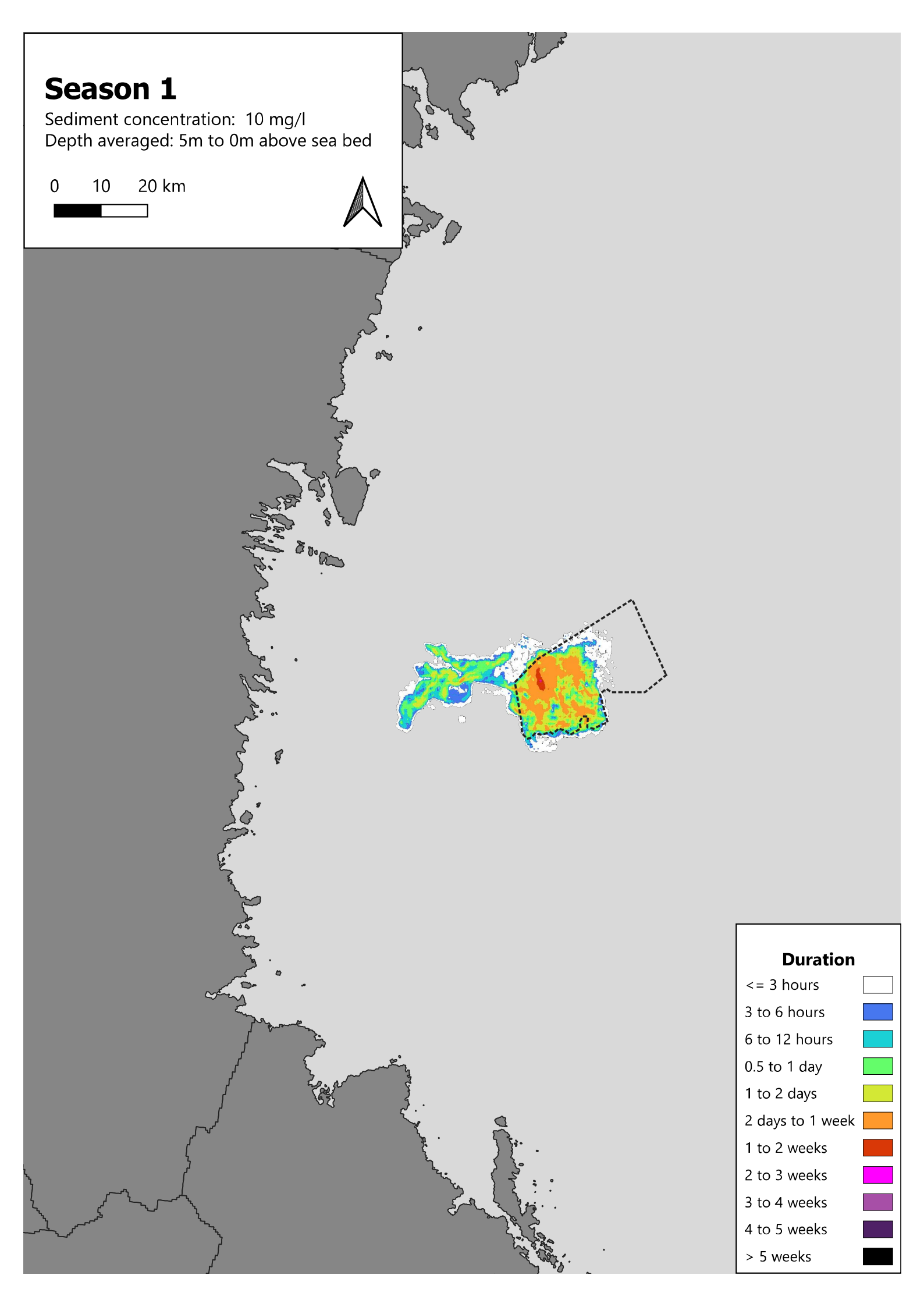


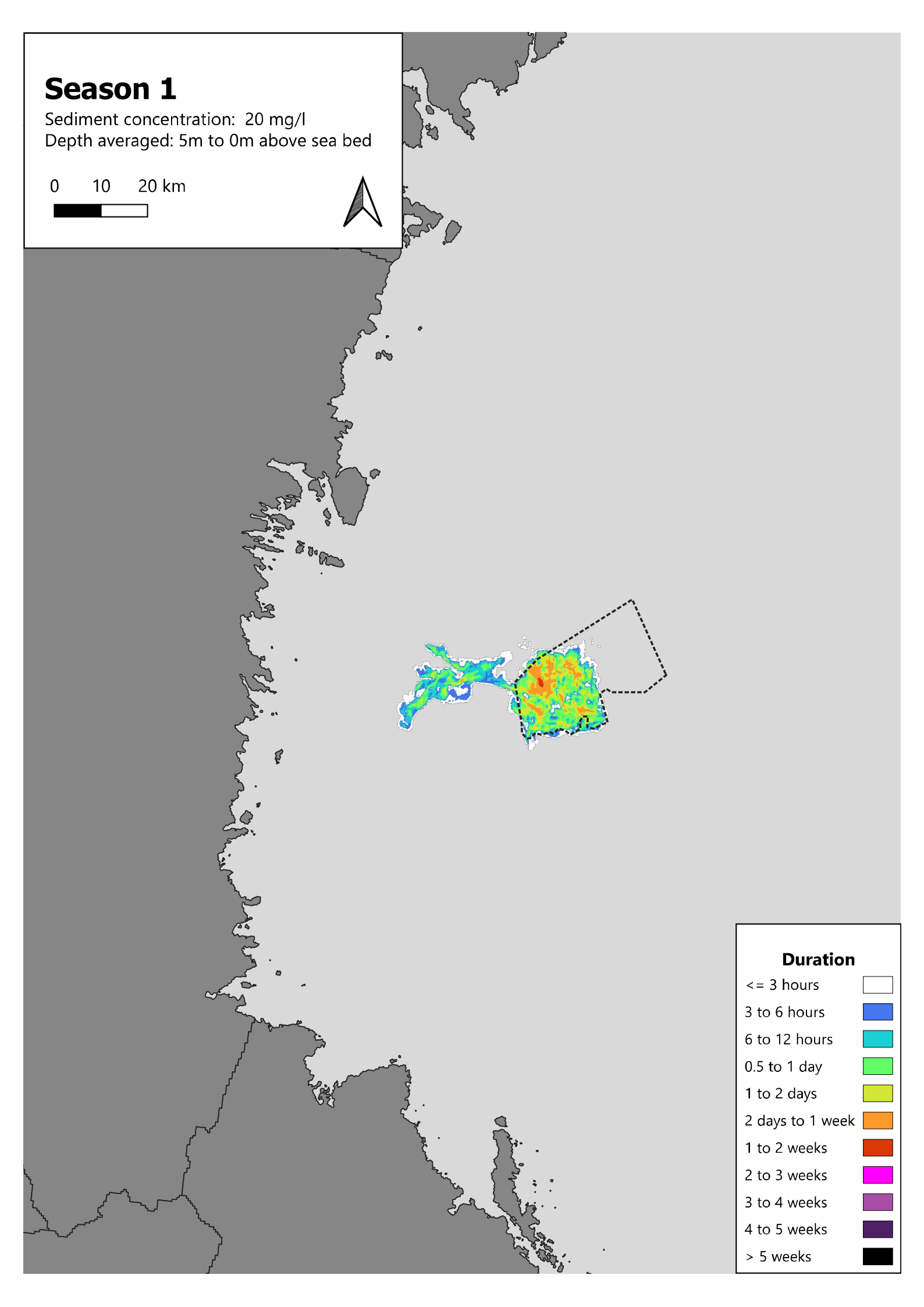


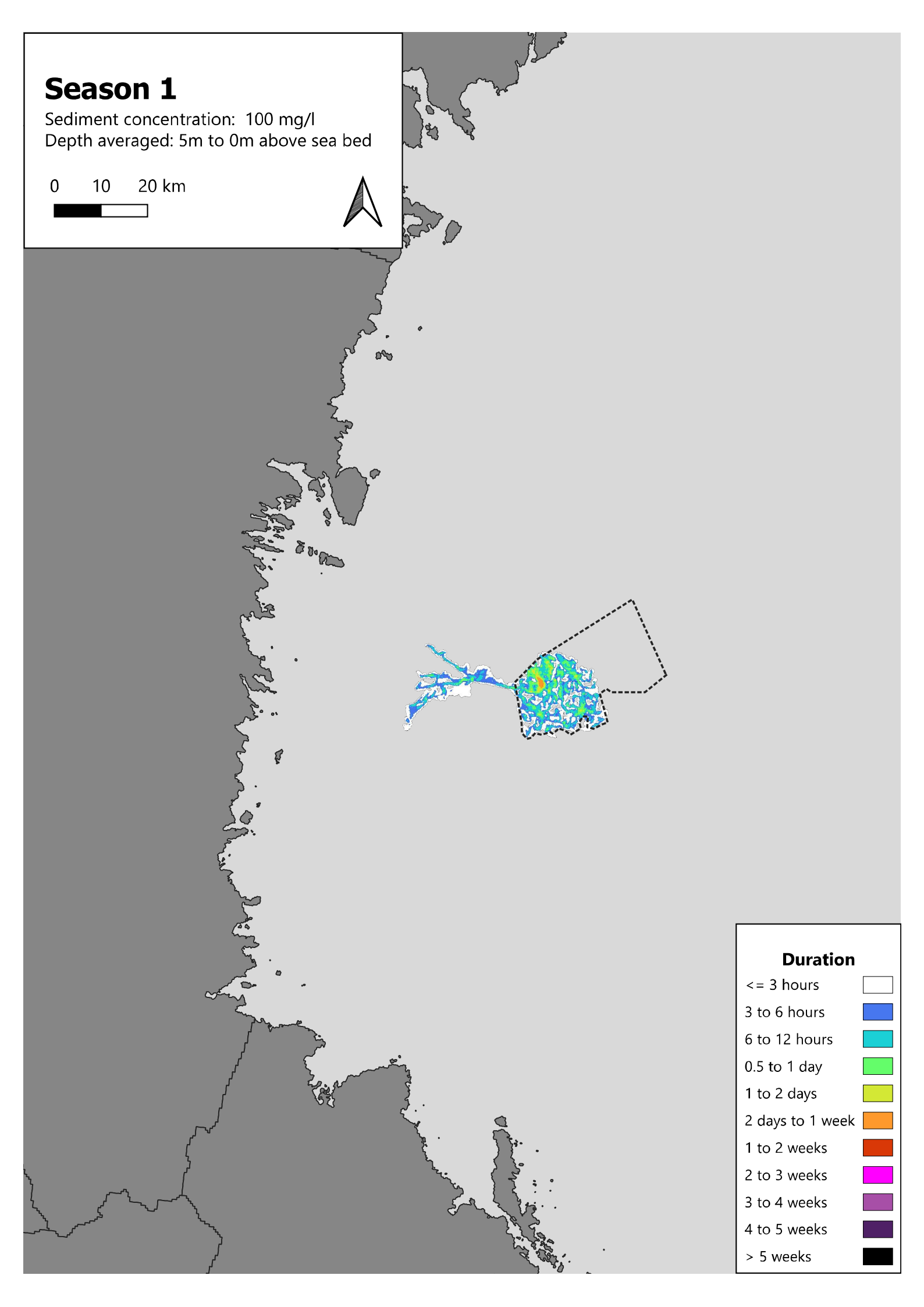


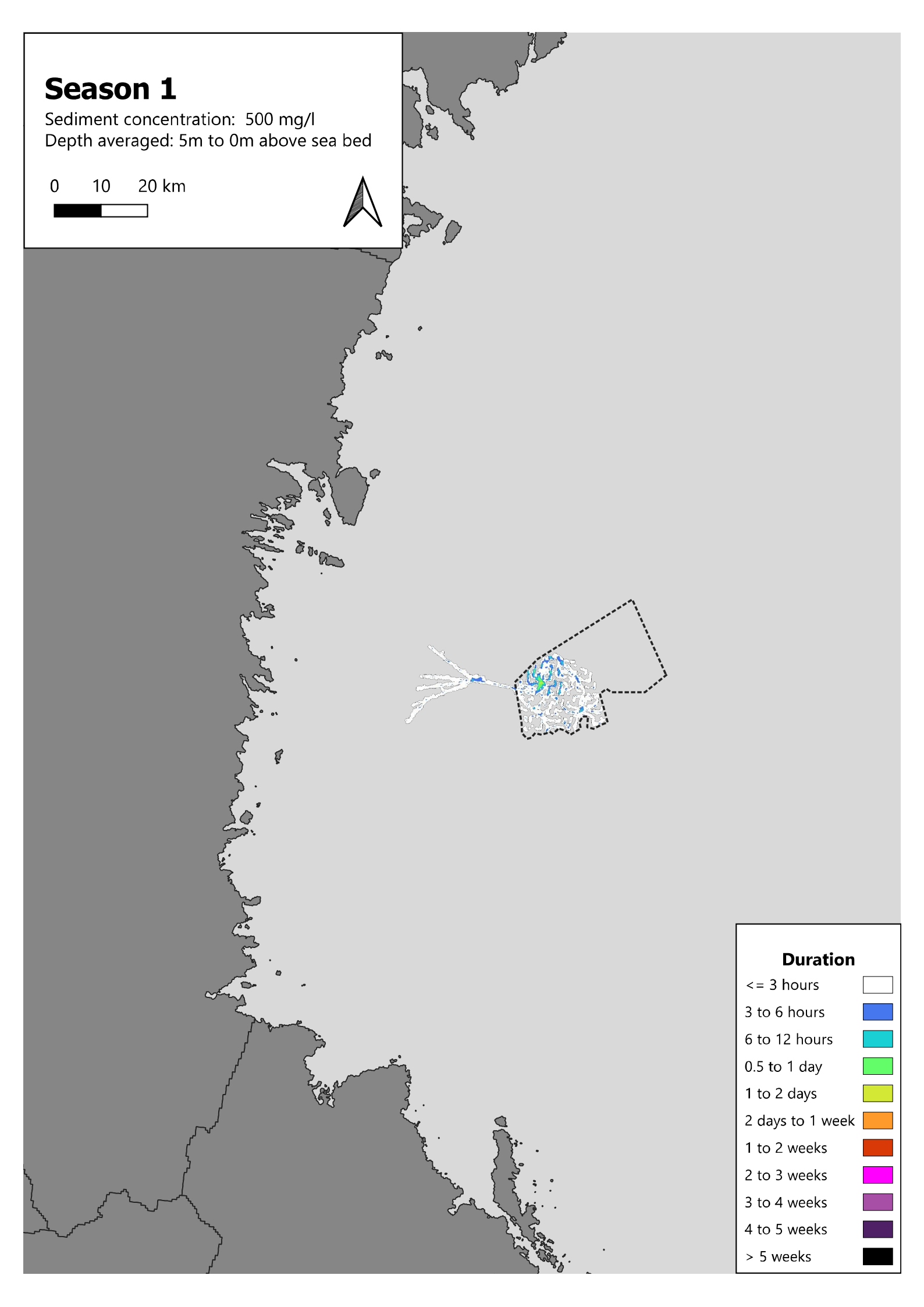


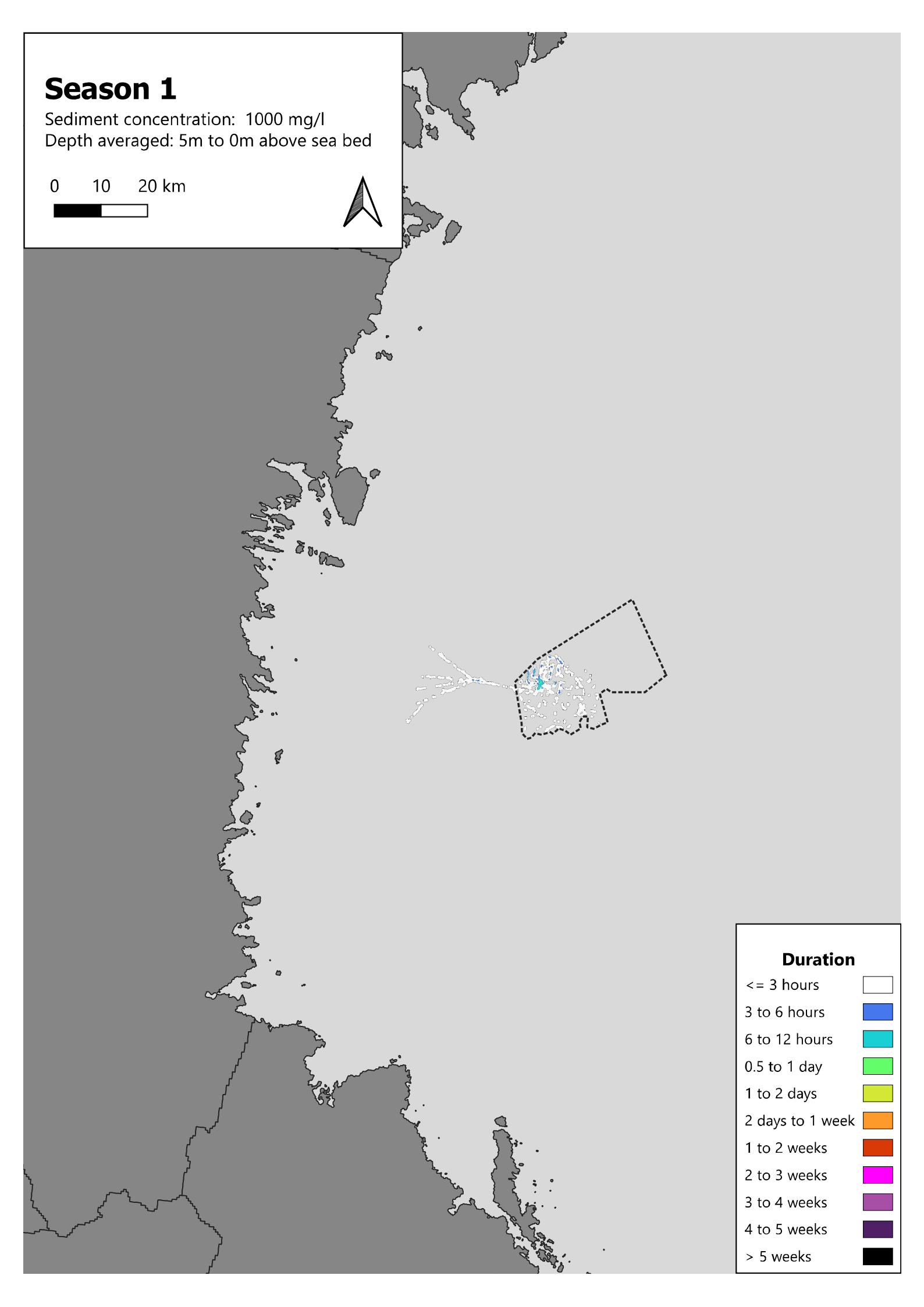






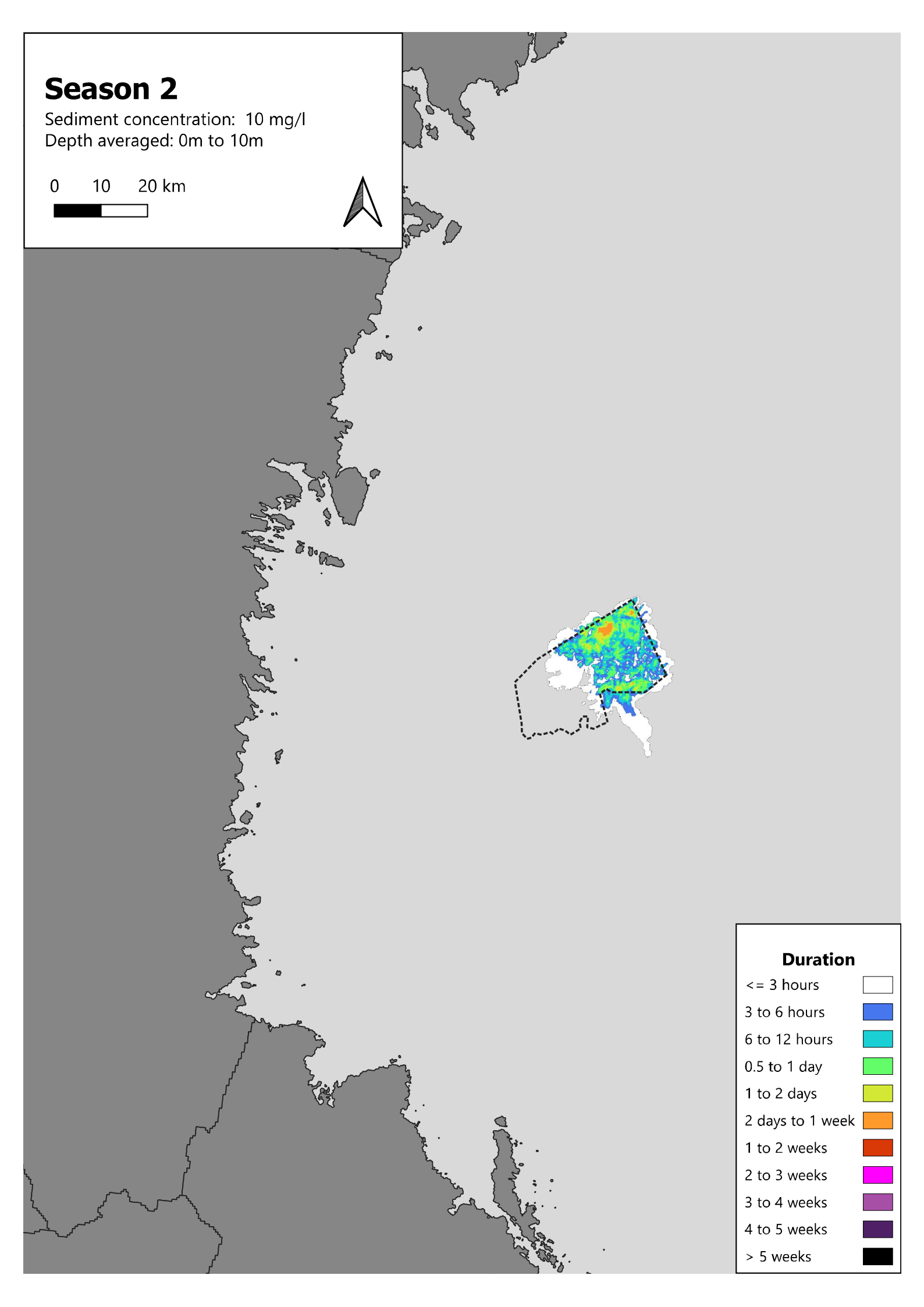


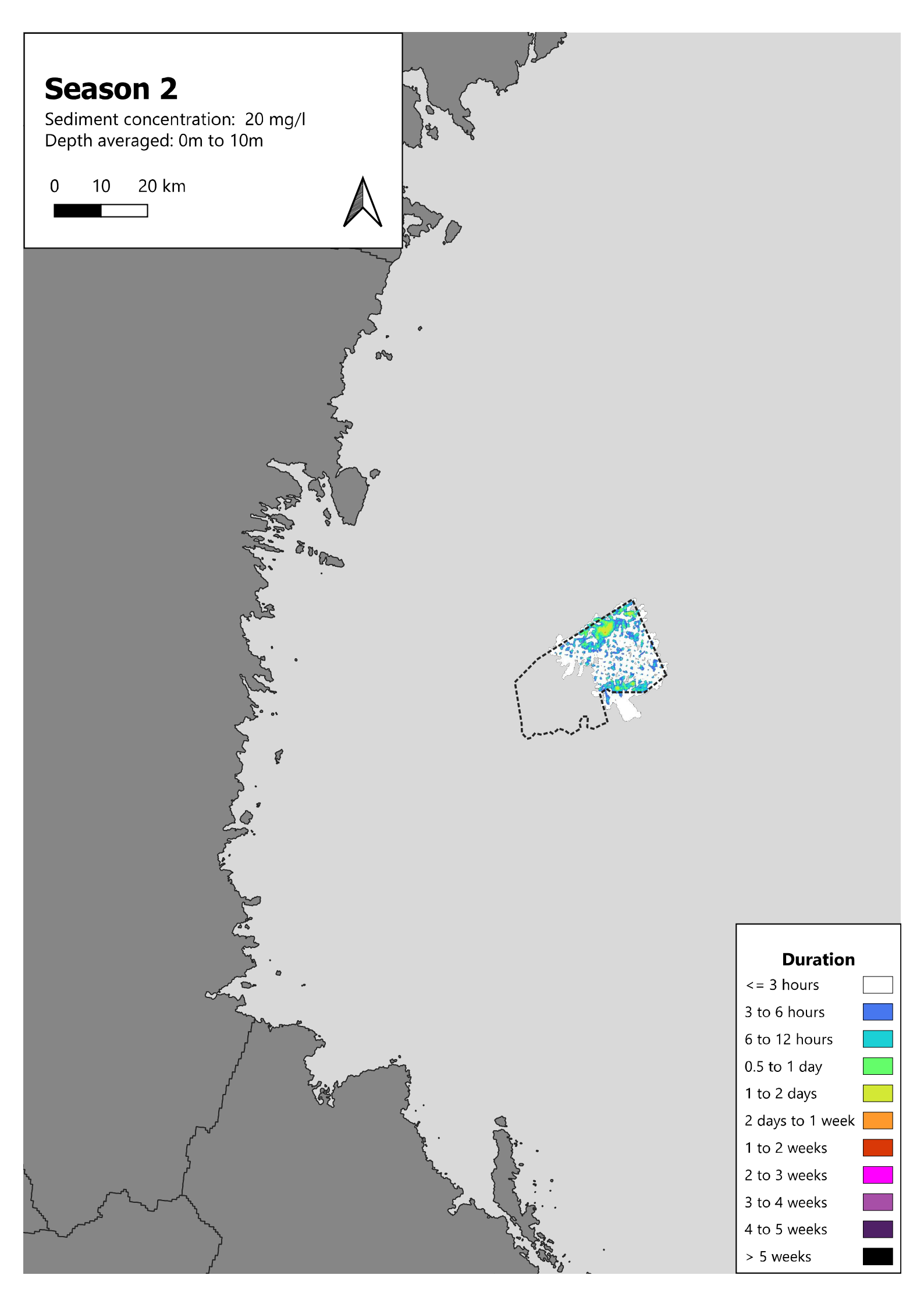


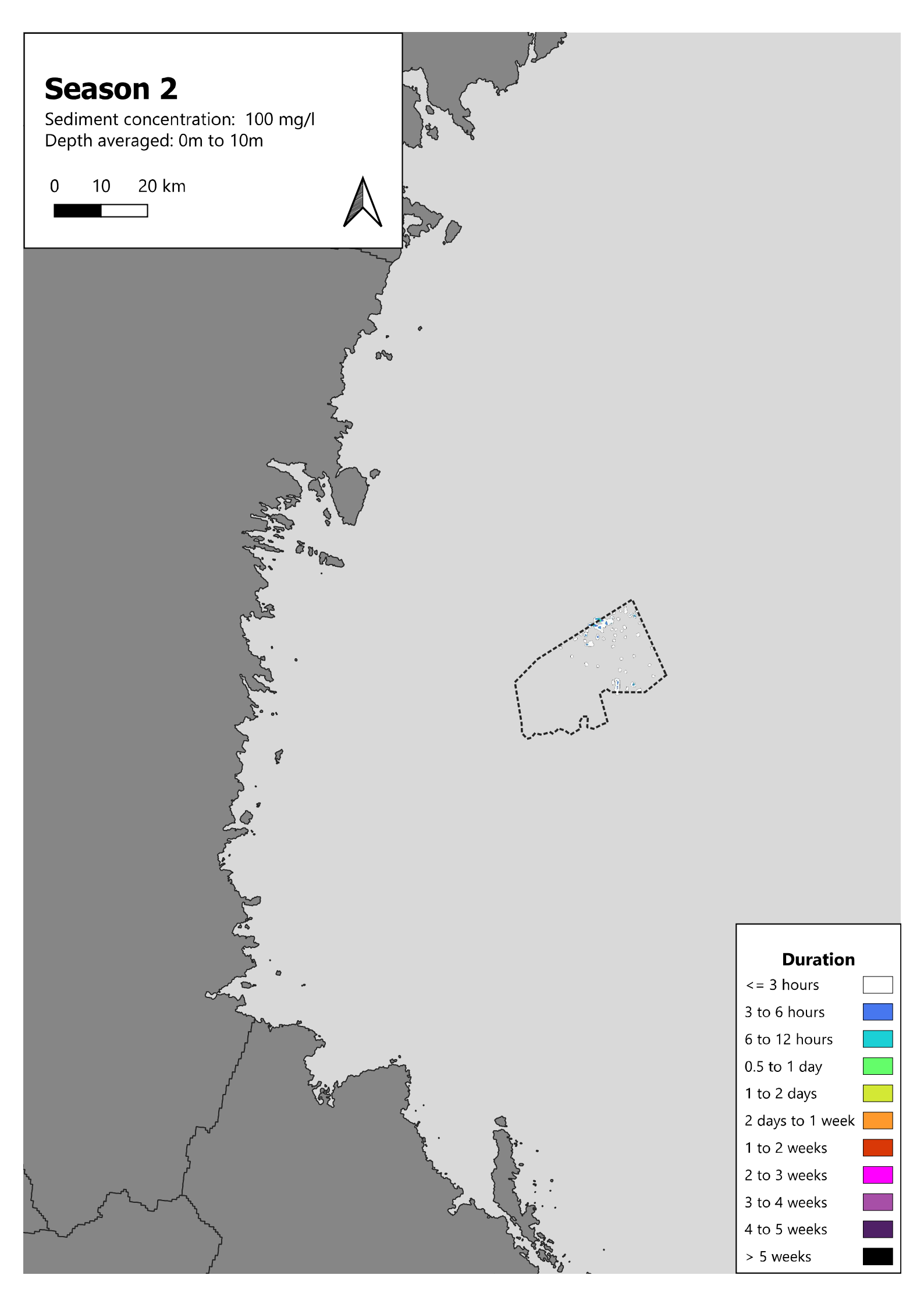


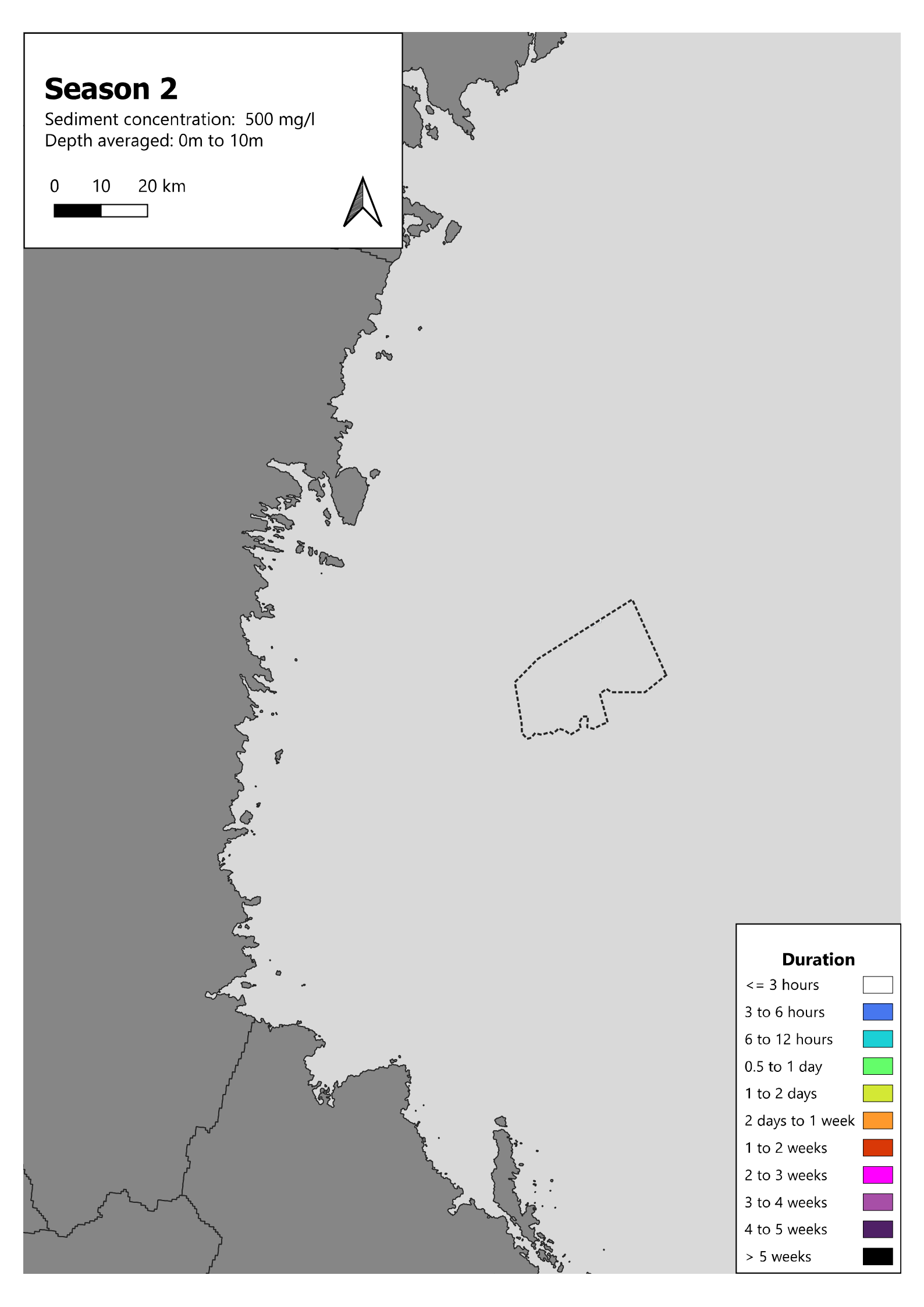


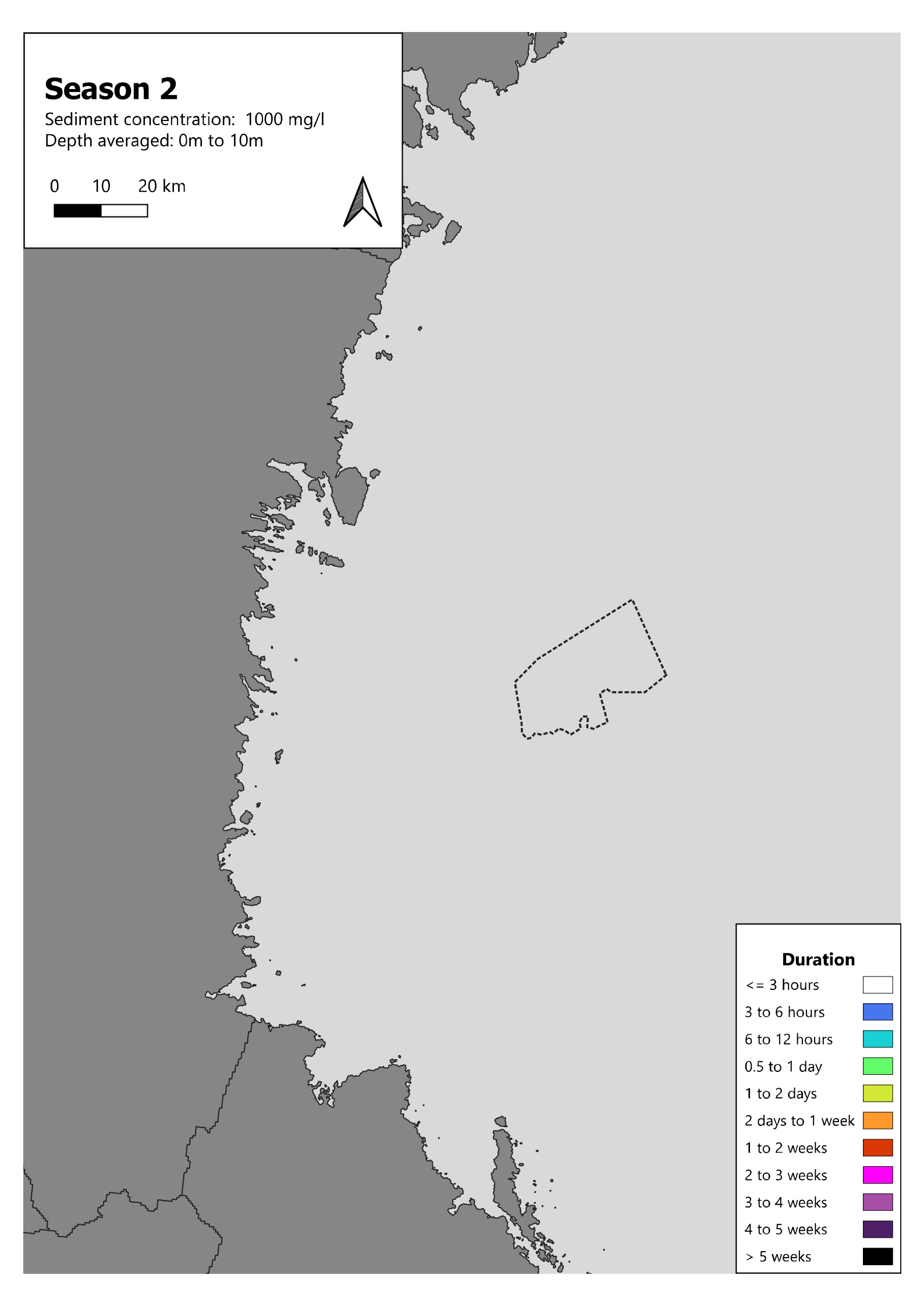
Appendix 18 Sediment dispersal: Concentration – Season 2
--

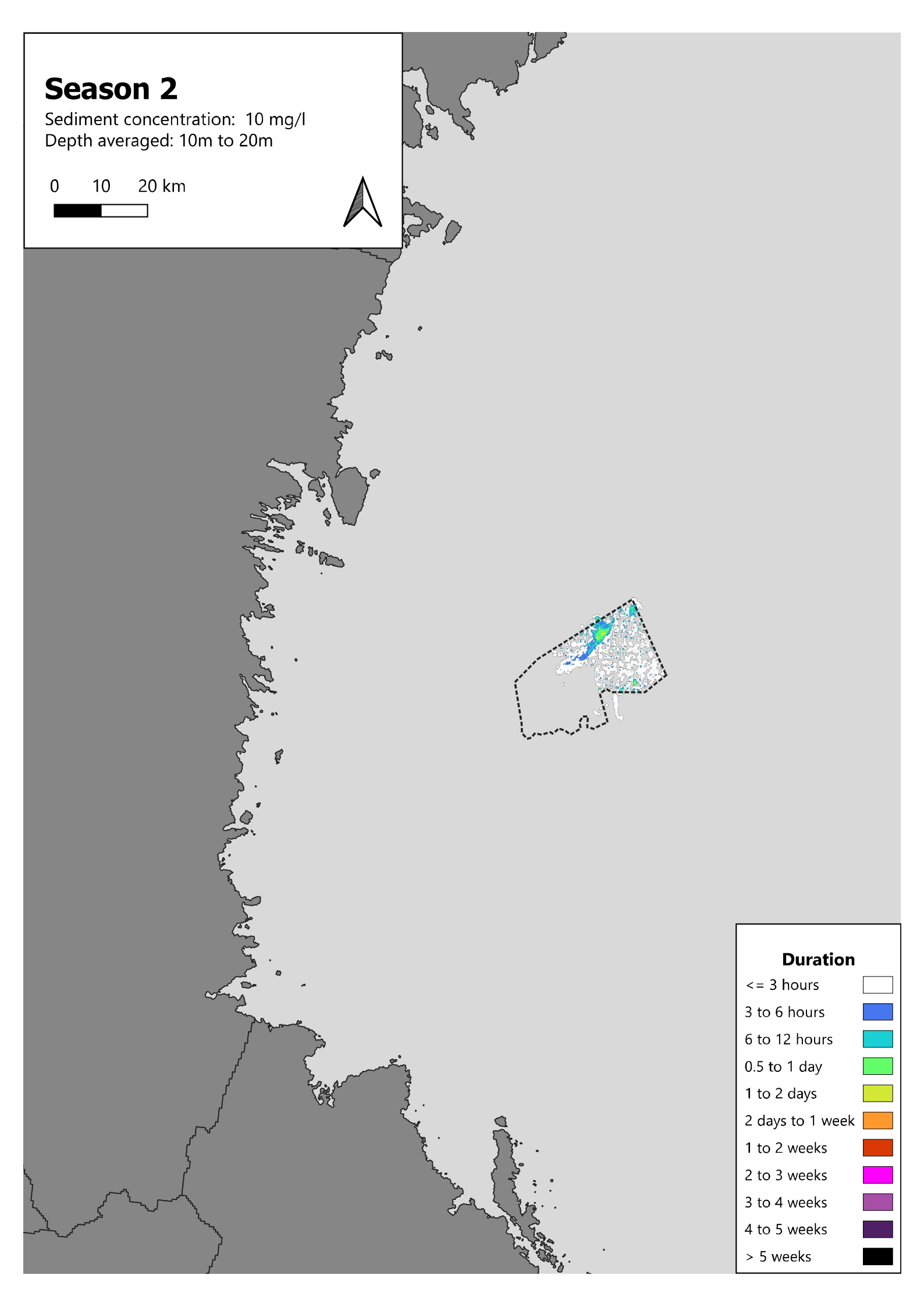


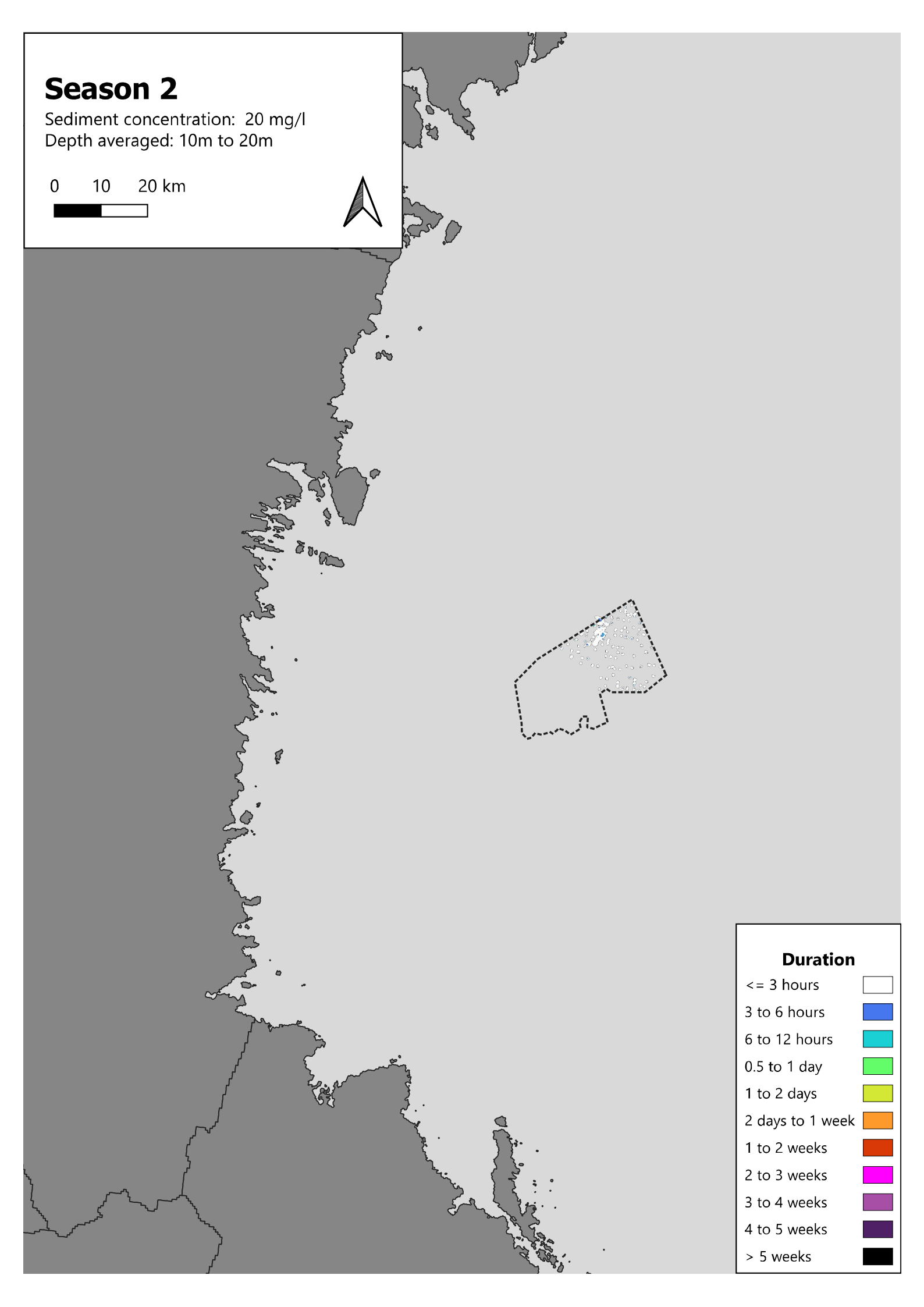


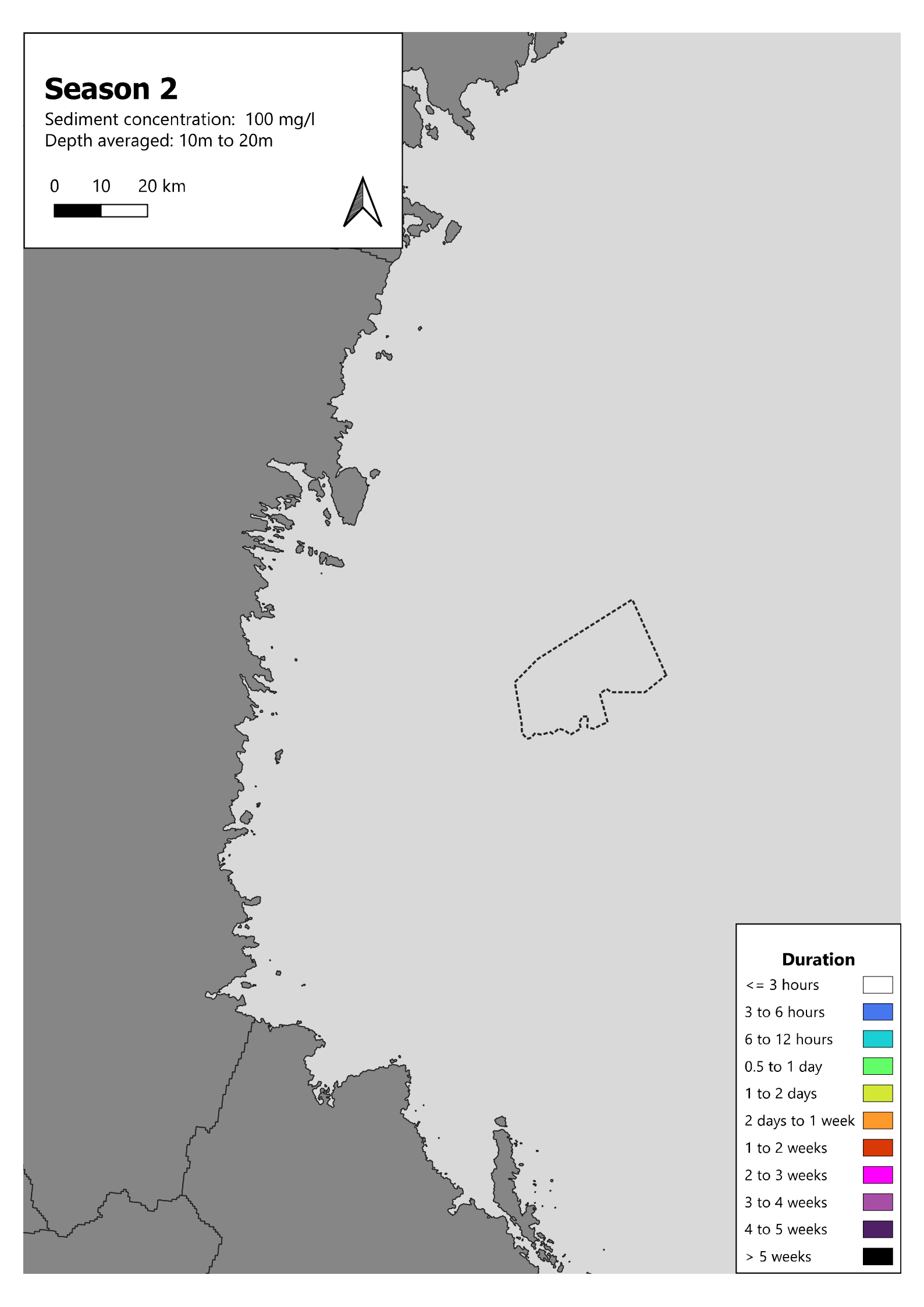


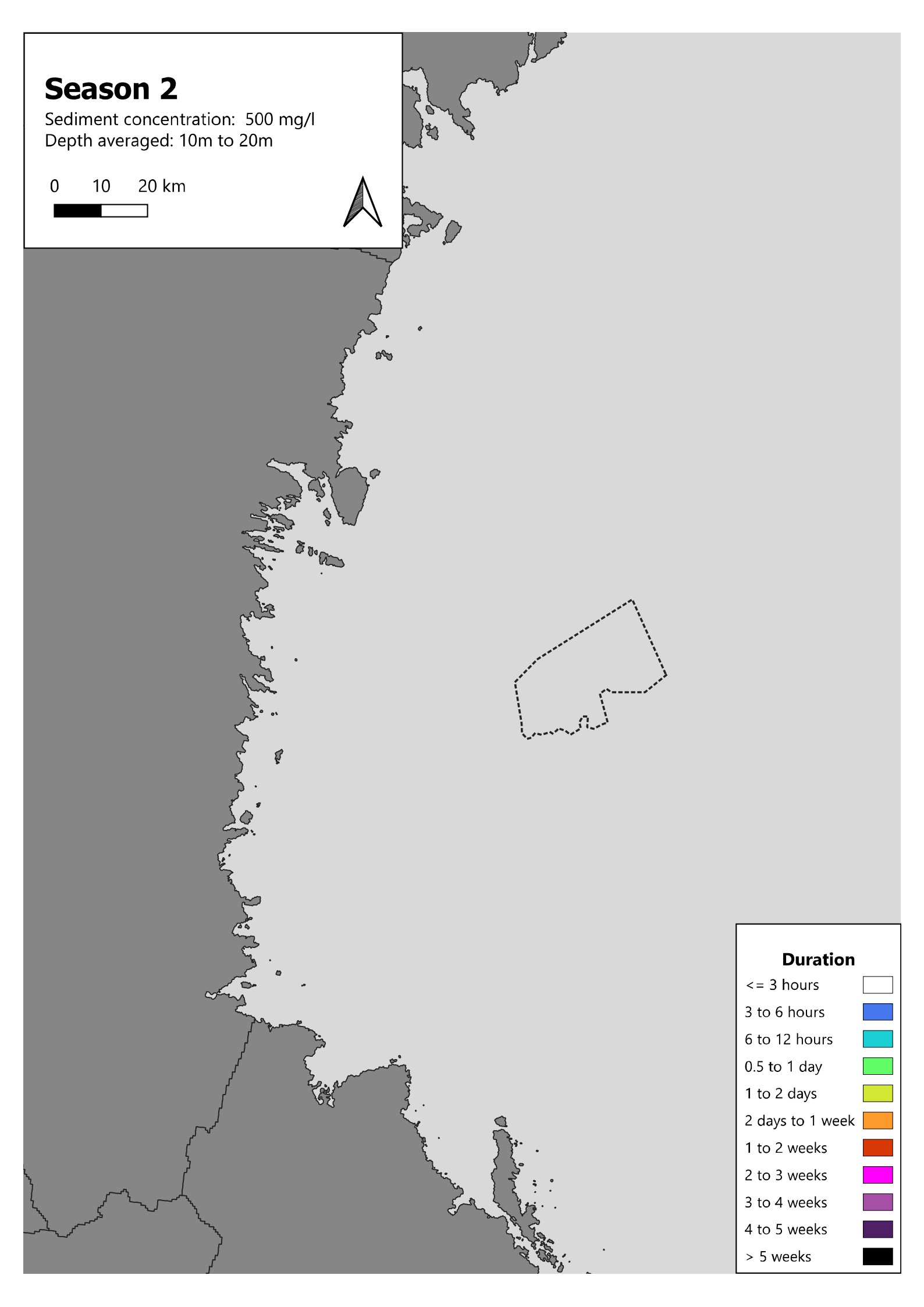


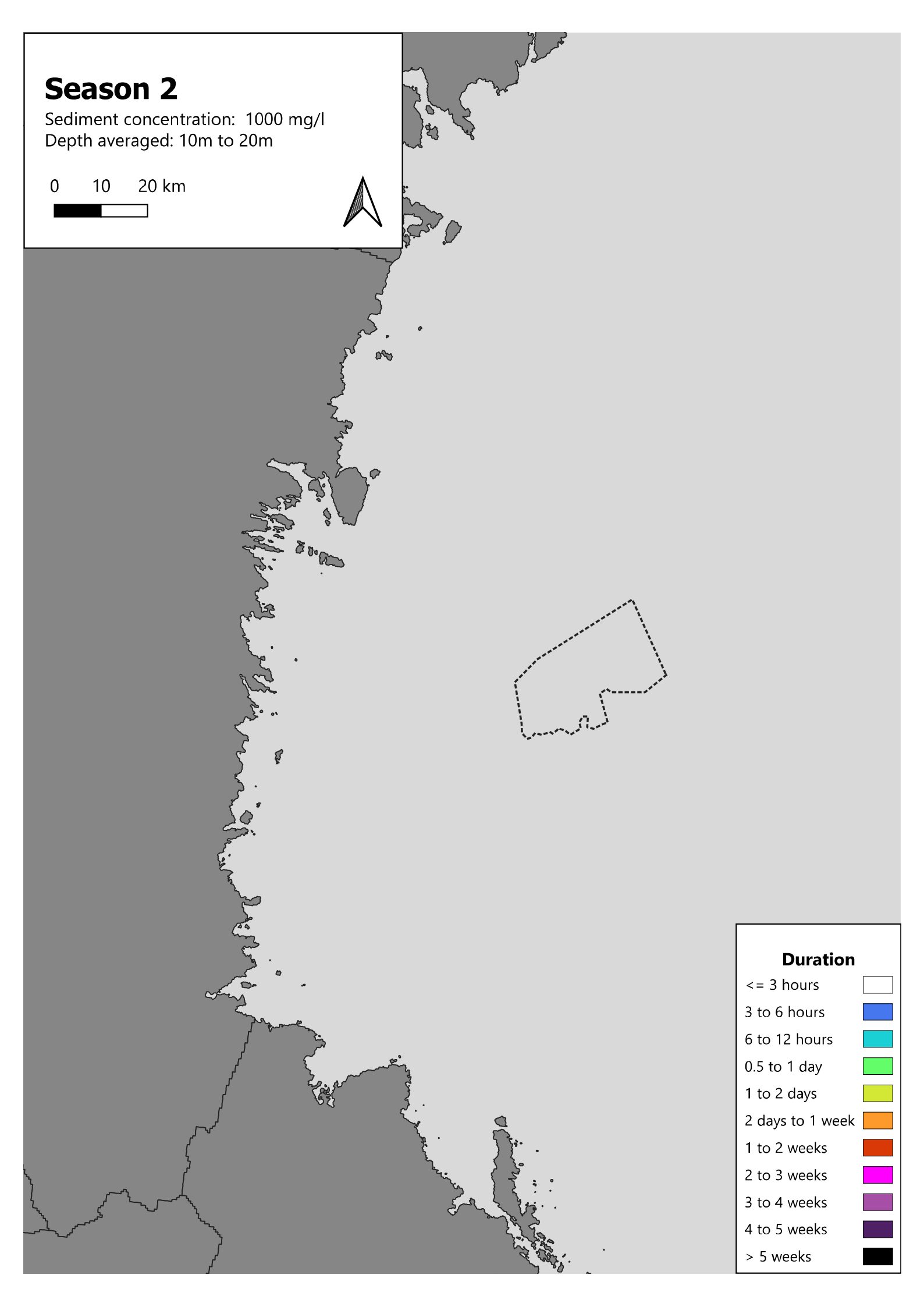


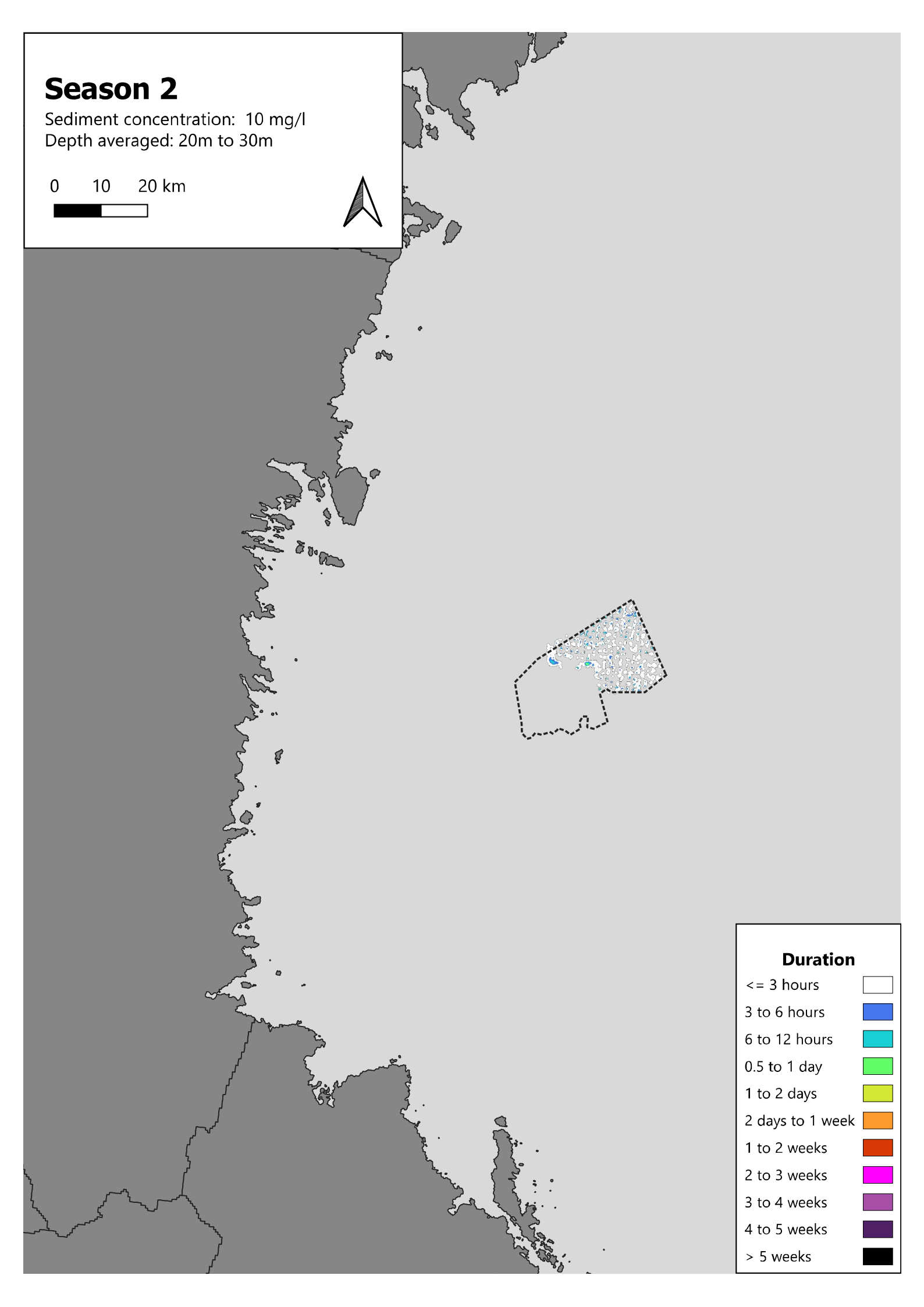


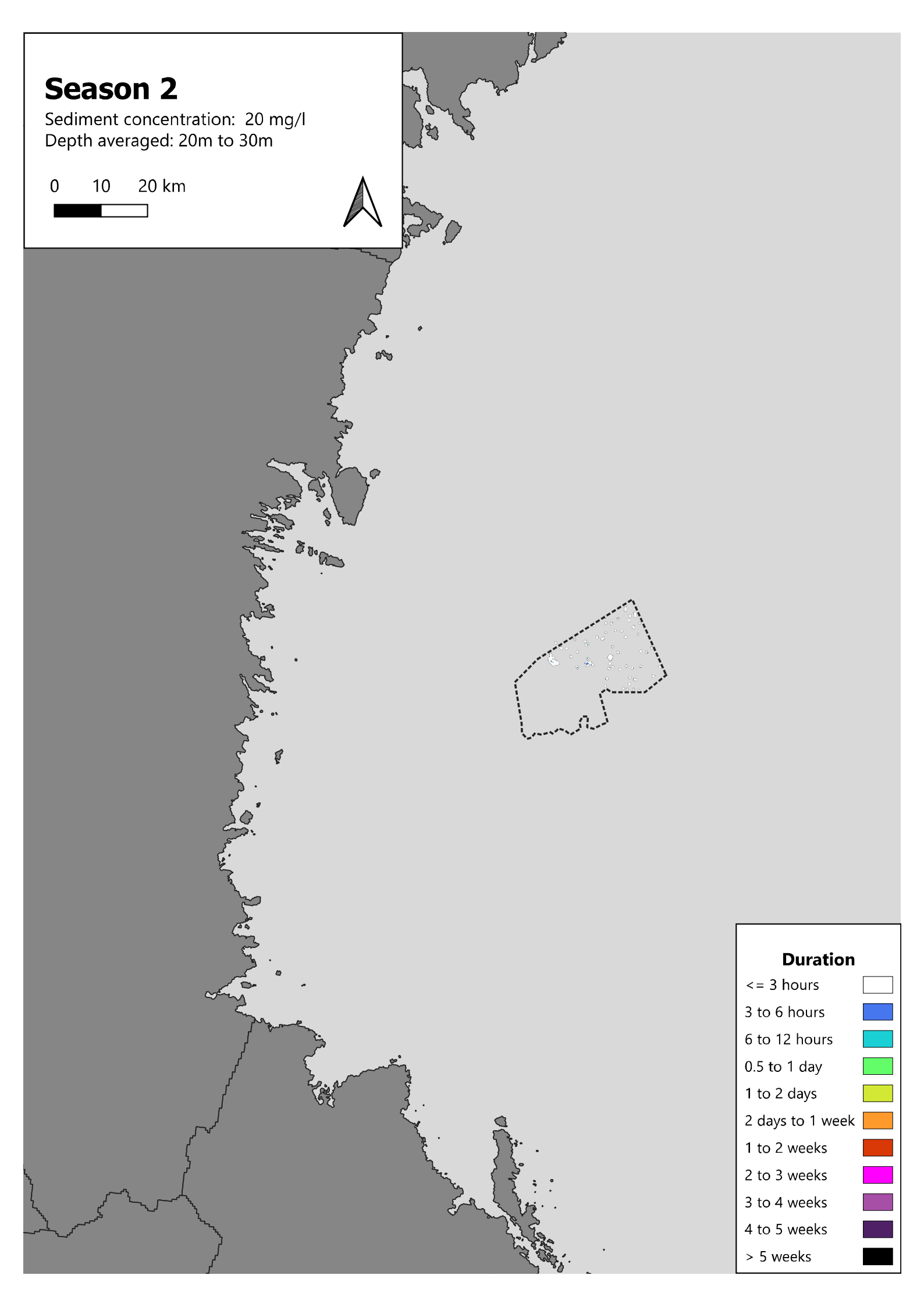


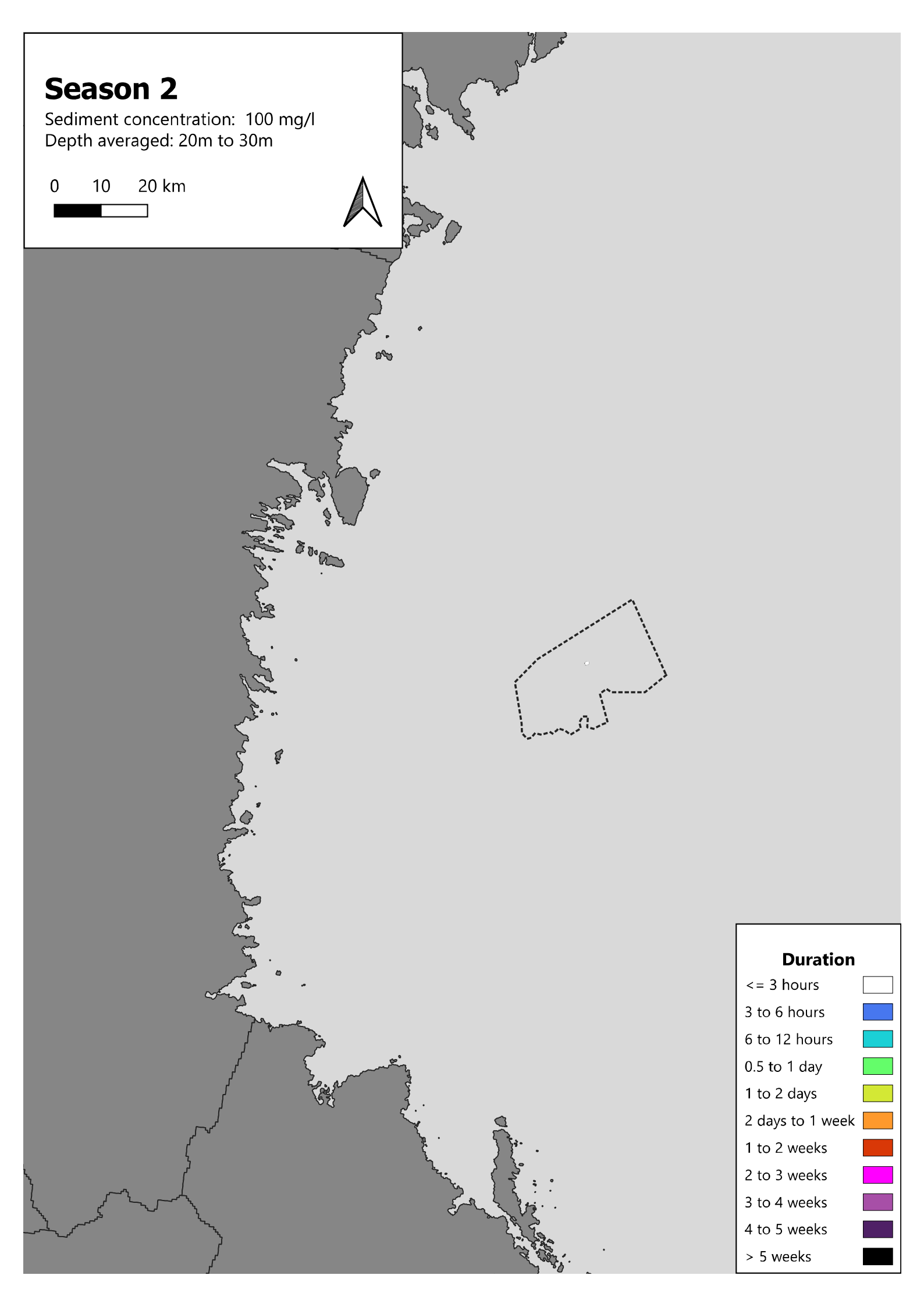


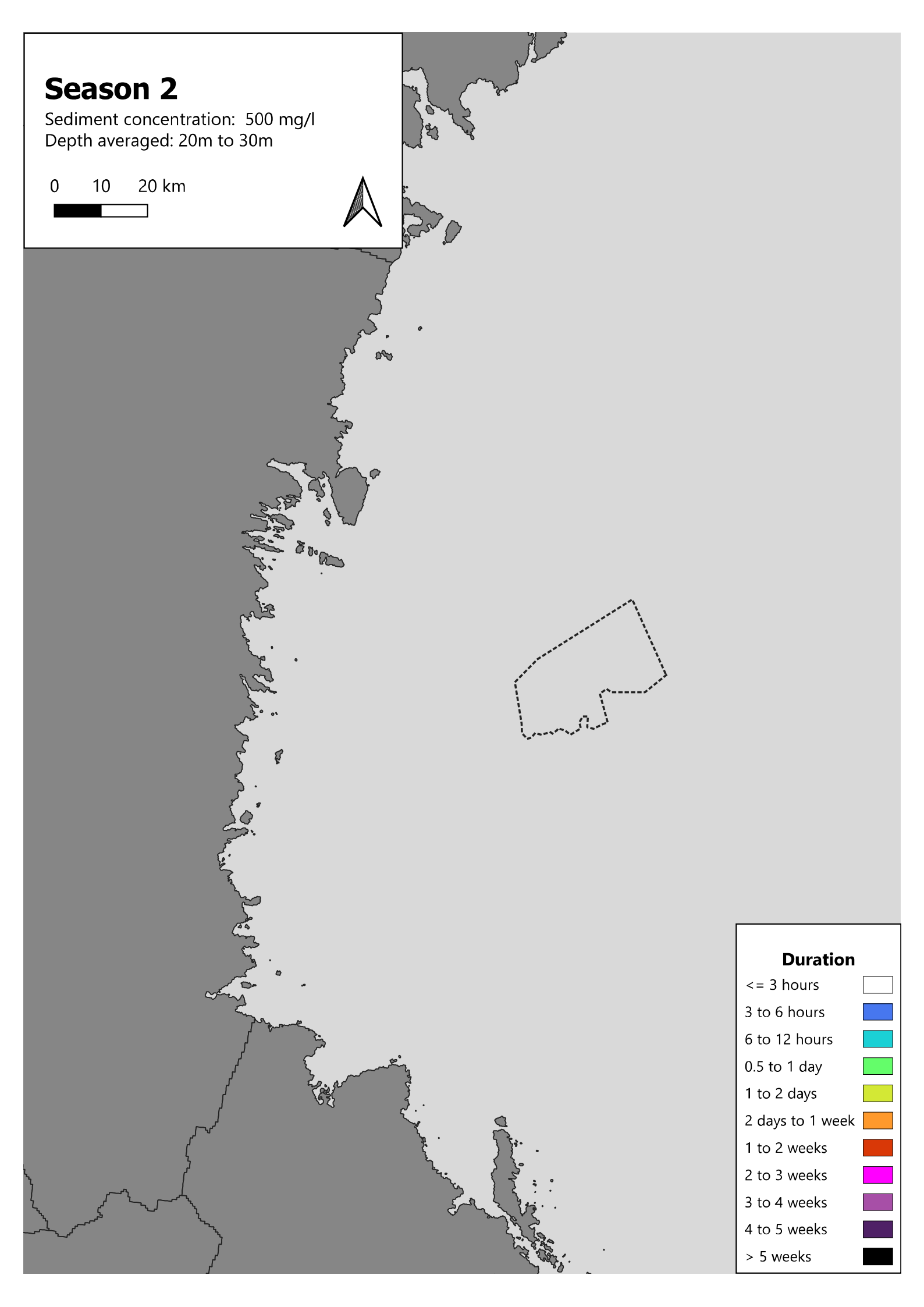


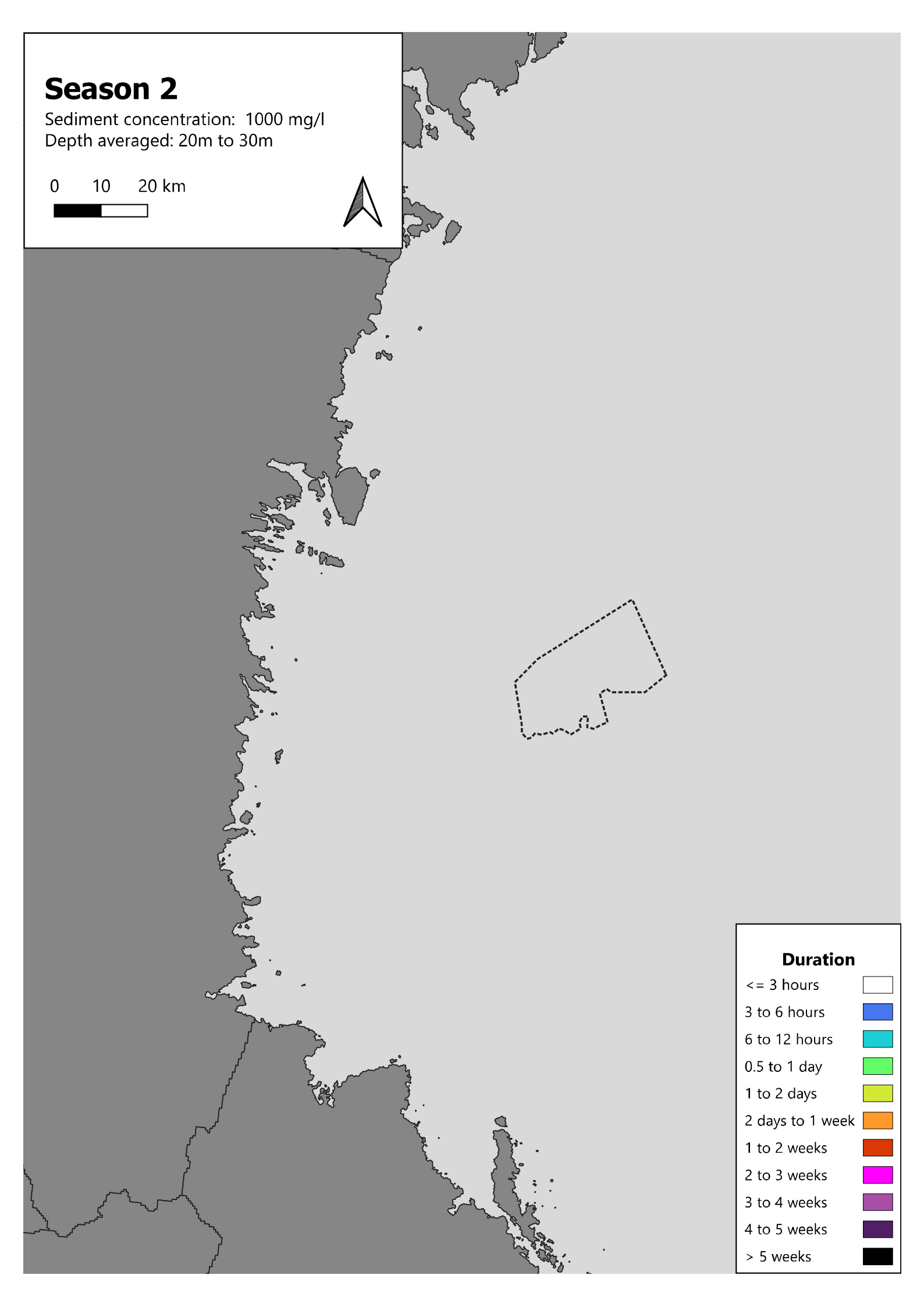


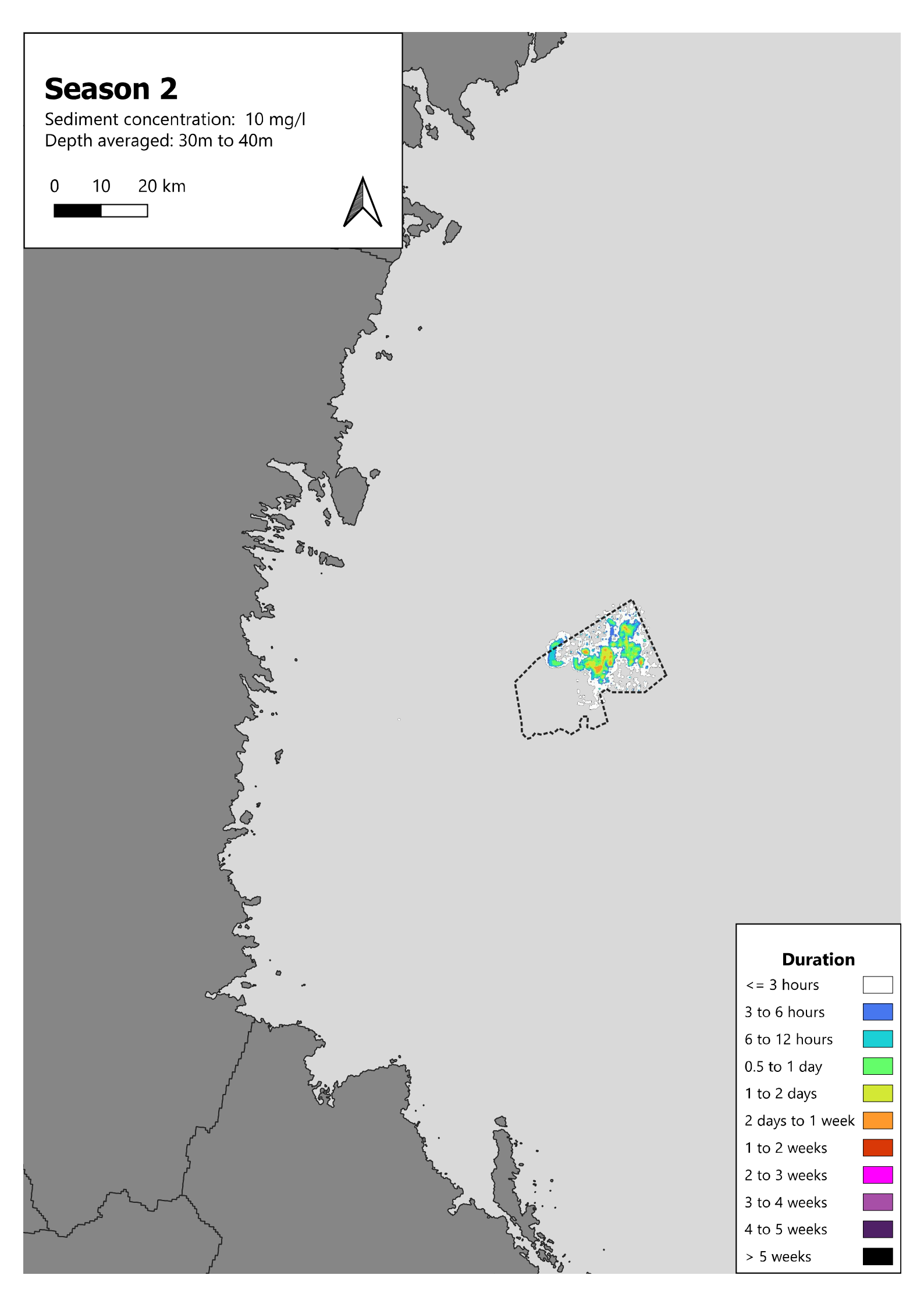


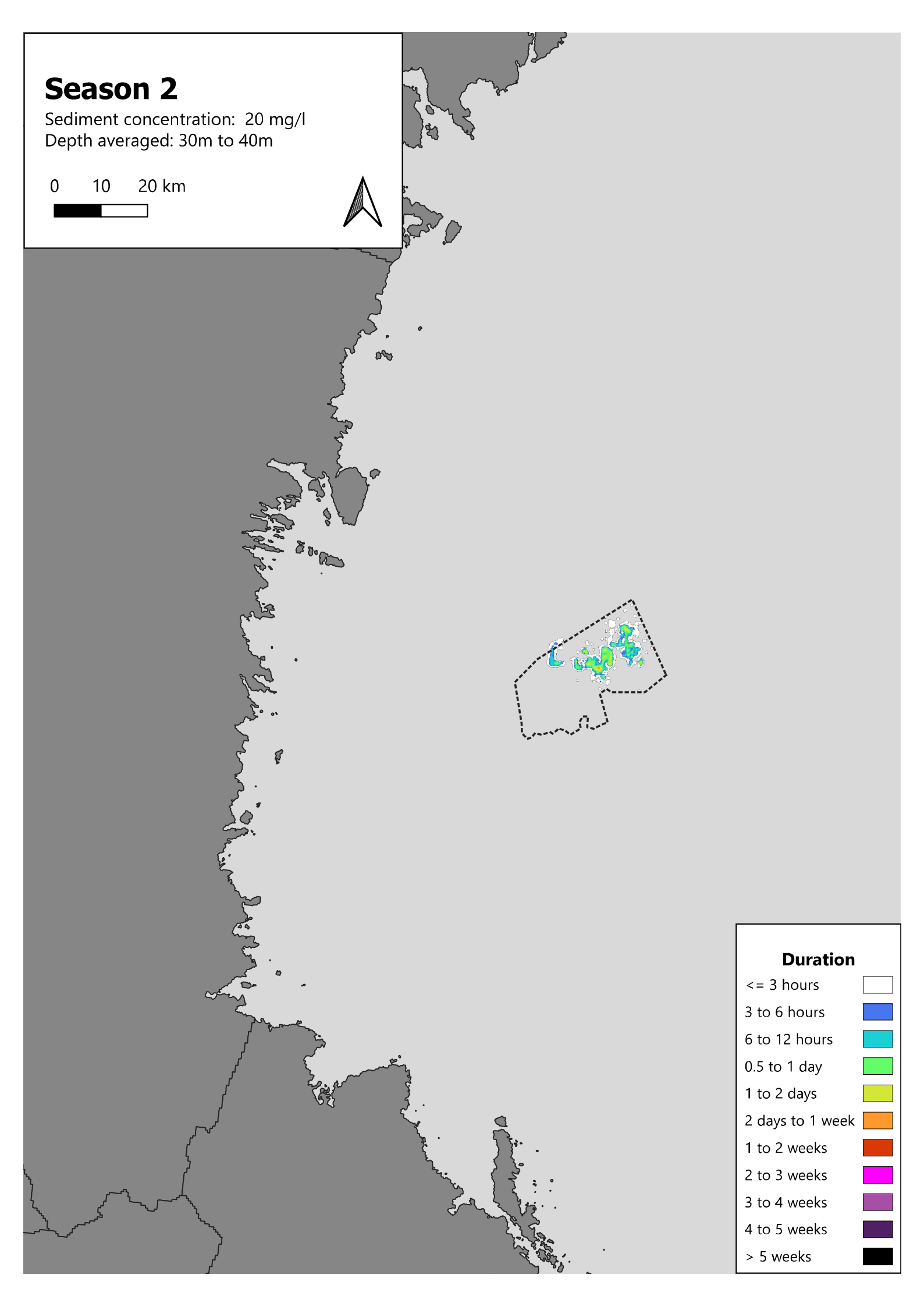


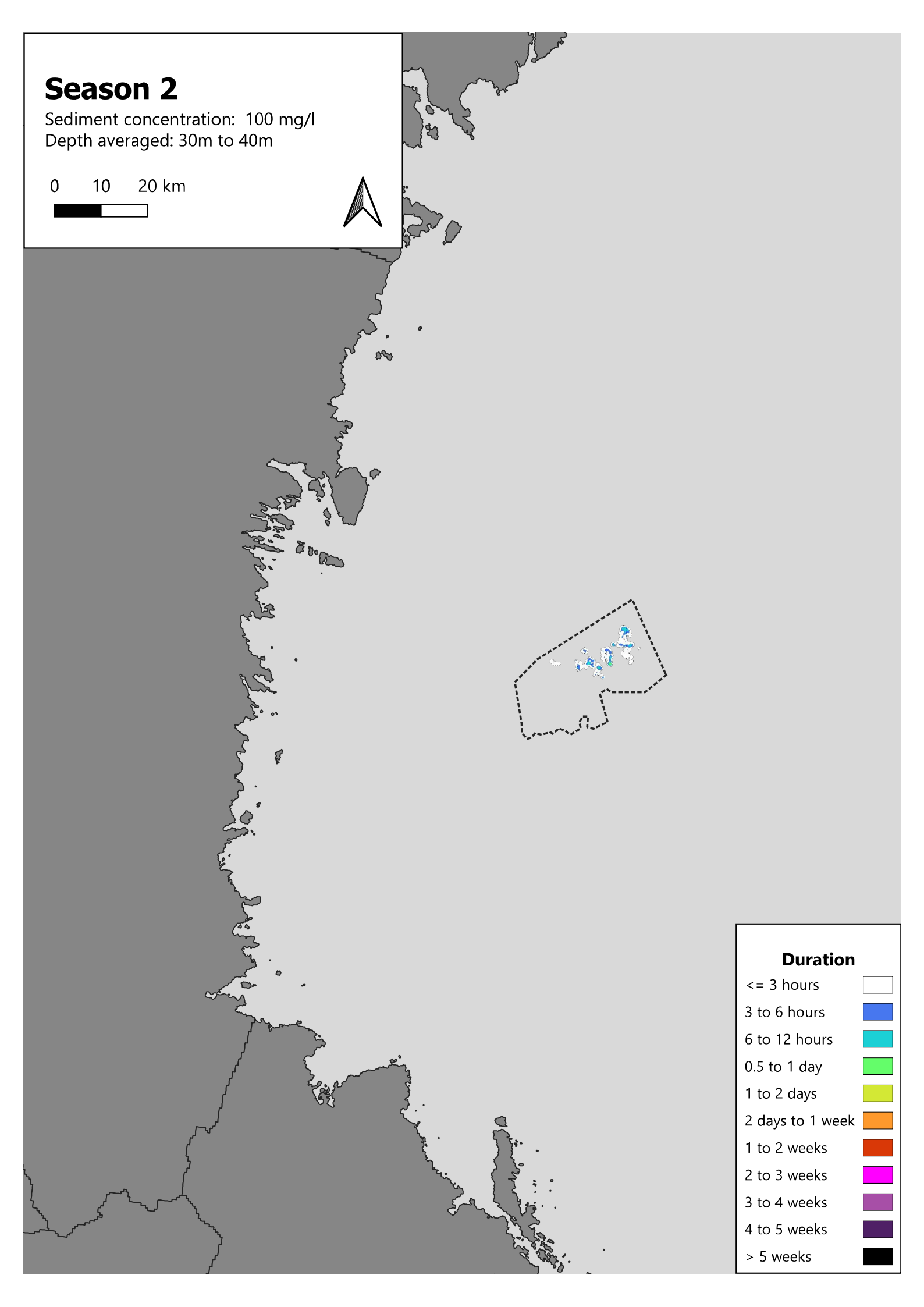


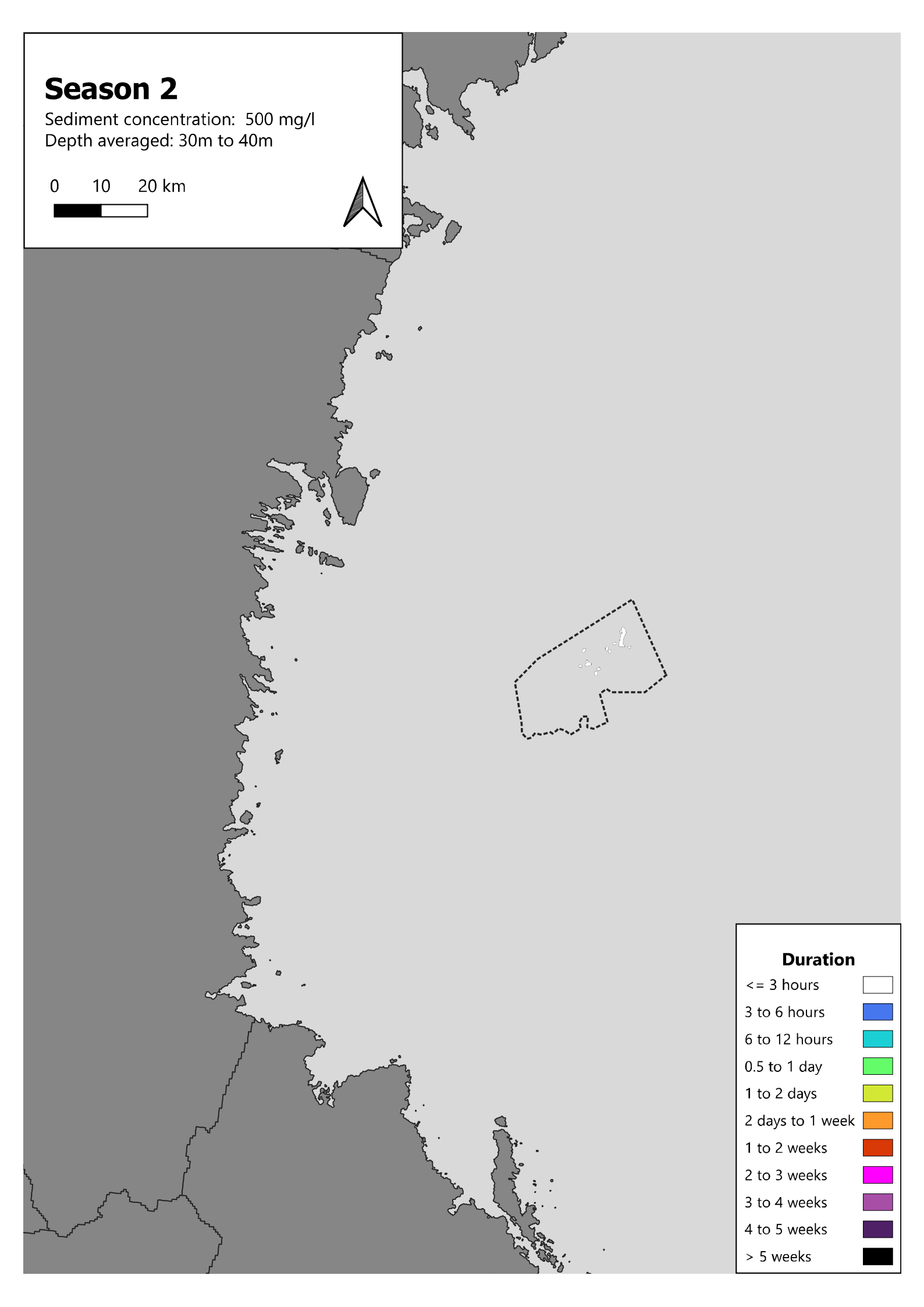


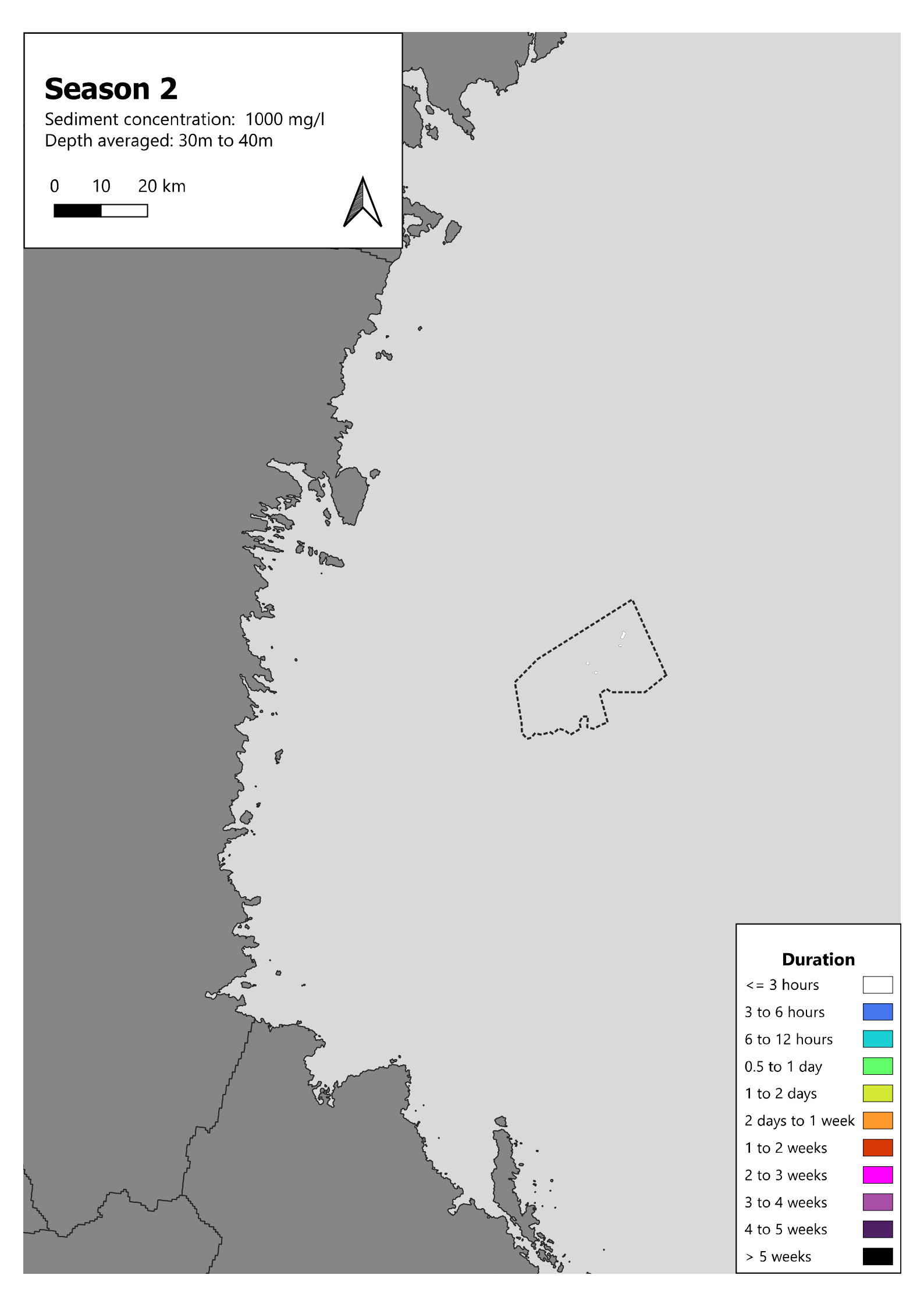


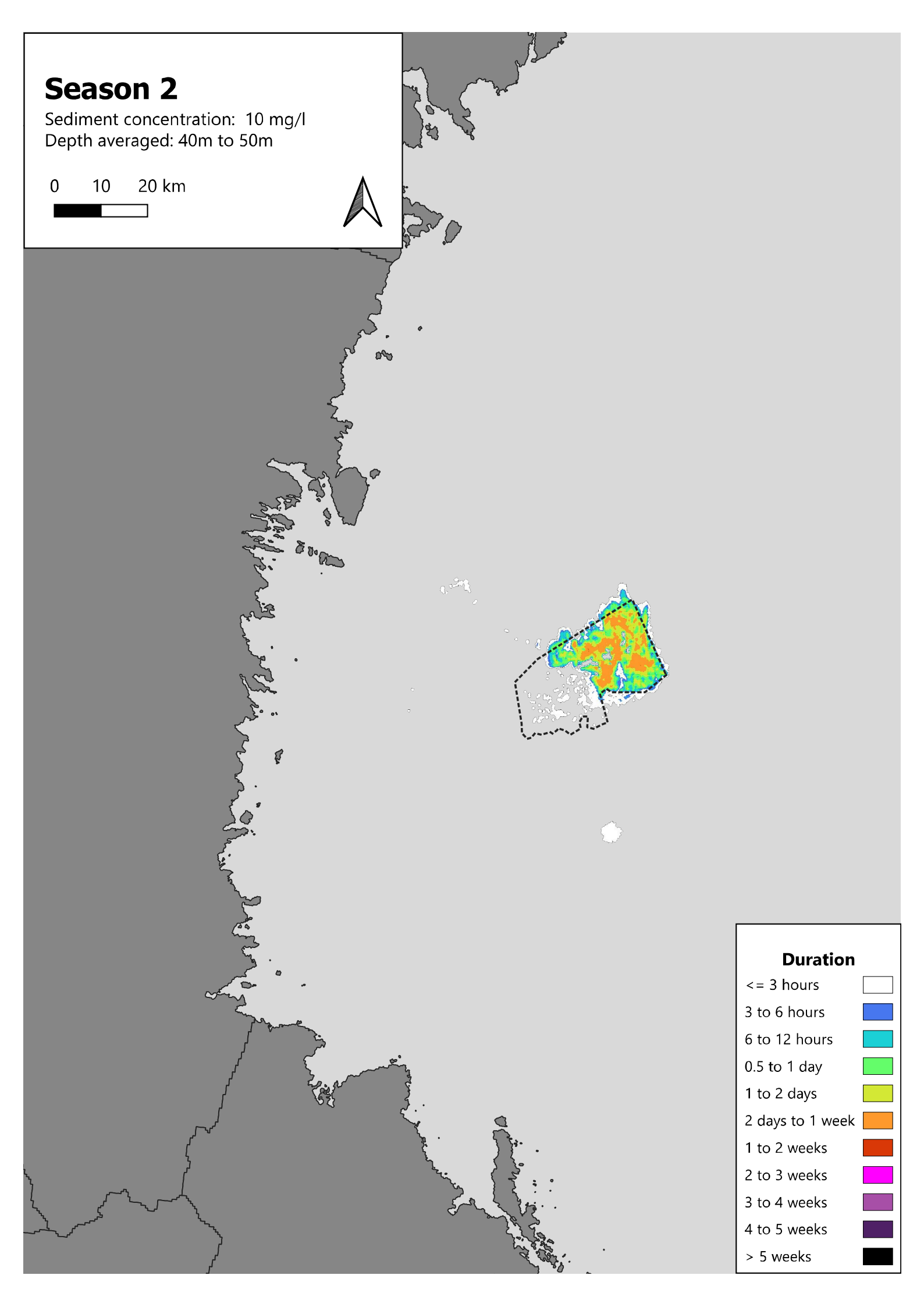


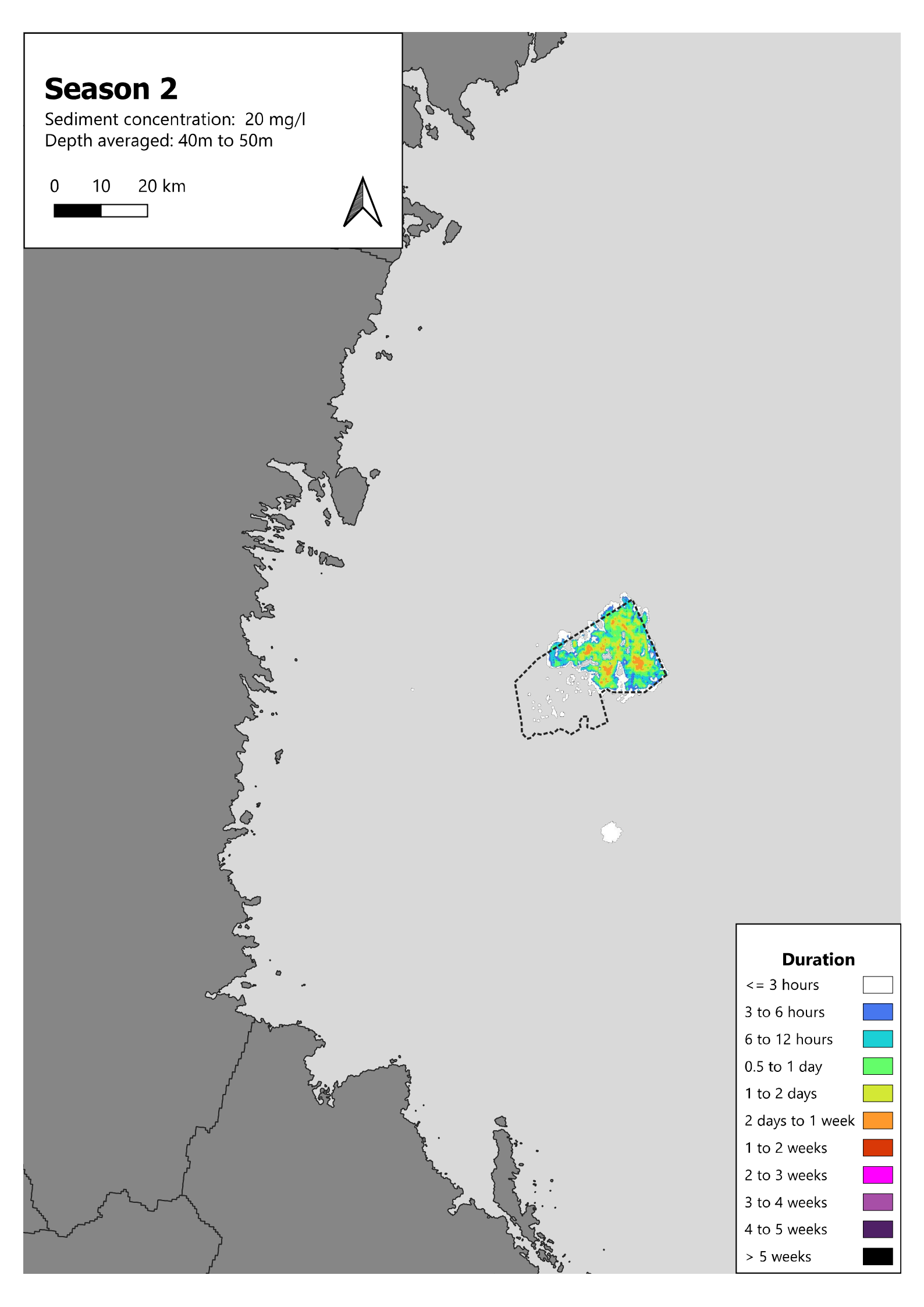


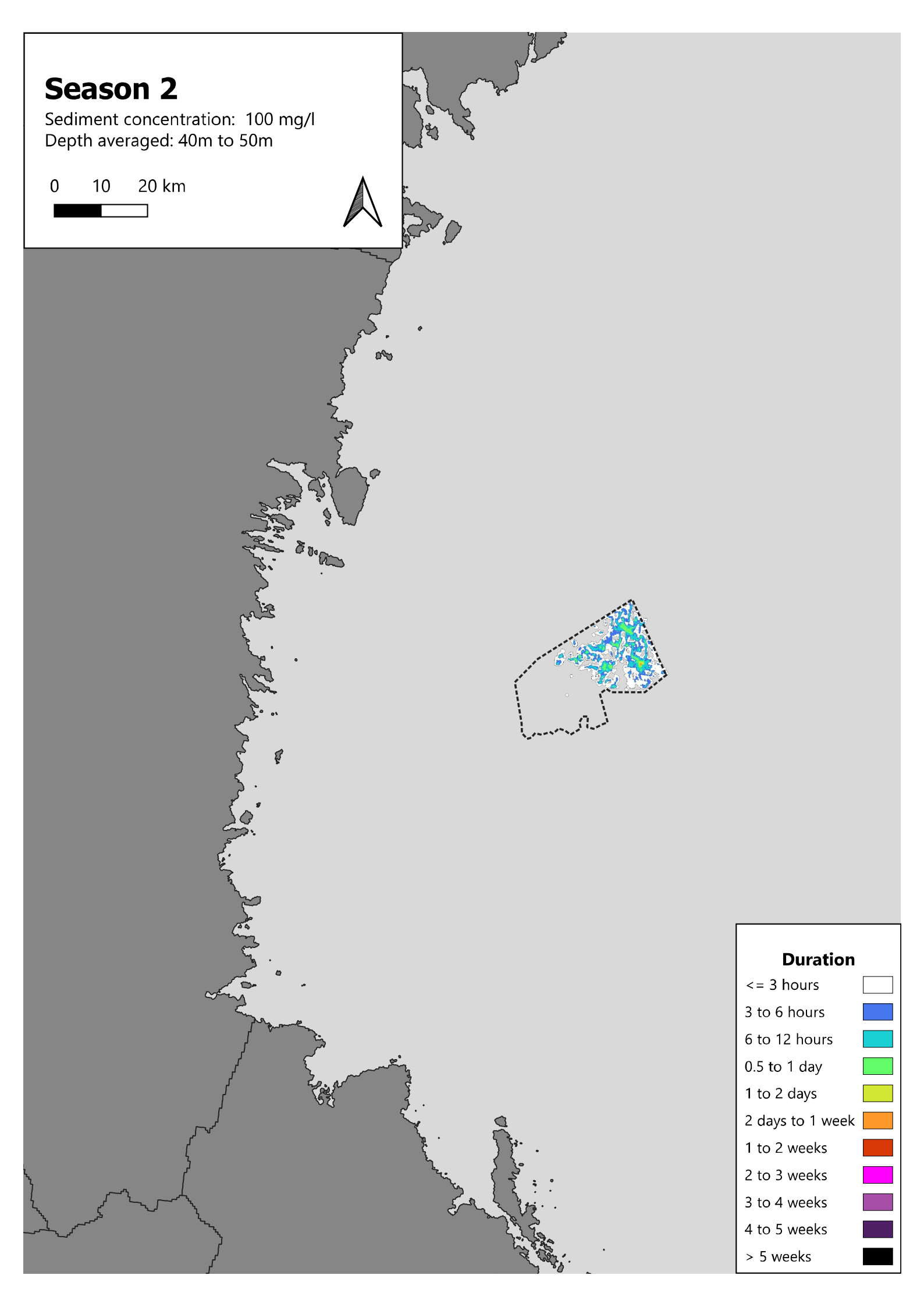


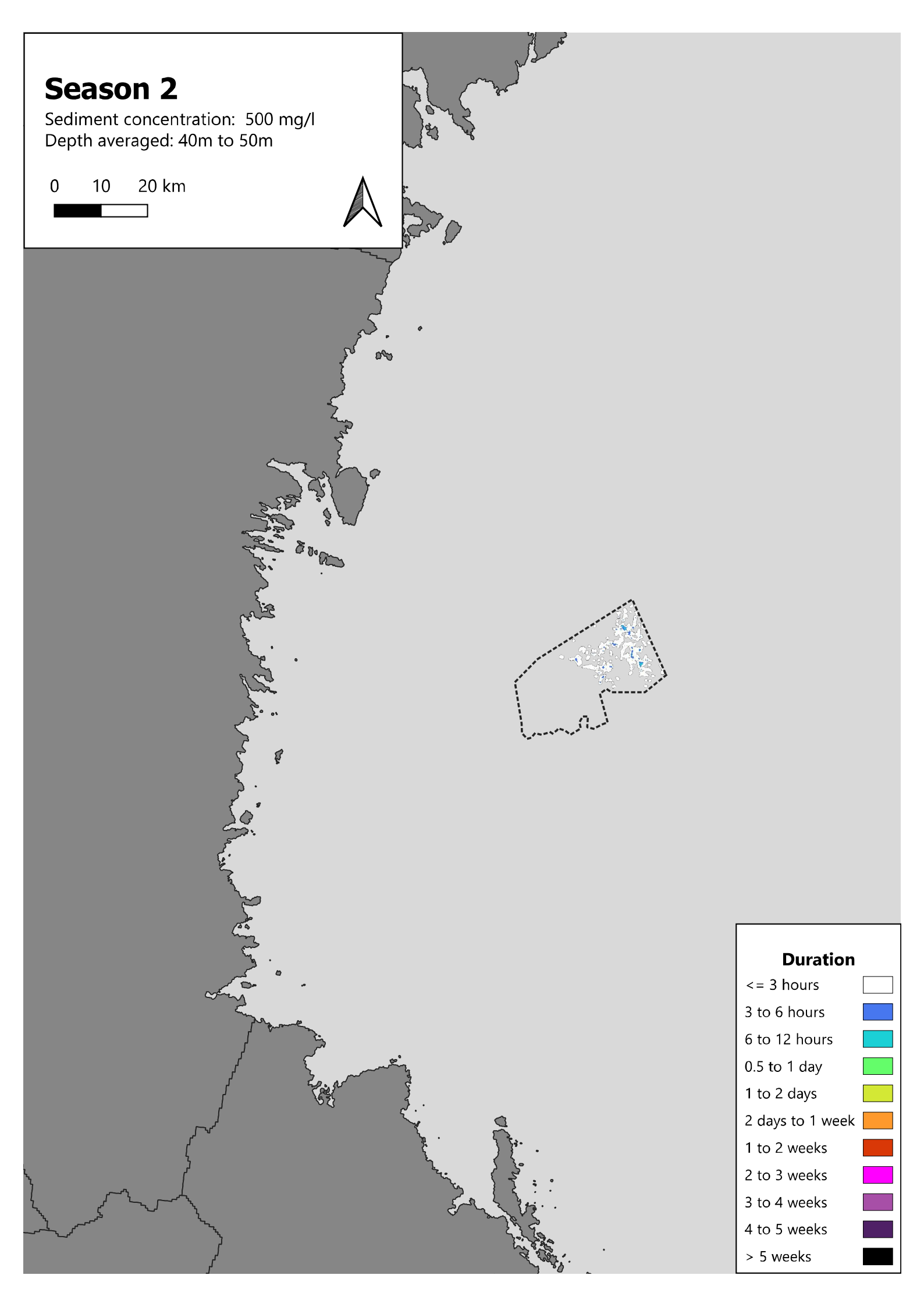


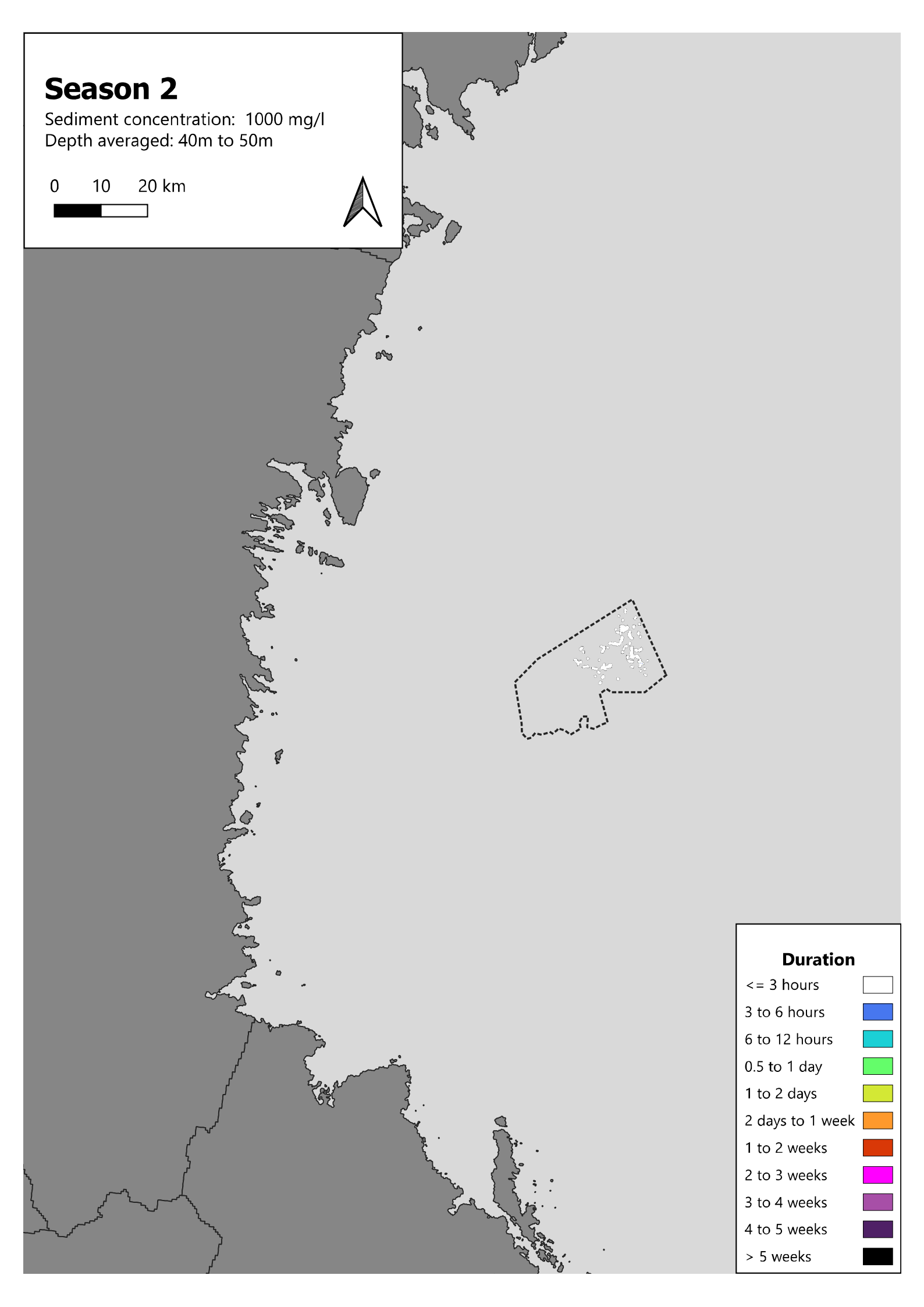


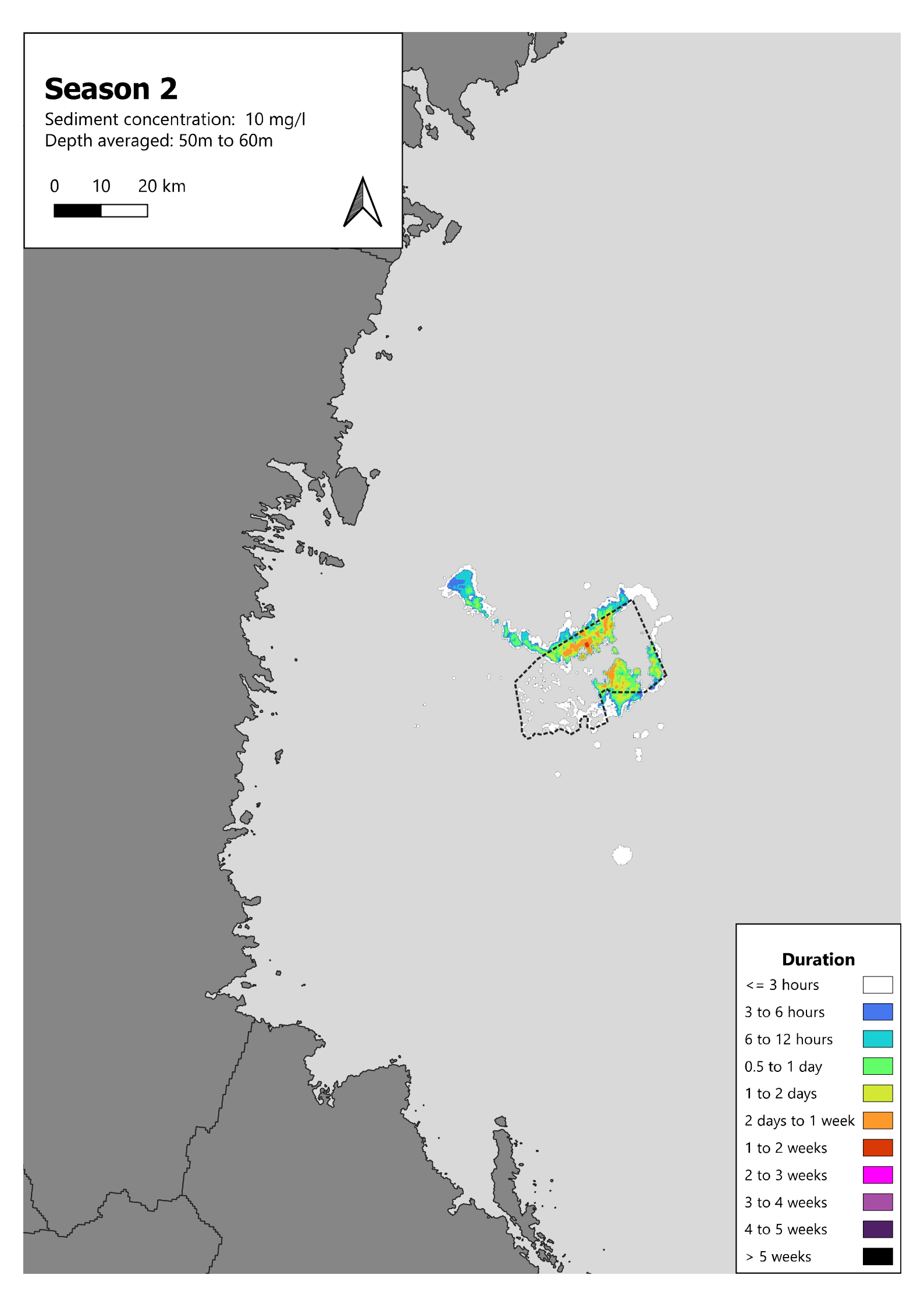


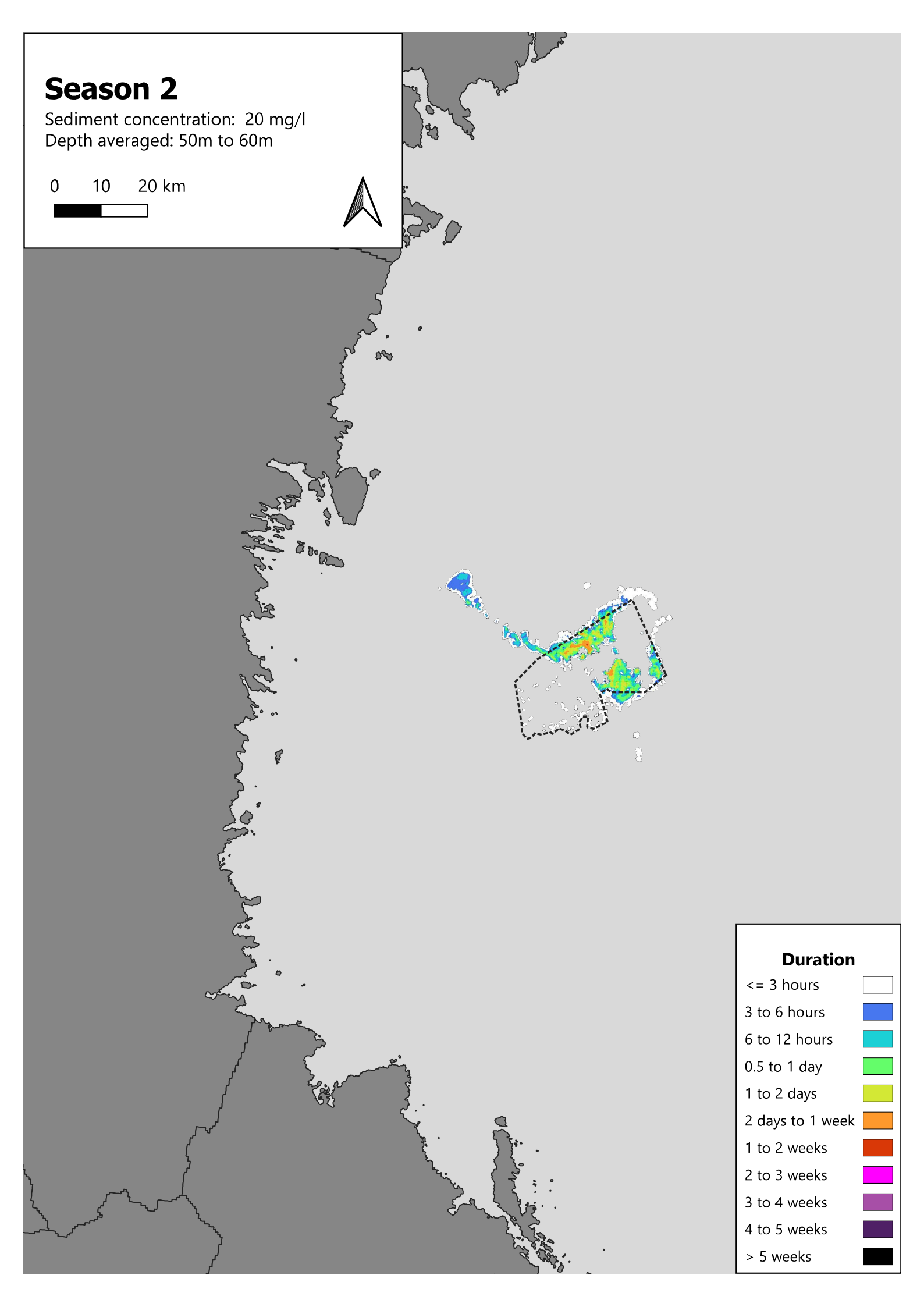


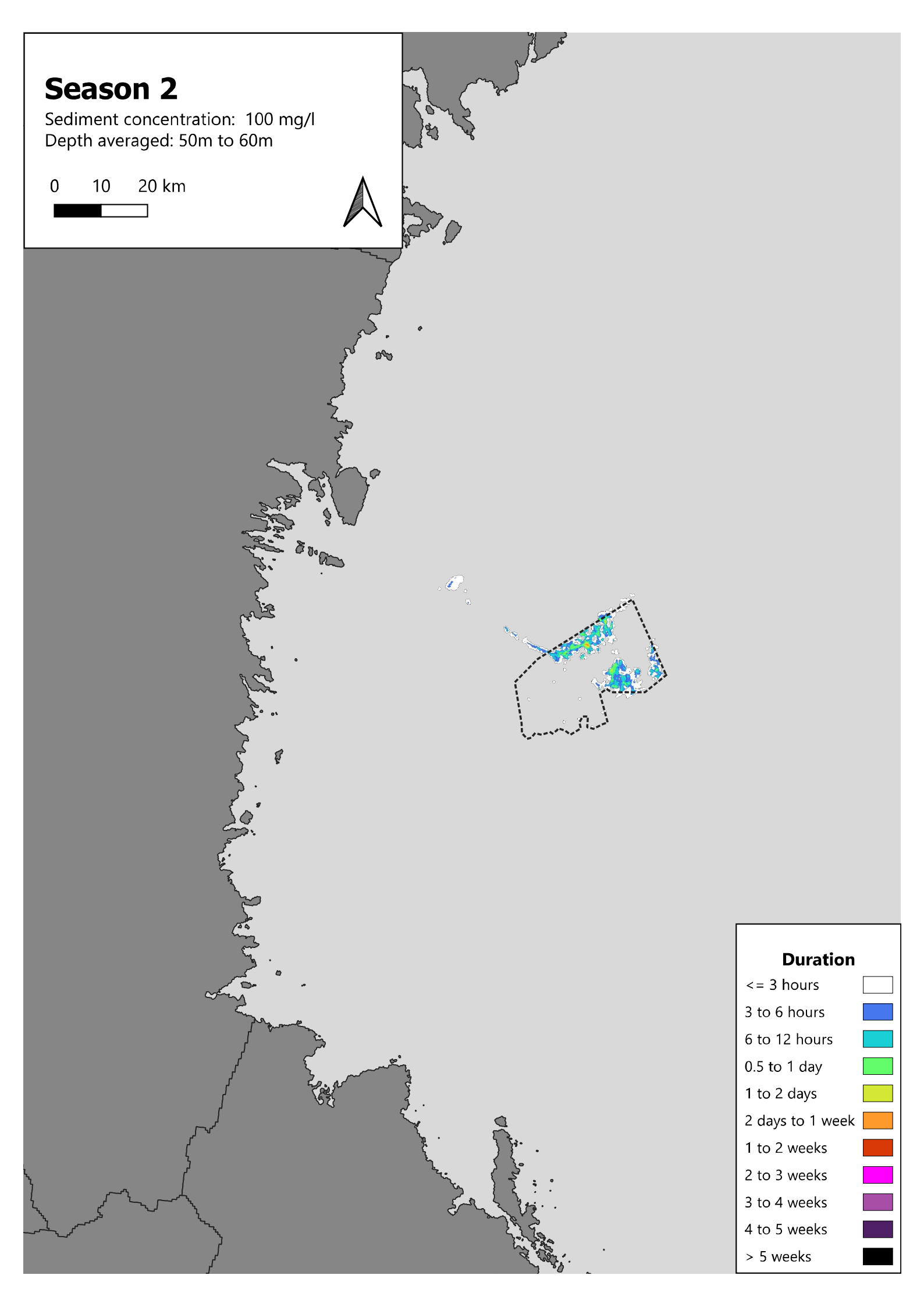


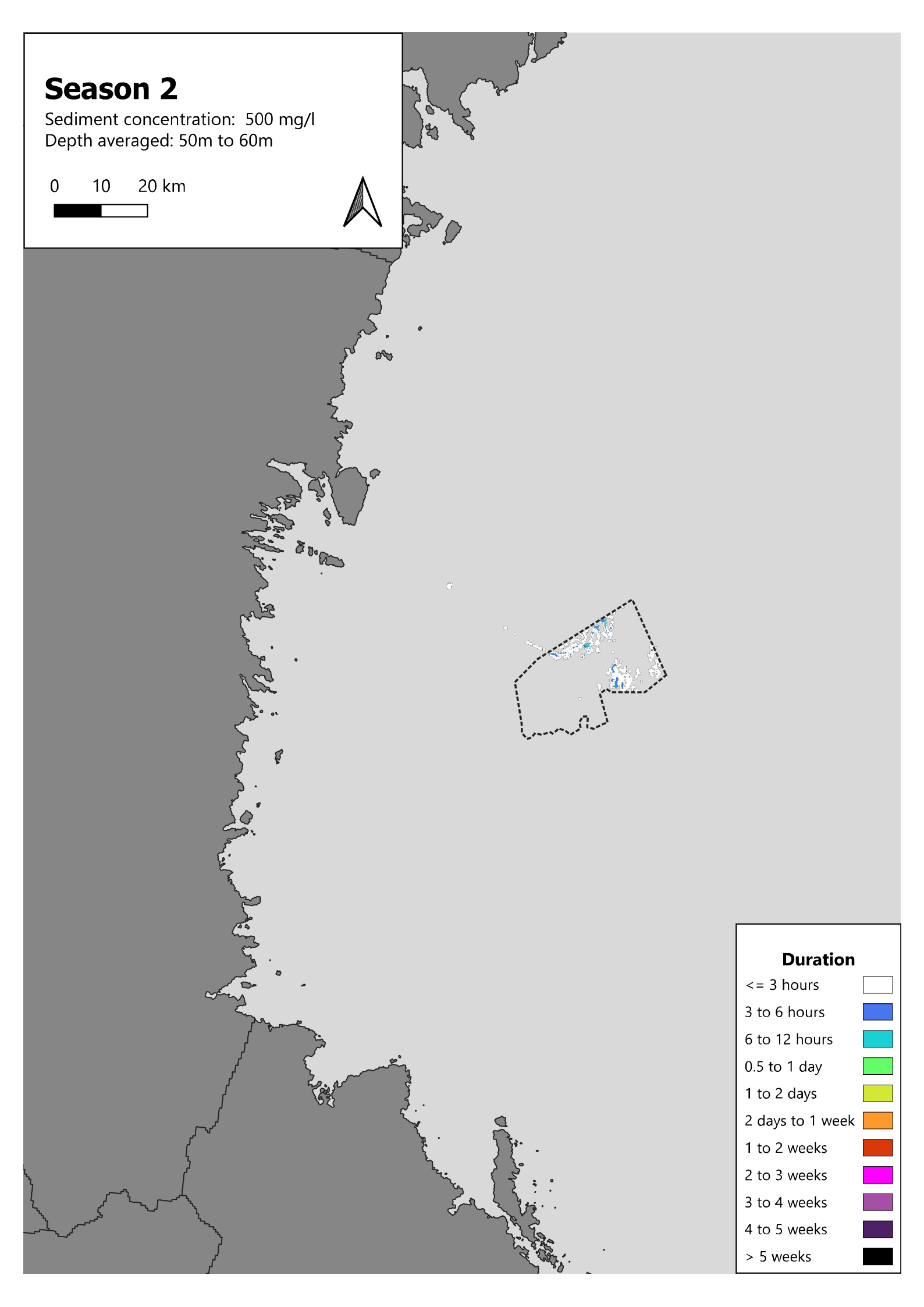


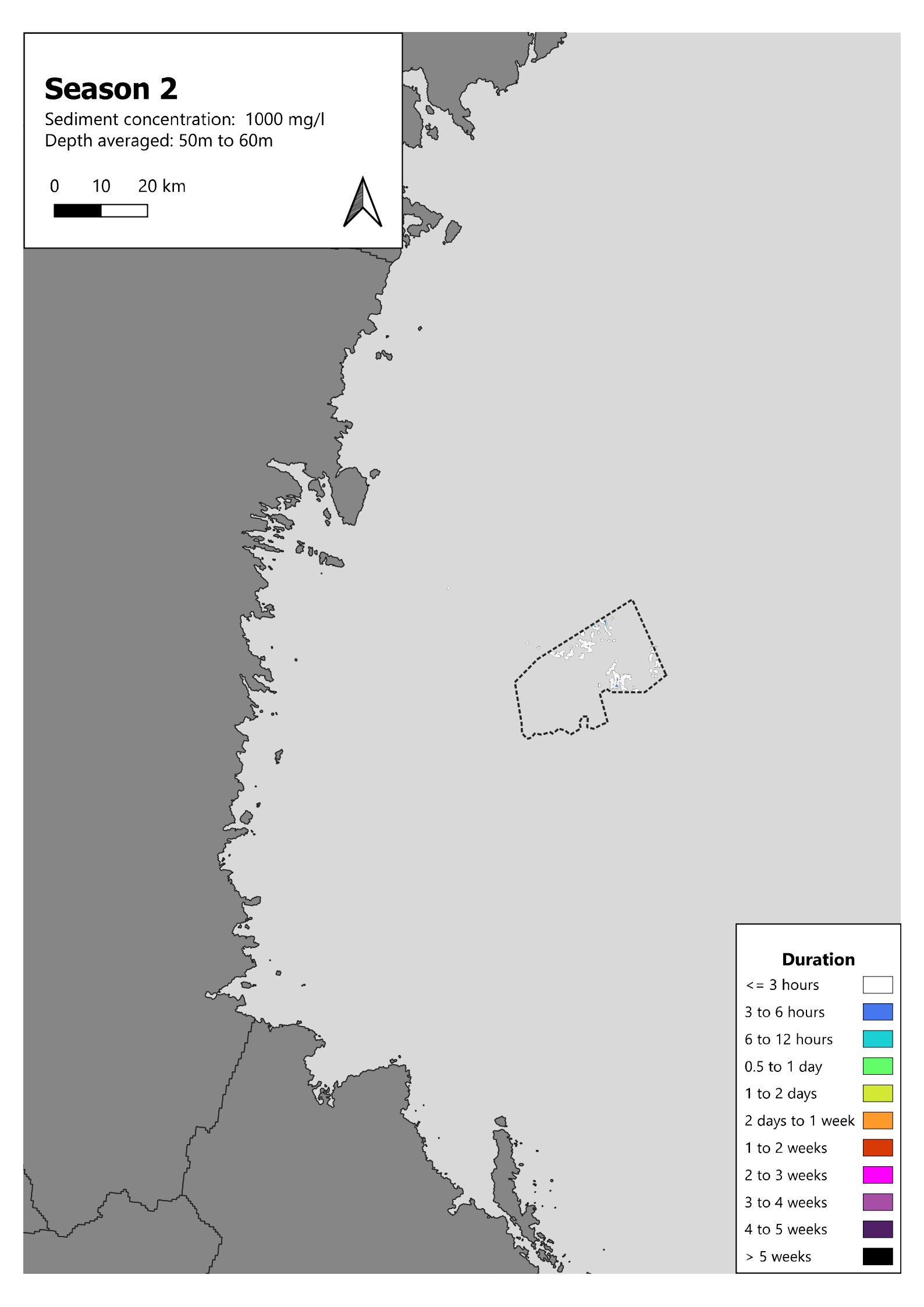


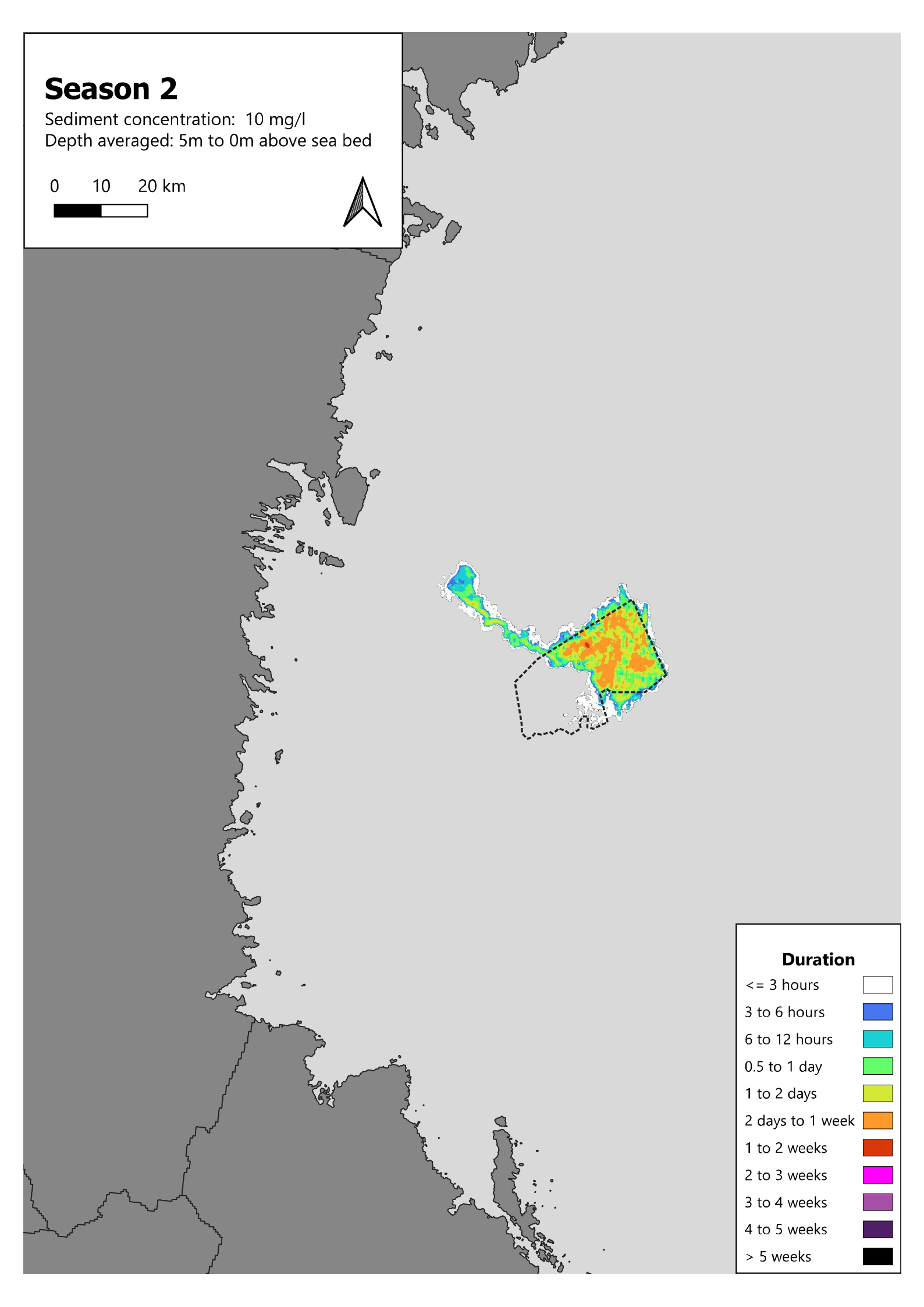


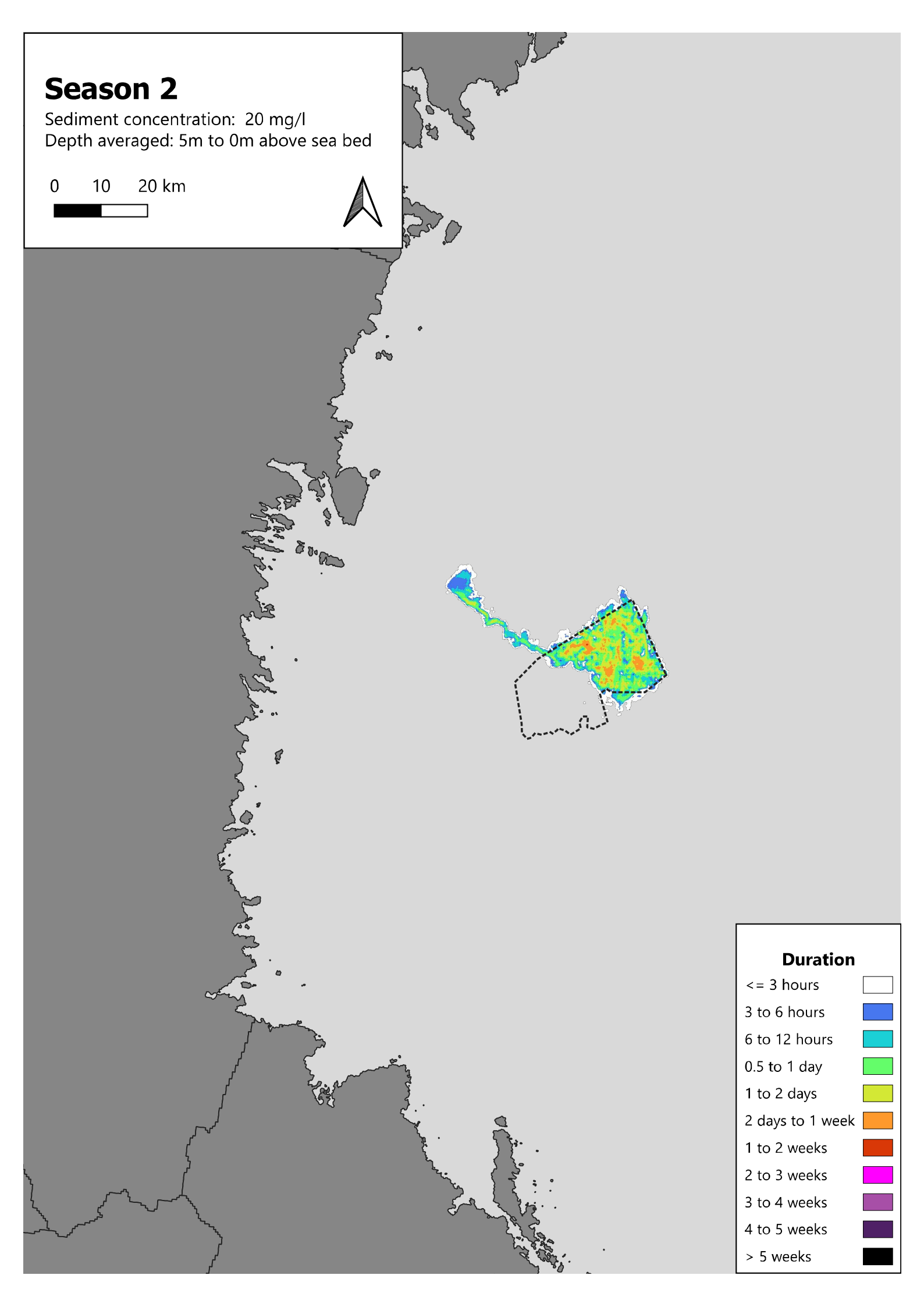


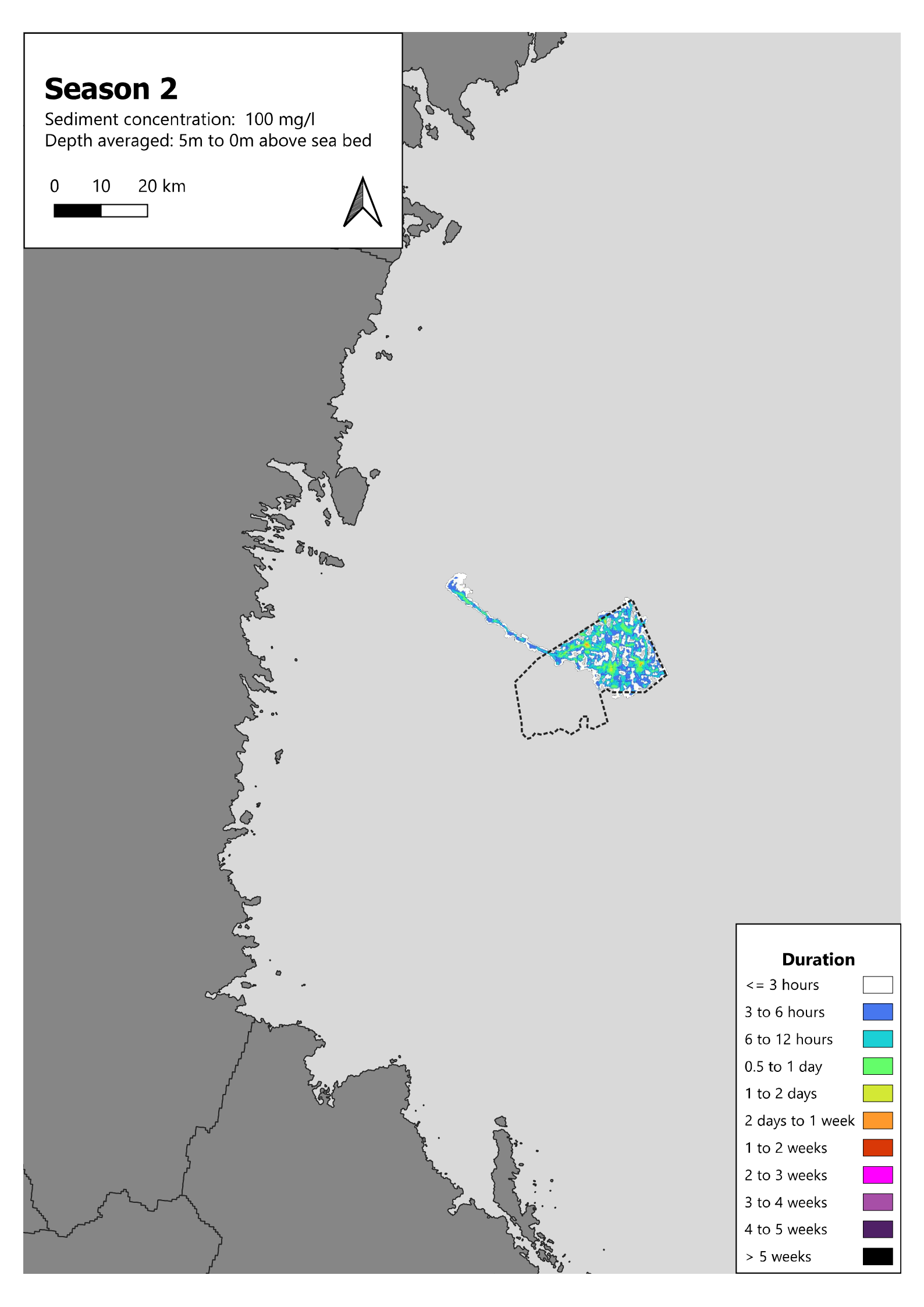


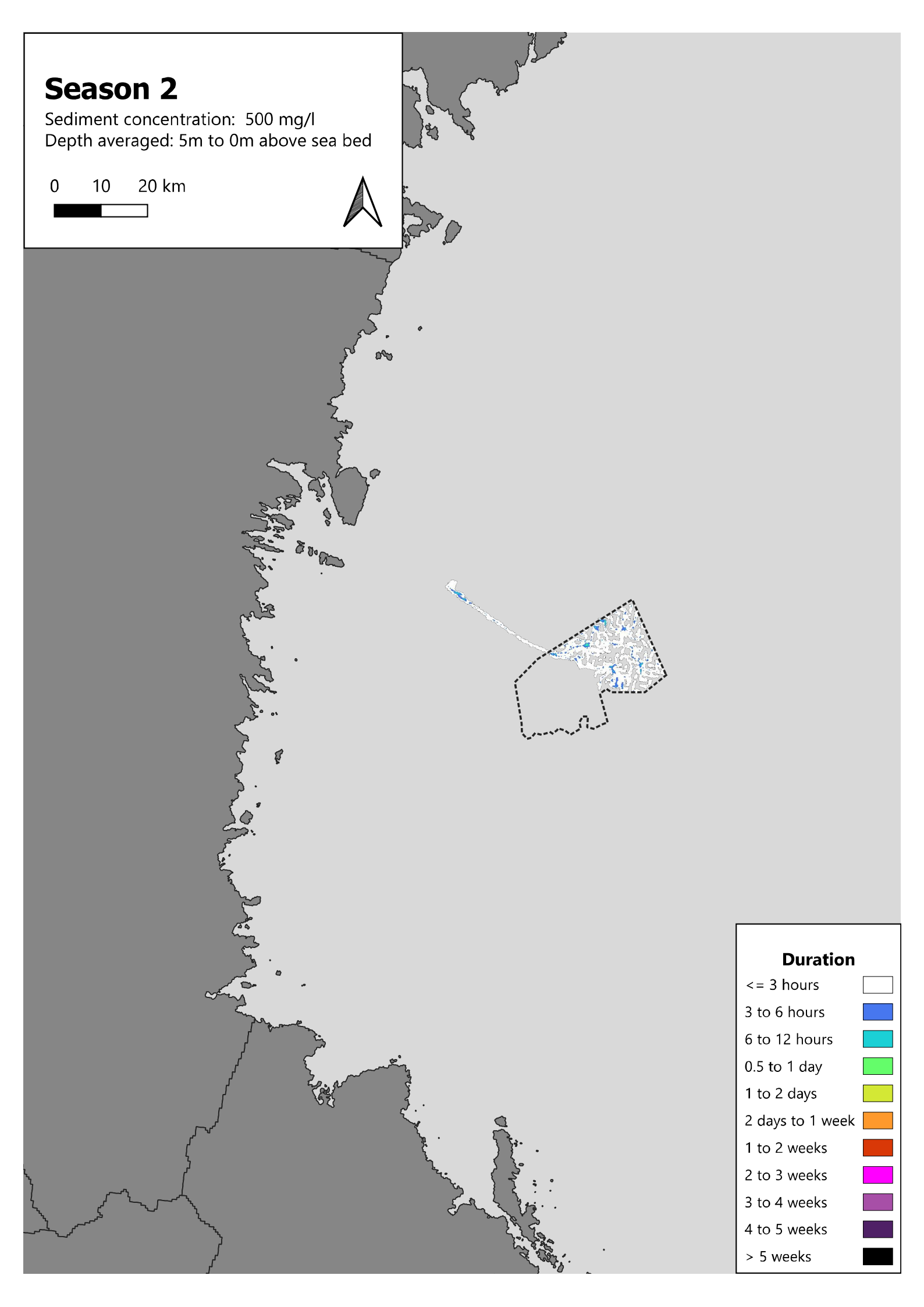


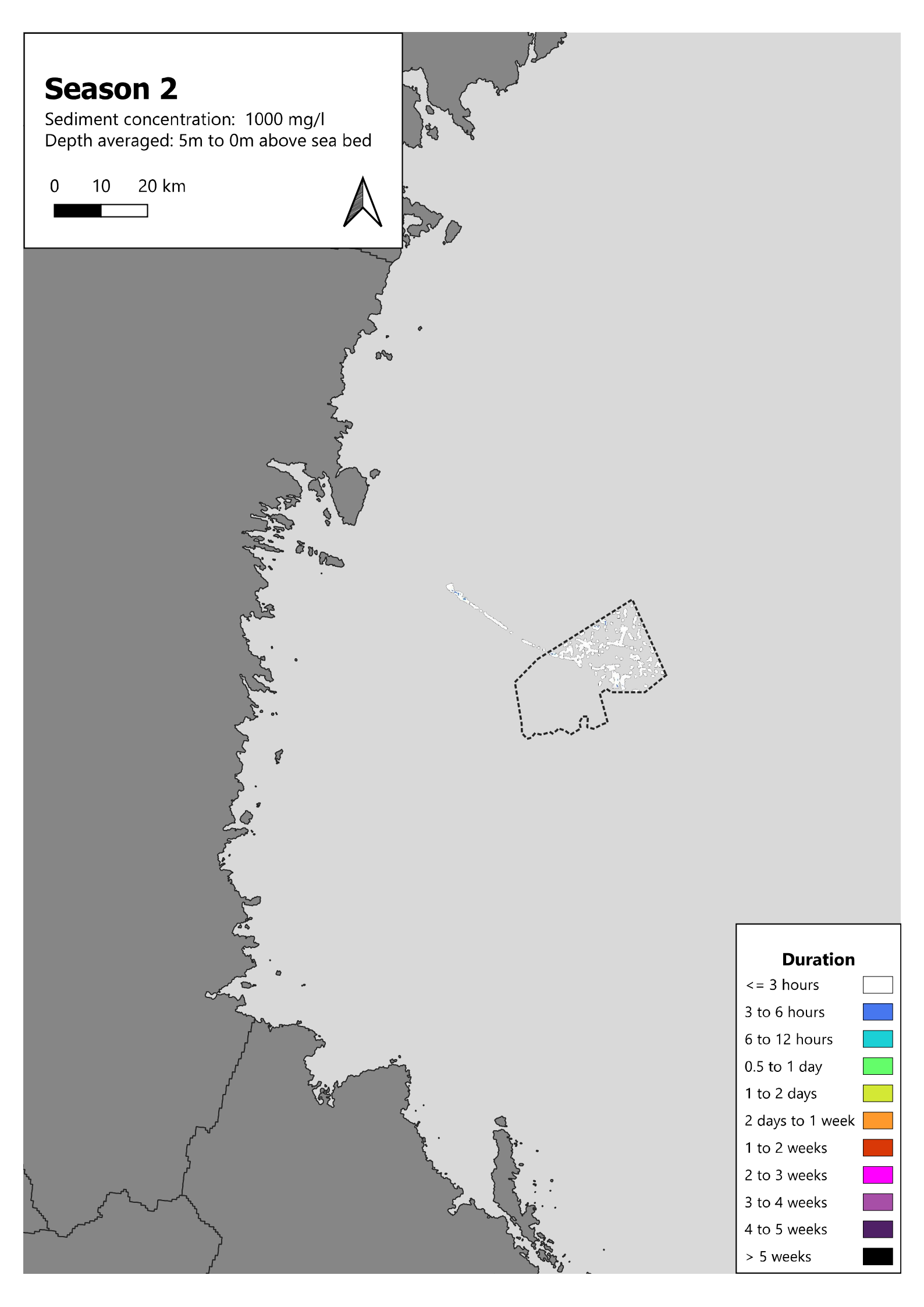








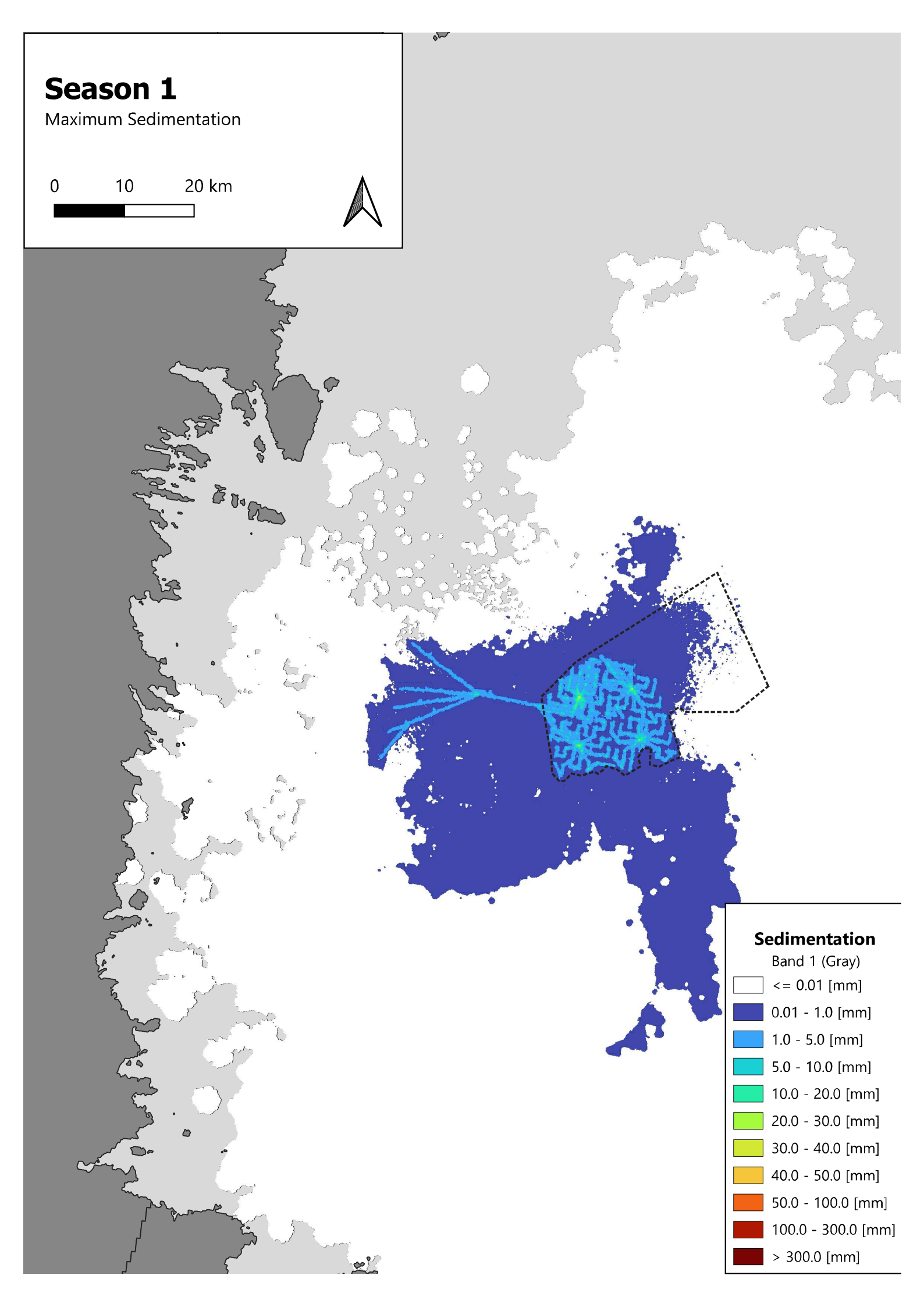


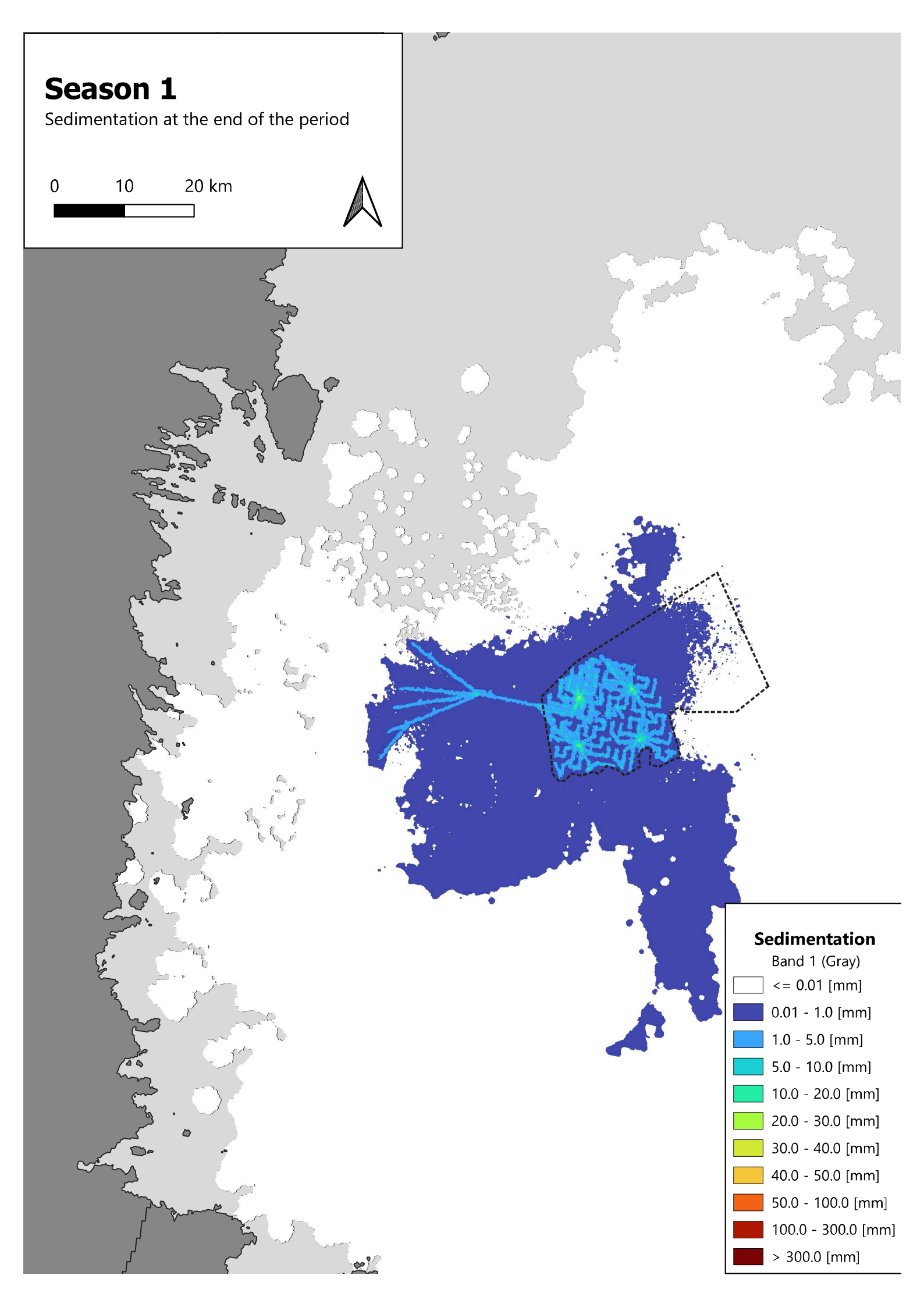




Appendix 19 Sediment dispersal: Sedimentation – seasc

Project ID: 10418781 Prepared by: AIRN Verified by: GVIG Approved by: TEB Document ID: 4S6X2MX43VNH-1644138503-81







Δr	٦ı	nen	div	20	Sedin	hent (dich	ersal.	Sedi	men	tation -	- seasor	12
ヘト	ᄱ	יו וסץ	UIX	20	Sedill	ICI IL I	aisp	cı sai.	Seal	111611	tation -	20201	1 4

